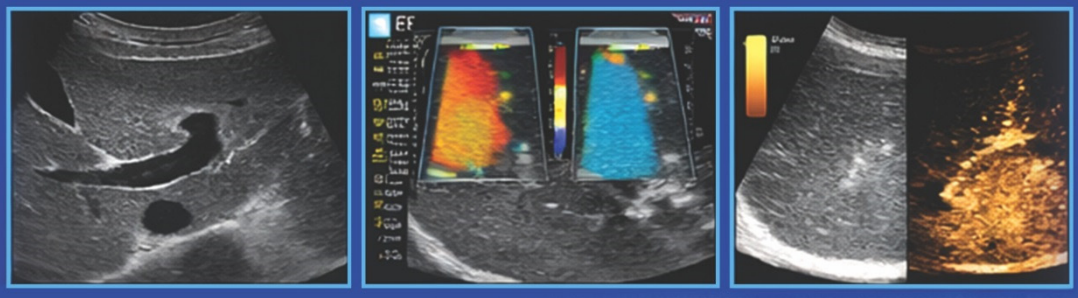
„VICTOR BABEŞ" UNIVERSITY
OF MEDICINE AND PHARMACY
FROM TIMISOARA

Multiparametric Ultrasound (MPUS)

for the Evaluation of the Liver





Edited by
Ioan Sporea, Alina Popescu, Roxana Şirli, Mirela Dănilă

HIPPOCRATE

„Victor Babeş" Publishing House
Timişoara, 2026

„Victor Babeș" Publishing House
Piața Eftimie Murgu nr. 2, cam. 316, 300041 Timișoara
Tel./Fax 0256 495 210
e-mail: evb@umft.ro
www.umft.ro/ro/organizare-evb/

General Director: Prof. univ. dr. Sorin Ursoniu

Collection: HIPPOCRATE

Collection coordinator: Prof. univ. dr. Andrei Motoc

Scientific Referent: Prof. univ. dr. Bogdan Timar

© 2026

All rights to this edition are reserved. Partial or full reproduction of the text, on any medium, without the written consent of the authors is prohibited and will be sanctioned according to the laws in force.

ISBN 978-606-786-556-1

CONTENT

1. Ultrasonography for the Hepatologist: Is It Really Necessary? 13

Ioan Sporea, Roxana Șirli

2. What does "multiparametric ultrasound" mean? 18

Alina Popescu, Ioan Sporea

3. Ultrasound anatomy of the liver 25

Ioan Sporea, Roxana Șirli

4.1. B-mode evaluation in diffuse liver diseases 36

Ioan Sporea, Alexandru Popa

4.2. Doppler Evaluation of the Liver: Technique, Clinical Value, Pitfalls, and Limitations 59

Ivica Grgurevic

4.3. Quantification of liver fat and inflammation using ultrasound 69

Ioan Sporea, Alexandru Popa, Raluca Lupușoru

5. Liver elastography for diffuse liver diseases. 84

5.1. Clinical applications—short history, indications 84

Roxana Şirli

5.2. Classification of elastographic methods and techniques 93

Felix Bende, Tudor Moga

5.3. Elastography in Chronic Viral Hepatitis 102

Ruxandra Mare, Roxana Şirli

5.4. Elastography for Metabolic Dysfunction-Associated Steatotic Liver Disease (MASLD) 119

Ioan Sporea, Alexandru Popa

5.5. The Role of Liver Elastography in Alcohol-Related Liver Disease 141

Camelia Nica, Alina Popescu

5.6. Elastography for other chronic hepatopathies (autoimmune hepatitis, primary biliary cholangitis, primary sclerosing cholangitis) 159

Alina Popescu, Tudor Moga, Raluca Lupușoru

5.7. Comparison of various elastographic techniques for liver fibrosis assessment 173

Ioan Sporea, Raluca Lupușoru

6. Ultrasound Screening for Steatotic Liver in Populations at Risk 194

Ioan Sporea, Ruxandra Mare

7. Endoscopic Ultrasound Elastography of the Liver 206

Bogdan Miuțescu, Călin Burciu, Adrian Burdan

8. Liver multiparametric ultrasound in pediatric population 221

Blerina Saraci (Qirinxhi), Durim Cela, Denis Qirinxhi

9. Multiparametric Ultrasound for Focal Liver Lesions..... 244

9.1. B-mode evaluation for Focal Liver Lesions (FLL) 244

Mirela Dănilă, Ana-Maria Ghiuchici

9.2. Why do we need Liver Contrast Enhanced Ultrasound (CEUS)? 273

Ioan Sporea

9.3. CEUS of the Liver: indications, technique, limitations 279

Tudor Moga, Alina Popescu

9.4. CEUS for benign focal liver lesions 287

Roxana Şirli, Tudor Moga

9.5. Contrast enhanced ultrasound (CEUS) for malignant lesions 301

Mirela Dănilă, Ana Maria Ghiuchici

9.6. Contrast-Enhanced Ultrasound (CEUS) for the Follow-Up of Percutaneous Treatment of Liver Tumors 328

Felix Bende, Tudor Moga

9.7. Evidence-Based Proofs of the Value of Contrast-Enhanced Ultrasound (CEUS) for Focal Liver Lesions (FLL) 338

Ioan Sporea, Raluca Lupușoru

9.8. Elastography for Focal Liver Lesions (FLL) 345

Ana-Maria Ghiuchici, Mirela Dănilă

10. Ultrasound for Hepatocellular Carcinoma (HCC) screening: when and how? 355

Mirela Dănilă, Ioan Sporea

11. Multiparametric Ultrasound for Portal Hypertension 366

11.1. Standard Ultrasound for Portal Hypertension 366

Ivica Grgurević

11.2. Value of Doppler ultrasound for the evaluation of Portal Hypertension 374

Ivica Grgurević

11.3. Portal vein thrombosis: value of standard ultrasound and contrast enhanced ultrasound (CEUS) 386

Mirela Dănilă, Ana Maria Ghiuchici

11.4. Liver and Spleen elastography and combination for portal hypertension 398

Felix Bende, Renata Bende, Iulia Rațiu

12. Point of Care Ultrasound (PoCUS) in Hepatology: when to use it and how to use it? 426

Ioan Sporea, Roxana Șirli

13. Handheld ultrasound devices: How to Use Them?..... 433

Alina Popescu, Tudor Moga

14. Comparison between Imaging Methods for Liver Evaluation..... 440

Durim Cela, Blerina Saraci, Denis Qirinxhi

15. Recent development of ultrasound for liver (PAT, Micro-flow, Image fusion ultrasongraphy, Drug delivery) 473

Felix Bende, Tudor Moga, Raluca Lupuşoru

16. Artificial Intelligence in Liver Ultrasound..... 484

Ioan Sporea, Alexandru Popa

Foreword

Over the past decade, the concept of multiparametric imaging has become increasingly important in modern medical diagnostics. Initially introduced in the field of magnetic resonance imaging, the term "multiparametric" has progressively expanded into other imaging modalities. In recent years, it has also become a reality in the field of ultrasound, where continuous technological developments have enabled the integration of multiple evaluation parameters within a single examination.

With the rapid evolution of ultrasound technology, clinicians now have access to a growing number of complementary imaging techniques. These modalities provide structural, functional, and hemodynamic information, allowing a more comprehensive assessment of organs and pathological processes. In hepatology in particular, the combination of conventional B-mode ultrasound, Doppler techniques, elastography, and contrast-enhanced ultrasound has opened new perspectives for the noninvasive evaluation of liver diseases.

This book, "Multiparametric Ultrasound (MPUS) for the Evaluation of the Liver," aims to present to clinicians and researchers the many facets of this modern diagnostic approach. It is addressed primarily to practitioners involved in liver ultrasound, but also to gastroenterologists, hepatologists, radiologists, and other specialists interested in advanced ultrasound techniques. The chapters explore both the current clinical applications of multiparametric ultrasound and the potential future developments of this rapidly evolving field.

The multiparametric facets of ultrasound also enable its use as a clinical tool, in a point-of-care setting, enabling a rapid diagnosis and a quick therapeutic decision, benefitting the patient and the doctor as well.

The book has been written by authors with extensive experience in hepatology and ultrasound imaging, performing a large number of examinations in their daily clinical practice. Their combined expertise ensures

that the content reflects both scientific evidence and practical clinical experience. Artificial intelligence tools have also been used as supportive instruments in the preparation and refinement of the manuscript, helping to achieve the best possible clarity and presentation.

As this work is published primarily as an English-language ebook, we believe it represents an efficient way to disseminate knowledge globally, reaching clinicians and researchers wherever ultrasound is practiced and appreciated.

We hope that this book will serve not only as a reference for current practice but also as a source of inspiration for the continued adoption of new ultrasound technologies in everyday clinical work. Enjoy the book and explore the possibilities offered by liver multiparametric ultrasound in your daily practice!

LIST OF AUTHORS

Editors

Ioan Sporea, MD, PhD, FEBGH, Doctor Honoris Causa – Professor of Gastroenterology, "Victor Babeș" University of Medicine and Pharmacy Timișoara, Romania; Regional Research Center in Advanced Hepatology of the Romanian Academy of Medical Sciences; World Federation of Ultrasound in Medicine and Biology (WFUMB) Past-Vice-President; Director of WFUMB Center of Education, Timișoara, Romania

Alina Popescu, MD, PhD – Professor of Gastroenterology, Head of the Department of Gastroenterology and Hepatology at "Pius Brînzeu" Clinical Emergency County Hospital Timișoara; Center for Advanced Research in Gastroenterology and Hepatology, "Victor Babeș" University of Medicine and Pharmacy, Timișoara, Romania; European Federation of Ultrasound in Medicine and Biology (EFSUMB) Honorary Treasurer; secretary of WFUMB Center of Education, Timișoara, Romania

Roxana Șirli, MD, PhD – Professor of Gastroenterology, Department of Gastroenterology and Hepatology, Center for Advanced Research in Gastroenterology and Hepatology, "Victor Babeș" University of Medicine and Pharmacy, Timișoara, Romania, "Pius Brînzeu" Clinical Emergency County Hospital Timișoara, Romania; WFUMB Center of Education, Timișoara, Romania

Mirela Dănilă, MD, PhD – Professor of Gastroenterology, Department of Gastroenterology and Hepatology, Center for Advanced Research in Gastroenterology and Hepatology, "Victor Babeș" University of Medicine and Pharmacy, Timișoara, Romania, "Pius Brînzeu" Clinical Emergency County Hospital Timișoara, Romania; WFUMB Center of Education, Timișoara, Romania

Co-authors

Felix Bende, MD, PhD – Department of Gastroenterology and Hepatology, Center for Advanced Research in Gastroenterology and Hepatology, "Victor Babeș" University of Medicine and Pharmacy, Timișoara, Romania, "Pius Brînzeu" Clinical Emergency County Hospital Timișoara, Romania; WFUMB Center of Education, Timișoara, Romania

Renata Bende MD, PhD – Department of Gastroenterology and Hepatology, Center for Advanced Research in Gastroenterology and Hepatology, "Victor Babeș" University of Medicine and Pharmacy, Timișoara, Romania, "Pius Brînzeu" Clinical Emergency County Hospital Timișoara, Romania; WFUMB Center of Education, Timișoara, Romania

Călin Burciu, MD, PhD - Department of Gastroenterology, Faculty of Medicine, Pharmacy and Dental Medicine, “Vasile Goldis” West University of Arad, Romania; Center for Advanced Research in Gastroenterology and Hepatology, "Victor Babeș" University of Medicine and Pharmacy, Timișoara, Romania

Adrian Burdan, MD, PhD student, Advanced Regional Research Center in Gastroenterology and Hepatology, "Victor Babes" University of Medicine and Pharmacy, Timisoara, Romania

Durim Cela, MD, PhD – Associate Professor of Radiology, University of Medicine, Tirana, Albania; Director of WFUMB Center of Education, Tirana, Albania

Anamaria Ghiuchici, MD, PhD – Department of Gastroenterology and Hepatology, Center for Advanced Research in Gastroenterology and Hepatology, "Victor Babeș" University of Medicine and Pharmacy, Timișoara, Romania, "Pius Brînzeu" Clinical Emergency County Hospital Timișoara, Romania; WFUMB Center of Education, Timișoara, Romania

Ivica Grgurević, MD, PhD, FEBGH, FRCP (London) – Professor of Gastroenterology; Consultant Gastroenterologist and Hepatologist, Department of Gastroenterology, Hepatology and Clinical Nutrition, University of Zagreb School of Medicine; Faculty of Pharmacy and Biochemistry; University Hospital Dubrava; Director of WFUMB Center of Education, Zagreb, Croatia

Raluca Lupușoru MD, PhD – Department of Gastroenterology and Hepatology, Center for Advanced Research in Gastroenterology and Hepatology, "Victor Babeș" University of Medicine and Pharmacy, Timișoara, Romania, "Pius Brînzeu" Clinical Emergency County Hospital Timișoara, Romania; WFUMB Center of Education, Timișoara, Romania

Ruxandra Mare, MD, PhD – Department of Gastroenterology and Hepatology, Center for Advanced Research in Gastroenterology and Hepatology, "Victor Babeș" University of Medicine and Pharmacy, Timișoara, Romania, "Pius Brînzeu" Clinical Emergency County Hospital Timișoara, Romania; WFUMB Center of Education, Timișoara, Romania

Bogdan Miuțescu, MD, PhD – Department of Gastroenterology and Hepatology, Center for Advanced Research in Gastroenterology and Hepatology, "Victor Babeș" University of Medicine and Pharmacy, Timișoara, Romania, "Pius Brînzeu" Clinical Emergency County Hospital Timișoara, Romania; WFUMB Center of Education, Timișoara, Romania

Tudor Moga, MD, PhD – Department of Gastroenterology and Hepatology, Center for Advanced Research in Gastroenterology and Hepatology, "Victor Babeș" University of Medicine and Pharmacy, Timișoara, Romania, "Pius Brînzeu" Clinical Emergency County Hospital Timișoara, Romania; WFUMB Center of Education, Timișoara, Romania

Camelia Nica, MD, PhD – Department of Gastroenterology and Hepatology, Center for Advanced Research in Gastroenterology and Hepatology, "Victor Babeș" University of Medicine and Pharmacy, Timișoara, Romania, "Pius Brînzeu" Clinical Emergency County Hospital Timișoara, Romania; WFUMB Center of Education, Timișoara, Romania

Alexandru Popa, MD, PhD – Department of Gastroenterology and Hepatology, Center for Advanced Research in Gastroenterology and Hepatology, "Victor Babeș" University of Medicine and Pharmacy, Timișoara, Romania, "Pius Brînzeu" Clinical Emergency County Hospital Timișoara, Romania; WFUMB Center of Education, Timișoara, Romania

Iulia Rațiu, MD, PhD – Department of Gastroenterology and Hepatology, Center for Advanced Research in Gastroenterology and Hepatology, "Victor Babeș" University of Medicine and Pharmacy, Timișoara, Romania, "Pius Brînzeu" Clinical Emergency County Hospital Timișoara, Romania; WFUMB Center of Education, Timișoara, Romania

Denis Qirinxhi, MD, PhD (c) - Radiologist at University Hospital Center "Mother Teresa," and Lecturer at the University of Medicine Tirana, Albania

Blerina Saraci, MD, PhD (c) - Radiologist at University Hospital Center "Mother Teresa" and Lecturer at the University of Medicine Tirana, Deputy Director of the Albanian Center for Education Tirana, Albania

1. Ultrasonography for the Hepatologist: Is It Really Necessary?

Ioan Sporea, Roxana Șirli

Abstract

Ultrasonography has transformed from a simple morphological tool into a multiparametric, dynamic, and indispensable imaging platform in hepatology. This review evaluates its role from conventional grayscale imaging to Doppler, liver and spleen elastography, and liver contrast-enhanced ultrasound (CEUS), analyzing its diagnostic value, clinical impact, and overall necessity. Evidence from international guidelines and landmark studies demonstrates that ultrasonography functions as a true "one stop shop" for hepatologists, dramatically improving diagnostic accuracy, reducing healthcare costs, and accelerating patient management.

Introduction

Ultrasonography (US) has been used in medical diagnostics for over 50 years. Initially valued for its accessibility and low cost, it has expanded into a central pillar of hepatology (1). The evolution of ultrasound — starting with standard (gray scale) ultrasound, continuing with Doppler examination, liver (and spleen) elastography, and liver contrast enhanced ultrasound (CEUS) — has enabled hepatologists to obtain rapid, accurate, bedside diagnoses within minutes. The purpose of this paper is to critically examine whether ultrasonography is truly indispensable in hepatology today (to be performed by hepatologist), supported by updated literature and modern clinical guidelines.

B-mode (grayscale) Ultrasonography in Diffuse and Focal Liver Diseases

Conventional US remains the first-line imaging modality for evaluating liver morphology, texture, and focal lesions. It accurately identifies steatosis, cirrhotic morphology (typical aspects being the nodular contour, a modified, heterogeneous liver, caudate lobe enlargement, and portal hypertension signs). Using the Artificial Intelligence (AI) tool the accuracy of such evaluation is increased (see the chapter Artificial Intelligence in ultrasonography). It is highly sensitive for detecting focal liver lesions (FLLs), prompting further characterization by CEUS or cross-sectional imaging. Numerous guidelines,

including EASL (European Association for the Study of the Liver) and AASLD (American Association for the Study of the Liver), endorse ultrasound as the fundamental tool for surveillance in chronic liver disease and hepatocellular carcinoma (HCC) screening programs (2, 3).

Doppler Ultrasound and Hemodynamic Evaluation

Doppler US adds functional hemodynamic assessment, critical in portal hypertension evaluation (4). It identifies portal vein flow direction, velocity, the presence of thrombosis, collateral circulation, splenic vein abnormalities, and hepatic artery changes. Doppler is essential in diagnosing Budd–Chiari syndrome, assessing transjugular intrahepatic portosystemic shunt (TIPS) function, and monitoring progression of chronic liver disease. More recently, microflow is used to assess the vascular pattern in focal liver lesions.

Elastography: A Noninvasive Revolution

Elastography has become the leading noninvasive method for staging liver fibrosis. Vibration Controlled Transient Elastography (VCTE) and ARFI technology-based Shear-Wave Elastography (SWE) (point SWE and 2D-SWE) have been validated against liver biopsy, with excellent performance for ruling out advanced fibrosis and cirrhosis (5,6,7,8). Liver stiffness measurement (LSM) as a marker of fibrosis is a valuable guide regarding prognosis, need for therapy and surveillance. Spleen stiffness measurement (SSM) improves prediction of clinically significant portal hypertension (CSPH) (4). EFSUMB (European Federation of Societies of Ultrasound in Medicine and Biology) guidelines strongly recommend elastography as a core component of liver evaluation (6). With the new modules for quantitative steatosis assessment, a very precise evaluation of the fat in the liver is provided in short time (8,9). New developments of technologies already existing in some ultrasound machines allow liver viscosity assessment, potentially making ultrasound helpful to differentiate between simple steatosis and steatohepatitis in patients with MASLD (Metabolic dysfunction Associated Steatotic Liver Disease) (10).

Contrast-Enhanced Ultrasound (CEUS)

CEUS provides real-time microvascular imaging using intravascular microbubble contrast agents. It achieves more than 90% accuracy in distinguishing benign from malignant focal liver lesions and offers dynamic characterization similar to CT/MR, but without nephrotoxicity or radiation

(11,12). CEUS is recommended by WFUMB (World Federation of Ultrasound in Medicine and Biology) and EFSUMB guidelines (11,12) as a primary problem-solving tool for liver incidental lesions discovered in standard ultrasound examination and for HCC characterization, especially when CT/MRI are inconclusive or contraindicated. Using the Li-RADS system the accuracy of the method is improved and allows uniform interpretation everywhere (13).

Ultrasound-Guided Interventions

Ultrasound is essential for guiding liver biopsies, drainages, tumor ablation (RFA, MWA, ethanol injection), and targeted sampling of focal liver lesions. It provides real-time visualization, high safety, low cost, and wide accessibility. It remains the preferred modality for percutaneous therapy of HCC/metastasis worldwide.

The "One-Stop-Shop" Concept in Hepatology

Modern high-end ultrasound systems integrate grayscale US, Doppler, elastography with fat quantification and CEUS into a single platform. This allows hepatologists to perform a comprehensive evaluation of the liver in less than 30 minutes, improving diagnostic confidence and reducing downstream imaging. This concept reflects the practical reality of hepatology today: ultrasound is not optional, but fundamental (1,15).

In some countries such as Germany, Japan, Italy or Romania, the training of gastroenterologists/hepatologists to use ultrasound in daily practice is an old tradition. Recently, EASL pays more attention for training hepatologists for the use of ultrasound in daily practice, but it seems to be a long way before this problem is solved at global level.

In our WFUMB Center of Education (COE) Timișoara, ultrasound and its recent developments are implemented in the curricula of our fellows in Gastroenterology/Hepatology, so that when they finish their fellowship, they can use ultrasound as a point of care method (PoCUS) in daily practice. Currently, in most countries around the world (especially in Anglo-Saxon ones) ultrasound is performed mainly by radiologists, but this method is entering more and more in the field of clinical specialties (Gastroenterology and Hepatology being in the first line).

Considering all the above, this book on Liver MPUS is dedicated to all the people that like and use ultrasound in their daily practice, no matter if they are clinicians or radiologists.

Conclusion

Ultrasonography is indispensable for hepatologists in their daily practice. It provides rapid, accurate, safe, and cost-effective assessment of liver structure, function, hemodynamics, fibrosis, and focal lesions. With liver elastography and CEUS, it has become a comprehensive diagnostic tool that significantly reduces the need for invasive procedures and for expensive imaging methods. The evidence overwhelmingly supports its role as a mandatory component of modern hepatology practice.

References

1. Sporea I. Ultrasound: “one stop shop” in hepatology. Med Ultrason. 2016; 18(2): 143-144.
2. European Association for the Study of the Liver. EASL Clinical Practice Guidelines: Management of hepatocellular carcinoma. J Hepatol. 2018 Jul;69(1):182-236.
3. Kim TH, Kim SY, Tang A, Lee JM. Comparison of international guidelines for noninvasive diagnosis of hepatocellular carcinoma: 2018 update. Clin Mol Hepatol. 2019; 25(3): 245-263.
4. de Franchis R, Bosch J, Garcia-Tsao G, Reiberger T, Ripoll C; Baveno VII Faculty. Baveno VII - Renewing consensus in portal hypertension. J Hepatol. 2022; 76(4): 959-974.
5. Ferraioli G, Filice C, Castera L, Choi BI, Sporea I, Wilson SR, et al. WFUMB guidelines and recommendations for clinical use of ultrasound elastography: Part 3: liver. Ultrasound Med Biol. 2015; 41(5): 1161-1179.
6. Dietrich CF, Bamber J, Berzigotti A, Bota S, Cantisani V, Castera L, et al. EFSUMB Guidelines and Recommendations on the Clinical Use of Liver Ultrasound Elastography, Update 2017 (Long Version). Ultraschall Med. 2017; 38(4): e16-e47.
7. Ferraioli G, Barr RG, Berzigotti A, Sporea I, Wong VW, Reiberger T et al. WFUMB Guideline/Guidance on Liver Multiparametric Ultrasound: Part 1. Update to 2018 Guidelines on Liver Ultrasound Elastography. Ultrasound Med Biol. 2024; 50(8): 1071-1087.
8. Ferraioli G, Barr RG, Berzigotti A, Sporea I, Wong VW, Reiberger T, et al. WFUMB Guidelines/Guidance on Liver Multiparametric Ultrasound. Part 2: Guidance on Liver Fat Quantification. Ultrasound Med Biol. 2024; 50(8): 1088-1098.
9. Shili-Masmoudi S, Wong GL, Hiriart JB, Liu K, Chermak F, Shu SS, et al. Liver stiffness measurement predicts long-term survival and complications in non-alcoholic fatty liver disease. Liver Int. 2020; 40(3): 581-589.

10. Paisant A, Roux M, Calame P, Lecharpentier A, Thevenot T, Aubé C, Boursier J. Liver viscosity: pathological significance and interest for the assessment of MASLD severity in clinical practice. Eur Radiol. 2025. Nov 19. doi: 10.1007/s00330-025-12142-7. Epub ahead of print.
11. Claudon M, Dietrich CF, Choi BI, Cosgrove DO, Kudo M, Nolsøe CP, et al. Guidelines and good clinical practice recommendations for contrast enhanced ultrasound (CEUS) in the liver--update 2012: a WFUMB-EFSUMB initiative in cooperation with representatives of AFSUMB, AIUM, ASUM, FLAUS and ICUS. Ultraschall Med. 2013; 34(1): 11-29.
12. Dietrich CF, Nolsøe CP, Barr RG, Berzigotti A, Burns PN, Cantisani V, et al. Guidelines and Good Clinical Practice Recommendations for Contrast-Enhanced Ultrasound (CEUS) in the Liver-Update 2020 WFUMB in Cooperation with EFSUMB, AFSUMB, AIUM, and FLAUS. Ultrasound Med Biol. 2020; 46(10): 2579-2604.
13. Elsayes KM, Kielar AZ, Chernyak V, Morshid A, Furlan A, Masch WR, et al. LI-RADS: a conceptual and historical review from its beginning to its recent integration into AASLD clinical practice guidance. J Hepatocell Carcinoma. 2019; 5(6): 49-69.
14.Cunha GM, Fowler KJ, Roudenko A, Taouli B, Fung AW, Elsayes KM, Markds RM, Cruite I, Horvat N, Chernyak V, Sirlin CB, Tang A. How to Use LI-RADS to Report Liver CT and MRI Observations. RadioGraphics 2021; 41: 1352–1367
15. Popescu A, Bende F, Sirli R, Sporea I. Redefining Diagnosis and Management in Hepatology with Multiparametric Ultrasound. EMJ Hepatol. 2025;13(1):66-75.

2. What does “multiparametric ultrasound” mean?

Alina Popescu, Ioan Sporea

Abstract

Multiparametric Ultrasound (MPUS) represents an integrated ultrasonographic approach that combines several advanced ultrasound techniques to improve diagnostic accuracy and expand the scope of conventional (gray scale) ultrasonography. Although ultrasound is often underestimated compared to other imaging modalities, the development of elastography and contrast-enhanced ultrasound (CEUS), in conjunction with real-time B-mode and Doppler imaging, now allows a multiparametric evaluation, comparable in concept to that used in cross-sectional imaging.

2.1. Introduction

Ultrasound (US) remains one of the most widely used imaging methods worldwide because it is real-time, dynamic, inexpensive, non-irradiating, repeatable, portable, and well accepted by patients (1). Despite these advantages, US has historically been regarded as the “Cinderella” of imaging, often overshadowed by CT and MRI (1). Criticisms include operator dependence and variable specificity and accuracy, particularly in the characterization of focal lesions.

However, as ultrasound technology has evolved, many of its former limitations have been addressed. Modern developments—especially liver CEUS and ultrasound-based elastography—now provide critical diagnostic information that was previously available only through CT or MRI. These advancements gave rise to the ***concept of multiparametric ultrasound (MPUS),*** first introduced in analogy with multiparametric MRI (2).

2.2. Definition of MPUS

MPUS refers to the combined use of multiple, complementary ultrasound techniques—each providing a distinct diagnostic “parameter”— to enhance diagnostic confidence and accuracy. Instead of relying solely on conventional B-mode imaging, MPUS integrates:

1. Conventional ultrasound (B-mode)
2. Doppler techniques (color, power, spectral Doppler)
3. 3D and 4D ultrasound
4. Ultrasound elastography (strain, shear-wave)
5. Contrast-enhanced ultrasound (CEUS)

This multiparametric approach allows a far more comprehensive evaluation of tissues and organs, addressing limitations related to vascular characterization, lesion stiffness, and microvascular perfusion that cannot be assessed with B-mode alone (1).

2.3. Why is MPUS needed?

Ultrasound is the most used imaging technique because it is cheap and can be performed everywhere. But in comparison with other imaging methods, when it is used without a specific contrast, the specificity of the method is not very high.

Although B-mode ultrasound is excellent for detection, its specificity—especially for focal lesions—can be limited. Historically, the inability to evaluate lesion vascularity with precision was a major criticism of US. Doppler techniques partly addressed this issue but lacked the microvascular resolution achievable with contrast-enhanced techniques.

The introduction of CEUS overcame this limitation by allowing real-time, dynamic evaluation of vascular patterns in a way analogous to CE-CT (Contrast enhanced-CT) and CE-MRI (Contrast enhanced-MRI). Likewise, elastography provides noninvasive information on tissue stiffness, essential in evaluating liver fibrosis or differentiating between benign and malignant lesions (3).

Thus, MPUS combines these strengths into one structured diagnostic pathway.

2.4. Components of MPUS

1. Conventional Ultrasound (B-mode)

- First-line assessment of morphology, echogenicity, and structural changes.

2. Doppler Ultrasound

- Evaluates blood flow, vascular anatomy, and hemodynamics.
- Limited for microvasculature, but essential for initial vascular characterization. More recently, with the use of the microflow technique, more information can be obtained for microvascularization.

3. 3D and 4D ultrasound

- These techniques provide detailed, high-definition, 3D still (3D) or moving (4D) ultrasound images, with most of the applications in obstetrics, but also useful in the characterization of focal lesions, allowing to better visualize detected structural abnormalities. They are highly valuable mainly for examining fetal anatomy and behavior, improving diagnostic certainty.

4. Elastography

- Provides quantitative or semiquantitative assessment of tissue stiffness.
- Particularly valuable for:
    - Diagnosing or excluding liver cirrhosis (high accuracy in <5 minutes), with high value in hepatology (3). Assessing stiffness of focal lesions in the liver, breast, prostate, and others.

5. Contrast-Enhanced Ultrasound (CEUS)

- Performed in the same session as conventional US (like a Point of Care method), requiring ~5-10 additional minutes. This technique, which has become like usual today, increases the accuracy of ultrasound evaluation (in some fields of US) to the level of CE-CT or CE-MRI.

Together, these modalities provide complementary information—morphological, vascular, stiffness-related, and perfusion-related—offering a complex and reliable diagnostic profile in many medical fields.

2.5. The MPUS Workflow: A "One-Stop Shop"

A typical MPUS assessment uses ***a stepwise algorithm***, particularly well established for liver evaluation:

1. Conventional US → detection of an abnormality or a lesion.
2. Elastography → assessment of underlying liver disease (e.g., advanced fibrosis or cirrhosis) and, in some cases, lesion stiffness.
3. CEUS → dynamic vascular characterization of a focal liver lesion and then differential diagnosis.

This "one-stop shop" strategy allows completion of a complex evaluation during a single ultrasound session, reducing patient stress, time, and the need for more expensive imaging modalities (3).

2.6. Clinical Applications of MPUS

2.6.1. Liver Imaging

The liver is the organ in which MPUS has become most fully developed.

- ***Focal liver lesions:***
    - US is highly sensitive for lesion detection. Vascular evaluation of the lesions can be performed with Doppler technique or with microvascular (microflow) assessment.
    - CEUS provides a more precise real-time vascular pattern evaluation.
    - Elastography determines whether lesions arise in a cirrhotic/advanced fibrosis or non-cirrhotic liver—a critical factor in lesion interpretation.
    - In case of morphological assessment, ultrasound guidance is the favorite method. Simple to use, it is very helpful for the procedure. The percutaneous treatment (RFA, Microwave Ablation, alcohol injection-PEIT) of malignant focal liver lesions is performed usually under ultrasound guidance and this method is very useful for the assessment of the treatment result or of the complications.

This combined approach significantly increases diagnostic accuracy and reduces dependence on CT or MRI for many patients.

- ***Chronic diffuse liver disease:***
    - Conventional US may raise the suspicion of these pathologies.
    - Elastography is now the main method to assess fibrosis and fatty quantification. In the last years, evaluation of viscoelastic (viscosity) properties of the liver has been used for differentiation between simple steatosis and steatohepatitis in patients with MASLD (Metabolic Dysfunction Associated Steatotic Liver Disease) (6, 7).
    - Elastography of the liver and of the spleen can evaluate complications such as portal hypertension (7).
    - If a liver biopsy is necessary (quite rare at this moment, having non-invasive methods), usually this is performed under ultrasound guidance.

2.6.2. Prostate Cancer

Multiple studies demonstrate the value of MPUS in detecting prostate cancer by integrating B-mode, Doppler, CEUS, and elastography (8-11). In many cases, transrectal ultrasound is used to guide prostate biopsy.

2.6.3. Thyroid and Parathyroid Imaging

MPUS helps differentiate benign from malignant nodules (12-14) and distinguish parathyroid lesions (15, 16). Ultrasound is used to guide the biopsy of a thyroid lesion or for guiding percutaneous procedures in the nodules.

2.6.4. Breast lesions

After the detection of a breast lesion by high-quality ultrasound, other ultrasound methods are used, mainly elastography. Strain (SE) or shear wave elastography (SWE) can be useful for the characterization of the lesions. In case of morphological diagnosis, ultrasound is the method for guiding the biopsy (17, 18).

2.6.5. Kidney Disease

Quantitative ultrasound parameters support the assessment of chronic kidney disease severity (19-21). Kidney biopsy is performed usually under ultrasound guidance.

These examples demonstrate that MPUS is not organ-specific but rather a versatile approach applicable across multiple clinical domains.

2.7. Advantages of MPUS

- Non-invasive and radiation-free
- Cost-effective and repeatable
- Real-time assessment
- Provides microvascular, structural, and biomechanical information
- Improves specificity and diagnostic accuracy
- Enhances patient comfort by consolidating evaluation in a single session and well accepted by patients.
- Reduces need for higher-cost imaging (CT/MRI) in many situations.

2.8. Limitations and Considerations

- MPUS is still *somewhat operator dependent,* though much of this can be minimized through adequate training.
- Availability of elastography and CEUS varies between institutions but is increasing in accessibility (due to the implementation of these methods inside middle-class ultrasound machines).
- Interpretation requires integration of multiple parameters, making expertise essential. Artificial Intelligence (AI) used in the field of ultrasound makes more accessible the integration of results in practice for people with less experience (22).

2.9. Conclusion

Multiparametric ultrasound (MPUS) represents a major advancement in modern ultrasonography. By integrating conventional US, Doppler, elastography, and CEUS, MPUS provides a comprehensive and highly accurate diagnostic approach that addresses many limitations traditionally associated with ultrasound.

US—far from being an outdated or limited modality—has evolved into a powerful, multi-technique imaging solution, that should be considered a first-line diagnostic tool in many clinical scenarios. MPUS is likely to continue expanding across organs and indications, reinforcing the central role of ultrasound in contemporary medical imaging.

References

1. Popescu A. Multiparametric ultrasound (MPUS) or "the many faces" of ultrasonography. Med Ultrason. 2019 Nov 24;21(4):369-370.
2. Sidhu PS. Multiparametric Ultrasound (MPUS) Imaging: Terminology Describing the Many Aspects of Ultrasonography. Ultraschall Med. 2015;36:315–317.
3. Sporea I. Ultrasound: "one stop shop" in hepatology. Med Ultrason. 2016 Jun;18(2):143-4.
4. Claudon M, Dietrich CF, Choi BI, Cosgrove DO, Kudo M, Nolsøe CP, et al. Guidelines and good clinical practice recommendations for contrast enhanced ultrasound (CEUS) in the liver--update 2012: a WFUMB-EFSUMB initiative in cooperation with representatives of AFSUMB, AIUM, ASUM, FLAUS and ICUS. Ultraschall Med. 2013 Feb;34(1):11-29.
5. Dietrich CF, Bamber J, Berzigotti A, Bota S, Cantisani V, Castera L, et al. EFSUMB Guidelines and Recommendations on the Clinical Use of Liver Ultrasound Elastography, Update 2017 (Short Version). Ultraschall Med. 2017 Aug;38(4):377-394.
6. Ferraioli G, Barr RG, Berzigotti A, Sporea I, Wong VW, Reiberger T, et al. WFUMB Guideline/Guidance on Liver Multiparametric Ultrasound: Part 1. Update to 2018 Guidelines on Liver Ultrasound Elastography. Ultrasound Med Biol. 2024 Aug;50(8):1071-1087.
7. de Franchis R, Bosch J, Garcia-Tsao G, Reiberger T, Ripoll C; Baveno VII Faculty. Baveno VII - Renewing consensus in portal hypertension. J Hepatol. 2022 Apr;76(4):959-974.
8. Postema A, Mischi M, de la Rosette JJ, Wijkstra H. Multiparametric ultrasound in the detection of prostate cancer: a systematic review. World J Urol. 2015;33:1651–1659.
9. Grey A, Ahmed HU. Multiparametric ultrasound in the diagnosis of prostate cancer. Curr Opin Urol. 2016 Jan;26(1):114-119..

10.Barr RG, Cosgrove D, Brock M, Cantisani V, Correas JM, Postema AW, et al. WFUMB Guidelines and Recommendations on the Clinical Use of Ultrasound Elastography: Part 5. Prostate. Ultrasound Med Biol. 2017 Jan;43(1):27-48.
11. Crisan N, Andras I, Radu C, Andras D, Coman RT, Tucan P, et al. Prostate ultrasound: back in business! Med Ultrason. 2017 Nov 29;19(4):423-429.
12. Cantisani V, D'Ambrosio F, Nielsen MB. Multiparametric Ultrasound of Thyroid Nodules: Where Do We Stand? Ultraschall Med. 2017;38:357–359.
13.Stoian D, Borlea A, Moisa-Luca L, Paul C. Multiparametric ultrasound-based assessment of overt hyperthyroid diffuse thyroid disease. Front Endocrinol (Lausanne). 2023 Dec 18;14:1300447.
14. Stoian D, Borlea A, Sporea I, Popa A, Moisa-Luca L, Popescu A. Assessment of Thyroid Stiffness and Viscosity in Autoimmune Thyroiditis Using Novel Ultrasound-Based Techniques. Biomedicines. 2023 Mar 17;11(3):938.
15. Isidori AM, Cantisani V, Giannetta E, et al. Multiparametric ultrasonography and ultrasound elastography in differentiating parathyroid lesions. Endocrine. 2017;57:335–343.
16.Amzar D, Cotoi L, Sporea I, Timar B, Schiller O, Schiller A, et al. Shear Wave Elastography in Patients with Primary and Secondary Hyperparathyroidism. J Clin Med. 2021 Feb 10;10(4):697.
17.Barr RG, Nakashima K, Amy D, Cosgrove D, Farrokh A, Schafer F, et al. WFUMB guidelines and recommendations for clinical use of ultrasound elastography: Part 2: breast. Ultrasound Med Biol. 2015 May;41(5):1148-60.
18. Tang L, Wang Y, Chen P, Chen M, Jiang L. Clinical use and adjustment of ultrasound elastography for breast lesions followed WFUMB guidelines and recommendations in the real world. Front Oncol. 2022 Nov 24;12:1022917.
19. Gao J, Perlman A, Kalache S, et al. Multiparametric Quantitative Ultrasound Imaging in Assessment of Chronic Kidney Disease. J Ultrasound Med. 2017;36:2245–2256.
20. Bob F, Bota S, Sporea I, Sirli R, Petrica L, Schiller A. Kidney shear wave speed values in subjects with and without renal pathology and inter-operator reproducibility of acoustic radiation force impulse elastography (ARFI)--preliminary results. PLoS One. 2014 Nov 26;9(11):e113761
21. Bob F, Grosu I, Sporea I, Bota S, Popescu A, Sima A, et al. Ultrasound-Based Shear Wave Elastography in the Assessment of Patients with Diabetic Kidney Disease. Ultrasound Med Biol. 2017 Oct;43(10):2159-2166.
22. Ding W, Meng Y, Ma J, Pang C, Wu J, Tian J, et al. Contrast-enhanced ultrasound-based AI model for multi-classification of focal liver lesions. J Hepatol. 2025 Aug;83(2):426-439.

3. Ultrasound anatomy of the liver

Ioan Sporea, Roxana Șirli

Abstract

Ultrasound remains the first-line imaging modality for the examination of the liver. In this chapter we review the normal ultrasound anatomy of the liver, with emphasis on the parenchymal appearance, hepatic and portal venous systems, Couinaud segmental anatomy, and the anatomical relationships at the hepatic hilum.

3.1. Introduction

The liver is the largest solid abdominal organ and is ideally positioned for ultrasound assessment, beneath the right hemidiaphragm. Recognition of normal liver anatomy is essential for accurate detection of focal and diffuse disease, for Doppler hemodynamic analysis, and for pre‑procedural planning. A systematic ultrasound approach, using longitudinal, transverse, and oblique sections, allows full coverage of the hepatic parenchyma and vascular landmarks. During ultrasound examination of the liver, it is mandatory to see all the segments of the liver; if one is "skipped", a possible lesion in that region can be missed. In practice, dynamic movements of the operator's hand during ultrasound examination allow liver examination in hundreds of planes. The great advantage of ultrasound examination is the mobility of the examination plane and the real time examination.

3.2. Ultrasound appearance of the normal liver

In normal subjects, the *hepatic parenchyma has a homogeneous echotexture* (Fig.3.1a and Fig 3.1b), slightly hyperechoic or isoechoic to the renal cortex (Fig 3.2) (1). Hepatic and portal veins are clearly visible when the liver is scanned dynamically using multiple planes. The intrahepatic bile ducts are typically not visible on ultrasound in normal conditions (1).

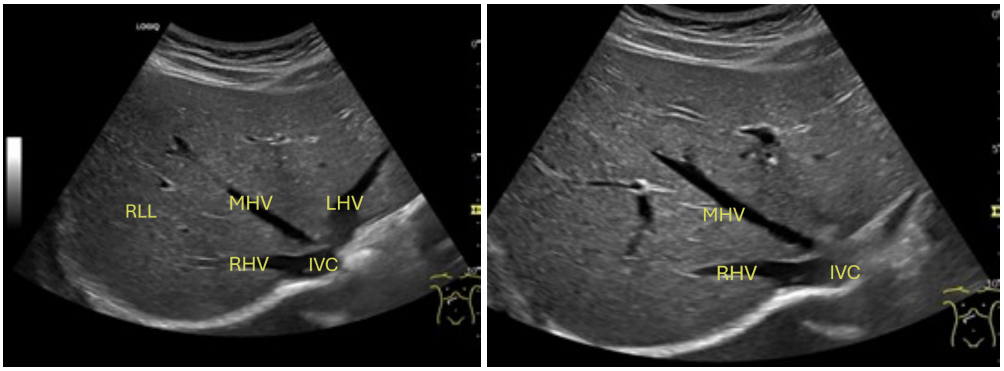


Fig. 3.1a and 3.1b Oblique subcostal sections of the liver. Normal structure of the liver (RLL – right liver lobe, IVC – inferior vena cava, RHV – right hepatic vein, MHV – middle hepatic vein, LHV – left hepatic vein)

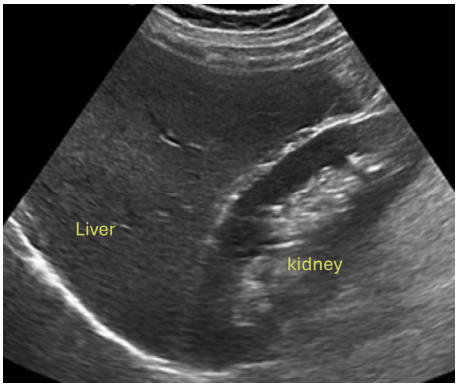


Fig. 3.2 The normal liver is slightly hyperechoic or isoechoic to the renal cortex

Reported reference values used in practice include a cranio-caudal diameter of approximately 17 cm and an antero-posterior diameter of approximately 15 cm, interpreted in the clinical context of body habitus and respiration. In practice, we don't recommend routine measurement of the liver size, due to its variability, related to the individual's height and weight.

Hepatic veins

Three main hepatic veins can usually be identified: the right, middle and left hepatic vein. They present thin, poorly echogenic walls and they drain into the inferior vena cava (IVC) (Fig.3.3 and Fig. 3.4). Oblique and subcostal sections improve the view of the hepatic veins confluence with the inferior vena cava

(IVC) (1). Not very often, all three hepatic veins can be seen in the same section, usually it is necessary to angulate the transducer to see all three, since they are situated in different planes. These vessels serve as intersegmental landmarks and are essential for mapping focal lesions and for Doppler waveform assessment (1). In steatotic livers, hepatic veins' walls can be slightly blurred (Fig.3.5)

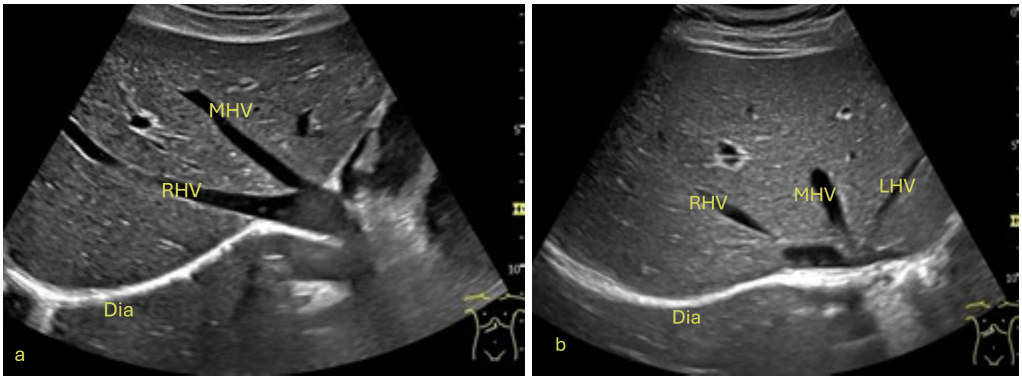


Fig. 3.3a and Fig. 3.3b Normal liver parenchyma with hepatic veins, the diaphragma situated posteriorly and superiorly (Dia – diaphragm, RHV – right hepatic vein, MHV – middle hepatic vein, LHV – left hepatic vein)

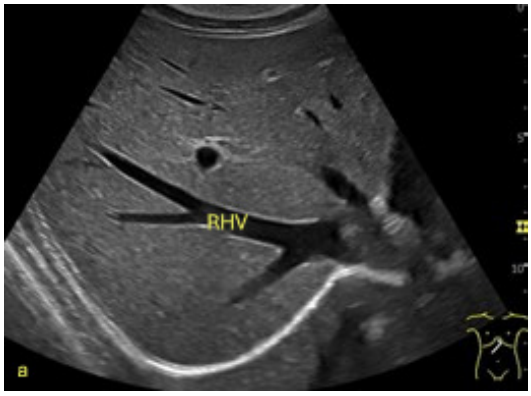


Fig. 3.4a Normal right hepatic vein (RHV) - thin, poorly echogenic walls.

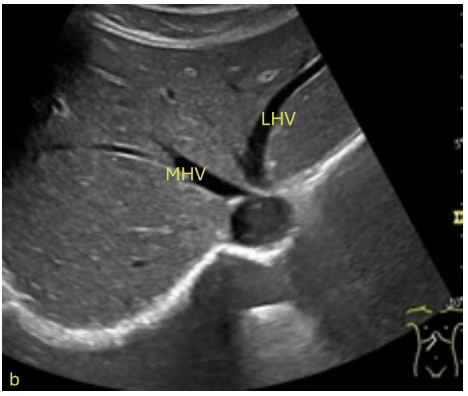


Fig. 3.4b Normal middle (MHV) and left hepatic veins (LHV)

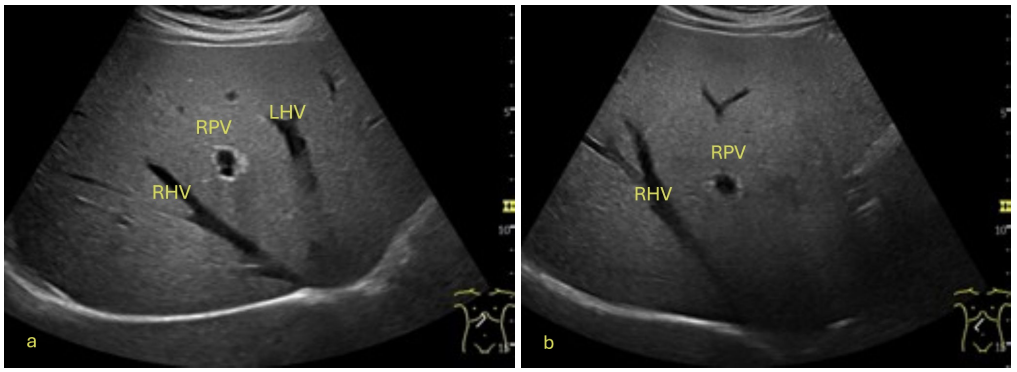


Fig.3.5a and Fig.3.5b Hepatic veins in steatotic liver (bright liver), the walls are slightly blurred (RHV – right hepatic vein, MHV – middle hepatic vein, RPV – right portal vein)

Portal vein

The portal vein has more echogenic walls than the hepatic veins, due to the periportal fibrous tissue. The main portal vein (examined by a subcostal approach with the transducer placed on a reference line connecting the right shoulder and the umbilicus) (Fig. 3.6) bifurcates into the right and left branches (best seen in oblique subcostal sections, parallel with the inferior margin of the ribs) (Fig. 3.7) (1). The portal venous system is fundamental for anatomical orientation and for assessing portal hypertension, collateral formation and surgical planning.

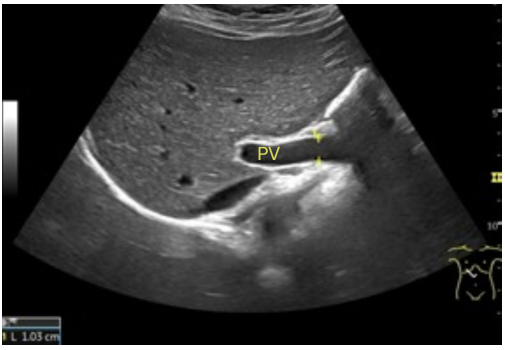


Fig. 3.6 Normal portal vein (PV) in the hilum

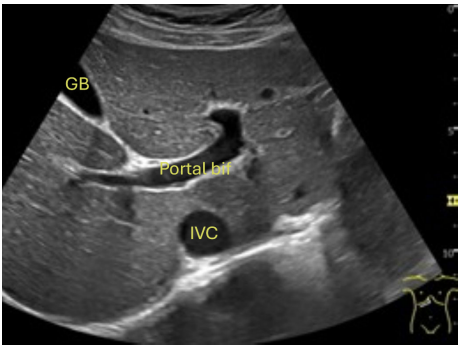


Fig. 3.7 Portal bifurcation (GB – gall bladder, IVC – inferior vena cava

Hepatic hilum and biliary-vascular relationships

At the hepatic hilum (examined by a subcostal approach with the transducer placed on a reference line connecting the right shoulder and the umbilicus, perpendicular to the costal ribs), the main biliary duct is situated anteriorly, the portal vein lies posteriorly, and the hepatic artery is interposed between them (Fig.3.8) (1). These relationships form a characteristic sonographic pattern, essential for the evaluation of obstructive jaundice, cholestatic disease, hilar tumors and post-surgical states. The normal size of the main biliary duct (MBD) is up to 6 mm, slightly larger in patients who underwent cholecystectomy (up to 10 mm) (2). The diameter of the MBD can increase 1 mm per decade after 60 years old (2). Since normal intrahepatic biliary ducts are not visible, their dilatation is an important indirect sign of obstruction.

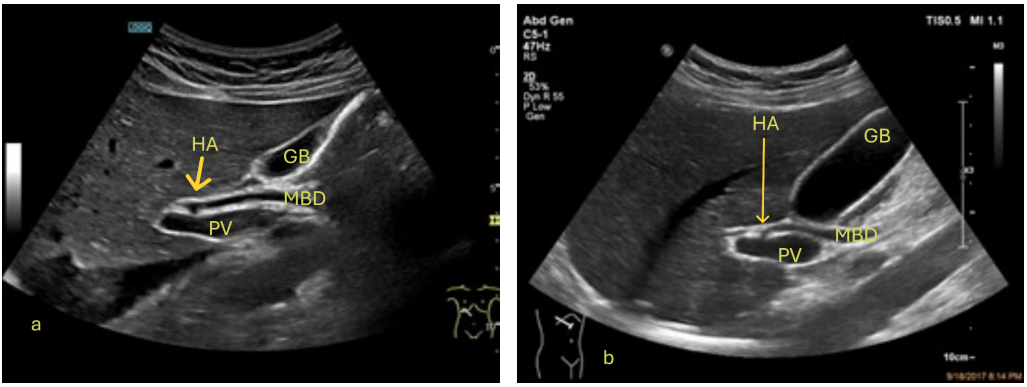


Fig.3.8a and Fig.3.8b Anatomy of the hepatic hilum (PV – portal vein, MBD – main biliary duct, HA – hepatic artery, GB – gall bladder)

Couinaud segmental anatomy

Functional hepatic anatomy follows the Couinaud segmentation system (3), which divides the liver into eight segments, each with its own vascular inflow, outflow and biliary drainage. Segment I corresponds to the caudate lobe, segments II–IV are part the left liver lobe, and segments V–VIII of the right liver lobe. Segment IV is commonly subdivided into IV a (superior) and IV b (inferior) (Fig. 3.9). Hepatic veins delimit intersegmental planes, whereas portal branches are intra-segmental (4).

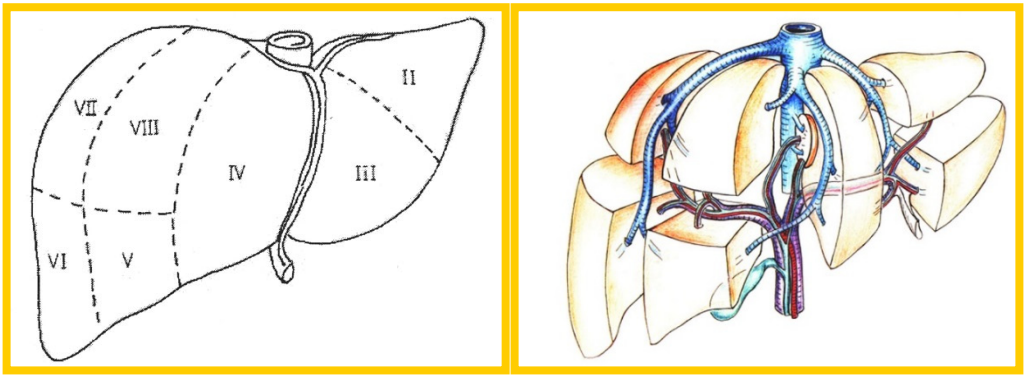


Fig. 3.9a and Fig. 3.9b Schematic segmentation of the liver (5)

In an oblique subcostal section, liver segments have a "shell-form" pattern, providing a useful orientation pattern in routine scanning to localize focal liver lesions (Fig.3.10).

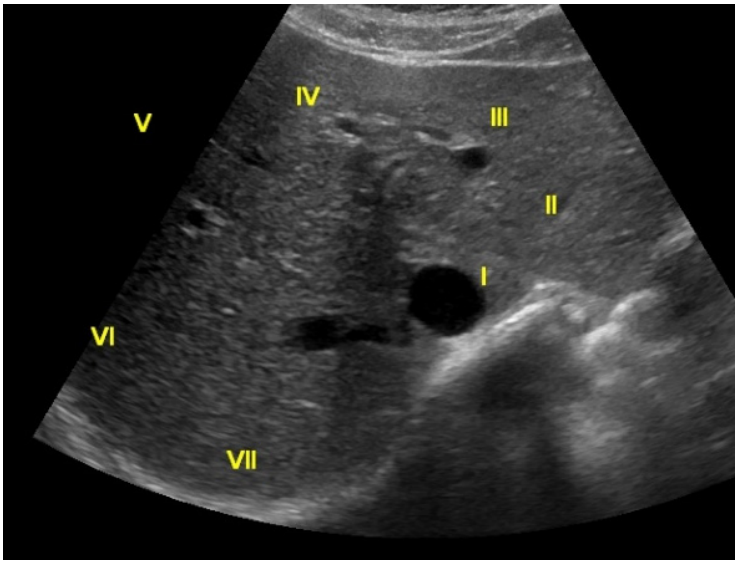


Fig.3.10 "Shell -form" pattern in subcostal oblique sections, with segments from I to VII, starting from segment I (caudate lobe) to segment VII, in counterclockwise direction.

When hepatic veins are seen (oblique subcostal sections), they are useful landmarks to delineate the liver segments as seen in Fig.3.11.

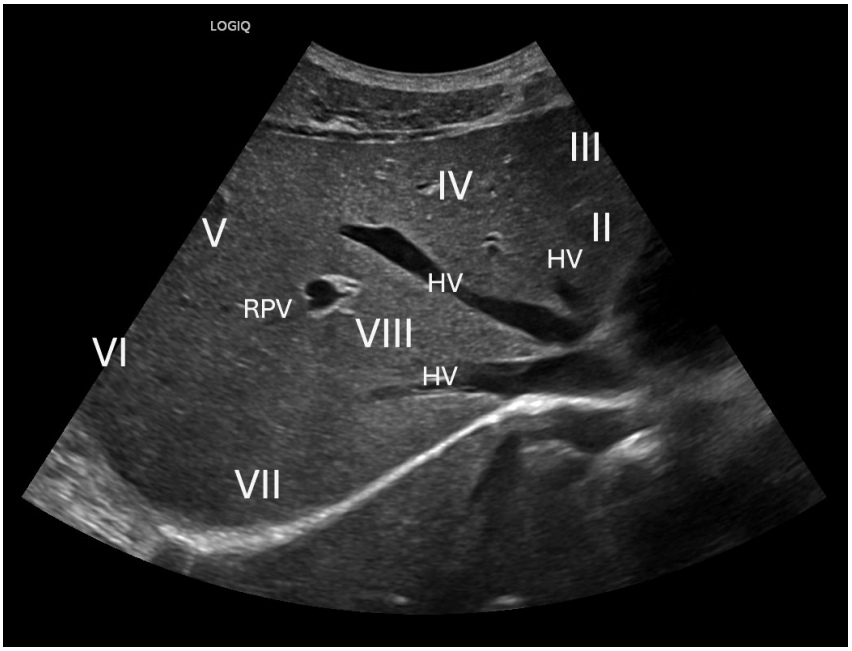


Fig.3.11 Liver segments (HV – hepatic vein, RPV – right portal vein)

Another modality to recognize liver segments is to use longitudinal sections in the left lobe, for segment 1,2 and 3 (Fig. 3.12), and in the right lobe (intercostal), for segment 5,6,7 and 8 (Fig. 3.13).

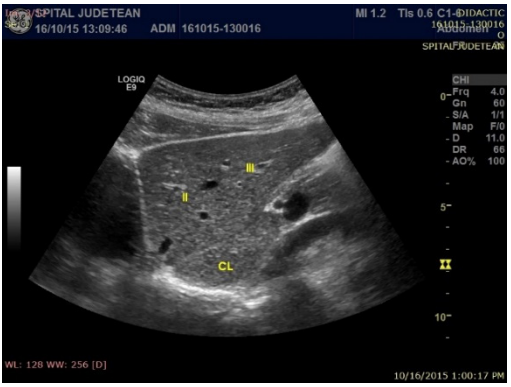


Fig. 3.12 Longitudinal section in left liver lobe

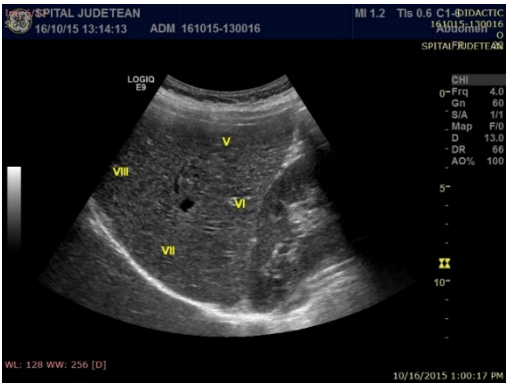


Fig. 3.13 Longitudinal section in the right liver lobe

To measure the caudate lobe, a longitudinal section in the epigastric region is performed. The normal antero-posterior diameter of the caudate lobe is less than 35 mm (Fig. 3.14).

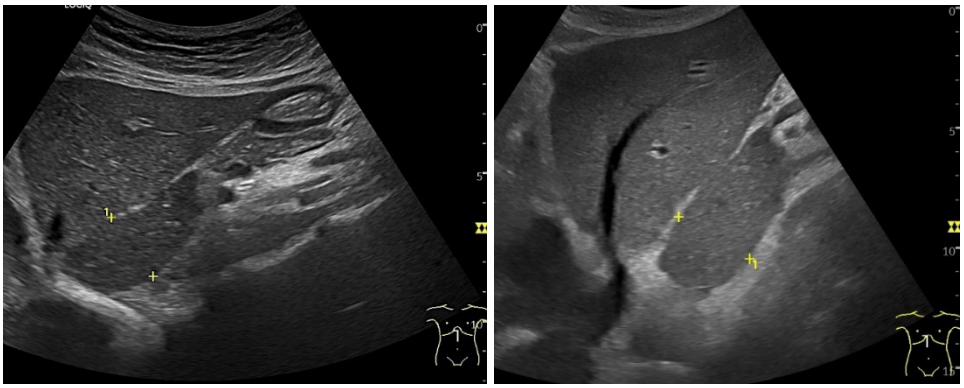


Fig. 3.14a and Fig. 3.14b Normal caudate lobe (markers)

Relations of the liver with neighboring organs

The liver is closely related to the right kidney (Fig.3.15) and the adrenal gland, to the inferior vena cava (Fig.3.16), gallbladder (Fig.3.17), stomach (and abdominal esophagus) (Fig.3.18), abdominal aorta (Fig. 3.19), pancreas (Fig.3.20) and to the posterior diaphragm (6). These relations help orientation during scanning and are relevant when evaluating perihepatic collections, diaphragmatic motion, retrohepatic venous pathologies or lesions extending from adjacent organs.

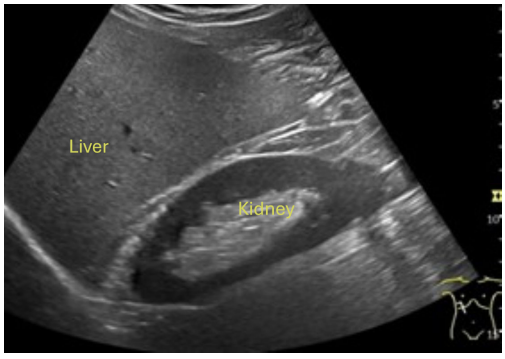


Fig.3.15 The Liver and right kidney

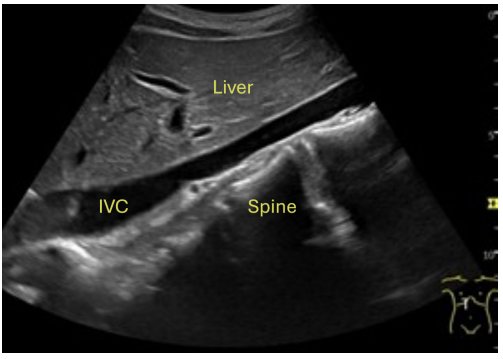


Fig.3.16 The inferior vena cava (IVC) behind the liver

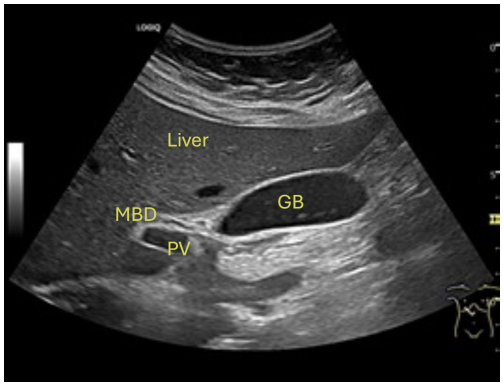


Fig.3.17 Liver and gallbladder (GB) in an oblique section (PV – portal vein, MBD – main biliary duct

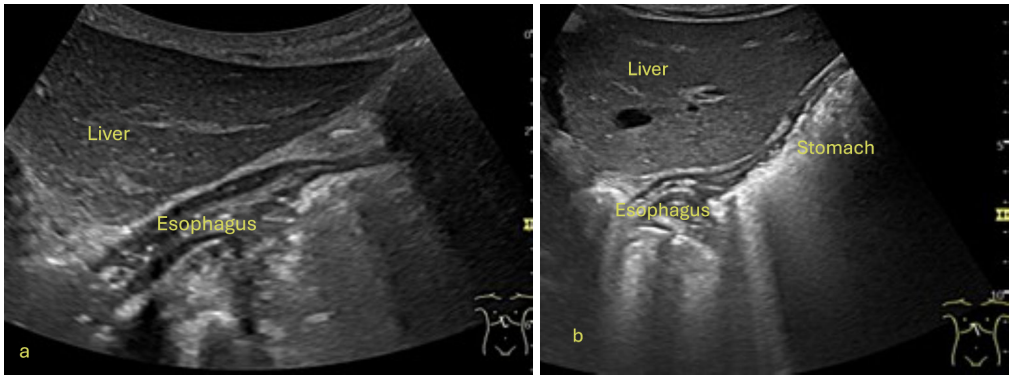


Fig.3.18a and Fig.3.18b Abdominal esophagus behind left liver

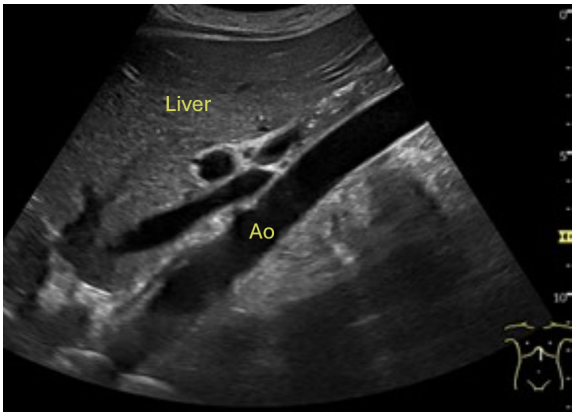


Fig. 3.19 Abdominal aorta (Ao) and left liver lobe

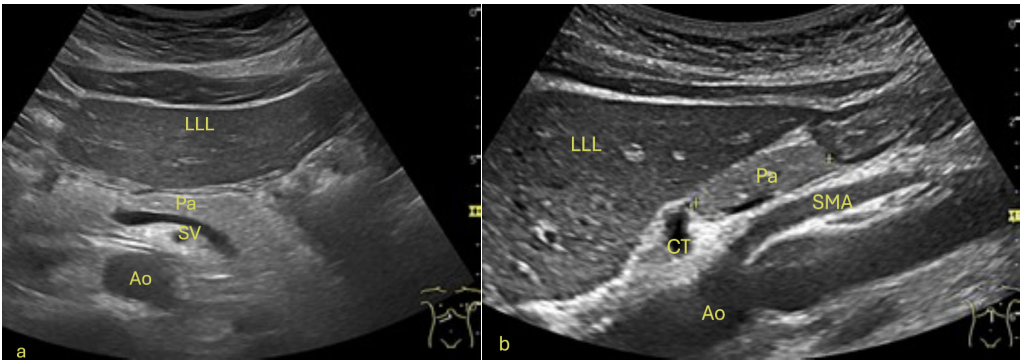


Fig.3.20a Left liver lobe (LLL) and the pancreas (Pa) in transverse section (SV – Splenic Vein, Ao – Aorta)

Fig.3.20b Left liver lobe (LLL) and the pancreatic body (Pa) in longitudinal section (SMA – superior mesenteric artery, CT – celiac trunk, Ao - Aorta

Systematic examination approach

A complete ultrasound examination should begin with the evaluation of the liver parenchyma, followed by the hepatic veins and inferior vena cava, the portal vein and its branches, and finally the biliary tree and hepatic hilum. Sweeping movements in longitudinal, transverse and oblique planes ensure that the entire hepatic volume is explored, increasing diagnostic confidence and reducing the risk of overlooking focal lesions.

Conclusion

Knowledge of the ultrasound anatomy of the liver is fundamental for clinical hepatology and abdominal imaging. Mastery of the parenchymal appearance, vascular landmarks, segmental anatomy, and hilar relationships supports accurate diagnosis, guides interventional procedures and facilitates effective multidisciplinary communication.

References

1. Dietrich CF, Choi BY. Examination of the liver, in Nuernberg D, Chammas C,Gilja OH, Sporea I, Sirli R: WFUMB Ultrasound Book. Edited by WFUMB (World Federation for Ultrasound in Medicine and Biology) 2021. Available at: https://indd.adobe.com/view/dc120eb3-45f0-45d4-9873-0a94c74cd44c

2. Popescu A, Elhakim S, Matteoni AC. Gallbladder and Bile Duct System – Sonopathology, in Nuernberg D, Chammas C,Gilja OH, Sporea I, Sirli R: WFUMB Ultrasound Book. Edited by WFUMB (World Federation for Ultrasound in Medicine and Biology) 2021. Available at: https://indd.adobe.com/view/d1cfd8f5-c5ef-4508-bc0a-f505b71964ce
3. Couinaud C. Le foie: études anatomiques et chirurgicales. Paris: Masson; 1957.
4. Lanz T, Wachsmuth W. Practical anatomy of the liver segments. Stuttgart: Thieme; 1993.
5. Fluture V. Rezecția hepatică. Timișoara: Editura de Vest; 2003.
6. Hofer M. Ultrasound Teaching Manual. 2nd ed. Stuttgart: Thieme; 1999.

4.1. B-mode evaluation in diffuse liver diseases

Ioan Sporea, Alexandru Popa

Abstract

B-mode ultrasound is a first-line, noninvasive imaging method for the evaluation of diffuse liver diseases. A systematic abdominal examination allows assessment of liver parenchymal echotexture, surface morphology, vascular structures, spleen size, and the presence of ascites or focal lesions. In chronic liver disease, ultrasound may show indirect signs such as splenomegaly and features of portal hypertension, although early stages can appear normal. B-mode imaging is particularly useful for detecting hepatic steatosis, characterized by increased liver echogenicity and increased hepato-renal contrast. However, its accuracy for staging liver fibrosis is limited, as typical findings mainly reflect advanced disease. Despite these limitations, conventional ultrasound remains an essential tool for initial evaluation, differential diagnosis of jaundice, and surveillance in patients with chronic liver disease.

When performing abdominal ultrasonography, we support a comprehensive examination of the entire abdomen, with a special emphasis on the region(s) of clinical relevance. According to the "WFUMB Ultrasound Book" (1), a systematic examination should be used for abdominal ultrasound evaluation. For liver examination, multiple sections are necessary so that a real 3D examination is performed. It is important to avoid missing some areas of the liver, where lesions can be hidden.

Under normal conditions, liver examination reveals a homogeneous hepatic structure, with clearly visible hepatic veins, and a portal vein that can be traced to the hepatic hilum (Fig. 4.1.1). The posterior aspect of the diaphragm should also be well visualized. When examining the spleen, the entire organ must be displayed, and its length measured from one pole to the other. The normal spleen size is typically less than 12 cm in length (Fig. 4.1.2), although some authors use a cutoff of less than 13 cm.

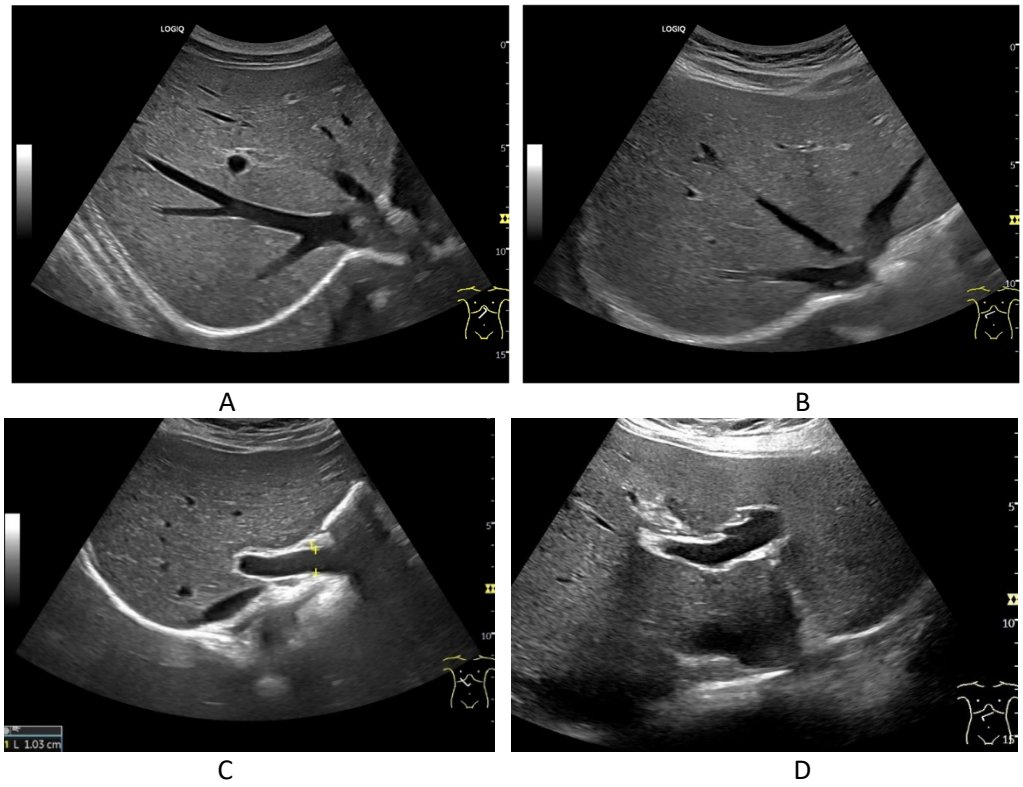


Figure 4.1.1 A-B. Oblique subcostal ultrasound view of the hepatic veins. C - Porta in the hilum. D - portal bifurcation

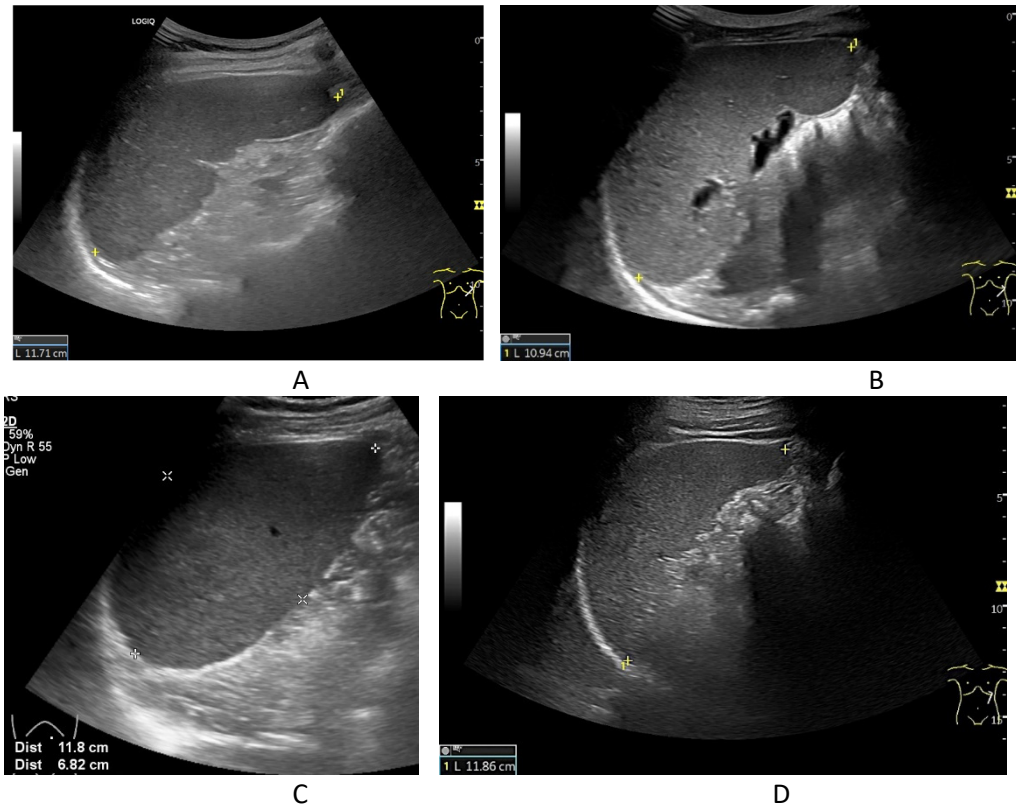


Figure 4.1.2 A-D. Ultrasound image of a normal spleen, within the normal range (<12 cm).

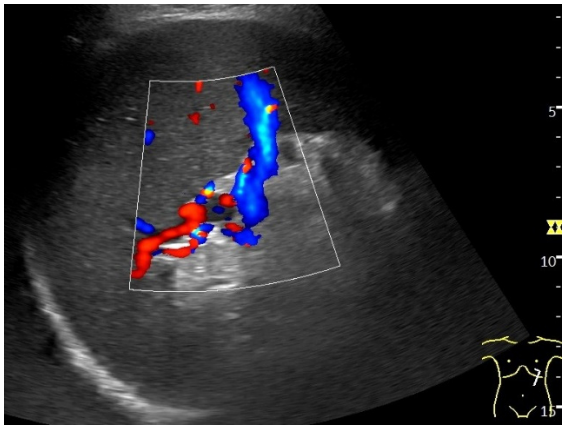


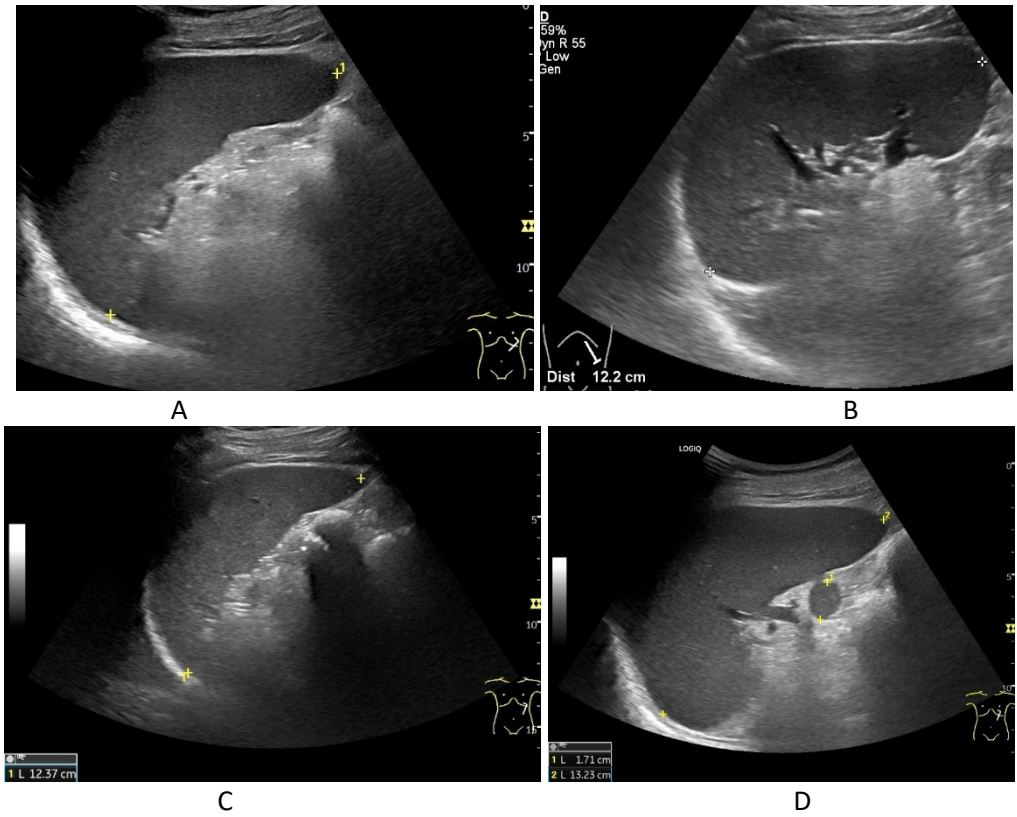
Figure 4.1.3. Color Doppler ultrasound of the spleen hilum

During liver ultrasound, the examination should be structured and comprehensive. Key items include parenchymal appearance (uniform versus coarse/inhomogeneous echotexture), assessment of liver surface morphology, confirmation of portal and hepatic vein patency, signs suggestive of steatosis, measurement of the extrahepatic bile duct and inspection of the intrahepatic ducts for dilatation, and a careful search for focal liver lesions.

From a clinical standpoint, liver abnormalities are typically encountered in two settings. First, relevant findings may be detected incidentally during a routine abdominal scan—such as a dysmorphic liver, splenomegaly, ascites, indirect signs of portal hypertension, or focal lesions. Second, ultrasound is frequently requested in a targeted work-up of liver-related complaints or laboratory abnormalities [e.g., elevated aminotransferases and/or bilirubin, jaundice, or cholestatic enzyme elevation (alkaline phosphatase and GGT)].

In ***chronic diffuse liver disease***, the conventional B-mode assessment should focus on liver parenchymal morphology, spleen size, signs of portal hypertension, and the presence and distribution of ascites. Although Doppler aspects are addressed in a dedicated section, evaluation of portal, hepatic, and splenic venous flow is often clinically informative. In parallel, ultrasound elastography has become an integral component of modern practice over the last two decades, enabling routine stiffness assessment in both the liver and spleen.

In chronic viral hepatitis, B-mode ultrasound may remain unremarkable, particularly in earlier stages. When morphological abnormalities are present, they generally indicate more advanced disease with substantial fibrosis. Mild splenomegaly (typically >12 cm) may be seen and should be documented with accurate measurements (Fig. 4.1.4).



A B C D

Figure 4.1.4 A-C. Mild splenomegaly (>12 cm).
D - Splenomegaly with accessory spleen.

Additionally, in chronic hepatitis B or C, as well as in autoimmune hepatitis and primary biliary cholangitis, enlarged ovoid hypoechoic lymph nodes can occasionally be identified at the hepatic hilum (approximately 2–4 cm in length and 1–1.5 cm in short axis (Figure 4.1.5). Conversely, detection of hilar lymphadenopathy on routine ultrasound should prompt consideration of chronic hepatopathy and appropriate laboratory evaluation.

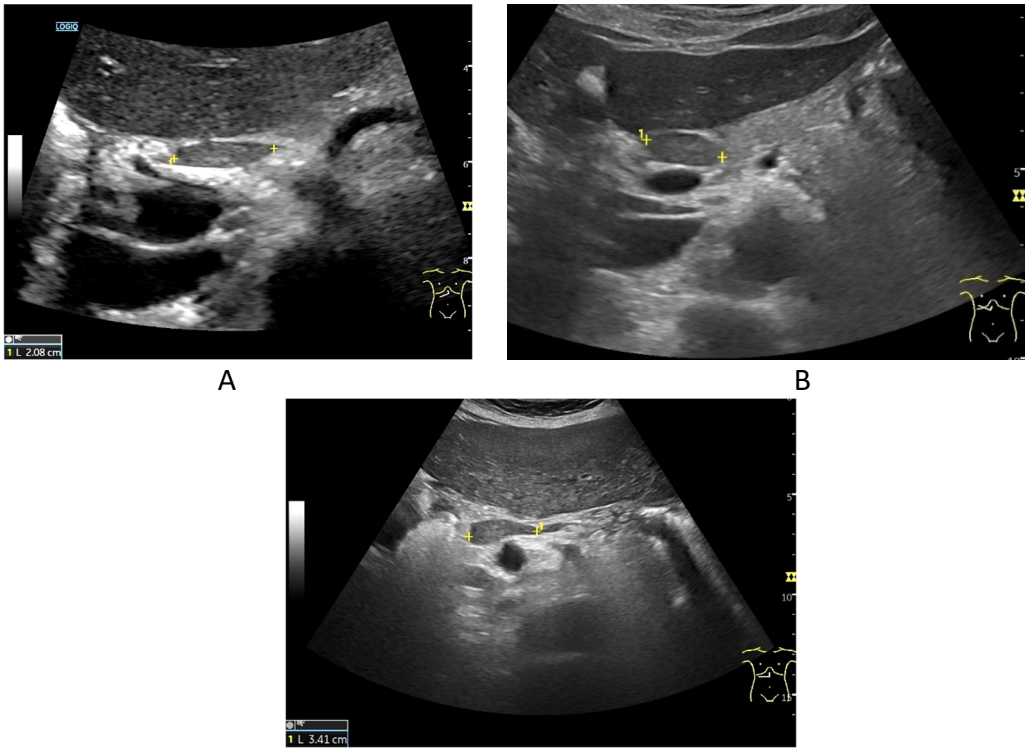


Figure 4.1. 5 A-C. Ultrasound imaging of inflammatory hepatic hilum lymph nodes: ovoid, hypoechoic structures

Conventional B-mode ultrasound remains a cornerstone for ***identifying hepatic steatosis***, a highly prevalent condition in industrialized settings, affecting roughly one-third of the adult population (2). In line with recent nomenclature updates, the umbrella term NAFLD (non-alcoholic Fatty Liver Disease) has been replaced by **metabolic dysfunction–associated steatotic liver disease (MASLD)** (3, 4).

For fatty liver assessment, standard ultrasound offers good diagnostic performance—particularly when steatosis is moderate or severe—and generally high specificity. The classic appearance is a diffusely increased parenchymal echogenicity ("bright liver") accompanied by progressive posterior beam attenuation (Figure 4.1.6 A). In routine practice, the degree of brightness and the extent of attenuation allow a pragmatic, semi-quantitative impression of severity (mild/moderate/severe), albeit with an unavoidable subjective component.

A useful sign is the hepato-renal index (Figure 4.1.6. B). Normally, the echogenicity of the right renal cortex approximates that of adjacent liver tissue. With steatosis, the liver becomes relatively hyperechoic compared with the kidney, increasing the liver-kidney contrast. Several studies, including those using histology as the reference standard, suggest that the hepato-renal index can be a robust indicator of steatosis and may, in certain contexts, outperform brightness/attenuation alone.

Accordingly, we routinely compare liver and right kidney echogenicity during examination. This approach should be interpreted cautiously in chronic kidney disease, where increased renal cortical echogenicity may blunt the contrast and reduce the reliability of hepato-renal comparison.

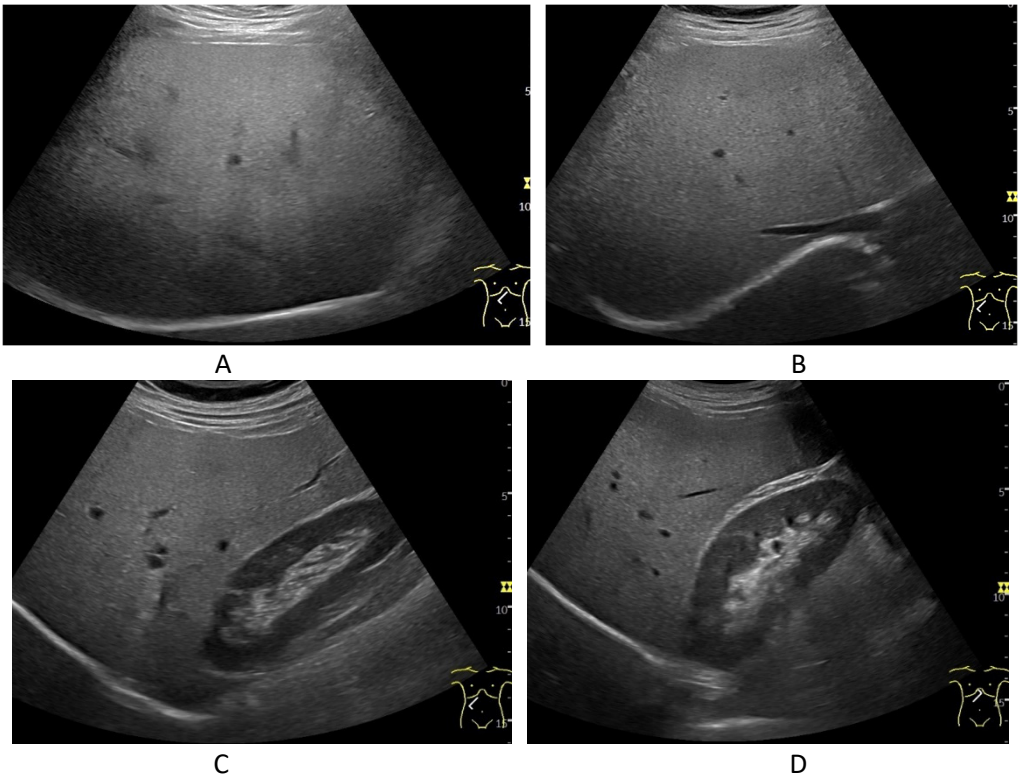


Figure 4.1.6 A-D. Ultrasound Assessment of Hepatic Steatosis: A-B Increased Liver Echogenicity with Posterior Attenuation and C-D. Increased Hepato-renal Index

Because B-mode evaluation of steatosis relies on visual impressions (Fig. 4.1.7), several semi-quantitative scoring approaches have been proposed to improve consistency, including the *Hamaguchi score* (5). This score

integrates four commonly used sonographic features: increased liver echogenicity (brightness), posterior beam attenuation, hepato-renal contrast, and vessel blurring (reduced definition of portal/hepatic vascular margins, sometimes with an apparent narrowing of the lumen). While such composite scores can increase objectivity compared with a purely descriptive assessment, they are not routinely implemented in everyday clinical reporting.

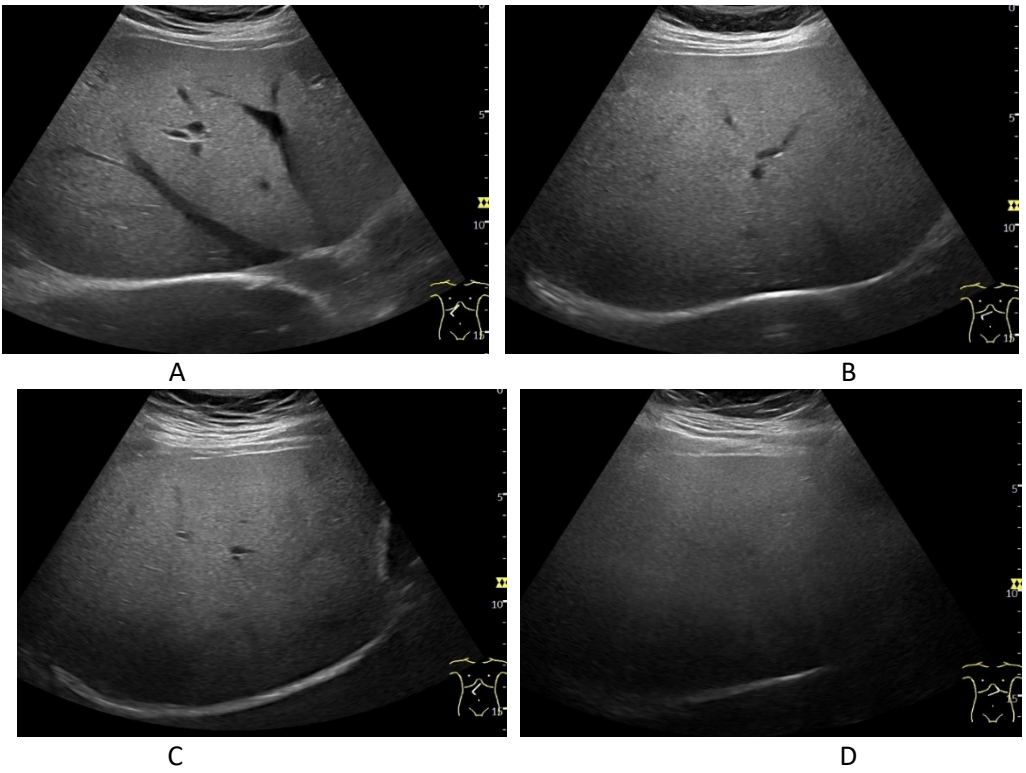


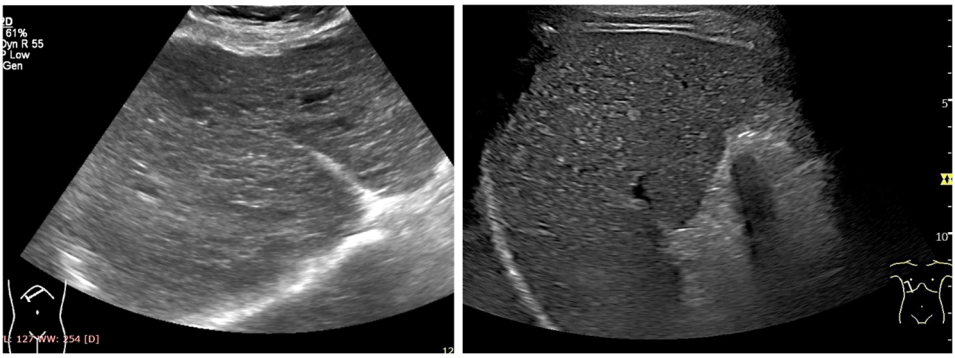
Figure 4.1.7 A-D. Different degrees of fatty infiltration (A- mild, B,C - moderate and D- severe)

Even with structured scoring, important limitations persist: inter- and intra-observer variability, differences in equipment performance and settings, and the difficulty of reliably tracking small changes in fat content over time using subjective criteria alone. More recent, objective modalities of fatty quantification using ultrasound waves (QUS methods) are used, with good results, in comparison with liver biopsy of MRI-PDFF (6, 7), but this will be presented in the next chapters.

Liver biopsy (when necessary) is performed under ultrasound guidance. Liver biopsy can be echo-assisted (usually with Menghini needle) or echo-guided. In both procedures, using ultrasound to guide biopsy, the risk of this invasive procedure is decreased. But, in the last years, the number of liver biopsies decreased greatly, because noninvasive (NIT) methods replaced this invasive procedure in many cases.

Conventional B-mode ultrasound is of limited value for ***fibrosis staging***, as it primarily identifies features of ***advanced disease,*** rather than early or moderate fibrosis (8). Sonographic findings that raise suspicion for significant fibrosis/cirrhosis include a coarse or heterogeneous parenchymal pattern, an irregular or nodular liver surface, caudate lobe hypertrophy, splenomegaly, indirect signs of portal hypertension, and gallbladder wall thickening (often related to portal hypertension and/or hypoalbuminemia). In one biopsy-controlled study in chronic hepatitis B, a composite assessment of these B-mode features achieved an accuracy of about 80% for compensated cirrhosis (9).

Evaluation of the liver surface becomes easier when perihepatic ascites is present, as the fluid interface improves delineation - particularly with a high-frequency linear transducer. Nevertheless, when standard ultrasound is benchmarked against biopsy for fibrosis detection in chronic hepatitis, sensitivity may be very low (around 25%) (8), despite a relatively preserved specificity (approximately 80%) (9), underscoring the need for ultrasound elastography or other noninvasive tools when fibrosis staging is clinically required.



A B

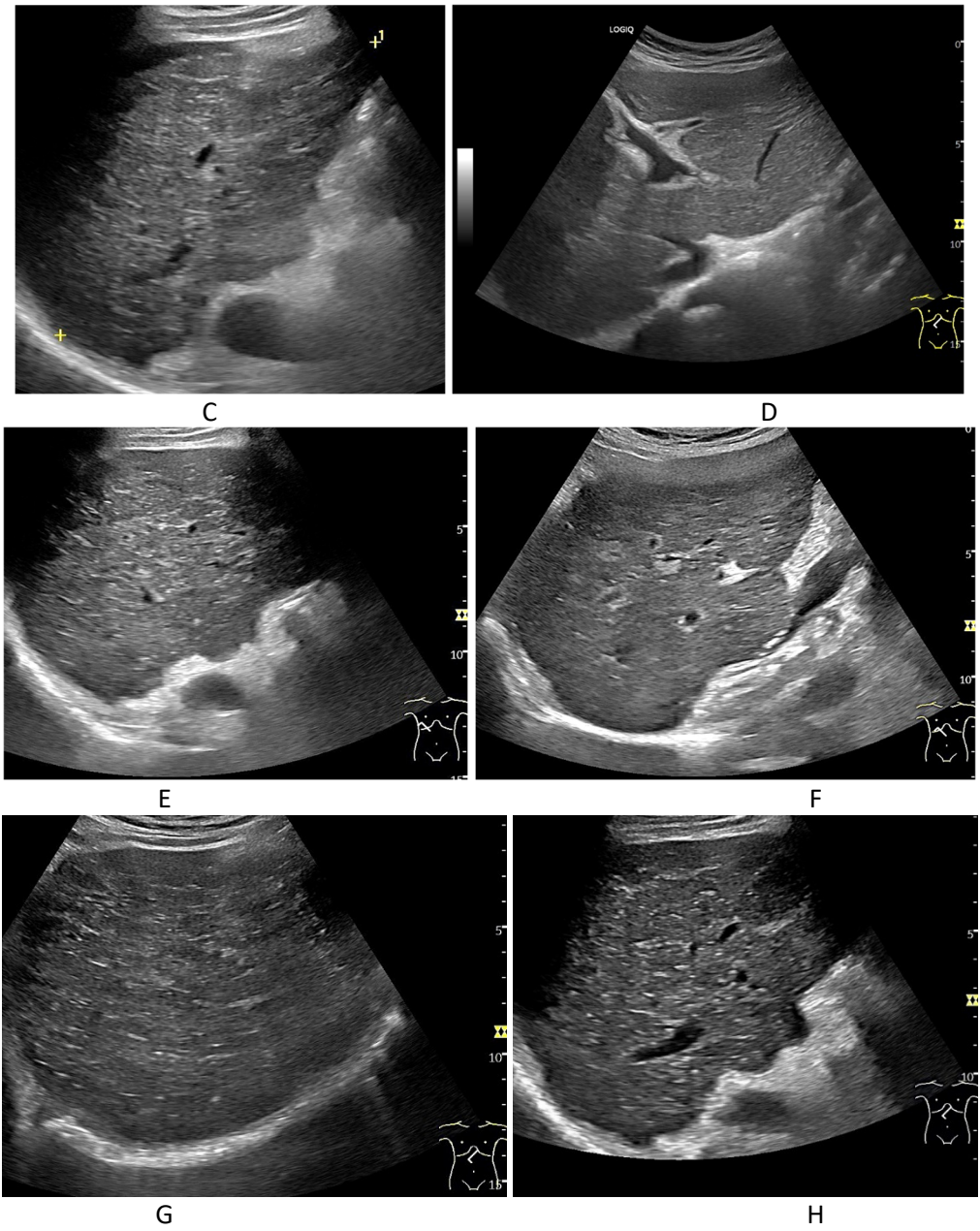


Figure 4.1.8 A-H. Heterogeneous (inhomogeneous) hepatic parenchyma in liver cirrhosis

Caudate lobe hypertrophy (segment I) is another morphologic feature that may support a diagnosis of liver cirrhosis. On ultrasound, the caudate lobe

can be assessed by measuring its anteroposterior diameter—typically from the posterior margin of the lobe to the ligamentum venosum. In most individuals, this dimension is generally <35 mm. In cirrhosis, the caudate lobe often enlarges beyond this threshold and may occasionally reach 50–60 mm, producing the characteristic prominence of segment I (Fig. 4.1.9.).

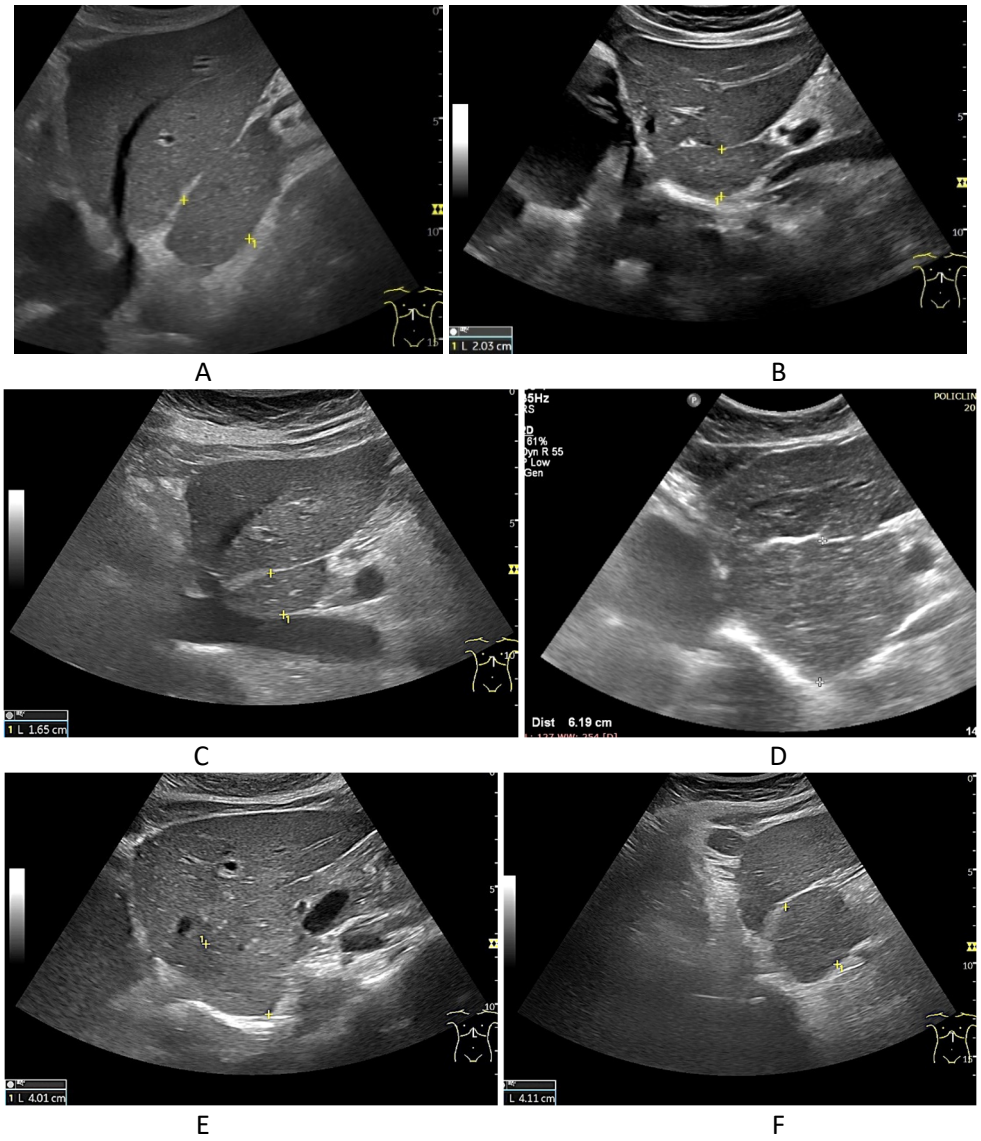


Figure 4.1.9 A-F. Ultrasound findings of normal (A,B,C) and enlarged caudate lobe (D,E,F)

Assessment of the portal venous system can provide indirect evidence of portal hypertension. On B-mode and Doppler imaging, suggestive features include a portal vein caliber increased at the hepatic hilum (commonly cited as >14 mm) (Fig. 4.1.10.), prominence of intrahepatic portal radicles, associated splenic vein dilatation, and, occasionally, splenic varices/collaterals. Another characteristic sign is *paraumbilical (umbilical) vein recanalization,* seen as a vascular channel arising from the left portal vein and coursing toward the umbilicus (Fig. 4.1.11).

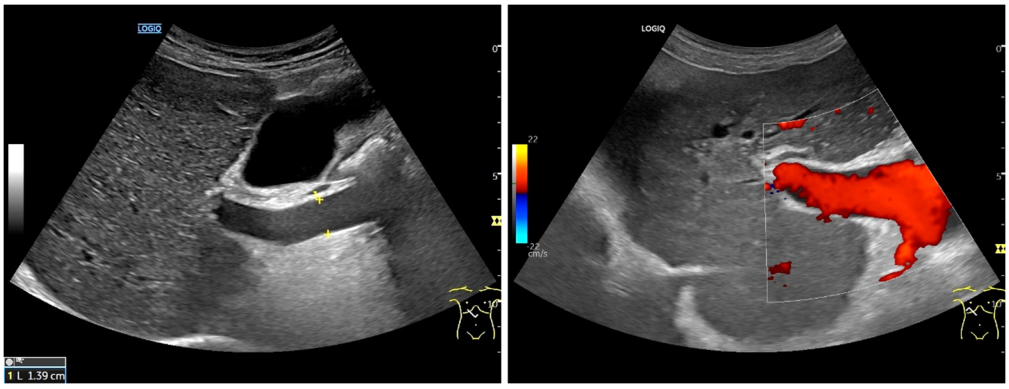
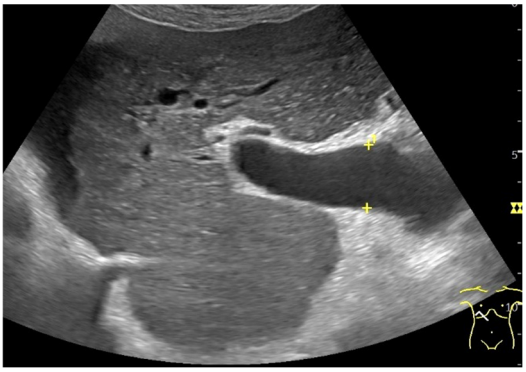
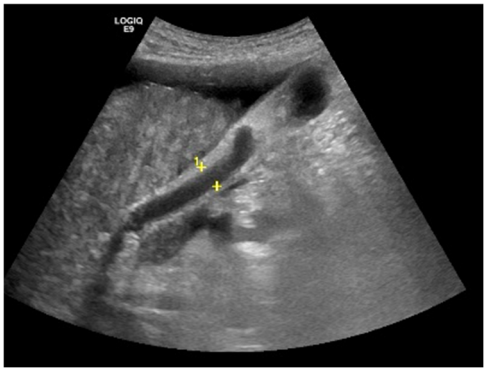


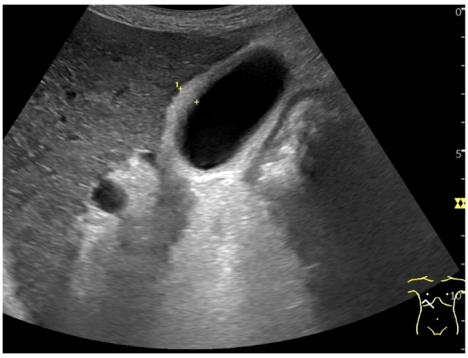
Figure 4.1.10 Evaluation of the Portal Vein. A - B-mode ultrasound demonstrating a portal vein diameter of approximately 14 mm at the hepatic hilum, suggestive of mild dilation. B - Color Doppler ultrasound confirming an enlarged portal vein lumen, consistent with early signs of portal hypertension.



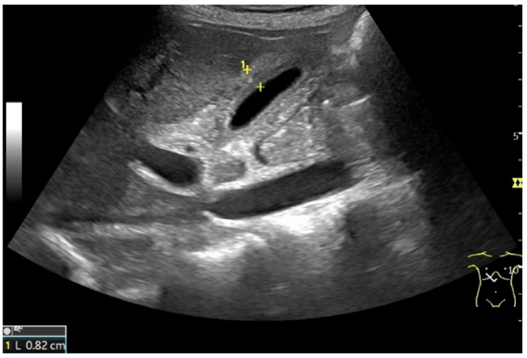
A



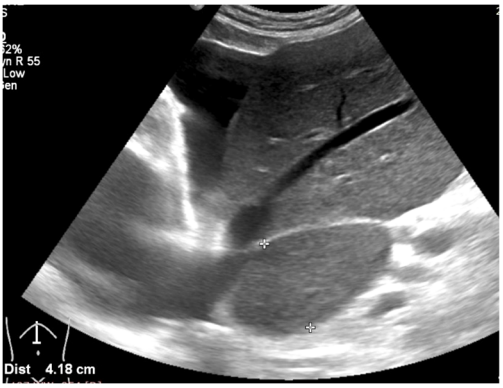
B



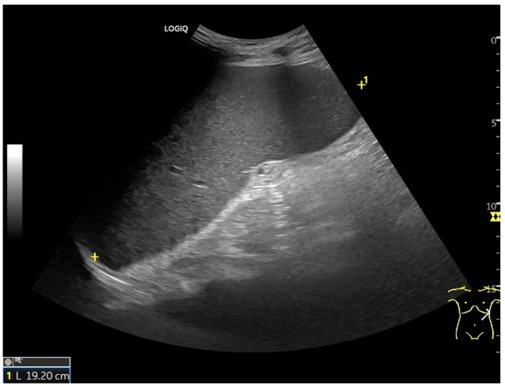
C



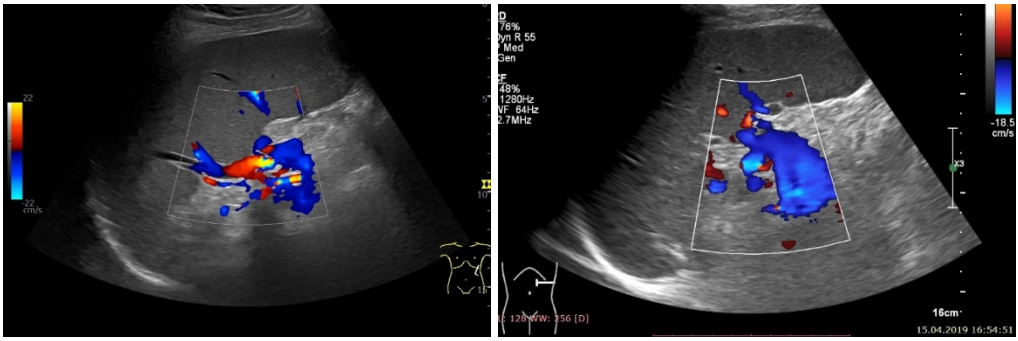
D



E



F



G H

Figure 4.1.11 A-H. Ultrasound Findings Indicative of Portal Hypertension and Liver Cirrhosis

A - A dilated portal vein is visible. B - Recanalization of the paraumbilical (umbilical) vein is evident, forming an abnormal vascular channel in the ligamentum teres. C, D - The gallbladder demonstrates a "double-layered" thickened wall, often associated with hypoalbuminemia and portal hypertension. E - Hypertrophy of the caudate lobe is observed. F - Splenomegaly is clearly depicted, a frequent finding in portal hypertension. G,H - Color Doppler imaging reveals splenic varices, confirming collateral circulation.

Ultrasound is extremely sensitive for the detection of ascites (Fig. 4.1.12), including small fluid volumes. Free fluid is most often first appreciated in dependent spaces such as the pelvis (e.g., the rectovesical pouch), and it may also be seen in perihepatic recesses or around the spleen. A pragmatic, semi-quantitative impression of ascitic volume can support therapeutic decisions, and repeated examinations are useful to monitor response and to fine-tune diuretic therapy. When therapeutic paracentesis is indicated, ultrasound guidance is recommended to improve safety and reduce the risk of inadvertent bowel injury.

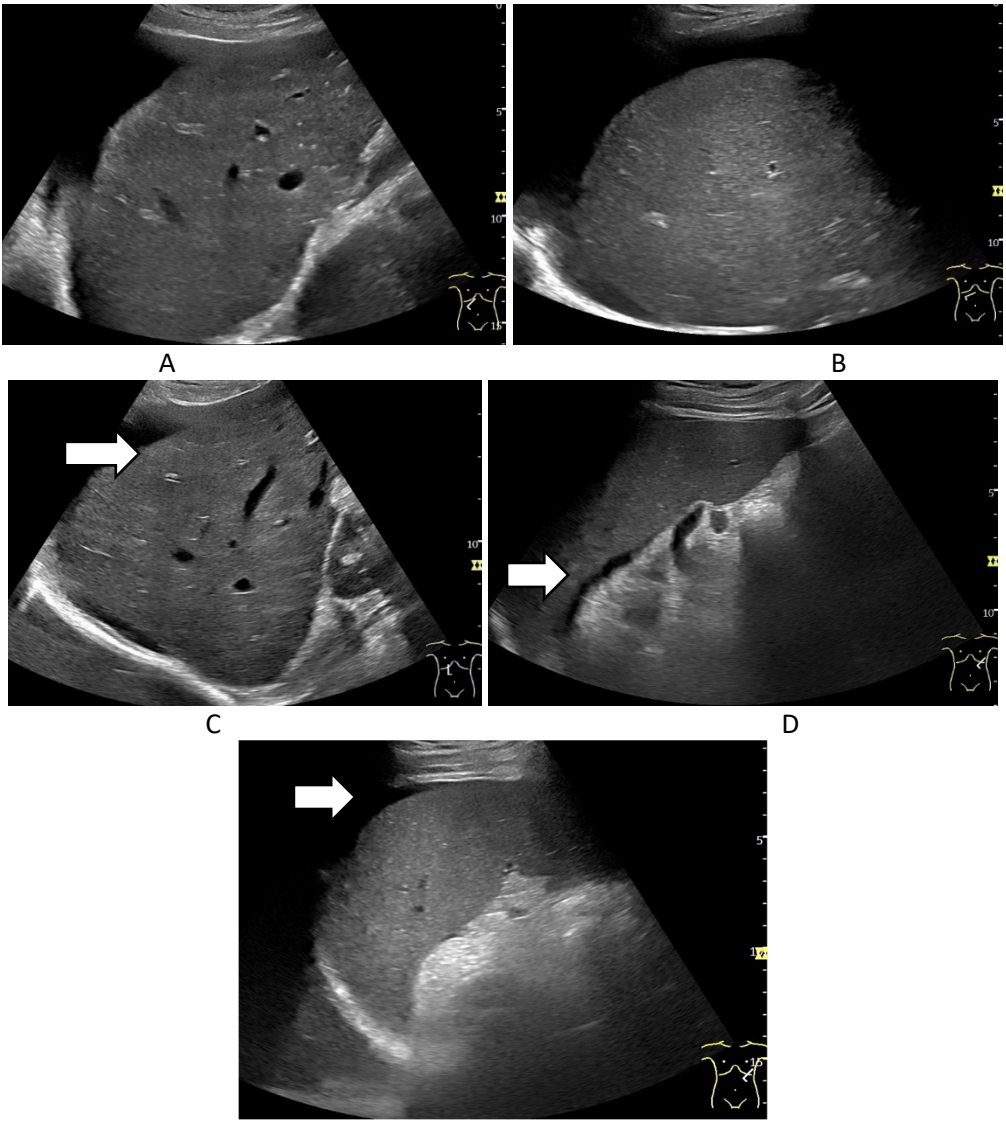
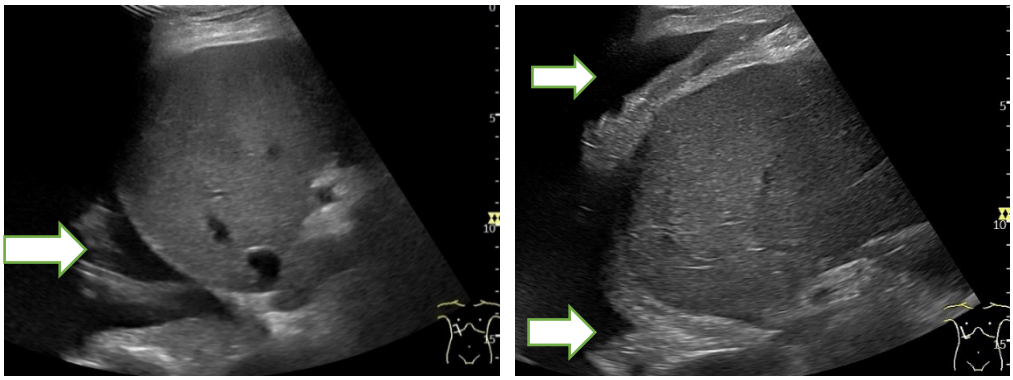


Figure 4.1.12. A-C Perihepatic ascites D-E. Small peri-splenic amount of ascites

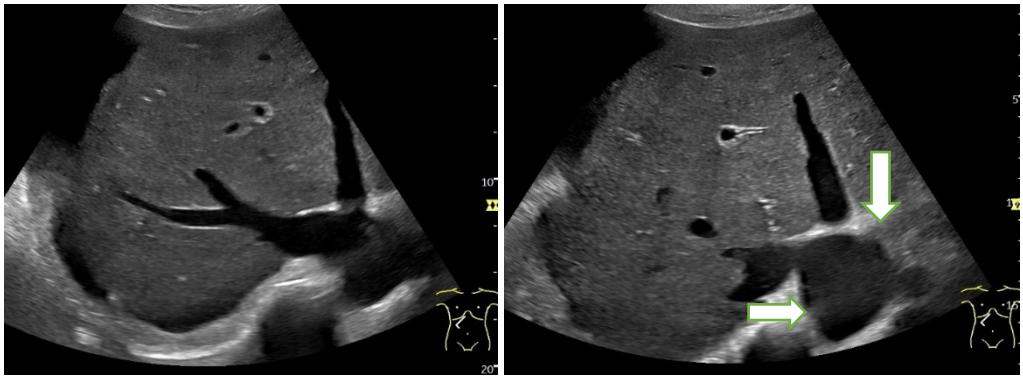
Ultrasound is also very helpful for the assessment of pleural effusion, showing the presence of the fluid and a semi-quantitative evaluation of the volume (Fig. 4.1.13). If thoracocentesis is necessary, ultrasound is used to guide this procedure.



A B

Figure 13 A-B Right pleural effusion

In the case of cardiac liver, dilated hepatic veins and dilatation of the inferior vena cava can be seen, as well as the presence of ascites (Fig. 4.1.14).



A B

Figure 4.1.14 A-B. Cardiac liver

In contrast, interpretation of liver echotexture changes remains challenging and largely subjective. Marked parenchymal inhomogeneity is frequently encountered in advanced cirrhosis, yet it may be minimal or absent in earlier stages. In primary biliary cholangitis, a coarse or abnormal liver texture is commonly described.

Given the limited performance of conventional B-mode ultrasound for identifying early-to-moderate fibrosis, additional techniques are needed for fibrosis assessment. Over the last two decades, ultrasound-based elastography has become a routine, noninvasive approach to estimate liver stiffness in

patients with suspected chronic liver disease (10, 11). All about ultrasound-based liver elastography will be presented in the next chapters.

Ultrasound findings in acute hepatitis. Conventional B-mode ultrasound is often non-specific and may be completely normal in acute hepatitis. When present, the most helpful clue is gallbladder wall thickening with a layered ("sandwich-like") appearance, sometimes described as "splitting" of the wall. This finding is common - particularly in acute viral hepatitis and is generally attributed to edema related to hypoalbuminemia and systemic inflammatory changes, rather than primary biliary obstruction. In a young or middle-aged patient with dyspeptic symptoms and jaundice, a layered gallbladder wall may therefore support the diagnosis of acute hepatitis in the appropriate clinical context.

Other low-specific findings may include a relatively hypoechoic liver parenchyma (reflecting edema and often difficult to appreciate without a reliable reference structure) and occasionally mild splenomegaly. However, splenomegaly more often suggests pre-existing chronic liver disease, on which an acute episode may supervene.

Overall, ultrasound has limited diagnostic specificity for confirming acute hepatitis itself; its greatest contribution is in the ***differential diagnosis of jaundice,*** primarily by distinguishing ***parenchymal jaundice*** (non-dilated bile ducts) from ***obstructive jaundice*** (ductal dilatation).

In **obstructive jaundice**, ultrasound characteristically shows biliary dilatation, involving intrahepatic ductal enlargement (often described as a "spider-like" pattern) and/or dilatation of the main bile duct (MBD). In most patients, the MBD is <7 mm (Fig. 4.1.15. A,B), with slightly larger diameters commonly encountered after cholecystectomy. In significant obstruction, the duct may become markedly enlarged ((Fig. 4.1.15. C,D), sometimes reaching 15–20 mm. Careful interrogation of the dilated ductal system may identify choledocholithiasis (with moderate sensitivity, particularly for small stones) or reveal an obstructing lesion at the pancreatic head. When the blockage is at the hepatic hilum (e.g., hilar cholangiocarcinoma), intrahepatic ducts are typically dilated, while the extrahepatic duct may remain of normal caliber.

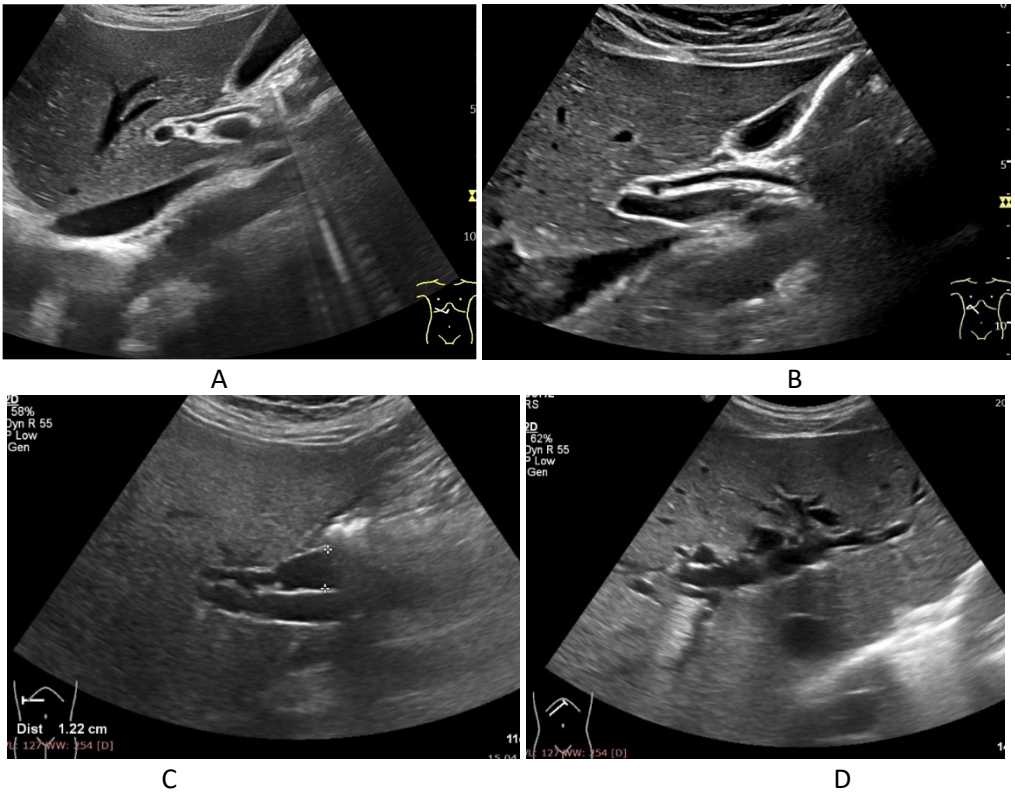


Figure 15 A-B Normal MBD; C-D. Ultrasound findings in obstructive jaundice: dilated intrahepatic (D) and extrahepatic bile ducts, including a prominent common bile duct (>12 mm) (C)

In patients with jaundice secondary to decompensated cirrhosis, ultrasound usually demonstrates typical features of advanced chronic liver disease - such as a coarse/heterogeneous echotexture, caudate lobe hypertrophy, splenomegaly, and ascites—while the intrahepatic and extrahepatic bile ducts remain non-dilated.

Ultrasound is likewise important in the assessment of hepatic vascular disorders, including Budd–Chiari syndrome and portal vein thrombosis. In Budd–Chiari syndrome, one or more hepatic veins may be poorly visualized, occluded, or markedly narrowed (Fig. 4.1.16), with secondary collateralization. In this setting, Doppler evaluation is essential, and contrast-enhanced ultrasound (CEUS) can provide additional diagnostic confidence and improve characterization when needed.

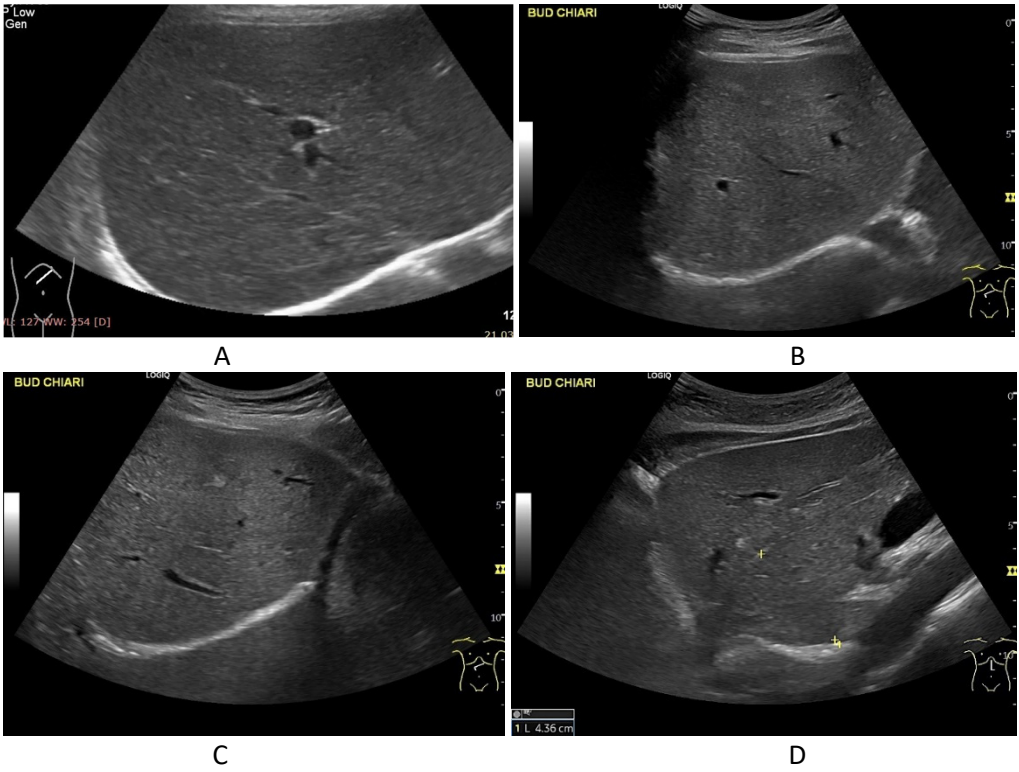
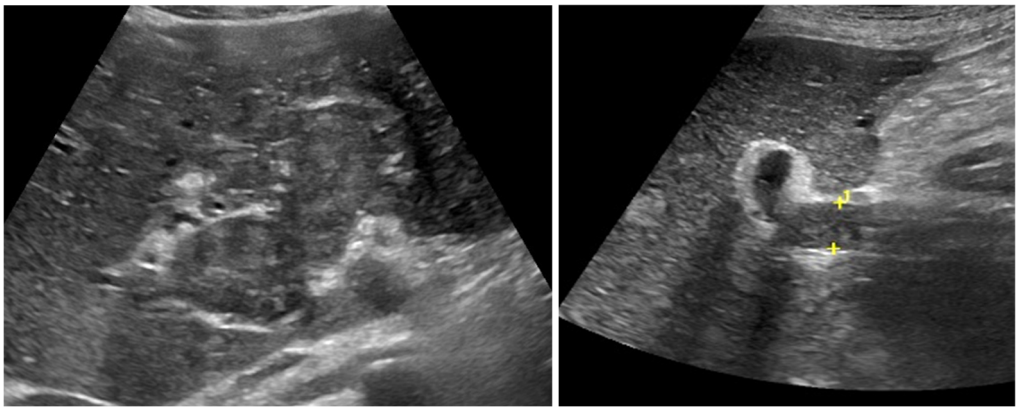


Figure 4.1.16 A-C. Ultrasound findings suggestive of Budd-Chiari syndrome: In this image, the expected hepatic veins are not clearly visualized. The hepatic veins appear absent. D. Caudate lobe hypertrophy

The examination of the portal vein can identify partial or complete thrombosis, typically seen on B-mode as intraluminal echogenic material replacing the normal anechoic flow channel (Fig. 4.1.17). Contrast-enhanced ultrasound (CEUS) is particularly valuable because it can distinguish benign thrombus from tumor (malignant) thrombus with high diagnostic accuracy (12, 13). In patients with cirrhosis and/or hepatic malignancy, a systematic survey of the entire portal venous system is therefore mandatory, as the presence and nature of portal thrombosis may significantly change staging and subsequent management.



A B

Figure 4.1.17 A-B. Two B-mode ultrasound images illustrating echogenic material within the lumen of the portal vein, consistent with portal thrombosis. The normally anechoic vascular channel appears partially or completely filled.

In patients with compensated advanced chronic liver disease (cACLD) or advanced fibrosis, ultrasound remains the backbone of ***hepatocellular carcinoma (HCC) surveillance*** (HCC screening) (Fig 4.1.18). This population carries an estimated annual HCC incidence in the ~1–5% range, influenced by underlying etiology, age, and sex. Most contemporary guidelines endorse ***6-month ultrasound surveillance***, commonly combined with ***alpha-fetoprotein (AFP)*** to improve early detection.

The effectiveness of surveillance depends heavily on examination quality. Sensitivity is maximized when scanning is performed by an experienced operator, with meticulous coverage of the entire liver—particularly in markedly heterogeneous cirrhotic parenchyma. Patient positioning and cooperation, as well as adequate equipment performance, are also important. When ultrasound examination is *suboptimal* (e.g., poor acoustic window, non-visualized segments, or extreme parenchymal heterogeneity), escalation to cross-sectional imaging - contrast-enhanced CT or MRI—is warranted.

Abbreviated MRI protocols have received increasing attention as a potential surveillance alternative in selected settings; however, implementing MRI-based surveillance at scale is constrained by costs, access, and workflow considerations, given the large number of patients who require long-term follow-up. Finally, it is important to emphasize that patients with cirrhosis who *achieve virological cure after HCV treatment should continue lifelong HCC surveillance*, as the risk of HCC is reduced but not eliminated.

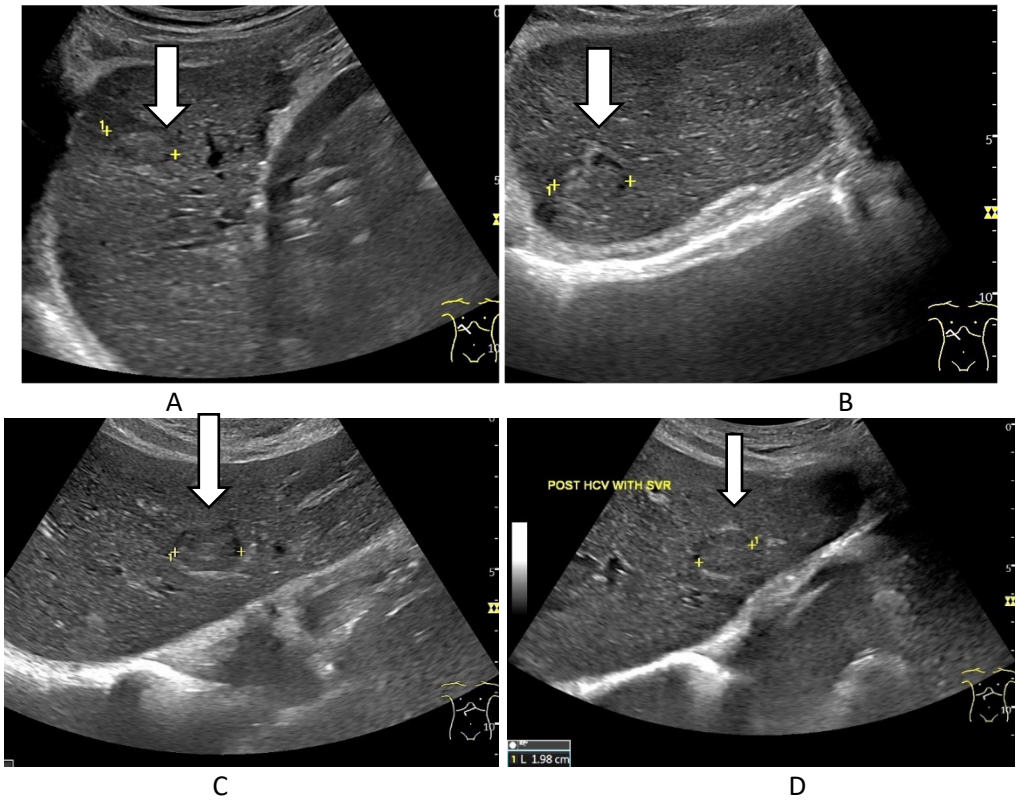


Figure 4.1.18 A-D. B-mode ultrasound images showing small hepatocellular carcinomas in the context of liver cirrhosis, found during HCC screening program.

In **summary**, ultrasound remains central to the assessment and longitudinal care of chronic liver disease, combining safety, wide availability, low cost, and real-time bedside applicability. Although limitations such as operator dependence and reduced image quality—particularly in obesity or in the presence of bowel gas—are well recognized, their impact can be substantially reduced through standardized acquisition protocols, structured reporting, and appropriate training.

With the new trend in hepatology, where the clinicians (hepatologists, gastroenterologists, internal medicine specialists, or general practitioners) perform ultrasound in daily practice, often like PoCUS (Point of Care Ultrasound) method, in the room of consultation, answers to clinical questions can be obtained (14). With such a strategy, quality of consultation is increased and waiting time for a final diagnosis is reduced.

References

1. Nürnberg D, Chammas MC, Gilja OH, Sporea I, Șirli R, editors. WFUMB Course Book. 1st ed.: World Federation for Ultrasound in Medicine and Biology (WFUMB); 2021. ISBN: 978-1-8384990-0-6.
2. Younossi ZM, Golabi P, Paik JM, Henry A, Van Dongen C, Henry L. The global epidemiology of nonalcoholic fatty liver disease (NAFLD) and nonalcoholic steatohepatitis (NASH): a systematic review. Hepatology. 2023 Apr 1;77(4):1335-1347.
3. Rinella ME, Sookoian S. From NAFLD to MASLD: updated naming and diagnosis criteria for fatty liver disease. J Lipid Res. 2024 Jan;65(1):100485.
4. Rinella ME, Neuschwander-Tetri BA, Siddiqui MS, Abdelmalek MF, Caldwell S, Barb D, et al. AASLD Practice Guidance on the clinical assessment and management of nonalcoholic fatty liver disease. Hepatology. 2023 May 1;77(5):1797-1835..
5. Hamaguchi M, Kojima T, Itoh Y, Harano Y, Fujii K, Nakajima T, et al. The severity of ultrasonographic findings in nonalcoholic fatty liver disease reflects the metabolic syndrome and visceral fat accumulation. Am J Gastroenterol. 2007 Dec;102(12):2708-15.
6. Sporea I, Șirli R, Popescu A, Stoian D. Textbook of Elastography. E-book: https://www.umft.ro/wp-content/upload/2024/10/TEXTBOOK-OF-ELASTOGRAPHY-21-oct.pdf
7. Ferraioli G, Barr RG, Berzigotti A, Sporea I, Wong VW, Reiberger T, et al. WFUMB Guidelines/Guidance on Liver Multiparametric Ultrasound. Part 2: Guidance on Liver Fat Quantification. Ultrasound Med Biol. 2024 Aug; 50(8):1088-1098.
8. D'Onofrio M, Martone E, Brunelli S, Faccioli N, Zamboni G, Zagni I, et al. Accuracy of ultrasound in the detection of liver fibrosis in chronic viral hepatitis. Radiol Med. 2005 Oct;110(4):341-348.
9. Zheng RQ, Wang QH, Lu MD, Xie SB, Ren J, Su ZZ, et al. Liver fibrosis in chronic viral hepatitis: an ultrasonographic study. World J Gastroenterol. 2003 Nov;9(11):2484-9.
10. Ferraioli G, Wong VW, Castera L, Berzigotti A, Sporea I, Dietrich CF, et al. Liver ultrasound elastography: An update to the World Federation for Ultrasound in Medicine and Biology guidelines and recommendations. Ultrasound Med Biol. 2018;44(12):2419-2440.
11. Ferraioli G, Barr RG, Berzigotti A, Sporea I, Wong VWS, Reiberger T, et al. WFUMB Guideline/Guidance on Liver Multiparametric Ultrasound: Part 1. Update to 2018 Guidelines on Liver Ultrasound Elastography. Ultrasound Med Biol. 2024;50(8):1071-1087.
12. Sporea I, Badea R, Popescu A, Spârchez Z, Sirli RL, Dănilă M, et al. Contrast-enhanced ultrasound (CEUS) for the evaluation of focal liver lesions - a prospective multicenter study of its usefulness in clinical practice. Ultraschall Med. 2014;35(3):259-266.

13. Dietrich CF, Nolsøe CP, Barr RG, Berzigotti A, Burns PN, et al. Guidelines and Good Clinical Practice Recommendations for Contrast-Enhanced Ultrasound (CEUS) in the Liver-Update 2020 WFUMB in Cooperation with EFSUMB, AFSUMB, AIUM, and FLAUS. Ultrasound Med Biol. 2020 Oct;46(10):2579-2604.
14. Sporea I, Popescu A, Puiu S, Cela D, Saraci B, Grgurevic I, Brkljacic B, Nurenberg D. Integrating Ultrasound in Clinical practice. “Victor Babeș” Publishing House, Timisoara 2025; ISBN 978-606-786-461-8

4.2. Doppler Evaluation of the Liver: Technique, Clinical Value, Pitfalls, and Limitations

Ivica Grgurevic

Abstract

Doppler ultrasonography is a key noninvasive technique for evaluating hepatic vascular hemodynamics and liver pathology. By combining grayscale, color, and spectral Doppler imaging, it enables assessment of vessel morphology, flow direction, velocity, and waveform characteristics.

The portal vein normally shows hepatopetal laminar flow, while conditions such as cirrhosis and portal hypertension may lead to dilation, reduced velocity, or flow reversal. The hepatic artery demonstrates a low-resistance waveform, with Doppler indices useful for detecting arterial stenosis or thrombosis. Hepatic venous waveforms normally display a triphasic pattern reflecting cardiac cycle changes but may become dampened in chronic liver disease or altered in cardiac disorders. Doppler evaluation of the splenic circulation also contributes to the assessment of portal hypertension.

Although highly valuable in clinical practice, Doppler examination is operator-dependent and influenced by technical and hemodynamic factors, requiring careful interpretation and correlation with other imaging modalities, when necessary.

4.2.1. Introduction

The liver is the largest parenchymal organ in the abdomen with an abundant blood supply. Approximately 70–75% of its blood volume is supplied by the portal vein (PV), while the remaining 25–30% is delivered by the hepatic artery (HA) (1). Venous outflow occurs through the hepatic veins into the inferior vena cava (IVC) and subsequently into the right atrium. The integrity of hepatic vascular circulation is essential for normal liver function, and both acute and chronic liver diseases are associated with characteristic alterations in vascular morphology and hemodynamics. In this setting, Doppler ultrasonography represents a fundamental tool in the noninvasive evaluation of hepatic vascular physiology and pathology.

4.2.2. Basic Principles and Doppler Modalities

Doppler assessment of hepatic vessels includes evaluation of vascular morphology, presence and direction of flow, flow velocity, and spectral waveform characteristics (2). Gray-scale (B-mode) ultrasonography is used for morphological assessment, color Doppler for detecting and mapping blood flow, and spectral (pulsed-wave) Doppler for quantitative velocity analysis and hemodynamic assessment. Doppler ultrasonography is based on the Doppler effect, first described by Christian Doppler, whereby ultrasound waves reflected from moving erythrocytes undergo a frequency shift proportional to blood flow velocity ($\Delta f=2f_0$ x u x $cos\emptyset/v$, where f_0 refers to emitted frequency, u to flow velocity, $\emptyset$ to the angle between the axis of the ultrasound wave relative to the direction of the blood flow in the interrogated vessel, and v to the ultrasound velocity in the tissue-approximately 1.540 cm/s in human body), which is then processed into visual and auditory signals.

Color Doppler superimposes flow information onto the gray-scale image. Blood flow directed toward the transducer is conventionally coded in red, whereas flow away from the transducer is coded in blue; thus, color assignment reflects direction relative to the probe rather than distinguishing arterial from venous flow. When the ultrasound beam is perpendicular (90°) to the vessel, no Doppler signal is detected because the cosine of 90° equals zero in the Doppler equation, resulting in an apparent absence of flow.

Pulsed-wave Doppler enables quantitative measurement of flow velocity within a defined sample volume. *Spectral Doppler* provides a graphical representation of velocities throughout the cardiac cycle, with distinct patterns observed in arteries and veins; within the liver, waveforms differ further between the PV and HV. In cases of very slow flow, power Doppler may be used. *Power Doppler* analyzes the amplitude (signal strength) rather than frequency shift and is therefore more sensitive to low-flow states. The signal intensity is proportional to the number of moving erythrocytes within the sampled volume. However, power Doppler does not provide information regarding flow direction or velocity.

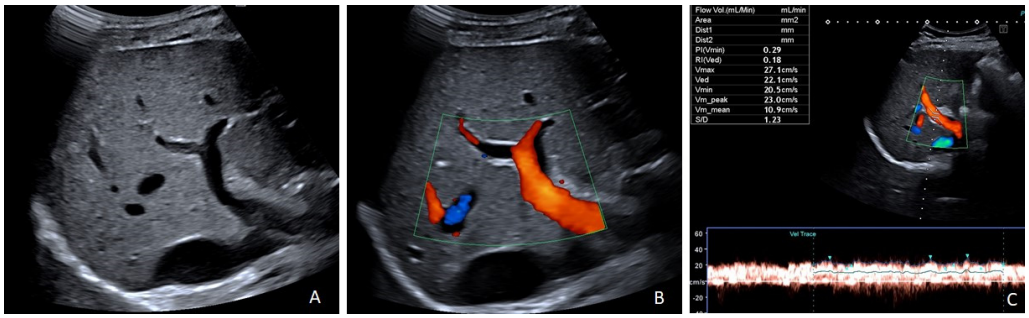


Fig. 4.2.1. Modalities of Doppler Ultrasound examination. A-Grey-scale (B-mode) image; B-Color Doppler-image of the blood flow is superimposed over grey-scale image. Red color-coded blood flow represents the direction towards the ultrasound probe, whereas blue-coded flow refers to the flow away from the probe (this modality is also known as Duplex Doppler); C-Pulse-wave Doppler analysis of the hemodynamics in the portal vein (also known as Spectral Doppler, or Triplex Doppler) demonstrates the waveform as the result of the blood flow direction, velocities, type of flow (laminar or turbulent), also reflecting cardiac cycle and respiration.

Accurate Doppler evaluation requires meticulous optimization of machine settings (3). The insonation angle should be maintained below 60° for reliable velocity measurements. Pulse repetition frequency (PRF) must be adjusted to avoid aliasing in high-velocity states, while maintaining sensitivity to low flow. Gain settings should be optimized to suppress background noise, without obscuring true vascular signals. Proper positioning and sizing of the sample volume within the vascular lumen are equally essential. A detailed discussion of Doppler physics and parameter optimization is beyond the scope of this chapter and is addressed extensively elsewhere in the literature.

4.2.3. Doppler Evaluation of Hepatic Vessels

a) Portal Vein

The portal vein is formed by the confluence of the splenic vein and the superior mesenteric vein (the inferior mesenteric vein most commonly drains into the splenic vein). An additional important tributary is the left gastric vein, which drains along the lesser curvature of the stomach into the portal vein. The portal vein thus conveys blood from the gastrointestinal tract and spleen to the liver and is essential for maintaining physiological function of these organs.

Upon entering the liver, the portal vein divides into right and left branches, each subsequently giving rise to anterior and posterior segmental branches. On grayscale imaging, the portal vein walls appear hyperechoic. Its

diameter is measured at the hepatic hilum and normally does not exceed 12–12.5 mm. Portal venous flow is laminar and hepatopetal (toward the liver), typically appearing as a homogeneous red signal on color Doppler when examined from a standard intercostal approach. Flow velocity exhibits mild respiratory and cardiac phasic variations; therefore, the mean peak velocity is measured. Mean peak velocity (Time averaged maximum velocity, Tamax) normally ranges from 20 to 40 cm/s, while the average mean velocity (Time Averaged Mean Velocity, TAMV) ranges between 15 and 30 cm/s (2, 4).

In pathological conditions, such as cirrhosis, increased intrahepatic vascular resistance leads to portal vein dilation (>12.5 mm), reduced flow velocity, and occasionally helical flow with increased spectral phasicity. Marked phasicity may also occur in arterioportal fistulas or elevated central venous pressure due to right-sided heart disease, where transmitted pulsations from hepatic veins affect portal flow. In advanced portal hypertension, flow reversal (hepatofugal flow) may occur, appearing blue on color Doppler and below the baseline on spectral Doppler (2, 4, 5).

In portal vein thrombosis, the Doppler signal is absent within the thrombosed segment (Fig. 4.2.2). Acute thrombi may be hypoechoic and easily overlooked on gray-scale imaging; therefore, Doppler assessment is essential, particularly in acute abdominal conditions. Chronic thrombosis results in increased thrombus echogenicity and development of collateral circulation, including periportal venous plexuses forming a portal cavernoma—identified as multiple serpiginous vascular channels at the hepatic hilum with venous spectral signals (6).

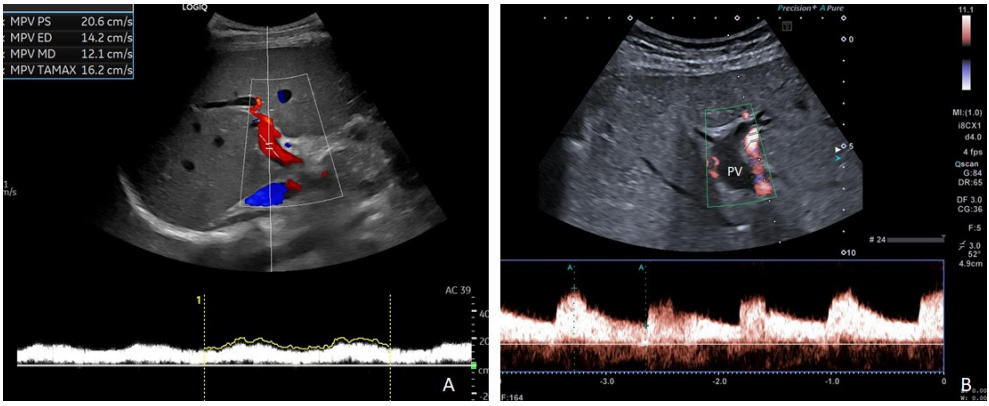


Fig. 4.2.2. Normal patent versus thrombosed portal vein. A-Spectral (triplex) Doppler from the patent portal vein, demonstrating hepatopetal flow (red-color coded). Thrombus is almost anechoic in this phase; B-Acute portal vein thrombosis: lack of Doppler signal in the portal vein, with normal signal from the adjacent hepatic artery.

Portal vein stenosis, most commonly iatrogenic (e.g., postoperative), produces an hourglass configuration with turbulent color flow at the stenotic site. Spectral Doppler demonstrates markedly increased velocities at the stenosis and post-stenotic turbulence, with bidirectional frequency components.

b) Hepatic Artery

The hepatic artery courses within the hepatoduodenal ligament, typically located between the portal vein and the common bile duct. After entering the liver, it divides into right and left branches and subsequently into segmental arterial branches that parallel the portal venous system and biliary tree.

On spectral Doppler, the hepatic artery demonstrates a low-resistance waveform characteristic of parenchymal arteries. This consists of a sharp systolic upstroke followed by continuous forward diastolic flow (Fig. 4.2.3.). Quantitative parameters include peak systolic velocity (PSV), end-diastolic velocity (EDV), resistive index [RI= (PSV − EDV) / PSV] and pulsatility index [PI=(PSV-EDV]/Tamax, where Tamax is measured by the device's software over one full cardiac cycle (from the beginning of systole to the end of diastole). Normal peak systolic velocity ranges between 30 and 75 cm/s, while the end-diastolic velocity ranges between 15 and 25 cm/s. Normal RI values ranges between 0.5 and 0.7, while normal PI values are up to 0.9 (2, 4, 5).

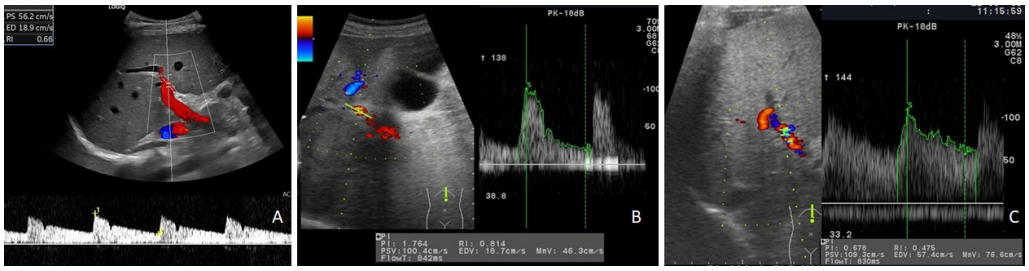


Fig. 4.2.3. Doppler images of the hepatic artery. A-normal low resistant waveform on spectral analysis in healthy person (Resistive index 0.66). B-In a patient with compensated cirrhosis: Spectral Doppler revealed increased hepatic artery RI of 0.81. C-Parvus-tardus waveform (high PSV and EDV, but low RI of 0.47) in a patient with cirrhosis and arterio-venous fistula.

In chronic liver disease, progressive fibrosis and architectural distortion increase intrahepatic vascular resistance, resulting in elevated RI values (typically due to reduced EDV).

In arterio-venous communications—seen in cirrhosis, hereditary hemorrhagic telangiectasia, or following interventional procedures such as liver biopsy—reduced distal resistance leads to increased diastolic flow and a decreased RI (<0.5) (7).

Hepatic artery stenosis, most commonly observed after liver transplantation, is characterized by markedly increased PSV at the stenotic site. Distal to the stenosis, a parvus–tardus waveform is observed, defined by reduced systolic velocity, prolonged systolic acceleration time (>80 m/s), and decreased RI (<0.5) (8, 9).

Hepatic artery thrombosis results in ischemia or infarction of the supplied hepatic territory. Doppler examination demonstrates absence of arterial flow, often accompanied by compensatory collateral circulation. Clinically, this condition is associated with abrupt and marked elevation of serum transaminases.

c) Hepatic Veins

The hepatic veins exhibit the most complex Doppler waveform morphology, due to their direct hemodynamic relationship with the right atrium and the absence of venous valves in between. They drain into the inferior vena cava, and their flow pattern reflects cyclic changes in right atrial pressure. Under normal conditions, the hepatic venous waveform is triphasic. When examined using a subcostal approach with the ultrasound probe directed toward the hepatic vein confluence, the waveform consists of:

- forward (over the baseline) „a-wave“ corresponding to atrial contraction,
- retrograde (below the baseline) „s-wave“ representative of ventricular systole, and
- retrograde „d-wave“ representative of ventricular diastole.

During atrial contraction, blood flows through the tricuspid valve into the right ventricle; however, due to the absence of valves in the hepatic veins, a portion of blood is transmitted retrogradely toward the liver—that is, toward the ultrasound transducer—resulting in a positive deflection on the spectral Doppler tracing. During ventricular systole, the tricuspid valve is closed, and blood flows from the liver toward the right atrium, moving away from the transducer; consequently, this phase is represented as a negative deflection on

the spectral waveform. During ventricular diastole, the tricuspid valve opens and blood flows from the right atrium into the right ventricle, while venous return from the liver continues toward the right atrium. As this flow direction remains away from the transducer, it is likewise displayed as a negative deflection on the spectral Doppler recording.

In chronic liver disease, reduced hepatic compliance secondary to steatosis and/or fibrosis leads to progressive dampening of waveform phasicity (10-12) (Fig. 4.2.4.). The triphasic pattern may become biphasic and eventually monophasic. However, the diagnostic performance of this finding is limited by interindividual variability and hemodynamic influences; therefore, Doppler findings alone are insufficient for reliable staging of fibrosis. Contemporary assessment of fibrosis relies more accurately on elastography.

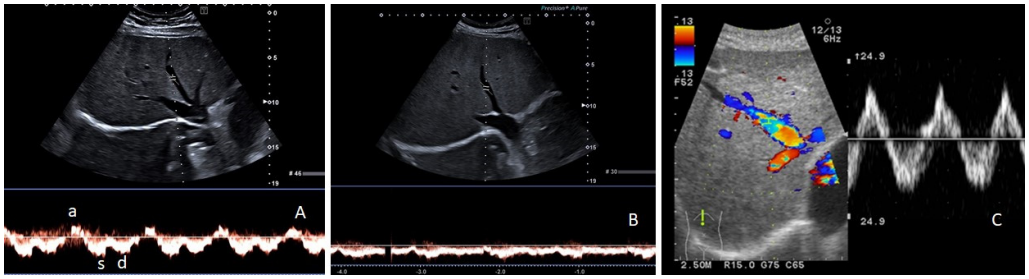


Fig. 4.2.4. Doppler images of the hepatic vein waveform in different conditions. A-Normal triphasic waveform in a healty individual: "a" wave over the baseline reflects atrial contraction, "s" wave below baseline reflects ventricular systole, and "d" wave reflects ventricular diastole. B-Biphasic waveform (reduced phasicity, lack of "a" wave) in a patient with liver steatosis and fibrosis; C-Increased phasicity in a patients with tricuspidal regurgitation and right-sided heart failure: note the lack of the systolic wave (the first one following atrial contraction; systolic wave is reverted and merged with "a" wave from the atrial contraction making a single huge deflection over the baseline ("a-s wave"), followed by a single negative deflection from the ventricular diastole.

Reduced phasicity may also occur in hepatic venous outflow obstruction, such as Budd–Chiari syndrome, characterized by partial or complete obstruction of the hepatic veins and/or inferior vena cava. Upstream from the obstruction, monophasic flow is typically observed, often accompanied by development of intrahepatic veno-venous collaterals (13).

Conversely, increased waveform pulsatility may be seen in conditions associated with elevated right-sided cardiac pressures or tricuspid

regurgitation. In right heart failure, elevated atrial pressures are transmitted to the hepatic veins, resulting in exaggerated pulsatility and increased waveform amplitude. In significant tricuspid regurgitation, systolic flow reversal may occur, producing a prominent positive systolic deflection (14).

In hepatic congestion, the hepatic veins are dilated (>8 mm in diameter when measured at least 2 cm proximal to their junction with the inferior vena cava), a finding readily demonstrated on gray-scale imaging.

d) Splenic artery

The spleen plays a crucial role and should be carefully evaluated when considering portal hypertension (PH), as it experiences both structural and hemodynamic alterations. In a normal spleen, blood flows in through the splenic artery and exits via the splenic vein, which contributes to the portal vein circulation. The Doppler waveform of the parenchymal branches of splenic artery typically shows a low-resistance pattern (Fig. 4.2.5.). Besides the resistance index (RI), the pulsatility index (PI) is also assessed. In individuals without portal hypertension, RI values should be below 0.63, while PI values should be under 1. The average blood flow velocity in the splenic vein at the splenic hilum for healthy individuals is generally below 15 cm/s (15, 16).

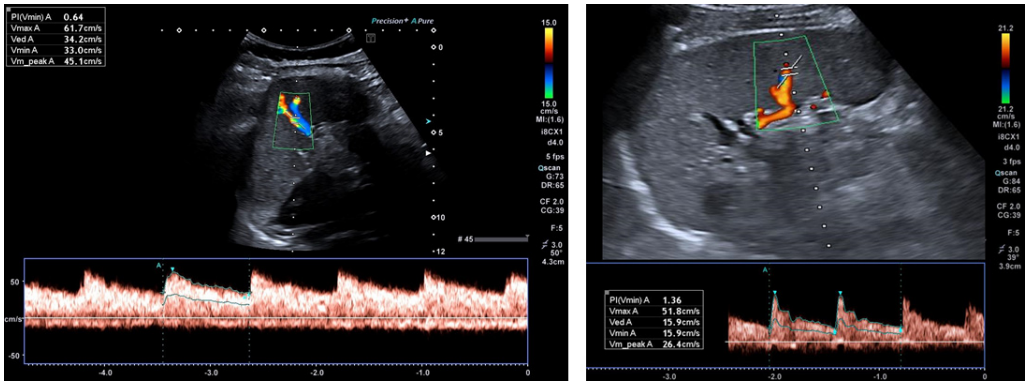


Fig. 4.2.5. Doppler Ultrasound of the splenic artery. A-normal splenic artery pulsatility index (SAPI) in a healthy person; B-increased SAPI 1.3 in a patient with portal hypertension

4.2.4. Pitfalls and Limitations of Doppler Evaluation

Doppler evaluation of the hepatic vasculature is operator-dependent and technically demanding. Inadequate angle correction, improper placement of the sample volume, suboptimal gain, or inappropriate pulse repetition

frequency may lead to significant velocity measurement errors or misinterpretation of flow direction. Respiratory motion, patient body habitus, bowel gas, and limited acoustic windows may further degrade image quality and reduce diagnostic reliability.

Physiological factors also represent important limitations. Portal and hepatic venous waveforms are influenced by respiration, cardiac function, and intravascular volume status; consequently, abnormal spectral patterns do not necessarily reflect primary hepatic pathology. In particular, reduced phasicity of the hepatic venous waveform lacks sufficient sensitivity and specificity for accurate staging of fibrosis and should not be used in isolation for this purpose (2-5, 17).

In addition, Doppler ultrasound has limited sensitivity for detecting very slow flow, small-caliber vessels, or deeply located vascular segments, despite the use of power Doppler. Differentiating between severe stenosis and near-occlusive thrombosis may occasionally be challenging. In these situations contrast-enhanced ultrasound (CEUS) or cross-sectional imaging modalities, such as contrast-enhanced CT or MRI, may be required.

In conclusion, Doppler ultrasonography provides comprehensive qualitative and quantitative assessment of hepatic vascular hemodynamics. Nevertheless, interpretation requires awareness of technical limitations, hemodynamic influences, and potential pitfalls to avoid misdiagnosis.

References

1. Burroughs, A.K. (2011). The Hepatic Artery, Portal Venous System and Portal Hypertension: The Hepatic Veins and Liver in Circulatory Failure. In Sherlock's Diseases of the Liver and Biliary System (eds J.S. Dooley, A.S.F. Lok, A.K. Burroughs and E.J. Heathcote), 12th Edition.

2. McNaughton DA, Abu-Yousef MM. Doppler US of the liver made simple. Radiographics. 2011 Jan-Feb;31(1):161-188.

3. Meola M, Ibeas J, Lasalle G, Petrucci I. Basics for performing a high-quality color Doppler sonography of the vascular access. J Vasc Access. 2021 Nov;22(1_suppl):18-31.

4. Berzigotti A, Piscaglia F. Ultrasound in portal hypertension--part 1. Ultraschall Med. 2011 Dec;32(6):548-568

5. Berzigotti A, Piscaglia F; EFSUMB Education and Professional Standards Committee. Ultrasound in portal hypertension--part 2--and EFSUMB recommendations for the performance and reporting of ultrasound examinations in portal hypertension. Ultraschall Med. 2012 Feb;33(1):8-32

6. Grgurevic I, Kujundzic M, Banic M, Kusec R, Bokun T, Vukelic-Markovic M, et al. Subtypes and clinical significance of common bile duct varices in portal vein thrombosis: diagnosis and follow-up by Doppler US and EUS. Abdom Radiol (NY). 2016 Mar;41(3):476-484.
7. Buscarini E, Danesino C, Olivieri C, Lupinacci G, De Grazia F, Reduzzi L, et al. Doppler ultrasonographic grading of hepatic vascular malformations in hereditary hemorrhagic telangiectasia -- results of extensive screening. Ultraschall Med. 2004 Sep;25(5):348-355.
8. Crossin JD, Muradali D, Wilson SR. US of liver transplants: normal and abnormal. Radiographics. 2003 Sep-Oct;23(5):1093-1114.
9. Dodd GD 3rd, Memel DS, Zajko AB, Baron RL, Santaguida LA. Hepatic artery stenosis and thrombosis in transplant recipients: Doppler diagnosis with resistive index and systolic acceleration time. Radiology 1994; 192(3):657-661.
10. Bolondi L, Li Bassi S, Gaiani S, Zironi G, Benzi G, Santi V, Barbara L. Liver cirrhosis: changes of Doppler waveform of hepatic veins. Radiology. 1991 Feb;178(2):513-516.
11. Kim SY, Jeong WK, Kim Y, Heo JN, Kim MY, Kim TY, Sohn JH. Changing waveform during respiration on hepatic vein Doppler sonography of severe portal hypertension: comparison with the damping index. J Ultrasound Med. 2011 Apr;30(4):455-462.
12. Kim MY, Baik SK, Park DH, Lim DW, Kim JW, Kim HS, et al. Damping index of Doppler hepatic vein waveform to assess the severity of portal hypertension and response to propranolol in liver cirrhosis: a prospective nonrandomized study. Liver Int. 2007 Oct;27(8):1103-1110.
13. Chawla Y, Kumar S, Dhiman RK, Suri S, Dilawari JB. Duplex Doppler sonography in patients with Budd-Chiari syndrome. J Gastroenterol Hepatol. 1999 Sep;14(9):904-907.
14. Sugawara Y, Yoshihisa A, Ishibashi S, Matsuda M, Yamadera Y, Ohara H, et al. Liver Congestion Assessed by Hepatic Vein Waveforms in Patients With Heart Failure. CJC Open. 2021 Feb 7;3(6):778-786.
15. Bolognesi M, Sacerdoti D, Merkel C, Gerunda G, Maffei-Faccioli A, Angeli P, et al. Splenic Doppler impedance indices: influence of different portal hemodynamic conditions. Hepatology 1996; 23(5): 1035-1040.
16. Piscaglia F, Donati G, Serra C et al. Value of splanchnic Doppler ultrasound in the diagnosis of portal hypertension. Ultrasound Med Biol 2001; 27: 893–899
17. Kim G, Cho YZ, Baik SK, Kim MY, Hong WK, Kwon SO. The accuracy of ultrasonography for the evaluation of portal hypertension in patients with cirrhosis: a systematic review. Korean J Radiol. 2015 Mar-Apr;16(2):314-324.

4.3. Quantification of liver fat and inflammation using ultrasound

Ioan Sporea, Alexandru Popa, Raluca Lupușoru

Abstract

The growing prevalence of metabolic dysfunction–associated steatotic liver disease (MASLD) has increased the need for reliable noninvasive methods for assessing hepatic steatosis and inflammatory activity. Ultrasound has become a key imaging modality, due to its wide availability, safety, and cost-effectiveness. This chapter reviews the evolution of ultrasound techniques for the quantitative assessment of liver fat and inflammation.

4.3.1. Introduction

Conventional B-mode ultrasonography remains widely used in clinical practice for the detection of steatosis through characteristic features such as increased liver echogenicity, posterior beam attenuation, and the hepato-renal index. However, the limitations of subjective interpretation have led to the development of more objective quantitative methods. Attenuation-based techniques, including the Controlled Attenuation Parameter (CAP) and Ultrasound Attenuation Parameter (UAP), provide standardized numerical estimates of hepatic fat content and have demonstrated good diagnostic performance compared with liver biopsy and MRI-PDFF.

More recently, quantitative ultrasound (QUS) technologies integrated into conventional ultrasound systems—such as attenuation imaging, backscatter analysis, and speed-of-sound estimation—have shown promising accuracy for steatosis grading and longitudinal monitoring. In addition, emerging ultrasound-derived parameters related to tissue dispersion and viscosity may offer indirect information about hepatic inflammatory activity. Although still under investigation, these multiparametric ultrasound approaches have the potential to improve noninvasive evaluation, risk stratification, and follow-up of patients with chronic liver disease.

4.3.2. Quantification of liver fat using ultrasound

Given the increasing prevalence of metabolic dysfunction-associated steatotic liver disease (MASLD), the noninvasive measurement of hepatic steatosis has emerged as a key element in the assessment of chronic liver disease. The development of ultrasound-based alternatives has been prompted by the invasive nature of liver biopsy and its limited utility for repeated

evaluation, even if it is still the gold standard for grading steatosis. Ultrasound continues to be the most accessible imaging modality for this purpose due to its widespread availability, safety, and affordability.

The evaluation of liver fat using ultrasonography has evolved over the last ten years from subjective visual interpretation to more objective and quantitative techniques. Although more recent attenuation-based and quantitative ultrasonography techniques now enable a more consistent measurement of hepatic fat content, conventional B-mode examination still plays a significant role in everyday practice. When combined, these approaches show how ultrasound has developed from a qualitative screening tool to a more thorough way of assessing and tracking liver steatosis.

For the evaluation of hepatic steatosis, ***conventional abdominal ultrasonography*** has long been recognized as a useful and accessible method. A semi-quantitative understanding of fat accumulation within the liver parenchyma is made possible by conventional sonographic signs such as a "bright liver," posterior beam attenuation, and an elevated hepato-renal index (Fig. 4.3.1). *Steatosis can be subjectively classified as mild, moderate, or severe* based on these visual characteristics. The *Hamaguchi score* is one of the most widely used structured scoring methods that have been proposed, in addition to these traditional findings. Hepato-renal contrast, liver brightness, deep attenuation, and vascular blurring—the latter of which refers to less distinct intrahepatic hepatic vein walls and relative luminal narrowing—are the four sonographic characteristics included in this score. Increased visceral adiposity and metabolic syndrome are linked to more severe ultrasonographic abnormalities in fatty liver disease, as demonstrated by Hamaguchi et al. (1).

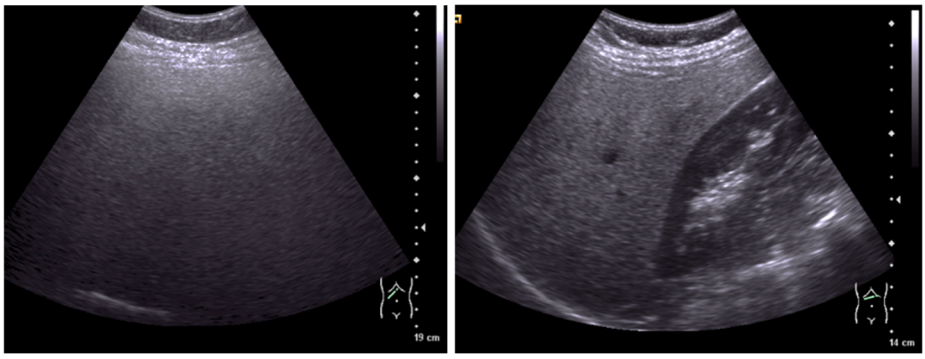


Fig. 4.3.1. Conventional ultrasound features of hepatic steatosis: "bright liver" with posterior beam attenuation (left panel) and an increased hepato-renal index (right panel).

These sonographic markers are nevertheless somewhat operator-dependent and intrinsically subjective, despite being simple to identify in routine practice. Nevertheless, a significant amount of research has demonstrated their clinical utility in identifying pertinent hepatic fat buildup. When compared to liver biopsy, conventional ultrasound showed a pooled sensitivity of 84.8% (95% CI: 79.5-88.9%) and a specificity of 93.6% (95% CI: 87.2-97.0%) for the diagnosis of moderate-to-severe steatosis in Hernaez et al.'s well-known meta-analysis, which comprised 49 studies and 4,720 people. Because moderate and severe steatosis are typically the categories with the most diagnostic and prognostic relevance, these findings help to explain why conventional ultrasonography still has significant clinical value for this purpose. However, this method has significant drawbacks, such as interobserver variability, reliance on imaging settings and equipment quality, decreased cross-center repeatability, and low precision when serial measurements are required to evaluate disease progression or regression across time (2).

More objective techniques (*quantitative methods*) for measuring liver fat have grown in significance due to the shortcomings of traditional B-mode assessment. The development of the FibroScan equipment (Echosens, Paris, France), which enables the measurement of steatosis using the Controlled Attenuation Parameter (CAP) and liver stiffness using vibration-controlled transient elastography (VCTE), was a significant advancement. CAP, which has been accessible on the FibroScan platform since 2010, measures the liver's ultrasonic attenuation, a characteristic that rises in tandem with the amount of fat in the liver. A numerical assessment of the severity of steatosis is provided by CAP values, which are given in decibels per meter (dB/m), typically falling between 100 and 400 dB/m (3).

One of the most reliable noninvasive techniques for assessing liver fat is CAP, which has been thoroughly investigated. AUROC scores for the detection and grading of steatosis were found to be between 0.82 and 0.87 in previous research comparing CAP with liver biopsy. Furthermore, AUROCs of 0.85 for ≥S1 steatosis, 0.88 for ≥S2, and 0.87 for ≥S3 were reported by Shi et al.'s meta-analysis, which combined data from 11 cohorts (4). By comparing CAP with MRI-PDFF instead of just histology, more recent data has improved the interpretation of CAP. For MRI-PDFF-defined steatosis (≥5%), the pooled sensitivity and specificity were 0.84 and 0.77, respectively, with an AUROC of 0.88; for MRI-PDFF ≥10%, the AUROC was 0.85, according to a 2024 comprehensive review and meta-analysis that included 8 studies and 1,116

patients at risk for MASLD. These findings highlight the importance of threshold tuning and context-specific interpretation, while also supporting the ongoing clinical value of CAP (5).

The cutoff values used to stage liver steatosis vary somewhat according to disease etiology and the reference standard applied. Using liver biopsy as the comparator, Eddowes et al. established one of the most commonly used sets of thresholds for MASLD patients: 294 dB/m for S1, 310 dB/m for S2, and 331 dB/m for S3 steatosis. For easy memorization, they are sometimes rounded to roughly 290, 310, and 330 dB/m in ordinary practice. The distinction between rule-in/rule-out thresholds and biopsy-based grading thresholds is highlighted by more recent MRI-PDFF-based investigations, which indicate that CAP values below around 249 dB/m may help rule out steatosis, while values above about 328 dB/m may strongly support its presence (6).

The M probe or the XL probe can be used to collect CAP; the latter is especially helpful for people who are obese. The practical question of whether distinct probe-specific thresholds are required has arisen as a result. As demonstrated by Chan et al. and corroborated by the prospective study of Eddowes et al (6, 7), the available data indicates that the same CAP cutoffs may be used for both probes, when grading hepatic steatosis.

The FibroTouch system (iLivTouch) (Fig 4.3.2), which makes use of the Ultrasound Attenuation Parameter (UAP), is another attenuation-based choice. AUROCs for diagnosing steatosis grades ≥S1, ≥S2, and S3 were 0.88, 0.93, and 0.88, respectively, in a prospective trial of 237 patients who had both FibroTouch and liver biopsy. The examination success rate was 96.5%. Values of 244, 269, and 296 dB/m were the corresponding suggested cutoffs. The use of a single probe for every patient, in conjunction with traditional ultrasound guidance prior to the quantitative assessment is a useful benefit of FibroTouch. This tool can evaluate stiffness and steatosis, much like FibroScan, and more recent iterations also seek to offer data on inflammatory activity (8).



Fig. 4.3.2. The iLivTouch system.

Quantitative ultrasound (QUS)

One of the most promising advancements in the noninvasive assessment of hepatic steatosis in recent years is quantitative ultrasonography (QUS). QUS offers objective numerical data obtained from ultrasound signal analysis, as opposed to simply visual assessment. QUS approaches can measure attenuation, backscatter, or speed of sound, depending on the manufacturer and software application. Some platforms integrate many physical parameters to enhance hepatic fat characterization. These techniques are very appealing as point-of-care tools since they are often quick, simple to use, and can be integrated straight into a standard abdominal ultrasound examination. These methods represent a significant advancement in ultrasound-based fat estimation and may be increasingly incorporated into standard hepatology practice, according to a WFUMB policy document and more recent reviews (9).

The smooth integration of QUS with conventional ultrasonography is one of its main advantages. Quantitative evaluation can frequently be carried out right away during the same examination when a traditional abdomen scan indicates fatty liver, providing an objective baseline measurement. Because numerical results can be compared over time more consistently than subjective visual impressions, this is especially helpful for longitudinal follow-up. While some methods provide fat fraction estimations in percentage values, QUS data can be expressed in dB/m, as with CAP, or in dB/cm/MHz, depending on the device. The following pictures will display different QUS varieties from different manufacturers (Fig. 4.3.3-4.3.9).

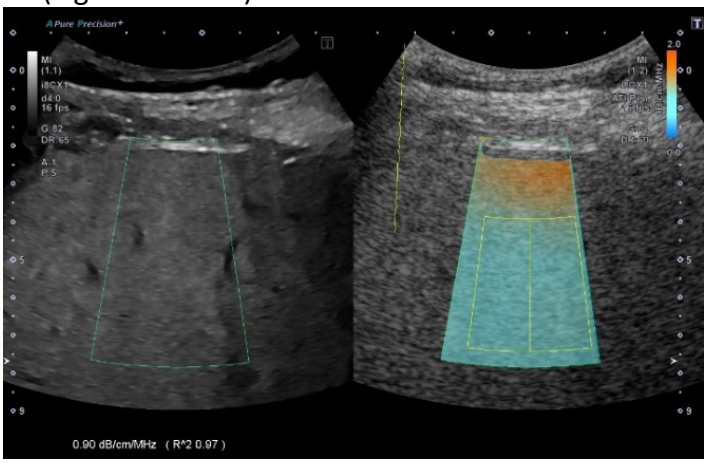


Fig. 4.3.3. ATI (Attenuation Imaging) from Canon™

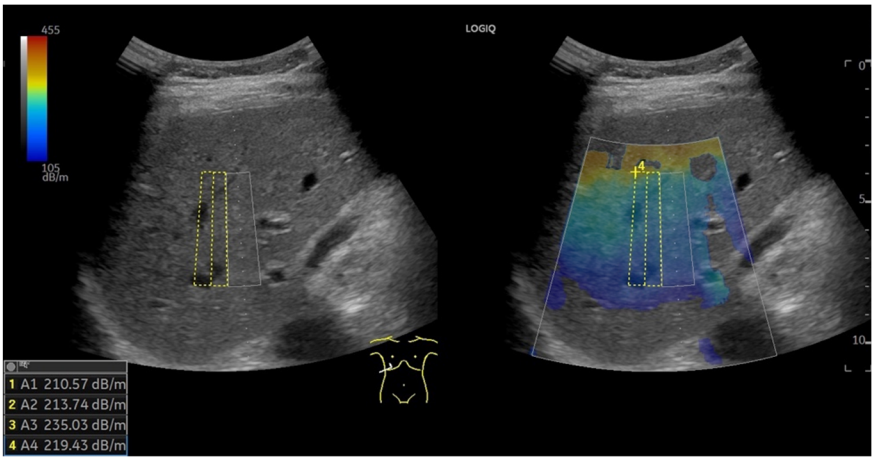


Fig. 4.3.4. UGAP (Ultrasound-Guided Attenuation Parameter) from General Electric™

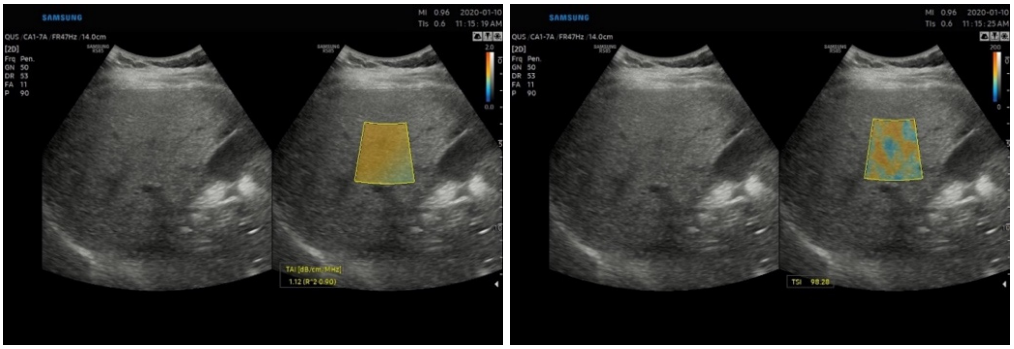


Fig. 4.3.5 TAI (Tissue Attenuation Imaging) (left panel) and TSI (Tissue Scatter distribution Imaging) (right panel) from Samsung™

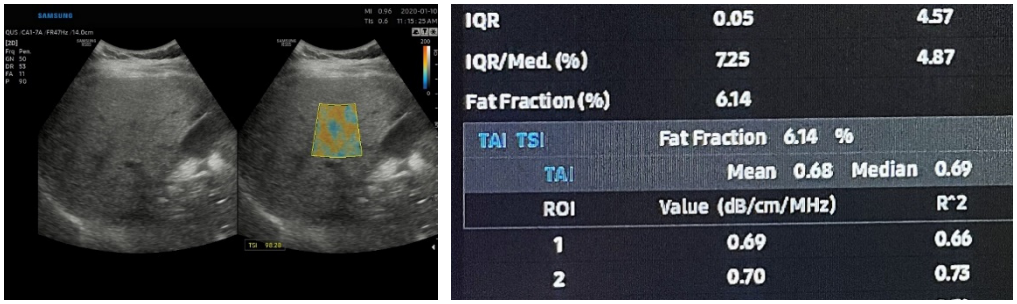


Fig. 4.3.6 Samsung™ steatosis estimation in % by means of TAI/TSI

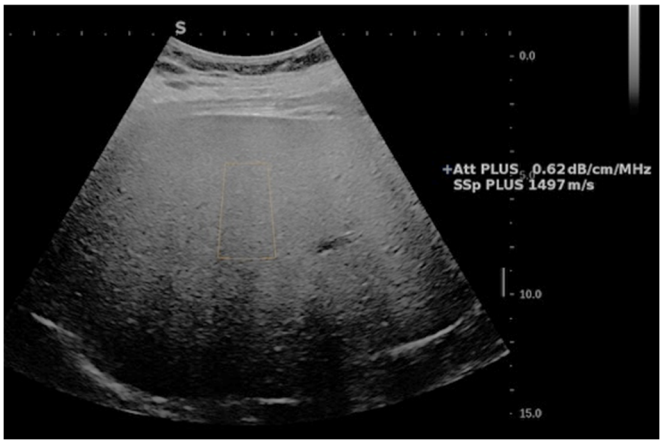


Fig. 4.3.7. Speed of Sound estimation (Att Plus and SSp Plus) from Aixplorer (Hologic™)

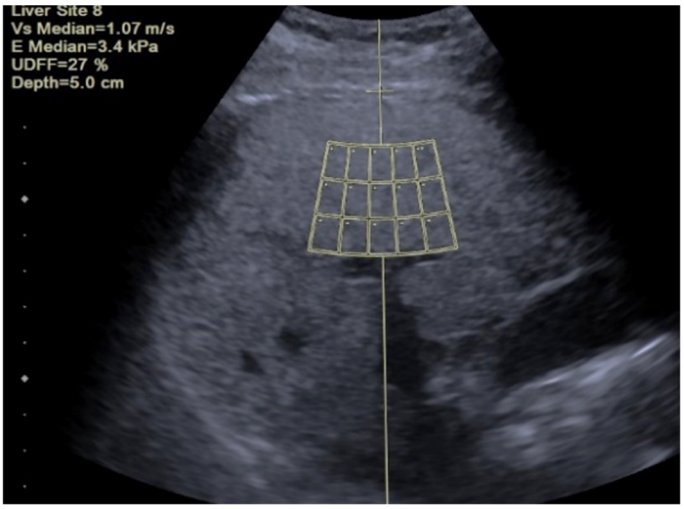


Fig. 4.3.8. UDFF (Ultrasound Derived Fat Fraction) from Siemens™: this method expresses fatty infiltration as a percentage.

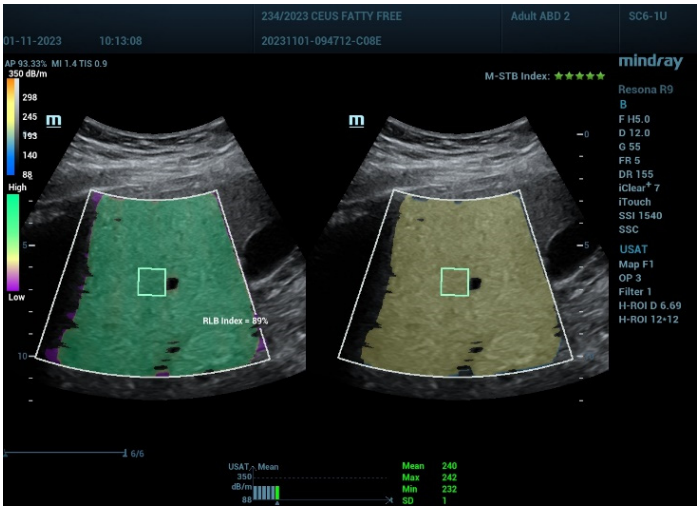


Fig. 4.3.9. USAT (UltraSound Attenuation Analysis) from Mindray™

Studies employing either liver biopsy or MRI-PDFF as the reference standard have verified the performance of these QUS approaches, and the growing body of evidence has made them more appealing for both first-line evaluation and follow-up in patients with MASLD. In fact, attenuation coefficient-based ultrasound techniques demonstrated diagnostic performance comparable to MRI-PDFF and superior to CAP for moderate and

severe steatosis, according to a recent meta-analysis comparing imaging tools for steatosis grading. This finding supports the idea that QUS is no longer only investigational but is becoming clinically relevant in routine practice (10).

Ferraioli et al. used MRI-PDFF as the reference to assess 114 people at risk for steatosis and 15 healthy controls for ATI. Compared to CAP, ATI had a stronger correlation (r=0.81 vs. r=0.65) with MRI-PDFF, indicating better quantitative performance. ATI demonstrated AUROCs ranging from 0.84 to 0.93 for steatosis grading in a different study by Bae et al. based on liver histology in 108 patients (10). More recently, an ultrasound-based steatosis grading system employing 2D-attenuation imaging was proposed by an individual-patient-data meta-analysis with external validation, which strengthened the evidence base for ATI-derived approaches and brought the field closer to more standardized deployment (11).

Fujiwara et al. examined 163 individuals with chronic liver disease who concurrently underwent liver biopsy, CAP, and UGAP. In that group, UGAP outperformed CAP with reported AUROCs of 0.900 for >S1, 0.953 for >S2, and 0.959 for S3 steatosis (12). Imajo et al. observed a substantial association between UGAP and MRI-PDFF, with an intraclass correlation coefficient of 0.768, in a different multicenter Japanese study, with 1,010 patients from six liver centers. Again, demonstrating the method's resilience, the AUROCs stayed high for differentiating steatosis grades. Although more extensive multicenter standardization is still desired, more recent real-world evidence from 2024 further supports the diagnostic use of UGAP in clinical practice (13).

Jeon et al. assessed 120 patients with clinically suspected NAFLD for the Samsung platform and compared MRI-PDFF with two QUS-derived parameters: scatter-based assessment from Tissue Scatter Distribution Imaging (TSI) and attenuation coefficient from Tissue Attenuation Imaging (TAI). With correlation coefficients of 0.659 for TAI and 0.727 for TSI, both measures showed a substantial association with MRI-PDFF. The AUROCs for TAI and TSI were 0.861 and 0.835, respectively, when utilizing MRI-PDFF thresholds of ≥5% and ≥10% hepatic fat, while TSI performed even better, with AUROCs of 0.964 and 0.935. These results demonstrate the great potential of QUS techniques based on attenuation and backscatter for noninvasive liver fat measurement (14).

Results from direct comparisons between QUS and CAP have also been instructive. In a study with 123 individuals, Jung et al. found that when MRI-PDFF was utilized as the reference standard, QUS achieved a considerably higher AUROC than CAP for the diagnosis of fatty liver disease (0.92 vs. 0.79,

p=0.03). This pattern is in line with more recent assessments that show a number of QUS algorithms integrated into traditional ultrasound equipment have diagnostic accuracy that is at least on par with, and sometimes even superior to CAP (15).

In general, the body of research on QUS in MASLD is growing quickly. Strong agreement with histology and, increasingly, with MRI-PDFF is consistently shown by current research. However, the discipline is still developing, especially in terms of defining globally recognized cutoff values for each vendor-specific platform, reproducibility standards, and standardized acquisition techniques. However, the evidence clearly shows that QUS has developed into a very promising and increasingly validated approach for the objective assessment of liver steatosis, with significant potential for routine use in risk stratification, screening, and long-term monitoring (16).

4.3.3. Quantification of Liver Inflammation Using Ultrasound

The degree of necroinflammatory activity, which contributes to continuous hepatocellular damage, fibrogenesis, and disease progression, is as important to the prognosis of chronic diffuse liver disorders as the stage of fibrosis (17). This is true for a wide range of etiologies, such as viral hepatitis, alcohol-related liver disease, autoimmune liver disorders, metabolic dysfunction-associated steatotic liver disease (MASLD), and other chronic hepatopathies. Even while liver biopsy is still the gold standard for evaluating inflammatory activity and related histological alterations, large-scale screening and recurrent follow-up are not appropriate due to its invasive nature, sampling variability, and limited feasibility. As a result, more focus has been placed on ultrasound-based methods that can record tissue viscoelastic characteristics that might indicate inflammatory alterations in the liver parenchyma.

From a clinical standpoint, non-invasive measurement of inflammation would supplement the well-established ultrasound-based assessment of fibrosis and steatosis. Such a strategy would enhance risk assessment, facilitate long-term monitoring, and possibly lessen the necessity for liver biopsies in certain patients. Specifically, the creation of a true multiparametric ultrasound (MPUS) framework for chronic liver illness would benefit from the capacity to evaluate inflammation, in addition to fat content and stiffness, during the same test. However, only a small number of manufacturers and studies have

investigated specific ultrasound-derived parameters for this purpose, and inflammation is currently the least validated of the three categories.

Patients with fatty liver disease provide the majority of the evidence that is currently accessible. Gao F et al. assessed radiofrequency (RF) and raw-data features in 259 patients with biopsy-proven NAFLD using the VCTE-based iLivTouch platform. They found two parameters that were merged into a quantitative ultrasound score. With an AUROC of 0.798 (95% CI 0.731–0.865) in the training set and 0.816 (95% CI 0.725–0.906) in the validation cohort, this score demonstrated a reasonable capacity to distinguish steatohepatitis (18). This work demonstrates the more general idea that ultrasound signal analysis may offer indirect information on inflammatory liver injury, albeit being generated from a cohort with MASLD.

In addition to VCTE-type systems, a number of studies have examined metrics related to inflammation derived from 2D Shear-Wave elastography (2D-SWE) platforms. Sugimoto et al. evaluated 2D-SWE-derived metrics, such as dispersion slope, attenuation coefficient, and shear-wave speed, for the characterization of inflammation, steatosis, fibrosis, and steatohepatitis in 120 patients having liver biopsies for suspected fatty liver disease. With AUCs of 0.95 for mild (A1), 0.81 for moderate (A2), and 0.85 for marked (A3) inflammation, dispersion slope excelled in evaluating lobular inflammation. In the same study, liver stiffness demonstrated AUROCs of 0.88 for F2, 0.90 for F3, and 0.95 for F4 fibrosis, whereas the attenuation coefficient obtained AUROCs of 0.88 for S1, 0.86 for S2, and 0.79 for S3 steatosis. The AUC for diagnosing steatohepatitis was 0.81 when dispersion slope, attenuation coefficient, and SWE were combined (19). These results lend credence to the hypothesis that dispersion-related metrics, in addition to traditional stiffness evaluation, may provide information on inflammatory activity.

Similarly, 102 individuals with fatty liver disease verified by biopsy had their shear-wave dispersion slope (SWDS), measured in (m/s)/kHz, assessed by Lee DH et al. (20). With AUROCs of 0.89, 0.85, and 0.78, respectively, SWDS detected lobular inflammatory activity in grades 1 through 3, demonstrating the best performance for mild inflammatory activity. The results are of broader relevance because they imply that shear-wave dispersion may represent tissue viscosity changes linked to inflammation, a process that may also be important in other chronic diffuse hepatopathies, even if they are once again restricted to a fatty liver cohort.

More recently, Jang JK et al. (21) assessed a multiparametric ultrasound approach that included liver stiffness, dispersion slope (DS) from 2D-SWE, and attenuation coefficient (AC) from ATI in prospective multicenter research involving 132 patients with biopsy-confirmed fatty liver disease. With an AUROC of 0.94 (95% CI 0.89–0.98; $p<0.05$), their straightforward score based on AC and DS demonstrated excellent diagnostic performance for steatohepatitis. Although this model was created for steatotic liver disease, it supports the idea that non-invasive disease evaluation may be improved by combining inflammation-sensitive measures with steatosis and fibrosis assessment.

Viscosity Plane-wave UltraSound (Vi.PLUS) has been investigated as an alternative method (Fig. 4.3.10) among 204 participants who did not get a liver biopsy. In multivariate studies,Vi. PLUS values were linked to liver stiffness and body mass index, as determined by the Aixplorer/Hologic ultrasonography instrument. The lack of histological confirmation restricts judgments on the diagnostic accuracy of viscosity measurements for liver inflammation, even if these results support technical feasibility and biological plausibility (22).

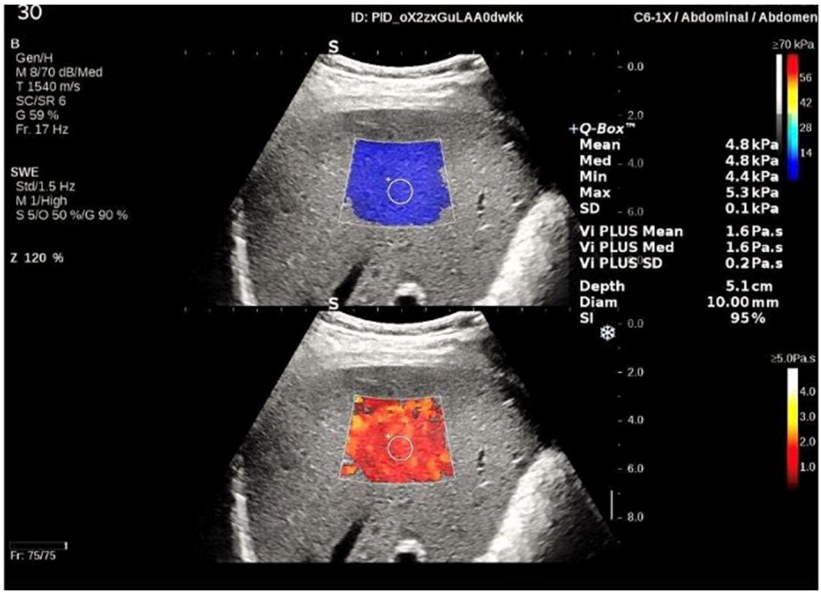


Fig. 4.3.10. *Liver viscosity assessment using Vi.PLUS integrated with 2D-SWE. The lower panel displays the viscosity map. Viscosity values are expressed in* pascal-seconds (Pa·s)*; in this example, the mean Vi.PLUS value is* 1.6 Pa·s*.*

Overall, the information that is now available indicates that components of hepatic inflammatory activity may be captured by ultrasound-derived measures relating to dispersion and viscosity. Nevertheless, the research is still mostly limited to MASLD/NAFLD groups, preliminary, and methodologically inconsistent. Their function in various chronic diffuse liver illnesses, such as autoimmune hepatitis, alcohol-related liver disease, chronic viral hepatitis, or cholestatic disorders, is still unclear and needs specific validation against histology and clinical consequences. Therefore, rather than being proven stand-alone indicators of hepatic inflammation, these methods should now be regarded as promising adjuncts (23).

In **conclusion,** ultrasound based fatty quantification is very useful for daily practice in MASLD patients. Easy to be used and with consistent results, is recommended for the accessibility and low cost. Evaluation of viscoelastic property of liver tissue with ultrasound is under research, but with some interesting results in patients with fatty liver.

References

1. Hamaguchi M, Kojima, T, Itoh Y, Harano Y, Fujii K, Nakajima T, et al. The Severity of Ultrasonographic Findings in Nonalcoholic Fatty Liver Disease Reflects the Metabolic Syndrome and Visceral Fat Accumulation. Am. J. Gastroenterol. 2007; 102: 2708–15.
2. Hernaez R, Lazo M, Bonekamp S, Kamel I, Brancati FL, Guallar E, Clark JM'. Diagnostic Accuracy and Reliability of Ultrasonography for the Detection of Fatty Liver: A Meta-Analysis. Hepatology 2011; 54: 1082–90.
3. Ferraioli G. Quantitative Assessment of Liver Steatosis Using Ultrasound Controlled Attenuation Parameter (Echosens). Journal of Medical Ultrasonics 2021; 48: 489–495.
4. Shi KQ, Tang JZ, Zhu X-L, Ying L, Li D-W, Gao J, et al. Controlled Attenuation Parameter for the Detection of Steatosis Severity in Chronic Liver Disease: A Meta-Analysis of Diagnostic Accuracy. J. Gastroenterol. Hepatol. 2014; 29: 1149–58.
5. Malandris K, Katsoula A, Liakos A, Bekiari E, Karagiannis T, Theocharidou E, et al. Accuracy of controlled attenuation parameter for liver steatosis in patients at risk for metabolic dysfunction-associated steatotic liver disease using magnetic resonance imaging: a systematic review and meta-analysis. Ann Gastroenterol. 2024 Sep-Oct;37(5):579-87.
6. Raeman R. Inflammation: The Straw That Broke the NAFLD Liver! Cell. Mol. Gastroenterol. Hepatol. 2022, 13, 1273–74.
7. Chan W-K, Nik Mustapha NR, Mahadeva S, Wong VW-S, Cheng JY-K, Wong GL-H. Can the Same Controlled Attenuation Parameter Cut-Offs Be Used for M and XL Probes for Diagnosing Hepatic Steatosis? J. Gastroenterol. Hepatol. 2018 ;33:1787–94.

8. Qu Y, Song, Y-Y, Chen C-W, Fu Q-C, Shi J-P, Xu Y, et al. Diagnostic Performance of FibroTouch Ultrasound Attenuation Parameter and Liver Stiffness Measurement in Assessing Hepatic Steatosis and Fibrosis in Patients With Nonalcoholic Fatty Liver Disease. Clin. Transl. Gastroenterol. 2021; 12: e00323.
9. Park J, Lee JM, Lee G, Jeon SK, Joo I. Quantitative Evaluation of Hepatic Steatosis Using Advanced Imaging Techniques: Focusing on New Quantitative Ultrasound Techniques. Korean J. Radiol. 2022;23:13–29.
10. Ferraioli G, Maiocchi L, Raciti MV, Tinelli C, De Silvestri A, Nichetti M, et al. Detection of Liver Steatosis With a Novel Ultrasound-Based Technique: A Pilot Study Using MRI-Derived Proton Density Fat Fraction as the Gold Standard. Clin. Transl. Gastroenterol. 2019; 10: e00081.
11. Hobeika C, Ronot M, Guiu B, Ferraioli G, Iijima H, Tada T, et al. Ultrasound-based steatosis grading system using 2D-attenuation imaging: An individual patient data meta-analysis with external validation. Hepatology 2025 Jan 1;81(1):212-27.
12. Fujiwara Y, Kuroda H, Abe T, Ishida K, Oguri T, Noguchi S, et al. The B-Mode Image-Guided Ultrasound Attenuation Parameter Accurately Detects Hepatic Steatosis in Chronic Liver Disease. Ultrasound Med. Biol. 2018; 44: 2223–32.
13. Imajo K, Toyoda H, Yasuda S, Suzuki Y, Sugimoto K, Kuroda H, et al. Utility of Ultrasound-Guided Attenuation Parameter for Grading Steatosis With Reference to MRI-PDFF in a Large Cohort. Clin. Gastroenterol. Hepatol. 2022; 20: 2533-41.e7.
14. Jeon SK, Lee JM, Joo I, Park SJ. Quantitative Ultrasound Radiofrequency Data Analysis for the Assessment of Hepatic Steatosis in Nonalcoholic Fatty Liver Disease Using Magnetic Resonance Imaging Proton Density Fat Fraction as the Reference Standard. Korean J. Radiol. 2021; 22: 1077–86.
15. Jung J, Han A, Madamba E, Bettencourt R, Loomba RR, Boehringer AS, et al. Direct Comparison of Quantitative US versus Controlled Attenuation Parameter for Liver Fat Assessment Using MRI Proton Density Fat Fraction as the Reference Standard in Patients Suspected of Having NAFLD. Radiology 2022; 304: 75–82.
16. Ferraioli G, Kumar V, Ozturk A, Nam K, de Korte CL, Barr RG. US Attenuation for Liver Fat Quantification: An AIUM-RSNA QIBA Pulse-Echo Quantitative Ultrasound Initiative. Radiology 2022; 302: 495–06.
17. Eddowes PJ, Sasso M, Allison M, Tsochatzis E, Anstee QM, Sheridan D, et al. Accuracy of FibroScan Controlled Attenuation Parameter and Liver Stiffness Measurement in Assessing Steatosis and Fibrosis in Patients With Nonalcoholic Fatty Liver Disease. Gastroenterology. 2019 May;156(6):1717-30.
18. Gao F, He Q, Li G, Huang O-Y, Tang L-J, Wang X-D, A Novel Quantitative Ultrasound Technique for Identifying Non-Alcoholic Steatohepatitis. Liver International 2022; 42: 80–91.
19. Sugimoto K, Moriyasu F, Oshiro H, Takeuchi H, Abe M, Yoshimasu Y, The Role of Multiparametric US of the Liver for the Evaluation of Nonalcoholic Steatohepatitis. Radiology 2020; 296: 532–40.

20. Lee DH, Cho EJ, Bae JS, Lee JY, Yu SJ, Kim H, et al. Accuracy of Two-Dimensional Shear Wave Elastography and Attenuation Imaging for Evaluation of Patients With Nonalcoholic Steatohepatitis. Clin. Gastroenterol. Hepatol. 2021; 19: 797-805.e7.
21. Jang JK, Lee ES, Seo JW, Kim YR, Kim SY, Cho YY, Lee DH. Two-Dimensional Shear-Wave Elastography and US Attenuation Imaging for Nonalcoholic Steatohepatitis Diagnosis: A Cross-Sectional, Multicenter Study. Radiology 2022;305:118–126.
22. Popa A, Sporea I, Bende F, Popescu A, Fofiu R, Borlea A, t al. The Non-Invasive Ultrasound-Based Assessment of Liver Viscosity in a Healthy Cohort. Diagnostics 2022; 12: 1451.
23. Barr RG. Multiparametric Ultrasound for Chronic Liver Disease. Radiol. Clin. North Am. 2025; 63: 13–28.

5. Liver elastography for diffuse liver diseases

5.1. Clinical applications—short history, indications

Roxana Şirli

Abstract

Ultrasound elastography is a noninvasive imaging method used to evaluate tissue stiffness, an important marker of liver fibrosis. The technique is based on the principle that diseased tissues become stiffer than normal ones. Two main elastographic approaches are used in clinical practice: strain elastography and shear-wave elastography. While strain elastography provides mainly qualitative information and has limited applicability in liver assessment, shear-waves elastography enables quantitative measurement of liver stiffness. Techniques such as Vibration Controlled Transient Elastography (VCTE) and ARFI-based methods (pSWE and 2D-SWE) have significantly improved the non-invasive evaluation of chronic liver diseases. Elastography is now widely validated and recommended in international guidelines for diagnosing and staging liver fibrosis and for predicting liver-related complications.

5.1.1. Introduction

Elasticity is an inherent characteristic of all materials, including tissues, to undergo deformation when subjected to an external force. The greater the elasticity of a tissue, the more it will deform; conversely, the stiffer the tissue (less elastic), the less it will deform to a stimulus of equivalent intensity. Palpation, a crucial component of clinical examination, is the most ancient technique for evaluating tissue elasticity. Certain diseases, such as malignant tumors and fibrotic tissue accumulation, result in increased tissue stiffness, whereas others, including inflammation and edema, cause a reduction in stiffness.

Elastography is a medical imaging modality that quantifies tissue stiffness (elasticity), with the names “elasticity” and “stiffness” serving as antonyms. Elastography has demonstrated its utility in the diagnosis and monitoring of several medical illnesses, particularly in chronic liver diseases, as well as in thyroid, breast, prostate, and vascular pathologies. It was derived from the correlation between the elastic characteristics of tissues and specific disorders.

The quantification of tissue deformation caused by an external stimulus can be made either parallel to the stimulus application (*strain elastography*) or perpendicular to it by evaluating the velocity of the shear waves produced within the tissue (*shear-wave elastography*).

The formula for estimating elasticity was developed in the seventeenth century, namely Hooke's law (1678) (1). It applies to solid structures exhibiting linear deformation. Tissue elasticity contrasts with that of solids, since it is a viscoelastic medium, impacted by elements outside the intensity of the stimulus, including the direction of stimulus delivery and the viscoelastic properties of the tissue. Nevertheless, a reasonably precise estimation of the tissues' elastic characteristics can be achieved using elastic moduli (1), as will be elucidated in the chapter about the technical aspects of elastography.

The initial investigations into the elasticity of viscoelastic materials commenced in 1951, when a mathematical model was constructed to predict the behavior of a sphere vibrating within a viscoelastic medium (2). Subsequently, utilizing a strobe, members of the same group quantified the velocity of thigh surface deformation induced by the vibration of a piston applied to the skin (3). This research served as the foundation for the creation of elastographic techniques employed to evaluate the elasticity of living tissues, utilizing either nuclear magnetic resonance or ultrasound.

5.1.2. Strain Elastography (SE)

The initial application of strain elastography (SE) was documented by Eisensher et al. in 1983, utilizing M-mode ultrasonography to monitor low-frequency (1.5 Hz) vibration-induced tissue displacement in breast and liver tissues, therefore successfully distinguishing benign tumors from malignant ones (4).

In the early 1990s, SE techniques were developed and integrated into standard ultrasound systems, utilizing light manual compression with the transducer as the stimulus for tissue deformation (5). In the mid-1990s, BB Golberg’s team established the initial clinical uses of SE for the assessment of breast nodules (6).

Since the mid-2000s, SE has demonstrated efficacy in the location and characterization of prostate nodules (7), as well as in guiding prostate puncture for prostate cancer diagnosis (8). During this period, SE was also utilized for the assessment of thyroid nodules (9).

Strain elastography is rarely used in liver evaluation because the deformation stimulus inadequately penetrates the liver, while the generated elastogram cannot yield numerical findings, rendering it solely a qualitative tool. Contemporary ultrasound devices utilize cardiac and respiratory motions or an acoustic impulse as stimuli for tissue deformation (10).

5.1.3. Shear-wave elastography (SWE)

Shear-wave elastography (SWE) measures the velocity of shear waves induced in tissues perpendicularly to the direction of the applied stimulus. SWE approaches are classified based on the mechanism of tissue stimulation and the approach employed to assess shear wave velocity as follows (10):

- Vibration Controlled Transient Elastography (VCTE), formerly referred to as Transient Elastography (TE), utilizes a mechanical impulse produced by a vibrator as the stimulus.
- SWE methodologies utilizing ARFI (Acoustic Radiation Force Impulse), wherein the stimulus is an acoustic pulse produced by the transducer.

a) Vibration-Controlled Transient Elastography (VCTE)

In the early 2000s, Laurent Sandrin and his team pioneered the technology of transient elastography, later called VCTE, creating a device known as FibroScan™ (Echosens, Paris, France) (11). A specialized transducer, affixed to the shaft of a vibrator, quantifies the velocity of the shear waves produced in the liver by the mechanical shock delivered by the vibrator. The value observed in m/s, indicative of liver stiffness, is automatically translated to kiloPascals (kPa) using the Young's modulus. VCTE was a significant advancement in the noninvasive assessment of liver fibrosis, now serving as one of the standard methodologies for evaluating chronic liver disorders (12-15).

It was observed that obesity constitutes a significant barrier to accurate liver stiffness measures using VCTE, particularly in individuals with a body mass index exceeding 40 kg/m², where the measurement failure rate reaches 88% (16). To mitigate this limitation, the XL probe was introduced in 2010, which yields valid data in around 60-80% of individuals who experienced unsuccessful readings with the M probe (17, 18). Simultaneously, the S probe was approved for pediatric application (19).

Numerous studies have been published over the years regarding the efficacy of VCTE in evaluating the severity of liver fibrosis in chronic liver

diseases, with meta-analyses confirming the method's value in both mixed patient cohorts (20-23) and specific pathologies, including chronic viral hepatitis (24, 25), alcohol-induced liver disease (26), metabolic dysfunction-associated steatotic liver disease (MASLD) (27), as well as rarer conditions such as cholestatic liver diseases (28), alpha-1 antitrypsin deficiency (29), liver damage in cystic fibrosis (30), and autoimmune liver disease (31). Furthermore, VCTE has demonstrated its efficacy as a predictor of portal hypertension (32, 33), hepatic mortality (34), and the incidence of hepatocellular carcinoma (35).

In 2011, Horia Ștefănescu published the inaugural study assessing the efficacy of VCTE in the spleen for predicting esophageal varices (36). This study employed specialized software that extends the measuring range, thus providing a novel perspective on the application of VCTE.

Considering the significant prevalence of steatotic liver disease and its correlation with fibrosis, the manufacturers of the FibroScan device have created an application specifically for quantifying steatosis, known as the Controlled Attenuation Parameter (CAP), which is integrated into the same apparatus, available on both the M probe since 2010 (37) and the XL probe since 2015 (38).

b) SWE techniques utilizing ARFI (Acoustic Radiation Force Impulse) technology

In all ARFI-based SWE approaches, the stimulus inducing tissue deformation is an acoustic impulse focused at a specific depth, which produces shear waves that propagate away from the application site. The ARFI-based SWE techniques used for measuring the shear velocity are classified as follows (10):

● ***Point shear wave elastography (pSWE)*** - a technique where the acoustic impulse is focused at a specific point, and the velocity of shear waves is quantified in a designated area, expressed in m/s, which can be converted to kPa.

● ***2D-SWE and 3D-SWE (real-time SWE)*** involve tissue stimulation at several locations using sonic impulses, followed by the measurement of shear waves velocity over a larger area. This form of elastography was made possible by advancements in ultrasound technology, yielding results that include both a numerical value (expressed in m/s or kPa) and an elastogram, a color-coded image overlaying the grayscale ultrasound image.

The ARFI approach, established in 1998 by Sarvazyan et al. (39), utilized an acoustic pulse to induce tissue deformation (shear waves), with the

propagation speed determined via ultrasonography. The primary benefit of this technology is that it necessitates no additional equipment (unlike FibroScan™), provided that the ARFI pulse and B-mode ultrasound for measuring shear wave velocity are incorporated within the same transducer. In the early 2000s, publications regarding the in vitro and in vivo applications of the ARFI approach commenced (40).

In 2007, Siemens developed the inaugural commercial implementation of the ***pSWE technology***, known as Virtual Touch Quantification - VTQ™. This was succeeded by the release of multiple articles corroborating this approach in comparison to liver biopsy and VCTE (41-43). At present, VTQ is accepted by international guidelines as a technique for evaluating liver fibrosis (13-15, 44). Subsequently, p-SWE techniques have been introduced on several platforms, Philips' ElastPQ™ approach being the most extensively described (45, 46).

Technological advancements have enabled the development of ***real-time SWE (2D-SWE and 3D-SWE***) where tissue stimulation occurs at multiple places in fast succession, rather than solely at a single spot as in p-SWE using ARFI. The velocity of shear waves produced by several ARFI pulses can be measured using ultrasonography transducers with an exceptionally high scan rate, approximately 10 pictures per second. This technology was introduced in 2004 (47) and served as the foundation for the advancement of 2D-SWE real-time elastography, subsequently incorporated into Supersonic Imagine's Aixplorer™ system. This method has clinical uses in assessing liver fibrosis (48-50), breast nodules (51), thyroid pathology, and prostate pathology, among others.

Subsequently, 2D-SWE was introduced on other platforms, including General Electric, Samsung, Canon, and Toshiba, with differing techniques employed among manufacturers to create the acoustic pulses and quantify shear wave velocity.

The following years witnessed several clinical validation trials of 2D-SWE techniques, juxtaposed with biopsies and alternative elastographic methods, for assessing liver fibrosis and pathologies of the thyroid, breast, and prostate, among others. They established that 2D-SWE elastographic techniques are effective approaches with high feasibility, now incorporated into worldwide guidelines (13-15, 44).

References

1. Ormachea J, Parker KJ. Elastography imaging: the 30-year perspective. Phys Med Biol. 2020; 65(24).
2. Helmholtz-Laplace O. Field and Impedance of an Oscillating Sphere in a Viscoelastic Medium with an Application to Biophysics. J Acoust Soc Am. 1951; 23:707–14.
3. Gierke HE, Oestreicher HL, Franke EK, Parrack HO, Wittern WW. Physics of vibrations in living tissues. J Appl Physiol. 1952; 4(12):886-900.
4. Eisensher A S-TE, Pelletier G, Jacquemard G. Rhythmic ultrasound palpation-echosismography. J Radiol. 1983; 64:225–61.
5. Ophir J, Cespedes I, Ponnekanti H, Yazdi Y, Li X. Elastography: a quantitative method for imaging the elasticity of biological tissues. Ultrasound Imaging. 1991; 13(2):111-34.
6. Shankar PM, Molthen R, Narayanan VM, Reid JM, Genis V, Forsberg F, et al. Studies on the use of non-Rayleigh statistics for ultrasonic tissue characterization. Ultrasound Med Biol. 1996; 22(7):873-82.
7. Taylor LS, Porter BC, Nadasdy G, di Sant'Agnese PA, Pasternack D, Wu Z, et al. Three-dimensional registration of prostate images from histology and ultrasound. Ultrasound Med Biol. 2004; 30(2):161-8.
8. König K, Scheipers U, Pesavento A, Lorenz A, Ermert H, Senge T. Initial experiences with real-time elastography guided biopsies of the prostate. J Urol. 2005; 174(1):115-7.
9. Rago T, Di Coscio G, Basolo F, Scutari M, Elisei R, Berti P, et al. Combined clinical, thyroid ultrasound and cytological features help to predict thyroid malignancy in follicular and Hupsilonrthle cell thyroid lesions: results from a series of 505 consecutive patients. Clin Endocrinol (Oxf). 2007; 66(1):13-20.
10. Shiina T, Nightingale KR, Palmeri ML, Hall TJ, Bamber JC, Barr RG, et al. WFUMB guidelines and recommendations for clinical use of ultrasound elastography: Part 1: basic principles and terminology. Ultrasound Med Biol. 2015; 41(5):1126-47.
11. Sandrin L, Fourquet B, Hasquenoph JM, Yon S, Fournier C, Mal F, et al. Transient elastography: a new noninvasive method for assessment of hepatic fibrosis. Ultrasound Med Biol. 2003; 29(12):1705-13.
12. European Association for Study of Liver. Asociación Latinoamericana para el Estudio del Higado. EASL-ALEH Clinical Practice Guidelines: Non-invasive tests for evaluation of liver disease severity and prognosis. J Hepatol. 2015; 63(1):237-64.
13. European Association for the Study of the Liver. Clinical Practice Guideline on non-invasive tests for evaluation of liver disease severity and prognosis - 2021 update. J Hepatol. 2021; 75(3):659-89.
14. Ferraioli G, Filice C, Castera L, Choi BI, Sporea I, Wilson SR, et al. WFUMB guidelines and recommendations for clinical use of ultrasound elastography: Part 3: liver. Ultrasound Med Biol. 2015; 41(5):1161-79.

15. Ferraioli G, Wong VW, Castera L, Berzigotti A, Sporea I, Dietrich CF, et al. Liver Ultrasound Elastography: An Update to the World Federation for Ultrasound in Medicine and Biology Guidelines and Recommendations. Ultrasound Med Biol. 2018; 44(12):2419-40.
16. Roulot D, Czernichow S, Le Clesiau H, Costes JL, Vergnaud AC, Beaugrand M. Liver stiffness values in apparently healthy subjects: influence of gender and metabolic syndrome. J Hepatol. 2008; 48(4):606-13.
17. de Ledinghen V, Vergniol J, Foucher J, El-Hajbi F, Merrouche W, Rigalleau V. Feasibility of liver transient elastography with FibroScan using a new probe for obese patients. Liver Int. 2010; 30(7):1043-8.
18. Sporea I, Sirli R, Mare R, Popescu A, Ivascu SC. Feasibility of Transient Elastography with M and XL probes in real life. Med Ultrasound. 2016; 18(1):7-10.
19. de Ledinghen V, Le Bail B, Rebouissoux L, Fournier C, Foucher J, Miette V, et al. Liver stiffness measurement in children using FibroScan: feasibility study and comparison with Fibrotest, aspartate transaminase to platelets ratio index, and liver biopsy. J Pediatr Gastroenterol Nutr. 2007; 45(4):443-50.
20. Friedrich-Rust M, Ong MF, Martens S, Sarrazin C, Bojunga J, Zeuzem S, Herrmann E. Performance of transient elastography for the staging of liver fibrosis: a meta-analysis. Gastroenterology. 2008; 134(4):960-74.
21. Stebbing J, Farouk L, Panos G, Anderson M, Jiao LR, Mandalia S, et al. A meta-analysis of transient elastography for the detection of hepatic fibrosis. J Clin Gastroenterol. 2010; 44(3):214-9.
22. Talwalkar JA, Kurtz DM, Schoenleber SJ, West CP, Montori VM. Ultrasound-based transient elastography for the detection of hepatic fibrosis: systematic review and meta-analysis. Clin Gastroenterol Hepatol. 2007; 5(10):1214-20.
23. Tsochatzis EA, Gurusamy KS, Ntaoula S, Cholongitas E, Davidson BR, Burroughs AK. Elastography for the diagnosis of severity of fibrosis in chronic liver disease: a meta-analysis of diagnostic accuracy. J Hepatol. 2011; 54(4):650-9.
24. Houot M, Ngo Y, Munteanu M, Marque S, Poynard T. Systematic review with meta-analysis: direct comparisons of biomarkers for the diagnosis of fibrosis in chronic hepatitis C and B. Aliment Pharmacol Ther. 2016; 43(1):16-29.
25. Li Y, Huang YS, Wang ZZ, Yang ZR, Sun F, Zhan SY, et al. Systematic review with meta-analysis: the diagnostic accuracy of transient elastography for the staging of liver fibrosis in patients with chronic hepatitis B. Aliment Pharmacol Ther. 2016; 43(4):458-69.
26. Pavlov CS, Casazza G, Nikolova D, Tsochatzis E, Gluud C. Systematic review with meta-analysis: diagnostic accuracy of transient elastography for staging of fibrosis in people with alcoholic liver disease. Pharmacol Ther Food. 2016; 43(5):575-85.
27. Mozes FE, Lee JA, Selvaraj EA, Jayaswal ANA, Trauner M, J Fellow, et al. Diagnostic accuracy of non-invasive tests for advanced fibrosis in patients with NAFLD: an individual patient data meta-analysis. Gut. 2022; 71(5):1006-19.

28. Manzo-Francisco LA, Aquino-Matus J, Vidana-Perez D, Uribe M, Chavez-Tapia N. Systematic review and meta-analysis: Transient elastography compared to liver biopsy for staging of liver fibrosis in primary biliary cholangitis. Ann Hepatol. 2023; 28(4):101107.
29. Huang DQ, Chan KE, Tan C, Zeng RW, Koh B, Ong EYH, et al. Meta-analysis: Prevalence of significant or advanced fibrosis in adults with alpha-1-antitrypsin deficiency. Pharmacol Ther Food. 2023; 58(2):152-8.
30. Martonosi AR, Soos A, Rumbus Z, Hegyi P, Izsak V, Pazmany P, et al. Non-invasive Diagnostic Tests in Cystic Fibrosis-Related Liver Disease: A Diagnostic Test Accuracy Network Meta-Analysis. Front Med (Lausanne). 2021;8:598382.
31. Chen H, Shen Y, Wu SD, Zhu Q, Weng CZ, Zhang J, et al. Diagnostic role of transient elastography in patients with autoimmune liver diseases: A systematic review and meta-analysis. World J Gastroenterol. 2023; 29(39):5503-25.
32. Kim G, Kim MY, Baik SK. Transient elastography versus hepatic venous pressure gradient for diagnosing portal hypertension: a systematic review and meta-analysis. Clin Mol Hepatol. 2017; 23(1):34-41.
33. Shi KQ, Fan YC, Pan ZZ, Lin XF, Liu WY, Chen YP, Zheng MH. Transient elastography: a meta-analysis of diagnostic accuracy in evaluation of portal hypertension in chronic liver disease. Liver Int. 2013; 33(1):62-71.
34. Wang J, Li J, Zhou Q, Zhang D, Bi Q, Wu Y, Huang W. Liver stiffness measurement predicted liver-related events and all-cause mortality: A systematic review and nonlinear dose-response meta-analysis. Common hepatol. 2018; 2(4):467-76.
35. Kim DY, Song KJ, Kim SU, Yoo EJ, Park JY, Ahn SH, Han KH. Transient elastography-based risk estimation of hepatitis B virus-related occurrence of hepatocellular carcinoma: development and validation of a predictive model. Onco Targets Ther. 2013;6:1463-9.
36. Stefanescu H, Grigorescu M, Lupsor M, Procopet B, Maniu A, Badea R. Spleen stiffness measurement using Fibroscan for the noninvasive assessment of esophageal varices in liver cirrhosis patients. J Gastroenterol Hepatol. 2011; 26(1):164-70.
37. Sasso M, Beaugrand M, de Ledinghen V, Douvin C, Marcellin P, Poupon R, et al. Controlled attenuation parameter (CAP): a novel VCTE guided ultrasonic attenuation measurement for the evaluation of hepatic steatosis: preliminary study and validation in a cohort of patients with chronic liver disease from various causes. Ultrasound Med Biol. 2010; 36(11):1825-35.
38. Sasso M, Audiere S, Kemgang A, Gaouar F, Corpechot C, Chazouilleres O, et al. Liver Steatosis Assessed by Controlled Attenuation Parameter (CAP) Measured with the XL Probe of the FibroScan: A Pilot Study Assessing Diagnostic Accuracy. Ultrasound Med Biol. 2016; 42(1):92-103.
39. Sarvazyan AP, Rudenko OV, Swanson SD, Fowlkes JB, Emelianov SY. Shear wave elasticity imaging: a new ultrasonic technology of medical diagnostics. Ultrasound Med Biol. 1998; 24(9):1419-35.

40. Nightingale K, McAleavey S, Trahey G. Shear-wave generation using acoustic radiation force: in vivo and ex vivo results. Ultrasound Med Biol. 2003; 29(12):1715-23.
41. Bota S, Herkner H, Sporea I, Salzl P, Sirli R, Neghina AM, Peck-Radosavljevic M. Meta-analysis: ARFI elastography versus transient elastography for the evaluation of liver fibrosis. Liver Int. 2013; 33(8):1138-47.
42. Friedrich-Rust M, Nierhoff J, Lupsor M, Sporea I, Fierbinteanu-Braticevici C, Strobel D, et al. Performance of Acoustic Radiation Force Impulse imaging for the staging of liver fibrosis: a pooled meta-analysis. J Viral Hepat. 2012; 19(2):E212-9.
43. Sporea I, Sirli RL, Deleanu A, Popescu A, Focsa M, Danila M, Tudora A. Acoustic radiation force impulse elastography as compared to transient elastography and liver biopsy in patients with chronic hepatopathies. Ultraschall Med. 2011; 32 Suppl 1:S46-52.
44. Barr RG, Wilson SR, Rubens D, Garcia-Tsao G, Ferraioli G. Update to the Society of Radiologists in Ultrasound Liver Elastography Consensus Statement. Radiology. 2020; 296(2):263-274.
45. Sporea I, Bota S, Gradinaru-Tascau O, Sirli R, Popescu A. Comparative study between two point Shear Wave Elastographic techniques: Acoustic Radiation Force Impulse (ARFI) elastography and ElastPQ. Med Ultrasound. 2014; 16(4):309-14.
46. Ma JJ, Ding H, Mao F, Sun HC, Xu C, Wang WP. Assessment of liver fibrosis with elastography point quantification technique in chronic hepatitis B virus patients: a comparison with liver pathological results. J Gastroenterol Hepatol. 2014; 29(4):814-9.
47. Bercoff J, Tanter M, Fink M. Supersonic shear imaging: a new technique for soft tissue elasticity mapping. IEEE Trans Ultrasonic Ferroelectr Freq Control. 2004; 51(4):396-409.
48. Bota S, Paternostro R, Etschmaier A, Schwarzer R, Salzl P, Mandorfer M, et al. Performance of 2-D shear wave elastography in liver fibrosis assessment compared with serologic tests and transient elastography in clinical routine. Ultrasound Med Biol. 2015; 41(9):2340-9.
49. Ferraioli G, Tinelli C, Dal Bello B, Zicchetti M, Filice G, Filice C, Liver Fibrosis Study G. Accuracy of real-time shear wave elastography for assessing liver fibrosis in chronic hepatitis C: a pilot study. Hepatology. 2012; 56(6):2125-33.
50. Herrmann E, de Ledinghen V, Cassinotto C, Chu WC, Leung VY, Ferraioli G, et al. Assessment of biopsy-proven liver fibrosis by two-dimensional shear wave elastography: An individual patient data-based meta-analysis. Hepatology. 2018; 67(1):260-72.
51. Evans A, Whelehan P, Thomson K, McLean D, Brauer K, Purdie C, et al. Quantitative shear wave ultrasound elastography: initial experience in solid breast masses. Breast Cancer Res. 2010; 12(6):R104.

5.2. Classification of elastographic methods and techniques

Felix Bende, Tudor Moga

Abstract

Liver elastography is a key noninvasive tool for evaluating diffuse liver diseases, particularly for staging fibrosis and assessing the risk of advanced chronic liver disease. Ultrasound-based elastography techniques are classified into strain elastography and shear wave elastography (SWE), according to the type of mechanical excitation and the physical parameter measured.

Strain elastography provides qualitative or semi-quantitative information based on tissue deformation and has limited value in diffuse liver disease. In contrast, SWE techniques—including vibration-controlled transient elastography (VCTE), point shear wave elastography (pSWE), and two-dimensional shear wave elastography (2D-SWE)—generate and track shear waves to provide quantitative measurements of liver stiffness expressed in m/s or kPa. Current WFUMB and EFSUMB guidelines recommend shear wave-based methods as first-line approaches for non-invasive fibrosis assessment, provided that standardized examination protocols, quality criteria, and potential confounding factors are carefully considered.

5.2.1. Introduction

Liver elastography has become an integral component in the noninvasive evaluation of diffuse liver diseases, particularly for the assessment of fibrosis and, more recently, steatosis and portal hypertension. According to the most recent guidelines issued by the World Federation for Ultrasound in Medicine and Biology (WFUMB) and the European Federation of Societies for Ultrasound in Medicine and Biology (EFSUMB), ultrasound-based elastography techniques can be classified based on the physical principle of excitation, the type of mechanical parameter measured, and the mode of image display (1–4).

Ultrasound elastography methods are broadly ***divided into***:

1. **Strain (deformation) elastography**
2. **Shear wave elastography (SWE)**

This classification reflects the type of mechanical stimulus applied and the way tissue response is quantified (3).

Strain elastography relies on quasi-static compression (external or physiological), whereas shear wave elastography is based on the generation and

tracking of dynamically induced shear waves, allowing quantitative assessment of tissue stiffness (4, 5).

From a technical perspective, elastography techniques may also be classified according to:

- The source of excitation (mechanical surface vibration vs. acoustic radiation force impulse – ARFI)
- The dimensionality of measurement (point measurement vs. two-dimensional or volumetric imaging)
- The physical parameter displayed (strain, shear wave velocity in m/s, or Young's modulus in kPa)

In diffuse liver diseases, shear wave-based methods are recommended for routine clinical practice due to their reproducibility, standardization, and quantitative output (1, 3).

5.2.2. Strain elastography

Strain elastography evaluates tissue deformation induced by external compression or internal physiological motion. The resulting strain map reflects relative tissue stiffness, displayed as a qualitative or semi-quantitative color-coded image superimposed on B-mode ultrasound (4, 5).

Because the applied stress is unknown and not uniform, strain elastography does not provide an absolute measure of Young's modulus. Instead, stiffness is inferred from relative differences within the region of interest. Although widely available on commercial ultrasound systems, strain elastography has limited clinical application in diffuse liver disease due to variability and lower diagnostic accuracy compared with shear wave-based techniques (4, 5).

Current WFUMB and EFSUMB recommendations do not support strain elastography as a primary method for staging liver fibrosis, but it may have adjunctive value in selected settings (1, 3).

5.2.3. Shear wave elastography (SWE)

Shear wave elastography encompasses techniques that generate mechanical shear waves within the liver and measure their propagation velocity. Because shear wave velocity is directly related to tissue stiffness, SWE provides quantitative and reproducible measurements expressed either in meters per second (m/s) or converted into Young's modulus (kPa) (1–4).

SWE techniques are further ***classified into***:

a) **Vibration-Controlled Transient Elastography (VCTE)**
b) **Point Shear Wave Elastography (pSWE)**
c) **Two-dimensional Shear Wave Elastography (2D-SWE) and** (Less commonly) **Three-dimensional SWE (3D-SWE)**
d) **Vibro-elastography**

a) Vibration-Controlled Transient Elastography (VCTE)

VCTE uses a mechanical piston integrated into a dedicated probe to generate a low-frequency vibration (approximately 50 Hz) at the skin surface, inducing a transient shear wave that propagates through the liver (6) (Fig. 5.2.1). Shear wave velocity is measured along a one-dimensional axis and converted into liver stiffness expressed in kPa.

VCTE is commercially available as FibroScan® and was specifically developed for liver applications. It samples a cylindrical volume of liver parenchyma significantly larger than a biopsy core and provides a median value of multiple valid measurements along with reliability parameters (e.g., IQR/median ratio) (3, 7). Controlled attenuation parameter (CAP) is a technology that quantifies liver steatosis by measuring the energy loss as the sound wave passes through the medium. Total attenuation at 3.5 MHz is expressed in dB/m, and steatosis is estimated using the same radiofrequency data as elastography, in the same location that stiffness is measured (7).

According to EFSUMB and WFUMB guidelines, VCTE is well validated for staging fibrosis in chronic viral hepatitis, MASLD, alcohol-related liver disease, and other chronic hepatopathies (1, 3). Limitations include the absence of B-mode guidance and unreliable measurements in patients with ascites (8, 9).

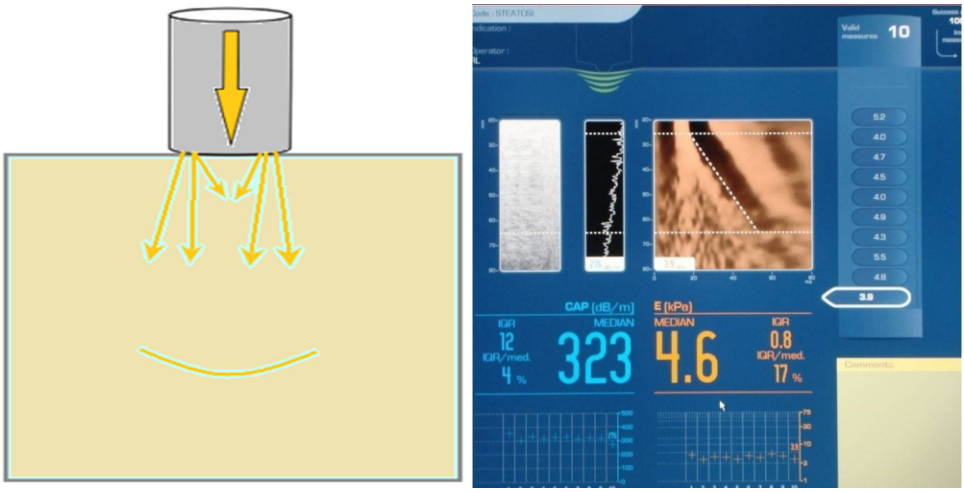


Fig. 5.2.1. The left image illustrates the schematic representation of the VCTE principle, where a mechanically induced impulse at the tissue surface generates shear waves that propagate outward from the point of application. The right image displays the FibroScan® device interface, where numerical values for the Controlled Attenuation Parameter (CAP) are shown on the left in blue (dB/m), while liver stiffness measurements (VCTE values) are displayed on the right in yellow (kPa).

b) Point Shear Wave Elastography (pSWE)

Point shear wave elastography uses acoustic radiation force impulse (ARFI) technology integrated into conventional ultrasound systems. A focused acoustic “push” pulse generates a localized shear wave at a predefined depth, and its velocity is measured within a small region of interest (ROI) (Fig. 5.2.2) (2, 4).

pSWE provides quantitative measurements in m/s or kPa and benefits from real-time B-mode guidance, allowing precise ROI placement while avoiding large vessels and artifacts. Ascites does not preclude measurement, representing an advantage over VCTE (1, 3).

Guidelines recommend the acquisition of multiple valid measurements and the use of reliability criteria such as IQR/median ratio (≤30% in kPa; stricter criteria may apply when values are expressed in m/s) (1, 3).

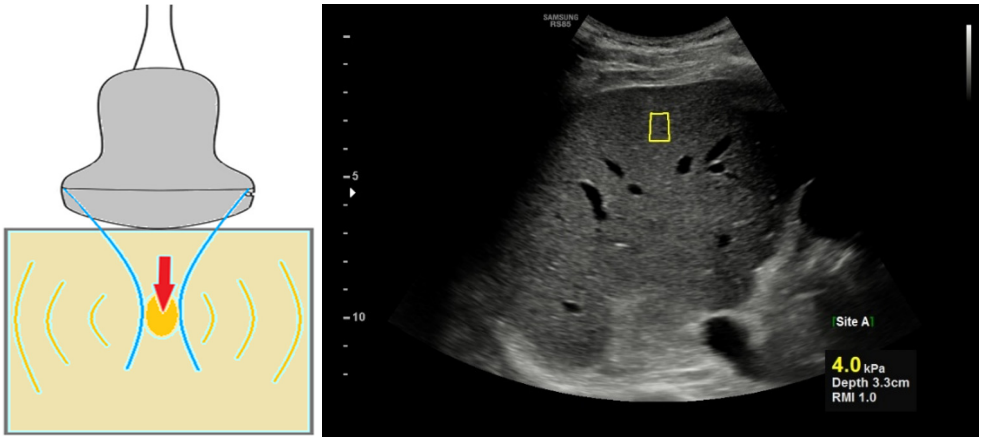


Fig. 5.2.2. The left image illustrates a schematic representation of the pSWE principle, where an ARFI impulse is generated at a controlled depth, inducing a lateral shear wave within a region of interest (ROI). The velocity of the shear wave is measured to assess tissue stiffness. The right image showcases pSWE elastography implemented on the Samsung system, where an ROI is positioned 1–2 cm below the liver capsule. The resulting liver stiffness measurement is displayed in kPa.

c) Two-Dimensional Shear Wave Elastography (2D-SWE)

Two-dimensional SWE is based on multiple sequential ARFI excitations that generate shear waves tracked in real time over a larger area, producing a color-coded elastogram superimposed on the B-mode image (Fig. 5.2.3) (2, 4). This technique allows both qualitative visualization of stiffness distribution and quantitative measurement within a selected ROI inside the elastographic map. Results are expressed as mean or median values in m/s or kPa, along with standard deviation and quality parameters.

2D-SWE evaluates a larger portion of liver parenchyma compared with pSWE and provides visual assessment of tissue homogeneity (Fig. 3). According to recent WFUMB and EFSUMB updates, 2D-SWE demonstrates high diagnostic performance for significant fibrosis and cirrhosis, with good intra- and interobserver reproducibility when quality criteria are respected (1–3).

The 2D SWE technique is an operator-dependent method, with experience playing a role in obtaining reliable results (10). Even though the method overcomes some of the previous limitations, it might have impaired results in patients with severe ascites, poor echoic window, obesity (BMI >30 kg/m^2), inability to hold their breath, increased wall thickness (≥25 mm), steatosis, waist circumference (≥ 102 cm), and recent food intake (2, 4, 11).

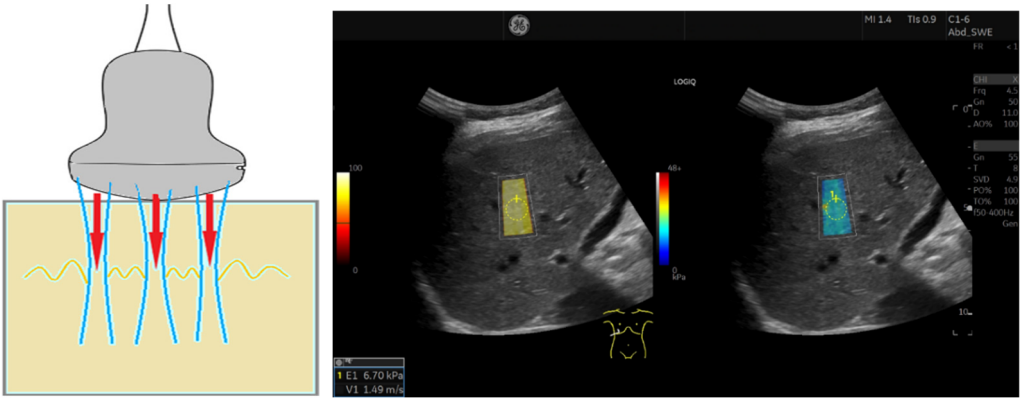


Fig. 5.2.3. The left image illustrates a schematic representation of the 2D-SWE elastography principle, where multiple ARFI impulses generate transverse shear waves for tissue stiffness assessment. The right image demonstrates 2D-SWE elastography implemented on the General Electric system. The elastogram, overlaid on the B-mode image, is positioned 1–2 cm below the liver capsule. A circular region of interest (ROI) is placed within the elastogram to measure liver stiffness. Additionally, a color-coded quality map (left image) is available to assist in ROI placement within the most homogeneous area. Results are expressed in kPa and m/s. This technique is supported by multiple ultrasound systems from various manufacturers, including SuperSonic Imagine/Hologic, GE Healthcare, Canon, Philips, Siemens, Mindray, and others.

Vibro-elastography

Vibro-elastography represents a category of elastographic techniques in which mechanical vibrations are used to generate shear waves within biological tissues. These waves propagate through the liver parenchyma, and their velocity is measured using ultrasound imaging in order to estimate tissue stiffness, which correlates with the degree of hepatic fibrosis. In contrast to acoustic radiation force–based techniques, vibro-elastography relies on externally generated mechanical stimulation that produces harmonic or transient shear waves across a larger portion of the liver. One of the most widely used vibration-based techniques is VCTE, commercially available as FibroScan®.

Recent developments in vibro-elastography include ***Time-Harmonic Elastography (THE)***, a technique that uses continuous multifrequency mechanical stimulation generated by a vibration device integrated into the examination bed. This method produces shear waves at multiple frequencies that propagate through the liver, allowing the generation of two-dimensional elastograms over a wider imaging field compared with conventional

elastography methods (12). Using this approach, liver stiffness can be measured across a large portion of the hepatic parenchyma, with penetration depths of up to approximately 13 cm below the body surface.

Another emerging vibration-based elastography technology is ***Velacur elastography*** (13, 14), which combines mechanical excitation with ultrasound tracking of shear waves. In this system, vibrations generated by an activation unit beneath the patient induce shear waves in the liver, while an ultrasound probe tracks tissue displacement. Velacur provides measurements of liver stiffness and ultrasound attenuation related to hepatic steatosis. Recent studies have also integrated artificial intelligence algorithms to automatically detect and segment shear waves, improving acquisition quality and assisting operators during point-of-care liver assessments.

Vibro-elastography techniques represent an important advance in the non-invasive evaluation of chronic liver diseases. By generating mechanically induced shear waves, they improve liver stiffness assessment and provide information on hepatic viscoelastic properties.

5.2.4. Technical considerations for diffuse liver disease assessment

For diffuse liver diseases, elastography should be performed in the right liver lobe via an intercostal approach, with the patient in a supine position and the right arm in maximal abduction. Measurements in the left lobe are discouraged due to increased variability (1, 3).

All guidelines emphasize that elastographic measurements should be made respecting the following conditions:

- Fasting for at least 2–3 hours before examination
- Breath-hold in an intermediate position during acquisition
- For pSWE and 2D-SWE placement of the ROI, at least 1.5 cm below the liver surface to avoid reverberation and parallel to the liver surface.
- Avoidance of large vessels and artifacts
- Use of reliability criteria (e.g., IQR/median ratio)

Confounding factors such as acute inflammation, cholestasis, hepatic congestion, recent food intake, and elevated transaminases may increase liver stiffness independently of fibrosis severity and must be considered in interpretation (1, 3).

5.2.5. Summary of classification

In diffuse liver diseases, ultrasound-based elastography techniques are classified as follows:

- **Strain elastography** – qualitative/semi-quantitative, limited role in fibrosis staging
- **Shear wave elastography (SWE)**
    - VCTE (mechanical surface excitation, dedicated device)
    - pSWE (ARFI-based, point measurement integrated into US systems)
    - 2D-SWE (real-time elastographic map with quantitative ROI analysis)

Current international guidelines from WFUMB and EFSUMB recommend shear wave elastography techniques as first-line non-invasive tools for fibrosis assessment in chronic liver diseases, with technique selection depending on availability, operator expertise, and patient-related factors (1-4).

References

1. Ferraioli G, Barr RG, Berzigotti A, Sporea I, Wong VW, Reiberger T, et al. WFUMB Guideline/Guidance on Liver Multiparametric Ultrasound: Part 1. Update to 2018 Guidelines on Liver Ultrasound Elastography. Ultrasound Med Biol. 2024 Aug;50(8):1071-1087.
2. Bamber J, Cosgrove D, Dietrich CF, Fromageau J, Bojunga J, Calliada F, et al. EFSUMB guidelines and recommendations on the clinical use of ultrasound elastography. Part 1: Basic principles and technology. Ultraschall Med. 2013 Apr;34(2):169-84.
3. Dietrich CF, Bamber J, Berzigotti A, Bota S, Cantisani V, Castera L, et al. EFSUMB Guidelines and Recommendations on the Clinical Use of Liver Ultrasound Elastography, Update 2017 (Long Version). Ultraschall Med. 2017 Aug;38(4):e16-e47. English Erratum in: Ultraschall Med. 2017 Aug;38(4):e48.
4. Shiina T, Nightingale KR, Palmeri ML, Hall TJ, Bamber JC, Barr RG, et al. WFUMB guidelines and recommendations for clinical use of ultrasound elastography: Part 1: basic principles and terminology. Ultrasound Med Biol. 2015 May;41(5):1126-47
5. Sigrist RMS, Liau J, Kaffas AE, Chammas MC, Willmann JK. Ultrasound Elastography: Review of Techniques and Clinical Applications. Theranostics. 2017 Mar 7;7(5):1303-1329.
6. Sandrin L, Tanter M, Gennisson JL, Catheline S, Fink M. Shear elasticity probe for soft tissues with 1-D transient elastography. IEEE Trans Ultrason Ferroelectr Freq Control. 2002 Apr;49(4):436-46.

7. Sasso M, Beaugrand M, de Ledinghen V, Douvin C, Marcellin P, Poupon R, et al. Controlled attenuation parameter (CAP): a novel VCTE™ guided ultrasonic attenuation measurement for the evaluation of hepatic steatosis: preliminary study and validation in a cohort of patients with chronic liver disease from various causes. Ultrasound Med Biol. 2010 Nov;36(11):1825-35.
8. Castéra L, Foucher J, Bernard PH, Carvalho F, Allaix D, Merrouche W, et al. Pitfalls of liver stiffness measurement: a 5-year prospective study of 13,369 examinations. Hepatology. 2010 Mar;51(3):828-35.
9. Sporea I, Şirli R. Hepatic Elastography Using Ultrasound Waves. Bentham Science: E-Book2016. p. 178. DOI: 10.2174/97816080546331120101.
10. Grădinaru-Taşcău O, Sporea I, Bota S, Jurchiş A, Popescu A, Popescu M, et al. Does experience play a role in the ability to perform liver stiffness measurements by means of supersonic shear imaging (SSI)? Med Ultrason. 2013 Sep;15(3):180-3.
11. Cassinotto C, Lapuyade B, Mouries A, Hiriart JB, Vergniol J, Gaye D, et al. Non-invasive assessment of liver fibrosis with impulse elastography: comparison of Supersonic Shear Imaging with ARFI and FibroScan®. J Hepatol. 2014 Sep;61(3):550-7.
12. Moga T, Sporea I, Lupușoru R, Popescu A, Popa A, Bota S, et al. Performance of a Noninvasive Time-Harmonic Elastography Technique for Liver Fibrosis Evaluation Using Vibration Controlled Transient Elastography as Reference Method. Diagnostics 2020, 10, 653.
13. Curry MP, Tam E, Schneider C, Abdelgelil N, Hassanien T, Afdhal NH. The Use of Noninvasive Velacur® for Discriminating between Volunteers and Patients with Chronic Liver Disease: A Feasibility Study. Int J Hepatol. 2024 Jan 17; 2024:8877130
14. Honarvar M, Lobo J, Schneider C, Wolfe N, Gawrieh S, Loomba R, et al. Deep Learning Based Shear Wave Detection and Segmentation Tool for Use in Point-of-Care for Chronic Liver Disease Assessments. Ultrasound Med Biol. 2024 Dec;50(12):1812-1820.

5.3. Elastography in Chronic Viral Hepatitis

Ruxandra Mare, Roxana Şirli

Abstract

Chronic viral hepatitis remains a major global cause of liver-related morbidity and mortality, despite major advances in antiviral therapy. Hepatitis C virus (HCV), hepatitis B virus (HBV), and hepatitis D virus (HDV) infections are major causes of progressive liver fibrosis, cirrhosis, portal hypertension, and hepatocellular carcinoma.

Although liver biopsy has traditionally served as the reference standard for fibrosis staging, its invasiveness, sample variability, and limited acceptance have prompted the development and broad adoption of noninvasive techniques. Among these, ultrasound-based elastography has emerged as a key tool for assessing fibrosis in chronic viral hepatitis, offering reliable, quantifiable, and clinically relevant data.

Elastography techniques are currently used extensively throughout the healthcare continuum, including baseline staging, treatment decision-making, prognostic classification, and long-term surveillance. This review summarizes the role of elastography in chronic viral hepatitis, focusing on vibration-controlled transient elastography (VCTE), point shear wave elastography (pSWE), two-dimensional shear wave elastography (2D-SWE), and emerging multiparametric ultrasound (MPUS) approaches.

5.3.1. Elastography Techniques in Chronic Viral Hepatitis - General Considerations

Chronic viral hepatitis remains a major global cause of liver-related morbidity and mortality, despite major advances in antiviral therapy (1). Ultrasound-based elastography assesses liver stiffness (LS) as a fibrosis surrogate by assessing the propagation of mechanically or acoustically produced shear waves across hepatic tissue. VCTE, pSWE, and 2D-SWE have different technical implementations but share similar strengths: non-invasiveness, repeatability, and high accuracy for diagnosing advanced fibrosis and cirrhosis (2-5).

The most thoroughly validated approach is VCTE (FibroScan®), which provides standardized liver stiffness measures (LSM) expressed in kilopascals (kPa), with specified quality criteria and universally accepted cut-offs. Point

Shear Wave Elastography (pSWE), integrated into traditional ultrasound systems, enables point-based stiffness measurements using B-mode guidance, whereas bidimensional Shear Wave Elastography (2D-SWE) provides real-time color-coded stiffness maps with quantitative sampling over broader regions of interest. Confounding factors such as necroinflammatory activity, cholestasis, congestion, and recent meal intake must be considered when interpreting results using any of the abovementioned techniques (2-5).

5.3.2. Role of elastography in chronic hepatitis C

a) Vibration-Controlled Transient Elastography (VCTE) (Fig. 5.3.1). Chronic hepatitis C (HCV) was the first chronic viral hepatitis in which elastography was extensively validated (4, 5). Early comparative studies demonstrated that VCTE has limited value in discriminating adjacent early fibrosis stages (F0–F2) but reliably identifies clinically significant fibrosis (≥F2) and cirrhosis, which historically guided treatment decisions. Thus, even if VCTE lacks sufficient accuracy to consistently differentiate adjacent early Metavir stages, particularly F0, F1, and F2, due to the significant overlap in their stiffness values, it remains clinically valuable since it distinguishes between no/mild fibrosis (F0–F1) and significant fibrosis (F2), which was a critical treatment choice threshold at that time.



Figure 5.3.1. Liver stiffness measurement using VCTE. Liver stiffness is displayed in yellow (5.4 kPa), while the Controlled Attenuation Parameter (CAP), as a marker of steatosis, is displayed in blue (155 dB/m).

VCTE is also highly effective in identifying HCV-related cirrhosis. In a French multicenter study coordinated by Beaugrand (6), 494 patients with chronic HCV hepatitis underwent both liver biopsy and VCTE. Fibrosis severity showed a significant correlation with LS (Spearman $r = 0.57$ and $p < 0.001$). The study proposed a cut-off of 7.5 kPa to separate F0–F1 from F2–F4, with a sensitivity of 67%, a specificity of 87%, an 86% PPV, a 68% NPV, and an overall diagnostic accuracy of 76%.

In a study conducted by our team (7) involving 407 treatment-naïve chronic HCV patients, LS had shown a significant correlation with fibrosis severity (Spearman $r = 0.605$, $P < 0.0001$). Two critical cut-offs were identified: for severe fibrosis (≥F2 Metavir), a threshold of 6.8 kPa yielded a sensitivity of 58.9%, a specificity of 89.1%, and an AUROC of 0.760. For cirrhosis, a threshold of 12.6 kPa resulted in a sensitivity of 92.1% and a specificity of 91.6%, with an AUROC of 0.953.

Over time, many studies evaluated VCTE for fibrosis staging and reported F0–F1 vs. F2–F4 cut-offs ranging from 6.8 to 7.3 kPa (7-9). In the meta-analysis by Friedrich-Rust (50 studies), the mean AUROC for significant fibrosis (F2) was 0.84, with a suggested cut-off of 7.6 kPa (10). In the meta-analysis by Tsochatzis (11), the calculated cut-off for F≥2 Metavir was also 7.6 kPa, with cumulative sensitivity 0.78 and cumulative specificity 0.89.

VCTE has a substantially higher predictive value for the presence of cirrhosis, with an AUROC of more than 0.95 (10,12). A 2016 meta-analysis of 24 papers found a Se of 84%, Sp of 90%, and AUROC of 0.95 for the prediction of cirrhosis in individuals with chronic HCV hepatitis (13). The proposed cut-off value for diagnosing HCV liver cirrhosis ranged between 12.5 and 15 kPa (11, 14).

Over time, especially after the treatment with highly efficient direct antiviral agents (DAAs) became available, the focus on separating fibrosis severity levels changed to detecting patients with compensated advanced chronic liver disease (cACLD) - those with severe fibrosis/cirrhosis who are at higher risk of developing clinically significant portal hypertension (CSPH), hepatocellular carcinoma (HCC), decompensating events, and liver failure.

More recent meta-analyses published between 2023 and 2025 confirmed the excellent performance of VCTE for predicting advanced fibrosis (≥F3), with AUROC values consistently above 0.90 (15, 16). In the era of DAAs, liver stiffness typically declines rapidly after viral eradication, reflecting resolution of necroinflammation; however, persistently elevated values after

sustained virologic response (SVR) identify patients at continued risk of portal hypertension and hepatocellular carcinoma (15-17).

As a practical approach, the Society of Radiologists in Ultrasound Consensus (18) proposed the *"rule of 5"* to stratify fibrosis severity in patients with chronic viral hepatitis, based on LS assessment by means of VCTE:

- LS ≤ 5 kPa - high probability of being normal;
- LS < 10 kPa in the absence of other known clinical signs - rules out cACLD (F3-F4 stages);
- LS 10-15 kPa - suggestive of cACLD - further tests needed for confirmation;
- LS > 15 kPa - highly suggestive of cACLD;
- An LS value of 20-25 kPa or higher indicates clinically significant portal hypertension.

Consensus guidelines also emphasize noninvasive risk stratification for portal hypertension complications. The Baveno VI criteria (LS ≤ 20 kPa and platelet count ≥ 150×10^9/L) have been validated as having a low likelihood of high-risk esophageal varices and a low risk of decompensation, thereby identifying patients in whom screening endoscopy can be avoided. The expanded Baveno VII consensus further highlights the role of non-invasive tests in routine care, particularly VCTE, to rule in and rule out compensated advanced chronic liver disease (cACLD) and CSPH (19, 20).

EASL guidelines recommend fibrosis severity assessment by noninvasive tests in each HCV patient prior to starting treatment to identify those with cACLD (at risk for complications even after SVR). The proposed cutoffs for VCTE are 10 kPa for F3 and 13 kPa for F4 (21).

An important clinical question in the management of patients with cirrhosis who achieve sustained virologic response (SVR) is whether standard surveillance for clinically significant portal hypertension (CSPH) and hepatocellular carcinoma (HCC) can be safely de-escalated.

Emerging evidence suggests that, among patients who achieve SVR, the regression of portal hypertension surrogates may further refine risk prediction. For example, when LS values fall below 12 kPa after SVR in patients with normal platelet counts, CSPH can effectively be excluded with high sensitivity, supporting the de-escalation of invasive hemodynamic assessment in those selected populations (20, 22).

However, even in the context of marked improvement in surrogate markers of portal hypertension after SVR, patients with established advanced

fibrosis or cirrhosis remain at persistent risk for HCC. Post-SVR liver stiffness levels are independently associated with HCC incidence across a range of LSM thresholds, and rates of HCC remain clinically significant even with lower stiffness values; therefore, ongoing surveillance for hepatocarcinogenesis is recommended irrespective of improvements in portal hypertension metrics (23, 24).

In summary, low-risk patients may safely defer routine screening endoscopy if they meet the Baveno VI/VII criteria after achieving SVR. However, current evidence supports continued participation in structured HCC surveillance programs for all individuals with advanced fibrosis or cirrhosis, irrespective of regression in portal hypertension measures.

b) Point shear wave elastography (pSWE), using Acoustic Radiation Force Impulse (ARFI)-based techniques [such as Virtual Touch Quantification (VTQ) and ElastPQ (Fig. 5.3.2)], is currently recognized as a validated non-invasive method for the assessment and longitudinal monitoring of liver fibrosis in patients with chronic HCV infection. The EFSUMB recommendations indicate that VTQ cut-off values between 1.21 and 1.34 m/s suggest significant fibrosis (F > 2), with AUROC values between 0.85 and 0.89, whereas values between 1.55 and 2 m/s signify cirrhosis, with AUROC values of 0.89–0.93 (25).

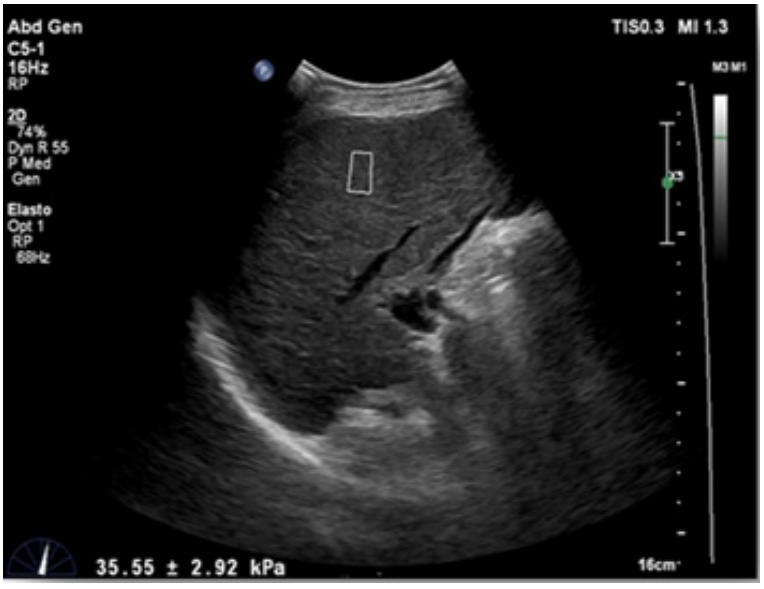


Figure 5.3 2. Evaluation of liver stiffness using pSWE (ElastPQ). The values displayed are compatible with liver cirrhosis.

The guidelines advocate using pSWE, specifically VTQ, as a primary instrument for evaluating the severity of liver fibrosis in individuals with persistent HCV infection, emphasizing its exceptional accuracy in ruling out cirrhosis (25). Evidence about the application of ElastPQ for assessing the severity of liver fibrosis in chronic HCV hepatitis is still scarce. A limited number of studies evaluated HCV cohorts utilizing liver biopsy as the reference standard. Pilot research indicated an AUROC of 0.80 for identifying significant fibrosis (F ≥ 2) and 0.95 for diagnosing cirrhosis (26). Additional studies evaluated the diagnostic efficacy of ElastPQ in comparison to VCTE as the reference method, revealing AUROC values ranging from 0.92 to 0.96 for severe fibrosis and from 0.83 to 0.95 for cirrhosis (27, 28).

Analogous to VCTE, liver stiffness measurements by pSWE techniques diminish after sustained virological response (SVR) following antiviral treatment (29, 30). Prospective research involving 336 patients, of whom 121 achieved sustained virologic response (SVR), demonstrated a diagnostic performance of 0.818 for identifying severe fibrosis (≥F2) and 0.981 for diagnosing cirrhosis (F4). The corresponding cut-off values were 1.26 m/s for ≥F2 and 1.49 m/s for F4 (30). A further study with 644 patients demonstrated a decrease in median LS values during sustained virologic response (SVR), but histological fibrosis evaluated via liver biopsy remained constant; in this cohort, 80.9% received biopsy at therapy onset and 19.1% at three years post-SVR (29).

The role of pSWE in forecasting cirrhosis-associated problems in individuals with chronic HCV infection, especially CSPH, will be discussed in a separate chapter.

c) Two-dimensional shear wave elastography (2D-SWE) is recommended by both EFSUMB and WFUMB guidelines as an ultrasound-based, non-invasive option for staging liver fibrosis in chronic hepatitis C (CHC), provided that acquisitions follow standardized quality measures (fasting, right-lobe intercostal approach, adequate depth below the capsule, avoidance of large vessels, and interpretation in clinical context) (4, 25). It is also based on ARFI technology – an acoustic impulse generates shear waves into the liver tissue; their speed is measured by various techniques (depending on the vendor) and is considered indicative of fibrosis severity.

In chronic hepatitis C (CHC) cohorts, diagnostic performance is typically rated as satisfactory to excellent: a meta-analysis of individual patient data utilizing Aixplorer 2D-SWE (Fig. 5.3.3) and liver biopsy (n=379 CHC) indicated an

AUROC of 0.863 for significant fibrosis (≥F2) and 0.929 for cirrhosis (F4) (31). In a biopsy-based prospective study involving 233 HCV patients, 2D-SWE demonstrated an AUROC of 0.915 for ≥F2 and 0.949 for F4, with incremental increases in shear-wave velocity corresponding to METAVIR stages (32).

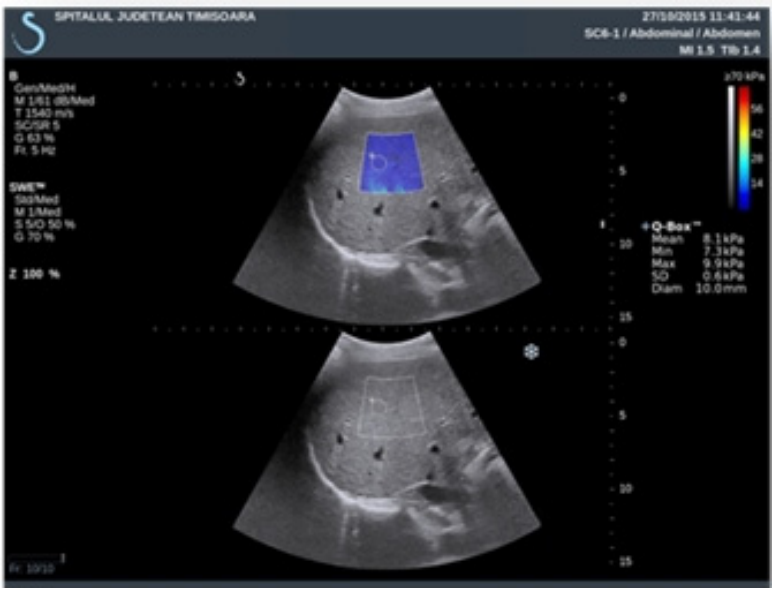


Figure 5.3.3. Liver stiffness measurement using 2D-SWE (Aixplorer). A color-coded elastography map overlaid on the B-mode ultrasound image allows quantitative assessment of LS.

Thresholds differ by platform and reference standard, prompting guidelines to emphasize the necessity for technique and vendor-specific cut-offs and local validation; however, generally reported values in chronic hepatitis C cluster around approximately 7–8 kPa for significant fibrosis (≥F2) and 10–12 kPa for cirrhosis. Sporea et al. proposed 2D-SWE cut-offs of >7.8 kPa for ≥F2 (AUROC 0.859) and >11.5 kPa for F4 (AUROC 0.914), using VCTE as the reference (33). In a biopsy-anchored validation cohort comprising mixed chronic liver disease (including HCV), a pragmatic rule-out threshold of 7.29 kPa for ≥F2 produced an AUROC of 0.84 with high sensitivity (95.4%) (34).

Recent studies have assessed individuals with chronic HCV infection utilizing various 2D-SWE approaches, yielding generally comparable outcomes. Our group conducted a study (35) comparing two 2D-SWE methods—2D-SWE.SSI (Aixplorer™) and 2D-SWE.GE (General Electric)—utilizing VCTE as the

reference standard in 208 consecutive HCV patients assessed during the same session. Liver stiffness measurements acquired by 2D-SWE.GE demonstrated a more robust connection with VCTE compared to that derived from 2D-SWE.SSI ($r = 0.75$ vs. $r = 0.57$; $p < 0.0001$), although no significant discrepancies were observed between the two methodologies regarding diagnosis accuracy for fibrosis stages $F \geq 2$, $F \geq 3$, or F4 (AUROCs 0.95–0.97; all $p > 0.29$). The 2D-SWE.GE approach was evaluated in comparison to liver biopsy in a population of 103 patients with persistent HBV or HCV infection (36). In patients with HCV, the thresholds were 7.81 kPa for $F \geq 2$, 9.00 kPa for $F \geq 3$, and 12.47 kPa for cirrhosis.

In a separate investigation involving 178 patients with chronic HCV hepatitis, researchers evaluated another 2D-SWE technique, ElastQ (Philips EPIQ 7), using VCTE as the reference method. The reported cut-off values were 8.15 kPa for ≥F2 (AUROC 0.899), 10.31 kPa for ≥F3 (AUROC 0.900), and 12.65 kPa for F4 (AUROC 0.899) (37).

Overall, 2D-SWE is endorsed by recommendations as a dependable first-line technique for fibrosis risk assessment in CHC, with best practices highlighting uniform acquisition and the use of etiology- and device-specific cut-offs.

A problem when using pSWE and 2D-SWE is that cut-off values are different for different vendors, which led to a lot of debate. In order to ease the use of pSWE and 2D-SWE in clinical practice, the Society of Radiologists in Ultrasound Consensus (18) proposed the *"rule of 4"* to stratify fibrosis severity in patients with chronic viral hepatitis, based on LS assessment by means of ARFI-based techniques, applicable both to pSWE and 2D-SWE:

- LS ≤ 5 kPa (1.3 m/s) - high probability of being normal;
- LS < 9 kPa (1.7 m/s) in the absence of other known clinical signs - rules out cACLD (F3-F4 stages);
- LS - 9 - 13 kPa (1.7 m/s - 2.1 m/s) - suggestive of cACLD, further tests needed for confirmation;
- LS > 13 kPa (2.1 m/s) – rules-in cACLD;
- LS ≥ 17 kPa (2.4 m/s) – suggestive of CSPH.

5.3.3. Role of elastography in chronic hepatitis B

Ultrasound elastography plays a key role in the noninvasive assessment and longitudinal monitoring of fibrosis in chronic hepatitis B (CHB).

a) Vibration-controlled transient elastography (VCTE - FibroScan®) is the most thoroughly validated method, with meta-analyses indicating strong diagnostic accuracy for fibrosis staging, yielding AUROC values of approximately 0.84 for significant fibrosis (≥F2) and 0.94 for cirrhosis (F4) (38). Commonly used cut-off values are approximately 7–8 kPa for ≥F2 and 11–13 kPa for F4, although these thresholds are affected by ALT activity and inflammatory status (39). To decrease fibrosis overestimation during hepatic flares, Chan et al. calculated ALT-adjusted liver stiffness cut-off values using VCTE. The cut-off for advanced fibrosis (F3) was 9 kPa in patients with normal ALT and 12 kPa in those with ALT higher than 5 times the upper limit of normal. For cirrhosis, the cut-offs were 12 kPa with normal ALT and 13.4 kPa with raised ALT, emphasizing the significance of aminotransferase levels (inflammation) in interpreting liver stiffness data (40). Measurements using VCTE must be analyzed within a biochemical framework; otherwise, there is a risk of overestimating the severity of fibrosis. Consequently, examination by VCTE is not advisable in cases of acute hepatitis or during exacerbations of chronic hepatitis caused by HBV (3, 5, 25).

VCTE has emerged as a recognized technique for assessing fibrosis in chronic hepatitis B virus (HBV) patients with normal ALT levels, demonstrating superior efficacy compared to serological testing (2, 3, 5, 25).

The latest EASL Guidelines on chronic hepatitis B (41) recommend that in all HBsAg+ patients, fibrosis severity should be assessed by non-invasive methods, including VCTE, for which the following thresholds should be used:

- >7 kPa for significant fibrosis (F≥2 Metavir)
- >8 kPa for advanced fibrosis (F≥3 Metavir)
- >11 kPa for cirrhosis (F4 Metavir)

In patients with chronic hepatitis B undergoing antiviral therapy, numerous studies have shown a substantial decrease in liver stiffness (LS) values over time, with the most pronounced reduction occurring within the initial 2–3 years of treatment, followed by relative stabilization thereafter (42-45). Nonetheless, as shown in chronic hepatitis C, a reduction in LS levels in cirrhotic patients following successful antiviral treatment should not result in the cessation of hepatocellular carcinoma monitoring (5, 25). Likewise, the Baveno VI/VII criteria for risk stratification related to portal hypertension should be utilized in individuals with chronic hepatitis B (46).

A specific subset consists of people with persistent HBeAg-negative HBV infection, previously referred to as inactive HBsAg carriers, characterized by HBsAg positivity, HBeAg negativity, HBV DNA levels below 2000 IU/ml, and

normal ALT levels. While the majority have modest illnesses, a minority may still demonstrate severe fibrosis and cirrhosis. In our investigation, the mean liver stiffness assessed by VCTE in HBeAg-negative infection was 5.6 ± 2.1 kPa, substantially greater than that of healthy controls (4.8 ± 1.2 kPa, p = 0.0002). Patients exhibiting undetectable HBV DNA demonstrated markedly lower stiffness values in contrast to those with detectable viremia (but lower than <2000 IU/ml): 4.9 ± 1.2 kPa vs. 6.7 ± 2.7 kPa, p < 0.001 (42). Current worldwide guidelines advocate for using VCTE to rule out severe fibrosis and to identify cirrhosis in this category of patients (5, 25, 41).

The role of VCTE in forecasting cirrhosis-related problems, especially clinically severe portal hypertension in chronic hepatitis B, will be discussed in a separate chapter.

b) Point shear-wave elastography (pSWE) demonstrates significant accuracy in HBV patients, especially for advanced fibrosis, with AUROC values ranging from 0.91 to 0.93 for ≥F3–F4 in the case of VTQ. Proposed cut-off values in chronic hepatitis B cohorts are approximately 1.3–1.4 m/s for ≥F2 and around 1.7 m/s for cirrhosis, highlighting the necessity for etiology-specific thresholds (48, 49). According to liver biopsy studies, VTQ elastography can diagnose fibrosis severity in chronic hepatitis B with similar performance to VCTE. The AUROC values for significant fibrosis (F≥2) ranged from 0.75 to 0.76 for VTQ and from 0.81 to 0.83 for VCTE, while for cirrhosis (F4), they ranged from 0.83 to 0.97 for VTQ and from 0.80 to 0.93 for VCTE (50-52). In a Romanian study (53 patients with chronic hepatitis B and 107 with chronic hepatitis C), VTQ had a similar incorrect measurement rate as VCTE (8.8% vs. 10.9%, p = 0.66). Mean VTQ liver stiffness values were similar across HBV and HCV cohorts for the same fibrosis stage. VTQ and VCTE struggled to discriminate F0, F1, or F≥2 in chronic hepatitis B patients but excelled in differentiating advanced fibrosis (F≥3) and cirrhosis (F4) from non-cirrhotic illness (53).

Although tested in fewer trials, ElastPQ has shown high accuracy for substantial fibrosis (AUROC 0.94–0.95) and very good accuracy for cirrhosis (AUROC 0.88–0.89) in chronic HBV (54, 55). EFSUMB guidelines recommend pSWE approaches, notably VTQ, for detecting cirrhosis in chronic hepatitis B patients (25).

The latest EASL Guidelines on chronic hepatitis B (41) also include pSWE techniques for the non-invasive assessment of fibrosis severity in HBV patients.

c) Two-dimensional shear-wave elastography (2D-SWE) enhances spatial sampling and reproducibility, with a CHB-specific meta-analysis indicating an AUROC of approximately 0.92 for ≥F2 and mean stiffness cut-offs between 7.5 and 8.0 kPa, while elevated thresholds are frequently necessary for patients undergoing prolonged antiviral treatment (31). A prospective multicenter study examined 602 chronic hepatitis B patients who underwent 2D-SWE utilizing ElastQ with liver biopsy as the reference standard. Liver stiffness values from 2D-SWE were substantially linked with the fibrosis stage ($r = 0.71$, $P < 0.001$). The best cut-off values were 5.72 kPa for ≥F1, 6.85 kPa for ≥F2, 7.43 kPa for ≥F3, and 8.03 kPa for cirrhosis (F4) (56).

The latest EASL Guidelines on chronic hepatitis B (42) also include 2D-SWE techniques for the non-invasive assessment of fibrosis severity in HBV patients.

The same problem when using pSWE and 2D-SWE in HBV patients is that cut-off values are different for different vendors. Per the recommendations of the Society of Radiologists in Ultrasound Consensus, the *"rule of 4"* mentioned in HCV patients can be used to stratify fibrosis severity in patients with chronic hepatitis B, as shown above (18).

5.3.4. Role of elastography in chronic hepatitis D

Ultrasound elastography is useful in diagnosing fibrosis severity in chronic hepatitis D (HDV), a condition that causes rapid fibrosis progression and early cirrhosis. Studies using liver biopsy as the reference standard have shown that VCTE provides reliable noninvasive fibrosis staging in HDV, with higher liver stiffness values at comparable histological stages than in HBV monoinfection, reflecting HDV's aggressive natural history (57, 58).

VCTE has excellent diagnostic performance for advanced fibrosis and cirrhosis, with reported AUROC values of 0.90-0.95 and cirrhosis cut-off values that are typically lower than those utilized in HBV, commonly in the 10-11 kPa range (57, 58). Reduced LS in patients receiving antiviral or anti-HDV therapy may occur as a result of decreased necroinflammation and possible fibrosis regression; however, as with other chronic viral hepatitis, improvements in stiffness values should not affect hepatocellular carcinoma surveillance in patients with cirrhosis (58). Overall, elastography is a useful tool in HDV for baseline fibrosis staging, risk stratification, and longitudinal follow-up, while interpretation is tricky because of the scarcity of HDV-specific cut-off values (57, 58).

5.3.5. Rule of 5 and Rule of 4: Pragmatic Interpretation of Liver Stiffness

As mentioned above, to address overlapping stiffness values between fibrosis stages and to align elastography with clinical decision-making, a pragmatic interpretation framework has been proposed. For VCTE, the "Rule of 5" suggests that liver stiffness values less than 5 kPa indicate a high probability of a normal liver, values lower than 10 kPa exclude compensated advanced chronic liver disease (cACLD) in the absence of clinical signs, values higher than 15 kPa strongly suggest cACLD, and values higher than 20–25 kPa indicate a high likelihood of clinically significant portal hypertension (59, 60).

For ARFI-based techniques (pSWE and 2D-SWE), an analogous "Rule of 4" has been proposed, using approximate thresholds of 5, 9, 13, and 17 kPa, respectively. These simplified rules, endorsed by expert consensus and incorporated into recent guidelines, facilitate harmonized interpretation across platforms and etiologies in chronic viral hepatitis and MASLD (18, 59-61).

In conclusion, elastography has emerged as an essential instrument in the management of chronic viral hepatitis. VCTE, pSWE, and 2D-SWE deliver precise and consistent evaluations of liver fibrosis across HCV, HBV, and HDV chronic infections, demonstrating reliable efficacy in detecting advanced disease and stratifying patients for surveillance protocols. The integration of multiparametric ultrasonography and the application of pragmatic interpretation frameworks, such as the Rule of 5 and Rule of 4, facilitate coherent and clinically significant decision-making across various viral etiologies.

References

1. World Health Organization. Global hepatitis report 2024. Geneva: WHO; 2024.
2. European Association for the Study of the Liver; Asociación Latinoamericana para el Estudio del Higado. EASL-ALEH Clinical Practice Guidelines: Non-invasive tests for evaluation of liver disease severity and prognosis. J Hepatol. 2015 Jul;63(1):237-64.
3. European Association for the Study of the Liver. EASL Clinical Practice Guidelines on non-invasive tests for evaluation of liver disease severity and prognosis - 2021 update. J Hepatol. 2021 Sep;75(3):659-689. doi: 10.1016/j.jhep.2021.05.025.
4. Ferraioli G, Filice C, Castera L, Choi BI, Sporea I, Wilson SR, et al. WFUMB Guidelines and Recommendations for Clinical Use of Ultrasound Elastography: Part 3: Liver. Ultrasound Med Biol. 2015;41(5):1161–1179. doi:10.1016/j.ultrasmedbio.2015.03.007

5. Ferraioli G, Wong VW, Castera L, Berzigotti A, Sporea I, Dietrich CF, et al. Liver Ultrasound Elastography: An Update to the World Federation for Ultrasound in Medicine and Biology Guidelines and Recommendations. Ultrasound Med Biol. 2018; 44(12):2419-40.
6. Ziol M, Douvin C, de Ledinghen V, Poupon R, Beaugrand M. Liver stiffness cut-off values in HCV patients: validation and comparison in an independent population. Hepatology. 2006; 44(4):269A-70A.
7. Sporea I, Sirli R, Deleanu A, Tudora A, Curescu M, Cornianu M, Lazar D. Comparison of the liver stiffness measurement by transient elastography with the liver biopsy. World J Gastroenterol. 2008; 14(42):6513-7
8. Castera L, Vergniol J, Foucher J, Le Bail B, Chanteloup E, Haaser M, et al. Prospective comparison of transient elastography, Fibrotest, APRI, and liver biopsy for the assessment of fibrosis in chronic hepatitis C. Gastroenterology. 2005; 128(2):343-50.
9. Ziol M, Handra-Luca A, Kettaneh A, Christidis C, Mal F, Kazemi F, et al. Noninvasive assessment of liver fibrosis by measurement of stiffness in patients with chronic hepatitis C. Hepatology. 2005; 41(1):48-54
10. Friedrich-Rust M, Ong MF, Martens S, Sarrazin C, Bojunga J, Zeuzem S, Herrmann E. Performance of transient elastography for the staging of liver fibrosis: a meta-analysis. Gastroenterology. 2008; 134(4):960-74
11. Tsochatzis EA, Gurusamy KS, Ntaoula S, Cholongitas E, Davidson BR, Burroughs AK. Elastography for the diagnosis of severity of fibrosis in chronic liver disease: a meta-analysis of diagnostic accuracy. J Hepatol. 2011; 54(4):650-9.
12. Shaheen AA, Wan AF, Myers RP. FibroTest and FibroScan for the prediction of hepatitis C-related fibrosis: a systematic review of diagnostic test accuracy. J Gastroenterol. 2007; 102(11):2589-600.
13. Ying HY, Lu LG, Jing DD, Ni XS. Accuracy of transient elastography in the assessment of chronic hepatitis C-related liver cirrhosis. Clin Invest Med. 2016; 39(5):E150-E60.
14. Castera L, Vergniol J, Foucher J, Le Bail B, Chanteloup E, Haaser M, et al. Prospective comparison of transient elastography, Fibrotest, APRI, and liver biopsy for the assessment of fibrosis in chronic hepatitis C. Gastroenterology. 2005; 128(2):343-50.
15. Singh S, Facciorusso A, Loomba R, Falck-Ytter Y. Magnitude and kinetics of decrease in liver stiffness after antiviral therapy in chronic hepatitis C: a systematic review and meta-analysis. Clin Gastroenterol Hepatol. 2023;21(2):278–89.e6.
16. Xiao G, Yang J, Yan L. Comparison of transient elastography, acoustic radiation force impulse, and shear wave elastography for staging liver fibrosis in chronic hepatitis C: updated meta-analysis. Hepatology. 2024;79(1):123–36
17. Semmler G, Meyer EL, Kozbial K, Schwabl P, Hametner S, Mandorfer M, et al. Liver stiffness after SVR predicts portal hypertension and hepatocellular carcinoma risk in chronic hepatitis C. J Hepatol. 2023;78(4):742–53

18. Barr RG, Ferraioli G, Palmeri ML, et al. Elastography Assessment of Liver Fibrosis: Society of Radiologists in Ultrasound Consensus Conference Statement. Radiology. 2015;276(3):845-61.
19. de Franchis R, Bosch J, Garcia-Tsao G, Reiberger T, Ripoll C, Abraldes JG, et al. Baveno VII – renewing consensus in portal hypertension. J Hepatol. 2022;76(4):959-74
20. Canillas L, Reig M, Abraldes JG, et al. Liver stiffness regression and exclusion of clinically significant portal hypertension after sustained virologic response. Hepatology. 2026;73(1):215-27.
21. European Association for the Study of the Liver; Clinical Practice Guidelines Panel. EASL recommendations on treatment of hepatitis C: Final update of the series☆. J Hepatol. 2020 Nov;73(5):1170-1218. Erratum in: J Hepatol. 2023 Feb;78(2):452
22. Bañares R, Bosch J. Refining non-invasive criteria for clinically significant portal hypertension in the era of etiologic cure. J Hepatol. 2025;82(2):312-20.
23. da Silva PGF, et al. Transient elastography and FIB-4 as predictors of HCC risk post-SVR. World J Gastroenterol. 2025;31(45):112318.
24. Nakatsuka T, et al. Pre-treatment vs post-treatment LSM as predictors of HCC after SVR. Hepatol Res. 2025;41031772
25. Dietrich CF, Bamber J, Berzigotti A, Bota S, Cantisani V, Castera L, et al. EFSUMB Guidelines and Recommendations on the Clinical Use of Liver Ultrasound Elastography, Update 2017 (Long Version). Ultraschall Med. 2017; 38(4):e48.
26. Ferraioli G, Tinelli C, Lissandrin R, Zicchetti M, Dal Bello B, Filice G, Filice C. Point shear wave elastography method for assessing liver stiffness. World J Gastroenterol. 2014; 20(16):4787-96.
27. Baldea V, Sporea I, Lupusoru R, Bende F, Mare R, Popescu A, Sirli R. Comparative Study Between the Diagnostic Performance of Point and 2-D Shear-Wave Elastography for the Non-invasive Assessment of Liver Fibrosis in Patients With Chronic Hepatitis C Using Transient Elastography as Reference. Ultrasound Med Biol. 2020; 46(11):2979-88
28. Mare R, Sporea I, Lupusoru R, Sirli R, Popescu A, Danila M, Pienar C. The value of ElastPQ for the evaluation of liver stiffness in patients with B and C chronic hepatopathies. Ultrasonics. 2017;77:144-51.
29. Chen SH, Lai HC, Chiang IP, Su WP, Lin CH, Kao JT, et al. Performance of Acoustic Radiation Force Impulse Elastography for Staging Liver Fibrosis in Patients With Chronic Hepatitis C After Viral Eradication. Clin Infect Dis. 2020; 70(1):114-22.
30. Tachi Y, Hirai T, Kojima Y, Miyata A, Ohara K, Ishizu Y, et al. Liver stiffness measurement using acoustic radiation force impulse elastography in hepatitis C virus-infected patients with a sustained virological response. Pharmacol Ther Food. 2016; 44(4):346-55.
31. Herrmann E, de Lédinghen V, Cassinotto C, Chu WCW, Leung VYF, Ferraioli G, et al. Assessment of biopsy-proven liver fibrosis by two-dimensional shear wave elastography: An individual patient data-based meta-analysis. Hepatology. 2018;67(1):260–72. doi:10.1002/hep.29179.

32. Abe T, Kuroda H, Fujiwara Y, Yoshida Y, Miyasaka A, Kamiyama N, et al. Accuracy of 2D shear wave elastography in the diagnosis of liver fibrosis in patients with chronic hepatitis C. J Clin Ultrasound. 2018. 46(5):319-327
33. Sporea I, Bota S, Grădinaru-Taşcău O, Sirli R, Popescu A, Jurchiş A. Which are the cut-off values of 2D-Shear Wave Elastography (2D-SWE) liver stiffness measurements predicting different stages of liver fibrosis, considering Transient Elastography (TE) as the reference method? Eur J Radiol. 2014;83(3):e118–e122
34. Dhyani M, Grajo JR, Bhan AK, Corey KE, Chung RT, Samir AE. Validation of Shear-wave Elastography Cutoff Values on the Supersonic Aixplorer for Practical Clinical Use in Liver Fibrosis Staging. Ultrasound Med Biol. 2017;43(9):1846–53
35. Baldea V, Bende F, Popescu A, Sirli R, Sporea I. Comparative study between two 2D-Shear Waves Elastography techniques for the non-invasive assessment of liver fibrosis in patients with chronic hepatitis C virus (HCV) infection. Med Ultrasound. 2021; 23(3):257-64.
36. Aksakal M, Oktar SO, Sendur HN, Esendagli G, Ozenirler S, Cindoruk M, Hizel K. Diagnostic performance of 2D shear wave elastography in predicting liver fibrosis in patients with chronic hepatitis B and C: a histopathological correlation study. Abdom Radiol (NY). 2021; 46(7):3238-44.
37. Villani R, Cavallone F, Romano AD, Bellanti F, Serviddio G. Two-Dimensional Shear Wave Elastography versus Transient Elastography: A Non-Invasive Comparison for the Assessment of Liver Fibrosis in Patients with Chronic Hepatitis C. Diagnostics (Basel). 2020; 10(5):313
38. Friedrich-Rust M, Ong MF, Martens S, Sarrazin C, Bojunga J, Zeuzem S, Herrmann E. Performance of transient elastography for the staging of liver fibrosis: a meta-analysis. Gastroenterology. 2008 Apr;134(4):960-74.
39. Marcellin P, Ziol M, Bedossa P, Douvin C, Poupon R, de Ledinghen V, Beaugrand M. Non-invasive assessment of liver fibrosis by stiffness measurement in patients with chronic hepatitis B. Liver Int. 2009; 29(2):242-7.
40. Chan HL, Wong GL, Choi PC, Chan AW, Chim AM, Yiu KK, et al. Alanine aminotransferase-based algorithms of liver stiffness measurement by transient elastography (Fibroscan) for liver fibrosis in chronic hepatitis B. J Viral Hepat. 2009; 16(1):36-44.
41. European Association for the Study of the Liver. EASL Clinical Practice Guidelines on the management of hepatitis B virus infection. J Hepatol. 2025 Aug;83(2):502-83.
42. Sporea I, Nicolita D, Sirli R, Deleanu A, Tudora A, Bota S. Assessment of noninvasive liver stiffness in inactive HBsAg carriers by transient elastography: Fibroscan in inactive HBsAg carriers. Hepat Mon. 2011; 11(3):182-5
43. Jang W, Yu SI, Sinn RH, Park SH, Park H, Park JY, et al. Longitudinal change of liver stiffness by transient elestography in chronic hepatitis B patients treated with nucleos(t)ide analogue. Clin Res Hepatol Gastroenterol. 2014; 38(2):195-200.

44. Kuo YH, Lu SN, Chen CH, Chang KC, Hung CH, Tai WC, et al. The changes of liver stiffness and its associated factors for chronic hepatitis B patients with entecavir therapy. PLoS One. 2014; 9(3):E93160.
45. Ogawa E, Furusyo N, Murata M, Ohnishi H, Toyoda K, Taniai H, et al. Longitudinal assessment of liver stiffness by transient elastography for chronic hepatitis B patients treated with nucleoside analog. Hepatol Res. 2011; 41(12):1178-88.
46. Lazar A, Sporea I, Popa A, Lupusoru R, Gherhardt D, Mare R, et al. Dynamic Changes in Liver Stiffness in Patients with Chronic Hepatitis B Undergoing Antiviral Therapy. Diagnostics (Basel). 2022; 12(11): 2646
47. Zhang X, Song J, Zhang Y, Wen B, Dai L, Xi R, et al. Baveno VII algorithm outperformed other models in ruling out high-risk varices in individuals with HBV-related cirrhosis. J Hepatol. 2023; 78(3):574-83
48. Friedrich-Rust M, Nierhoff J, Lupsor M, Sporea I, Fierbinteanu-Braticevici C, Strobel D, et al. Performance of Acoustic Radiation Force Impulse imaging for the staging of liver fibrosis: a pooled meta-analysis. J Viral Hepat. 2012; 19(2):E212-9.
49. Nierhoff J, Chavez Ortiz AA, Herrmann E, Zeuzem S, Friedrich-Rust M. The efficiency of acoustic radiation force impulse imaging for the staging of liver fibrosis: a meta-analysis. Eur Radiol. 2013; 23(11):3040-53.
50. Dong DR, Hao MN, Li C, Peng Z, Liu X, Wang GP, Ma AL. Acoustic radiation force impulse elastography, FibroScan(R), Forns' index and their combination in the assessment of liver fibrosis in patients with chronic hepatitis B, and the impact of inflammatory activity and steatosis on these diagnostic methods. Mol Med Rep. 2015; 11(6):4174-82.
51. Friedrich-Rust M, Buggisch P, de Knegt RJ, Dries V, Shi Y, Matschenz K, et al. Acoustic radiation force impulse imaging for non-invasive assessment of liver fibrosis in chronic hepatitis B. J Viral Hepat. 2013; 20(4):240-7.
52. Zhang D, Chen M, Wang R, Liu Y, Zhang D, Liu L, Zhou G. Comparison of acoustic radiation force impulse imaging and transient elastography for non-invasive assessment of liver fibrosis in patients with chronic hepatitis B. Ultrasound Med Biol. 2015; 41(1):7-14.
53. Sporea I, Sirli R, Bota S, Popescu A, Sendroiu M, Jurchis A. Comparative study concerning the value of acoustic radiation force impulse elastography (ARFI) in comparison with transient elastography (TE) for the assessment of liver fibrosis in patients with chronic hepatitis B and C. Ultrasound Med Biol. 2012; 38(8):1310-6.
54. Lu Q, Lu C, Li J, Ling W, Qi X, He D, et al. Stiffness Value and Serum Biomarkers in Liver Fibrosis Staging: Study in Large Surgical Specimens in Patients with Chronic Hepatitis B. Radiology. 2016; 280(1):290-9.
55. Ma JJ, Ding H, Mao F, Sun HC, Xu C, Wang WP. Assessment of liver fibrosis with elastography point quantification technique in chronic hepatitis B virus patients: a comparison with liver pathological results. J Gastroenterol Hepatol. 2014; 29(4):814-9.

56. Song L, Zhao L, Deng J, Luo Y, Zhang Y, Wang M, et al. Staging liver fibrosis in patients with chronic hepatitis B using two-dimensional shear wave elastography based on histopathological findings: a prospective multicenter study. Quant Imaging Med Surg. 2023;13(4):2376–87.
57. Wranke A, Serrano BC, Heidrich B, Dalekos G, Yalçin K, Tabak F et al. Antiviral treatment and liver-related complications in hepatitis delta. Hepatology. 2017;65(2):414–425.
58. European Association for the Study of the Liver. EASL clinical practice guidelines on hepatitis delta virus. J Hepatol. 2023;79(2):433–460.
59. Augustin S, Pons M, Maurice JB, Bureau C, Stefanescu H, Ney M, et al. Expanding the Baveno VI criteria for the screening of varices in patients with compensated advanced chronic liver disease. Hepatology. 2017; 66(6):1980-8.
60. by Franchis R, Baveno VIF. Expanding consensus in portal hypertension: Report of the Baveno VI Consensus Workshop: Stratifying risk and individualizing care for portal hypertension. J Hepatol. 2015; 63(3):743-52.
61. Ferraioli G, Barr RG, Berzigotti A, Sporea I, Wong VW, Reiberger T, et al. WFUMB Guideline/Guidance on Liver Multiparametric Ultrasound: Part 1. Update to 2018 Guidelines on Liver Ultrasound Elastography. Ultrasound Med Biol. 2024 Aug;50(8):1071-1087.

5.4. Elastography for Metabolic Dysfunction-Associated Steatotic Liver Disease (MASLD)

Ioan Sporea, Alexandru Popa

Abstract

Metabolic Dysfunction–Associated Steatotic Liver Disease (MASLD) has become the leading cause of chronic liver disease worldwide, driven by the global epidemic of obesity and type 2 diabetes. As liver biopsy is unsuitable for large-scale screening and follow-up, non-invasive imaging, particularly ultrasound, plays a central role in disease assessment. Multiparametric ultrasound (MPUS) integrates conventional B-mode imaging, quantitative ultrasound (QUS) techniques for steatosis quantification, and elastography for liver stiffness evaluation as a surrogate of liver biopsy. Attenuation-based parameters, backscatter-derived indices, and speed-of-sound measurements enable objective estimation of hepatic fat, while Vibration-Controlled Transient Elastography (VCTE) and Acoustic Radiation Force Impulse (ARFI)–based shear-wave elastography provide validated tools for fibrosis staging and portal hypertension risk stratification. Emerging dispersion and viscosity-related parameters show promise in reflecting necro-inflammatory activity, potentially supporting non-invasive identification of metabolic steatohepatitis (MASH). By combining fat, fibrosis, and inflammation metrics in a single session, MPUS offers a rapid, point-of-care, and scalable strategy for risk stratification, longitudinal monitoring, and reduction of biopsy need in MASLD.

5.4.1. Introduction

Steatotic liver disease is currently the most common condition encountered in hepatology. As outcomes in viral hepatitis have improved markedly—through highly effective HCV cures and long-term HBV suppression—the clinical and research focus has increasingly shifted toward metabolic liver disease, which now drives a substantial share of liver-related burden worldwide.

Recent epidemiological data estimate that roughly 30% of adults in the general population have fatty liver, with notable geographic variability (1-3). The burden is substantially higher in type 2 diabetes mellitus (T2DM) patients, where prevalence approaches two-thirds and a considerable proportion already

show clinically significant fibrosis, including a meaningful subset with advanced fibrosis—supporting the need for scalable detection and staging strategies (4).

Terminology of this condition has evolved accordingly, from Non-Alcoholic Fatty Liver Disease (NAFLD) to Metabolic Dysfunction–Associated Fatty Liver Disease (MAFLD) and, most recently, to MASLD (Metabolic Dysfunction–Associated Steatotic Liver Disease), aiming to better reflect underlying pathophysiology and clinical phenotypes (5).

Histologically, steatotic liver is defined by fat charge in more than 5% of hepatocytes. Although liver biopsy remains the reference standard for morphological assessment, its invasiveness limits its use for screening and longitudinal monitoring. Among non-invasive imaging methods, ultrasound is the most accessible and widely used, while CT entails ionizing radiation and MRI-based techniques, including MRI-PDFF (MRI Proton Density Fat Fraction), a reference standard for fat quantification, are limited by cost and availability in routine practice.

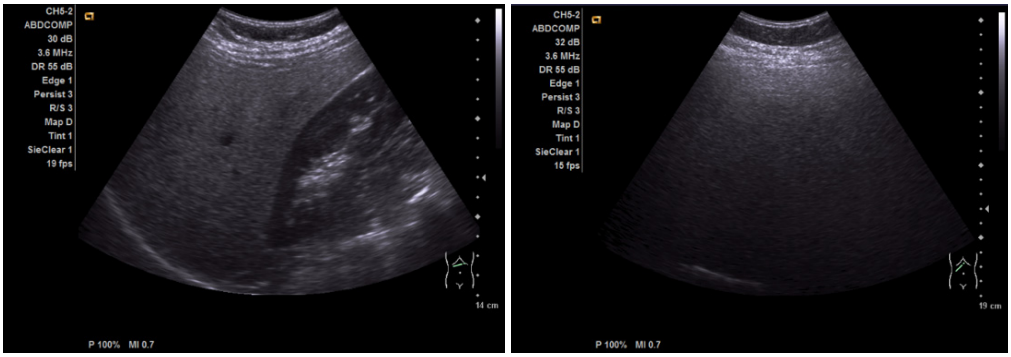
Multiparametric ultrasound (MPUS) offers a pragmatic, point-of-care approach by combining complementary ultrasound techniques within a single platform. Beyond conventional B-mode imaging, ***MPUS integrates quantitative tools for steatosis assessment*** and ***elastography-based liver stiffness*** as a surrogate for fibrosis, with emerging parameters that may capture ***viscoelastic properties***, potentially related to inflammation. By providing rapid, non-invasive assessment during a single visit, MPUS may support screening, risk stratification, and follow-up in patients with MASLD.

5.4.2. Evaluation of steatosis in MASLD patients using ultrasound

A. Conventional ultrasound

Classic B-mode ultrasound remains a pragmatic first-line tool for detecting steatosis. Fatty liver appears as a “bright” liver due to increased parenchymal echogenicity, with posterior beam attenuation and blurring of intrahepatic vessels, with increased hepato-renal index (Fig. 5.4.1). Semi-quantitative grading scales classify steatosis as mild, moderate, or severe based on these visual features. Scoring systems such as the Hamaguchi score incorporate the hepato-renal index, brightness, deep attenuation, and vessel blurring, aiming to standardize interpretation (6). A meta-analysis comparing B-mode US with liver biopsy reported sensitivities around 85% and specificities >90 % for moderate to severe steatosis, but accuracy was much lower for mild steatosis, because echogenic changes may be subtle and confounded by

fibrosis or inflammation (7). Moreover, B-mode US has limited reproducibility and a sensitivity of only 73.3% for detecting steatosis above 0–5% liver fat (7). These limitations have driven the development of quantitative ultrasound (QUS) techniques.



A B

Fig. 5.4.1. Conventional B-mode ultrasound in hepatic steatosis. (A) Increased hepato-renal index*, demonstrating the marked contrast between hyperechoic liver tissue and the relatively hypoechoic right kidney. (B) "Bright liver"—increased parenchymal echogenicity with posterior beam attenuation.*

B. Quantitative techniques

a) Controlled Attenuation Parameter (CAP)

The Controlled Attenuation Parameter (CAP) embedded in the FibroScan device (Echosens) was the first ultrasound-based quantitative tool for hepatic steatosis quantification. CAP measures the ultrasound beam attenuation (in decibels per meter) during Vibration Controlled Transient Elastography (VCTE). The technique simultaneously provides liver stiffness measurement (LSM) for fibrosis staging and CAP values (100–400 dB/m) for fat assessment (8). CAP correlates with histological steatosis grades. Meta-analyses have reported areas under the receiver operating characteristic curve (AUROC) values of 0.85–0.88 for distinguishing between steatosis grades and have suggested cutoffs around 290 dB/m, 310 dB/m, and 330 dB/m for mild (S1), moderate (S2), and severe (S3) steatosis, respectively (9, 10). A 2025 Italian single-center biopsy-based study (120 patients) compared CAP with newer multiparametric ultrasound parameters and found that, for identifying moderate-to-severe steatosis (S ≥ 2), CAP had an AUROC of 0.83 (95% CI 0.75–0.91); a cut-off of 275 dB/m yielded 94.5% sensitivity and 66.0% specificity (11). CAP's performance drops in the presence of advanced fibrosis; this

retrospective study also reported that in patients with chronic hepatitis B, CAP was less reliable for detecting steatosis when fibrosis stages were F2–F4 (12). Studies comparing CAP performed with M and XL probes suggested similar thresholds can be applied in obese and non-obese individuals, although measurement failure is more common in severe obesity (13).

b) Quantitative ultrasound (QUS)

Recently, quantitative ultrasound (QUS) has emerged as a rapidly evolving approach for the objective, point-of-care assessment of hepatic steatosis, moving beyond subjective B-mode grading. Commercial ultrasound systems implement QUS using different physical biomarkers—most commonly the ***attenuation coefficient***, ***backscatter-related parameters***, and ***speed of sound***—each reflecting distinct interactions between the ultrasound beam and liver tissue (Fig. 5.4.2) (14).

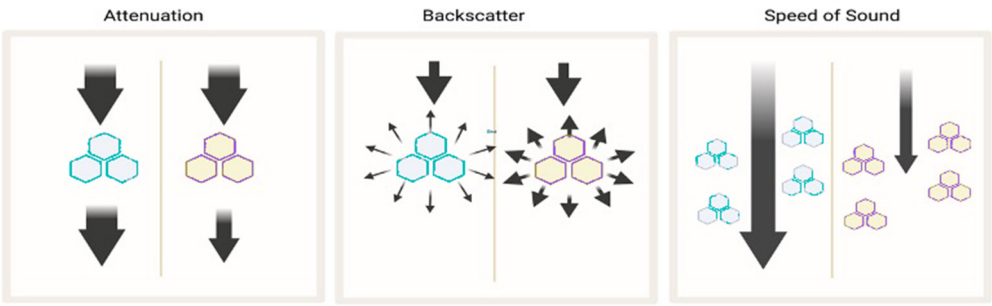


Fig. 5.4.2 (14). Schematic representation of the three principal physical parameters used in quantitative ultrasound (QUS): attenuation coefficient, backscatter coefficient, and speed of sound, each reflecting distinct interactions between the ultrasound beam and hepatic tissue

Tables 5.4.I and 5.4.II summarize the main commercially available, ultrasound-integrated QUS approaches for liver steatosis quantification, grouped into attenuation-based (AC), backscatter/scatter-derived (BSC), speed-of-sound (SoS), and multivariate fat-fraction methods. Fig. 5.4.3–5.4.5 present examples of QUS on different platforms.

Table 5.4.I The main commercially available, ultrasound-integrated QUS approaches for liver steatosis quantification.

Attenuation-based techniques (AC)		
Vendor / platform	**Commercial feature name**	**Output**
Canon (Aplio)	**ATI – Attenuation Imaging**	dB/cm/MHz
GE HealthCare (LOGIQ)	**UGAP – Ultrasound-Guided Attenuation Parameter**	dB/cm/MHz
Samsung Medison	**TAI – Tissue Attenuation Imaging**	dB/cm/MHz
Supersonic Imagine / Hologic (Aixplorer MACH)	**Att PLUS – Attenuation PLUS**	dB/cm/MHz
FUJIFILM/Hitachi (ARIETTA)	**iATT – Attenuation Measurement**	dB/cm/MHz
Mindray	**USAT – Ultrasound Attenuation Analysis**	dB/cm/MHz
Philips	**LFQ – Liver Fat Quantification**	dB/cm/MHz
Esaote	**QAI – Q-Attenuation Imaging**	dB/cm/MHz
Speed-of-Sound techniques (SoS)		
Supersonic Imagine Hologic (Fig. 4)	**SSp PLUS – Sound Speed PLUS**	m/s
Mindray	**SSI – Sound Speed Index**	m/s

Table 5.4.II Ultrasound-integrated QUS approaches for liver steatosis quantification using multivariate methods.

Multivariate methods using AC ± backscatter ± other QUS features			
Vendor / platform	**Commercial name**	**Uses**	**Output**
Siemens Healthineers	**UDFF – Ultrasound-Derived Fat Fraction**	Uses AC + backscatter-related features	% fat fraction
GE HealthCare	**UGFF – Ultrasound-Guided Fat Fraction** (Fig. 5)	Integrates Attenuation + backscatter coefficient + signal-to-noise ratio	% fat fraction

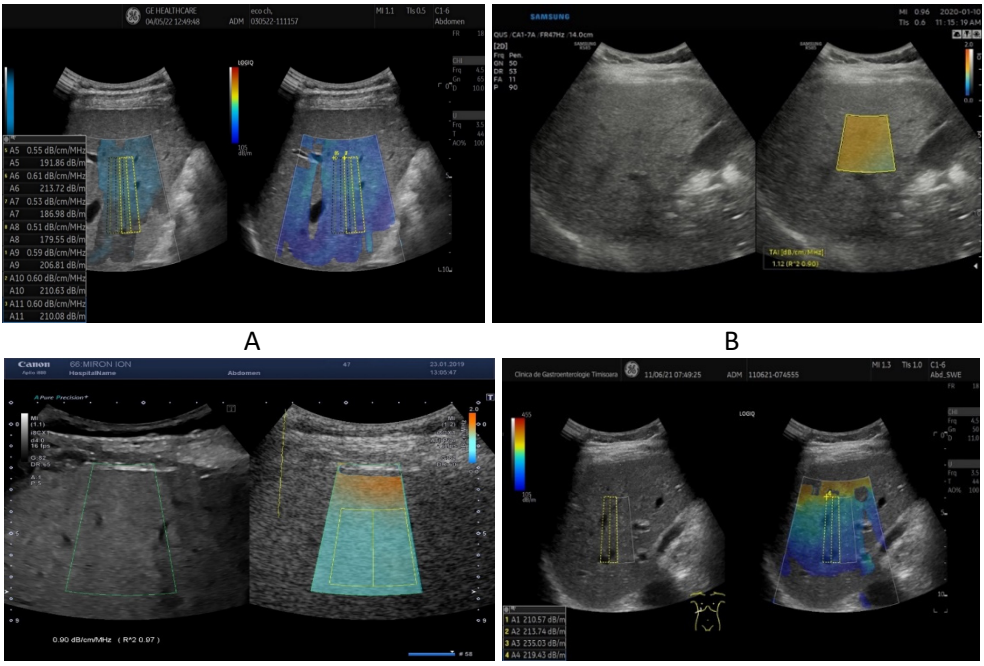


Fig. 5.4.3. Representative vendor implementations of attenuation‑based liver fat quantification: (A) ultrasound‑guided attenuation parameter (UGAP, GE LOGIQ); (B) tissue attenuation imaging (TAI, Samsung); (C) attenuation imaging (ATI, Canon); and (D) combined Att PLUS and Sound‑Speed PLUS measurements (Hologic/Aixplorer). Each panel shows ROI placement and decibel/centimeter/megahertz outputs for hepatic fat estimation.

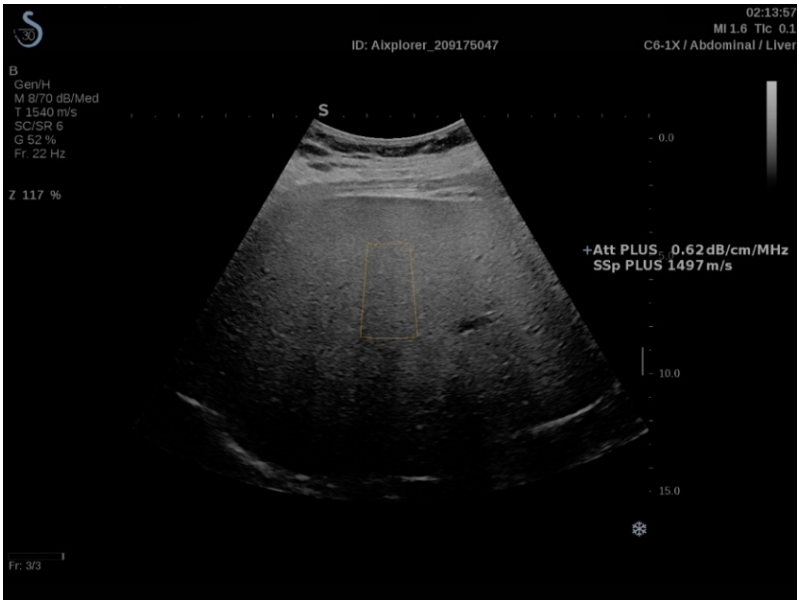


Fig. 5.4.4. Combined attenuation and sound-speed measurement (Att PLUS + SSp PLUS, Hologic/Aixplorer), illustrating speed-of-sound estimation and its integration with attenuation quantification

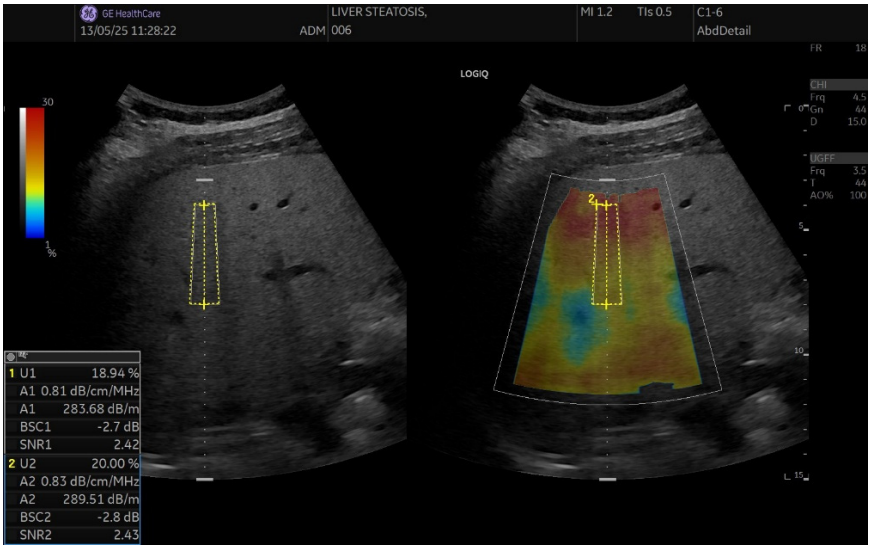


Fig. 5.4.5. Examples of multivariate approaches that integrate attenuation and backscatter features: The ultrasound-guided fat fraction (UGFF) *module displays a fat fraction map overlaid on B-mode images and provides quantitative percentage outputs.*

5.4.3. Liver fibrosis evaluation using ultrasound in patients with MASLD

A. Vibration-controlled transient elastography (VCTE)

Patients with liver steatosis can have their liver fibrosis assessed immediately after their hepatic steatosis, using ultrasound-based methods to measure liver stiffness. Although liver stiffness is correlated with liver fibrosis, assessments of stiffness may be impacted by other factors, excepting fibrosis, including right heart failure, increased aminotransferases, extrahepatic cholestasis, or non-fasting status. These confounding variables may lead to an overestimation of fibrosis severity. To ensure that the results are taken into account within the proper clinical context, we advocate that only trained personnel who also know the patient's history should perform this assessment.

Early elastography studies compared stiffness measurements with liver biopsy, stratifying results by fibrosis stages on the METAVIR scale (F1–F4). More recently, however, hepatologists adopted the concept of compensated advanced chronic liver disease (cACLD) introduced in the Baveno VI consensus. This terminology shifts attention away from minor distinctions between absent or mild fibrosis (F0–F1) and instead focuses on differentiating significant fibrosis, advanced fibrosis, and cirrhosis.

In practice, **shear waves ultrasound-based elastographic methods (SWE)** are used for liver fibrosis evaluation. There are two main SWE categories: Vibration-Controlled Transient Elastography (VCTE), which delivers an external mechanical pulse at low frequency, and Acoustic Radiation Force Impulse (ARFI) techniques, in which the transducer itself generates the stimulus that deforms the liver. ARFI methods include point SWE (pSWE) and two-dimensional SWE (2D‑SWE). VCTE outputs are expressed in kilopascals (kPa), while ARFI systems report shear-wave velocity in m/s or convert it to kPa (15, 16).

Feasibility exceeds 90% for most elastographic methods. VCTE requires in adults two probes—an M probe and an XL probe for obese patients—and cannot be used in the presence of ascites. Routine calibration of VCTE probes adds cost. Across all elastography techniques, the ratio of interquartile range to median (IQR/median) should be below 30 % to ensure reliability; 2D-SWE systems incorporate their own quality metrics. Many ultrasound platforms now provide both pSWE and 2D-SWE. Having dual modules is advantageous: if 2D-SWE is sometimes not feasible or offers unreliable results according to the quality criteria, pSWE often yields interpretable results, ensuring that patients still receive a valid stiffness measurement.

VCTE is available in both FibroScan and FibroTouch devices. Comparative research, such as the study by Xu et al., demonstrated equivalent performance between these systems (17). In a prospective cohort of 435 patients with chronic liver disease who underwent biopsy, the AUROC values for detecting significant fibrosis, severe fibrosis, and cirrhosis were similar for FibroTouch and FibroScan (17). The correlation between stiffness measurements was strong ($r = 0.85$, $p < 0.001$), and there were no significant differences in sensitivity, specificity, negative predictive value, positive predictive value, or overall diagnostic accuracy (17).

Multiple studies and meta-analyses have proposed cutoff values for VCTE, accounting for underlying etiology. Recent Baveno VI and Baveno VII consensus statements advocate a simplified "rule of 5" classification of stiffness measurements, helping clinicians stratify patients more easily according to severity of disease (18, 19).

Below is a visual representation of the ***Liver Stiffness Measurement (LSM) scale*** based on the Baveno VI and VII consensus statements (Fig. 5.4.6). The diagram illustrates the "rule of five" cutoffs (5-10-15-20-25 kPa) that the guidelines use to stratify risk and guide management. According to Baveno VII, LSM < 10 kPa rules out compensated advanced chronic liver disease (cACLD); values ≥ 15 kPa are highly suggestive of cACLD; and ≥ 25 kPa are sufficient to rule in clinically significant portal hypertension (CSPH) in patients with cACLD. The scale also notes that LSM ≤ 15 kPa together with a platelet count ≥ 150×10^9/L rules out CSPH, whereas LSM values of 20–25 kPa combined with low platelets (≤ 150×10^9/L) or 15–20 kPa with very low platelets (≤ 110×10^9/L) indicate a high probability of CSPH.

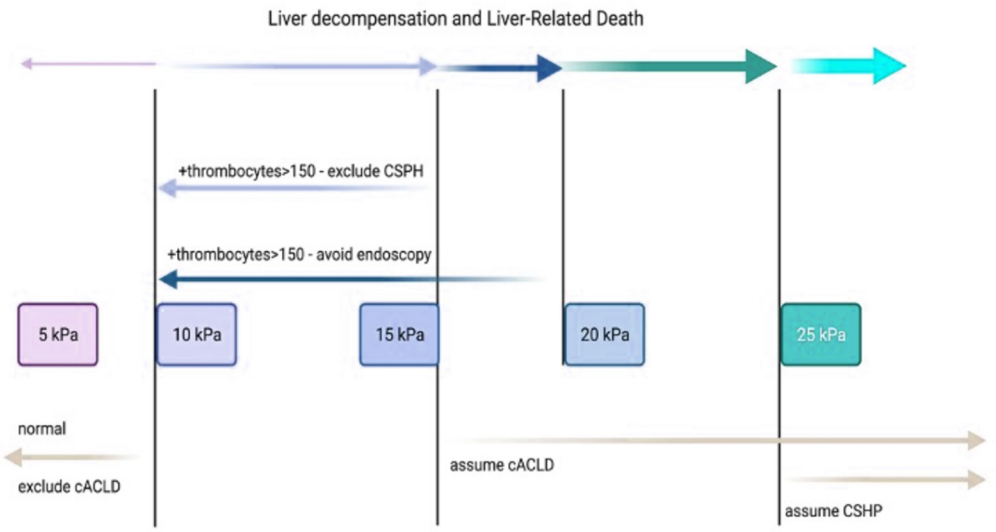


Fig. 5.4.6. Rule ‑of ‑five diagram (5–10–15–20–25 kPa) modified from the Baveno VII consensus showing how VCTE thresholds stratify normal liver, exclude compensated advanced chronic liver disease (cACLD), suggest cACLD, and indicate clinically significant portal hypertension (CSPH); annotations highlight the role of platelet count and recommend when to avoid endoscopy.

How to use this scale in practice:

- ***Normal (< 5 kPa):*** liver stiffness values under 5 kPa indicate a normal liver parenchyma.
- ***LSM < 10 kPa:*** this threshold effectively excludes cACLD; patients with ongoing liver injury should be monitored, but advanced fibrosis is unlikely.
- ***LSM 10–15 kPa:*** these values correspond to “probable cACLD”; repeat measurements and additional tests (e.g., fibrosis markers) are recommended.
- ***LSM 15–20 kPa:*** values ≥ 15 kPa are highly suggestive of cACLD; however, LSM ≤ 15 kPa with platelets ≥ 150×10^9/L rules out CSPH, emphasizing the combined use of stiffness and platelet count.
- ***LSM 20–25 kPa:*** this zone denotes increasing risk of CSPH. Patients with 20–25 kPa and platelets < 150×10^9/L or 15–20 kPa and platelets < 110×10^9/L have a ≥60% risk of CSPH and should be considered for endoscopic evaluation.

- ***LSM ≥ 25 kPa:*** this cutoff rules in CSPH with high specificity and positive predictive value. Such patients are at substantial risk of variceal bleeding and decompensation and should be managed accordingly.

B. ARFI (Acoustic Radiation Force Impulse) techniques

Acoustic Radiation Force Impulse (ARFI)–based shear-wave elastography (SWE) has the major advantage of being embedded in standard diagnostic ultrasound systems. This enables a comprehensive, single-session workflow that combines conventional B-mode assessment, Doppler evaluation, liver fat quantification, and liver stiffness measurement. In addition, when a focal liver lesion is identified during the same examination, contrast-enhanced ultrasound (CEUS) can be performed immediately, further consolidating the multiparametric ultrasound (MPUS) concept in routine practice (20-25).

Although vendor implementations differ in user interface, quality metrics, and reporting formats, all ARFI techniques share the same physical principle: a focused ultrasound "push" pulse generated by the transducer induces localized tissue displacement, generating shear waves whose propagation speed is measured and converted into stiffness values. ARFI methods are generally categorized as **point SWE (pSWE)**—providing a single numeric estimate within a small ROI (Table 5.4.III)—and **two-dimensional SWE (2D-SWE)**—providing a color-coded stiffness map (elastogram) over a larger sampling box, with quantitative readouts obtained from a selected ROI (Table 5.4.IV). Table 2 illustrates representative pSWE and 2D-SWE implementations across vendors.

From a practical standpoint, ARFI-based SWE is easy to implement and mirrors the patient positioning used for VCTE. The patient is examined in the supine position with the right arm maximally abducted to widen the intercostal spaces. The transducer is placed intercostally to obtain an optimal acoustic window in the right liver lobe, aiming for the clearest B-mode image and avoiding large vessels and bile ducts.

For **pSWE**, a small measurement box (commonly around ***10 × 5 mm***) is positioned **1–*2 cm below the liver capsule***, targeting a homogeneous parenchymal area and carefully avoiding vascular structures. The patient is asked to hold the breath in a neutral position (brief apnea), and the system acquires ***5–10 valid measurements***, with the ***median*** reported as the final result.

For **2D-SWE**, a larger sampling box (approximately ***3 × 2 cm***) is placed in a similar subcapsular location. Several short cine loops are acquired; a region

of interest (ROI) is then positioned within the elastogram in each loop to extract quantitative values. In routine settings, ***3–5 valid measurements*** are typically sufficient, and the system reports the ***median*** stiffness value (16). Because 2D-SWE provides a color-coded elastogram, it also allows visual assessment of measurement stability and facilitates ROI placement in the most reliable (homogeneous) parenchymal region.

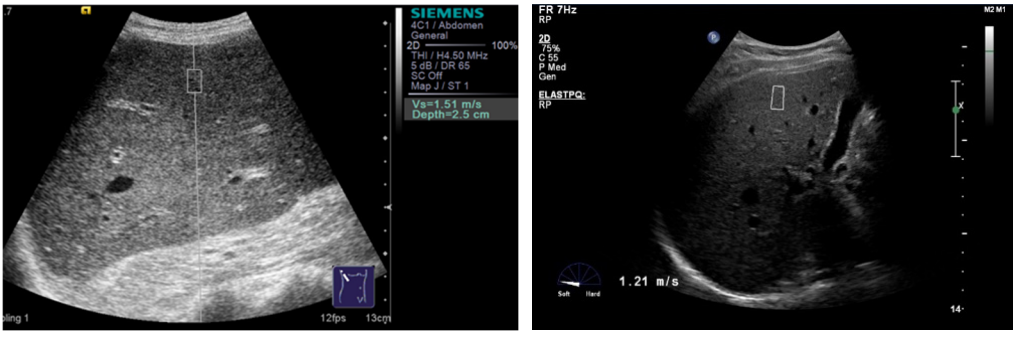
Vendor-specific cut-offs historically complicated the interpretation of ARFI stiffness values. To support harmonized clinical use, Barr and colleagues proposed a simplified algorithm—the **"Rule of 4"**—to interpret ARFI-based stiffness values, particularly in patients with viral hepatitis and NAFLD/MASLD (26).

The recommended thresholds are

- **≤ 5 kPa (≈ 1.3 m/s):** high likelihood of a normal liver.
- **< 9 kPa (≈ 1.7 m/s):** cACLD is unlikely in the absence of other clinical signs; if clinical suspicion persists, additional testing may be required.
- ***9–13 kPa (≈ 1.7–2.1 m/s):*** possible cACLD; confirmatory tests are recommended.
- ***> 13 kPa (≈ 2.1 m/s):*** cACLD is ruled in.
- ***> 17 kPa (≈ 2.4 m/s):*** suggestive of clinically significant portal hypertension (CSPH).

Table 5.4.III – Main types of pSWE, proprietary techniques, and measurement output according to the vendor

Point shear-wave elastography (pSWE / ARFI point SWE)		
Vendor / platform	**Commercial feature name**	**Output**
Siemens Healthineers (ACUSON) (Fig. 5.4.7.A)	**VTQ– Virtual Touch Quantification**	m/s (± kPa)
Philips (EPIQ / Affiniti) (Fig. 5.4.7.B)	**ElastPQ – Point Quantification**	m/s (± kPa)
Samsung Medison	**S-SWE – S-shear wave elastography**	kPa (± m/s) + reliability index
Mindray	**STQ – Sound Touch Quantification**	m/s (± kPa)
FUJIFILM / Hitachi (ARIETTA)	**SWM – Shear Wave Measurement**	m/s (± kPa) + reliability index
Esaote	**QElaXto (pSWE)**	m/s (± kPa)
GE HealthCare (LOGIQ)	**pSWE (point SWE module)**	m/s (± kPa)
Canon Medical (Aplio)	**pSWE (point SWE module)**	m/s (± kPa)

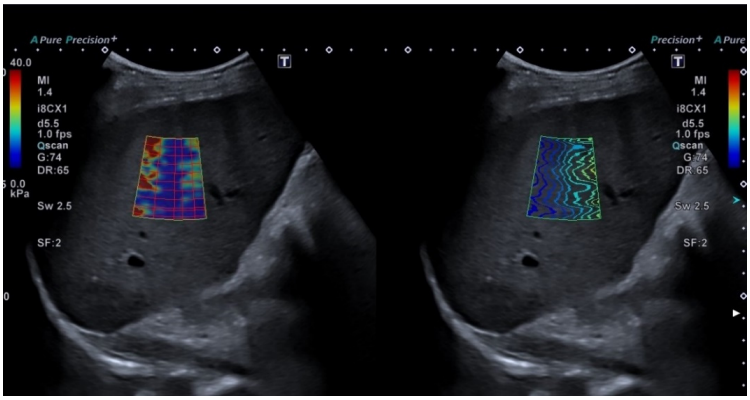


A B

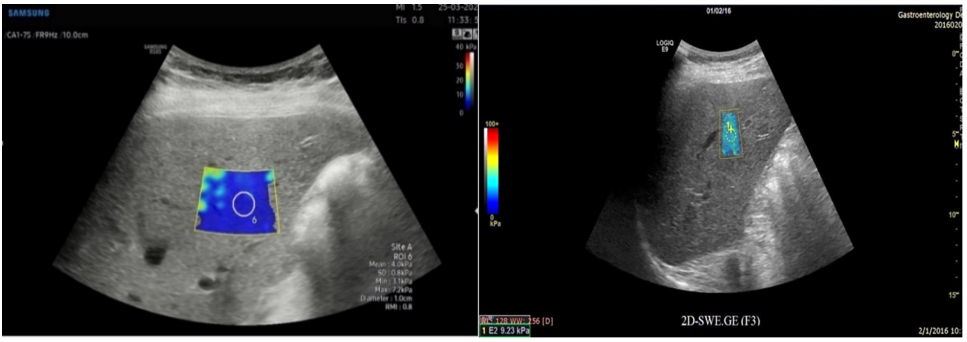
Fig. 5.4.7. Vendor examples of pSWE measurements: A- Virtual Touch Quantification (VTQ) on Siemens ACUSON. B- ElastPQ on Philips EPIQ, showing small ROIs placed 1–2 cm below the liver capsule and corresponding shear ‑wave velocity or kiloPascal values.

Table 5.4.III – Main types of 2D-SWE, proprietary techniques, and measurement output according to the vendor

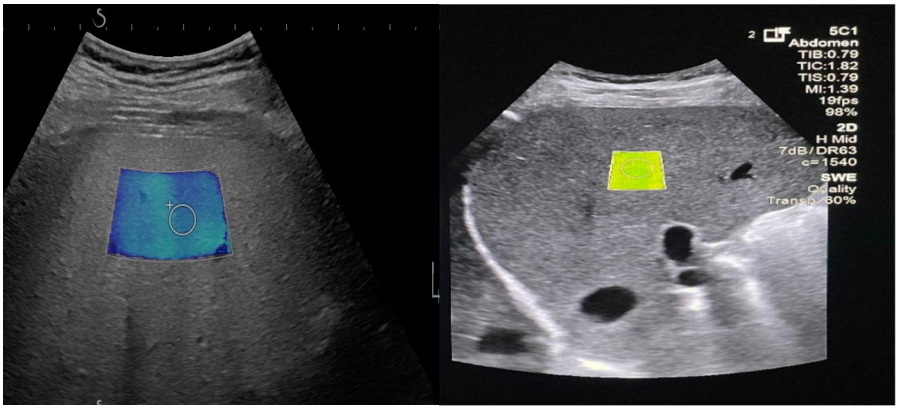
Two-dimensional shear-wave elastography (2D-SWE / ARFI 2D SWE)		
Vendor / platform	**Commercial feature name**	**Output**
Siemens Healthineers (ACUSON)	**VTIQ – Virtual Touch IQ**	m/s (± kPa) + elastogram / quality map
Philips (EPIQ / Affiniti)	**ElastQ Imaging (2D-SWE)**	kPa (± m/s) + confidence map
GE HealthCare (LOGIQ) (Fig. 5.4.8.C)	**2D-SWE (Shear Wave Elastography)**	kPa (± m/s) + quality tools
Canon Medical (Aplio) (Fig. 5.4.8.A)	**2D-SWE (with propagation / quality control)**	kPa (± m/s) + propagation map
Samsung Medison (Fig. 5.4.8.B)	**2D-SWE (SWE module)**	kPa (± m/s) + quality map
Mindray	**STE – Sound Touch Elastography**	kPa (± m/s) + elastogram
FUJIFILM/Hitachi (ARIETTA) (Fig. 5.4.8.E)	**2D-SWE (SWE module)**	kPa (± m/s) + elastogram
Esaote	**QElaXto 2D**	kPa (± m/s) + elastogram
Supersonic Imagine / Hologic (Aixplorer) (Fig. 5.4.8.D)	**ShearWave Elastography (SWE)**	kPa (± m/s) + elastogram



A



B C



D E

Fig. 5.4.8. Two‑dimensional shear‑wave elastography (2D‑SWE) methods. Color-coded elastograms and quality maps from various 2D‑SWE platforms, including Canon Medical (with propagation map) (A), Samsung (S‑SWE module) (B), GE (Shear Wave Elastography) (C), Hologic/Aixplorer (ShearWave Elastography) (D), Hitachi (2D‑SWE module) (E). Each panel demonstrates real‑time stiffness mapping and ROI placement for quantitative liver stiffness assessment.

5.4.4. Liver inflammation assessment

In patients with fatty liver disease, prognosis is driven not only by the presence of advanced fibrosis but also by the degree of necroinflammatory activity and hepatocyte ballooning (27). Although liver biopsy remains the reference standard for assessing these histological features, its invasive nature and limited feasibility make it impractical at the population level, particularly given the global burden of steatotic liver disease. Consequently, in recent years, ultrasound manufacturers and research groups have increasingly focused on techniques aimed at capturing the ***viscoelastic properties*** of liver tissue, which may reflect inflammatory activity. If inflammation could be assessed alongside steatosis and fibrosis within the same examination, ultrasound would evolve into a *truly multiparametric modality for comprehensive MASLD evaluation*.

Clinically, patients with isolated steatosis generally have a more favorable course than those with steatohepatitis—now termed ***metabolic dysfunction–associated steatohepatitis (MASH)***—*which* carries a higher risk of progression to advanced fibrosis and cirrhosis. Therefore, a reliable ***non-invasive tool*** able to detect inflammatory activity (and to support differentiation between simple steatosis and MASH) could substantially improve clinical triage and monitoring, reducing reliance on liver biopsy. At present, however, only a limited number of manufacturers and publications address inflammation using dedicated ultrasound-derived parameters.

Using the VCTE-based iLivTouch platform, Gao F et al. evaluated radiofrequency (RF) and raw data features in 259 patients with biopsy-proven NAFLD and identified two parameters that were combined into a QUS score (28). This score showed a moderate ability to discriminate NASH, with an AUROC of 0.798 (95% CI 0.731–0.865) in the training set and 0.816 (95% CI 0.725–0.906) in the validation cohort (28).

Beyond VCTE-type systems, several studies have examined inflammation-related metrics derived from 2D-SWE–based platforms. Sugimoto K et al. studied 120 patients undergoing liver biopsy for suspected steatotic liver disease, with histology graded by an expert pathologist according to the NASH Clinical Research Network criteria (29). The authors assessed 2D-SWE–derived parameters—including ***dispersion slope***, *attenuation coefficient, and shear-wave speed*—for their ability to characterize inflammation, steatosis, fibrosis, and NASH. Dispersion slope performed particularly well for grading lobular inflammation, with AUCs of 0.95 for mild (A1), 0.81 for moderate (A2), and 0.85 for marked (A3) inflammation. In the same study, the attenuation

coefficient (steatosis) achieved AUROCs of 0.88 for S1, 0.86 for S2, and 0.79 for S3, while liver stiffness showed AUROCs of 0.88 for F2, 0.90 for F3, and 0.95 for F4 fibrosis. When dispersion slope, attenuation coefficient, and SWE were combined, the AUC for diagnosing NASH was 0.81 (29).

Similarly, Lee DH et al. investigated ***shear-wave dispersion slope (SWDS),*** expressed in m/s/kHz, derived from 2D-SWE in 102 patients with biopsy-confirmed steatotic liver disease. SWDS was able to identify lobular inflammatory activity across grades 1 to 3, with AUROCs of 0.89, 0.85, and 0.78, respectively, demonstrating the highest performance for mild inflammatory activity (30).

More recently, Jang JK et al. performed a prospective multicenter study including 132 patients with biopsy-confirmed fatty liver and evaluated a multiparametric ultrasound strategy incorporating attenuation coefficient (AC) from ATI, liver stiffness, and dispersion slope (DS) from 2D-SWE (31). They proposed a simple risk score by summing unweighted scores of AC and DS, which demonstrated high diagnostic performance for NASH, with an AUROC of 0.94 (95% CI 0.89–0.98; $p<0.05$) (31).

Another approach to inflammation assessment has been explored with ***Viscosity Plane-wave UltraSound (Vi.PLUS)***. In a cohort of 204 subjects who did not undergo liver biopsy (32), Vi.PLUS values were associated with body mass index and liver stiffness measured on the same Hologic ultrasound platform in multivariate regression analyses. While these findings support biological plausibility and technical feasibility, the absence of histological reference limits conclusions regarding diagnostic accuracy for inflammation (32).

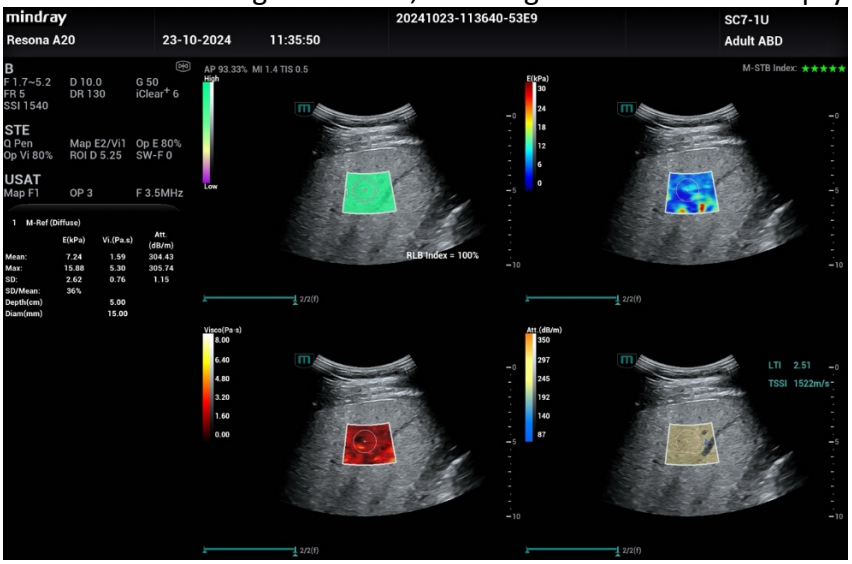
Overall, although early data suggest that ultrasound-derived dispersion- and viscosity-related metrics may capture aspects of inflammatory activity, evidence remains limited and further validation is required. Nevertheless, the direction of development is clinically relevant: ***combining modules*** for ***steatosis quantification***, ***fibrosis/stiffness estimation***, and ***inflammation-related viscoelastic assessment*** within a single ultrasound system would enable a practical MPUS framework for MASLD, with *particular value in non-invasive differentiation between simple steatosis and MASH*, as well as longitudinal follow-up (33).

To simultaneously quantify steatosis, fibrosis and inflammation in a single session, manufacturers are moving towards **multiparametric ultrasound (MPUS)**. This approach combines attenuation-based and sound-speed imaging for steatosis, shear-wave elastography for stiffness, and emerging viscosity or

dispersion measurements for inflammation (33). For example, ***plane-wave systems*** that include *Attenuation Plus* and *Sound Speed-Plus* modules measure liver steatosis, while *ShearWave-PLUS* quantifies stiffness, while *Viscosity-PLUS* derives the shear-wave dispersion slope to reflect necro-inflammation (34).

Clinical studies show that adding viscosity improves disease stratification: multiparametric ultrasound can noninvasively assess steatosis, inflammation, fibrosis, and liver viscosity markedly improves identification of metabolic-associated steatohepatitis (MASH). A 2021 multicenter study combined liver stiffness, attenuation coefficient, and dispersion slope into a *LAD-NASH* score and achieved an AUC of 0.86–0.88 in derivation and validation cohorts for identifying high-risk MASH, potentially avoiding 59% of biopsies (35).

More broadly, expert reviews note that a multiparametric US exam can include B-mode imaging, liver stiffness evaluation, quantitative fat measurement, and dispersion imaging, offering a rapid and relatively inexpensive assessment of chronic liver disease. Early research into shear-wave dispersion indicates that viscosity measurements correlate better with necroinflammatory activity than do stiffness values, suggesting they may help discriminate MASH from simple steatosis. Although only a handful of high-end systems currently offer all three modules (Fig. 9), these studies illustrate how simultaneous measurement of fat, stiffness, and viscosity could enhance the noninvasive characterization of metabolic dysfunction–associated steatotic liver disease and refine triage decisions, reducing reliance on liver biopsy.

A 

B



Fig. 5.4.9. Multiparametric ultrasound assessment of steatosis, fibrosis, and inflammation.

Mindray Resona A20 outputs: (A) simultaneous acquisition of B‑mode imaging, shear‑wave elastography (elasticity), viscosity map (Vi.PLUS) and attenuation map (USAT) from the same liver region; (B) radar plot summarizing median attenuation, viscosity, and elasticity values across steatosis stages (S0–S3) and inflammatory grades (G0–G3), enabling integrated evaluation of hepatic fat, stiffness, and necro‑inflammatory activity.

References

1. Younossi Z, Koenig A, Abdelatif D, Fazel Y, Henry L, Wymer M. Global Epidemiology of Nonalcoholic Fatty Liver Disease—Meta-Analytic Assessment of Prevalence, Incidence, and Outcomes. Hepatology 2016, 64, 73–84

2. Younossi Z, Golabi P, Paik J, Henry A, Van Dongen C, Henry L. The Global Epidemiology of Nonalcoholic Fatty Liver Disease (NAFLD) and Nonalcoholic Steatohepatitis (NASH): A Systematic Review. Hepatology 2023, 77, 1335–47

3. Younossi Z, Golabi P, de Avila L, Paik J, Srishord M, Fukui N, et al. The Global Epidemiology of NAFLD and NASH in Patients with Type 2 Diabetes: A Systematic Review and Meta-Analysis. J. Hepatol. 2019, 71, 793–801,

4. En Li Cho E, Ang C, Quek J, Fu C, Lim L, Heng Z, et al . Global Prevalence of Non-Alcoholic Fatty Liver Disease in Type 2 Diabetes Mellitus: An Updated Systematic Review and Meta-Analysis. Gut 2023, 72, 2138–2148.
5. Rinella M, Lazarus J, Ratziu V, Francque S, Sanyal A, Kanwal F, et al. A Multisociety Delphi Consensus Statement on New Fatty Liver Disease Nomenclature. Hepatology 2023, 78, 1966–86.
6. Hamaguchi M, Kojima T, Itoh Y, Harano Y, Fujii K, Nakajima T, et al. The Severity of Ultrasonographic Findings in Nonalcoholic Fatty Liver Disease Reflects the Metabolic Syndrome and Visceral Fat Accumulation. Am. J. Gastroenterol. 2007, 102, 2708–15
7. Hernaez R, Lazo M, Bonekamp S, Kamel I, Brancati F, Guallar E, et al. Diagnostic Accuracy and Reliability of Ultrasonography for the Detection of Fatty Liver: A Meta-Analysis. Hepatology 2011, 54, 1082–90.
8. Ferraioli G. Quantitative Assessment of Liver Steatosis Using Ultrasound Controlled Attenuation Parameter (Echosens). Journal of Medical Ultrasonics 2021, 48, 489–95.
9. Lupsor-Platon M, Feier D, Stefănescu H, Tamas A, Botan E, Sparchez Z et al. Diagnostic Accuracy of Controlled Attenuation Parameter Measured by Transient Elastography for the Non-Invasive Assessment of Liver Steatosis: A Prospective Study. Journal of Gastrointestinal and Liver Diseases 2015, 24, 35–42.
10. Karlas T, Petroff D, Sasso M, Fan J, Mi Y, de Lédinghen V et al. Individual Patient Data Meta-Analysis of Controlled Attenuation Parameter (CAP) Technology for Assessing Steatosis. J. Hepatol. 2017, 66, 1022–30.
11. Liguori A, Ainora M, Gialleonardo L, Viceconti N, Petrucci L, Esposto G, et al. Multiparametric Ultrasound for Non-Invasive Assessment of Liver Steatosis, Fibrosis, and Inflammation in Metabolic Dysfunction-Associated Steatotic Liver Disease. World J. Gastroenterol. 2025, 31, 105518.
12. Park HJ, Kang HJ, Kim SY, Yoon S, Baek S, Song IH, et al. Effects of Hepatic Fibrosis on the Quantification of Hepatic Steatosis Using the Controlled Attenuation Parameter in Patients with Chronic Hepatitis B. Ultrasonography 2024, 44, 83–91.
13. Chan WK, Nik Mustapha NR, Mahadeva S, Wong VWS, Cheng JYK, Wong GLH. Can the Same Controlled Attenuation Parameter Cut-Offs Be Used for M and XL Probes for Diagnosing Hepatic Steatosis? J. Gastroenterol. Hepatol. 2018, 33, 1787–94.
14. Park J, Lee JM, Lee G, Jeon SK, Joo I. Quantitative Evaluation of Hepatic Steatosis Using Advanced Imaging Techniques: Focusing on New Quantitative Ultrasound Techniques. Korean J. Radiol. 2022, 23, 13–29.
15. Dietrich CF, Bamber J, Berzigotti A, Bota S, Cantisani V, Castera L, et al. EFSUMB Guidelines and Recommendations on the Clinical Use of Liver Ultrasound Elastography, Update 2017 (Long Version). Ultraschall in der Medizin 2017. Aug;38(4):e16-e47
16. Cosgrove D, Piscaglia F, Bamber J, Bojunga J, Correas J, Gilja OH, et al. EFSUMB Guidelines and Recommendations on the Clinical Use of Ultrasound Elastography part 2: Clinical Applications. Ultraschall in der Medizin 2013, 34, 238–53.

17. Xu Y, Liu Y, Cao Z, Wang L, Li Z, Sheng Z, et al. Comparison of FibroTouch and FibroScan for staging fibrosis in chronic liver disease: Single-center prospective study. Dig Liver Dis. 2019 Sep;51(9):1323-1329.
18. de Franchis R, Bosch J, Garcia-Tsao G, Reiberger T, Ripoll C. Baveno VII - Renewing Consensus in Portal Hypertension. J. Hepatol. 2022, 76, 959–74.
19. de Franchis, R. Expanding Consensus in Portal Hypertension: Report of the Baveno VI Consensus Workshop: Stratifying Risk and Individualizing Care for Portal Hypertension. J. Hepatol. 2015, 63, 743–52.
20. Cassinotto C, Boursier J, de Lédinghen V, Lebigot J, Lapuyade B, et al. Liver Stiffness in Nonalcoholic Fatty Liver Disease: A Comparison of Supersonic Shear Imaging, FibroScan, and ARFI with Liver Biopsy. Hepatology 2016, 63, 1817–27.
21. Lefebvre T, Wartelle-Bladou C, Wong P, Sebastiani G, Giard JM, Castel H, et al. Prospective Comparison of Transient, Point Shear Wave, and Magnetic Resonance Elastography for Staging Liver Fibrosis. Eur. Radiol. 2019, 29, 6477–88.
22. Xiao G, Zhu S, Xiao X, Yan L, Yang J, Wu G. Comparison of Laboratory Tests, Ultrasound, or Magnetic Resonance Elastography to Detect Fibrosis in Patients with Nonalcoholic Fatty Liver Disease: A Meta-Analysis. Hepatology 2017, 66, 1486–1501.
23. Furlan A, Tublin M, Yu L, Chopra K, Lippello A, Behari J. Comparison of 2D Shear Wave Elastography, Transient Elastography, and MR Elastography for the Diagnosis of Fibrosis in Patients With Nonalcoholic Fatty Liver Disease. AJR Am. J. Roentgenol. 2020, 214, W20–W26.
24. Selvaraj E, Mózes F, Jayaswal A, Zafarmand M, Vali Y, Lee J, et al. Diagnostic Accuracy of Elastography and Magnetic Resonance Imaging in Patients with NAFLD: A Systematic Review and Meta-Analysis. J. Hepatol. 2021, 75, 770–85.
25. Imajo K, Honda Y, Kobayashi T, Nagai K, Ozaki A, Iwaki M, et al. Direct Comparison of US and MR Elastography for Staging Liver Fibrosis in Patients With Nonalcoholic Fatty Liver Disease. Clin. Gastroenterol. Hepatol. 2022, 20, 908-17.e11.
26. Barr R, Wilson S, Rubens D, Garcia-Tsao G, Ferraioli G. Update to the Society of Radiologists in Ultrasound Liver Elastography Consensus Statement. Radiology 2020, 296, 263–74
27. Raeman R. Inflammation: The Straw That Broke the NAFLD Liver! Cell. Mol. Gastroenterol. Hepatol. 2022, 13, 1273–74.
28. Gao F, He Q, Li G, Huang OY, Tang LJ, Wang XD, et al. A Novel Quantitative Ultrasound Technique for Identifying Non-Alcoholic Steatohepatitis. Liver International 2022, 42, 80–91.
29. Sugimoto K, Moriyasu F, Oshiro H, Takeuchi H, Abe M, Yoshimasu Y, et al. The Role of Multiparametric US of the Liver for the Evaluation of Nonalcoholic Steatohepatitis. Radiology 2020, 296, 532–40.
30. Lee DH, Cho EJ, Bae JS, Lee JY, Yu SJ, Kim H, et al. Accuracy of Two-Dimensional Shear Wave Elastography and Attenuation Imaging for Evaluation of Patients With Nonalcoholic Steatohepatitis. Clin. Gastroenterol. Hepatol. 2021, 19, 797-805.e7.

31. Jang JK, Lee ES, Seo JW, Kim YR, Kim SY, Cho YY, Lee DH. Two-Dimensional Shear-Wave Elastography and US Attenuation Imaging for Nonalcoholic Steatohepatitis Diagnosis: A Cross-Sectional, Multicenter Study. Radiology 2022, 305, 118–16.
32. Popa A, Sporea I, Bende F, Popescu A, Fofiu R, Borlea A, et al. The Non-Invasive Ultrasound-Based Assessment of Liver Viscosity in a Healthy Cohort. Diagnostics 2022, 12, 1451.
33. Barr RG. Multiparametric Ultrasound for Chronic Liver Disease. Radiol. Clin. North Am. 2025, 63, 13–28.
34. Popa A, Bende F, Șirli R, Popescu A, Bâldea V, Lupușoru R, et al. Quantification of Liver Fibrosis, Steatosis, and Viscosity Using Multiparametric Ultrasound in Patients with Non-Alcoholic Liver Disease: A “Real-Life” Cohort Study. Diagnostics 2021, 11, 783.
35. Sugimoto K, Lee DH, Lee JY, Yu SJ, Moriyasu F, Sakamaki K, et al. Multiparametric US for Identifying Patients with High-Risk NASH: A Derivation and Validation Study. Radiology 2021, 301, 625–34.

5.5. The Role of Liver Elastography in Alcohol-Related Liver Disease

Camelia Nica, Alina Popescu

Abstract

Alcohol-related liver disease (ALD) is a leading cause of advanced chronic liver disease worldwide and remains a major driver of liver-related morbidity and mortality. Disease progression ranges from steatosis to steatohepatitis and cirrhosis, with the fibrosis stage representing the principal determinant of prognosis. Accurate fibrosis assessment is therefore central to risk stratification and clinical decision-making. While liver biopsy has historically been the reference standard, its invasiveness and limitations have accelerated the development of noninvasive alternatives.

Over the past decade, elastography has emerged as a pivotal modality in the evaluation of ALD. Vibration-controlled transient elastography has demonstrated high diagnostic accuracy for advanced fibrosis and cirrhosis and has become widely adopted in clinical practice. More recently, point shear wave elastography and two-dimensional shear wave elastography have expanded diagnostic capabilities, enabling integration into conventional ultrasound platforms. Importantly, elastography in ALD requires careful interpretation due to the influence of inflammation and dynamic changes associated with alcohol exposure and abstinence.

Elastography now represents a cornerstone of noninvasive assessment in ALD, facilitating early detection, longitudinal monitoring, and the implementation of structured, cost-effective screening strategies.

5.5 1. Introduction

Alcohol-related liver disease (ALD) remains one of the leading causes of chronic liver disease worldwide and represents a major contributor to liver-related mortality. According to global epidemiological data, more than 40% of liver-related deaths are attributable to alcohol consumption (1, 2). In Europe, ALD is currently one of the most frequent indications for liver transplantation, and its burden continues to increase (3). Alcohol-related liver disease (ALD) and metabolic-and alcohol-related liver disease (MetALD) account for an estimated 20 million cases of compensated cirrhosis globally and are responsible for more than 330,000 cirrhosis-related deaths annually (4).

MASLD is defined by the presence of hepatic steatosis in combination with at least one cardiometabolic risk factor and a self-reported alcohol intake below 20 g/day in women and 30 g/day in men. MetALD describes the frequent clinical scenario in which individuals with MASLD consume alcohol above the MASLD thresholds but below those required for an ALD diagnosis (5).

Diagnosis of ALD is suspected when alcohol consumption is >50 g/d in females and >60 g/d in males and clinical and/or biological modifications suggestive of liver injury or extrahepatic manifestations of alcohol use disorder (AUD) occur (6). Because a high proportion of patients with AUD do not express clinical symptoms or laboratory abnormalities, asymptomatic patients with a harmful use of alcohol should undergo appropriate screening investigations (7).

ALD follows the typical progression of chronic liver diseases, including alcoholic liver steatosis, steatohepatitis, fibrosis, and liver cirrhosis. Approximately 90% of heavy drinkers will develop liver steatosis, and 5%–10% will develop liver cirrhosis in 5 years (8). Despite this high morbidity and mortality, the ALD research field is largely overlooked and underprioritized (9).

Liver cirrhosis is the main predictor for survival (10), so early recognition of fibrosis is the most important objective in this category of patients. Moreover, disease progression can be halted or even partially reversed with sustained abstinence (6), further emphasizing the need for early identification. ALD remains underestimated due to bad reporting of real alcohol consumption and lack of specific investigations. Shifting from late diagnosis to early detection is a complex task that will need to be tackled from multiple angles simultaneously (Figure 5.5.1).

The main points to address in front of a patient with ALD from the hepatological point of view would be the evaluation of liver steatosis, inflammation, and fibrosis.

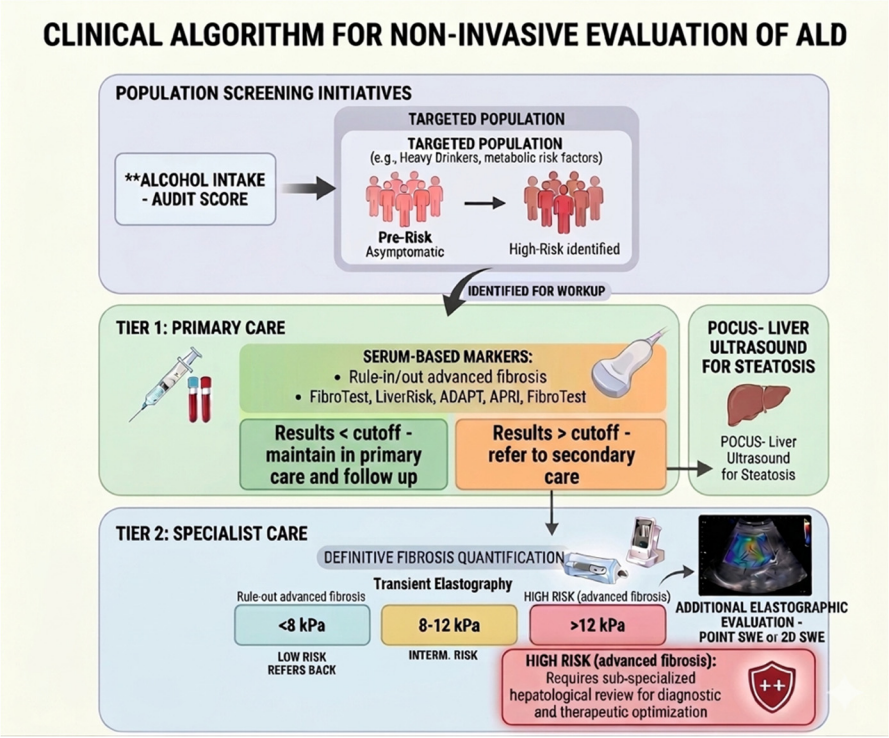


Figure 5.5.1 Algorithm of non-invasive evaluation in alcoholic liver disease. Created using Gemini 3 Flash

From a hepatological perspective, evaluation of ALD requires assessment of hepatic steatosis, necroinflammatory activity, and fibrosis stage. While liver biopsy remains the gold standard for diagnosis and staging (6), it is invasive, associated with a complication rate of approximately 7%, and subject to sampling variability (11). These limitations have driven the development of noninvasive diagnostic methods, including serum biomarkers and elastography techniques (12).

In patients with suspected ALD (presence of alcohol use disorder-AUD, abnormal liver tests or extrahepatic manifestations of AUD, and no other causes of chronic liver disease) noninvasive tests can be transferred into clinical practice for the detection of advanced fibrosis. Physical and biological approaches are complementary, and both methods should be used, starting with primary care, to facilitate the early detection of ALD. First of all, patients should be routinely screened for AUD using the AUDIT questionnaire (6). Further, patients can be easily assessed by primary care using patented or non-

patented biological scores, and in case of liver fibrosis presence, redirected to a 2nd line assessment made by a liver specialist to validate the results by elastography methods. All patients with AUD need to be referred to a specialized withdrawal center. Follow-up can be performed by primary care or, in the case of advanced liver fibrosis, by liver clinic units for specific investigation (12).

5.5.2. Evaluation of liver fibrosis, steatosis and inflammation in ALD

5.5.2.1. Serum based markers

Serum-based fibrosis assessment in ALD can be performed using patented or non-patented biomarkers. Among patented tests, the Enhanced Liver Fibrosis (ELF™) test and FibroTest (FT) are the most extensively studied. A meta-analysis evaluating ELF demonstrated good performance for histological fibrosis staging (13). In biopsy-proven ALD, ELF and FT showed comparable diagnostic accuracy for advanced fibrosis, with AUROC values of 0.92 and 0.90, respectively (14). ELF values below 10.5 and FT values below 0.58 were able to reliably rule out advanced fibrosis (14).

Non-patented indicators such as the aspartate aminotransferase-to-platelet ratio index (APRI) (15), fibrosis-4 index (FIB-4) (16), AST/ALT ratio (17), and age-platelet index have also been evaluated in ALD. However, comparative analyses suggest that ELF and FT outperform indirect markers for the diagnosis of advanced fibrosis in this population (12, 18).

The LiverRisk score incorporates routinely collected clinical and biochemical parameters—age, gender, fasting glucose, cholesterol, AST, ALT, gamma-glutamyltransferase, and platelet count—and was derived using three liver stiffness measurement thresholds as the reference standard (19).

Direct fibrosis tests, which reflect extracellular matrix turnover, include the ELF test—one of the most extensively validated and used blood-based tests—and N-terminal type III collagen propeptide (PRO-C3), which can be used alone or in combination with age, diabetes, and platelet count in the ADAPT algorithm (20).

The diagnostic performance of ELF is good, with AUROCs of 0.90-0.92 for detecting advanced fibrosis in patients with ALD from primary, secondary, and tertiary care settings (14). In a meta-analysis on the diagnostic accuracy of ELF for staging fibrosis across etiologies, the optimized cutoffs for detecting advanced fibrosis and cirrhosis were higher in ALD compared to other etiologies, with a numerically higher performance of ELF. However, these

results were limited by ALD being the least studied etiology. PROC3 and ADAPT were compared to non-patented NITs in a cohort of 426 patients with ALD, which revealed AUROCs for detecting advanced fibrosis of 0.85 for PRO-C3 and 0.88 for ADAPT (20). The prevalence of advanced fibrosis influences the performance of diagnostic tests. FIB-4 has been extensively tested as a first-line screening test to rule out advanced fibrosis in low-prevalence populations. In contrast, evidence supporting the use of PRO-C3 and ADAPT is limited, which should be considered when interpreting their performance.

The European Association for the Study of the Liver (EASL) noninvasive tests clinical practice guidelines advise using FIB-4 as the initial assessment in patients at risk of ALD. If the FIB-4 result is positive (FIB-4>1.3), liver stiffness measurement (LSM) using VCTE should be performed. When LSM exceeds 8 kPa, it should be further supplemented with a patented serum test such as the Enhanced Liver Fibrosis (ELF) test (22).

From an economic perspective, although patented tests are more costly, non-invasive fibrosis assessment strategies have proven cost-effective by preventing progression to decompensated disease stages (Table 5.5.I) (23, 24).

Table 5.5.I. Comparison and performance of biological tests for the diagnosis of advanced fibrosis (F3) in studies with biopsy-proven ALD. Abbreviations: APRI—aspartate transaminase-platelet ratio index; FIB-4—fibrosis 4 index; ELF—Enhanced Liver Fibrosis; FT—Fibrotest; AUC—area under the curve; Se—sensitivity; Sp—specificity.

Test	**AUROC**	**Rule-in Cutoff F3**	**Se%**	**Sp%**	**Best Use**
APRI (14)	0.80	≥1	38%	90%	Initial triage
FIB-4 (16)	0.85	≥3.25	58%	91%	Triage in primary care
AST/ALT ratio (17)	0.76	<1	85%	46%	Triage
Age-platelet index (14)	0.81	≥6.0	65%	85%	Triage
ELF test(14)	0.92	≥ 10.5	79%	91%	Specialty screening
FibroTest (14)	0.90	≥ 0.58	67%	87%	Secondary care confirmation
ADAPT algorithm (20)	0.87	> 6.3287	91%	73%	Specialty screening

5.5.2.2. Ultrasound-based methods

Hepatic steatosis is defined by the accumulation of fat—primarily triglycerides—within hepatocytes, and it is considered pathological when fat content exceeds 5%. It is typically asymptomatic and is mainly associated with alcohol consumption and metabolic risk factors. In patients with alcohol use disorder (AUD), hepatic steatosis may be reversible with sustained abstinence. The severity of steatosis correlates with the degree of lobular inflammation and fibrosis (25). Approximately 90% of individuals with AUD develop hepatic steatosis (8).

Liver biopsy remains the gold standard for assessing steatosis; however, it has significant limitations, including potential complications, sampling variability, its invasive nature, and poor patient acceptance for repeated follow-up evaluations (11). Consequently, noninvasive methods have been developed to facilitate the assessment of patients at risk of liver steatosis.

Since fat accumulation alters the echogenic appearance of the liver, B-mode ultrasound (US) is the first-line imaging modality for screening and evaluating fatty liver (12). It is safe, widely available, accessible, repeatable, and cost-effective, with reported sensitivity ranging from 60% to 94% and specificity from 88% to 95% for detecting steatosis (26). Nevertheless, its diagnostic performance is superior for severe steatosis compared to mild forms, it is operator-dependent, and it does not provide information regarding the presence of fibrosis (27). Magnetic resonance imaging–proton density fat fraction (MRI-PDFF) is regarded as the most sensitive and specific technique for quantifying liver steatosis (28). However, it is not suitable as a point-of-care tool due to the need for specialized radiological assessment, high costs, and limited availability. Furthermore, MRI may not be feasible in obese or claustrophobic patients or in those with implanted metallic devices or pacemakers (28).

A) Ultrasound-based methods for liver steatosis assessment in ALD

A novel non-invasive ultrasound-based parameter, the Controlled Attenuation Parameter (CAP), has been developed for the evaluation of liver steatosis. CAP is performed at the same time as VCTE and is integrated into the FibroScan device (Echosens, Paris, France), enabling simultaneous assessment of steatosis and fibrosis during the same examination (29). CAP measures ultrasound attenuation, a physical property reflecting the loss of ultrasound energy as it propagates through tissue; fat is known to increase attenuation (30). Initially, CAP was developed using the M probe with a central frequency

of 3.5 MHz (30). However, its performance was reduced in overweight and obese patients due to increased subcutaneous fat thickness. To address this limitation, the XL probe, operating at 2.5 MHz and measuring at a depth of 7.5 cm, was introduced (31). CAP values are expressed in decibels per meter (dB/m), ranging from 100 to 400 dB/m. CAP results are displayed only when liver stiffness measurements (LSM) are valid. It is recommended as a point-of-care method for detecting liver steatosis by the World Federation for Ultrasound in Medicine and Biology (WFUMB) (32).

CAP has demonstrated good diagnostic accuracy for steatosis in studies and meta-analyses involving mixed patient cohorts (29), particularly in non-alcoholic fatty liver disease (NAFLD) (33).

In alcohol-related liver disease (ALD), data are limited to a single study by Thiele M. et al. (34), which included 562 patients with ALD who underwent CAP assessment, B-mode ultrasound, and liver biopsy. In this study, CAP outperformed conventional ultrasound steatosis patterns. A CAP value >290 dB/m ruled in steatosis with 88% specificity, whereas values <220 dB/m ruled out steatosis with 90% sensitivity. CAP demonstrated AUROCs of 0.77, 0.78, and 0.82 for mild, moderate, and severe steatosis, respectively. Higher CAP values were observed in patients with ALD and concomitant metabolic syndrome (MetS), with a mean difference of 40 dB/m (302±64 in patients with MetS vs 262±55 in those without MetS; $P<0.001$). Similarly, patients with BMI ≥30 kg/m² had CAP values higher by 49 dB/m (311±48) in obese patients vs. 261±57 in patients with BMI <30 ($P<0.001$) (34). In the same multicenter study, 293 patients admitted for alcohol detoxification showed a mean CAP decrease of 32±47 dB/m, with similar reductions in patients with ALD regardless of MetS status; however, CAP values did not significantly decrease in obese individuals following detoxification. There was no evidence that CAP influenced liver stiffness measurements by VCTE or vice versa. The diagnostic performance of CAP appears lower in mild steatosis compared to other etiologies, and optimal cut-offs vary across studies, possibly reflecting differences in alcohol consumption patterns at the time of evaluation.

The clinical definition of MetALD describes the intersection of alcohol consumption and metabolic risk factors, such as obesity or type 2 diabetes (35). Elastography plays a pivotal role in this new entity, as MetALD patients often exhibit more rapid fibrosis progression than those with MASLD alone. In this context, combining liver stiffness measurements with steatosis quantification allows for comprehensive phenotypic characterization, though massive steatosis can sometimes interfere with shear wave propagation (35).

In addition, several ultrasound manufacturers have developed new ultrasound-based software tools for steatosis quantification, primarily based on the assessment of ultrasound beam attenuation (quantitative ultrasound methods—QUS). These include Ultrasound-Guided Attenuation Parameter (UGAP) from General Electric Healthcare, Attenuation Imaging (ATI) developed by Canon, Attenuation (ATT) from Hitachi, SSp.PLUS (Sound Speed Plane-wave UltraSound) and Att.PLUS (Attenuation Plane-wave UltraSound) from Supersonic Imagine, and TAI™ (Tissue Attenuation Image) and TSI™ (Tissue Scatter-distribution Image) along with USFF (ultrasound fat fraction) from Samsung. Table 5.5.II presents the available published data regarding the evaluation of liver steatosis using QUS methods.

Table 5.5.II. Optimal Thresholds for Non-Invasive Staging of Hepatic Steatosis Using Multiparametric Ultrasound Parameters. Abbreviations: ATI-Attenuation Imaging, USFF-Ultrasound Fat Fraction, UGAP-Ultrasound-Guided Attenuation Parameter, CAP-Controlled Attenuation Parameter

Technique (Machine)	**Parameter**	**S3 (Severe)**	**ALD Patients Included**
ATI (36) (Canon)	dB/cm/MHz	>0.77	**Mixed cohort; ~15% ALD**
USFF (37) (Samsung)	%	>10.0	**169 total; ~12% ALD**
UGAP (38) (GE)	dB/cm/MHz	>0.77	**Mixed cohort; ~20% ALD**
CAP (34) (FibroScan)	dB/m	>290	**562 total; 100% ALD**

B) Ultrasound-based elastography methods for liver fibrosis assessment in ALD

The modern management of ALD has shifted from simple fibrosis staging toward the identification and monitoring of compensated advanced chronic liver disease (cACLD) (35). According to the Baveno VII consensus and pivotal longitudinal studies, liver stiffness measurement (LSM) is no longer merely a diagnostic "snapshot" but a dynamic prognostic marker (39). The LSM threshold of 10 kPa serves as the sentinel for cACLD; patients with ALD and LSM ≥10 kPa face a 19-fold higher risk of decompensation compared to those below this threshold, establishing VCTE as a critical triage tool in primary care and addiction clinics (40).

Beyond baseline staging, longitudinal monitoring of LSM provides critical dynamic insights into disease trajectory and patient survival. Recent data indicates that patients classified as "increasers"—those demonstrating an LSM elevation of ≥20 kPa from baseline over time—face a 3.2-fold increased risk of mortality. Conversely, clinical regression, defined by a decrease in LSM to <10 kPa or a reduction of ≥ 20% from the baseline value, is associated with significantly improved survival and a reduced risk of clinical events. This finding supports the clinical recommendation for annual elastographic surveillance in high-risk patients to detect "silent" disease progression before clinical decompensation occurs (40). The integration of advanced elastographic methods into ALD and MetALD management pathways facilitates the early identification of candidates for esophageal varices screening, adhering to the Baveno VII "Rule of 20/25" (39).

Vibration-controlled transient elastography (VCTE) (FibroScan, Echosens, Paris, France), the first elastography technique developed, remains the most widely used method, as it is noninvasive, rapid, and reproducible, with lower sampling errors (41, 42). Major published studies in alcohol-related liver disease (Table 5.5.III) demonstrate strong performance in the diagnosis of liver cirrhosis with AUROCs ranging from 0.87 (43) to 0.97 (44, 45). However, the established cut-off values differ quite a bit, most likely due to the presence of inflammation in these patients, triggered by recent alcohol consumption and assessed by AST levels. Several studies performed by Mueller et al. (44, 46) show that absolute alcohol withdrawal leads to a 13% reduction of liver stiffness (LS) after one week, and even a 40% reduction in alcohol consumption can lead to a 17% reduction of LS (44, 45, 46). In another study, LS improved in almost 80% of patients admitted for alcohol detoxification due to the coexistence of inflammation seen by AST >100 U/ml (29). Preliminary observational data on long-term abstinence, observed over a period of more than 5 years, shows an LS decrease by 50%, while LS increases by 22% if alcohol consumption continues (46). These dynamics are critical when using liver stiffness to predict and monitor the risk of decompensation and mortality in patients with ALD.

Table 5.5.III. Elastography in patients with alcoholic liver disease performed by VCTE

Reference	**Number of patients *(n)***	**Elastography method**	**Cut-off values for liver cirrhosis**
Anastasiou 2010 (47)	14 patients	VCTE	>12.5 kPa
Boursier 2009 (48)	106 patients	VCTE	>17.3 kPa
de Ledinghen 2012 (49)	34 patients	VCTE	>12.5 kPa
Fernandez 2012 (50)	139 patients	VCTE	>18 kPa
Janssens 2010 (51)	49 patients	VCTE	>21.1 kPa
Lemoine 2008 (52)	48 patients	VCTE	>34.9 kPa
Mueller 2010 (45)	101 patients	VCTE	>11.5 kPa
Nahon 2008 (43)	147 patients	VCTE	>22.6 kPa
Nguyen-Khac 2008 (24)	103 patients	VCTE	>19.5 kPa
Muller 2015 (53)	364 patients	VCTE	>12.5 kPa
Voican 2017 (54)	188 patients	VCTE	>20.8 kPa
Kim 2009 (55)	45 patients	VCTE	>25.8kPa

Following VCTE, other ultrasound-based methods have been developed, such as point Share Wave Elastography (pSWE), Two-Dimensional Share Wave Elastography (2D-SWE), or Time-Harmonic Elastography, all of them embedded in regular ultrasound systems (56-64).

Few studies present data on the performance of pSWE or 2D-SWE in ALD, most with a small number of included patients, showing a wide range of values. The Thiele study from 2016 (63), which included 199 patients and utilized 2D-SWE, established cut-off values of >10.2 kPa for F2 and >16.4 kPa for F4. In studies focusing on pSWE, Kiani 2016 (65) analyzed 69 patients and reported thresholds of >1.63 m/s for F2, >1.84 m/s for F3, and >1.94 m/s for F4. Zhang 2015 (66) evaluated 112 patients and identified lower cut-off values of >1.27 m/s for F2, >1.40 m/s for F3, and >1.65 m/s for F4. Finally, Cho Y 2020 (67) analyzed a larger cohort of 251 patients, establishing thresholds of >1.46 m/s for F2, >1.47 m/s for F3, and >1.66 m/s for F4. Collectively, these results highlight the variability in optimal thresholds across different elastography techniques and study populations within the ALD landscape.

The collective data underscores that while 2D-SWE and pSWE are valuable alternatives to VCTE, there is significant heterogeneity in threshold values depending on the study population and equipment used. While VCTE thresholds for cirrhosis are frequently reported above 12.5 kPa, the 2D-SWE

findings from Thiele 2016 (65) suggest a higher rule-in threshold of >16.4 kPa for F4. While VCTE and 2D-SWE are typically reported in kiloPascals, pSWE is frequently measured in meters per second. Using the simplified conversion $E = 3V^2$, the pSWE threshold of >1.94 m/s (65) for cirrhosis approximately aligns with 11.3 kPa, which is similar to the VCTE rule-in threshold of >11.5 kPa (45, 65). This variability emphasizes that thresholds are not interchangeable across vendors and must be interpreted within the context of the specific equipment used.

Future research in early diagnosis of ALD should focus on integrated non-invasive diagnostic strategies combining elastography with circulating fibrosis biomarkers and objective markers of alcohol exposure. Recent studies have shown that panels of serum biomarkers may provide prognostic information comparable to liver biopsy in early ALD (67), while biomarkers reflecting alcohol consumption, such as phosphatidylethanol (PEth), may further improve risk stratification when combined with non-invasive fibrosis tests (68). In addition, longitudinal studies evaluating liver stiffness trajectories may help predict clinically relevant outcomes and guide individualized patient management. Ultimately, the continued integration of elastography with emerging biomarkers and multidimensional non-invasive diagnostic strategies will be essential to enable earlier detection, improved prognostic stratification, and more personalized management of patients with alcohol-related liver disease.

There are some **take-home messages.**

- Alcohol-related liver disease is a dynamic and progressive condition, ranging from steatosis to steatohepatitis and cirrhosis, with fibrosis stage representing the strongest predictor of morbidity and mortality.
- Most patients with ALD remain asymptomatic until advanced stages, making structured screening in high-risk populations (alcohol use disorder, elevated transaminases, metabolic risk factors) essential.
- Non-invasive tests (NITs) have replaced liver biopsy as first-line tools for fibrosis assessment, enabling safe, repeatable, and cost-effective evaluation. Use simple serum markers (e.g., FIB-4) for initial triage, and confirm with elastography. Cirrhosis is typically suggested by ≥12–15 kPa (VCTE) or ~1.8 m/s (pSWE).

- **Liver stiffness in ALD is highly inflammation-sensitive.** AST >100 U/L, hyperbilirubinemia, and active alcoholic hepatitis can falsely elevate stiffness.
- **Alcohol abstinence significantly reduces liver stiffness,** sometimes within weeks; repeat measurement after detoxification may be necessary before definitive staging.
- **Elastography reflects both fibrosis and reversible inflammatory/ hemodynamic components**, requiring contextual interpretation.
- Sequential screening strategies are recommended. Combining serum scores and elastography enables earlier detection, better risk stratification, cost-effective screening, and precision management—particularly relevant in the era of MetALD.

Future ideas:

- **Develop inflammation-adjusted, ALD-specific stiffness thresholds** that reflect the dynamic biology of alcohol-related liver injury.
- **Shift from single measurements to stiffness trajectories** to predict decompensation, portal hypertension, and mortality.
- **Integrate elastography into AI-driven, multiparametric precision models** combining clinical, biochemical, metabolic, and behavioral data.
- **Validate elastography as a surrogate endpoint in therapeutic trials** and expand its implementation into primary care and addiction medicine screening pathways.

5.5.3. Conclusion

Elastography has redefined the noninvasive assessment of alcohol-related liver disease, enabling accurate fibrosis staging without the limitations of liver biopsy. VCTE remains the most validated modality in ALD, while point shear wave and two-dimensional shear wave elastography provide comparable diagnostic performance with the advantage of integration into conventional ultrasound platforms.

However, ALD presents distinct biological challenges. Liver stiffness is strongly influenced by necroinflammatory activity and recent alcohol exposure, necessitating contextual interpretation and, in many cases, longitudinal reassessment after abstinence. In this dynamic disease, elastography reflects not only structural fibrosis but also reversible components of hepatic injury.

When incorporated into sequential diagnostic pathways alongside serum biomarkers, elastography enhances risk stratification and supports

earlier detection of advanced fibrosis. The next critical step is outcome-driven validation—establishing ALD-specific thresholds, defining stiffness trajectories predictive of clinical events, and integrating elastography into precision-based management algorithms.

Elastography is no longer an adjunct tool in ALD; it is central to modern, non-invasive, and patient-centered hepatology care.

References

1. Kim D, Li AA, Gadiparthi C, Khan MA, Cholankeril G, Glenn JS, Ahmed A. Changing trends in etiology-based and ethnicity-based annual mortality rates of chronic liver disease and cirrhosis in the United States from 2007 through 2016. Gastroenterology. 2018;155:1154-63.e3.
2. Sepanlou SG, Safiri S, Bisignano C, Ikuta KS, Merat S, Saberifiroozi M, , et al. The global, regional, and national burden of cirrhosis by cause in 195 countries and territories, 1990–2017: a systematic analysis for the Global Burden of Disease Study 2017. Lancet Gastroenterol Hepatol. 2020;5:245-66.
3. Sweatt SK, Gower BA, Chieh AY, Liu Y, Li L. Physiol Behav. 2016;176:139-48.
4. GBD 2017 Cirrhosis Collaborators. The global, regional, and national burden of cirrhosis by cause in 195 countries and territories, 1990–2017: a systematic analysis for the Global Burden of Disease Study 2017. Lancet Gastroenterol Hepatol. 2020;5:245-66.
5. Rinella ME, Lazarus JV, Ratziu V, Francque SM, Sanyal AJ, Kanwal F et al. A multisociety Delphi consensus statement on new fatty liver disease nomenclature. J Hepatol. 2023;79:1542-56.
6. Thursz M, Gual A, Lackner C, Mathurin P, Moreno C, Spahr L, et al. EASL Clinical Practice Guidelines: management of alcohol-related liver disease. J Hepatol. 2018;69:154-81.
7. Askgaard G, Leon DA, Kjær MS, Deleuran T, Gerds TA, Tolstrup JS. Risk for alcoholic liver cirrhosis after an initial hospital contact with alcohol problems: a nationwide prospective cohort study. Hepatology. 2017;65:929-37.
8. Gao B, Bataller R. Alcoholic liver disease: pathogenesis and new therapeutic targets. Gastroenterology. 2011;141:1572-85.
9. Amonker S, Houshmand A, Hinkson A, Rowe I, Parker R. Prevalence of alcohol-associated liver disease: a systematic review and meta-analysis. Hepatol Commun. 2023;7.
10. Seitz HK, Bataller R, Cortez-Pinto H, Gao B, Gual A, Lackner C, et al. Alcoholic liver disease. Nat Rev Dis Primers. 2018; Aug 16;4(1):16.

11. Filingeri V, Francioso S, Sforza D, Santopaolo F, Oddi FM, Tisone G. A retrospective analysis of 1,011 percutaneous liver biopsies performed in patients with liver transplantation or liver disease: ultrasonography can reduce complications? Eur Rev Med Pharmacol Sci. 2016;20:3609-17.
12. Moreno C, Mueller S, Szabo G. Non-invasive diagnosis and biomarkers in alcohol-related liver disease. J Hepatol. 2019;70:273-83.
13. Xie Q, Zhou X, Huang P, Wei J, Wang W, Zheng S. The performance of enhanced liver fibrosis (ELF) test for the staging of liver fibrosis: a meta-analysis. PLoS One. 2014;9:e92772.
14. Thiele M, Madsen BS, Hansen JF, Detlefsen S, Antonsen S, Krag A. Accuracy of the enhanced liver fibrosis test vs. FibroTest, elastography, and indirect markers in detection of advanced fibrosis in patients with alcoholic liver disease. Gastroenterology. 2018;154:1369-79.
15. Wai CT, Greenson JK, Fontana RJ, Kalbfleisch JD, Marrero JA, Conjeevaram HS, Lok AS. A simple noninvasive index can predict both significant fibrosis and cirrhosis in patients with chronic hepatitis C. Hepatology. 2003;38:518-26.
16. Sterling RK, Lissen E, Clumeck N, Sola R, Correa MC, Montaner J, et al. Development of a simple noninvasive index to predict significant fibrosis in patients with HIV-HCV coinfection. Hepatology. 2006;43:1317-25.
17. Williams ALB, Hoofnagle JH. Ratio of serum aspartate to alanine aminotransferase in chronic hepatitis: relationship to cirrhosis. Gastroenterology. 1988;95:734-9.
18. Hadefi A, Degré D, Trépo E, Moreno C. Noninvasive diagnosis in alcohol-related liver disease. Health Sci Rep. 2020;3:e146.
19. Serra-Burriel M, Juanola A, Serra-Burriel F, Thiele M, Graupera I, Pose E, et al. Development, validation, and prognostic evaluation of a risk score for long-term liver-related outcomes in the general population: a multicohort study. Lancet. 2023;402:988-96.
20. Madsen BS, Thiele M, Detlefsen S, Kjaergaard M, Møller LS, Trebicka J, et al. PRO-C3 and ADAPT algorithm accurately identify patients with advanced fibrosis due to alcohol-related liver disease. Aliment Pharmacol Ther. 2021;54:699-708.
21. European Association for the Study of the Liver. EASL Clinical Practice Guidelines on non-invasive tests for evaluation of liver disease severity and prognosis – 2021 update. J Hepatol. 2021;75:659-89.
22. Jin W, Lin Z, Xin Y, Jiang X, Dong Q, Xuan S. Diagnostic accuracy of the aspartate aminotransferase-to-platelet ratio index for the prediction of hepatitis B-related fibrosis: a meta-analysis. BMC Gastroenterol. 2012;12:14.
23. Asphaug L, Thiele M, Krag A, Melberg HO. Cost-effectiveness of noninvasive screening for alcohol-related liver fibrosis. Hepatology. 2020;71:2093-104.

24. Nguyen-Khac E, Chatelain D, Tramier B, Decrombecque C, Robert B, Joly JP, et al. Assessment of asymptomatic liver fibrosis in alcoholic patients using Fibroscan: prospective comparison with seven non-invasive laboratory tests. Aliment Pharmacol Ther. 2008;28:1188-98.
25. Chalasani N, Wilson L, Kleiner DE, Cummings OW, Brunt EM, Ünalp A. Relationship of steatosis grade and zonal location to histological features of steatohepatitis in adult patients with non-alcoholic fatty liver disease. J Hepatol. 2008;48:829-34.
26. Lupşor-Platon M, Stefănescu H, Mureşan D, Florea M, Szász ME, Maniu A, Badea R. Noninvasive assessment of liver steatosis using ultrasound methods. Med Ultrason. 2014;16:236-45.
27. Schwenzer NF, Springer F, Schraml C, Stefan N, Machann J, Schick F. Non-invasive assessment and quantification of liver steatosis by ultrasound, computed tomography and magnetic resonance. J Hepatol. 2009;51:433-45.
28. Zhang Y, Fowler KJ, Hamilton G, Cui JY, Sy EZ, Balanay M, et al. Liver fat imaging: a clinical overview of ultrasound, CT, and MR imaging. Br J Radiol. 2018;91:20170959.
29. Karlas T, Petroff D, Sasso M, Fan JG, Mi YQ, de Lédinghen V, et al. Individual patient data meta-analysis of controlled attenuation parameter technology for assessing steatosis. J Hepatol. 2017;66:1022-30.
30. Sasso M, Beaugrand M, de Lédinghen V, Douvin C, Marcellin P, Poupon R, et al. Controlled attenuation parameter: a novel VCTE-guided ultrasonic attenuation measurement for the evaluation of hepatic steatosis. Ultrasound Med Biol. 2010;36:1825-35.
31. Sasso M, Audière S, Kemgang A, Gaouar F, Corpechot C, Chazouillères O, et al. Liver steatosis assessed by controlled attenuation parameter measured with the XL probe of the FibroScan. Ultrasound Med Biol. 2016;42:92-103.
32. Ferraioli G, Wong VWS, Castera L, Berzigotti A, Sporea I, Dietrich CF, et al. Liver ultrasound elastography: an update to the World Federation for Ultrasound in Medicine and Biology guidelines and recommendations. Ultrasound Med Biol. 2018;44:2419-40.
33. Eddowes PJ, Sasso M, Allison M, Tsochatzis E, Anstee QM, Sheridan D, et al. Accuracy of FibroScan controlled attenuation parameter and liver stiffness measurement in assessing steatosis and fibrosis in patients with nonalcoholic fatty liver disease. Gastroenterology. 2019;156:1717-30.
34. Thiele M, Rausch V, Fluhr G, Kjærgaard M, Piecha F, Mueller J, et al. Controlled attenuation parameter and alcoholic hepatic steatosis: diagnostic accuracy and role of alcohol detoxification. J Hepatol. 2018;68:1025-32.
35. Johansen S, Thiele M, Krag A. Non-invasive tests for MetALD and alcohol-related liver disease. JHEP Rep. 2025;7:101569.

36. Nishimura T, Tada T, Akita T, Kondo R, Suzuki Y, Imajo K, et al. Diagnostic performance of attenuation imaging versus controlled attenuation parameter for hepatic steatosis with MRI-based proton density fat fraction as the reference standard: a prospective multicenter study. J Gastroenterol. 2025;60:727-37.
37. Nica C, Sporea I, Popa A, Lupușoru R, Voicu Stan Erimescu M, Șirli R, et al. The value of ultrasound fat fraction as compared to controlled attenuation parameter for the severity of liver steatosis assessment: preliminary results. Med Ultrason. 2026.
38. Byenfeldt M, Grönlund C, Nasr P, Lindam A, Ekstedt M, Lundberg P, Kihlberg J. A comparative study between ultrasound-guided attenuation parameter, controlled attenuation parameter, and proton density fat fraction for assessment of hepatic steatosis. Scand J Gastroenterol. 2026;61:124-32.
39. Baveno VII Faculty. Baveno VII – renewing consensus in portal hypertension. J Hepatol. 2022;76:959-74.
40. Thorhauge KH, Semmler G, Johansen S, Lindvig KP, Kjærgaard M, Hansen JK, et al. Using liver stiffness to predict and monitor the risk of decompensation and mortality in patients with alcohol-related liver disease. J Hepatol. 2024;81:23-32.
41. Dietrich CF, Bamber J, Berzigotti A, Bota S, Cantisani V, Castera L, et al. EFSUMB guidelines and recommendations on the clinical use of liver ultrasound elastography: update 2017. Ultraschall Med. 2017;38:e16-47.
42. Moreno C, Mueller S, Szabo G. Non-invasive diagnosis and biomarkers in alcohol-related liver disease. J Hepatol. 2019;70:273-83.
43. Nahon P, Kettaneh A, Tengher-Barna I, Ziol M, de Lédinghen V, Douvin C et al. Assessment of liver fibrosis using transient elastography in patients with alcoholic liver disease. J Hepatol. 2008;49:1062-8.
44. Mueller S, Luderer M, Zhang D, Meulien D, Brach BS, Schou MB. Open-label study with nalmefene as needed use in alcohol-dependent patients with evidence of elevated liver stiffness and/or hepatic steatosis. Alcohol Alcohol. 2020;55:63-70.
45. Mueller S, Millonig G, Sarovska L, Friedrich S, Reimann FM, Pritsch M, et al. Increased liver stiffness in alcoholic liver disease: differentiating fibrosis from steatohepatitis. World J Gastroenterol. 2010;16:966-72.
46. Mueller S. Liver elastography: clinical use and interpretation. Cham: Springer; 2020.
47. Anastasiou J, Alisa A, Virtue S, Portmann B, Murray-Lyon I, Williams R. Noninvasive markers of fibrosis and inflammation in clinical practice: prospective comparison with liver biopsy. Eur J Gastroenterol Hepatol. 2010;22:474-80.
48. Boursier J, Vergniol J, Sawadogo A, Dakka T, Michalak S, Gallois Y, et al. The combination of a blood test and Fibroscan improves the non-invasive diagnosis of liver fibrosis. Liver Int. 2009;29:1507-15.
49. de Lédinghen V, Wong VWS, Vergniol J, Wong GLH, Foucher J, Chu SHT, et al. Diagnosis of liver fibrosis and cirrhosis using liver stiffness measurement: comparison between M and XL probe of FibroScan. J Hepatol. 2012;56:833-9.

50. Fernandez M, Trépo E, Degré D, Gustot T, Verset L, Demetter P, et al. Transient elastography using Fibroscan is the most reliable noninvasive method for the diagnosis of advanced fibrosis and cirrhosis in alcoholic liver disease. Eur J Gastroenterol Hepatol. 2015;27:1074-9.
51. Janssens F, De Suray N, Piessevaux H, Horsmans Y, De Timary P, Stärkel P. Can transient elastography replace liver histology for determination of advanced fibrosis in alcoholic patients: a real-life study. J Clin Gastroenterol. 2010;44:575-82.
52. Lemoine M, Katsahian S, Ziol M, Nahon P, Ganne-Carrie N, Kazemi F, et al. Liver stiffness measurement as a predictive tool of clinically significant portal hypertension in patients with compensated hepatitis C virus or alcohol-related cirrhosis. Aliment Pharmacol Ther. 2008;28:1102-11.
53. Mueller S, Englert S, Seitz HK, Badea RI, Erhardt A, Bozaari B, et al. Inflammation-adapted liver stiffness values for improved fibrosis staging in patients with hepatitis C virus and alcoholic liver disease. Liver Int. 2015;35:2514-21.
54. Nguyen-Khac E, Thiele M, Voican C, Nahon P, Moreno C, Boursier J, et al. Non-invasive diagnosis of liver fibrosis in patients with alcohol-related liver disease by transient elastography: an individual patient data meta-analysis. Lancet Gastroenterol Hepatol. 2018;3:614-25.
55. Hu WY. 印刷杂志. 2003.
56. Popa A, Șirli R, Popescu A, Bâldea V, Lupușoru R, Bende F, et al. Ultrasound-based quantification of fibrosis and steatosis with a new software considering transient elastography as reference in patients with chronic liver diseases. Ultrasound Med Biol. 2021.
57. Moga T, Sporea I, Lupus R, Popescu A, Popa A, Bota S, et al. Performance of a noninvasive time-harmonic elastography technique for liver fibrosis evaluation using vibration-controlled transient elastography as reference method. Diagnostics (Basel). 2020;10:653.
58. Popa A, Bende F, Șirli R, Popescu A, Bâldea V, Lupușoru R et al. Quantification of liver fibrosis, steatosis, and viscosity using multiparametric ultrasound in patients with non-alcoholic liver disease: a real-life cohort study. Diagnostics (Basel). 2021;11:783.
59. Ferraioli G, Maiocchi L, Lissandrin R, Tinelli C, De Silvestri A, Filice C. Accuracy of the ElastPQ technique for the assessment of liver fibrosis in patients with chronic hepatitis C: a real-life single center study. J Gastrointestin Liver Dis. 2016;25:331-5.
60. Herrmann E, de Lédinghen V, Cassinotto C, Chu WCW, Leung VYF, Ferraioli G, et al. Assessment of biopsy-proven liver fibrosis by two-dimensional shear wave elastography: an individual patient data-based meta-analysis. Hepatology. 2018;67:260-72.

61. Bende F, Sporea I, Şirli R, Nistorescu S, Fofiu R, Bâldea V, Popescu A. The performance of a two-dimensional shear-wave elastography technique for predicting different stages of liver fibrosis using transient elastography as the control method. Ultrasound Q. 2020.
62. Foncea C, Popescu A, Lupușoru R, Fofiu R, Șirli R, Danilă M, Sporea I. Comparative study between pSWE and 2D-SWE techniques integrated in the same ultrasound machine, with transient elastography as the reference method. Med Ultrason. 2020;22:13-19.
63. Thiele M, Detlefsen S, Sevelsted Møller L, Madsen BS, Fuglsang Hansen J, Fialla AD, et al. Transient and two-dimensional shear-wave elastography provide comparable assessment of alcoholic liver fibrosis and cirrhosis. Gastroenterology. 2016;150:123-33.
64. Kiani A, Brun V, Lainé F, Turlin B, Morcet J, Michalak S et al. Acoustic radiation force impulse imaging for assessing liver fibrosis in alcoholic liver disease. World J Gastroenterol. 2016;22:4926-35.
65. Zhang D, Li P, Chen M, Liu L, Liu Y, Zhao Y, Wang R. Non-invasive assessment of liver fibrosis in patients with alcoholic liver disease using acoustic radiation force impulse elastography. Abdom Imaging. 2014;40:723-9.
66. Cho Y, Choi YI, Oh S, Han J, Joo SK, Lee DH, et al. Point shear wave elastography predicts fibrosis severity and steatohepatitis in alcohol-related liver disease. Hepatol Int. 2020;14:270-80.
67. Rasmussen DN, Thiele M, Johansen S, Kjærgaard M, Lindvig KP, Israelsen M, et al. Prognostic performance of seven biomarkers compared to liver biopsy in early alcohol-related liver disease. J Hepatol. 2021;75:1017-25.
68. Torp N, Johansen S, Jensen EL, Maagaard M, Semmler G, Andersen ML, et al. Prognostic performance of phosphatidylethanol with noninvasive liver fibrosis tests in alcohol-related liver disease. Gastroenterology. 2025.

5.6. Elastography for other chronic hepatopathies (autoimmune hepatitis, primary biliary cholangitis, primary sclerosing cholangitis)

Alina Popescu, Tudor Moga, Raluca Lupușoru

Abstract

Ultrasound elastography has become an essential noninvasive method for assessing liver fibrosis in chronic liver diseases. In autoimmune and cholestatic liver disorders—particularly autoimmune hepatitis (AIH), primary biliary cholangitis (PBC), and primary sclerosing cholangitis (PSC)—accurate evaluation of fibrosis stage and disease progression is crucial for guiding therapy and predicting long-term outcomes. Several ultrasound-based elastography techniques, including vibration-controlled transient elastography (VCTE), point shear-wave elastography (pSWE), and two-dimensional shear-wave elastography (2D-SWE), allow quantitative assessment of liver stiffness as an indicator of fibrosis and have been widely validated in clinical practice.

In autoimmune hepatitis, elastography provides reliable evaluation of fibrosis when inflammatory activity is controlled and may help monitor treatment response and disease progression. In primary biliary cholangitis, liver stiffness measurements correlate with histological fibrosis stages and have significant prognostic value, particularly when integrated with biochemical risk models and longitudinal follow-up. In primary sclerosing cholangitis, elastography contributes to risk stratification and assessment of portal hypertension, although interpretation may be complicated by cholestasis and biliary obstruction.

This chapter reviews the current evidence regarding the diagnostic performance, prognostic significance, and technical considerations of ultrasound elastography in autoimmune and cholestatic liver diseases, highlighting its role as a valuable noninvasive tool in modern hepatology.

5.6.1. Introduction

Assessment of liver fibrosis is essential in the management of chronic liver diseases because the fibrosis stage strongly influences prognosis, therapeutic decisions, and the risk of complications such as cirrhosis and portal hypertension. Traditionally, liver biopsy has been considered the reference standard for fibrosis staging; however, its invasiveness, sampling variability,

and potential complications have encouraged the development of noninvasive diagnostic techniques (1–3).

Among these, ultrasound elastography has emerged as one of the most widely used methods for the non-invasive evaluation of hepatic fibrosis, with several ultrasound-based elastography techniques being available, including vibration-controlled transient elastography (VCTE), point shear-wave elastography (pSWE), and two-dimensional shear-wave elastography (2D-SWE) (4–7).

These techniques enable rapid, reproducible, and noninvasive measurement of liver stiffness as a marker for fibrosis and have been extensively validated in various chronic liver diseases. Their clinical application has expanded beyond viral hepatitis and metabolic liver disease to include autoimmune and cholestatic liver disorders such as autoimmune hepatitis (AIH), primary biliary cholangitis (PBC), and primary sclerosing cholangitis (PSC) (6–9).

Autoimmune and cholestatic liver diseases represent a heterogeneous group of conditions characterized by immune-mediated hepatic injury and progressive fibrosis. Accurate assessment of fibrosis stages and disease progression is critical for monitoring treatment responses and predicting long-term outcomes in these disorders. In recent years, numerous studies have investigated the diagnostic accuracy and prognostic significance of ultrasound elastography in these diseases (7–11).

This chapter summarizes current evidence regarding the role of ultrasound elastography in the evaluation of autoimmune hepatitis, primary biliary cholangitis, and primary sclerosing cholangitis, focusing on diagnostic performance, prognostic implications, and technical considerations.

5.6.2. Liver Elastography in Autoimmune Hepatitis

A) Diagnostic performance

Autoimmune hepatitis is a chronic inflammatory liver disease characterized by immune-mediated hepatocellular injury that may progress to fibrosis and cirrhosis if untreated. Monitoring fibrosis progression in AIH is essential for disease management, and elastography has emerged as a valuable non-invasive tool in this setting.

Several studies have demonstrated that ***VCTE*** correlates well with histological fibrosis stage in patients with AIH. Early work by Hartl and colleagues showed that the diagnostic performance of VCTE is strongly

influenced by inflammatory activity, highlighting the importance of timing when performing liver stiffness measurements (1). During periods of active hepatitis, elevated aminotransferase levels may lead to transient increases in liver stiffness, potentially resulting in overestimation of fibrosis severity. Consequently, elastography measurements obtained during active disease should be interpreted cautiously (1, 12).

Subsequent studies confirmed that elastography becomes more reliable once biochemical remission is achieved. In patients with controlled inflammatory activity, liver stiffness measurements demonstrate a good correlation with the fibrosis stage and can distinguish between mild fibrosis and advanced disease (2, 4, 5).

Meta-analyses evaluating non-invasive methods for fibrosis staging in autoimmune liver diseases have confirmed the diagnostic value of elastography. These analyses reported good sensitivity and specificity for detecting advanced fibrosis and cirrhosis, particularly when VCTE is used (7, 8).

Beyond VCTE, other ultrasound-based techniques have been investigated in AIH. ***Point shear-wave elastography and 2D-SWE*** have demonstrated promising results for fibrosis staging, with diagnostic accuracy comparable to VCTE in several studies (9–11).

pSWE and 2D-SWE offer the advantage of real-time visualization of hepatic tissue, allowing the operator to select an optimal region of interest while avoiding large vessels or artifacts. This may improve measurement reliability and reproducibility in clinical practice (11).

Furthermore, recent studies have explored additional elastography-derived parameters, including shear-wave dispersion, which may reflect inflammatory changes within the liver parenchyma. These advanced parameters may enhance the ability of ultrasound elastography to differentiate between inflammatory activity and fibrosis in AIH (13).

B) Prognostic implications

In addition to its diagnostic role, elastography may provide important prognostic information in patients with autoimmune hepatitis. Longitudinal studies have shown that liver stiffness measurements are associated with disease progression and clinical outcomes. Higher baseline stiffness values have been linked to increased risk of cirrhosis, portal hypertension, and liver-related complications. Monitoring changes in stiffness over time may therefore help identify patients at higher risk of disease progression (14).

Several studies have demonstrated that reductions in liver stiffness can occur following successful immunosuppressive therapy, suggesting improvements in inflammatory activity or the regression of fibrosis. Conversely, persistently elevated stiffness values may indicate ongoing disease activity or advanced fibrosis despite treatment (5, 14).

More recent investigations have also explored the relationship between elastography parameters and histopathological features in AIH. These studies suggest that ultrasound elastography may offer new information about the pathophysiology of autoimmune liver injury and fibrogenesis (13).

5.6.3. Elastography in Primary Biliary Cholangitis

A) Diagnostic performance

Primary biliary cholangitis is a chronic cholestatic liver disease characterized by immune-mediated destruction of intrahepatic bile ducts, leading to progressive fibrosis and eventually cirrhosis. Accurate assessment of fibrosis stage is crucial for predicting disease progression and guiding treatment decisions.

Ultrasound elastography has been extensively investigated as a non-invasive tool for fibrosis assessment in patients with PBC. Multiple studies have demonstrated strong correlations between liver stiffness measurements and histological fibrosis stage (15–17).

VCTE has been shown to accurately identify advanced fibrosis and cirrhosis in PBC patients, and dual cut-off approaches have been proposed to improve diagnostic accuracy at different stages of disease progression (15).

Systematic reviews and meta-analyses comparing elastography with liver biopsy have confirmed that elastography provides reliable noninvasive assessment of hepatic fibrosis in PBC. These findings support its use as a routine clinical tool for fibrosis staging and disease monitoring (18).

In addition to VCTE, other ultrasound-based techniques have been investigated for fibrosis assessment in PBC. ***2D-SWE*** has shown promising results in several studies, demonstrating good correlation with histological fibrosis stage and reliable diagnostic accuracy, and may also help predict the presence of portal hypertension and esophageal varices (19, 20).

2D-SWE also allows evaluation of larger areas of hepatic tissue, which may reduce sampling variability compared with point-based methods. Moreover, integration with conventional ultrasound imaging enables the operator to avoid vascular structures and other artifacts during measurement.

B) Prognostic implications

Beyond fibrosis staging, LSM has important prognostic implications in patients with PBC. Several studies have shown that higher liver stiffness values are associated with more advanced disease and an increased risk of clinical complications, including portal hypertension, hepatic decompensation, and liver transplantation (21–23).

Longitudinal studies have demonstrated that liver stiffness values measured by VCTE correlate with long-term clinical outcomes in PBC. Patients with elevated baseline stiffness values tend to experience faster disease progression and higher rates of liver-related complications (21, 22).

Large international cohort studies have confirmed the prognostic value of elastography in PBC. These studies demonstrated that LSM significantly improves prediction of clinical outcomes when incorporated into prognostic models, highlighting its value as a non-invasive biomarker of disease severity (23).

Dynamic changes in liver stiffness over time may also provide valuable information regarding disease evolution. Increasing stiffness values during follow-up may reflect progressive fibrosis, while stable or decreasing values may indicate a favorable disease course or response to therapy (24).

C) Relationship with biochemical response

Biochemical response to ursodeoxycholic acid (UDCA) therapy is a key determinant of prognosis in PBC. Several prognostic scoring systems, such as the GLOBE score and the UK-PBC score, incorporate biochemical parameters to estimate long-term outcomes.

Recent research has explored the relationship between elastography findings and biochemical response in PBC. These studies suggest that LSM provide complementary prognostic information to biochemical markers. In some cases, elastography may identify patients at increased risk of disease progression even when biochemical parameters appear relatively stable (24, 25).

The integration of elastography with biochemical risk scores may therefore improve risk stratification and facilitate individualized patient management. This combined approach may help clinicians identify patients who require closer monitoring or escalation of therapy.

Emerging elastography parameters such as shear-wave dispersion imaging have also been explored in cholestatic liver diseases. Preliminary

studies suggest that these techniques may provide additional information about tissue viscoelastic properties and inflammatory activity, although further research is needed to establish their clinical role (26).

5.6.4. Elastography in Primary Sclerosing Cholangitis

A) Diagnostic performance

Primary sclerosing cholangitis is a chronic cholestatic liver disease characterized by inflammation and fibrosis of intrahepatic and extrahepatic bile ducts. Disease progression is highly variable, and reliable tools for assessing fibrosis and predicting outcomes are essential for patient management.

Ultrasound elastography has been investigated as a noninvasive method for evaluating fibrosis severity in PSC. Several studies have demonstrated that liver stiffness measurements correlate with histological fibrosis stage and may reflect disease severity (27–29).

However, interpretation of elastography findings in PSC can be challenging due to the complex pathophysiology of the disease. Biliary obstruction, cholestasis, and inflammatory changes may influence liver stiffness independently of fibrosis. As a result, elastography values should be interpreted cautiously and always considered in conjunction with clinical and imaging findings (27).

B) Prognostic value

Despite these limitations, elastography has demonstrated prognostic significance in PSC. Elevated liver stiffness values have been associated with an increased risk of hepatic decompensation, portal hypertension, and reduced transplant-free survival (28, 30).

Longitudinal studies comparing elastography with other biomarkers such as alkaline phosphatase and Enhanced Liver Fibrosis (ELF) scores have shown that changes in liver stiffness may reflect disease progression over time (28). These findings suggest that elastography may be useful for monitoring disease course in PSC patients.

Recent systematic reviews have highlighted the potential of elastography for risk stratification in PSC. However, further research is needed to establish standardized stiffness thresholds and determine optimal monitoring strategies (30).

C) Advanced imaging approaches

Recent studies have evaluated advanced elastography techniques for PSC assessment. ***pSWE*** integrated into conventional ultrasound systems has demonstrated feasibility and diagnostic utility in PSC patients (29), particularly because it can be integrated into standard ultrasound examinations. This allows the operator to place the sampling region under B-mode guidance, potentially reducing the influence of visible vascular or biliary structures.

Additionally, comparative studies have examined the relationship between LSM and imaging findings obtained through magnetic resonance cholangiopancreatography (MRCP). These investigations suggest that combining elastography with cross-sectional imaging may improve risk stratification in PSC (31).

Magnetic resonance elastography (MRE) has also shown promise for evaluating hepatic fibrosis in PSC, although its availability and cost may limit widespread clinical use. Ultrasound elastography therefore remains an attractive option due to its accessibility and ease of implementation in routine clinical practice.

Recent studies have shown that elastography can improve risk stratification by identifying patients with persistent structural liver damage despite apparently favorable biochemical evolution. In this context, 2D-SWE and VCTE may provide complementary information, especially when interpreted together with histology, biochemical response to UDCA, and long-term prognostic models. Data from recent cohort studies suggest that baseline stiffness, as well as its trajectory over time, correlates with adverse outcomes such as hepatic decompensation, portal hypertension, and transplant-related endpoints (31–35).

More specifically, contemporary PSC literature supports a dynamic interpretation of elastography. Patients with persistently increased liver stiffness despite biochemical response may remain at increased clinical risk, whereas declining stiffness values may reflect more favorable disease evolution. This has reinforced the concept that elastography should not be interpreted in isolation but rather as part of a broader multiparametric framework that also includes alkaline phosphatase, bilirubin, albumin, platelet count, and validated prognostic scores (33–35).

PSC remains one of the most challenging autoimmune-associated cholestatic diseases for the noninvasive evaluation of fibrosis. Unlike AIH, where inflammation is the main confounder, or PBC, where fibrosis progression

often follows a relatively interpretable pattern, PSC is marked by segmental biliary obstruction, heterogeneous parenchymal injury, and fluctuating cholestasis. For this reason, liver stiffness values in PSC may reflect not only fibrosis but also transient increases in biliary pressure and inflammatory changes (36–40).

Available studies nevertheless support a clinically meaningful role for elastography in PSC. Liver stiffness has been associated with fibrosis burden, portal hypertension, and long-term prognosis, while repeated measurements may help identify disease progression. Comparative studies using different ultrasound platforms have shown that elastography is feasible in PSC, although inter-system variability remains a relevant issue and underlines the need for careful interpretation of serial values, particularly when patients are followed on different machines or across centers (37, 38).

In parallel, systematic reviews suggest that elastography may contribute to risk stratification in PSC but emphasize that no single technique has yet fully solved the problem of heterogeneity in fibrosis distribution or the confounding effect of dominant strictures (39–41).

Another important concept in PSC is the integration of elastography with cross-sectional imaging. Studies comparing MRCP findings with liver stiffness have suggested that both structural biliary abnormalities and stiffness values contribute to prognostic assessment. Therefore, elastography in PSC should be interpreted together with cholangiographic severity, biochemical trends, and clinical evidence of portal hypertension rather than as a standalone marker (42, 43).

5.6.5. Technical Considerations and Methodological Standards

The expanding clinical role of ultrasound elastography has also brought renewed attention to technical standardization. Several foundational studies and consensus papers have established the methodological basis for reliable stiffness assessment, including patient preparation, acquisition quality, reproducibility, and the influence of operator experience (44–48).

An essential point is that liver stiffness does not equate exclusively to fibrosis. Increased stiffness may also result from portal hypertension, hepatic congestion, cholestasis, and marked necroinflammation. This is particularly relevant in autoimmune and cholestatic liver disease, where biochemical flares, biliary obstruction, and hemodynamic changes can lead to overestimation of fibrosis if measurements are interpreted too simplistically (49–51).

As elastography evolved, attention expanded from liver stiffness alone to the broader hemodynamic consequences of chronic liver disease, especially portal hypertension. In this area, spleen stiffness has emerged as an important complementary tool. Studies in chronic liver disease populations have shown that spleen stiffness may correlate more closely than liver stiffness with clinically significant portal hypertension and the presence of esophageal varices (52–55).

This concept is particularly attractive in PSC, where liver fibrosis may be highly heterogeneous and where biliary changes can distort the interpretation of parenchymal stiffness. In such settings, spleen stiffness may offer a more global reflection of portal pressure burden. Although the standardization of spleen stiffness is still less mature than that of liver stiffness, the accumulated data suggest that it may become increasingly relevant for identifying patients at higher risk of portal hypertensive complications (52–55).

5.6.6. Reproducibility, Cut-offs, and Remaining Limitations

A major challenge across the elastography literature is the reproducibility of measurements and the transferability of cutoff values between technologies, disease etiologies, and clinical settings. Earlier reproducibility studies demonstrated that VCTE can achieve good repeatability under standardized conditions but also highlighted the effect of operator experience, obesity, narrow intercostal spaces, and technical failures (56).

Subsequent studies of point and 2D-SWE methods confirmed that technique-specific differences matter, meaning that values derived from one platform cannot always be directly translated to another. This is particularly important when reviewing studies in AIH, PBC, and PSC together, because the literature often combines VCTE, pSWE techniques, and 2D-SWE in ways that are clinically informative but not always numerically interchangeable (57–59).

Meta-analytic work has also shown that stiffness thresholds for significant fibrosis, advanced fibrosis, and cirrhosis vary depending on etiology and study design. For this reason, a single universal cut-off is unlikely to be appropriate for all autoimmune and cholestatic liver diseases. Instead, clinically useful interpretation requires attention to disease type, inflammatory state, cholestasis, treatment status, and the specific elastography technology used (60, 61).

5.6.7. Conclusions

Despite these limitations related to the pathogeny of these diseases but also to the relatively small number of patients and studies related to the usefulness of elastography in the assessment of severity and prognosis, which did not allow obtaining highly accurate cutoff values, the latest guidelines suggest that for PBC, VTCE cutoff values of 8 and 15 kPa can be used to stratify low-, medium-, and high-risk groups for liver-related events (45), and a cutoff of 10 kPa can rule in severe fibrosis/cACLD (62), while in PSC a VCTE cutoff value of 9.5 kPa can be used to support the diagnosis of advanced fibrosis in compensated patients with normal bilirubin and without high-grade stenosis. Also, in AIH there are no validated cutoff values, but a VCTE liver stiffness measurement of 8 kPa may be suggestive of advanced tissue damage (45). Also, VCTE can be used in these patients to monitor the disease course together with aminotransferases and IgG and to stage liver fibrosis after at least 6 months of immunosuppressive therapy (62).

New cohort data, updated reviews, and late-generation studies continue to refine the performance characteristics of elastography in autoimmune liver disorders and PSC, but they also show that standardization remains incomplete. In practical terms, elastography is best viewed as a powerful decision-support tool rather than an isolated substitute for the full clinical picture (61–63).

References

1. Hartl J, Denzer U, Ehlken H, Zenouzi R, Peiseler M, Sebode M, et al. Transient elastography in autoimmune hepatitis: Timing determines the impact of inflammation and fibrosis. J Hepatol. 2016;65(4):769-75.
2. Xu Q, Sheng L, Bao H, Chen X, Guo C, Li H, et al. Evaluation of transient elastography in assessing liver fibrosis in patients with autoimmune hepatitis. J Gastroenterol Hepatol. 2017;32(3):639-44.
3. Wang X, Li Y, Jiang L, Zhou M, Zhang X, Wen H. Performance of 2D-shear wave elastography in autoimmune hepatitis-primary biliary cholangitis overlap syndrome. Abdom Radiol (NY). 2023;48(4):1290-97.
4. Mahmud N, Doshi SD, Forde KA, Khungar V. Transient elastography reliably estimates liver fibrosis in autoimmune hepatitis. Clin Exp Hepatol. 2019;5(3):244-49.
5. Paranaguá-Vezozzo DC, Terrabuio DRB, Reinoso-Pereira GL, Moutinho R, Ono SK, Salas VW, et al. Liver elastography can predict degree of advanced fibrosis for autoimmune hepatitis in biochemical remission. JGH Open. 2023;7(4):272-77.

6. Lytvyak E, Hirschfield G, Shreekumar D, Wong YJ, Montano-Loza AJ. Pathogenesis, non-invasive assessments, and treatment of hepatic fibrosis in autoimmune liver diseases. Liver Int. 2025. Aug;45(8):e70190.
7. An J, Chon YE, Kim G, Kim MN, Kim HY, Lee HA, et al. Diagnostic accuracy of vibration-controlled transient elastography for staging liver fibrosis in autoimmune liver diseases: A systematic review and meta-analysis. Clin Mol Hepatol. 2024;30(Suppl):S134-46.
8. Chen H, Shen Y, Wu SD, Zhu Q, Weng CZ, Zhang J, et al. Diagnostic role of transient elastography in patients with autoimmune liver diseases: A systematic review and meta-analysis. World J Gastroenterol. 2023;29(39):5503-25.
9. Wu HM, Sheng L, Wang Q, Bao H, Miao Q, Xiao X, et al. Performance of transient elastography in assessing liver fibrosis in autoimmune hepatitis-primary biliary cholangitis overlap syndrome. World J Gastroenterol. 2018;24(6):737-43.
10. Park DW, Lee YJ, Chang W, Park JH, Lee KH, Kim YH, et al. Diagnostic performance of point shear wave elastography for hepatic fibrosis in patients with autoimmune liver disease. PLoS One. 2019;14(3):e0212771.
11. Wu S, Yang Z, Zhou J, Zeng N, He Z, Zhan S, et al. Diagnostic accuracy of non-invasive tests for staging liver fibrosis in autoimmune hepatitis. Hepatol Int. 2019;13(1):91-101.
12. Goertz RS, Gaßmann L, Strobel D, Wildner D, Schellhaas B, Neurath MF, et al. Acoustic radiation force impulse elastography in autoimmune and cholestatic liver diseases. Ann Hepatol. 2019;18(1):23-29.
13. Hartl J, Ehlken H, Sebode M, Peiseler M, Krech T, Zenouzi R, et al. Usefulness of biochemical remission and transient elastography in monitoring disease course in autoimmune hepatitis. J Hepatol. 2018;68(4):754-63.
14. Dong Y, Potthoff A, Klinger C, Barreiros AP, Pietrawski D, Dietrich CF. Ultrasound findings in autoimmune hepatitis. World J Gastroenterol. 2018;24(15):1583-90.
15. Méndez-Sánchez N, Qi X. The usefulness of transient elastography in patients with autoimmune hepatitis—when can we use it? Ann Transl Med. 2018;6(15):309.
16. Soh EG, Lee YH, Kim YR, Yoon KH, Choi KH. Usefulness of 2D shear wave elastography for the evaluation of hepatic fibrosis and treatment response in patients with autoimmune hepatitis. Ultrasonography. 2022;41(4):740-49.
17. Xing X, Yan Y, Shen Y, Xue M, Wang X, Luo X, et al. Liver fibrosis with two-dimensional shear-wave elastography in patients with autoimmune hepatitis. Expert Rev Gastroenterol Hepatol. 2020;14(7):631-38.
18. Olivas I, Arvaniti P, Gabeta S, Torres S, Del Barrio M, Díaz-González A, et al. Liver stiffness measurement predicts clinical outcomes in autoimmune hepatitis. JHEP Rep. 2024;6(11):101213.
19. Hazzan R, Regev-Sadeh T, Dola T, Shemer-Shamay H, Umansky A, Zigmond E, et al. Ultrasound shear wave elastography and shear wave dispersion in autoimmune hepatitis. Ultrasound Med Biol. 2025;51(5):823-29.

20. Rasool N, Hyder A, Tareen K, Ahmed I, Iqbal S, Siddiqui MK, et al. Diagnostic performance of shear-wave elastography in autoimmune hepatitis. Cureus. 2025;17(1):e76789.
21. Peta V, Sandler Y, Deckmyn O, Duroselle O, Vinnitskaya E, Khomeriki S, et al. Diagnostic performance of FibroTest-ActiTest, transient elastography, and FIB-4 index in autoimmune hepatitis. World J Hepatol. 2025;17(3):104534.
22. Kim KA. Transient elastography for assessing liver fibrosis in autoimmune liver diseases: Editorial. Clin Mol Hepatol. 2025;31(1):275-76.
23. Cristoferi L, Calvaruso V, Overi D, Viganò M, Rigamonti C, Degasperi E, et al. Accuracy of transient elastography in assessing fibrosis at diagnosis in naïve patients with primary biliary cholangitis. Hepatology. 2021;74(3):1496-1508.
24. Chen JL, Hou YX, Liu Y, Jiang YY, Wang XB. Real-world performance of transient elastography in Chinese patients with primary biliary cholangitis. World J Gastroenterol. 2025;31(41):111256.
25. Corpechot C, Gaouar F, El Naggar A, Kemgang A, Wendum D, Poupon R, et al. Baseline values and changes in liver stiffness measured by transient elastography are associated with severity of fibrosis and outcomes. Gastroenterology. 2014;146(4):970-79.
26. Corpechot C, Carrat F, Poujol-Robert A, Gaouar F, Wendum D, Chazouillères O, et al. Noninvasive elastography-based assessment of liver fibrosis progression and prognosis in PBC. Hepatology. 2012;56(1):198-208.
27. Floreani A, Cazzagon N, Martines D, Cavalletto L, Baldo V, Chemello L. Performance and utility of transient elastography and noninvasive markers of liver fibrosis in PBC. Dig Liver Dis. 2011;43(11):887-92.
28. Manzo-Francisco LA, Aquino-Matus J, Vidaña-Pérez D, Uribe M, Chavez-Tapia N. Transient elastography compared to liver biopsy for staging fibrosis in PBC: systematic review. Ann Hepatol. 2023;28(4):101107.
29. Osman KT, Maselli DB, Idilman IS, Rowan DJ, Viehman JK, Harmsen WS, et al. Liver stiffness measured by MR or transient elastography predicts outcomes in PBC. J Clin Gastroenterol. 2021;55(5):449-57.
30. Schulz M, Wilde AB, Demir M, Müller T, Tacke F, Wree A. Shear wave elastography and shear wave dispersion imaging in primary biliary cholangitis. Quant Imaging Med Surg. 2022;12(2):1235-42.
31. Zhang Y, Meng F, Hu X, Zhang T, Han X, Han J, et al. Comparative diagnostic efficacy of 2D-SWE and transient elastography in PBC. BMC Gastroenterol. 2024;24:396.
32. Yan Y, Xing X, Lu Q, Wang X, Luo X, Yang L. Assessment of biopsy proven liver fibrosis by 2D-SWE in PBC. Dig Liver Dis. 2020;52(5):555-60.
33. Corpechot C, Carrat F, Gaouar F, Chau F, Hirschfield G, Gulamhusein A, et al. Liver stiffness measurement improves outcome prediction in PBC. J Hepatol. 2022;77(6):1545-53.

34. Lam L, Soret PA, Lemoinne S, Hansen B, Hirschfield G, Gulamhusein A, et al. Dynamics of liver stiffness measurement and clinical course of PBC. Clin Gastroenterol Hepatol. 2024;22(12):2432-41.
35. Wong YJ, Lam L, Soret PA, Lemoinne S, Hansen B, Hirschfield G, et al. Prognostic value of liver stiffness measurement vs biochemical response in PBC. J Hepatol. 2026;84(2):275-83.
36. Ehlken H, Lohse AW, Schramm C. Transient elastography in primary sclerosing cholangitis. Gastroenterology. 2014;147(2):542-43.
37. Mjelle AB, Fossdal G, Gilja OH, Vesterhus M. Liver elastography in PSC using three different scanner systems. Ultrasound Med Biol. 2020;46(8):1854-64.
38. Fossdal G, Mjelle AB, Wiencke K, Bjørk I, Gilja OH, Folseraas T, et al. Fluctuating biomarkers in PSC: comparison of ALP, liver stiffness and ELF. JHEP Rep. 2021;3(5):100328.
39. Roccarina D, Saffioti F, Rosselli M, Marshall A, Pinzani M, Thorburn D. Utility of ElastPQ point shear wave elastography in PSC. JHEP Rep. 2023;5(11):100873.
40. Russo MW. Noninvasive prognostic models, imaging, and elastography in PSC. World J Hepatol. 2023;15(9):1013-1020.
41. Hashemi P, Boyer JL, Langdon JH. Utility of elastography in PSC: systematic review. J Magn Reson Imaging. 2026;63(4):938-58.
42. Mjelle AB, Mulabecirovic A, Hausken T, Havre RF, Gilja OH, Vesterhus M. Ultrasound and point shear wave elastography in PSC. Ultrasound Med Biol. 2016;42(9):2146-55.
43. Tafur M, Cheung A, Menezes RJ, Feld J, Janssen H, Hirschfield GM, et al. Risk stratification in PSC using MRCP vs liver stiffness. Eur Radiol. 2020;30(7):3735-47.
44. Boursier J, Zarski JP, de Ledinghen V, Rousselet MC, Sturm N, Lebail B, et al. Determination of reliability criteria for liver stiffness evaluation by transient elastography. Hepatology. 2013;57(3):1182-91.
45. Ferraioli G, Wong VW, Castera L, Berzigotti A, Sporea I, Dietrich CF, et al. Liver ultrasound elastography: An update to the World Federation for Ultrasound in Medicine and Biology guidelines and recommendations. Ultrasound Med Biol. 2018;44(12):2419-40.
46. Barr RG, Wilson SR, Rubens D, Garcia-Tsao G, Ferraioli G. Update to the Society of Radiologists in Ultrasound liver elastography consensus statement. Radiology. 2020;296(2):263-74.
47. Dietrich CF, Bamber J, Berzigotti A, Bota S, Cantisani V, Castera L, et al. EFSUMB guidelines and recommendations on the clinical use of ultrasound elastography. Ultraschall Med. 2017;38(4):377-94.
48. Cosgrove D, Piscaglia F, Bamber J, Bojunga J, Correas JM, Gilja OH, et al. EFSUMB guidelines and recommendations on the clinical use of ultrasound elastography. Part 2: Clinical applications. Ultraschall Med. 2013;34(3):238-53.

49. Millonig G, Reimann FM, Friedrich S, Fonouni H, Mehrabi A, Büchler MW, et al. Extrahepatic cholestasis increases liver stiffness irrespective of fibrosis. Hepatology. 2008;48(5):1718-23.
50. Arena U, Vizzutti F, Corti G, Ambu S, Stasi C, Bresci S, et al. Acute viral hepatitis increases liver stiffness values measured by transient elastography. Hepatology. 2008;47(2):380-84.
51. Vizzutti F, Arena U, Marra F, Pinzani M. Non-invasive diagnosis of portal hypertension in cirrhosis by elastography. Liver Int. 2014;34(6):1026-33.
52. Colecchia A, Montrone L, Scaioli E, Bacchi-Reggiani ML, Colli A, Casazza G, et al. Measurement of spleen stiffness for evaluation of portal hypertension and esophageal varices. Hepatology. 2012;56(2):644-51.
53. Stefanescu H, Marasco G, Calès P, Fraquelli M, Rosselli M, Bolognesi M, et al. Spleen stiffness measurement using elastography for predicting portal hypertension. J Hepatol. 2020;73(2):313-24.
54. Berzigotti A. Non-invasive evaluation of portal hypertension using ultrasound elastography. J Hepatol. 2017;67(2):399-11.
55. Giuffrè M, Fourquet B, Abraldes JG, Berzigotti A. Elastography in portal hypertension and variceal risk assessment. Clin Gastroenterol Hepatol. 2022;20(1):9-18.
56. Fraquelli M, Rigamonti C, Casazza G, Donato MF, Ronchi G, Conte D, et al. Reproducibility of transient elastography in the evaluation of liver fibrosis. Gut. 2007;56(7):968-73.
57. Sporea I, Bota S, Gradinaru-Tascau O, Sirli R, Popescu A. Comparative study between transient elastography and acoustic radiation force impulse elastography. World J Gastroenterol. 2013;19(30):4924-31.
58. Friedrich-Rust M, Nierhoff J, Lupsor M, Sporea I, Fierbinteanu-Braticevici C, Strobel D, et al. Performance of acoustic radiation force impulse imaging for the staging of liver fibrosis. Hepatology. 2012;55(3):833-41.
59. Ferraioli G, Filice C, Castera L, Choi BI, Sporea I, Wilson SR, et al. WFUMB guidelines and recommendations for clinical use of ultrasound elastography. Ultrasound Med Biol. 2015;41(5):1126-47.
60. Singh S, Venkatesh SK, Wang Z, Miller FH, Motosugi U, Low RN, et al. Diagnostic performance of elastography for staging liver fibrosis: systematic review and meta-analysis. Clin Gastroenterol Hepatol. 2015;13(3):440-51.
61. Dietrich CF, Barr RG, Farrokh A, Dighe M, Hocke M, Jenssen C, et al. Elastography in liver disease: update and clinical applications. World J Gastroenterol. 2021;27(16):1800-20.
62. European Association for the Study of the Liver (EASL). Clinical practice guidelines on non-invasive tests for evaluation of liver disease severity and prognosis. J Hepatol. 2021;75(3):659-89.
63. Castera L, Friedrich-Rust M, Loomba R. Non-invasive assessment of liver disease in patients with chronic liver disease. Nat Rev Gastroenterol Hepatol. 2019;16(9):571-86.

5.7. Comparison of various elastographic techniques for liver fibrosis assessment

Ioan Sporea, Raluca Lupușoru

Abstract

Liver elastography has become a cornerstone in the non-invasive assessment of liver fibrosis, progressively replacing liver biopsy in routine clinical practice. Current international guidelines (EFSUMB, WFUMB, EASL) recognize Shear Wave Elastography (SWE) - including Vibration Controlled Transient Elastography (VCTE), point SWE (pSWE), and two-dimensional SWE (2D-SWE) - as validated methods for fibrosis staging.

Comparative studies demonstrate similar diagnostic performance among ultrasound-based techniques when system-specific cut-off values are applied. VCTE, the first widely implemented method, has extensive validation across chronic viral hepatitis, MAFLD, alcoholic liver disease, and cholestatic disorders. pSWE and 2D-SWE provide comparable accuracy, with higher feasibility in certain patient subgroups and the advantage of B-mode guidance.

Magnetic resonance elastography (MRE) consistently shows superior diagnostic accuracy, particularly for advanced fibrosis and cirrhosis, and in obese or MAFLD patients. Meta-analyses report AUROC values >0.90 for MRE across fibrosis stages. However, cost, availability, and need for specialized radiological infrastructure limit its widespread use.

Ultrasound-based elastography remains the most accessible and practical tool for daily clinical evaluation. Awareness of confounding factors and proper use of validated cut-off values are essential. Overall, both ultrasound-based elastography and MRE provide reliable, evidence-based strategies for non-invasive liver fibrosis assessment.

5.7.1. Introduction

Considering the increased numbers of elastographic techniques, evaluating their suitability for clinical application is a reasonable concern. Ultrasound-based elastography and magnetic resonance elastography (MRE) can be used for liver elastography. The latter was primarily developed in the United States, perhaps because of the high obesity rate in the region, which makes ultrasound-based elastography less feasible.

Ultrasound based elastography was divided into Shear Wave Elastography (SWE) and Strain Elastography (SE) by the significant guidelines, issued by EFSUMB and WFUMB (1, 2). Although several Japanese studies showed promising results for strain elastography for liver fibrosis evaluation, both guidelines emphasize that only SWE is prepared for clinical application for liver fibrosis assessment (3).

The updated WFUMB guidelines confirm the clinical use of Vibration Controlled Transient Elastography (VCTE), point shear wave elastography (pSWE), and two-dimensional shear wave elastography (2D-SWE) for staging liver fibrosis. The diagnostic performance of these methods is generally comparable, when system-specific cut-off values are applied during validation. However, potential confounding factors—such as hepatic inflammation, cholestasis, and cardiac congestion—must be carefully considered when interpreting liver stiffness measurements. Operator experience also plays a significant role in ensuring reliable acquisition and accurate interpretation of results (4).

In addition to the previously published EFSUMB and WFUMB recommendations, more recent international guidelines further consolidated the role of elastography in clinical practice. The 2021 update of the European Association for the Study of the Liver (EASL) Clinical Practice Guidelines emphasized that non-invasive tests, including VCTE, pSWE, 2D-SWE, and MRE, should be used as first-line tools for fibrosis assessment, significantly reducing the need for liver biopsy. The guidelines also highlighted that cut-off values are system-specific and etiology-dependent and that MRE may be particularly useful for obese patients or in cases with unreliable ultrasound measurements (5).

Comparing SWE approaches will be the main topic of this chapter. The US probe induces shear waves in the liver for elastographic measurements in all SWE techniques. Either kPa or meters/seconds are used to express the results. Point SWE (pSWE) and 2D-SWE are two subclasses of SWE using Acoustic Radiation Force Impulse (Fig.5.7.1).

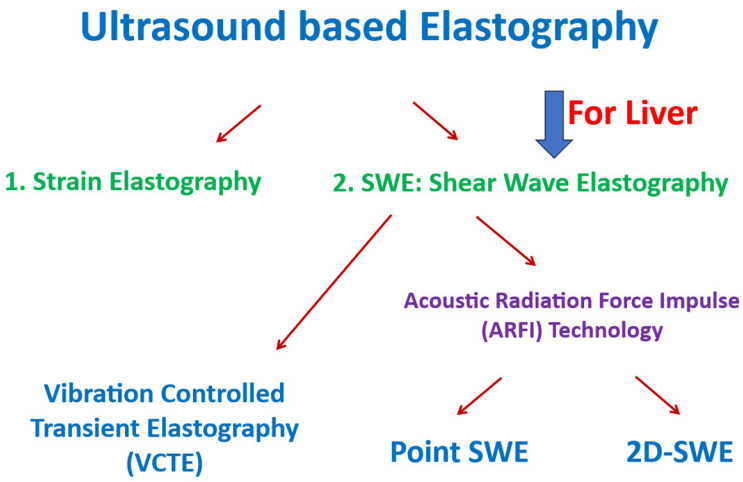


Fig. 5.7.1: US-based elastographic method classification

5.7.2. Feasibility of different elatography techniques

The practicality of ultrasound-based elastographic techniques is a crucial criterion that is impacted by several variables, including the patient's gender, abdominal circumference, and level of obesity.

The feasibility of VCTE using only the M probe (in normal-weight subjects) is only 70-85% (6-8) but using both M and XL (for obese) probes, it can reach 93.5% (9). For point SWE, where the measuring box is small, the feasibility is usually higher than 95%. For 2D-SWE, where the box is larger, the feasibility is lower, especially in patients with advanced fibrosis (in which the liver is heterogenous), and a good experience in abdominal ultrasound is needed for good acquisitions (10-13) (Table 5.7.I).

Table 5.7.I. Feasibility of different elastography techniques

Study	**Number of subjects with valid measurements/ Feasibility**	**Elastography method**	**No. of subjects evaluated**
Castera L 2015; Hepatology.	10.903 (86.4%)	VCTE	12.949
Sirli R 2013; Eur J. Radiol.	5827 (71.9%)	VCTE	8.218
Sporea I 2016; Med. Ultrason.	3.024 (93.5%)	VCTE	3.235
Grădinaru-Tascău O 2013; Med.Ultrason.	324 (87.1%)	SSI (2D-SWE)	371
Bota S 2013; Liver Int.	pSWE : 1138 (97.9%) VCTE : 1087 (93.4%)	VCTE, ARFI	1163
Cassinotto C 2016; Hepatology	VCTE:223 (76.6%) 2D-SWE :232 (79.7%) pSWE: 236 (81%)	VCTE, SSI, ARFI	291
Lee MS 2018; PLoS	VCTE:74(78.7%) 2D-SWE:69(73.4%) pSWE:82(88.3%)	VCTE, SSI, ARFI	94

5.7.3. Comparison between the performance of techniques

Extensive research comparing various elastographic techniques has been published. Liver biopsies were considered the gold standard for some of these publications. This approach was no longer feasible in subsequent research, since the number of liver biopsies performed fell precipitously as non-invasive techniques became available (1). However, given that VCTE was approved as a reliable tool for fibrosis assessment by numerous guidelines, such as those published by the European Association for the Study of the Liver (5), some subsequent studies considered VCTE as a reference method.

EFSUMB and WFUMB guidelines (1, 2) underline that the cut-off values of liver elastography for different stages of fibrosis are system dependent and that they must be known for every system used in practice. The cutoff values for the newly developed elastographic techniques (and currently all the important ultrasound companies have implemented elastographic modules on

their systems) have been calculated considering either liver biopsy, VCTE, or MRE as the reference method.

From a temporal perspective, VCTE was the first liver elastographic method on the market. More than 2100 published papers proved this method's value for liver fibrosis evaluation in HCV and HBV chronic hepatitis, in MASLD, in alcoholic liver disease (ALD), in cholestatic liver diseases, and in post-transplant patients, mainly considering liver biopsy as the gold standard. The second-generation elastographic method that appeared on the market was point SWE (pSWE). The first system based on the ARFI technique was Virtual Touch Quantification (VTQ) from Siemens.

Many ***comparative studies between different ultrasound-based elastographic methods*** have been published during this time**.**

A) Point SWE (Table 5.7.II)

A comparison between VCTE and VTQ (ARFI) was performed by Lupșor M (14) in chronic hepatitis C patients, with liver biopsy as the gold standard. In a cohort of 112 consecutive patients, the diagnostic accuracy of these two elastographic methods was comparable only for the prediction of severe fibrosis and cirrhosis, but for earlier stages of fibrosis, VCTE performed better.

In a multicenter study in 400 HCV chronic hepatitis patients, with liver biopsy as the gold standard, VTQ was compared to VCTE (15). In this study, the correlation with histological fibrosis was similar between VTQ and VCTE (0.689 vs 0.728, with a p=0.28).

In a prospective European multicenter study, VTQ was compared with VCTE, also with liver biopsy as the gold standard (16). A total of 241 HCV patients from 7 European centers were evaluated. A comparison between the accuracy of pSWE and VCTE revealed no significant difference between the methods for all stages of fibrosis (0.81 vs 0.85 for F≥2; p=0.15; 0.88 vs 0.92 for F≥3; p=0.11; and 0.89 vs 0.94 for cirrhosis; p=0.19). The conclusion of the study was that the diagnostic accuracy of VCTE and pSWE (VTQ) was comparable in HCV patients.

Later, a meta-analysis was performed to compare VCTE with pSWE (VTQ) (11). In this meta-analysis, 1163 patients with chronic hepatopathies were analyzed. The feasibility of VTQ was 97.9%, and for VCTE it was 93.4% (p<0.001). For predicting significant fibrosis (F≥2), VCTE had a sensitivity of 0.78 (95% CI: 0.72-0.83) and a specificity of 0.84 (95% CI: 0.75-0.90), while for VTQ, the sensitivity was 0.74 (95% CI: 0.66-0.80) and the specificity was 0.83 (95% CI:

0.75-0.90). For the diagnosis of liver cirrhosis, the sensitivity was 0.89 (95% CI: 0.80-0.94) for VCTE and the specificity 0.87 (95% CI: 0.81-0.91), while for VTQ the sensitivity was 0.87 (95% CI: 0.79-0.92) and the specificity 0.87 (95% CI: 0.75-0.90). There were no significant differences between the diagnostic odds ratio of these two methods regarding the detection of significant fibrosis [mean difference in rDOR=0.27 (95% CI: 0.69-0.14)] or cirrhosis [mean difference in rDOR=0.12 (95% CI: 0.29-0.52)]. The results of this meta-analysis in a substantial cohort of patients are proof of this method's utility for clinical use, at least in some types of patients.

When using validated cut-off values, other meta-analyses have confirmed that ultrasound-based elastographic methods demonstrate comparable diagnostic performance. A comprehensive meta-analysis published by Tsochatzis et al. (17) showed the high accuracy of elastography for advanced fibrosis and cirrhosis, with only minimal differences between the VCTE and SWE techniques. These findings support the concept that all shear wave–based ultrasound methods can be reliably used in clinical practice, provided that appropriate system-specific thresholds are applied.

In a recently published paper, an Italian group compared VCTE with ElastPQ (a pSWE method) (18). Liver stiffness measurements with ElastPQ and VCTE have been obtained in 361 patients from a cohort of 406 individuals with chronic liver diseases of diverse etiology, who underwent liver biopsy. In this comparative study, ElastPQ values correlated well with the histologic fibrosis score ($r = 0.718$; $p < 0.001$). For ElastPQ, the AUROC values were 0.856 for significant fibrosis (F≥2), 0.951 for advanced fibrosis (F≥3), and 0.965 for cirrhosis. The diagnostic accuracy of ElastPQ and VCTE was found to be superimposable at each stage of liver fibrosis. The conclusion of this comparative study was that ElastPQ and VCTE identified patients with fibrosis and liver cirrhosis with a similar level of accuracy.

Table 5.7.II. Comparative performance of pSWE techniques

Study	**Elastography techniques**	**No. of subjects/ Etiology**	**Performance of methods**	
Lupșor M 2009; JGLD	VTQ vs VCTE	112 HCV	VCTE (AUROC)	VTQ (AUROC)
			≥F1:0.918 ≥F2:0.961 ≥F3:0.957 F4:0.970	≥F1:0.725 ≥F2:0.869 ≥F3:0.900 F4:0.936
Sporea I 2011; EJR	VTQ vs VCTE	400 HCV		VTQ (AUROC)
				≥F1: 0.779 ≥F2:0.792 ≥F3:0.829 F4:0.842
Friedrich-Rust M 2015; Ultraschall Med.	VTQ vs VCTE	241 HCV	VCTE (Spearman's r)	VTQ (Spearman's r)
			≥F2:0.85 ≥F3:0.92 F4:0.94	≥F2:0.81 ≥F3:0.88 F4:0.89
Bota S 2013; Liver Int.	VTQ vs VCTE	1163 CLD	VCTE (sROC)	VTQ (sROC)
			≥F2:0.87 F4:0.93	≥F2:0.85 F4:0.93
Conti F 2019; Clin Gastroenterol Hepatol.		406 CLD	VCTE (AUROC)	ELASTPQ (AUROC)
			SUPERIMPOSABLE	≥F2:0.856 ≥F3:0.951 F4:0.965
Tsochatzis EA 2018; J Hepatol.	VCTE vs. SWE (meta-analysis)	Multiple studies; CLD	VCTE (AUROC) ≥F2: 0.80-0.88 ≥F3: 0.85-0.92 F4: 0.90-0.95	SWE (AUROC) ≥F2: 0.82-0.89 ≥F3: 0.87-0.93 F4: 0.90-0.96

B) 2D-SWE (Table 5.7.III)

Table 5.7.III. Comparative performance of 2D-SWE techniques

Study.	**Elastography techniques**	**No. of subjects Etiology**	**Performance of methods**		
Cassinotto C 2014; J Hepatol	VTQ (ARFI) vs VCTE vs SSI	349 CLD	VCTE (AUROC)	VTQ (ARFI) (AUROC)	SSI (AUROC)
			≥F1:0.86 ≥F2:0.84 ≥F3:0.87 F4:0.90	≥F1:0.84 ≥F2:0.81 ≥F3:0.89 F4:0.90	≥F1:0.89 ≥F2:0.88 ≥F3:0.93 F4:0.93
Cassinotto C 2016; Hepatology	VTQ (ARFI) vs VCTE vs SSI	291 NAFLD	VCTE (AUROC)	VTQ (ARFI)	SSI (AUROC)
			≥F2:0.82 ≥F3:0.86 F4:0.87	≥F2:0.77 ≥F3:0.84 F4:0.84	≥F2:0.86 ≥F3:0.89 F4:0.88
Lee MS 2017; PLoS One	VTQ (ARFI) vs VCTE vs SSI	94 NAFLD	VCTE (AUROC)	VTQ (ARFI)	SSI (AUROC)
			≥F2:0.757 ≥F3:0.870	≥F2:0.657 ≥F3:0.873	≥F2:0.759 ≥F3:0.809
Hermann E 2018; Hepatology	VCTE vs SSI	665 CLD	VCTE (Differences in AUROC)		SSI (AUROC)
			≥F2: -5.3% ≥F3: -3.4% F4:-1.8%		≥F2:0.864 ≥F3:0.908 F4:0.931
Sporea I 2013; Ultrasound Med Biol.	VTQ (ARFI) vs SSI	334 CLD	VTQ (ARFI) (Accuracy%)		SSI (Accuracy%)
			≥F2:72.2 F4:78.2		≥F2:74.4 F4:85.8
Mulazzani L 2017; J Ultrasound	pSWE.Esaote vs SSI	108 CLD	2D.SWE.SSI vs pSWE.ESA (Lin's Analysis)		
			<15.2 kPa		>15.2 kPa
			Precision: 0.737 Accuracy: 0.861		Precision: 0.559 Accuracy: 0.998
	VCTE vs SSI	402 VHB	VCTE (AUROC)		SSI (AUROC)

Yongyan G 2018; Radiology			F4:0.80	F4:0.87	
Sporea I 2018; Med Ultrason	VTQ vs SSI vs ElastPQ	127 CLD	VTQ (Accuracy%)	ElastPQ (Accuracy%)	SSI (Accuracy%)
			F<2:82 F2/F3:84.1 F4:93.9	F<2:86 F2/F3:84 F4:94	F<2:80 F2/F3:85.3 F4:94

In 2D-SWE, a color-coded image and numeric values are displayed as the result of elastographic assessment, which evaluates tissue stiffness. The advantages of 2D-SWE are multipoint evaluation, real-time evaluation, a large area of interrogation, and high-rate frame acquisition (in Aixplorer from SuperSonic Imagine/Hologic). Several comparative studies have been performed, two of them by a French group (Cassinoto et al) in chronic hepatitis (12) and NAFLD/MASLD patients (19), respectively. In the first one, including a cohort of 349 patients with chronic hepatopathies in whom liver biopsy was performed to assess liver fibrosis, three ultrasound-based elastography methods were compared: VCTE (FibroScan with M and XL probes), 2D-SWE (Supersonic Shear Imaging-SSI), and point SWE (VTQ with ARFI technology). All three elastographic techniques significantly correlated with histological fibrosis: $r=0.79$, $p<0.00001$ for SSI, $r=0.70$, $p<0.00001$ for VCTE, and $r=0.64$, $p<0.00001$ for VTQ. The AUROCs for different methods and stages of fibrosis were 0.88 for SSI, 0.84 for VCTE, and 0.81 for VTQ for significant fibrosis, while for cirrhosis they were 0.93 for SSI, 0.90 for VCTE, and 0.90 for VTQ. The conclusion of this study was that there were no significant differences between the systems for significant fibrosis and cirrhosis.

The second paper of the same group included 291 NAFLD/MASLD patients, in which the performance of elastographic systems was studied. All have been evaluated by means of liver biopsy in two French university hospitals, by 2D-SWE (SSI), VCTE, and point SWE (VTQ). For significant fibrosis (F≥2), the AUROCs were 0.86, 0.82, and 0.77, while for cirrhosis, 0.88, 0.87, and 0.84, respectively. Regarding feasibility, VTQ (ARFI) had the highest one—99.3%, vs. SSI - 87% and TE - 85.6%. The factors associated with failed measurements were waist circumference, BMI, and intercostal wall thickness. In the same study, the authors found that the cut-off values for SSI and TE were quite similar for predicting the same stages of fibrosis.

A similar study was performed by Lee et al (13) comparing VCTE, SSI, and VTQ with liver biopsy in 94 patients with NAFLD/MASLD. The rate of unreliable and failed results was 21.3% for VCTE, 26.6% for SSI, and for VTQ, only 11.7%. In this study, the AUROC's for significant fibrosis (F≥2) were 0.757, 0.759, and 0.657, and for advanced fibrosis (F≥3), they were 0.870, 0.809, and 0.873, respectively. This study also concluded that all three elastographic methods had similar diagnostic performance in NAFLD/MASLD patients.

In a multicenter study (13 centers from 9 countries) published by Hermann et al. (20), the accuracy of SSI (2D-SWE) for staging liver fibrosis (liver biopsy as reference) was evaluated in 1134 patients with viral and non-viral chronic liver diseases. In 665 subjects, SSI was also compared to VCTE. In the comparative study group, 2D-SWE (SSI) performed better than VCTE for all stages of fibrosis and significantly better for F≥2 and liver cirrhosis ($p<0.001$ and $p=0.007$).

In a comparative study between VTQ (ARFI) and 2D-SWE (SSI), considering VCTE as the reference method (21), 332 consecutive patients were evaluated on the same day by the three methods, but reliable liver stiffness measurements were obtained only in 184 cases (55.4%) by all three. Higher body mass index and older age were associated with unreliable measurements. Reliable measurements have been obtained in a significantly higher percentage of cases by VTQ than by VCTE (M probe) or by SSI: 92.1% vs. 72.2% ($p<0.0001$) and vs. 71.3%, ($p<0.0001$). This study also demonstrated that VTQ and SSI have similar accuracy in diagnosing significant fibrosis and liver cirrhosis.

A comparison between pSWE from Esaote (pSWE.ESA) and SSI (2D-SWE), considering VCTE as the reference method, was performed in a cohort of 81 patients with chronic liver diseases (22). Spearman's correlation coefficients between VCTE and pSWE.EAS and SSI were 0.849 and 0.878, respectively. According to this study, the correlation was less strict in higher liver stiffness values (>15.2 kPa), but this does not influence the staging of fibrosis, since all are in the cirrhotic range.

In another study, a comparison between 2D-SWE (SSI) and VCTE was performed in HBV patients, considering liver biopsy as the gold standard (23). The study included a cohort of 402 subjects with chronic hepatitis B (154 with chronic B infection and 248 with chronic B hepatitis). The AUROC of 2D-SWE to predict cirrhosis was 0.87 (95% confidence interval [CI]: 0.83-0.90), higher than that of VCTE—0.80 (95% CI: 0.68-0.88).

Another comparative paper between elastographic methods was published by a Romanian group (24). It was a prospective study on 127 consecutive patients with chronic liver diseases of mixed etiologies. In the same day, these patients were evaluated by four elastographic methods: TE, VTQ (pSWE), ElastPQ (pSWE) and SSI (2D-SWE), VCTE being the reference method. Regarding feasibility, valid measurements were obtained in 116/127 cases with VTQ, in 108/127 with SSI, in 111/127 with TE and in 109/127 with ElastPQ, so that the final analysis was performed in 82 subjects, who had reliable measurements by all four methods. This study showed that the accuracies of VTQ, SSI and ElastPQ for diagnosing significant/severe fibrosis and liver cirrhosis were quite similar: 84.1%, 85.3%, and 84% ($p>0.05$) and 93.9%, 94%, and 94% ($p>0.05$), respectively (25).

Considering the results of all the published studies that showed similar performance of various ultrasound-based liver elastography methods, it is safe to consider that any of them can be used for liver fibrosis assessment (25), keeping in mind that specific cut-off values should be used for each system.

C) MRE (Table 5.7.IV)

Comparative studies have also been performed between ultrasound-based elastographic methods and magnetic resonance elastography (MRE).

The first one was published in 2008 by Huwart L et al. (26) in a prospective cohort of 141 patients with chronic liver diseases, all evaluated by liver biopsy, MRE and VCTE. Reliable values were obtained in 133/141 patients (94%) by MRE and in 118/141 subjects (84%) with the M probe by VCTE, so that the comparison was performed in 96 cases. The AUROCs for MRE were higher as compared to VCTE (0.994 for $F \geq 2$; 0.985 for $F \geq 3$ and 0.998 for $F=4$ for MRE and 0.837, 0.709, and 0.849 for VCTE). The conclusion of this study was that the feasibility and the accuracy of MRE are superior to VCTE.

A comparative study regarding the performance of MRE and VCTE in chronic hepatitis B and C was performed in 103 patients with liver biopsy (27). The comparison was possible in 85 subjects (65 HBV, 19 HCV and 1 co-infected). In this study, VCTE and MRE had comparable accuracies (AUROC for $F \geq 2$: 0.914 VCTE vs. 0.909 MRE, $p=0.89$; for $F \geq 3$: 0.895 VCTE vs. 0.928 MRE, $p=0.42$).

In a retrospective study on 113 patients with chronic liver diseases, all with liver biopsy or liver resection (28), the AUROCs of MRE for all the stages of fibrosis were higher than for VCTE (0.98 vs 0.87 for $F \geq 2$: $p=0.0003$; 0.97 vs 0.93 for cirrhosis: $p<0.0308$).

In a systematic meta-analysis in HBV chronic hepatitis (29), the performance of MRE was evaluated in 1470 patients and of VCTE in 3641 patients. AUROC values for MRE and VCTE for detecting significant fibrosis, advanced fibrosis and cirrhosis were 0.981 vs. 0.796 ($p<0.001$), 0.972 vs. 0.893 ($p<0.001$), and 0.972 vs. 0.905 ($p<0.001$). The conclusion of this meta-analysis was that MRE is more accurate than VCTE for the assessment of liver fibrosis in HBV patients.

Another meta-analysis that compared TE and 2D-SWE (SSI) with MRE was performed in patients with nonalcoholic fatty liver disease (NAFLD/MASLD) (30). A total of 13,046 NAFLD/MASLD subjects were included, the prevalence of significant fibrosis, advanced fibrosis, and cirrhosis being 45.0%, 24.0%, and 9.4%, respectively. The sensitivities and specificities of VCTE, 2D-SWE, and MRE for detecting advanced fibrosis were 0.87 and 0.79, 0.90 and 0.93, and 0.84 and 0.90, respectively. In this meta-analysis, the AUROC values for VCTE with M probe, XL probe, 2D-SWE, and MRE for diagnosing F≥3 were 0.88, 0.85, 0.95, and 0.96, respectively. The conclusion of this study was that MRE and 2D-SWE have the highest accuracy for correct staging of fibrosis in NAFLD/MASLD patients.

Another study compared MRE with VCTE in NAFLD patients (31). This study included 142 patients with NAFLD/MASLD and a mean body mass index of 28.1 kg/m², all with liver biopsies. The AUROC of VCTE to predict $F \geq 2$ was 0.82 (95% CI: 0.74-0.89), whereas MRE had an AUROC value of 0.91 (95% CI: 0.86-0.96), $p = 0.001$. In the same study, the authors compared CAP (Controlled Attenuation Parameter) from FibroScan with PDFF (proton density fat fraction) from MRI. CAP measurements identified patients with hepatic steatosis grade ≥2 with an AUROC value of 0.73 (95% CI: 0.64-0.81), and PDFF identified them with an AUROC value of 0.90 (95% CI: 0.82-0.97), $p < 0.001$.

A large individual patient data meta-analysis by Karlas et al. (32) confirmed that Controlled Attenuation Parameter (CAP) provides acceptable diagnostic performance for detecting hepatic steatosis but shows variability depending on patient characteristics. Compared to MRI-based proton density fat fraction (PDFF), MRI techniques demonstrate superior accuracy and reproducibility, particularly for grading steatosis severity.

In a study performed by Park CC et al (33), a cohort of 104 patients with NAFLD/MASLD was included. All patients were evaluated by liver biopsy, VCTE, and MRE. MRE detected any fibrosis (stage 1 or more) with an AUROC of 0.82 (95% CI: 0.74-0.91), which was significantly higher than that of VCTE (AUROC,

0.67; 95% CI, 0.56-0.78). Regarding different stages of fibrosis, MRE detected fibrosis stage 2, 3, or 4 with AUROC values of 0.89 (95% CI, 0.83-0.96), 0.87 (95% CI, 0.78-0.96), and 0.87 (95% CI, 0.71-1.00), respectively; VCTE detected fibrosis stage 2, 3, or 4 with AUROC values of 0.86 (95% CI, 0.77-0.95), 0.80 (95% CI, 0.67-0.93), and 0.69 (95% CI, 0.45-0.94). Regarding steatosis assessment, MRI-PDFF detected any steatosis with an AUROC of 0.99 (95% CI, 0.98-1.00), significantly higher than that of CAP (AUROC, 0.85; 95% CI, 0.75-0.96). At the same time, MRI-PDFF identified steatosis grade 2 or 3 with AUROC values of 0.90 (95% CI, 0.82-0.97) and 0.92 (95% CI, 0.84-0.99), and CAP identified steatosis grade 2 or 3 with AUROC values of 0.70 (95% CI, 0.58-0.82) and 0.73 (95% CI, 0.58-0.89). The conclusion of this study was that MRE with PDFF is more accurate than VCTE with CAP for the evaluation of fibrosis and steatosis in NAFLD/MASLD patients.

Another comparison was performed between MRE and a pSWE technique—VTQ (ARFI) (34) in a cohort of 125 patients with NAFLD/MASLD, with a mean BMI of 31.8 (±7.0) kg/m^2. MRE AUROCs for diagnosing F≥2, F≥3 and F=4 was 0.885 (95% CI 0.816-0.953), 0.934 (95% CI 0.863-1.000), and 0.882 (95% CI 0.729-1.000), while for VTQ (ARFI) the AUROCs were 0.848 (95% CI 0.776-0.921), 0.896 (95% CI 0.824-0.968), and 0.862 (95% CI 0.721-1.000). Considering the influence of obesity, MRE was superior to VCTE in obese subjects, but not in non-obese (p=0.722). The conclusion of this study was that MRE is more accurate than pSWE for liver fibrosis assessment in NAFLD/MASLD patients, especially in obese subjects.

A direct comparative study between MRE and 2D-SWE demonstrated similar diagnostic performance for the detection of significant fibrosis, while MRE showed superior accuracy for advanced fibrosis and cirrhosis. The conclusion of the study was that based on these findings, 2D-SWE may be considered a reliable and accessible alternative when MRE is not available (35).

Another study has evaluated the diagnostic performance of VCTE against MRE. In a study (36), MRE demonstrated superior diagnostic accuracy for advanced fibrosis and cirrhosis, while VCTE showed comparable performance for significant fibrosis (F≥2). The authors concluded that VCTE represents a valid and accessible alternative when MRE is unavailable, particularly in routine clinical settings.

Table 5.7.IV. Comparative performance of MRE vs. ultrasound-based elastographic techniques.

Study	**Elastography techniques**	**No. of subjects Etiology**	**Performance of methods**		
Huwart L 2008; Gastroenterology	MRE vs VCTE	96 CLD	VCTE (AUROC)	MRE (AUROC)	
			≥F2:0.837 ≥F3:0.709 F4:0.849	≥F2:0.994 ≥F3:0.985 F4:0.998	
Bohte AE 2014; Eur Radiol	MRE vs VCTE	85 HBV, HCV	VCTE (AUROC)	MRE (AUROC)	
			≥F2:0.914 ≥F3:0.895	≥F2:0.909 ≥F3:0.928	
Ichikawa S 2015; Magn Reson Imaging	MRE vs VCTE	113 CLD	VCTE (AUROC)	MRE (AUROC)	
			≥F1:0.87 ≥F2:0.87 F4:0.93	≥F1:0.97 ≥F2:0.98 F4:0.97	
Xiao H 2017; PLoS One	MRE vs VCTE	3641 CLD	VCTE (AUROC)	MRE (AUROC)	
			≥F2:0.796 ≥F3:0.893 F4:0.905	≥F2:0.981 ≥F3:0.972 F4:0.972	
Xiao G 2017; Hepatology	MRE vs VCTE vs SSI	13.046 NAFLD	TE (AUROC)	SSI (AUROC)	MRE (AUROC)
			≥F2:0.83(M) ≥F3:0.87(M) F4:0.92(M)	≥F2:0.89 ≥F3:0.91 F4:0.97	≥F2:0.88 ≥F3:0.93 F4:0.92
			≥F2:0.82(XL) ≥F3:0.86(XL) F4:0.94(XL)		
Imajo K 2016; Gastroenterology	MRE vs VCTE	142 NAFLD	TE (AUROC)	MRE (AUROC)	
			≥F2:0.82	≥F2:0.91	
Park CC 2017; Gastroenterology	MRE vs VCTE	104 NAFLD	TE (AUROC)	MRE (AUROC)	
			≥F1:0.67 ≥F2:0.86 ≥F3:0.80 F4:0.69	≥F1:0.82 ≥F2:0.89 ≥F3:0.87 F4:0.87	

Cui J 2016; Hepatology	MRE vs VTQ (ARFI)	125 NAFLD	VTQ (ARFI) (AUROC)	MRE (AUROC)
			≥F1:0.66 ≥F2:0.84 ≥F3:0.89 F4:0.86	≥F1:0.79 ≥F2:0.88 ≥F3:0.93 F4:0.88
Hsu C 2019ș Clin Gastroenterol Hepatol.	MRE vs VCTE	230 NAFLD	VCTE (AUROC) ≥F2:0.87 ≥F3:0.84 F4:0.84	MRE (AUROC) ≥F2: 0.92 ≥F3: 0.93 F4: 0.94
Singh S 2020; Gastroenterology	MRE (meta-analysis)	Mixed chronic liver diseases		MRE (AUROC) ≥F2: >0.90 ≥F3: >0.90 F4: >0.90

The superiority of MRE in fibrosis staging has been further confirmed by a large systematic review and meta-analysis published in Gastroenterology (Singh et al., 2020). The analysis reported AUROC values exceeding 0.90 for all clinically relevant stages of fibrosis across multiple etiologies. MRE showed particularly strong performance in NAFLD/MASLD and obese patients, where ultrasound-based techniques may have reduced feasibility (35).

Furthermore, the 2024 update of the WFUMB Guidelines reinforced the clinical utility of shear wave elastography methods while acknowledging the higher diagnostic accuracy and reproducibility of MRE. However, cost, availability, and the need for specialized radiological infrastructure remain limiting factors for widespread implementation (4).

By the end of this chapter, we can say that numerous studies have demonstrated comparable outcomes for various ultrasound-based elastographic techniques in terms of performance and viability.

According to this perspective, all ultrasound-based elastographic techniques—VCTE, pSWE, and 2D-SWE—can be applied in clinical settings (37, 38).

The primary finding, however, is that different systems have varying cut-off values, which practitioners need to be aware of and utilize.

Most of the published research supports MRE when comparing it to ultrasound-based elastography. In contrast to US-based elastography, which can be performed by both radiologists and clinicians in a point-of-care scenario, we must consider the expense of MRE, the availability of such devices, and the fact that it can only be performed by radiologists.

Ultrasound-based elastographic modules (pSWE or 2D-SWE) are now a feature of almost all high-end and even some medium-class ultrasound systems (Philips, GE, Siemens, and others). This eliminates confounding variables by allowing the practitioner to do elastography after an ultrasound examination, when all clinical information is already available (e.g., nonfasting patient, obstructive jaundice, elevated aminotransferases, right heart failure) (39).

Considering more recent evidence and updated international guidelines, it can be concluded that ultrasound-based elastographic methods (VCTE, pSWE, and 2D-SWE) provide comparable diagnostic performance for liver fibrosis assessment and are suitable for routine clinical practice, when appropriate cut-off values are used. However, magnetic resonance elastography consistently demonstrates superior diagnostic accuracy, particularly in patients with NAFLD/MASLD, obesity, or unreliable ultrasound measurements.

Despite its higher diagnostic performance, the broader implementation of MRE is limited by cost, availability, and the requirement for radiological expertise. Therefore, ultrasound-based elastography remains the most accessible and widely used tool for fibrosis assessment in daily clinical practice.

5.7.4. Summary of the advantages and disadvantages of various elastographic techniques

The following are each technique's benefits and drawbacks:

1. Using a mechanical push, VCTE is simple to do (technicians perform it in some countries), but it is a blind study that cannot be carried out on individuals who have ascites.

2. Point SWE: Although the measuring box is small (around 10/5 mm), it is very simple to execute, employs an ultrasound image for measurement, and allows the operator to observe and select the region of interest (avoiding the liver capsule and large vessels). It can be utilized in patients with ascites.

3. Some ultrasound experience is required for 2D-SWE; the investigative area is larger and can be chosen using a B-mode ultrasound image; the elastographic assessment is shown with numerical values and in a color-coded manner; and it can be carried out on ascites-affected people (6).

In 2015, EASL issued guidelines regarding the non-invasive methods for liver diseases severity assessment, in which the advantages and disadvantages of all these methods are presented (40). This guideline was followed by an updated guideline on this topic in 2021 (5).

Table 3. Respective advantages and disadvantages of currently available non-invasive methods in patients with chronic liver disease.

Serum biomarkers	Measurement of liver stiffness			
	Transient elastography	ARFI (pSWE)	2D-SWE	MR elastography
Advantages				
• Good reproducibility • High applicability (95%) • No cost and wide availability (non-patented) • Well validated • Can be performed in the outpatient clinic	• Most widely used and validated technique: standard to be beaten • User-friendly (performed at bedside; rapid, easy to learn) • High range of values (2-75 kPa) • Quality criteria well defined • Good reproducibility • High performance for cirrhosis (AUROC >0.9) • Prognostic value in cirrhosis	• Can be implemented on a regular US machine • ROI smaller than TE but location chosen by the operator • Higher applicability than TE (ascites and obesity) • Performance equivalent to that of TE for significant fibrosis and cirrhosis	• Can be implemented on a regular US machine • ROI can be adjusted in size and location and chosen by the operator • Measures liver stiffness in real-time • High range of values (2-150 kPa) • Good applicability • High performance for cirrhosis	• Can be implemented on a regular MRI machine • Examination of the whole liver • Higher applicability than TE (ascites and obesity) • High performance for cirrhosis
Disadvantages				
• Non-specific of the liver • Unable to discriminate between intermediate stages of fibrosis • Performance not as good as TE for cirrhosis • Cost and limited availability (proprietary) • Limitations (hemolysis, Gilbert syndrome, inflammation…)	• Requires a dedicated device • ROI cannot be chosen • Unable to discriminate between intermediate stages of fibrosis • Applicability (80%) lower than serum biomarker: (obesity, ascites, operator experience) • False positive in case of acute hepatitis, extra-hepatic cholestasis, liver congestion, food intake and excessive alcohol intake	• Unable to discriminate between intermediate stages of fibrosis • Units (m/sec) different from that of TE (kPa) • Narrow range of values • (0.5-4.4 m/sec) • Quality criteria not well defined • Prognostic value in cirrhosis?	• Further validation warranted • Unable to discriminate between intermediate stages of fibrosis • Quality criteria not well defined • Learning curve? • Influence of inflammation?	• Further validation warranted especially in comparison with TE • Not applicable in case of iron overload • Requires a MRI facility • Time-consuming • Costly

ROI, region of interest.

Fig. 5.7.2. Advantages and disadvantages of non-invasive tools for fibrosis assessment in chronic hepatitis (EASL-ALEH Clinical Practice Guidelines: Non-invasive tests for evaluation of liver disease severity and prognosis. Journal of Hepatology. 2015;63(1):237-64)

References

1. Sporea I, Bota S, Peck-Radosavljevic M, Sirli R, Tanaka H, Iijima H, et al. Acoustic Radiation Force Impulse elastography for fibrosis evaluation in patients with chronic hepatitis C: an international multicenter study. European journal of radiology. 2012;81(12):4112-8.

2. Friedrich-Rust M, Lupsor M, de Knegt R, Dries V, Buggisch P, Gebel M, et al. Point Shear Wave Elastography by Acoustic Radiation Force Impulse Quantification in Comparison to Transient Elastography for the Noninvasive Assessment of Liver Fibrosis in Chronic Hepatitis C: A Prospective International Multicenter Study. Ultraschall in der Medizin. 2015;36(3):239-47.

3. Fujimoto K, Kato M, Kudo M, Yada N, Shiina T, Ueshima K, et al. Novel image analysis method using ultrasound elastography for noninvasive evaluation of hepatic fibrosis in patients with chronic hepatitis C. Oncology. 2013;84 Suppl 1:3-12.

4. Ferraioli G, Barr RG, Berzigotti A, Sporea I, Wong VW, Reiberger T, et al. WFUMB Guideline/Guidance on Liver Multiparametric Ultrasound: Part 1. Update to 2018 Guidelines on Liver Ultrasound Elastography. Ultrasound Med Biol. 2024 Aug;50(8):1071-87.
5. European Association for the Study of the Liver. EASL Clinical Practice Guidelines on non-invasive tests for evaluation of liver disease severity and prognosis - 2021 update. J Hepatol. 2021 Sep;75(3):659-689.
6. Castera L, Foucher J, Bernard PH, Carvalho F, Allaix D, Merrouche W, et al. Pitfalls of liver stiffness measurement: a 5-year prospective study of 13,369 examinations. Hepatology (Baltimore, Md). 2010;51(3):828-35.
7. Sirli R, Sporea I, Bota S, Jurchis A. Factors influencing reliability of liver stiffness measurements using transient elastography (M-probe)-monocentric experience. European journal of radiology. 2013;82(8):e313-6
8. Sporea I, Sirli R, Mare R, Popescu A, Ivascu SC. Feasibility of Transient Elastography with M and XL probes in real life. Medical ultrasonography. 2016;18(1):7-10.
9. Sirli R, Sporea I, Bota S, Jurchis A. Factors influencing reliability of liver stiffness measurements using transient elastography (M-probe)-monocentric experience. European journal of radiology. 2013;82(8):e313-6
10. Sporea I, Popescu A, Gheorghe L, Cijevschi Prelipcean C, Sparchez Z, Voiosu R. "Quo vadis" liver biopsy? A multi-centre Romanian study regarding the number of liver biopsies performed for chronic viral hepatitis. Journal of gastrointestinal and liver diseases: JGLD. 2012;21(3):326.
11. Bota S, Herkner H, Sporea I, Salzl P, Sirli R, Neghina AM, et al. Meta-analysis: ARFI elastography versus transient elastography for the evaluation of liver fibrosis. Liver international: official journal of the International Association for the Study of the Liver. 2013;33(8):1138-47.
12. Cassinotto C, Boursier J, de Ledinghen V, Lebigot J, Lapuyade B, Cales P, et al. Liver stiffness in nonalcoholic fatty liver disease: A comparison of supersonic shear imaging, FibroScan, and ARFI with liver biopsy. Hepatology. 2016;63(6):1817-27.
13. Lee MS, Bae JM, Joo SK, Woo H, Lee DH, Jung YJ, et al. Correction: Prospective comparison among transient elastography, supersonic shear imaging, and ARFI imaging for predicting fibrosis in nonalcoholic fatty liver disease. PloS one. 2018;13(6):e0200055.
14. Lupșor M, Badea R, Ștefănescu H, Spârchez Z, Branda H, Șerban A, et al. Performance of a new elastographic method (ARFI technology) compared to unidimensional transient elastography in the noninvasive assessment of chronic hepatitis C. Preliminary results. J gastrointest liver dis JGLD. 2009;18(3):303-10.
15. Sporea I, Bota S, Peck-Radosavljevic M, Șirli R, Tanaka H, Iijima H, et al. Acoustic Radiation Force Impulse elastography for fibrosis evaluation in patients with chronic hepatitis C: an international multicenter study. European journal of radiology. 2012;81(12):4112-8.

16. Friedrich-Rust M, Lupsor M, de Knegt R, Dries V, Buggisch P, Gebel M, et al. Point Shear Wave Elastography by Acoustic Radiation Force Impulse Quantification in Comparison to Transient Elastography for the Noninvasive Assessment of Liver Fibrosis in Chronic Hepatitis C: A Prospective International Multicenter Study. Ultraschall in der Medizin . 2015;36(3):239-47.
17. Tsochatzis EA, Gurusamy KS, Ntaoula S, Cholongitas E, Davidson BR, Burroughs AK. Elastography for fibrosis severity in chronic liver disease: meta-analysis. J Hepatol. 2011 Apr;54(4):650-9.
18. Conti F, Serra C, Vukotic R, Felicani C, Mazzotta E, Gitto S, et al. Assessment of Liver Fibrosis With Elastography Point Quantification vs Other Noninvasive Methods. Clinical gastroenterology and hepatology: the official clinical practice journal of the American Gastroenterological Association. 2019;17(3):510-7.e3.
19. Cassinotto C, Lapuyade B, Mouries A, Hiriart JB, Vergniol J, Gaye D, et al. Non-invasive assessment of liver fibrosis with impulse elastography: comparison of Supersonic Shear Imaging with ARFI and FibroScan(R). Journal of hepatology. 2014;61(3):550-7.
20. Herrmann E, de Ledinghen V, Cassinotto C, Chu WC, Leung VY, Ferraioli G, et al. Assessment of biopsy-proven liver fibrosis by two-dimensional shear wave elastography: An individual patient data-based meta-analysis. Hepatology. 2018;67(1):260-72.
21. Sporea I, Bota S, Jurchis A, Sirli R, Gradinaru-Tascau O, Popescu A, et al. Acoustic radiation force impulse and supersonic shear imaging versus transient elastography for liver fibrosis assessment. Ultrasound in medicine & biology. 2013;39(11):1933-41.
22. Mulazzani L, Salvatore V, Ravaioli F, Allegretti G, Matassoni F, Granata R, et al. Point shear wave ultrasound elastography with Esaote compared to real-time 2D shear wave elastography with supersonic imagine for the quantification of liver stiffness. Journal of ultrasound. 2017;20(3):213-25.
23. Gao Y, Zheng J, Liang P, Tong M, Wang J, Wu C, et al. Liver Fibrosis with Two-dimensional US Shear-Wave Elastography in Participants with Chronic Hepatitis B: A Prospective Multicenter Study. Radiology. 2018;289(2):407-15.
24. Sporea I, Mare R, Lupusoru R, Popescu A, Danila M, Bende F, et al. Comparative study between four ultrasound Shear Waves Elastographic methods for liver fibrosis assessment. Medical ultrasonography. 2018;20(3):265-71.
25. Sporea I. One or more elastographic methods for liver fibrosis assessment? Medical ultrasonography. 2015;17(2):137-8.
26. Huwart L, Sempoux C, Vicaut E, Salameh N, Annet L, Danse E, et al. Magnetic resonance elastography for the noninvasive staging of liver fibrosis. Gastroenterology. 2008;135(1):32-40.

27. Bohte AE, de Niet A, Jansen L, Bipat S, Nederveen AJ, Verheij J, et al. Non-invasive evaluation of liver fibrosis: a comparison of ultrasound-based transient elastography and MR elastography in patients with viral hepatitis B and C. European radiology. 2014;24(3):638-48.
28. Ichikawa S, Motosugi U, Morisaka H, Sano K, Ichikawa T, Tatsumi A, et al. Comparison of the diagnostic accuracies of magnetic resonance elastography and transient elastography for hepatic fibrosis. Magnetic resonance imaging. 2015;33(1):26-30.
29. Xiao H, Shi M, Xie Y, Chi X. Comparison of diagnostic accuracy of magnetic resonance elastography and Fibroscan for detecting liver fibrosis in chronic hepatitis B patients: A systematic review and meta-analysis. PloS one. 2017;12(11):e0186660.
30. Xiao G, Zhu S, Xiao X, Yan L, Yang J, Wu G. Comparison of laboratory tests, ultrasound, or magnetic resonance elastography to detect fibrosis in patients with nonalcoholic fatty liver disease: A meta-analysis. Hepatology (.2017;66(5):1486-501.
31. Imajo K, Kessoku T, Honda Y, Tomeno W, Ogawa Y, Mawatari H, et al. Magnetic Resonance Imaging More Accurately Classifies Steatosis and Fibrosis in Patients With Nonalcoholic Fatty Liver Disease Than Transient Elastography. Gastroenterology. 2016;150(3):626-37.e.
32. Karlas T, Petroff D, Sasso M, Fan JG, Mi YQ, de Lédinghen V, et al. Individual patient data meta-analysis of controlled attenuation parameter (CAP) technology for assessing steatosis. J Hepatol. 2017 May;66(5):1022-1030.
33. Park CC, Nguyen P, Hernandez C, Bettencourt R, Ramirez K, Fortney L, et al. Magnetic Resonance Elastography vs Transient Elastography in Detection of Fibrosis and Noninvasive Measurement of Steatosis in Patients With Biopsy-Proven Nonalcoholic Fatty Liver Disease. Gastroenterology. 2017;152(3):598-607.e2.
34. Cui J, Heba E, Hernandez C, Haufe W, Hooker J, Andre MP, et al. Magnetic resonance elastography is superior to acoustic radiation force impulse for the Diagnosis of fibrosis in patients with biopsy-proven nonalcoholic fatty liver disease: A prospective study. Hepatology (Baltimore, Md). 2016;63(2):453-61.
35. Singh S, Venkatesh SK, Wang Z, Miller FH, Motosugi U, Low RN et al. Magnetic resonance elastography for staging liver fibrosis: a systematic review and meta-analysis. *Clin Gastroenterol Hepatol. 2015 Mar;13(3):440-451*
36. Hsu C, Caussy C, Imajo K, Chen J, Singh S, Kaulback K, et al. Magnetic Resonance vs Transient Elastography Analysis of Patients With Nonalcoholic Fatty Liver Disease: A Systematic Review and Pooled Analysis of Individual Participants. Clin Gastroenterol Hepatol. 2019 Mar;17(4):630-637.e8.
37. Dietrich CF, Bamber J, Berzigotti A, Bota S, Cantisani V, Castera L, et al. EFSUMB Guidelines and Recommendations on the Clinical Use of Liver Ultrasound Elastography, Update 2017 (Long Version). Ultraschall in der Medizin. 2017;38(4):e16-e47.

38. Ferraioli G, Wong VW, Castera L, Berzigotti A, Sporea I, Dietrich CF, et al. Liver Ultrasound Elastography: An Update to the World Federation for Ultrasound in Medicine and Biology Guidelines and Recommendations. Ultrasound in medicine & biology. 2018;44(12):2419-40.
39. Sporea I. Clinical elastography. Medical Ultrasonography. 2018;20(3):263-4.
40. EASL-ALEH Clinical Practice Guidelines: Non-invasive tests for evaluation of liver disease severity and prognosis. Journal of hepatology. 2015;63(1):237-64.

6. Ultrasound Screening for Steatotic Liver in Populations at Risk

Ioan Sporea, Ruxandra Mare

Abstract

Metabolic dysfunction–associated steatotic liver disease (MASLD) is the most prevalent chronic liver disease worldwide, closely linked to obesity, type 2 diabetes, and metabolic syndrome, with a markedly higher prevalence in high-risk populations.

The fibrosis stage represents the main predictor of liver-related and overall mortality, yet disease progression is usually asymptomatic, leading to delayed diagnosis and justifying structured screening strategies in at-risk groups.

General population-wide screening is not cost-effective due to the high prevalence of isolated steatosis and low prevalence of steatohepatitis (MASH), whereas targeted screening for MASH with fibrosis in patients with T2DM, obesity, metabolic syndrome, dyslipidemia, or combined metabolic risk factors is evidence-based and clinically justified.

Recent data show a substantial burden of significant and advanced fibrosis in these groups, including in non-obese individuals with metabolic dysfunction, supporting risk-based rather than BMI-based screening approaches.

6.1. Introduction

Metabolic dysfunction–associated steatotic liver disease (MASLD), previously termed non-alcoholic fatty liver disease (NAFLD), is currently the most prevalent chronic liver disease worldwide and closely parallels the global epidemics of obesity, type 2 diabetes mellitus (T2DM), and other cardiometabolic disorders (1, 2). Approximately 30% of the adult population has hepatic steatosis, while prevalence exceeds 60–70% in high-risk groups such as patients with T2DM or metabolic syndrome (3). Although most individuals with MASLD have non-progressive steatosis, a significant proportion develop metabolic dysfunction–associated steatohepatitis (MASH), progressive fibrosis, cirrhosis, and hepatocellular carcinoma.

The fibrosis stage is the strongest predictor of liver-related and all-cause mortality in MASLD (4). Because disease progression is typically asymptomatic, diagnosis is often delayed until advanced stages. These epidemiological and

clinical considerations provide a strong rationale for structured screening strategies, focused on populations at increased metabolic risk, using non-invasive, accurate, and cost-effective methods.

6.2. Rationale for screening populations at risk

General population-wide screening for MASLD is not cost-effective because of the high prevalence of isolated steatosis and the relatively low short-term risk of liver-related outcomes in this population. In contrast, targeted screening for MASH with fibrosis in clearly defined high-risk groups is feasible and evidence-based. These groups include patients with T2DM, obesity with metabolic complications, metabolic syndrome, dyslipidemia, and individuals with combined metabolic risk factors and moderate alcohol intake (MetALD) (2, 5).

Systematic reviews and meta-analyses consistently demonstrate a high burden of clinically significant fibrosis in these populations. A large meta-analysis published in 2023 reported pooled prevalences of significant fibrosis (≥F2) and advanced fibrosis (≥F3) of approximately 35% and 15%, respectively, among patients with T2DM (6). Importantly, MASLD is also prevalent in non-obese individuals with metabolic dysfunction, among whom up to 10–15% may harbor significant fibrosis, particularly in the presence of T2DM or dyslipidemia (7). These findings support screening strategies based on metabolic risk, rather than using body mass index alone.

6.3. Who should perform screening and by whom?

Screening for MASLD should be embedded within routine care pathways for individuals with metabolic dysfunction and is optimally initiated in primary care and diabetology/endocrinology settings, where most at-risk patients are already managed. Recent population-based evidence supports a more refined, risk-enriched approach to case finding, using simple clinical variables. Even though FIB-4 and non-alcoholic fatty liver fibrosis (NFS) scores are highly used in clinical practice, patients who have risk factors (obesity, diabetes, or alcohol) for developing chronic liver disease are more likely to receive a false-negative result (8), making both scores suboptimal for screening.

The recently developed *metabolic dysfunction–associated fibrosis 5 score* (MAF-5), comprising waist circumference, body mass index (calculated as kg/m²), the presence of diabetes, aspartate aminotransferase, and platelet levels, provides a validated framework to define who should undergo liver-focused screening. In a large population-based analysis including 21,797

individuals with metabolic dysfunction, the MAF-5 score stratified subjects into low-, intermediate-, and high-risk categories for significant fibrosis (LSM ≥8 kPa), with observed fibrosis prevalences of 3.3%, 7.9%, and 28.1%, respectively (9). Importantly, approximately 25% of the general population with metabolic dysfunction were classified as high risk (MAF-5 ≥1), identifying a subgroup with a markedly enriched prevalence of clinically relevant liver disease suitable for targeted imaging-based screening. At the populational level, MAF-5 outperforms FIB-4 and complements ELF by providing age-independent risk stratification, superior discrimination for significant fibrosis (AUROC 0.81 vs 0.61), and efficient identification of a metabolically defined high-risk subgroup suitable for targeted ultrasound-based screening, without the cost and scalability constraints of biomarker panels (9).

Accordingly, primary care physicians and diabetologists should identify patients with metabolic dysfunction and apply a simple risk stratification step (e.g., MAF-5). Individuals classified as intermediate or high risk should undergo targeted ultrasound screening, ideally in centers capable of performing B-mode imaging, quantitative steatosis assessment, and ultrasound-based elastography in a single visit.

6.4. Assessment of liver steatosis - The first step in the diagnosis of MASLD

6.4.1. Conventional B-mode ultrasound

B-mode ultrasound remains the most widely available first-line imaging modality for detecting hepatic steatosis because of its low cost, portability, and patient acceptability. Its diagnostic performance is strongly dependent on the severity of steatosis. A classic meta-analysis comparing ultrasound to liver histology reported a pooled sensitivity of 84.8% and a pooled specificity of 93.6% for detecting moderate-to-severe steatosis (AUROC 0.93), but lower sensitivity for mild disease (10). More recent reviews emphasize that qualitative B-mode criteria (“bright liver,” hepatorenal contrast, posterior attenuation, and vascular blurring) perform best once liver fat exceeds ~20%, whereas steatosis in the 5–20% range may be missed in a substantial proportion of cases (11).

In contemporary screening discussions, the main value of conventional ultrasound is therefore to find cases of clinically overt steatosis in high-risk populations and as a platform to integrate quantitative measurements (QUS) and ultrasound-based elastography in a single visit. Importantly, a 2023 systematic literature review and meta-analysis evaluating Point-of-Care

Ultrasound (PoCUS) performed by trained general practitioners found a pooled sensitivity of 93% (95% CI 85–98) and a pooled specificity of 98% (95% CI 96–99) for steatosis detection when using formal ultrasound as the comparator standard (12). While this does not address histologic accuracy directly, it supports the feasibility of deploying B-mode patterns reliably in frontline settings.

6.4.2. Quantitative ultrasound techniques

Quantitative ultrasound methods have been developed to overcome these limitations. The Controlled Attenuation Parameter (CAP), implemented in the vibration-controlled transient elastography (VCTE) system, provides an objective estimate of hepatic fat content and can be obtained simultaneously with liver stiffness measurement (LSM). Meta-analyses report AUROC values around 0.85–0.88 for the detection of any steatosis and higher grades in MASLD (13). Nevertheless, CAP is not recommended as a first-line technique due to its limited availability and paucity of studies in comparison to conventional ultrasound (14). While there are no well-defined reference values, values exceeding 275 dB/mm can be employed to diagnose steatosis due to their positive predictive value (PPV) and sensitivity (Se) of over 90% (14).

In addition, several ultrasound manufacturers have implemented quantitative ultrasound (QUS) techniques directly within conventional ultrasound systems. Unlike CAP, these methods provide B-mode image-guided sampling, can be performed during a standard abdominal ultrasound examination, and yield continuous quantitative metrics that are suitable for longitudinal monitoring.

A) Ultrasound-integrated QUS approaches for steatosis quantification

a) Attenuation-based techniques (AC/ATI/UGAP/TAI/Att.PLUS)

Attenuation-based QUS estimates the attenuation coefficient (AC) (typically in dB/cm/MHz or dB/m/MHz) from raw radiofrequency data. In MASLD/NAFLD cohorts, 2D image-guided attenuation methods—including Attenuation Imaging (ATI), ultrasound-guided attenuation parameter (UGAP) (Fig. 6.1), and tissue attenuation imaging (TAI)—have shown consistently high discriminative ability for steatosis detection and grading.

Across multiple prospective studies summarized in a recent radiology review, ATI demonstrated AUROC ranges of 0.76–0.97 for mild steatosis, 0.86–

0.99 for moderate steatosis, and 0.79–0.97 for severe steatosis, depending on the reference standard and thresholds (15).

In a prospective MASLD cohort using MRI-PDFF as reference, UGAP showed good-to-excellent performance for steatosis grading (reported AUC range 0.80–0.94) and performed comparably to CAP in a direct subgroup comparison (16).

For vendor-integrated TAI (Samsung), a prospective study using MRI-PDFF thresholds of ≥5% and ≥10% reported AUCs of 0.89 and 0.93, respectively, with excellent interobserver reproducibility (ICC 0.95) (17).

When attenuation and sound speed are measured in parallel (e.g., Att.PLUS), a prospective pilot comparison against MR-PDFF/histology reported an AUC of 0.79 for differentiating S0 vs S1–S3 and 0.93 for differentiating S0–S1 vs S2–S3 (18).

Attenuation-based approaches are particularly attractive for liver steatosis screening because they can be embedded in routine ultrasound workflows, permitting ROI placement under B-mode guidance (avoiding vessels and artifacts), and provide quantitative outputs that can be tracked over time. Key implementation challenges include inter-vendor variability, variability in acquisition/ROI depth, and potential confounding due to advanced fibrosis; these issues have prompted calls for standardization of measurement protocols (15).

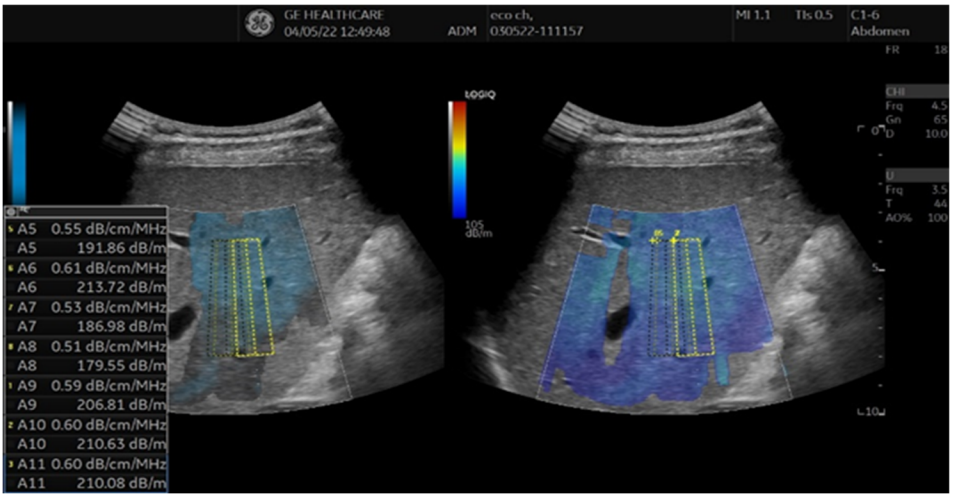


Fig 6.1 Evaluation of steatosis by the ultrasound-guided attenuation parameter (UGAP)
(left panel – mitigation map; right panel – quality map)

b) Backscatter/scatter-derived techniques (BSC/TSI/Nakagami; integrated fat fraction)

Backscatter-based methods quantify tissue microstructure using properties of the backscattered signal. Two clinically deployed examples are tissue scatter distribution imaging (TSI) (Nakagami parameter-based speckle statistics) and investigational/advanced metrics such as the backscatter coefficient (BSC).

In the same prospective Samsung-based study, TSI achieved AUCs of 0.87 (for ≥5% steatosis assessed by MRI-PDFF) and 0.86 (for ≥10% steatosis assessed by MRI-PDFF), with moderate interobserver reproducibility (ICC 0.73). Notably, TSI values were influenced by liver stiffness in multivariable models, suggesting potential interaction with fibrosis (17).

Reviews of advanced QUS report that BSC-based approaches can show high diagnostic performance against MRI-PDFF thresholds (e.g., AUROC up to 0.95 for MRI-PDFF ≥5% in selected datasets), although performance varies across implementations and reference standards (19).

An emerging direction is ultrasound-derived fat fraction (UDFF) (Fig. 6.2.), which combines attenuation and backscatter information to *directly estimate liver fat as a percentage*. A 2025 systematic review focusing on ultrasound-derived fat fraction reported pooled sensitivity around 90%, specificity around 84%, and pooled AUC approximately 0.93 versus MRI-PDFF (11). This estimation as a percentage is very useful for the clinician, allowing a rapid interpretation. Currently, other ultrasound companies have implemented this facility of direct steatosis estimation as a percentage as well.

Scatter-derived metrics may complement attenuation by providing information less directly tied to beam attenuation, while integrated fat-fraction approaches may be easier to interpret for clinicians and patients. Current limitations include heterogeneous implementations, limited cross-vendor standardization, and the need for robust validation in obesity and in coexisting fibrosis.

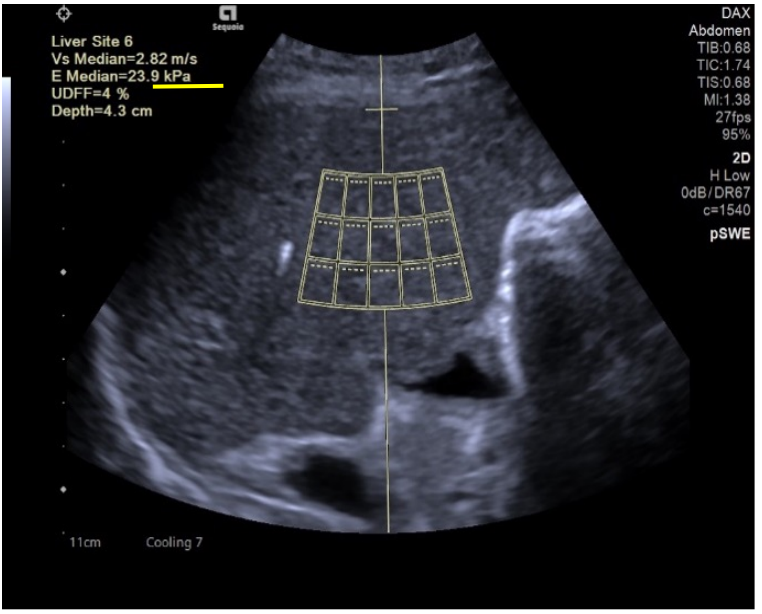


Fig 6.2. Evaluation of steatosis (UDFF) and fibrosis. In this case UDFF is 4%, thus no steatosis, and liver stiffness is 23.9 kPa—cirrhosis.

c) Speed-of-sound techniques (SoS/SSp.PLUS/CUTE)

Speed-of-sound (SoS) approaches exploit the fact that ultrasound propagates more slowly through fat-enriched tissue, enabling fat quantification without relying on attenuation alone.

In a first-in-human phase II diagnostic study, computed ultrasound tomography in echo mode (CUTE)–derived SoS distinguished steatotic from normal livers with AUC 0.97 (95% CI 0.93–1.0), sensitivity 90.9%, and specificity 95.5%, using CAP/B-mode–based inclusion criteria (20).

In a prospective pilot study, combined attenuation and sound-speed parameters (Att.PLUS and SSp.PLUS) showed similar accuracy for detecting any steatosis (AUC 0.79 vs 0.78 for S0 vs S1–S3), while attenuation performed better for detecting more severe steatosis (AUC 0.93 vs 0.89 for S0–S1 vs S2–S3) (18).

SoS can serve as an independent physical marker of tissue composition and may provide a useful “dual check” when combined with attenuation, potentially improving robustness in challenging examinations. The evidence base remains smaller than for attenuation-based techniques, and thresholds may be context-dependent.

Overall, ultrasound-integrated QUS techniques are transitioning from proof-of-concept toward clinical deployment. In the screening setting, their main advantages are quantification, image-guided ROI selection, and potential for serial monitoring during lifestyle or pharmacologic interventions. The priority for broad implementation is standardization of acquisition protocols and clinically meaningful cut-offs, ideally harmonized across vendors.

6.5. Assessment of liver fibrosis—the primary prognostic factor for patients with MASLD

6.5.1. Vibration-Controlled Transient Elastography (VCTE) is the most extensively validated noninvasive technique for fibrosis assessment in MASLD. Pooled AUROC values for the diagnosis of advanced fibrosis range between 0.85 and 0.90 and exceed 0.90 for cirrhosis (21, 22). The availability of XL probes has significantly improved feasibility in obese patients, a key consideration in MASLD screening programs (23). Nevertheless, LSM values may be influenced by confounding factors such as acute inflammation in the liver, extrahepatic cholestasis, hepatic congestion, or recent food intake, which must be considered during interpretation of the results.

6.5.2. Point and two-dimensional shear wave elastography are increasingly used alternatives embedded in standard ultrasound systems. When performed by experienced operators, these techniques show diagnostic accuracy comparable to VCTE for advanced fibrosis (24, 25). Their main advantage is the ability to perform fibrosis assessment during a conventional abdominal ultrasound examination under direct visual control.

6.5.3. Combi-elastography integrates shear wave elastography with strain elastography-derived parameters using a single ultrasound platform. Recent prospective studies in biopsy-proven MASLD demonstrate that combi-elastography provides diagnostic performance comparable to VCTE for significant fibrosis and high-risk MASH, while offering additional information on inflammatory activity (26). These multiparametric approaches may enable comprehensive, one-stop ultrasound-based evaluation in screening settings.

A proposed screening algorithm is presented in Fig 6.3.

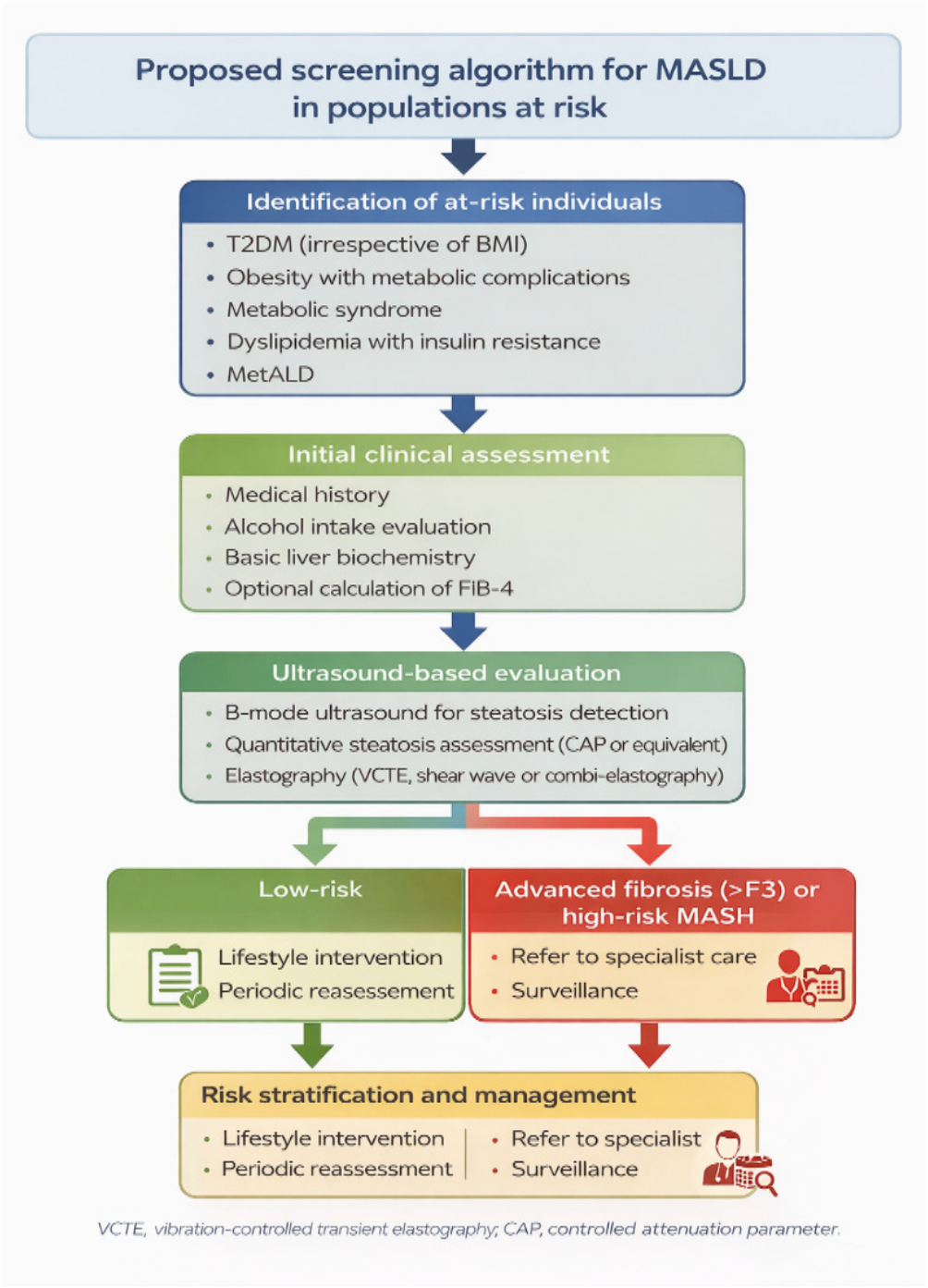


Fig. 6.3 Screening algorithm for MASLD in population at risk

6.6. Cost-effectiveness of screening in MASLD

Health economic models demonstrate that ultrasound-based screening targeted at high-risk populations is cost-effective and, in some age groups, cost-saving (24, 27, 28). Benefits are greatest when screening is initiated before the development of advanced fibrosis, particularly in patients aged 40–65 years with metabolic syndrome or T2DM.

6.7. Future directions

Future MASLD screening strategies are likely to incorporate artificial intelligence–assisted risk prediction, opportunistic screening using routinely acquired imaging or laboratory data, and increasingly sophisticated multi-parametric ultrasound techniques (29, 30, 31). AI-based models integrating demographic, metabolic, laboratory, and imaging data may further refine risk stratification and optimize resource allocation. In parallel, standardization and validation of multiparametric ultrasound platforms may enable true one-stop evaluation of steatosis, fibrosis, and inflammatory activity at the point of care.

References

1. Younossi ZM, Golabi P, Paik JM, Henry A, Van Dongen C, Henry L. The global epidemiology of nonalcoholic fatty liver disease (NAFLD) and nonalcoholic steatohepatitis (NASH): a systematic review. Hepatology. 2023 Apr 1;77(4):1335-47.
2. Eslam M, Newsome PN, Sarin SK, Anstee QM, Targher G, Romero-Gomez M, et al. A new definition for metabolic dysfunction-associated fatty liver disease: An international expert consensus statement. J Hepatol. 2020 Jul;73(1):202-9.
3. Younossi ZM, Golabi P, de Avila L, Paik JM, Srishord M, Fukui N, et al. The global epidemiology of NAFLD and NASH in patients with type 2 diabetes: A systematic review and meta-analysis. J Hepatol. 2019 Oct;71(4):793-1.
4. Angulo P, Kleiner DE, Dam-Larsen S, Adams LA, Bjornsson ES, Charatcharoenwitthaya P, et al. Liver Fibrosis, but No Other Histologic Features, Is Associated With Long-term Outcomes of Patients With Nonalcoholic Fatty Liver Disease. Gastroenterology. 2015 Aug;149(2):389-97.e10.
5. Rinella ME, Lazarus JV, Ratziu V, Francque SM, Sanyal AJ, Kanwal F et al. NAFLD Nomenclature consensus group. A multisociety Delphi consensus statement on new fatty liver disease nomenclature. Hepatology. 2023 Dec 1;78(6):1966-1986
6. Mantovani A, Petracca G, Beatrice G, Csermely A, Lonardo A, Tilg H, et al. Nonalcoholic fatty liver disease and risk of incident diabetes mellitus: a meta-analysis. Metabolism. 2023;141:155390.

7. Ye Q, Zou B, Yeo YH, Li J, Huang DQ, Wu Y, et al. Global prevalence, incidence, and outcomes of non-obese or lean non-alcoholic fatty liver disease: a systematic review and meta-analysis. Lancet Gastroenterol Hepatol. 2020 Aug;5(8):739-752.
8. Graupera I, Thiele M, Serra-Burriel M, Caballeria L, Roulot D, Wong GL, et al. Investigators of the LiverScreen Consortium. Low Accuracy of FIB-4 and NAFLD Fibrosis Scores for Screening for Liver Fibrosis in the Population. Clin Gastroenterol Hepatol. 2022 Nov;20(11):2567-76.e6.
9. van Kleef LA, Francque SM, Prieto-Ortiz JE, Sonneveld MJ, Sanchez-Luque CB, Prieto-Ortiz RG, et al. Metabolic Dysfunction-Associated Fibrosis 5 (MAF-5) Score Predicts Liver Fibrosis Risk and Outcome in the General Population With Metabolic Dysfunction. Gastroenterology. 2024 Jul;167(2):357-67.e9.
10. Hernaez R, Lazo M, Bonekamp S, Kamel I, Brancati FL, Guallar E, Clark JM. Diagnostic accuracy and reliability of ultrasonography for the detection of fatty liver: a meta-analysis. Hepatology. 2011 Sep 2;54(3):1082-90.
11. Kavvadas D, Rafailidis V, Liakos A, Sinakos E, Partovi S, Papamitsou T, Prassopoulos P. Quantitative Ultrasound for Hepatic Steatosis: A Systematic Review Highlighting the Diagnostic Performance of Ultrasound-Derived Fat Fraction. Diagnostics (Basel). 2025 Oct 20;15(20):2640.
12. Hernandez O, Yeb ZKS, Nagi T, Haider MA, Vallejo C, Ahson F. Exploring the Use of Point of Care Ultrasound in Screening for Non-Alcoholic Fatty Liver Disease: A Systematic Literature Review and Meta-Analysis. Arch Gastroenterol Res. 2023;4(1):4-11
13. Karlas T, Petroff D, Sasso M, Fan JG, Mi YQ, de Lédinghen V, et al. Individual patient data meta-analysis of controlled attenuation parameter for diagnosing hepatic steatosis. J Hepatol. 2017;66(5):1022–30.
14. European Association for the Study of the Liver. EASL clinical practice guidelines on non-invasive tests for evaluation of liver disease severity and prognosis—2021 update. J Hepatol. 2021;75(3):659–89.
15. Lee DH. Attenuation-based quantitative evaluation of hepatic steatosis: concepts and clinical considerations. J Korean Soc Radiol. 2025;86(3):321–34.
16. Huang YL, Sun C, Wang Y, Cheng J, Wang SW, Wei L et al. Ultrasound-guided attenuation parameter for identifying metabolic dysfunction-associated steatotic liver disease: a prospective study. Ultrasonography. 2025 Mar;44(2):134-44.
17. Rónaszéki AD, Budai BK, Csongrády B, Stollmayer R, Hagymási K, Werling K, et al. Tissue attenuation imaging and tissue scatter imaging for quantitative ultrasound evaluation of hepatic steatosis. Medicine (Baltimore). 2022 Aug 19;101(33):e29708.
18. Gottfriedova H, Dezortova M, Sedivy P, Pajuelo D, Burian M, Sticova E, et al. Comparison of ultrasound to MR and histological methods for liver fat quantification. Eur J Radiol. 2025 Feb;183:111931.
19. Park J, Lee JM, Lee G, Jeon SK, Joo I. Quantitative evaluation of hepatic steatosis using advanced imaging techniques: focusing on new quantitative ultrasound techniques. Korean J Radiol. 2022;23(1):13–29.

20. Stähli P, Becchetti C, Korta Martiartu N, Berzigotti A, Frenz M, Jaeger M. First-in-human diagnostic study of hepatic steatosis with computed ultrasound tomography in echo mode. Commun Med (Lond). 2023;3(1):176.
21. Talwalkar JA, Kurtz DM, Schoenleber SJ, West CP, Montori VM. Ultrasound-based transient elastography for the detection of hepatic fibrosis: systematic review and meta-analysis. Clin Gastroenterol Hepatol. 2007;5(10):1214–1220.
22. Friedrich-Rust M, Ong MF, Martens S, Sarrazin C, Bojunga J, Zeuzem S, Herrmann E. Performance of transient elastography for the staging of liver fibrosis: a meta-analysis. Gastroenterology. 2008 Apr;134(4):960-74.
23. Berger A, Shili S, Zuberbuhler F, Hiriart JB, Lannes A, Chermak F, et al. Liver Stiffness Measurement With FibroScan: Use the Right Probe in the Right Conditions! Clin Transl Gastroenterol. 2019 Apr;10(4):e00023.
24. Jiang W, Huang S, Teng H, Wang P, Wu M, Zhou X, Ran H. Diagnostic accuracy of point shear wave elastography and transient elastography for staging hepatic fibrosis in patients with non-alcoholic fatty liver disease: a meta-analysis. BMJ Open. 2018;8(8):e021787.
25. Herrmann E, de Lédinghen V, Cassinotto C, Chu WC, Leung VY, Ferraioli G, et al. Assessment of biopsy-proven liver fibrosis by two-dimensional shear wave elastography: An individual patient data-based meta-analysis. Hepatology. 2018 Jan;67(1):260-72.
26. Lee YK, Lee DH, Joo SK, Jang H, So YH, Jang S, et al. Innovative Target Exploration of NAFLD (ITEN) Consortium. Combi-Elastography versus Transient Elastography for Assessing the Histological Severity of Metabolic Dysfunction-Associated Steatotic Liver Disease. Gut Liver. 2024 Nov 15;18(6):1048-1059.
27. Zhang E, Wartelle-Bladou C, Lepanto L, Lachaine J, Cloutier G, Tang A. Cost-utility analysis of nonalcoholic steatohepatitis screening. Eur Radiol. 2015 Nov;25(11):3282-94.
28. Younossi ZM, Paik JM, Henry L, Stepanova M, Nader F. Pharmaco-Economic Assessment of Screening Strategies for High-Risk MASLD in Primary Care. Liver Int. 2025 Apr;45(4):e16119.
29. Li J, Chen J, Zeng X, Lyu G, Lin S, He S. Update of machine learning for ultrasound diagnosis of metabolic dysfunction-associated steatotic liver disease: a bright future for deep learning. Peer J. 2025 Jun 30;13:e19645.
30. Perveen S, Shahbaz M, Keshavjee K, Guergachi A. A Systematic Machine Learning Based Approach for the Diagnosis of Non-Alcoholic Fatty Liver Disease Risk and Progression. Sci Rep. 2018 Feb 1;8(1):2112.
31. Gheorghe E, Nicolau C, Kamal A, Udristoiu A, Gruionu L, Saftoiu A. Artificial Intelligence (AI)-Enhanced Ultrasound Techniques Used in Non-Alcoholic Fatty Liver Disease: Are They Ready for Prime Time? Applied Sciences 2023, 13(8), 5080.

7. Endoscopic Ultrasound Elastography of the Liver

Bogdan Miuțescu, Călin Burciu, Adrian Burdan

Abstract

Endoscopic ultrasound shear-wave elastography (EUS-SWE) represents an emerging modality for quantitative assessment of liver stiffness as a marker of fibrosis, which complements established transabdominal noninvasive tests. By providing a near-field acoustic window through the gastric or duodenal wall, EUS-SWE may overcome limitations related to obesity, ascites, and suboptimal intercostal access that affect conventional vibration-controlled transient elastography and other ultrasound-based techniques.

Current evidence from biopsy-anchored and comparative studies suggests that EUS-SWE demonstrates diagnostic performance comparable to transabdominal elastography for the detection of advanced fibrosis and cirrhosis, with potential advantages in technically challenging populations. Beyond fibrosis staging, EUS-SWE enables integration into an "endo-hepatology" workflow, combining bilobar liver stiffness assessment with portal pressure gradient measurement and targeted liver biopsy within a single session. Despite promising results, methodological heterogeneity, inter-lobar variability, and lack of standardized cutoffs currently limit widespread clinical implementation.

Future research should focus on multicenter validation, protocol harmonization, outcome-based thresholds, and integration into multiparametric ultrasound strategies. Within this framework, EUS-SWE should be considered a complementary, situationally advantageous tool rather than a first-line population screening modality.

7.1. Introduction

Ultrasound elastography has become a standard noninvasive method for assessing liver fibrosis, although its diagnostic performance may vary across patient populations because of well-recognized technical limitations.

Transabdominal elastography techniques, while widely used, are particularly affected by body habitus and acoustic window quality. Increased subcutaneous adipose tissue in obese individuals attenuates ultrasound signals and reduces penetration depth, leading to higher failure rates and increased measurement variability. The introduction of XL probes for vibration-controlled

transient elastography (VCTE) has significantly improved feasibility and reduced failure rates in morbidly obese patients (1, 2).

Ascites is another important limitation, particularly for VCTE, because free intraperitoneal fluid interferes with shear-wave propagation and may preclude reliable measurements, as described in elastography guidelines and review studies (3, 5). Other acoustic window limitations, including narrow intercostal spaces and rib shadowing, have also been described in general elastography recommendations (3).

Endoscopic ultrasound (EUS)–based elastography offers an alternative approach by shifting liver stiffness assessment from transabdominal to endoluminal. By enabling near-field imaging through the gastric or duodenal wall, EUS provides a more stable acoustic window that may mitigate limitations related to obesity or intercostal anatomy (4, 5). The proximity of the transducer to the liver improves signal acquisition and allows precise placement of the region of interest under real-time B-mode guidance, avoiding vessels, bile ducts, and focal lesions (4, 5, 10).

Within this framework, EUS elastography should be considered a complementary modality rather than a replacement for transabdominal elastography, particularly useful in technically challenging cases and as part of a multiparametric ultrasound (MPUS) evaluation.

7.2. Physical Principles of EUS Elastography

EUS elastography evaluates tissue mechanical properties by linking extracellular matrix accumulation to increased tissue stiffness. Currently, two main elastographic techniques are available on EUS platforms: strain elastography and shear-wave elastography.

7.2.1. Strain Elastography

Strain elastography provides a qualitative or semi-quantitative assessment of tissue stiffness by measuring tissue deformation in response to internal physiological motion or slight probe compression (Fig. 8.1). Tissue stiffness is typically expressed as a strain ratio comparing the target region to a reference tissue (6).

Early studies demonstrated the feasibility of liver assessment; however, strain elastography remains operator-dependent and lacks standardized cutoff values for fibrosis staging. Measurement variability related to compression

technique and reference tissue selection limits its role to complementary assessment when quantitative techniques are unavailable (6, 10).

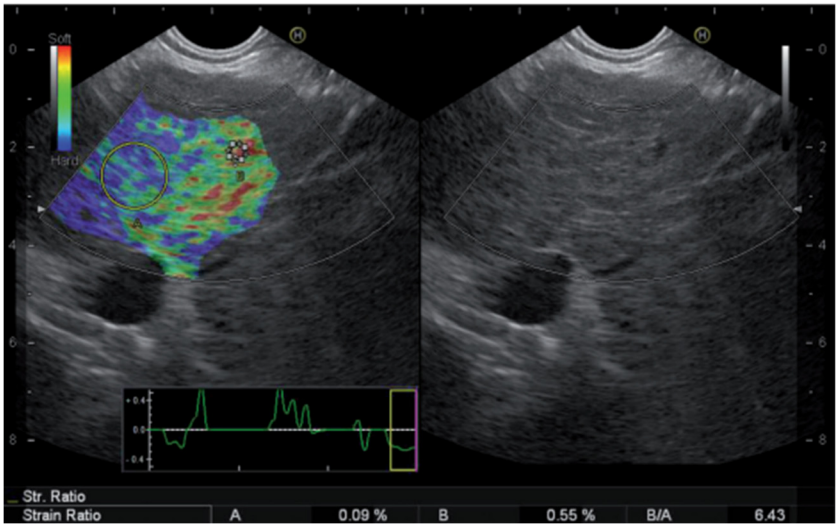


Fig. 8.1. Strain measurement using endoscopic ultrasound strain elastography.

7.2.2. Shear-Wave Elastography

Shear-wave elastography (SWE) quantifies tissue stiffness by measuring the velocity of shear waves generated by acoustic radiation force impulses, with results reported either in m/s or kPa, depending on the elasticity model (8).

When performed via EUS, SWE benefits from near-field acquisition, shorter propagation distances, and improved probe stability, which may reduce acoustic attenuation and improve measurement reproducibility compared with transabdominal approaches (4, 5, 9). Direct B-mode visualization enables accurate ROI placement within homogeneous parenchyma, avoiding vascular and biliary structures, consistent with technical recommendations (Fig. 8.2.) (10).

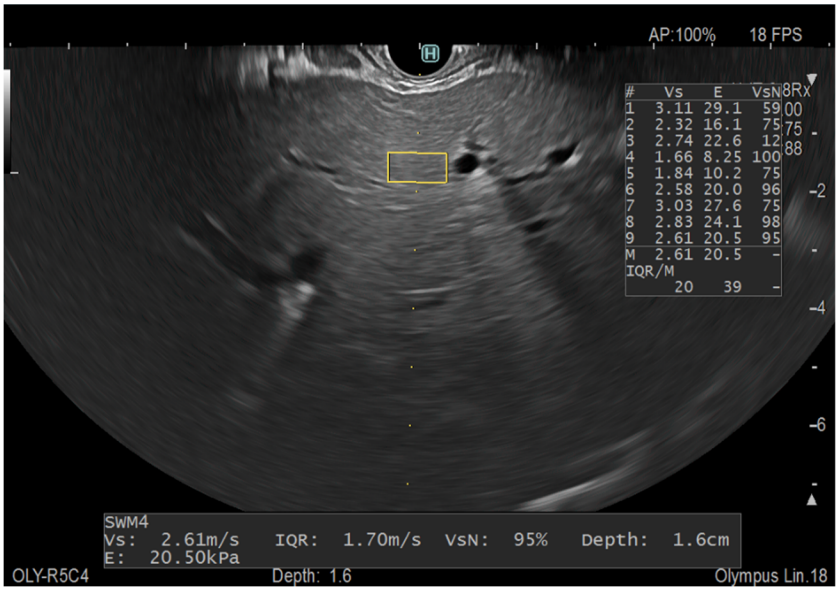


Fig. 8.2. Endoscopic Ultrasound Shear Wave Elastography of the left hepatic lobe

7.2.3. Technical Constraints Specific to EUS

Despite its advantages, EUS elastography has inherent limitations. Excessive compression from the echoendoscope tip may artificially increase stiffness values, particularly during transgastric assessment of the left lobe. Cardiac and respiratory motion may introduce variability, and the gastrointestinal wall can act as an intermediate acoustic medium, contributing to artifacts.

Sampling depth is more limited than with transabdominal techniques, restricting assessment to liver segments adjacent to the gastrointestinal tract. Furthermore, the need for sedation, specialized equipment, and operator expertise limits widespread adoption to tertiary referral centers (10, 15).

7.3. Technique and Best Practice

7.3.1. Left-Lobe Approach (Transgastric)

The transgastric approach to the left hepatic lobe is the most commonly used technique because of excellent visualization and stable probe positioning. Measurements should target homogeneous parenchyma while avoiding vessels, bile ducts, and focal lesions, in line with elastography recommendations (13, 15).

Left-lobe measurements may be affected by cardiac motion and probe compression; therefore, minimal insufflation and gentle scope manipulation are recommended to reduce artifacts and improve reproducibility (10, 15).

7.3.2. Right-Lobe Approach (Transduodenal)

Assessment of the right liver lobe from the duodenal bulb, or the second portion of the duodenum, is technically more challenging but may be less affected by cardiac motion. When feasible, evaluation of both lobes is recommended to reduce sampling variability and improve the representativeness of liver stiffness measurements (10, 12).

7.3.3. Measurement Protocol

Standardized acquisition protocols are essential to ensure reproducibility. Recommendations include selecting homogeneous parenchyma, avoiding vascular structures, minimizing respiratory motion, and acquiring multiple measurements under B-mode guidance (13, 15). Most studies recommend obtaining at least 5–10 valid measurements per lobe and using the median for analysis (13).

Quality criteria adapted from VCTE include maintaining an interquartile range-to-median ratio (IQR/M) below 0.30 and a success rate ≥60%, both of which are associated with improved measurement reliability (14).

Common pitfalls include excessive insufflation, which causes parenchymal compression; improper ROI placement; and inclusion of vascular or biliary structures, all of which may lead to falsely elevated stiffness values. Operator-dependent variability in probe pressure remains an important limitation, underscoring the need for standardized technique and training (10, 15).

7.4. Clinical applications

Current evidence supports endoscopic EUS-SWE as a quantitative liver stiffness measurement (LSM) modality that can be performed during diagnostic or interventional EUS and is best positioned as an adjunct to established noninvasive tests (NITs) rather than as a replacement for first-line transabdominal elastography. Contemporary liver guidelines emphasize stepwise risk stratification using serum markers and ultrasound-based elastography, with confirmatory or invasive testing reserved for indeterminate or high-risk scenarios (16, 17).

Across biopsy-anchored human studies to date, EUS-SWE performance for fibrosis staging is broadly comparable to VCTE in mixed etiology cohorts and appears particularly useful when VCTE is unreliable or technically limited. In a prospective tandem study in predominantly obese patients with suspected NAFLD undergoing first biopsy, VCTE was unreliable in 19% (8/42), whereas EUS-SWE was technically successful in all cases. AUROC values for advanced fibrosis and cirrhosis ranged from approximately 0.78–0.87 and 0.90–0.96, respectively, depending on lobe and comparator (9). In a separate cirrhosis-focused case-control study (n=59), both VCTE and EUS-SWE achieved AUROC >0.95 for diagnosing cirrhosis, but EUS-SWE showed higher observed agreement—particularly in the left lobe—and provided moderate concordance metrics (ICC ~0.55–0.64) against VCTE (18).

Methodological heterogeneity remains the principal barrier to clinical standardization: studies differ in platform, region-of-interest (ROI) geometry and depth, reliability indicators (e.g., IQR/median criteria in VCTE versus net effective shear-wave velocity thresholds in some EUS implementations), number of shots, and—critically—the hepatic lobe sampled. Editorial and experimental work has begun to define workable acquisition parameters (e.g., ROI length of about 1–1.5 cm, shallow depth of ~1 cm), but clinical cutoffs remain provisional and likely platform- and lobe-specific (19, 20).

Beyond fibrosis staging, the most compelling “added value” indication is advanced disease phenotyping within an endohepatology workflow, where EUS can integrate parenchymal stiffness, portal pressure gradient (PPG), and bilobar liver biopsy (LB) in a single session. In a single-center experience (n=25), mean EUS liver elastography was 24.1 kPa, and mean PPG was 4.6 mmHg. Portal hypertension (PPG >5 mmHg) and clinically significant portal hypertension (PPG >10 mmHg) were present in 44% and 12%, respectively, and both PPG and stiffness were higher with significant or advanced fibrosis on histology (23). A randomized controlled trial comparing an EUS approach (PPG+LB) with transjugular PPG+LB found higher rates of combined adequate biopsy plus reliable pressure measurement with EUS (82.8% vs. 41.4%) without excess adverse events, supporting the feasibility of a consolidated “one-stop” assessment (24).

7.5. Diagnostic applications

EUS SWE should be conceptualized as a stiffness biomarker obtained via an internal acoustic window, offering two potential advantages over transabdominal approaches: (i) reduced dependence on the anterior abdominal wall and intercostal acoustic limitations, which are clinically salient in obesity and other scenarios where VCTE may fail or become unreliable; and (ii) the ability to interrogate both hepatic lobes during the same endoscopic session, thereby potentially mitigating sampling error and enabling explicit assessment of interlobar variability. These theoretical advantages are repeatedly observed in early clinical experience, but their translation into reproducible cutoffs and clear clinical decision points remains an active research problem (9, 19).

With respect to liver fibrosis staging, the best-characterized application is fibrosis risk stratification in patients already selected for biopsy because of discordant or unreliable NITs. In a prospective tandem cohort study conducted at a Veterans Affairs center (n=42; mean BMI 32.5±7.4 kg/m²; obesity in 67%), EUS-SWE was performed in both lobes immediately before EUS-guided liver biopsy using a linear echoendoscope and a 19-gauge Franseen needle. Reliability was defined by a net effective shear-wave velocity >60%, and technical success was defined as ≥10 valid elasticity values per lobe (median reported as the final LSM) (9). Within this cohort, the cross-validated AUROC for advanced fibrosis (F≥3) was 0.8676 for VCTE, 0.7986 for left-lobe EUS-SWE, and 0.7827 for right-lobe EUS-SWE; for cirrhosis, the corresponding AUROC values were 0.8971, 0.9583, and 0.8971, respectively (9). Importantly, VCTE was unreliable in 19% (8/42), and all of those patients still had successful EUS-SWE acquisition (9). This is a clinically meaningful distinction: guideline frameworks emphasize that diagnostic value depends not only on AUROC but also on applicability and reliability in the target population (16).

The same study illustrates why cut-off selection is non-trivial and why “single universal thresholds” are currently premature. Using Youden-optimized thresholds, cut-offs for advanced fibrosis were 24.0 kPa in the left lobe (sensitivity 0.5822, specificity 0.9333) and 18.0 kPa in the right lobe (sensitivity 0.7500, specificity 0.8571) (9). When sensitivity was fixed at 0.90 (a choice that might be favored for screening or triage), the right-lobe advanced fibrosis cut-off fell to 10.8 kPa (sensitivity 0.9167, specificity 0.5000), whereas a specificity-fixed 0.90 scenario yielded a right-lobe advanced fibrosis cut-off of 22.5 kPa (sensitivity 0.5833, specificity 0.8929). (9). These ranges—spanning roughly 11

to 23 kPa for the same clinical target (advanced fibrosis) depending on the chosen operating point—underscore the need to pre-specify clinical intent (rule-out triage versus rule-in confirmation) before proposing cut-offs, consistent with the broader biomarker development logic referenced by the investigators (9).

A second prospective cohort study focused explicitly on reproducibility underscores the importance of lobe selection and within-session variability. In 52 consecutive patients referred for EUS-guided liver biopsy, VCTE was performed first, followed by two consecutive EUS-SWE measurements in the left lobe and two in the right lobe, with subsequent bilobar EUS-guided biopsy. Right-lobe EUS-SWE correlated strongly with histological fibrosis stage (Spearman $\rho=0.571$; $p<0.0001$), whereas left-lobe correlation was more modest ($\rho=0.368$; $p=0.0079$); variance between paired consecutive EUS-SWE measurements was 3.5-fold higher in the left lobe than in the right (11). This finding is consistent with the practical observation that the left lobe is more susceptible to artifacts from cardiac motion, gastric compression, and respiratory excursion; the key clinical implication is that protocols relying predominantly on left-lobe acquisition may require stricter quality controls or higher shot counts to stabilize estimates (11, 19).

7.5.1. Obesity and MASLD represent the most plausible near-term "niche-to-mainstream" pathway for EUS-SWE, largely because steep increases in adiposity compromise transabdominal acoustic access and increase failure or unreliability rates in VCTE and other ultrasound elastography methods (16, 17). In a 2025 pilot study targeting this problem (n=62; mean BMI 40.74 kg/m²), EUS-SWE outperformed FIB-4 for discriminating significant fibrosis (F2; AUROC 0.87 vs 0.61) and advanced fibrosis (F3; AUROC 0.93 vs 0.63) and showed a strong AUROC for cirrhosis (F4; 0.95). EUS-SWE was also superior to VCTE for predicting advanced fibrosis and cirrhosis ($p=0.0067$ and $p=0.0022$, respectively) (12). The study additionally proposed pragmatic cut-offs by anchoring to sensitivity and specificity fixed at 90%: for F2, these thresholds were 7.50 kPa (90% sensitivity) and 9.82 kPa (90% specificity); for F3, they were 8.48 and 10.20 kPa, respectively; for F4, they were 11.30 and 14.60 kPa (12). While these numbers are attractive for algorithmic risk stratification, they should be considered provisional until reproduced across platforms, with explicit attention to lobe selection and quality metrics—especially given the substantially higher kPa ranges reported for similar fibrosis targets in other cohorts and devices (9, 11).

7.5.2. Ascites and advanced disease**,** including portal hypertension, represent a second high-impact context where EUS-SWE may add value—less as a replacement for standard NITs and more as a way to unify diagnosis, staging, and complication risk assessment in patients already undergoing endoscopic evaluation. Standard NIT pathways rely heavily on VCTE and other elastography tools to stratify compensated advanced chronic liver disease and clinically significant portal hypertension, with consensus frameworks (e.g., Baveno VII) embedding LSM thresholds into decisions such as variceal screening strategies (21). The intrinsic limitation is that decompensated states (including tense ascites), body habitus, and anatomical constraints can make transabdominal measurements unreliable or impossible, precisely when decisions about portal hypertension and complications are most clinically urgent (16, 21).

In this setting, EUS-based workflows are conceptually compelling because they can combine parenchymal stiffness with direct hemodynamic measurement. In a single-center, mixed prospective-retrospective study of concomitant EUS liver elastography, EUS PPG, and EUS-guided liver biopsy (n=25), technical success was 100%, with diagnostic yield in all patients (mean portal tracts 14.3) and no significant adverse events reported. Mean EUS liver elastography was 24.1 kPa, and mean PPG was 4.6 mmHg; portal hypertension (PPG>5 mmHg) and clinically significant portal hypertension (PPG>10 mmHg) were present in 44% and 12% of patients, respectively. Patients with significant fibrosis (F2–F4) had higher PPG (5.9 vs 2.8 mmHg; p=0.003) and higher stiffness (30.0 vs 15.6 kPa; p=0.02) than those with F0–F1 fibrosis, and analogous differences were seen for advanced fibrosis (F3–F4) versus F0–F2 (23). These data support a biologically coherent model in which stiffness and portal pressures are complementary rather than redundant: stiffness is strongly related to fibrosis but also influenced by inflammation and congestion, whereas PPG provides a more direct readout of portal hypertension physiology (16, 23).

A related and increasingly practical extension is ***splenic EUS-SWE*** for portal hypertension phenotyping. In a cohort study of patients undergoing EUS-SWE spleen measurements (n=142), only 9.2% (13/142) had clinically significant portal hypertension, but mean spleen stiffness was significantly higher in that group (37.6±8.5 kPa vs. 29.1±9.9 kPa; p=0.003), with an AUROC of 0.74 (22). The low CSPH prevalence in that cohort highlights a crucial methodological point: predictive values will change markedly depending on pretest probability, and future studies should therefore recruit enriched high-risk populations (e.g.,

suspected advanced chronic liver disease or decompensation) if the goal is to define clinically actionable spleen stiffness thresholds (16, 22).

The interaction between interlobar variability and clinical phenotype deserves careful attention. In the cirrhosis case-control study (n=59), median EUS-SWE values in cirrhosis were 27 kPa (right) and 25 kPa (left), compared with 5.6 and 6.5 kPa in controls; agreement for cirrhosis diagnosis was 93.2% (right) and 96.6% (left), compared with 91.5% for VCTE (18). Yet the same study reported only moderate concordance between VCTE and EUS-SWE, with intraclass correlation coefficients of 0.641 (right) and 0.548 (left), indicating non-negligible systematic and random differences between modalities and lobes, even when diagnostic AUROCs appear similarly high (18). The practical consequence is that future standardization should not only define what constitutes a valid EUS-SWE acquisition but also clarify which lobe is intended as the clinical reference (right-lobed, bilobar median, or worst lobe) and how that choice interacts with portal hypertension and heterogeneous fibrosis distribution.

7.5.3. Focal lesion characterization. Regarding focal lesion characterization, the evidence base for EUS-SWE in hepatic lesions remains limited, and the most defensible near-term role is as an adjunct to lesion detection and biopsy targeting rather than a stand-alone discriminator of benign versus malignant pathology. Experimental work suggests that EUS-SWE can yield accurate stiffness estimates in small targets only when the ROI is fully contained within the lesion and that shallow ROI placement improves measurement accuracy (20). In practical hepatology, EUS already contributes meaningfully to detecting and sampling small left-lobe lesions that may be missed on cross-sectional imaging; EUS-SWE could, in principle, add a quantitative descriptor of lesion stiffness to guide targeting of the most representative area for tissue acquisition, but robust performance metrics, lesion-specific cut-offs, and prospective comparative trials against contrast-enhanced ultrasound or MRI are not yet established (20).

Finally, integration into multiparametric ultrasound (MPUS) and procedural synergy arguably make EUS-SWE clinically distinctive. MPUS guidance documents highlight the strategic value of combining multiple ultrasound biomarkers—typically stiffness, fat quantification, and Doppler-derived hemodynamic signals—to improve diagnostic confidence and prognostication (17). Although classic MPUS is transabdominal, EUS enables a

parallel “endo-MPUS” concept: high-resolution B-mode assessment, Doppler evaluation of portal and hepatic venous flow, liver and spleen stiffness by SWE, targeted bilobar biopsy, and—where indicated—direct PPG measurement, all performed during a single sedated procedure (23, 24). This consolidation may be particularly efficient when the patient has another EUS indication (biliary or pancreatic evaluation, variceal assessment, or unexplained abnormal liver tests requiring tissue confirmation) and when transabdominal elastography is nondiagnostic (9, 12). The incremental procedural burden appears modest: registry materials for an obesity/MASLD EUS-SWE study describe an additional 2–3 minutes to perform SWE beyond the standard examination, a detail that—while not a peer-reviewed endpoint—sets a plausible expectation for real-world workflow modeling (25).

A provisional clinical algorithm consistent with guideline logic can be articulated as follows in prose: transabdominal NITs remain first-line for most patients; EUS-SWE becomes reasonable when (i) VCTE or other transabdominal elastography is unreliable or infeasible, particularly in severe obesity; (ii) the patient is already scheduled for EUS for another indication, making incremental risk and time small; or (iii) an integrated endo-hepatology assessment is required, where stiffness adds context to PPG and/or optimizes biopsy strategy by directing bilobar sampling to representative parenchyma while avoiding vessels and artifact-prone regions (16, 23, 24).

7.6. Critical comparison with transabdominal elastography within MPUS

Head-to-head comparisons indicate that EUS-SWE can approximate VCTE accuracy for fibrosis staging while offering greater applicability in selected populations. In the biopsy-controlled tandem cohort (n=42), VCTE AUROC for advanced fibrosis was 0.8676, and EUS-SWE AUROC values were 0.7986 (left) and 0.7827 (right), with no significant AUROC differences reported. Yet VCTE was unreliable in 19%, whereas EUS-SWE remained feasible in all (9). In a cirrhosis-enriched case-control study (n=59), VCTE, right-lobe EUS-SWE, and left-lobe EUS-SWE each had AUROC ≥0.95 for diagnosing cirrhosis, but EUS-SWE achieved higher sensitivity (96.6% for both lobes) than VCTE (82.8%) at the study’s selected cut-offs, with only moderate ICC concordance between modalities (18). These data support a nuanced inference: EUS-SWE and VCTE are not interchangeable in absolute kPa numbers, but EUS-SWE can produce

clinically meaningful stratification—especially for rule-in of cirrhosis or advanced disease—within its own acquisition framework.

Compared with point shear-wave elastography (pSWE) and 2D-SWE integrated into conventional ultrasound systems, EUS-SWE has a different "cost-benefit geometry." Transabdominal pSWE/2D-SWE are widely available, do not require sedation, and fit naturally into MPUS pathways; the WFUMB MPUS guidance explicitly positions these tools as part of a broader non-invasive framework (17). EUS-SWE, by contrast, requires endoscopy infrastructure and specialist expertise and is therefore unlikely to be a population screening modality. Its comparative advantage is situational: obesity and other acoustic limitations; the need for bilobar access; and the opportunity to combine with EUS-guided biopsy or portal pressure measurement within a single diagnostic encounter (12, 23, 24).

The most "critical" technical distinction for clinicians is that EUS-SWE is currently more heterogeneous in implementation than VCTE, with variability in ROI control and reliability indices across platforms. Editorial guidance has stressed that shear-wave methods are more objective than strain elastography but require standardization, and experimental work identified ROI size and depth as the dominant determinants of accuracy for EUS-SWE (19, 20). Until acquisition parameters and quality criteria are harmonized—analogous to how VCTE technical criteria (e.g., IQR/median ratio) have been embedded into practice—comparative performance claims should be interpreted as platform-specific rather than universal truths (9, 16, 19).

7.7. Future perspectives

The next phase of EUS-SWE development should be judged by whether it can move from promising feasibility to standardized, outcome-relevant clinical utility. Several priorities follow from the existing evidence.

First, *protocol harmonization and cut-off validation* must be multicenter and biopsy-controlled. The range of reported cut-offs for the same fibrosis target—sometimes within a single study, depending on sensitivity/specificity constraints—makes clear that single-center thresholds cannot be simply exported (9, 12). A credible approach would be a multicenter design with at least several hundred participants, stratified by etiology (MASLD/MASH, viral hepatitis, alcohol-related liver disease) and BMI categories, using a pre-specified acquisition protocol (lobe, ROI size and depth, minimum number of valid shots, and explicit quality filters). The primary endpoint should be biopsy-

defined advanced fibrosis (F3–F4), with secondary endpoints for clinically meaningful states such as cirrhosis and portal hypertension, acknowledging that guidelines emphasize prognostic endpoints beyond histological stage alone (16, 21).

Second, *lobe strategy and artifact management* should be treated as first-class research questions, not minor technical footnotes. Evidence that left-lobe EUS-SWE can have markedly higher within-session variance than right-lobe measurements suggests that right-lobe-dominant protocols may offer more reproducible staging unless additional averaging or advanced motion compensation is implemented (11). Future studies should therefore report inter- and intra-observer ICCs separately for each lobe, include breath-control or motion-tracking strategies, and evaluate whether bilobar averaging improves classification or merely dilutes clinically relevant heterogeneity.

Third, *integration with endohepatology outcomes* is likely to be the "killer application" if it can be shown to alter management. The combination of EUS-elasticity with PPG and bilobar biopsy already appears technically feasible and safe in early studies, and an RCT suggests that EUS may outperform transjugular approaches for both reliable portal pressure measurements and adequate biopsy specimens (23, 24). The appropriate next step is longitudinal cohort work linking baseline EUS-SWE and EUS-PPG values to decompensation, variceal development, and mortality, aligned with consensus frameworks that define portal hypertension as a determinant of outcomes and therapeutic thresholds (21). Such cohorts should intentionally include patients with ascites or other conditions where transabdominal elastography is problematic, because this is precisely where incremental value is most plausible.

Fourth, *the learning curve and implementation science* deserve explicit measurement. Existing publications define feasibility and reproducibility but do not yet provide granular learning curve thresholds (e.g., the number of supervised procedures required to achieve stable ICCs or error rates by operator experience) (19, 20). Pragmatically, training studies should randomize operators by experience level, use phantoms and in vivo targets, and report how quality indicators (e.g., failure rate, within-session coefficient of variation, agreement with reference standards) evolve over time.

Finally, *health economic* positioning should be tested in realistic pathways. Because EUS requires sedation and specialized equipment, it will not compete with VCTE or pSWE as a low-cost, scalable screening tool. Its value proposition likely depends on shared-session efficiency (adding EUS-SWE

during an already indicated EUS) and avoiding additional diagnostic steps (repeat failed VCTE, separate biopsy sessions, or transjugular pressure measurements). Early operational descriptions suggest that SWE adds only minutes to an EUS examination, but formal economic evaluations are needed, ideally embedded within pragmatic trials comparing the “standard NIT pathway” versus the “endo-hepatology one-stop pathway” for selected high-risk subgroups (25, 24).

Fig. and diagram development should reflect what currently drives measurement error and clinical interpretation. A schematic of ROI placement should emphasize shallow depth, avoidance of vessels, proximity to the capsule, and differences between left-lobe transgastric and right-lobe transduodenal access; a second diagram could show how EUS-SWE, EUS-PPG, and bilobar EUS-LB integrate into a single procedural workflow, including suggested reporting elements (lobe, kPa distribution, quality indicators, and contemporaneous PPG). These choices are directly motivated by standardization editorials, experimental optimization work, and observed interlobar variance in clinical cohorts (11, 19, 20, 23).

References

1. Castéra L, Foucher J, Bernard PH, et al. Pitfalls of liver stiffness measurement: A 5-year prospective study of 13,369 examinations. J Hepatol. 2010;51:828–835.
2. Myers RP, Pomier-Layrargues G, Kirsch R, et al. Feasibility and diagnostic performance of FibroScan in morbidly obese patients. Hepatology. 2012;55:199–208.
3. Wong VWS, Vergniol J, Wong GLH, et al. Diagnosis of fibrosis and cirrhosis using liver stiffness measurement in NAFLD. Hepatology. 2010;51:454–462.
4. Song JE, Lee JH, Kim JW, et al. Clinical applications of endoscopic ultrasound elastography. Clin Endosc. 2018;51:354–360.
5. Cui XW, Ignee A, Jenssen C, et al. Endoscopic ultrasound elastography: Current status and future perspectives. World J Gastroenterol. 2015;21:13212–13224.
6. Shiina T, Nightingale KR, Palmeri ML, et al. WFUMB guidelines and recommendations for clinical use of ultrasound elastography: Part 1—Basic principles and terminology. Ultrasound Med Biol. 2015;41:1126–1147.
7. Schulman AR, Chan WW, Ryou M, et al. Endoscopic ultrasound elastography distinguishes benign from malignant liver disease. Endosc Ultrasound. 2018;7:242–249.
8. Nightingale K, Palmeri M, Trahey G. Acoustic radiation force impulse imaging: A review. Ultrasound Med Biol. 2011;37:175–193.

9. Kohli DR, Mettman D, Andraws N, et al. Comparative accuracy of endosonographic shear wave elastography and transcutaneous liver stiffness measurement: A pilot study. Gastrointest Endosc. 2023;97:35–41.
10. Dietrich CF, Jenssen C, Arcidiacono PG, et al. Endoscopic ultrasound: Elastographic and contrast-enhanced applications. Endosc Ultrasound. 2021;10:149–160.
11. Diehl DL, Sangwan V, Khurana S, et al. Reproducibility of EUS-guided shear wave elastography for assessment of hepatic fibrosis. Gastrointest Endosc. 2025;101:659–662.
12. Wang TJ, Jirapinyo P, Shah R, et al. EUS-guided shear wave elastography for fibrosis screening in MASLD. Gastrointest Endosc. 2025;101:456–462.e1.
13. Ferraioli G, Wong VWS, Castéra L, et al. Liver elastography: An update of current evidence. Clin Gastroenterol Hepatol. 2019;17:210–218.
14. Boursier J, Zarski JP, de Ledinghen V, et al. Determination of reliability criteria for liver stiffness evaluation. J Hepatol. 2013;58:744–750.
15. Dietrich CF, Bamber J, Berzigotti A, et al. EFSUMB guidelines on liver ultrasound elastography: Update 2020. Ultrasound Int Open. 2020;6:E2–E15.
16. European Association for the Study of the Liver (EASL). Clinical Practice Guidelines on non-invasive tests for evaluation of liver disease severity and prognosis. J Hepatol. 2021;75:659–689.
17. Dietrich CF, Bamber J, Berzigotti A, et al. WFUMB position paper on multiparametric ultrasound (MPUS) in liver disease. Ultrasound Med Biol. 2020;46:2927–2946.
18. AbiMansour J, Chin JYL, Kaur J, et al. Endoscopic ultrasound-based shear-wave elastography for detection of advanced liver disease. J Clin Gastroenterol. 2025;59:256–261.
19. Iglesias-García J, Lariño-Noia J, Abdulkader I, et al. Endoscopic ultrasound shear-wave elastography: Technical aspects and clinical applications. Endoscopy. 2021;53:267–276.
20. Iglesias-García J, de la Iglesia-García D, et al. Optimization of region-of-interest size and depth in EUS-SWE: Experimental study. Diagnostics (Basel). 2023;13:815.
21. de Franchis R, Bosch J, Garcia-Tsao G, et al. Baveno VII – Renewing consensus in portal hypertension. J Hepatol. 2022;76:959–974.
22. AbiMansour J, Chin JYL, Kaur J, et al. Endoscopic ultrasound-based shear-wave elastography of the spleen for detection of clinically significant portal hypertension. J Clin Gastroenterol. 2024;58:724–731.
23. Zhang XM, Li Q, et al. Endoscopic ultrasound-guided portal pressure gradient measurement combined with liver elastography and biopsy: A single-center experience. Endosc Ultrasound. 2023;12:274–281.
24. Huang JY, Samarasena JB, et al. Randomized controlled trial comparing EUS-guided portal pressure gradient measurement and liver biopsy with the transjugular approach. Gastrointest Endosc. 2023;98:765–774.
25. Wang TJ, Jirapinyo P, Shah R, et al. Operational feasibility of integrating EUS shear-wave elastography into routine endoscopic workflow. Gastrointest Endosc. 2025;101:456–462.

8. Liver multiparametric ultrasound in pediatric population

Blerina Saraci (Qirinxhi), Durim Cela, Denis Qirinxhi

Abstract

Multiparametric ultrasound (MPUS) represents an integrated imaging framework for comprehensive evaluation of pediatric liver disease. By combining grayscale morphology, Doppler-derived hemodynamic assessment, shear wave elastography, and contrast-enhanced ultrasound (CEUS), MPUS enables multidimensional characterization of hepatic structure, vascular dynamics, and tissue biomechanics within a single examination.

This chapter synthesizes current European and international recommendations regarding advanced ultrasound applications in pediatric hepatology, including focal liver lesions, metabolic dysfunction–associated steatotic liver disease (MASLD), chronic hepatitis, biliary atresia, portal hypertension, and post-transplant surveillance. Emphasis is placed on age-adjusted reference values and technique-specific stiffness thresholds.

Integration of morphological, hemodynamic, and elastographic parameters enhances diagnostic stratification beyond structural imaging alone. When interpreted within clinical context, multiparametric ultrasound constitutes a robust, radiation-free strategy for longitudinal pediatric liver assessment, with potential to reduce reliance on invasive procedures and support evidence-based care pathways.

The quantitative thresholds presented reflect a synthesis of published pediatric cohorts and international ultrasound guidelines rather than single-source recommendations.

8.1. Introduction

The diagnostic landscape of pediatric liver disease has undergone substantial transformation, reflecting broader shifts in contemporary medical imaging toward integration, quantification, and precision. In childhood, liver pathology unfolds within a dynamic developmental environment, where anatomical maturation, evolving vascular physiology, and age-specific disease expression challenge simplified interpretative models derived from adult practice. Consequently, pediatric hepatology demands imaging strategies that are adaptable, reproducible, and biologically contextualized.

Within this framework, ultrasound has progressively expanded beyond its traditional role as a structural modality. Its intrinsic advantages—absence of ionizing radiation, real-time capability, and suitability for serial evaluation—render it uniquely aligned with the safety and longitudinal monitoring requirements of pediatric care. However, its contemporary relevance lies not merely in accessibility but in its capacity to integrate multiple dimensions of hepatic assessment within a single examination.

The convergence of grayscale morphology, Doppler-derived hemodynamic interrogation, quantitative elastography, and contrast-enhanced ultrasound (CEUS) has given rise to a multiparametric imaging paradigm. This approach enables simultaneous evaluation of parenchymal architecture, vascular adaptation, tissue biomechanics, and microvascular perfusion. Rather than functioning as isolated techniques, these components collectively contribute to a cohesive diagnostic framework.

Elastography has emerged as a pivotal noninvasive surrogate for fibrosis staging, while Doppler assessment provides insight into portal hemodynamics and vascular complications. CEUS further extends diagnostic capability by enabling dynamic perfusion analysis without radiation exposure or nephrotoxicity—an advantage of particular relevance in children. In parallel, the increasing recognition of metabolic dysfunction–associated steatotic liver disease (MASLD) and other chronic pediatric liver conditions underscores the necessity for quantitative and longitudinal imaging biomarkers.

As pediatric hepatology continues to evolve, multiparametric ultrasound occupies an increasingly strategic position at the intersection of safety, diagnostic depth, and precision-oriented care. Its integration into clinical workflows reflects not only technological advancement, but also a conceptual redefinition of how pediatric liver disease is evaluated and monitored.

This chapter examines the technical principles, validated thresholds, and clinical applications of multiparametric ultrasound in the pediatric liver, emphasizing age-adapted methodology and future directions in evidence-based, precision imaging.

8.2. Normal Pediatric Liver Dimensions on Ultrasound

Physiological liver growth in childhood reflects continuous structural remodeling and vascular adaptation. For this reason, sonographic evaluation of hepatic size in pediatric patients requires strict age-adjusted interpretation rather than application of static reference thresholds. Developmental stage,

somatic growth, and body composition all influence normal dimensional parameters.

In routine practice, the most reproducible measurement is the craniocaudal length of the right hepatic lobe obtained along the midclavicular line during quiet respiration (Table 8.I). When performed using standardized technique, this parameter allows consistent longitudinal comparison across follow-up examinations. Intercostal acquisition in the supine or slight left lateral decubitus position is generally preferred to minimize obliquity and measurement variability.

Table 8.I. Approximate age-related reference ranges of the right liver lobe in children

Age Group	**Right Lobe Length (cm)**
Neonates	4.5–6 cm
1–5 years	6–9 cm
6–12 years	9–12 cm
Adolescents	12–15 cm

These values should be regarded as general orientation ranges rather than absolute cutoffs. Liver size correlates not only with chronological age but also with height, body surface area, and overall somatic development. Mild deviations from reference values may therefore reflect constitutional variation rather than pathology.

Importantly, assessment of hepatomegaly must incorporate additional parameters. Concomitant evaluation of splenic size, portal venous diameter and flow velocity, and hepatic parenchymal echotexture enhances diagnostic confidence. Reliance on isolated linear measurements risks both overdiagnosis and under-recognition of clinically significant disease.

Standardization of acquisition technique and awareness of interobserver variability remain essential for reproducible pediatric liver assessment, particularly in longitudinal follow-up contexts.

8.3. Pediatric Liver Elastography

8.3.1. Physical Principles

Ultrasound-based liver elastography provides quantitative estimation of hepatic stiffness by measuring the propagation velocity of mechanically induced shear waves through the parenchyma. From a biomechanical perspective, stiffness values reflect a composite response of hepatic tissue rather than

fibrosis alone. Fibrotic matrix deposition, inflammatory cellular infiltration, cholestatic pressure changes, vascular congestion, and interstitial edema may all influence measured values to varying degrees.

In pediatric populations, interpretation requires particular caution. Ongoing developmental changes in liver architecture, variable parenchymal thickness, and disease-specific remodeling patterns may modify stiffness behavior. Sustained elevation of stiffness is most commonly associated with progressive fibrotic remodeling, whereas transient increases may occur during acute inflammatory or hemodynamic disturbances. Consequently, elastographic findings should always be contextualized within biochemical and clinical parameters.

8.3.2. Normal Values and Cut-Offs

In healthy children, liver stiffness values most frequently fall within a range of approximately 3.0–5.5 kPa, although minor variation may occur depending on acquisition protocol and system calibration. These values should be regarded as orientation ranges rather than strict diagnostic cutoffs.

Mild stiffness elevation (approximately 6–7 kPa) may correspond to early fibrotic remodeling but may also reflect inflammatory activity. Measurements exceeding 9–12 kPa are more often observed in advanced fibrosis stages, acknowledging technique-specific variability and disease-dependent factors.

Reported stiffness ranges derive from heterogeneous pediatric studies with varying etiologies, acquisition protocols, and vendor platforms; therefore, values should be interpreted as orientation ranges rather than absolute diagnostic cut-offs.

Approximate orientation ranges for fibrosis-associated liver stiffness (kPa) in pediatric cohorts are as follows: F=0 (Normal) 3.0–5.5 kPa; F1 6–7.5 kPa; F2 7.5–9 kPa; F3–F4 > 9–12 kPa.

Overlap between stages is recognized, and interpretation should integrate laboratory findings and imaging context.

8.3.3. Technique Consideration: 2D-SWE vs. Point SWE

Two-dimensional shear wave elastography (2D-SWE) provides real-time color-coded stiffness mapping, allowing broader parenchymal sampling and visualization of spatial heterogeneity. This may reduce sampling bias and enhance reproducibility when technically feasible.

Point shear wave elastography (pSWE) relies on single-region sampling and remains widely available. Although technically straightforward, its smaller sampling volume may introduce modest variability, particularly in small intercostal windows common in pediatric patients.

Both techniques derive stiffness from shear wave velocity using comparable physical principles, yet absolute thresholds may differ slightly between platforms. For this reason, stiffness values should be interpreted according to the specific technology employed rather than applied universally (Table 8.II).

Table 8.II. Approximate liver stiffness thresholds for fibrosis staging using Point Shear Wave Elastography (pSWE) and Two-Dimensional Shear Wave Elastography (2D-SWE) in Pediatric Patients

Fibrosis Stage	**pSWE (kPa)**	**2D-SWE (kPa)**
F0–F1	3.0–6.0	3.0–5.5
F2	6.0–8.5	6.0–8.0
F3	8.50–10.5	8.0–10.0
F4	11.0–13.0	10.0–12.0

Values are approximate ranges synthesized from published pediatric elastography studies and international recommendations, including WFUMB guidelines. Thresholds may vary according to vendor platform, probe characteristics, acquisition protocol, and underlying inflammatory activity. Stiffness values should therefore be interpreted within the appropriate clinical context.

Absolute stiffness values may vary between ultrasound systems due to differences in shear wave generation, calibration algorithms, and region-of-interest sampling methodology.

8.3.4. Quality Control in Pediatric Examinations

Optimal ROI placement in pediatric liver elastography should be adapted according to patient age and hepatic parenchymal thickness. In school-aged children and adolescents, the sampling box is ideally positioned 2–5 cm below the hepatic capsule within the right lobe using an intercostal approach. In neonates and young infants, reduced liver depth necessitates shallower placement, typically 1–2 cm below the capsule, while carefully avoiding subcapsular artifacts.

Due to the anatomical proximity of the heart, particularly in small infants, cardiac-induced motion artifacts must be recognized and minimized. Measurements in the right lobe are generally preferred to reduce motion interference. In cooperative children, brief breath-hold acquisition improves measurement stability; however, in neonates and infants, free-breathing acquisition is typically performed, with repeated measurements to ensure reliability.

Fasting for 3–4 hours is recommended when age and clinical condition permit, as postprandial hepatic blood flow variations may influence stiffness values. Sedation is generally avoided solely for elastography purposes. When sedation is required for other clinical indications, its potential hemodynamic effects should be considered during interpretation.

The ROI must exclude large vascular structures, biliary branches, and focal lesions. Acquisition of at least 10 valid measurements with an interquartile range-to-median ratio (IQR/median) ≤30% is recommended to ensure reproducibility across pediatric age groups.

In the pediatric population we often have the challenge of the small surface area compared to the standard ultrasound probe able to perform elastography and the need for a dedicated elastography probe, which often increases the costs of the equipment.

Interobserver agreement in pediatric elastography has been reported as good to excellent in experienced centers, although operator expertise and patient cooperation remain important determinants of reproducibility.

8.3.5. Etiology-Specific Variation

Stiffness behavior varies according to the underlying disease mechanism. Acute viral hepatitis may produce transient elevation secondary to inflammatory infiltration and edema. Autoimmune hepatitis may demonstrate disproportionately increased stiffness during active inflammatory phases independent of established fibrosis.

Cholestatic disorders, including biliary atresia, may elevate stiffness via increased intrahepatic pressure and structural remodeling. In MASLD, isolated steatosis typically exerts limited direct impact on stiffness unless accompanied by inflammatory activity or fibrotic progression.

8.3.6. Inflammation versus Fibrosis: Pathophysiological Considerations

Fibrosis contributes to sustained stiffness elevation through extracellular matrix deposition and architectural distortion. In contrast, acute inflammation increases stiffness primarily through cellular infiltration and interstitial edema without necessarily implying irreversible structural change.

Transient inflammatory activity may produce temporary elevation in stiffness values with subsequent normalization, whereas progressive fibrotic remodeling results in sustained and cumulative stiffness increase over time. The curves are schematic and intended for educational representation rather than longitudinal patient-level data (Fig. 8.1).

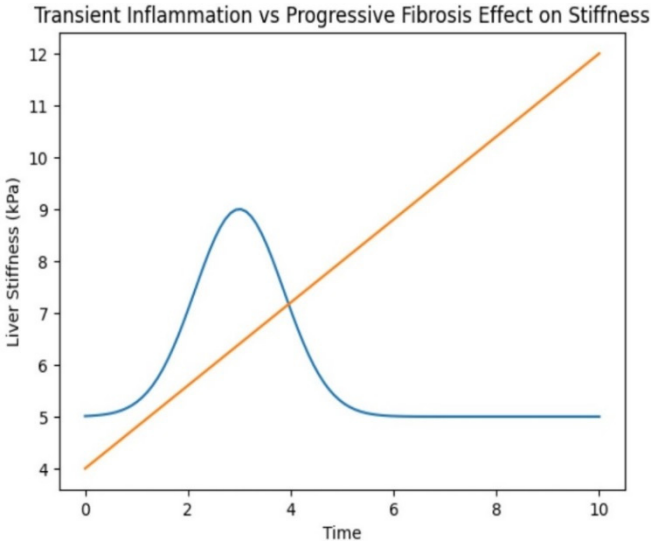


Fig. 8.1. Conceptual illustration of differential liver stiffness behavior in transient inflammation versus progressive fibrosis.

Elevated aminotransferase levels may therefore indicate inflammatory activity rather than advanced fibrosis. Reassessment after biochemical stabilization may help differentiate transient from persistent stiffness elevation, particularly in pediatric patients with fluctuating disease activity.

8.3.7. Spleen as a non-invasive biomarker

Assessment of portal hypertension in pediatric patients increasingly incorporates spleen stiffness measurement as a complementary non-invasive biomarker. Beyond reflecting splenic congestion, increased spleen stiffness may mirror the hemodynamic consequences of elevated portal pressure and

evolving architectural remodeling. Although pediatric-specific validation remains more limited than adult datasets, emerging evidence suggests a progressive association between higher spleen stiffness values and the likelihood of clinically significant portal hypertension. This relationship, while not strictly linear, may be conceptually represented as a sigmoid risk curve, reflecting gradual escalation of probability rather than abrupt threshold transition (Fig. 8.2).

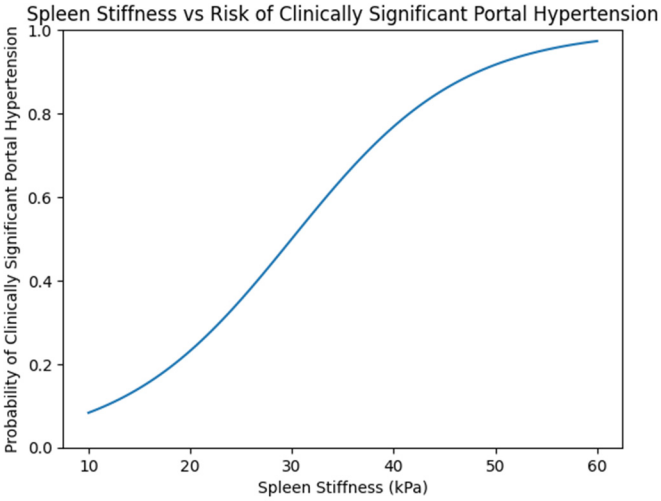


Fig. 8.2. Conceptual relationship between spleen stiffness values and estimated probability of clinically significant portal hypertension.

The sigmoid curve illustrates the progressive increase in risk with rising spleen stiffness measurements, reflecting trends reported in adult and emerging pediatric literature. This representation is schematic and does not correspond to a validated predictive model or patient-level dataset.

8.3.8. Suggested Clinical Algorithm

Elastography should be regarded as one component within a multiparametric diagnostic strategy. Adequate acquisition standards represent a prerequisite for interpretation. Stiffness values gain clinical relevance only when integrated with morphological assessment, Doppler-derived hemodynamic findings, laboratory markers, and longitudinal trends.

In cases of persistent stiffness elevation with uncertain etiology, further diagnostic evaluation—including histopathological sampling in selected patients—may be considered within multidisciplinary decision-making.

Table 8.III. Etiology-Specific Determinants of Liver Stiffness in Children

Etiology	**Predominant pathophysiological driver**	**Impact on Stiffness Interpretation**
Acute viral hepatitis	Inflammatory infiltration and parenchymal edema	May produce transient stiffness elevation; reassessment after biochemical stabilization is advisable
Chronic HBV/HCV	Progressive extracellular matrix deposition and architectural remodeling	Stiffness values generally correlate with fibrosis stage when inflammatory activity is stable
Autoimmune hepatitis	Immune-mediated inflammatory activity with or without fibrosis	Elevation may reflect inflammatory flare; reassessment after therapeutic control improves accuracy
Biliary atresia	Cholestasis-associated pressure changes and secondary fibrosis	Stiffness may carry prognostic implications in disease progression
MASLD	Fibrosis with variable low-grade inflammatory component	Isolated steatosis exerts limited direct mechanical impact unless fibrosis is present

8.4. Contrast-Enhanced Ultrasound (CEUS)

While elastography provides quantitative insight into the biomechanical properties of hepatic parenchyma, stiffness assessment alone cannot fully characterize vascular behavior or microcirculatory dynamics. Fibrotic remodeling, inflammatory activity, and cholestatic processes influence tissue elasticity; however, perfusion patterns and enhancement kinetics require complementary functional evaluation.

In this context, contrast-enhanced ultrasound (CEUS) extends the multiparametric framework beyond structural and biomechanical assessment by enabling real-time visualization of microvascular perfusion. Unlike elastography, which reflects mechanical tissue properties, CEUS interrogates

vascular distribution and temporal enhancement behavior, thereby offering additional diagnostic depth in focal and diffuse pediatric liver disease.

The integration of elastographic stiffness quantification with perfusion-sensitive imaging creates a more comprehensive diagnostic platform. Whereas elastography contributes to fibrosis staging and risk stratification, CEUS enhances lesion characterization and functional vascular assessment without ionizing radiation or nephrotoxic contrast agents.

Together, these techniques reinforce the concept of multiparametric ultrasound as an integrative imaging strategy rather than a collection of isolated modalities.

8.4.1. Microbubble Contrast Agents

Contrast-enhanced ultrasound utilizes gas-filled microbubble contrast agents that remain strictly confined to the intravascular compartment. Unlike iodinated or gadolinium-based agents, microbubbles do not undergo renal excretion and do not expose patients to ionizing radiation. Their purely intravascular distribution allows real-time assessment of tissue perfusion and vascular architecture.

In pediatric imaging, this safety profile is particularly advantageous. The absence of radiation and nephrotoxicity aligns with contemporary radiation-sparing principles and supports the use of CEUS as a problem-solving modality when lesion characterization requires functional vascular assessment.

8.4.2. Enhancement Phases

Hepatic CEUS evaluation is based on dynamic assessment of enhancement kinetics across three principal phases:

- Arterial phase (approximately 10–30 seconds)
- Portal venous phase (approximately 30–120 seconds)
- Late phase (>120 seconds)

Phase timing definitions follow established international CEUS criteria and may demonstrate minor physiological variation depending on cardiac output and age-related hemodynamics.

Lesion characterization depends not solely on enhancement intensity but on temporal behavior. The presence or absence of washout, the pattern of arterial filling, and the persistence of enhancement in late phases provide critical information regarding biological behavior.

8.4.3. Hemangioma: Characteristic Enhancement Pattern (Table 8.IV.)

Pediatric hepatic hemangioma is among the most common benign hepatic tumors in infancy. Typically, it demonstrates a pattern with peripheral nodular discontinuous arterial enhancement, followed by progressive centripetal fill-in during portal and late phases, without true washout. Malignant lesions typically demonstrate washout in the late phase.

On grayscale imaging, hepatic hemangiomas are typically well-defined and often hyperechoic, particularly when small. Larger lesions may demonstrate internal heterogeneity.

Color Doppler commonly reveals peripheral or moderate internal vascularity (Fig. 8.3.). In infantile high-flow variants, arterial enlargement and arteriovenous shunting may be observed. Spectral Doppler may demonstrate low-resistance arterial waveforms, reflecting vascular channel composition.

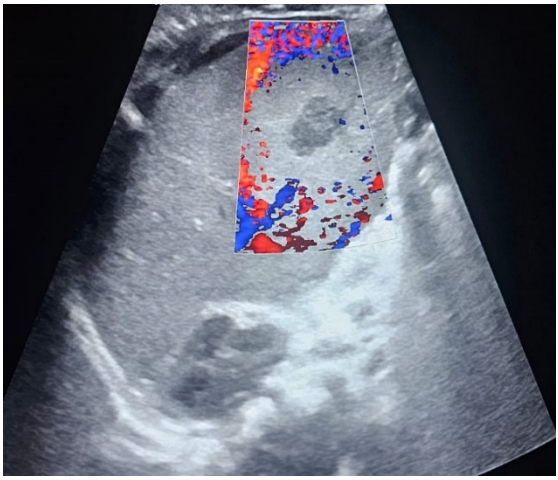


Fig. 8.3. Color Doppler ultrasound appearance of neonatal hepatic hemangioma.

On CEUS, hemangiomas characteristically demonstrate peripheral nodular discontinuous enhancement during the arterial phase, followed by progressive centripetal fill-in during portal and late phases. Sustained enhancement without true washout supports benign vascular etiology.

8.4.4. Hepatoblastoma *(Table 8.IV.)*

Hepatoblastoma is the most common primary malignant hepatic tumor of early childhood. Sonographically, it frequently appears as a heterogeneous solid mass, often large at presentation and occasionally associated with calcifications.

Color Doppler typically demonstrates marked internal vascularity with disorganized arterial branching. Spectral Doppler may show low-resistance arterial flow with elevated peak systolic velocities, reflecting tumoral neoangiogenesis and increased metabolic demand. Doppler ultrasound findings alone may be insufficient for definitive differentiation; contrast-enhanced imaging like CEUS and clinicobiochemical correlation are often required for accurate diagnosis.

On CEUS, hepatoblastoma often exhibits rapid and heterogeneous arterial hyperenhancement followed by early or progressive washout during portal or late phases. The presence of washout is strongly suggestive of malignancy in the appropriate clinical context.

Serum alpha-fetoprotein (AFP) levels, interpreted according to age-adjusted norms, provide important complementary diagnostic information.

Enhancement behavior should always be interpreted in conjunction with clinical presentation and laboratory markers, as overlap in perfusion characteristics may occur in atypical or treated lesions.

Table 8.IV. Comparative Gray-Scale and Doppler Ultrasound Features in Pediatric Hepatic Hemangioma and Hepatoblastoma

Features	**Hepatic Hemangioma**	**Hepatic Hepatoblastoma**
Gray-Scale	Well-defined, typically hyperechoic and homogeneous when small; larger lesions may appear heterogeneous	Heterogeneous solid mass, often large at presentation; may contain calcifications; margins frequently irregular
Color Doppler Findings	Peripheral or moderate internal vascularity; feeding artery may be present; high-flow shunts in infantile variants	Marked internal vascularity with chaotic architecture and prominent intratumoral arteries
Spectral Doppler Characteristics	Low-resistance arterial waveform; possible elevated peak systolic velocities in high-flow lesions	Low-resistance arterial flow reflecting neovascularization; elevated peak systolic velocities; possible vascular displacement or invasion

.

8.4.5. Key differences between benign vs. malignant focal liver lesions (Table 8.V.)

Differentiation between benign vascular tumors and malignant hepatic neoplasms relies on integration of structural and hemodynamic parameters.

Benign lesions such as hemangiomas tend to exhibit well-defined margins, organized vascular patterns, and absence of vascular invasion. In contrast, malignant tumors more commonly demonstrate irregular contours, chaotic intratumoral vascular architecture, prominent feeding arteries, and potential involvement of adjacent vascular structures. No single Doppler parameter is pathognomonic; rather, diagnostic confidence arises from the convergence of multiple imaging and clinical features.

Table 8.V. Comparative Ultrasound Findings in Pediatric Hepatic Hemangioma and Hepatoblastoma

Feature	**Hemangioma**	**Hepatoblastoma**
Margins	Well-defined	Often irregular
Internal vascularity	Mild to moderate	Marked and chaotic
Vascular architecture	Peripheral or organized	Disorganized
Feeding artery	May be present	Often prominent
Arteriovenous shunt	Possible (infantile type)	Rare
Vessel invasion	Absent	Possible

8.4.6. Integrative Diagnostic Strategy

Assessment of a pediatric focal liver lesion should follow a structured yet integrative approach. Grayscale imaging establishes lesion morphology, size, and calcification status. Doppler evaluation refines vascular characterization, while spectral analysis provides quantitative hemodynamic insight.

Laboratory markers, particularly AFP, further contextualize imaging findings. When conventional ultrasound remains indeterminate, CEUS offers dynamic perfusion assessment that frequently allows noninvasive characterization. Magnetic resonance imaging may serve as a complementary modality in selected cases.

Histopathological confirmation is reserved for situations in which imaging findings remain inconclusive or discordant with clinical and biochemical data.

8.4.7. Suggested Diagnostic Algorithm

Evaluation of a pediatric focal liver lesion should follow an integrative pathway beginning with grayscale assessment of lesion morphology, margins, and internal architecture. Doppler interrogation refines vascular characterization, while spectral analysis provides quantitative hemodynamic information. Laboratory correlation, particularly age-adjusted AFP levels, further contextualizes imaging findings. When uncertainty persists, CEUS or magnetic resonance imaging may provide definitive perfusion characterization. Histopathological sampling is reserved for cases in which imaging and clinical data remain discordant.

8.4.8. Clinical Indications for CEUS in Children

CEUS is most frequently applied in the evaluation of indeterminate focal liver lesions detected on baseline ultrasound. It is particularly useful in suspected hemangioma, focal nodular hyperplasia (FNH) (Fig. 8.4-8.5.), FNH-like lesions, and other vascular tumors where enhancement kinetics provide decisive diagnostic information.

In pediatric abdominal trauma, CEUS may aid in assessing parenchymal injury and perfusion abnormalities in hemodynamically stable patients, potentially reducing reliance on computed tomography.

CEUS also supports longitudinal follow-up of known lesions and monitoring of treatment response. By providing dynamic perfusion data without radiation exposure, CEUS contributes to minimizing cross-sectional imaging when clinically appropriate.

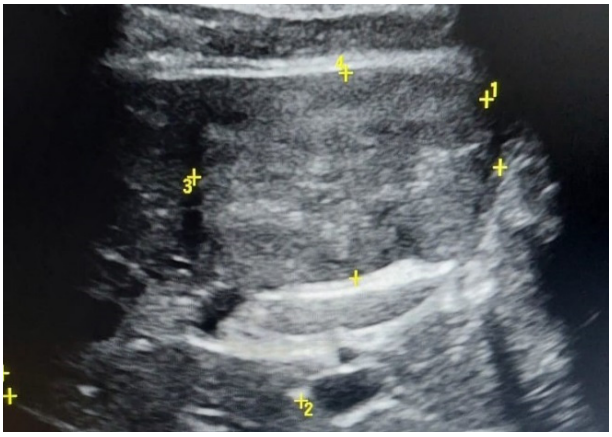


Fig. 8.4. B-mode ultrasound appearance of focal nodular hyperplasia

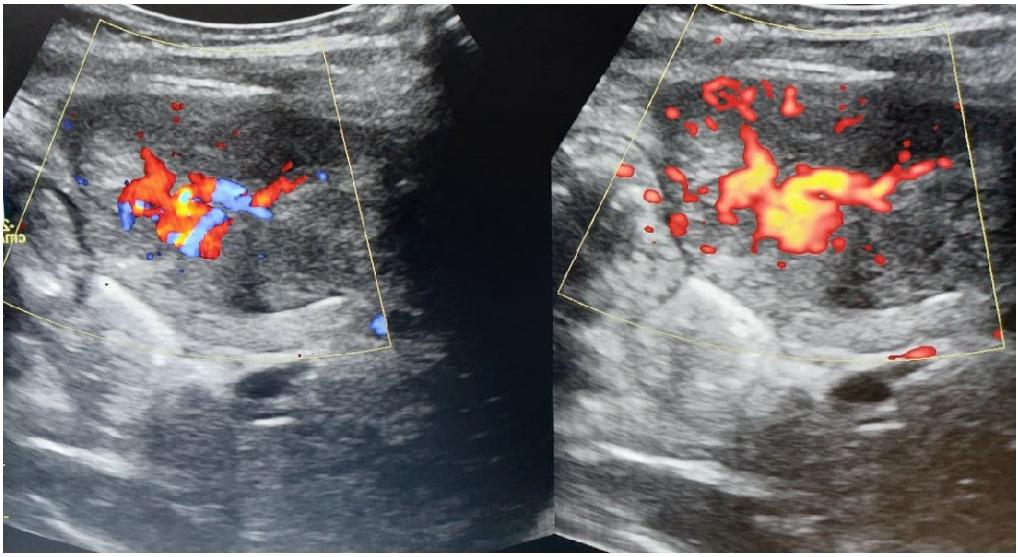


Fig. 8.5. Color Doppler (left panel) and Power Doppler (right panel) findings of focal nodular hyperplasia

8.5. Quantitative Assessment of Pediatric Steatosis

8.5.1. Rationale

The rising prevalence of MASLD in children has increased the need for reliable, noninvasive quantification of hepatic fat content. While conventional B-mode ultrasound may suggest steatosis through increased echogenicity, subjective assessment lacks reproducibility and sensitivity for mild disease. Quantitative ultrasound-based techniques aim to overcome these limitations by providing objective measurements related to hepatic fat deposition.

8.5.2. Controlled Attenuation Parameter (CAP)

The controlled attenuation parameter (CAP), obtained during transient elastography, estimates hepatic fat content by measuring ultrasound signal attenuation within the liver parenchyma. CAP values are expressed in decibels per meter (dB/m), with higher values corresponding to increased fat accumulation.

Although threshold ranges vary depending on population and device calibration, values above approximately 240–260 dB/m have been associated with steatosis in pediatric and adult cohorts. Interpretation should consider body habitus, fibrosis stage, and technical factors that may influence measurement reliability.

CAP provides a convenient adjunct to stiffness assessment, enabling simultaneous evaluation of fibrosis and steatosis within a single examination framework.

Pediatric validation data for CAP remain more limited than adult datasets, and body habitus as well as probe selection may influence attenuation measurements.

8.5.3. Ultrasound Attenuation Imaging

Modern ultrasound systems incorporate attenuation coefficient imaging techniques that quantify acoustic attenuation in units such as dB/cm/MHz. These methods assess the rate at which ultrasound energy diminishes as it traverses hepatic tissue, a property that increases in the presence of fat infiltration.

Reported attenuation coefficients around 0.60–0.70 dB/cm/MHz may suggest hepatic steatosis, though device-specific calibration and pediatric validation remain important considerations. Compared with visual grading, quantitative attenuation imaging enhances reproducibility and allows longitudinal monitoring of hepatic fat burden.

8.5.4. MRI-Proton Density Fat Fraction (MRI-PDFF) as Reference Standard

Magnetic resonance imaging–proton density fat fraction (MRI-PDFF) is widely regarded as the non-invasive reference standard for quantification of hepatic fat content. MRI-PDFF provides a continuous, reproducible estimate of fat fraction across the entire liver, independent of acoustic window limitations.

While MRI offers high diagnostic accuracy, its availability, cost, and need for patient cooperation may limit routine application in pediatric populations. Consequently, quantitative ultrasound techniques represent attractive first-line tools, with MRI reserved for validation, complex cases, or research settings.

8.5.5. Integrated Multiparametric Interpretation

Optimal evaluation of pediatric liver disease requires integration of structural, hemodynamic, biomechanical, and biochemical parameters rather than reliance on a single imaging metric.

B-mode echogenicity provides a preliminary assessment of parenchymal texture and focal abnormalities. Doppler interrogation contributes vascular and hemodynamic insight, particularly in the evaluation of portal

hypertension and focal lesion characterization. Elastography quantifies tissue stiffness and supports fibrosis risk stratification, while attenuation-based techniques offer objective estimation of hepatic fat burden.

These imaging findings must be interpreted alongside biochemical markers, including aminotransferases and disease-specific laboratory parameters. Diagnostic confidence emerges from the convergence of morphological, functional, and quantitative data within the broader clinical context.

Multiparametric ultrasound therefore represents not merely a combination of techniques, but an integrated diagnostic framework tailored to the pediatric population. Diagnostic confidence increases non-linearly as complementary parameters (morphology, Doppler, elastography, and CEUS) are integrated. The curve represents a theoretical framework rather than empirical patient-level data (Fig. 8.6).

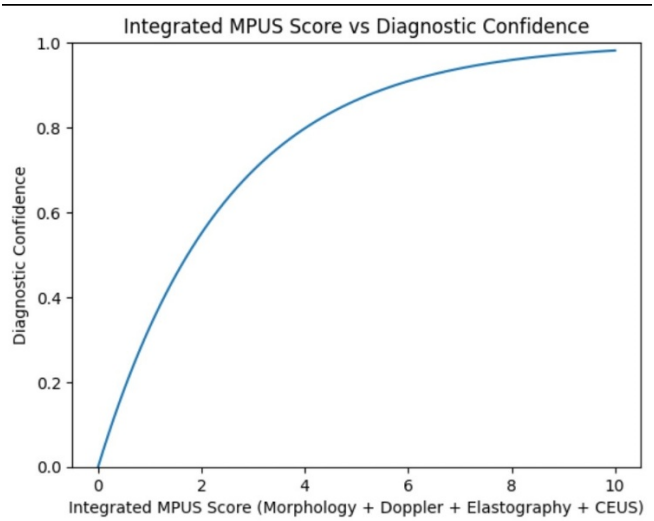


Fig. 8.6. Conceptual model illustrating the relationship between integrated multiparametric ultrasound (MPUS) score and diagnostic confidence.

8.6. Ultrasound-Guided Liver Biopsy in Pediatric Patients

8.6.1. Introduction

Despite significant advances in noninvasive imaging, percutaneous liver biopsy remains an important diagnostic tool in selected pediatric cases. It is particularly relevant when imaging findings are inconclusive, when precise histopathological staging is required, or when discordance exists between clinical presentation and non-invasive assessment.

Real-time ultrasound guidance enhances procedural safety by allowing continuous visualization of hepatic parenchyma, vascular structures, and adjacent organs. This reduces the risk of complications and improves sampling accuracy compared with blind techniques.

Biopsy should not be viewed as a routine first-line procedure but rather as a complementary modality reserved for situations in which noninvasive methods cannot provide sufficient diagnostic clarity.

8.6.2. Indications

In contemporary pediatric hepatology, liver biopsy is reserved for situations in which noninvasive imaging and laboratory evaluation do not provide sufficient diagnostic certainty. The procedure should be considered within a multidisciplinary framework and performed only when the anticipated diagnostic yield outweighs procedural risk.

Common clinical scenarios include:

- Persistent unexplained elevation of liver enzymes, particularly when biochemical abnormalities remain discordant with imaging findings.
- Suspected autoimmune hepatitis requiring histopathological confirmation and grading of inflammatory activity.
- Evaluation of metabolic or genetic liver diseases, including disorders such as Wilson disease, where tissue copper quantification or architectural assessment may be required.
- Assessment of cholestatic disorders, including biliary atresia, especially when clinical and imaging data are inconclusive.
- Discordance between elastography findings and overall clinical presentation, particularly when unexpectedly elevated stiffness values require clarification.
- Post–liver transplantation graft dysfunction, when differentiation between rejection, recurrence, or other pathology is necessary.
- Infiltrative or storage disorders in which parenchymal architecture cannot be adequately characterized by imaging alone.

Biopsy should therefore be viewed as a targeted diagnostic intervention rather than a routine extension of imaging evaluation.

8.6.3. Contraindications

Contraindications to percutaneous liver biopsy in children may be categorized as absolute or relative, and careful pre-procedural assessment is essential (Table 8.VI).

Absolute contraindications include uncorrected coagulopathy and severe thrombocytopenia, both of which substantially increase the risk of hemorrhagic complications.

Relative contraindications include severe ascites, which may compromise needle trajectory and increase bleeding risk, and lack of patient cooperation when safe sedation or anesthesia cannot be ensured. In such cases, alternative approaches—such as transjugular biopsy—may be considered in specialized centers.

Pre-procedural laboratory evaluation, including platelet count and coagulation profile, should be systematically performed to minimize risk.

Table 8.VI. Liver biopsy contraindications

Absolute	***Relative***
Uncorrected coagulopathy	Severe ascites
Severe thrombocytopenia	Uncooperative patient without sedation

8.6.4. Technical Considerations

In pediatric patients, percutaneous liver biopsy is most commonly performed using a right intercostal approach targeting the right hepatic lobe, which generally provides adequate parenchymal thickness while minimizing risk to adjacent organs. Real-time ultrasound guidance allows continuous visualization of needle trajectory and vascular structures, thereby enhancing procedural precision and safety.

Sedation or general anesthesia is frequently required in younger children to ensure immobility and optimize sampling accuracy. Pre-procedural evaluation includes assessment of coagulation profile, platelet count, and detailed ultrasound mapping of hepatic vascular anatomy. Particular attention should be given to identifying large intrahepatic vessels and potential anatomical variants.

Selection of needle gauge and sampling technique should balance diagnostic yield with procedural risk. Adequate core length and number of portal tracts remain critical for reliable histopathological interpretation.

8.6.5. Complications and Safety Profile

When performed under standardized protocols and appropriate patient selection, ultrasound-guided liver biopsy in children demonstrates a favorable safety profile.

Minor discomfort at the puncture site represents the most frequently reported adverse event and is generally self-limited. Minor bleeding may occur but is typically manageable with conservative observation. Major complications, including significant hemorrhage or injury to adjacent structures, are rare in experienced centers.

Most complications manifest within the first few hours following the procedure, underscoring the importance of post-biopsy monitoring. Hemodynamic observation and clinical assessment during the immediate post-procedural period are essential components of safe practice.

Overall complication rates in pediatric series remain low, particularly when contraindications are carefully excluded and procedural expertise is maintained.

8.6.6. Liver Biopsy vs. Elastography (Table 8.VII)

Elastography has transformed pediatric hepatology by enabling noninvasive estimation of liver stiffness and fibrosis risk. Its reproducibility and patient tolerability make it an attractive first-line assessment tool in many clinical scenarios.

However, elastography evaluates mechanical properties rather than cellular architecture. It cannot directly characterize inflammatory activity, quantify specific storage disorders, or identify subtle histological patterns. Consequently, biopsy remains indispensable when detailed architectural analysis or etiological clarification is required.

Rather than representing competing modalities, elastography and biopsy should be viewed as complementary. Non-invasive assessment may reduce the need for invasive sampling in many children, while biopsy retains its role in complex, discordant, or diagnostically uncertain cases.

Table 8.VII. Summary table-comparative overview: elastography vs. liver biopsy

Feature	Elastography	Liver Biopsy
Fibrosis assessment	Non-invasive quantitative stiffness estimation	Definitive architectural staging
Inflammation grading	Indirect assessment	Direct histopathological evaluation
Etiological clarification	Limited	Comprehensive
Invasiveness	Non-invasive and repeatable	Invasive
Suitability for longitudinal monitoring	Highly suitable	Not appropriate for frequent repetition

8.7. Conclusion

The evolution of pediatric liver ultrasound reflects a broader transformation in medical imaging toward integration, quantification, and patient-centered safety. What was once primarily an anatomical examination has developed into a multiparametric platform capable of combining morphological assessment, vascular analysis, tissue biomechanics, perfusion characterization, and fat quantification within a single radiation-free evaluation.

This integrated approach is particularly meaningful in pediatric care, where minimizing invasiveness is a fundamental principle. By enabling early detection, dynamic monitoring, and risk stratification, multiparametric ultrasound supports informed therapeutic decision-making while limiting exposure to ionizing radiation and unnecessary invasive procedures.

As quantitative standardization improves and pediatric-specific validation expands, the diagnostic gap between imaging biomarkers and histopathology continues to narrow. Within this convergence of technology, biology, and clinical reasoning, noninvasive precision emerges not simply as a technical advancement but as an ethical commitment to safer and more individualized care for children.

Pediatric ultrasound, particularly its multiparametric evolution (MPUS), continues to rely on a high level of operator expertise and contextual clinical interpretation.

The framework presented represents a synthesis of current literature and clinical experience rather than prescriptive diagnostic algorithms.

The integration of artificial intelligence into MPUS workflows is expected to enhance reproducibility, quantitative standardization, and decision support, while preserving the central role of expert-driven assessment in pediatric hepatology.

Selective references

1. Riccabona M. Ultrasound of the liver in children. Eur Radiol. 2016;26:323–335.
2. Darge K, Anupindi SA, Keener H. Pediatric liver ultrasound: state of the art. Pediatr Radiol. 2018;48:123–135.
3. Ferraioli G, Filice C, Castera L, Choi BI, Sporea I, et al. WFUMB guidelines and recommendations for clinical use of ultrasound elastography: Part 3: liver. Ultrasound Med Biol. 2015 May;41(5):1161-79.
4. Ferraioli G, Barr RG, Berzigotti A, Sporea I, Wong VW, Reiberger T, et al. WFUMB Guideline/Guidance on Liver Multiparametric Ultrasound: Part 1. Update to 2018 Guidelines on Liver Ultrasound Elastography. Ultrasound Med Biol. 2024 Aug;50(8):1071-87
5. Dietrich CF, Bamber J, Berzigotti A, Bota S, Cantisani V, Castera L, et al. EFSUMB Guidelines and Recommendations on the Clinical Use of Liver Ultrasound Elastography, Update 2017 (Long Version). Ultraschall Med. 2017 Aug;38(4):e16-e47. Erratum in: Ultraschall Med. 2017 Aug;38(4):e48.
6. Ferraioli G, Wong VW, Castera L, et al. Liver ultrasound elastography: an update. Radiology. 2019;292:546–556.
7. Shneider BL, Bosch J, de Franchis R, Emre SH, Groszmann RJ, Ling SC, et al; expert panel of the Children's Hospital of Pittsburgh of UPMC. Portal hypertension in children: expert pediatric opinion on the report of the Baveno V Consensus Workshop on Methodology of Diagnosis and Therapy in Portal Hypertension. Pediatr Transplant. 2012 Aug;16(5):426-37.
8. Colecchia A, Ravaioli F, Marasco G, Colli A, Dajti E, Di Biase AR, et al. A combined model based on spleen stiffness measurement and Baveno VI criteria to rule out high-risk varices in advanced chronic liver disease. J Hepatol. 2018 Aug;69(2):308-317.
9. Dietrich CF, Averkiou MA, Nielsen MB, et al. How to perform contrast-enhanced ultrasound (CEUS) in children. World J Gastroenterol. 2015;21:11393–11407.
10. Piscaglia F, Nolsoe C, Dietrich CF, et al. EFSUMB guidelines and recommendations on the clinical practice of CEUS. Ultraschall Med. 2012;33:33–59.
11. Riccabona M, Lobo ML, Augdal TA, Avni F, Blickman J, Bruno C, Damasio MB, Darge K, Mentzel HJ, Napolitano M, Ntoulia A, Papadopoulou F, Petit P, Woźniak MM, Ording-Müller LS. European Society of Paediatric Radiology Abdominal Imaging Task Force

recommendations in paediatric uroradiology, part X: how to perform paediatric gastrointestinal ultrasonography, use gadolinium as a contrast agent in children, follow up paediatric testicular microlithiasis, and an update on paediatric contrast-enhanced ultrasound. Pediatr Radiol. 2018 Sep;48(10):1528-1536.
12. European Society for Pediatric Gastroenterology, Hepatology and Nutrition (ESPGHAN); European Association for the Study of the Liver (EASL); North American Society for Pediatric Gastroenterology, Hepatology, and Nutrition (NASPGHAN); Latin-American Society for Pediatric Gastroenterology, Hepatology, and Nutrition (LASPGHAN); Asian Pan-Pacific Society for Pediatric Gastroenterology, Hepatology and Nutrition (APPSPGHAN); Pan Arab Society for Pediatric Gastroenterology and Nutrition (PASPGHAN); Commonwealth Association of Paediatric Gastroenterology & Nutrition (CAPGAN); Federation of International Societies of Pediatric Hepatology, Gastroenterology and Nutrition (FISPGHAN). Paediatric steatotic liver disease has unique characteristics: A multisociety statement endorsing the new nomenclature. J Pediatr Gastroenterol Nutr. 2024 May;78(5):1190-1196.
13. Ferraioli G, Calcaterra V, Lissandrin R, Guazzotti M, Maiocchi L, Tinelli C, et al. Noninvasive assessment of liver steatosis in children: the clinical value of controlled attenuation parameter. BMC Gastroenterol. 2017 May 4;17(1):61.
14 .Nightingale K. Acoustic Radiation Force Impulse imaging: a review. J Ultrasound Med. 2011;30:547–558.
15. European Association for the Study of the Liver. EASL Clinical Practice Guidelines on non-invasive tests for evaluation of liver disease severity and prognosis - 2021 update. J Hepatol. 2021 Sep;75(3):659-689
16. Dezsőfi A, Baumann U, Dhawan A, Durmaz O, Fischler B, Hadzic N et al; ESPGHAN Hepatology Committee. Liver biopsy in children: position paper of the ESPGHAN Hepatology Committee. J Pediatr Gastroenterol Nutr. 2015 Mar;60(3):408-20.
17. Rockey DC, Caldwell SH, Goodman ZD, et al. Liver biopsy. Hepatology. 2009 Mar;49(3):1017-44
18. Cao LL, Peng M, Xie X, Chen GQ, Huang SY, Wang JY et al. Artificial intelligence in liver ultrasound. World J Gastroenterol. 2022 Jul 21;28(27):3398-3409.
19. Karlas T, Petroff D, Sasso M, Fan JG, Mi YQ, de Lédinghen V, et al. Individual patient data meta-analysis of controlled attenuation parameter (CAP) technology for assessing steatosis. J Hepatol. 2017 May;66(5):1022-1030.
20. Caussy C, Brissot J, Singh S, Bassirian S, Hernandez C, Bettencourt R, et al. Prospective, Same-Day, Direct Comparison of Controlled Attenuation Parameter With the M vs the XL Probe in Patients With Nonalcoholic Fatty Liver Disease, Using Magnetic Resonance Imaging-Proton Density Fat Fraction as the Standard. Clin Gastroenterol Hepatol. 2020 Jul;18(8):1842-1850.e6.
21. Popescu A, Bende F, Sirli R, Sporea I. Redefining Diagnosis and Management in Hepatology with Multiparametric Ultrasound. EMJ Hepatol. 2025;13(1):66-75. https://doi.org/10.33590/emjhepatol/NTCU1425

9. Multiparametric Ultrasound for Focal Liver Lesions

9.1. B-mode evaluation for Focal Liver Lesions (FLL)

Mirela Dănilă, Ana-Maria Ghiuchici

Abstract

The increasing use of US (US) has led to more frequent detection of focal liver lesions (FLLs) in clinical practice. B-mode US is widely accessible and non-invasive, serving as the primary imaging modality for tissue characterization. Although most incidentally detected lesions are benign, malignant tumors can also be identified. Clinical history, risk factors, and precise B-mode pattern recognition are important for accurate diagnosis and management. This chapter discusses the US features of the most common FLLs encountered in clinical practice.

9.1.1. Introduction

The expansion of imaging methods, particularly US (US), has increased the frequency of liver tumor detection in medical practice. US is widely used to diagnose focal liver lesions (FLLs) because it is an inexpensive, non-invasive method for visualizing tissue characteristics.

The liver is a common site for tumors, including primary tumors originating within the liver and secondary tumors metastasizing from other cancers such as colon, breast, and lung cancers, among others.

Most FLLs are benign and incidentally discovered in asymptomatic patients; however, malignant tumors may also be detected incidentally, including in advanced stages, among patients presenting minor symptoms.

Risk factors for malignancy, including liver cirrhosis, hepatitis with severe fibrosis, or a history of malignancy, increase suspicion of a malignant tumor. Consequently, medical history and clinical examination are important steps in classifying FLLs detected by US. Subsequent contrast-enhanced examinations (CEUS, CT, or MRI) characterize the lesion and facilitate diagnosis. If these contrast examinations are inconclusive, biopsy and pathological analysis of the FLL provide a definitive diagnosis.

FLLs can be classified according to several analytical criteria:

- Nature of the lesion: benign or malignant.
- Echogenicity of tumors: cystic or solid.

• Tissue of origin: epithelial or mesenchymal.
• Cellular origin: hepatocytes or bile duct cells.
• Lesion type: primary or metastatic.

9.1.2. Benign focal liver lesions

1. Cystic lesions of the liver

a) Typical liver cysts.

A ***simple cyst***, also referred to as a ***biliary cyst***, is the most common type of liver cyst. These cysts are generally congenital, arising from an abnormal bile duct that fails to connect to the biliary tree, leading to the gradual accumulation of secretions. Hepatic cysts are estimated to affect 15-18% of the population (1, 2).

On US examination, simple cysts exhibit characteristic features including anechoic content, thin walls, round or oval shape, absence of intralesional septa, and posterior acoustic enhancement (Fig. 9.1.1; Fig. 9.1.2). This enhancement occurs due to higher transmission speed and lower attenuation of US waves as they pass from solid hepatic tissue into the cyst's fluid content. These cysts are typically single and unilocular, with multilocular forms being rare (Fig. 9.1.3 – Fig. 9.1.6). US demonstrates over 90% diagnostic accuracy for hepatic cysts and effectively distinguishes between simple and complex cysts (3, 4).

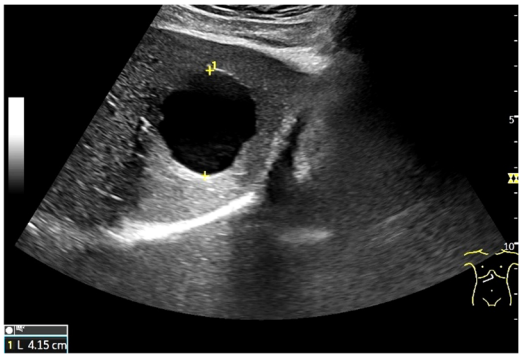


Figure 9.1.1. Biliary cyst - 4.15 cm anechoic lesion with thin, irregular walls and post-cystic enhancement.



Figure 9.1.2. Biliary cyst - 4 cm anechoic lesion with thin, irregular walls and post-cystic enhancement.

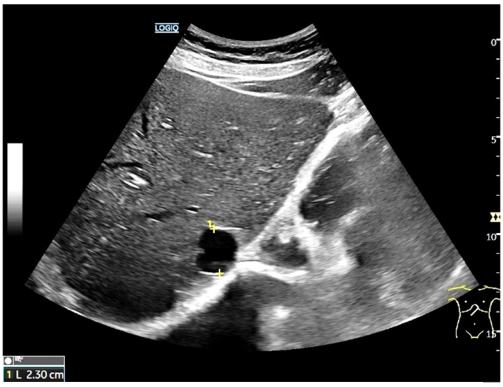


Figure 9.1.3. Biliary cyst - small anechoic lesion with thin, irregular wall.

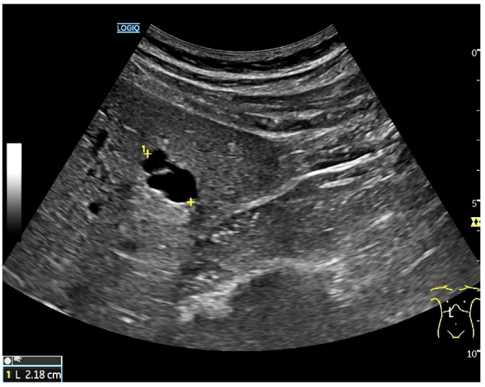


Figure 9.1.4. Biliary cyst - small anechoic lesion with thin, irregular walls.

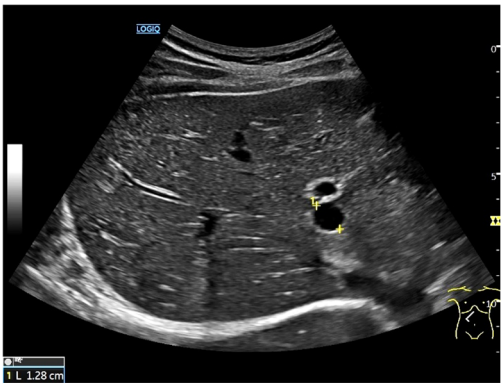


Figure 9.1.5. Small biliary cyst - anechoic lesion with thin walls and post-cystic enhancement next to the



Figure 9.1.6. Small biliary cyst - anechoic lesion with thin, irregular walls and post-cystic enhancement;

Most hepatic cysts measure less than 3 cm in diameter; however, some may exceed 30 cm. Large biliary cysts (Fig. 9.1.7; Fig. 9.1.8) are more likely to cause symptoms and complications, including spontaneous hemorrhage, infection, torsion of pedunculated cysts, rupture, or local biliary obstruction.

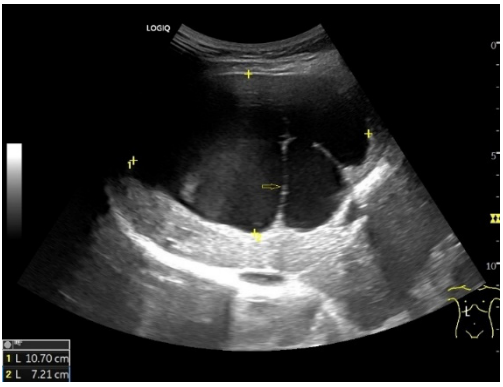


Figure 9.1.7. Giant biliary cyst - anechoic lesion with thin, irregular walls and thin septa.

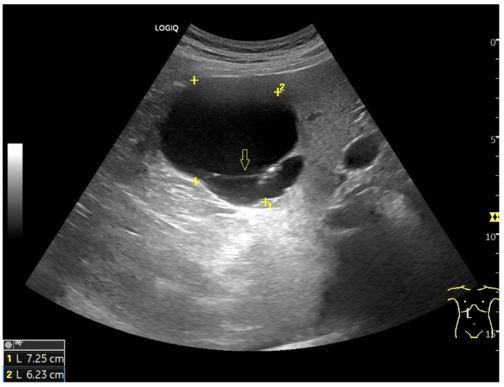


Figure 9.1.8. Biliary cyst - large anechoic lesion with thin, irregular walls and thin septa.

Simple cysts are typically incidental findings on US in asymptomatic patients, and no further follow-up is required after detection.

In patients presenting with multiple cysts, differential diagnosis should include polycystic liver disease, characterized by the presence of more than 20 cysts and frequently associated with polycystic kidney disease.

Atypical cystic lesions are characterized by features such as multiple or thick septa, calcifications, irregular walls, solid papillary projections, and echo-structural heterogeneity. Evaluation of these lesions requires contrast-enhanced imaging techniques.

Differential diagnosis of simple cysts is rarely necessary; however, other lesions with similar US appearances include liver abscesses, cystic liver metastases, and hydatid cyst type I.

b) Polycystic liver disease is a rare genetic disorder involving the presence of numerous cysts of varying sizes in the liver and kidneys. Isolated polycystic liver disease is extremely rare. Most cases are asymptomatic and detected during routine imaging. When symptoms occur, they typically result from pressure exerted by an enlarged liver on adjacent organs.

US examinations reveal multiple cystic liver lesions exhibiting characteristics similar to simple cysts, including anechoic content, thin walls, and round or oval shapes (Fig. 9.1.9 A, B).

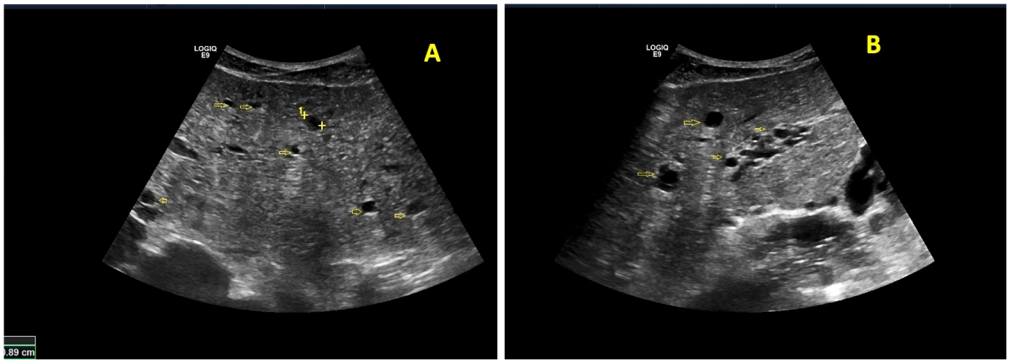


Figure 9.1.9 A, B. Polycystic liver. Multiple small anechoic lesions with thin, irregular walls are seen in the liver.

c) Hydatid cysts are typically caused by infection with the larval stage of the parasite Echinococcus granulosus. This parasite produces cystic lesions in organs such as the liver and lungs. Infection occurs through ingestion of water or food contaminated with eggs. These eggs release oncospheres that penetrate the intestinal wall, enter the portal system, and subsequently travel to the liver and other organs. Although echinococcosis can affect any organ, the liver and lungs are most commonly involved, accounting for 90% of cases.

Over a period of 5 to 20 years, the oncosphere can develop into a thick-walled hydatid cyst containing secondary cysts within the liver (5).

Patients are typically asymptomatic until cyst enlargement leads to complications. The onset of symptoms and complications depends on factors including cyst size, blood parasite levels, and cyst location.

US demonstrates a sensitivity of 90–95% for diagnosing liver hydatid cysts, with cyst appearance during scanning dependent on its developmental stage (6). Findings range from purely cystic to completely solid, allowing classification of liver hydatid cysts into six categories.

In 1994, the World Health Organization Informal Working Group on Echinococcosis (WHO-IWGE) proposed the development of a WHO-standardized US classification, which was adopted in 2003 (WHO-IWGE, 2003) and updated in 2010 (7, 8, 9). This classification is widely used alongside the Gharbi classification (10). Both are detailed in Tables 9.1.I and 9.1.II.

Table 9.1.I. US classification of hydatid cysts according to the WHO-IWGE

Stage	US Features	Key Characteristics	Activity
CE 1	Unilocular anechoic cyst with double line sign (Fig. 9.1.10; Fig. 9.1.11 - yellow arrow).	Simple cyst appearance.	Active
CE 2	Cyst with multiple internal septations (Fig. 9.1.11).	Septa represent walls of daughter cysts; multivesicular, rosette, or honeycomb appearance.	Active
CE 3A	Detached parasitic layers (Fig. 9.1.12).	Floating membranes (water-lily sign).	Active
CE 3B	Daughter cysts within a solid matrix (Fig. 9.1.13).	Predominantly solid with embedded daughter cysts.	Active
CE 4	Heterogeneous hypoechoic and hyperechoic contents (Fig. 9.1.14).	“Ball of wool” sign; absence of daughter cysts.	Inactive
CE 5	Thick solid and calcified wall (Fig. 9.1.15).	Heavily calcified cyst.	Inactive

Table 9.1.II. Gharbi Classification of Hydatid Cysts

Type	US Features	Key Characteristics / Description	Activity
Type I	Homogeneous anechoic fluid cyst with well-defined wall	Simple “rock-water” cyst appearance.	Active
Type II	Cyst with detached membrane	Fluid-filled cyst with separation of the parasitic membrane (endo-cyst) from the cyst wall.	Active
Type III	Multivesicular cyst	Contains daughter vesicles; “honeycomb” appearance	Active
Type IV	Pseudotumoral form	Non-homogeneous content; parenchymal or mixed (solid–liquid) appearance due to hydatid sand.	Transitional / degenerating
Type V	Calcified cyst	Thick calcified wall; inactive lesion.	Inactive

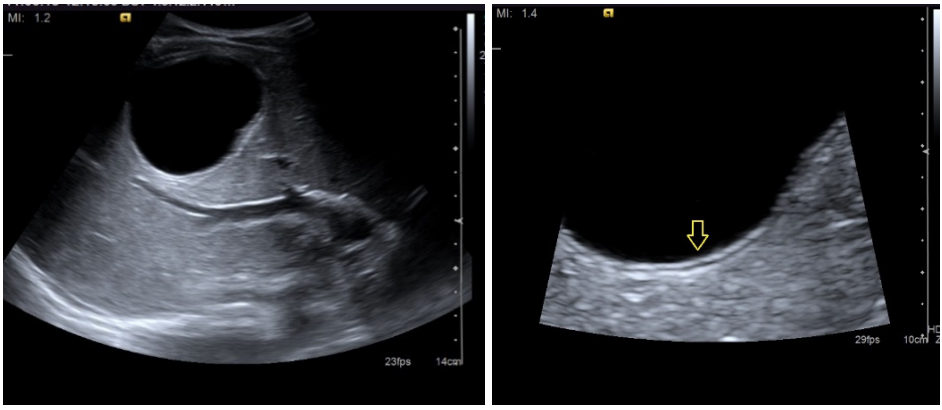


Figure 9.1.10 Hydatid cyst CE 1. Homogeneous anechoic fluid cyst with well-defined wall (double line sign – yellow arrow).

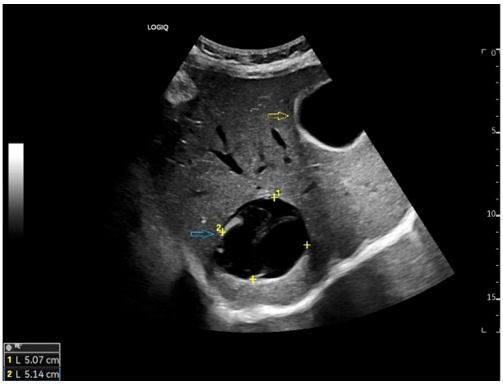


Figure 9.1.11. CE 1 Hydatid Cyst (yellow arrow) – anechoic content, thick walls; CE 2 Hydatid Cyst (blue arrow) – anechoic content, thick walls, and internal septations

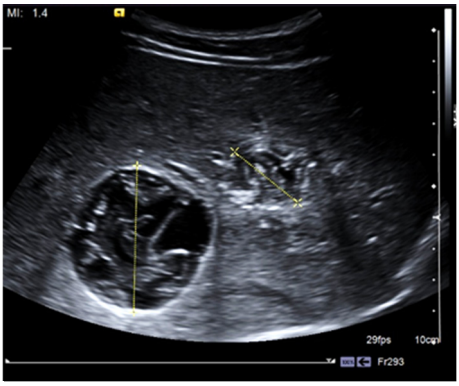


Figure 9.1.12. CE 3A Hydatid Cysts – an/hypoechoic content, thick walls, detached endomembrane "water-lily" sign

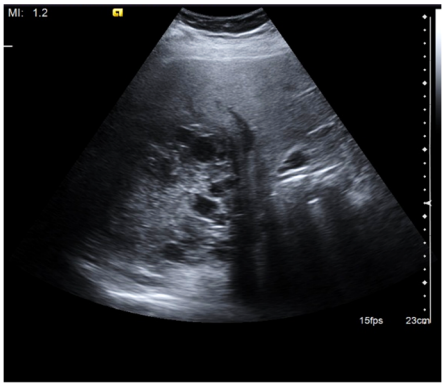


Figure 9.1.13. CE 3B Hydatid Cyst – daughter cysts within a solid matrix.

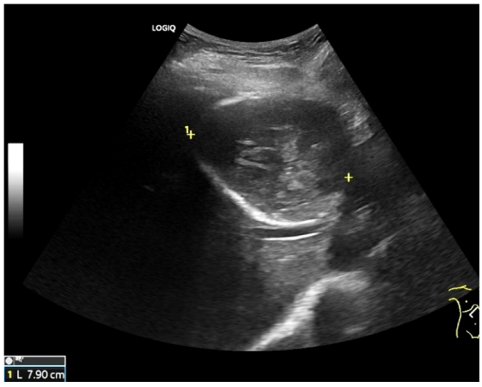


Figure 9.1.14. CE 4 Hydatid Cyst – heterogeneous hypo/hyperechoic contents, "ball of wool" sign; absence of daughter cysts

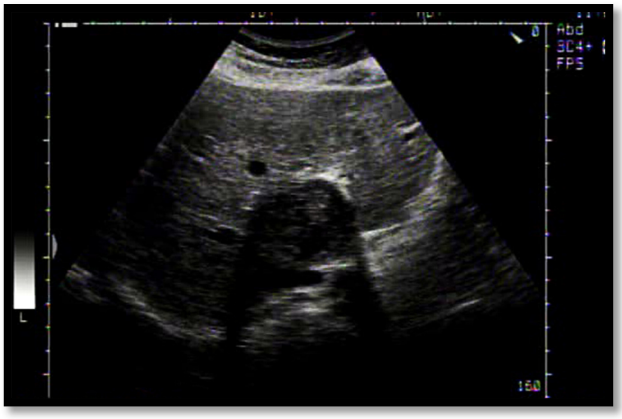


Figure 9.1.15. CE 5 Hydatid Cyst – thick solid and calcified wall

Diagnosis of hydatid cyst is established based on suggestive US imaging and detection of anti-echinococcus antibodies.

Active cysts require treatment to prevent complications, including infection, rupture, and mass effect on adjacent structures. Some complications are potentially life-threatening and necessitate prompt diagnosis and urgent intervention.

Rupture of hepatic hydatid cysts is a common complication. Minor leaks induce mild allergic reactions, whereas major ruptures can provoke full anaphylactic reactions, potentially fatal if untreated. In communicating ruptures, hydatid material may enter the bile ducts, causing obstruction, or spread into the peritoneal cavity or adjacent organs (11). An example of hydatid material in the biliary tract is shown in Fig. 9.1.16.

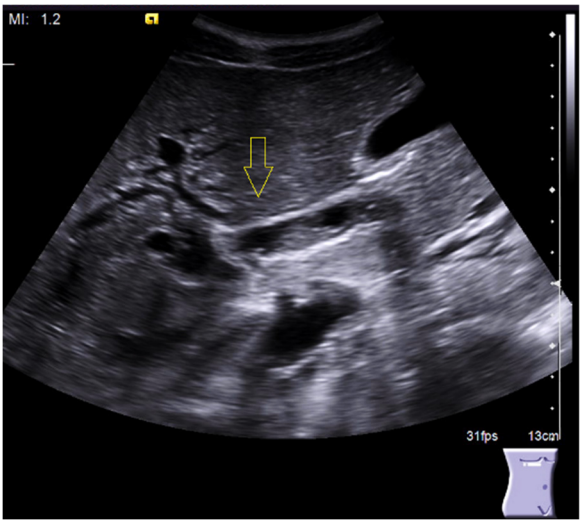


Figure 9.1.16. Communicating rupture – hydatid material in the common bile duct causing biliary obstruction.

WHO-IWGE experts recommend the following (7):

- CE1 and CE3a cysts larger than 5 cm must be treated with PAIR (percutaneous aspiration, injection, and re-aspiration), whereas smaller cysts may be managed with medical therapy alone (Albendazole or Mebendazole).
- For CE2 and CE3b parasitic cysts, surgery is the preferred treatment method compared to percutaneous or medical therapy.
- Follow-up is recommended for patients with asymptomatic or inactive parasitic cysts classified as stages CE4 or CE5.
- Surgical treatment is recommended for patients presenting with single or multiple complicated parasitic cysts.

d) Liver abscesses result from infections that destroy tissue, causing necrosis and pus accumulation in the liver. Although bacterial infections are the most common cause, fungal and parasitic infections can also lead to abscess formation.

Infections of the biliary tree, including cholangitis and cholecystitis, represent the most frequent cause of liver abscesses, accounting for 30–70% of cases (13).

Additional common causes include abdominal infections, such as diverticulitis or appendicitis, and distant infections disseminated via the bloodstream, such as pneumonia. The predominant bacterial species implicated in liver abscesses are Escherichia coli and Klebsiella pneumoniae.

On US examination, a liver abscess appears as an imprecisely defined lesion of variable size, which may be solitary or multiple. Echogenicity varies from hypoechoic to hyperechoic (Fig. 9.1.17; Fig. 9.1.18). Internal septa or cavitary debris may be observed. An anechoic component indicates the need for drainage or aspiration.

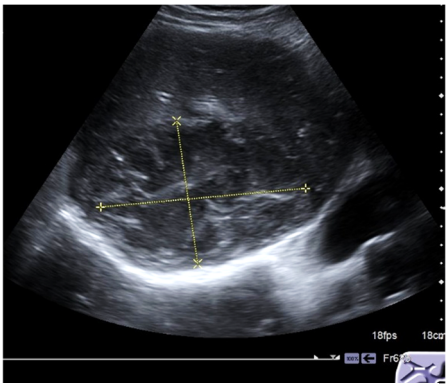


Figure 9.1.17. Liver abscess - heterogeneous hypoechoic, poorly delineated lesion, with small areas of anechoic content

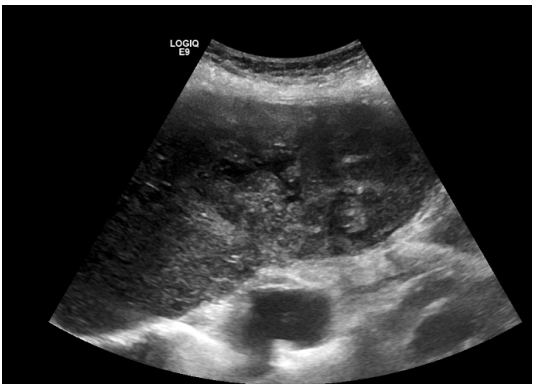


Figure 9.1.18. Liver abscess – heterogeneous hypo/hyperechoic, poorly delineated lesion, with small areas of anechoic content

Suspicion of a liver abscess arises when a hepatic mass is identified in conjunction with symptoms including abdominal pain, fever, chills, and abnormal laboratory findings such as leukocytosis and elevated inflammatory markers (e.g., ESR, fibrinogen, and CRP).

US is typically the preferred imaging modality for diagnosing liver abscesses, demonstrating a sensitivity of 85%, while computed tomography offers a higher sensitivity of 97% (14, 15).

Management of liver abscesses involves antibiotic therapy combined with US- or CT-guided drainage. Surgical drainage is indicated only when percutaneous drainage is not feasible. US-guided aspiration is essential for definitive diagnosis and to guide targeted antibiotic treatment.

Small abscesses measuring 3-4 cm or less (Fig. 9.1.19; Fig. 9.1.20) may be managed solely with antibiotic therapy. In contrast, abscesses exceeding 5 cm are preferably treated with catheter drainage rather than percutaneous aspiration, owing to a significantly higher success rate (100% versus 68%) (16).

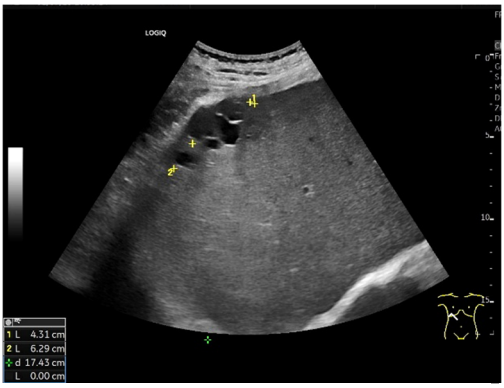


Figure 9.1.19. Small liver abscess - anechoic, poorly delineated lesion with septa



Figure 9.1.20. Small liver abscess - hyperchoic, poorly delineated lesion, with small areas of anechoic content

e) Liver hematoma refers to a collection of blood within the liver parenchyma.

The primary causes of hepatic hematoma include:

- Trauma: due to its relative inelasticity and extensive vascularization, the liver is susceptible to injury during severe trauma.
- Iatrogenic causes: US-guided interventional procedures, including liver biopsies and percutaneous therapies, as well as surgical interventions, may result in vascular injury.
- Liver tumors complicated by hemorrhage.
- Coagulopathies.

Hepatic hematoma is suspected when a hepatic lesion is identified in patients exhibiting signs of hemorrhagic shock following trauma or medical procedures. Alternatively, it may be detected in patients presenting with right hypochondrial pain or in asymptomatic individuals.

The US appearance of a hepatic hematoma varies with the timing of diagnosis. An acute hematoma initially appears hyperechoic and homogeneous. Subsequent US examinations reveal changes in size and echotexture, with the hematoma becoming hypoechoic and inhomogeneous over time (Fig. 9.1.21). Chronic hematomas may present as cystic lesions on US (17).

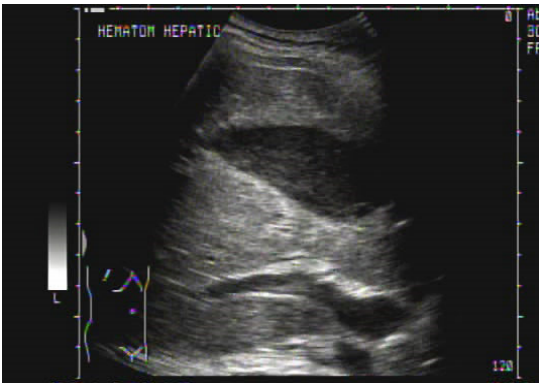


Figure 9.1.21. Liver hematoma: hypoechoic inhomogeneous lesion inside the liver parenchyma in a patient who underwent liver biopsy 24 hours prior.

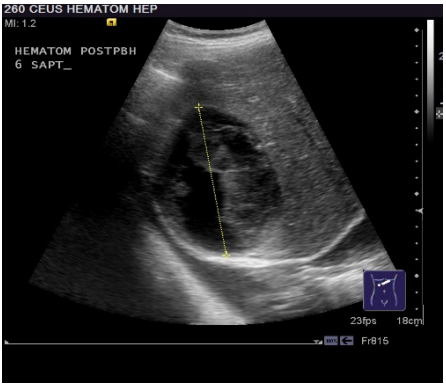


Figure 9.1.22. Liver hematoma: hypo/hyperechoic inhomogeneous lesion inside the liver parenchyma in a patient who underwent liver biopsy 6 weeks prior.

2. Solid lesions of the liver

a) Hemangiomas represent the most common benign liver tumors. They originate from mesenchymal vascular tissue and consist of blood-filled cavities lined by endothelial cells.

The prevalence of hemangiomas ranges from 0.4% to 20% in autopsy studies and from 2.5% to 5.1% in literature reviews. These lesions occur more frequently in women than in men, with a female-to-male ratio of 4 to 6:1 (18, 19, 20). Hepatic hemangiomas are typically small, measuring less than 3 cm, and may be solitary or multiple. Larger lesions can cause symptoms and complications related to compression.

Hepatic hemangiomas are classified into three primary histological subtypes: cavernous hemangioma, capillary hemangioma (also termed 'flash-filling' hemangioma), and sclerosed hemangioma.

Standard US is frequently the initial imaging modality for detecting hemangiomas. In certain cases, this technique suffices to confirm the diagnosis without additional imaging.

On US, hepatic hemangiomas typically appear as homogeneous, well-defined, hyperechoic lesions with posterior acoustic enhancement, ranging in size (Fig. 9.1.22 – 9.1.25). Color Doppler imaging reveals no vascular pattern within these lesions.

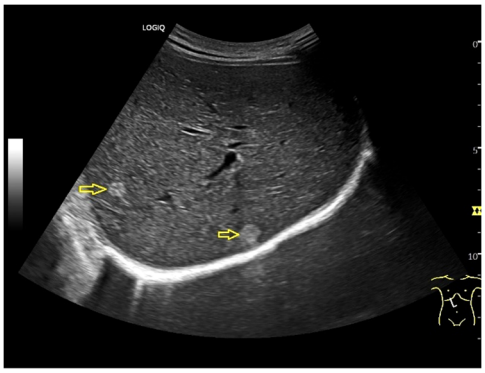


Figure 9.1.22. Typical small hemangiomas – B-mode US: hyperechoic, well delineated, homogeneous lesions.

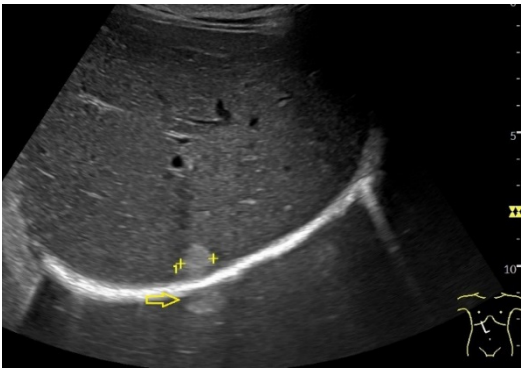


Figure 9.1.23. Typical hemangioma – small hyperechoic, well delineated, homogeneous subdiaphragmatic lesion, "mirror effect" (yellow arrow)

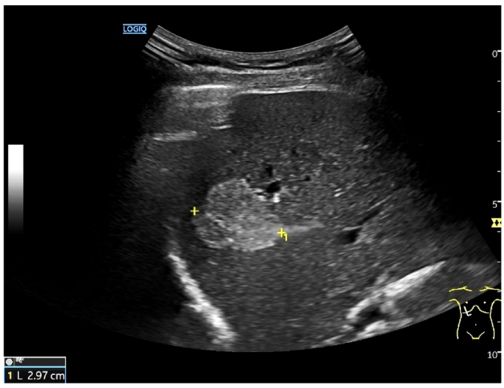


Fig. 9.1.24. Typical hemangioma – 3cm hyperechoic, well delineated, homogeneous lesion

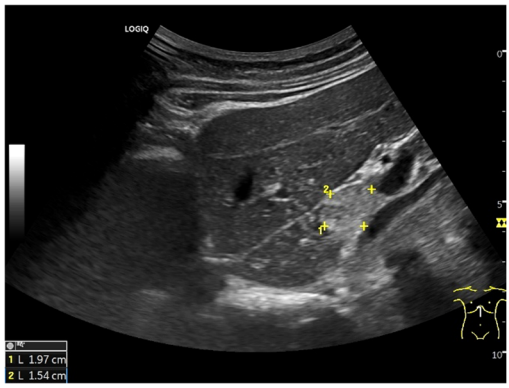


Fig. 9.1.25. Typical hemangioma – 2cm hyperechoic, well delineated, homogeneous lesion in the caudate lobe

Large hemangiomas may exhibit atypical US features, including heterogeneous echotexture. In such cases, second-level imaging modalities—contrast-enhanced US (CEUS), enhanced MRI, or CT—are required for characterization (Fig. 9.1.26; Fig. 9.1.27). These modalities are also necessary for hemangiomas identified in patients with a history of cancer or chronic liver disease.

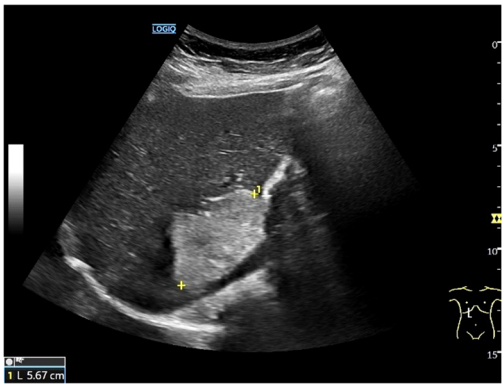


Fig. 9.1.26. Typical hemangioma – hyperechoic, well delineated, omogeneous lesion, > 3 cm in diameter. Posterior enhancement is visible.

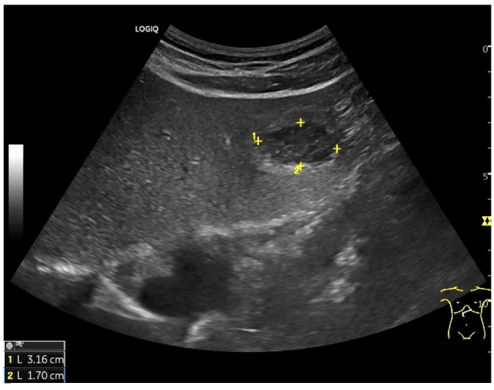


Fig. 9.1.27. Atypical hemangioma – 3.2 cm hypoechoic, well delineated, homogeneous lesion.

Management of hemangiomas is generally conservative. Routine monitoring is unnecessary for typical hemangiomas unless they coexist with chronic liver disease or associated malignant pathology. Biopsy of suspected hemangiomas should be avoided, when possible, because of the risk of bleeding. Surgical intervention is indicated for hemangiomas complicated by intralesional hemorrhage, rupture, or compression symptoms, especially in large lesions.

b) Focal nodular hyperplasia (FNH) is the second most common benign liver tumor, with an estimated prevalence of 0.3–3% in autopsy studies (20).

FNH is a pseudotumor resulting from a hyperplastic reaction to a vascular malformation, typically secondary to an aberrant dystrophic artery or vascular lesion that disrupts local blood flow.

Although FNH occurs more frequently in women than men, no confirmed association with sex hormone consumption exists, unlike hepatic adenomas (21). Due to the absence of this correlation, monitoring FNH during pregnancy is unnecessary, in contrast to hepatic adenomas.

Consequently, differentiating FNH from hepatic adenoma is essential in clinical practice and can be achieved using contrast-enhanced imaging. When imaging is inconclusive, a biopsy may be required for definitive diagnosis.

FNH exhibits variable B-mode US appearances, typically presenting as slightly hypoechoic or isoechoic lesions; hyperechoic presentations are rare. A central scar is visible in up to one-third of cases, aiding diagnosis. Color Doppler imaging demonstrates the lesion's hypervascularity with central vascularity (Fig. 9.1.28 -9.1.33).



Fig. 9.1.28. Isoechoic, slightly hypoechoic FNH – – deforming the middle hepatic vein.

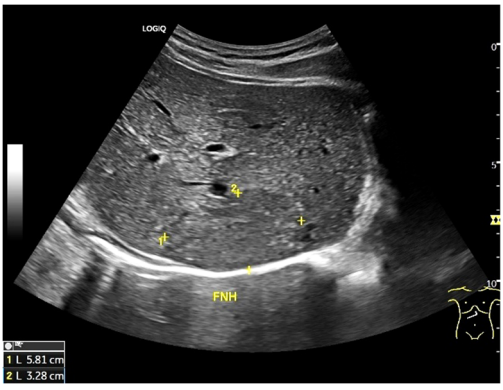


Fig. 9.1.29. Isoechoic, slightly hypoechoic 6 cm FNH in the right liver lobe.

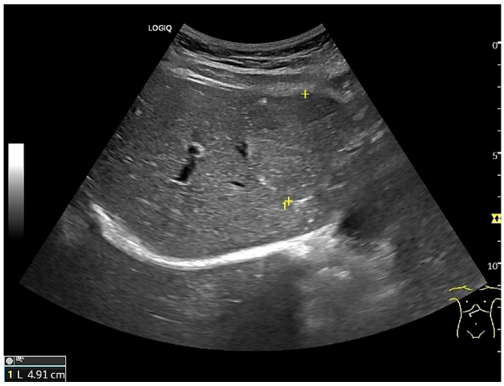


Fig. 9.1.30. Isoechoic FNH.

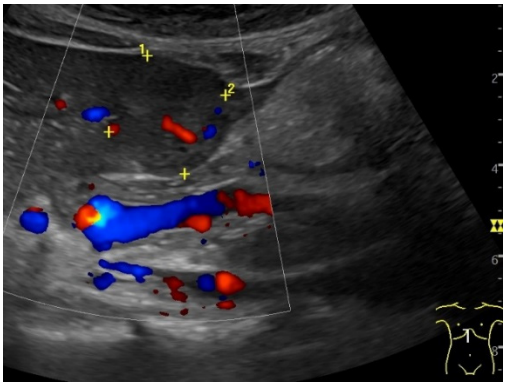


Fig. 9.1.31. Isoechoic FNH – color Doppler "spoke wheel" pattern; feeding artery visible.

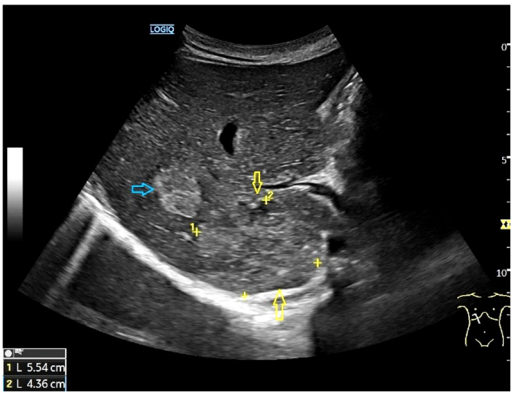


Fig. 9.1.32. Isoechoic FNH (yellow arrow); typical hepatic hemangioma – 4.3 cm hyperechoic, well delineated lesion (blue arrow).

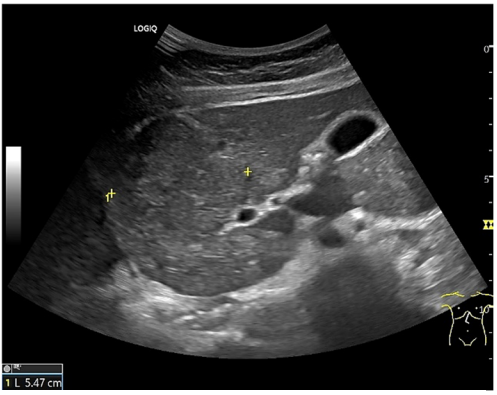


Fig. 9.1.33. Large isoechoic FNH.

c) Hepatocellular adenoma **(HCA)** is the third most common benign hepatic neoplasm, with a prevalence of approximately 0.007% to 0.012% (22). It is predominantly diagnosed in women under 50 years and is associated with oral contraceptive use. In men, liver adenomas may be linked to anabolic steroid use.

Additional risk factors for adenoma development include glycogen storage diseases, obesity, metabolic syndrome, and diabetes mellitus.

Hepatic adenomas are typically solitary; however, multiple lesions occur in up to 30% of patients.

On B-mode US, adenomas generally appear as isoechoic lesions (Fig. 9.1.34) relative to the surrounding parenchyma. In patients with steatosis and hyperechoic liver parenchyma, adenomas may present as hypoechoic (Fig. 9.1.35).

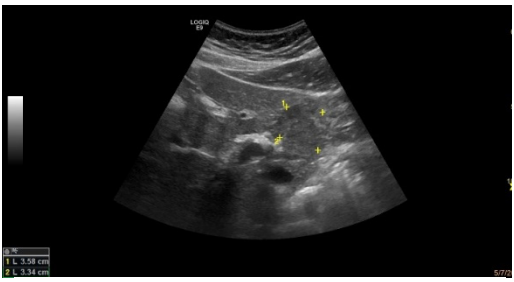


Fig. 9.1.34. Hepatic adenoma- isoechoic lesion in the left liver lobe



Fig. 9.1.35. Liver steatosis; hepatic adenoma- hypoechoic lesion.

Tumors exceeding 5 cm may exhibit altered appearances due to hemorrhage, necrosis, or fibrosis, resulting in inhomogeneity. Progressive imaging changes may indicate malignant transformation, warranting biopsy and histopathological evaluation.

Color Doppler imaging typically demonstrates a homogeneous vascular distribution predominantly at the periphery, contrasting with the central vascularity observed in FNH.

Adenomas are associated with an elevated risk of hemorrhage and/or malignant transformation.

Management of hepatocellular adenomas (HCAs) may be conservative for patients with small, asymptomatic lesions. Complication risk depends on lesion size, sex, and clinical and molecular subtypes.

Asymptomatic HCAs in females measuring less than 5 cm can be managed conservatively unless imaging suggests a β-catenin-mutated subtype, which is less frequently associated with complications such as hemorrhage or malignancy (23). Discontinuation of exogenous hormonal therapy is recommended (24).

β-catenin-mutated HCAs have a higher risk of malignant transformation compared to other subtypes and should be resected regardless of size.

Females with adenomas larger than 5 cm should be monitored for six months and discontinue exogenous hormone use (25).

Hepatic adenomas in men are frequently β-catenin-mutated and carry a higher risk of malignant transformation. Consequently, curative treatment, including resection or ablation, is recommended regardless of tumor size or subtype (25, 26).

d) Focal fatty alterations

Focal fatty alterations, including fatty infiltration (Fig. 9.1.36) and focal sparing (Fig. 9.1.37), may present as well-defined lesions mimicking tumors. These alterations are typically benign and associated with conditions such as diabetes, obesity, and dyslipidemia.

These focal liver lesions exhibit a geographic pattern on US and are commonly located adjacent to the gallbladder, portal vein bifurcation, falciform ligament, and subcapsular parenchyma.



Fig. 9.1.36. Focal fatty infiltration - hyperechoic area with neat, map-line delineation



Fig. 9.1.37. Focal fatty sparing - triangular hypoechoic area with neat, map-line delineation.

Other rare benign liver tumors

Biliary hamartomas**,** or von Meyenburg complexes, are bile duct malformations appearing as multiple small cystic lesions on US. They are often incidental findings and may be associated with Caroli's disease.

Other ***rare benign liver tumors***, including angiomyolipoma, mesenchymal hamartoma, hepatic lipoma, and solitary fibrous tumor of the liver, lack characteristic US features. Management is determined on a case-by-case basis.

9.1.3. Malignant focal liver lesion

The liver is a frequent site for both primary and secondary (metastatic) malignant tumors. Consequently, liver tumors are classified as either primary or secondary.

Primary malignant liver tumors may arise from any hepatic cell type; however, the most common are hepatocellular carcinoma, originating from hepatocytes, and cholangiocarcinoma, arising from the epithelial cells of the bile ducts.

a) Hepatocellular carcinoma

Hepatocellular carcinoma (HCC) is the most common primary malignant liver tumor, representing up to 90% of cases. It typically develops in the context of liver cirrhosis of various etiologies or severe hepatic fibrosis.

Accordingly, clinical guidelines recommend surveillance of at-risk patients to enable early detection of HCC at stages amenable to curative treatment.

Details regarding HCC screening are presented in a separate chapter.

US frequently serves as the initial imaging modality to raise the suspicion of hepatocellular HCC, especially in patients with advanced liver disease undergoing surveillance. In individuals without prior liver disease, HCC suspicion arises when US identifies a solitary liver mass accompanied by signs of cirrhosis, including liver heterogeneity, irregular liver surface, or caudate lobe enlargement.

The US appearance of hepatocellular carcinoma varies with lesion size and the echogenicity of adjacent liver tissue. Small nodules under 3 cm typically appear hypoechoic, while larger nodules display heterogeneous echotexture (Fig. 9.1.38 - 9.1.41). Hyperechoic presentations may also occur (Fig. 9.1.42; Fig. 9.1.44; Fig. 9.1.47). HCC lesions are generally well-defined, occasionally surrounded by a thin hypoechoic rim indicative of a capsule. Typically solitary, but multiple nodules can also be observed (Fig. 9.1.46).

Additional US features suggestive of HCC include a mosaic pattern within the liver nodule and a nodule-in-nodule appearance (Fig. 9.1.43), which is more evident on contrast-enhanced US (27).

Moribana et al. classified hepatocellular carcinoma (HCC) into two types based on halo presence: type 1 nodules with halos and type 2 nodules without halos. Type 2 nodules are further subdivided into 2a, 2b, and 2c subtypes (28), distinguished by echogenicity and margin definition. Malignant potential progressively increases across these subtypes.

On Doppler US, HCC appears as a hypervascular tumor exhibiting a characteristic basket pattern on color Doppler imaging.

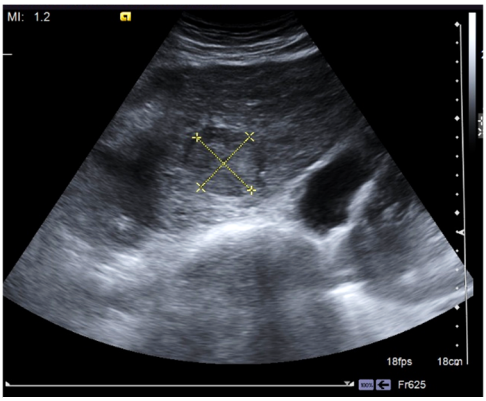


Fig. 9.1.38. Conventional B-mode US: slightly hyperechoic HCC nodule.

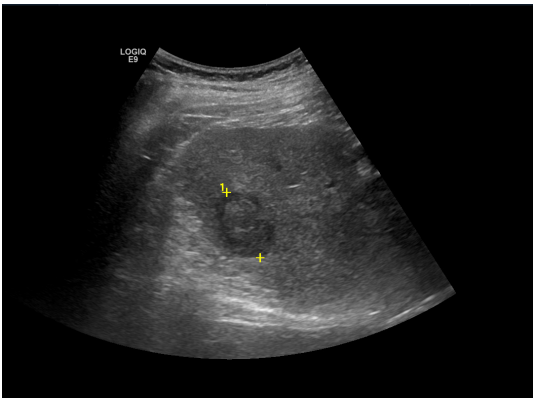


Fig. 9.1.39. Conventional B-mode US: hypoechoic HCC nodule.

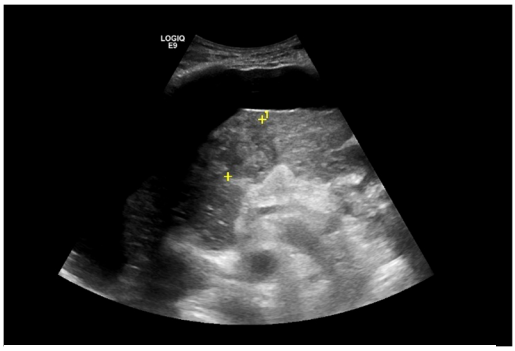


Fig. 9.1.40. Conventional B-mode US: hypoechoic 3 cm HCC in a patient with liver cirrhosis and ascites.

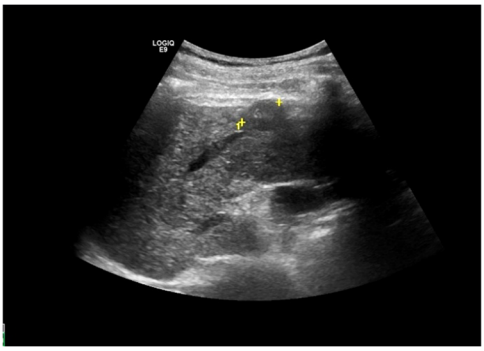


Fig. 9.1.41. Conventional B-mode US: hypoechoic 1.8 cm HCC in a patient with liver cirrhosis.

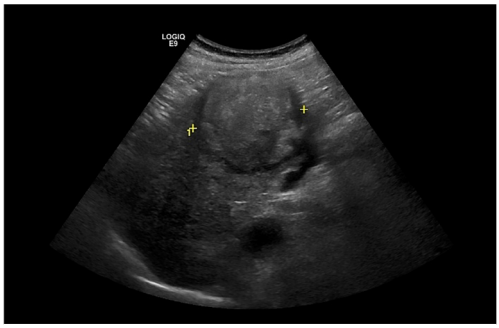


Fig. 9.1.42. Conventional B-mode US: slightly hyperechoic 6 cm HCC nodule with halo in a patient with liver cirrhosis.

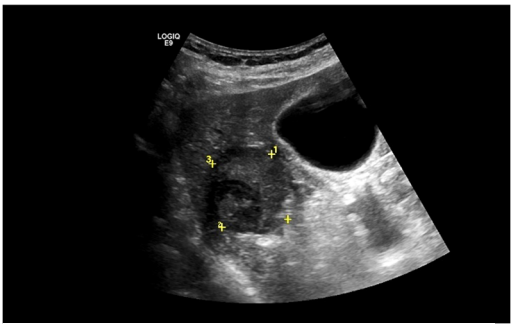


Fig. 9.1.43. Conventional B-mode US: hypoechoic 4.5 cm HCC in a patient with liver cirrhosis; nodule-in-nodule appearance.

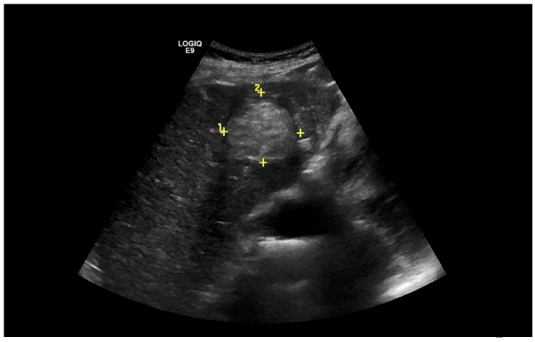


Fig. 9.1.44. Conventional B-mode US: hyperechoic HCC nodule.



Fig. 9.1.45. Conventional B-mode US: hypoechoic HCC nodule in a patient with liver cirrhosis; heterogeneous liver structure.

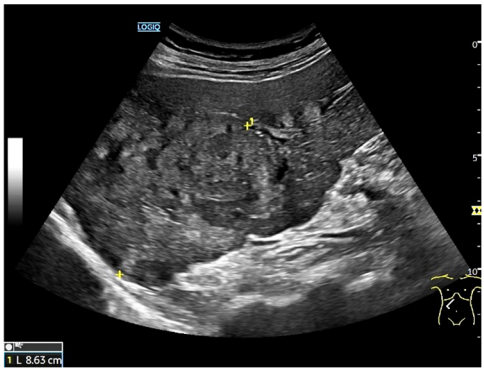


Fig. 9.1.46. Conventional B-mode US - large heterogeneous multicentric HCC.

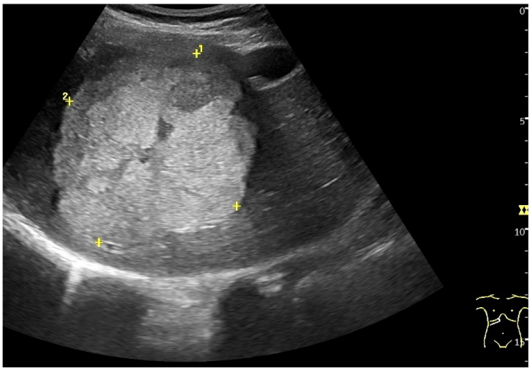


Fig. 9.1.47. Conventional B-mode US: hyperechoic, slightly inhomogeneous large HCC nodule.

Vascular invasion is common in HCC, with portal vein tumor thrombosis (PVTT) the most common form of macrovascular invasion. It is essential to assess the port system in patients with hepatocellular carcinoma (HCC) in order to rule out portal vein thrombosis, which is a common complication with a significant impact on prognosis.

b) Cholangiocarcinoma (CCA) is the second most common primary liver cancer, though considerably less prevalent than hepatocellular carcinoma (29). It arises from the biliary epithelium and may develop anywhere along the biliary tract, from intrahepatic bile ducts to the ampulla of Vater. Anatomically, CCA is classified into three types: perihilar (pCCA), the most frequent form comprising 50–60% of cases; intrahepatic (iCCA), representing 10% of cases; and distal (dCCA) (29, 30).

The US appearance of cholangiocarcinoma varies according to tumor type and location. Perihilar and distal CCAs are typically small tumors often not visualized on US; however, they induce dilation of intrahepatic bile ducts in perihilar CCA and dilation of both intrahepatic and extrahepatic bile ducts in distal CCA.

In certain cases, intraductal polypoid tumors or bile duct wall thickening may be observed alongside bile duct dilation.

US has a sensitivity of 87%–96% for detecting ductal masses or wall thickening in hilar and extrahepatic cholangiocarcinoma, but this depends on the operator's expertise (31, 32).

An intrahepatic CCA is typically characterized by an intrahepatic mass that exhibits variable echogenicity, often hypoechoic. These masses can vary in size and are more or less clearly delineated. The US appearance of CCA is usually indistinguishable from other liver lesions, such as HCC or liver metastases (Fig. 9.1.48 - 9.1.50).

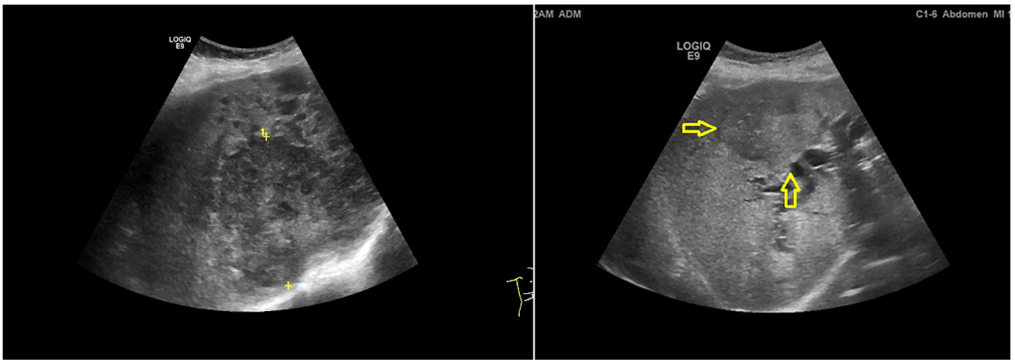


Fig. 9.1.48. iCCA and small liver metastases -hyperechoic, irregular, large liver mass; multiple small hypoechoic liver lesions.

Fig. 9.1.49. iCCA - 7 cm slightly hyperechoic liver lesion causing biliary obstruction.



Fig. 9.1.50. Biopsy-proven iCCA - large liver mass slightly hypoechoic in conventional US B-mode.

c) Liver metastases represent the most common liver malignancy and frequently originate from colorectal, gastric, pancreatic, lung, and breast cancers. They may also arise from neuroendocrine tumors, gastrointestinal stromal tumors, renal cell carcinomas, and lymphomas.

Liver metastases exhibit considerable variability in echogenicity and number. They are typically multiple but may present as solitary lesions. Occasionally, metastases manifest as diffuse, irregular hepatic texture rather than discrete masses.

The echogenicity of liver metastases varies and may suggest the primary tumor type. Hyperechoic metastases (Fig. 9.1.51) are more frequently associated with gastrointestinal cancers, renal cell carcinoma, carcinoid tumors, choriocarcinoma, pancreatic islet cell tumors, leukemia, and AIDS-associated Kaposi's sarcoma (33).



Fig. 9.1.51. Liver metastases. Conventional US B-mode: multiple hyperechoic focal liver lesions with hyperechoic halo.

Hypoechoic metastases (Fig. 9.1.52 – 9.1.54) may arise from various cancers but are particularly common in lymphomas, melanomas, and carcinomas of the pancreas, lung, and cervix.

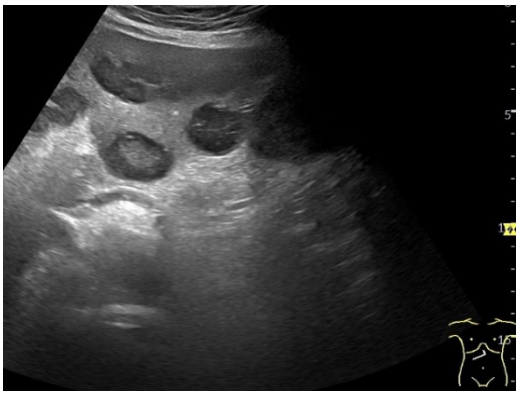


Fig. 9.1.52. Liver metastases. Conventional US B-mode: multiple hypoechoic focal liver lesions

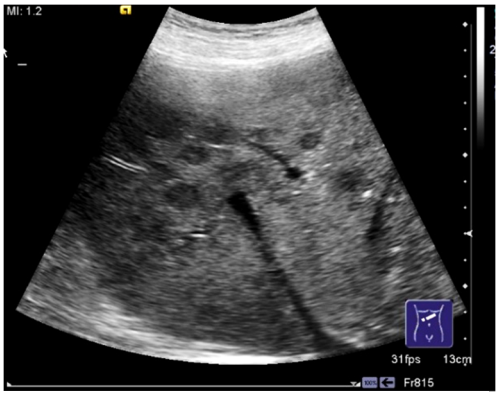


Fig. 9.1.53. Liver metastases. Conventional US B-mode: multiple hypoechoic small focal liver lesions



Fig. 9.1.54. Multiple confluent liver metastases in a patient diagnosed with pancreatic cancer.

Isoechoic and infiltrative metastases are poorly defined and challenging to detect. They may be suspected when adjacent structures are compressed or when alterations in liver contour are observed.

The most characteristic ultrasonographic appearance of metastases is the bull's eye or target pattern. Such metastases occur in bronchogenic carcinoma, breast and colon cancers, and primary malignant liver neoplasms such as HCC.

Cystic metastases (Fig. 9.1.55) are rare and typically arise from cancers with cystic components, such as cystadenocarcinomas. Differential diagnosis is necessary to distinguish these metastases from other cystic liver lesions, including abscesses, hematomas, simple cysts, and hydatid cysts. Clinical context often aids in diagnosis.



Fig. 9.1.55. Multiple cystic metastases.

Other malignant primary liver lesions

Hepatic epithelioid hemangioendothelioma (HEH) is a rare liver cancer originating from vascular endothelial cells. US typically reveals a hypoechoic tumor associated with liver capsule retraction (Fig. 9.1.56).

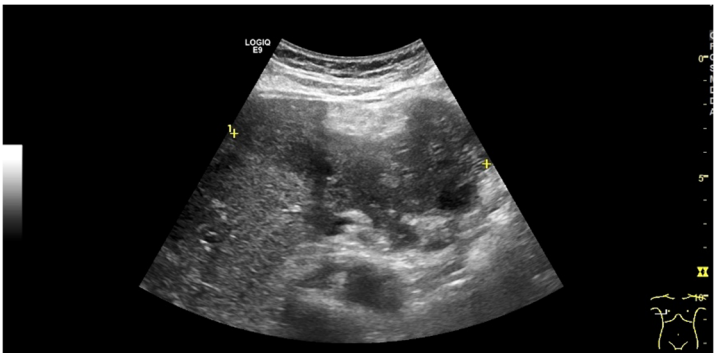


Fig. 9.1.56. Hepatic epithelioid hemangioendothelioma. US B-mode - 10 cm hypoechoic liver lesion with mixed echotexture located in the left hepatic lobe, accompanied by retraction of the liver capsule at this site.

Fibrolamellar hepatocellular carcinoma is a rare primary liver cancer subtype, constituting less than 1% of all primary liver tumors (34). This type of hepatocellular carcinoma typically affects young patients with no history of liver disease.

References

1. Marrero JA, Ahn J, Rajender Reddy K, American College of Gastroenterology. ACG clinical guideline: the diagnosis and management of focal liver lesions. Am J Gastroenterol 2014; 109:1328e47.
2. Lantinga MA, Gevers TJG, Drenth JPH. Evaluation of hepatic cystic lesions. World J Gastroenterol 2013; 19: 3543e54.
3. Lantinga MA, Gevers TJ, Drenth JP. Evaluation of hepatic cystic lesions. World J Gastroenterol 2013;19(23):3543–54.
4. Mavilia MG, Pakala T, Molina M, Wu GY. Differentiating cystic liver lesions: a Review of imaging modalities, diagnosis and management. J Clin Transl Hepatol 2018;6(2):208–16
5. Agudelo Higuita NI, Brunetti E, McCloskey C. Cystic echinococcosis. J Clin Microbiol 2016; 54: 518e23.
6. Dhar P, Chaudhary A, Desai R, Agarwal A, Sachdev A. Current trends in the diagnosis and management of cystic hydatid disease of the liver. J Commun Dis 1996 28:221–230.
7. Group WIW (2003) International classification of ultrasound images in cystic echinococcosis for application in clinical and field epidemiological settings. Acta Trop 85:253.
8. Brunetti E, Kern P, Vuitton D. Expert Consensus for the Diagnosis and Treatment of Cystic and Alveolar Echinococcosis in Humans. Acta Trop. 2010;114(1):1-16.
9. Mirabile E, Solomon N, Fields P, Macpherson C. Progress Towards International Adoption of the World Health Organization Ultrasound Classification of Cystic Echinococcosis. Acta Trop. 2019;189:6.
10. Gharbi H, Hassine W, Brauner M, Dupuch K. Ultrasound Examination of the Hydatic Liver. Radiology. 1981;139(2):459-63.
11. Vidili G, De Sio I, D'Onofrio M, Mirk P, Bertolotto M, Schiavone C. SIUMB experts committee. SIUMB guidelines and recommendations for the correct use of ultrasound in the management of patients with focal liver disease. J Ultrasound. 2019 Mar;22(1):41-51.

12. Pompili M, Ardito F, Brunetti E, Cabibbo G, Calliada F, Cillo U, et al. Benign liver lesions 2022: Guideline for clinical practice of Associazione Italiana Studio del Fegato (AISF), Società Italiana di Radiologia Medica e Interventistica (SIRM), Società Italiana di Chirurgia (SIC), Società Italiana di Ultrasonologia in Medicina e Biologia (SIUMB), Associazione Italiana di Chirurgia Epatobilio-Pancreatica (AICEP), Società Italiana Trapianti d'Organo (SITO), Società Italiana di Anatomia Patologica e Citologia Diagnostica (SIAPEC-IAP) - Part I - Cystic lesions. Dig Liver Dis. 2022 Nov;54(11):1469-1478.
13. Khim G, Em S, Mo S, Townell N: Liver abscess: diagnostic and management issues found in the low resource setting. British Medical Bulletin 2019;132(1):45–52.
14. Halvorsen RA, Korobkin M, Foster WL, Silverman PM, Thompson WM. The variable CT appearance of hepatic abscesses. Am J Roentgenol 1984;142(05):941–946.
15. Lee NK, Kim S, Lee JW, et al. CT differentiation of pyogenic liver abscesses caused by Klebsiella pneumoniae vs non-Klebsiella pneumoniae. Br J Radiol 2011;84(1002):518–525 16.
16. Kumar R, Ranjan A, Narayan R, Priyadarshi RN, Anand U Shalimar. Evidence-based therapeutic dilemma in the management of uncomplicated amebic liver abscess: A systematic review and meta-analysis. Indian J Gastroenterol 2019;38(06):498–508.
17. A. Manenti, L. Roncati, G. Manco, A. Farinetti, F. Coppi. Hepatic hematoma: A challenging, emergency disease. Surgery Open Digestive Advance Volume 10, June 2023, 100084.
18. Mocchegiani F, Vincenzi P, Coletta M, Agostini A, Marzioni M, Baroni GS, et al. Prevalence and clinical outcome of hepatic haemangioma with specific reference to the risk of rupture: A large retrospective cross-sectional study. *Dig Liver Dis*. 2016 Mar. 48 (3):309-14.
19. Horta G, López M, Dotte A, Chesta C, Castro A, Palavecino P, et al. Benign focal liver lesions detected by computed tomography: review of 1,184 examinations. *Rev Med Chil*. 2015 Feb. 143 (2):197-202.
20. Vilgrain V, Uzan F, Brancatelli G, Federle MP, Zappa M, Menu Y, et al. Prevalence of hepatic hemangioma in patients with focal nodular hyperplasia: MR imaging analysis. Radiology 2003;229(1):75–9.
21. Wanless IR, Albrecht S, Bilbao J, Frei JV, Heathcote EJ, Roberts EA, et al. Multiple focal nodular hyperplasia of the liver associated with vascular malformations of various organs and neoplasia of the brain: A new syndrome. Mod Pathol 1989;2(5):456–62.
22. Rooks JB, Ory HW, Ishak KG, Strauss LT, Greenspan JR, Hill AP, et al. Epidemiology of hepatocellular adenoma. The role of oral contraceptive use. JAMA 1979;242(7):644–8.
23. van der Windt DJ, Kok NF, Hussain SM, Zondervan PE, Alwayn IP, de Man RA, et al. Case-orientated approach to the management of hepatocellular adenoma. Br J Surg 2006;93(12):1495–502.

24. B¨uhler H, Pirovino M, Akobiantz A, Altorfer J, Weitzel M, Maranta, et al. Regression of liver cell adenoma. A follow-up study of three consecutive patients after discontinuation of oral contraceptive use. Gastroenterology 1982;82(4):775–82.
25. Frenette C, Mendiratta-Lala M, Salgia R, Wong RJ, Sauer BG, Pillai A. ACG Clinical Guideline: Focal Liver Lesions. Am J Gastroenterol. 2024 Jul 1;119(7):1235-1271.
26. Farges O, Ferreira N, Dokmak S, Belghiti J, Bedossa P, Paradis V, et al. Changing trends in malignant transformation of hepatocellular adenoma. Gut 2011;60(1):85–9.
27. Kim WK, Meyer A, Möllmann H, Rolf A, Möllmann S, Blumenstein J, et al. Cyclic changes in area- and perimeter-derived effective dimensions of the aortic annulus measured with multislice computed tomography and comparison with metric intraoperative sizing. Clin Res Cardiol 2016;105(7):622-62.
28. Moribata K, Tamai H, Shingaki N, Mori Y, Enomoto S, Shiraki T, et al. Assessment of malignant potential of small hypervascular hepatocellular carcinoma using B-mode ultrasonography. Hepatol Res 2011;41(3):233-239.
29. Khan SA, Tavolari S, Brandi G. Cholangiocarcinoma: Epidemiology and risk factors. Liver International. 2019;39(S1):19-31.
30. Shin DW, Moon S-H, Kim JH. Diagnosis of cholangiocarcinoma. Diagnostics. 2023;13(2):233.
31. Hann LE, Greatrex KV, Bach AM, Fong Y, Blumgart LH. Cholangiocarcinoma at the hepatic hilus: sonographic findings. Am J Roentgenol 1997;/168:/985_9.
32. Robledo R, Muro A, Prieto ML. Extrahepatic bile duct carcinoma: US characteristics and accuracy in demonstration of tumors. Radiology 1996;/198:/869_73.
33. Matos AP, Altun E, Ramalho M, Velloni F, AlObaidy M, Semelka RC. An overview of imaging techniques for liver metastases management. Expert Rev Gastroenterol Hepatol. 2015;9: 1561–1576.
34. Frenette C, Mendiratta-Lala M, Salgia R, Wong RJ, Sauer BG, Pillai A. ACG Clinical Guideline: Focal Liver Lesions. Am J Gastroenterol. 2024 Jul 1;119(7):1235-1271.

9.2. Why do we need Liver Contrast Enhanced Ultrasound (CEUS)?

Ioan Sporea

Abstract

Contrast-enhanced ultrasound (CEUS) is an essential imaging modality for evaluating focal liver lesions (FLLs). Although conventional B-mode ultrasound demonstrates high sensitivity for lesion detection, its specificity is limited. CEUS improves diagnostic accuracy by enabling real-time assessment of lesion vascularity and permitting reliable differentiation between benign and malignant liver lesions.

This chapter presents the clinical rationale for liver CEUS, technical aspects of the examination, diagnostic performance compared with contrast-enhanced computed tomography (CE-CT) and magnetic resonance imaging (CE-MRI), safety profile, cost-effectiveness, and future perspectives, including artificial intelligence (AI).

9.2.1. Introduction

Medical imaging is indispensable in modern clinical practice. Contrast-enhanced techniques are routinely used in computed tomography (CT) and magnetic resonance imaging (MRI) to improve lesion characterization. Consequently, the application of contrast agents in ultrasound imaging is a logical advancement. Contrast-enhanced ultrasound (CEUS) represents an evolution of conventional ultrasonography, enabling real-time evaluation of tissue perfusion without ionizing radiation or nephrotoxic contrast agents.

9.2.2. Indications for Liver CEUS

CEUS is indicated when a FLL is detected on baseline ultrasound and further characterization is required. In some cases, lesions may be missed on standard ultrasound due to heterogeneous liver parenchyma or limited acoustic windows. Therefore, CEUS is recommended only when the lesion is clearly visible on standard ultrasound (1). Additionally, in oncological patients, CEUS facilitates the detection of liver metastases or a higher number of lesions than standard ultrasound (2).

International guidelines recommend CEUS as a first-line contrast imaging modality for characterizing FLLs visible on conventional ultrasound (3).

9.2.3. Technical Aspects of Liver CEUS

The CEUS examination typically lasts approximately 10 minutes, including venous access placement, contrast agent preparation, injection, and real-time observation of arterial, portal, and late phases for up to five minutes. Common contrast agents include SonoVue® and Sonazoid® (2). SonoVue® is a widely used second-generation contrast agent. Sonazoid® is used in select regions, such as some Asian countries and Norway, and provides prolonged retention due to phagocytosis by Kupffer cells. Low mechanical index imaging is essential to prevent microbubble destruction.

Convex transducers are preferred for liver imaging during CEUS, whereas linear probes may be advantageous for superficial lesions. Optimal venous access is obtained via a 20-gauge cannula in the left antecubital vein to minimize microbubble disruption. Repeated injections are feasible and beneficial in cases involving multiple lesions or when the initial enhancement pattern is inconclusive (4).

9.2.4. Safety Profile of CEUS

Ultrasound contrast agents have an excellent safety profile. Severe anaphylactoid reactions are extremely rare, occurring at approximately 0.001% frequency, with no recorded mortality (5,6). Unlike iodinated or gadolinium-based contrast agents, CEUS is safe for patients with renal failure and does not involve ionizing radiation.

9.2.5. Diagnostic Performance of CEUS

Multiple studies have demonstrated that CEUS significantly improves diagnostic accuracy compared with standard ultrasound. The rate of indeterminate diagnoses is markedly reduced, with overall accuracy reaching approximately 85–90% (7). The hallmark of malignancy on CEUS is contrast washout during the portal and late phases, whereas benign lesions typically retain contrast. This vascular behavior enables reliable differentiation between benign and malignant FLLs (1,2,3).

9.2.6. Multicenter and Meta-Analytical Evidence

Large multicenter studies, including Romanian cohorts (7), have confirmed the high diagnostic performance of CEUS, correctly differentiating malignant from benign lesions in approximately 88% of cases (7). Meta-analyses

encompassing over 8,000 lesions reported pooled sensitivities and specificities exceeding 90% for diagnosing malignant liver lesions (8).

Another meta-analysis of 25 studies (9) indicated that the diagnostic value of CEUS for FLLs is comparable to that of CE-CT and CE-MRI. This conclusion was corroborated by a subsequent meta-analysis (10).

Some studies (7) have demonstrated that CEUS diagnostic accuracy varies among lesion types, being higher for hemangiomas, focal nodular hyperplasia, and liver metastases, but lower for adenomas and cholangiocarcinomas (7,11,12,13,14).

9.2.7. Cost-Effectiveness of Liver CEUS

Economic evaluations consistently demonstrate that CEUS is more cost-effective than CE-CT and CE-MRI for evaluating FLLs (15). Studies comparing traditional diagnostic pathways with CEUS-based strategies report significant cost savings (16), especially when CEUS is performed in experienced centers (17). These findings support the use of CEUS as a first-line contrast imaging modality for FLLs (9).

9.2.8. CEUS as a Point-of-Care Ultrasound Tool

Ultrasound has increasingly evolved into a point-of-care ultrasound (PoCUS) modality, particularly in hepatology and gastroenterology. In several countries, including Germany, Italy, Japan, and Romania, CEUS is frequently performed directly in the consultation room, facilitating immediate clinical decision-making. Although standard liver ultrasound demonstrates high sensitivity, its specificity for characterizing FLLs is limited. CEUS significantly enhances specificity by visualizing microvascular patterns in real time, enabling definitive diagnosis in many cases without the need for additional cross-sectional imaging.

9.2.9. Future Perspectives: Artificial Intelligence

Recent developments in artificial intelligence have further enhanced the diagnostic value of CEUS (18). AI-based models demonstrate diagnostic accuracy comparable to that of expert radiologists and superior to that of less experienced operators (19, 20). Integration of AI into CEUS workflows may expand access to high-quality liver imaging and enable rapid diagnosis of focal liver lesions.

9.2.10. Conclusions

Liver CEUS is a safe, rapid, and cost-effective imaging modality that significantly improves the characterization of FLLs. Its diagnostic performance is comparable to that of contrast-enhanced CT and MRI, with additional advantages including real-time imaging, no radiation exposure, and an excellent safety profile. Operator experience remains critical; however, emerging technologies and artificial intelligence are expected to further enhance CEUS's role in routine clinical practice. Despite these benefits, liver CEUS remains underutilized in clinical settings, underscoring the need to promote its broader adoption (21,22).

References

1. Claudon M, Dietrich CF, Choi BI, Cosgrove DO, Kudo M, Nolsøe CP, et al. Guidelines and good clinical practice recommendations for contrast enhanced ultrasound (CEUS) in the liver--update 2012: a WFUMB-EFSUMB initiative in cooperation with representatives of AFSUMB, AIUM, ASUM, FLAUS and ICUS. Ultraschall Med. 2013 Feb;34(1):11-29.

2. Dietrich CF, Nolsøe CP, Barr RG, Berzigotti A, Burns PN, Cantisani V, et al. Guidelines and Good Clinical Practice Recommendations for Contrast Enhanced Ultrasound (CEUS) in the Liver - Update 2020 - WFUMB in Cooperation with EFSUMB, AFSUMB, AIUM, and FLAUS. Ultraschall Med. 2020 Oct;41(5):562-585.

3. Sporea I, Badea R, Brisc C, Ioanițescu S, Moga T, Popescu A, et al. Romanian National Guidelines on Contrast Enhanced Ultrasound in clinical practice. Med Ultrason. 2017 Nov 29;19(4):401-415.

4. Dietrich CF, Averkiou M, Nielsen MB, Barr RG, Burns PN, Calliada F, et al. How to perform Contrast-Enhanced Ultrasound (CEUS). Ultrasound Int Open. 2018 Jan;4(1):E2-E15.

5. Piscaglia F, Bolondi L; Italian Society for Ultrasound in Medicine and Biology (SIUMB) Study Group on Ultrasound Contrast Agents. The safety of Sonovue in abdominal applications: retrospective analysis of 23188 investigations. Ultrasound Med Biol. 2006 Sep;32(9):1369-75.

6. Li Q, Yang K, Ji Y, Liu H, Fei X, Zhang Y, et al. Safety Analysis of Adverse Events of Ultrasound Contrast Agent Lumason/SonoVue in 49,100 Patients. Ultrasound Med Biol. 2023 Feb;49(2):454-459.

7.Sporea I, Săndulescu DL, Şirli R, Popescu A, Danilă M, Spârchez Z, et al. Contrast-Enhanced Ultrasound for the Characterization of Malignant versus Benign Focal Liver Lesions in a Prospective Multicenter Experience - The SRUMB Study. J Gastrointestin Liver Dis. 2019 Jun 1;28:191-196.

8. Friedrich-Rust M, Klopffleisch T, Nierhoff J, Herrmann E, Vermehren J, Schneider MD, et al. Contrast-Enhanced Ultrasound for the differentiation of benign and malignant focal liver lesions: a meta-analysis. Liver Int. 2013 May;33(5):739-55.
9.Xie L, Guang Y, Ding H, Cai A, Huang Y. Diagnostic value of contrast-enhanced ultrasound, computed tomography and magnetic resonance imaging for focal liver lesions: a meta-analysis. Ultrasound Med Biol. 2011 Jun;37(6):854-61.
10. Guang Y, Xie L, Ding H, Cai A, Huang Y. Diagnosis value of focal liver lesions with SonoVue®-enhanced ultrasound compared with contrast-enhanced computed tomography and contrast-enhanced MRI: a meta-analysis. J Cancer Res Clin Oncol. 2011 Nov;137(11):1595-605.
11. Moga TV, Lupusoru R, Danila M, Ghiuchici AM, Popescu A, et al. Challenges in Diagnosing Focal Liver Lesions Using Contrast-Enhanced Ultrasound. Diagnostics (Basel). 2024 Dec 28;15(1):46.
12.Şirli R, Sporea I, Săndulescu DL, Popescu A, Dănilă M, Săftoiu A, et al. Contrast enhanced ultrasound for the diagnosis of liver hemangiomas - results of a Romanian multicentre study. Med Ultrason. 2015 Dec;17(4):444-50.
13. Şirli R, Sporea I, Popescu A, Dănilă M, Săndulescu DL, Săftoiu A, et al. Contrast-enhanced ultrasound for the assessment of focal nodular hyperplasia - results of a multicentre study. Med Ultrason. 2021 May 20;23(2):140-146.
14. Dănilă M, Popescu A, Sirli R, Sporea I, Martie A, Sendroiu M. Contrast enhanced ultrasound (CEUS) in the evaluation of liver metastases. Med Ultrason. 2010 Sep;12(3):233-7.
15. Westwood M, Joore M, Grutters J, Redekop K, Armstrong N, Lee K, et al. Contrast-enhanced ultrasound using SonoVue® (sulphur hexafluoride microbubbles) compared with contrast-enhanced computed tomography and contrast-enhanced magnetic resonance imaging for the characterisation of focal liver lesions and detection of liver metastases: a systematic review and cost-effectiveness analysis. Health Technol Assess. 2013 Apr;17(16):1-243.
16.Romanini L, Passamonti M, Aiani L, Cabassa P, Raieli G, Montermini I, et al. Economic assessment of contrast-enhanced ultrasonography for evaluation of focal liver lesions: a multicentre Italian experience. Eur Radiol. 2007 Dec;17 Suppl 6:F99-106..
17. Giesel FL, Delorme S, Sibbel R, Kauczor HU, Krix M. Kontrastverstärkter Ultraschall zur Charakterisierung von inzidentellen Leberläsionen - eine ökonomische Betrachtung im Vergleich zur Mehrphasen-Computertomografie [Contrast-enhanced ultrasound for the characterization of incidental liver lesions - an economical evaluation in comparison with multi-phase computed tomography]. Ultraschall Med. 2009 Jun;30(3):259-68.
18. Moga TV, David C, Popescu A, Lupusoru R, Heredea D, Ghiuchici AM, et al. Multiparametric Ultrasound Approach Using a Tree-Based Decision Classifier for Inconclusive Focal Liver Lesions Evaluated by Contrast Enhanced Ultrasound. J Pers Med. 2021 Dec 20;11(12):1388.

19. Ding W, Meng Y, Ma J, Pang C, Wu J, Tian J, et al. Contrast-enhanced ultrasound-based AI model for multi-classification of focal liver lesions. J Hepatol. 2025 Aug;83(2):426-439.
20. Hu HT, Wang W, Chen LD, Ruan SM, Chen SL, Li X, et al. M. Artificial intelligence assists identifying malignant versus benign liver lesions using contrast-enhanced ultrasound. J Gastroenterol Hepatol. 2021 Oct;36(10):2875-2883.
21.Sporea I. Why isn't Contrast Enhanced Ultrasound for Focal Liver Lesions used more in daily practice? Med Ultrason.2016 Mar;18(1):5-6.
22.Yusuf GT, Sidhu PS. The benefits of CEUS and why we don't use more CEUS in clinical practice in the United Kingdom. Br. J Radiol.2026 Feb 3:tqag025.

9.3. CEUS of the Liver: indications, technique, limitations

Tudor Moga, Alina Popescu

Abstract

Contrast-enhanced ultrasound (CEUS) using second-generation ultrasound contrast agents (UCAs) is recommended as the first-line contrast imaging modality for the characterization of focal liver lesions (FLL), particularly for differentiating benign from malignant lesions, but also for detecting liver metastasis, for liver tumor treatment monitoring, and for interventional procedures guidance.

The technique is a safe one that requires low mechanical index ultrasound applications, and the UCA remains strictly intravascular and allows the visualization of the vascular pattern in the arterial, portal venous and late phases.

9.3.1. Indications of CEUS

Ultrasound contrast agents (UCAs) are gas-filled microbubbles stabilized by a lipid or phospholipid shell, with a diameter of approximately 1–10 µm, enabling exclusive intravascular distribution and detailed depiction of both macro- and microvascular architecture. Currently used second-generation agents for liver imaging include sulfur hexafluoride (SonoVue®), perflutren (Definity®/Luminity®/Optison®), and perfluorobutane (Sonazoid®), while older agents, such as Levovist®, are no longer in production or not licensed for hepatic use.

Contrast-enhanced ultrasound (CEUS) is recommended as the first-line contrast imaging modality for the characterization of focal liver lesions (FLL), particularly incidental focal liver lesions (IFLL), owing to its high diagnostic accuracy (~90%) for differentiating benign from malignant lesions, comparable to CE-MRI (1). CEUS enables real-time evaluation of enhancement patterns across arterial, portal-venous, and late phases, with late-phase washout serving as a key hallmark of malignancy (2, 3). It is non-ionizing, safe in renal impairment, and associated with a very low rate of adverse events, making it preferable to contrast-enhanced CT in many cases. In contrast to CT and MRI contrast media, which diffuse rapidly into the interstitial space, UCAs remain confined to the vascular compartment, functioning as pure blood pool agents; moreover, the administered volume (typically 1–2 mL) is substantially lower

than that used in cross-sectional imaging. Certain agents, particularly Sonazoid®, undergo additional uptake by Kupffer cells approximately 10–15 minutes after injection, generating a post-vascular (Kupffer) phase that enables prolonged whole-liver assessment and improves differentiation between benign and malignant focal liver lesions, especially in cirrhotic patients (4). Furthermore, CEUS can be performed immediately following conventional ultrasound in the same session, facilitating rapid diagnosis and reducing unnecessary cross-sectional imaging (1).

CEUS of the liver is primarily indicated for the **characterization and detection of FLLs**. Its role is particularly relevant in the following clinical contexts:

A. Characterization and detection of Focal Liver Lesions

- ***Differentiation between benign and malignant lesions*** in non-cirrhotic liver (3).
- ***Evaluation of nodules in cirrhotic liver***, including characterization according to CEUS LI-RADS criteria (5).
- ***Assessment of small or indeterminate lesions*** detected on baseline ultrasound (1).
- ***Characterization of inconclusive lesions at CT or MR imaging*** (6).
- ***Detection of liver metastasis in the late phase*** (6).

B. Evaluation of Tumor Vascularity

- Real-time analysis of **arterial wash-in and venous/late wash-out patterns**.
- Identification of hyperenhancement, isoenhancement, or hypo-enhancement relative to adjacent liver parenchyma (6).

C. Treatment Monitoring

- Assessment of response to (7, 8):
    - Radiofrequency ablation
    - Cryotherapy
    - Antiangiogenic or oncologic therapies
- Detection of residual viable tumor immediately post-ablation.

D. Guidance for Interventions

- CEUS-guided biopsy to (9):
    - Target viable (enhancing) tumor tissue
    - Avoid necrotic areas
- Evaluation of post-interventional complications (e.g., infarction, bleeding) (10).

E. Pediatric Applications

- Characterization of focal liver lesions (approved indication in some regions).

In experienced hands, CEUS provides diagnostic performance comparable to CT or MRI in many scenarios (11).

9.3.2. Technique

High-quality CEUS examination of the liver depends on meticulous optimization of technical parameters and a clear understanding of microbubble behavior and contrast kinetics. The technique should be performed using ultrasound systems equipped with dedicated contrast-specific nonlinear imaging modes, which allow selective visualization of microbubble signals while effectively suppressing background tissue echoes. Low mechanical index (MI) imaging is essential, typically maintained below 0.1–0.2, in order to minimize microbubble destruction and preserve continuous real-time assessment of enhancement patterns. Excessive acoustic power may lead to premature bubble disruption, signal loss, and misinterpretation of wash-in or wash-out dynamics.

The use of a dual-display mode is strongly recommended. This format simultaneously shows the contrast-specific image alongside a low-MI fundamental B-mode image. Such parallel visualization facilitates precise lesion localization, helps maintain the imaging plane during respiratory motion, and ensures accurate correlation between morphological findings and dynamic enhancement characteristics (12).

Table 9.3.I. Vascular Phases of Liver CEUS (6)

Phase	Approximate Timing After Injection	Hemodynamic Background	Main Diagnostic Purpose	Key Imaging Features
Arterial Phase (AP)	~10–30 seconds	Predominantly hepatic arterial supply	Characterization of early vascular behavior	Evaluation of arterial hyperenhancement pattern and vascular architecture
Portal Venous Phase (PVP)	~30–120 seconds	Combined portal venous and arterial perfusion	Comparison with surrounding liver parenchyma	Assessment of relative enhancement (hyper-, iso-, or hypo-enhancement)
Late (Sinusoidal) Phase (LP)	Up to 4–6 minutes	Sinusoidal distribution within liver microcirculation	Detection of wash-out	Identification of hypoenhancement, a key feature suggestive of malignancy
Post-vascular (Kupffer) Phase*	Variable (typically ≥10 minutes, depending on agent)	Phagocytosis by Kupffer cells (reticuloendothelial uptake)	Evaluation of Kupffer cell activity	Persistent parenchymal enhancement; defects correspond to lesions lacking Kupffer cells

Contrast Administration

Contrast administration in liver CEUS is typically performed using an intravenous bolus technique. For sulfur hexafluoride microbubble agents (SonoVue™), a dose of approximately 1.2–2.4 mL is commonly used in adult liver applications, depending on equipment settings and clinical indication. The contrast bolus should be injected at a controlled rate of about 1–2 mL per second to avoid excessive pressure that could lead to premature microbubble disruption. Immediately after contrast delivery, a saline flush of 5–10 mL is administered to ensure complete transit of the agent into the systemic circulation.

Peripheral venous access is preferred (Fig. 1), ideally via a 20-gauge cannula or larger, in order to minimize mechanical destruction of microbubbles during injection. The contrast timer should be started at the beginning of the injection to allow accurate temporal assessment of arterial, portal venous, and late phases. In more complex diagnostic scenarios—such as when multiple

lesions require characterization or when initial imaging is inconclusive—repeated injections may be necessary, provided adequate time is allowed for microbubble clearance between administrations (4, 6).



Fig. 9.3.1. Syringe and three-way stopcock configuration for CEUS (SonoVue™) administration. The recommended venous access is the left antecubital vein, which optimizes operator ergonomics.

Image Optimization

Proper parameter adjustment is essential (12):

- **Mechanical Index (MI):** Low to avoid microbubble destruction.
- **Gain:** Slightly above noise level to avoid signal saturation.
- **Dynamic Range:**
  - Narrow for low-perfusion visualization
  - Wide for quantification
- **Frame Rate:** ≥10 Hz during arterial phase.
- **Focus:** Positioned just below target lesion.
- Avoid continuous high-MI scanning to prevent bubble destruction.

9.3.3. Limitations

Despite its advantages, CEUS has several limitations:

a. Operator Dependence

Despite its advantages, CEUS remains significantly operator dependent. Diagnostic accuracy is strongly influenced by the examiner's experience, both in image acquisition and interpretation. Proper evaluation requires familiarity with microbubble kinetics, phase timing, and typical enhancement patterns of benign and malignant lesions. Insufficient technical expertise or limited experience may increase the risk of misinterpretation, making structured training and regular practice essential (6, 12).

b. Limited Field of View

In contrast to CT or MRI, which provide cross-sectional imaging of the entire liver in a single acquisition, CEUS allows evaluation of only one region at a time. Consequently, comprehensive assessment of the liver requires careful and systematic scanning of all segments, which may increase examination time and demands sustained operator attention (13).

c. Depth Limitations

CEUS provides optimal visualization for lesions located within approximately 12–15 cm from the transducer. Beyond this depth, image quality and contrast sensitivity progressively decrease. Diagnostic performance may therefore be reduced in obese patients, in individuals with advanced cirrhosis where acoustic windows are compromised, and in cases of deeply situated lesions, where attenuation and limited penetration can hinder accurate assessment (14).

d. Artifacts

CEUS is susceptible to several technical artifacts that may compromise image interpretation. The most frequent pitfalls include (14):

- **Microbubble destruction**, typically caused by an excessively high mechanical index (MI).
- **Acoustic shadowing**, usually related to an excessive contrast dose and high microbubble concentration.
- **Signal saturation**, resulting from overly high gain settings or excessive contrast administration.
- **Nonlinear propagation artifacts,** which may simulate true enhancement and lead to false-positive interpretation.
- **Pseudo enhancement following ablative therapy**, potentially mimicking residual viable tumor.

A progressive technical imbalance may lead to the so-called **"CEUS circle of disaster"**, characterized by the following sequence:

High MI → microbubble destruction → increased contrast dose → attenuation/shadowing → further increase in MI → additional microbubble destruction.

Careful adjustment of technical parameters is essential to prevent this cascade and maintain diagnostic reliability.

e. Quantitative limitations

Quantitative assessment using time–intensity curve (TIC) analysis requires strict control of technical conditions. Reliable measurements depend

on minimizing patient motion and maintaining a stable probe position throughout acquisition, as even minor displacement may significantly affect perfusion parameters.

In addition, variability between ultrasound systems limits the direct transferability of mechanical index (MI) values and quantitative settings. Differences in software algorithms and signal processing reduce standardization across platforms, which may affect reproducibility of quantitative results (15).

References

1. Șirli R, Popescu A, Jenssen C, Möller K, Lim A, Dong Y, et al. WFUMB Review Paper. Incidental Findings in Otherwise Healthy Subjects, How to Manage: Liver. Cancers 2024, 16, 2908.
2. Strobel D, Seitz K, Blank W, Schuler A, Dietrich C, von Herbay A, et al. Contrast-enhanced ultrasound for the characterization of focal liver lesions—Diagnostic accuracy in clinical practice (DEGUM multicenter trial) Ultraschall Med. 2008;29:499–505.
3. Friedrich-Rust M, Klopffleisch T, Nierhoff J, Herrmann E, Vermehren J, Schneider MD, et al. Contrast-Enhanced Ultrasound for the differentiation of benign and malignant focal liver lesions: A meta-analysis. Liver Int. 2013;33:739–755.
4. Sporea I, Badea R, Brisc C, Ioanițescu S, Moga T, Popescu A, et al. Romanian National Guidelines on Contrast Enhanced Ultrasound in clinical practice. Med. Ultrason. 2017;19:401–415.
5. Piscaglia F, Wilson SR, Lyshchik A, Cosgrove D, Dietrich CF, Jang HJ, et al. American College of Radiology Contrast Enhanced Ultrasound Liver Imaging Reporting and Data System (CEUS LI-RADS) for the diagnosis of Hepatocellular Carcinoma: a pictorial essay. Ultraschall in der Medizin - European Journal of Ultrasound. 2017;38(03):320–324.
6. Dietrich CF, Nolsøe CP, Barr RG, Berzigotti A, Burns PN, Cantisani V, et al. Guidelines Good Clinical Practice Recommendations for Contrast-Enhanced Ultrasound (CEUS) in the Liver-Update 2020 WFUMB in Cooperation with, EFSUMB, AFSUMB, AIUM and FLAUS. Ultrasound Med. Biol. 2020;46: 2579–2604
7. Faccia M, Garcovich M, Ainora ME, Riccardi L, Pompili M, Gasbarrini A, et al. Contrast-Enhanced Ultrasound for Monitoring Treatment Response in Different Stages of Hepatocellular Carcinoma. Cancers (Basel). 2022 Jan 18;14(3):481.
8. Eisenbrey JR, Gabriel H, Savsani E, Lyshchik A. Contrast-enhanced ultrasound (CEUS) in HCC diagnosis and assessment of tumor response to locoregional therapies. Abdom Radiol (NY). 2021 Aug;46(8):3579-3595.
9. Lorentzen T, Nolsoe CP, Ewertsen C, Nielsen MB, Leen E, Havre RF, et al. EFSUMB Guidelines on Interventional Ultrasound (INVUS), Part I. General aspects (long version). Ultraschall Med. 2015;36(5):E1–E14.

10. Sparchez Z, Mocan T, Craciun R, Sparchez M, Nolsøe C. Contrast enhancement for ultrasound-guided interventions: when to use it and what to expect? Ultrasonography. 2022 Apr;41(2):263-278.
11. Darge K, Papadopoulou F, Ntoulia A, Bulas DI, Coley BD, Fordham LA, et al. Safety of contrast-enhanced ultrasound in children for non-cardiac applications: A review by the Society for Pediatric Radiology CEUS Task Force. Pediatr Radiol. 2013;43(9):1063-1073.
12. Dietrich CF, Averkiou M, Nielsen MB, Barr RG, Burns PN, Calliada F, et al. How to perform Contrast-Enhanced Ultrasound (CEUS). Ultrasound Int Open. 2018;4(1):E2-E15.
13. Claudon M, Dietrich CF, Choi BI, Cosgrove DO, Kudo M, Nolsoe CP, et al. Guidelines and good clinical practice recommendations for Contrast Enhanced Ultrasound (CEUS) in the liver – update 2012: A WFUMB-EFSUMB initiative. Ultrasound Med Biol. 2013;39:187–210.
14. Dietrich CF, Ignee A, Greis C, Cui XW, Schreiber-Dietrich D, Hocke M. Artifacts and pitfalls in contrast-enhanced ultrasound of the liver. Ultraschall Med. 2014;35:108–125.
15. Dietrich CF, Averkiou MA, Correas JM, Lassau N, Leen E, Piscaglia F. An EFSUMB introduction into Dynamic Contrast-Enhanced Ultrasound (DCE-US) for quantification of tumour perfusion. Ultraschall Med. 2012;33:344–351.

9.4. CEUS for benign focal liver lesions

Roxana Şirli, Tudor Moga

Abstract

Focal liver lesions (FLLs) are frequently detected during routine ultrasound examinations, most often as incidental findings, with the majority being benign. Contrast-enhanced ultrasound (CEUS), integrated within multiparametric ultrasound (MPUS), has become a key noninvasive technique for their characterization. Using strictly intravascular microbubble contrast agents, CEUS enables real-time evaluation of lesion vascularity and dynamic enhancement behavior during arterial, portal venous, and late phases. The most reliable criterion for malignancy is washout in the portal or late phase, whereas benign solid lesions typically remain iso- or hyperenhancing.

Characteristic CEUS patterns allow confident diagnosis of common benign lesions, including hemangiomas, focal nodular hyperplasia, focal fatty alterations, and liver abscesses. Hepatocellular adenoma remains a diagnostic challenge, often requiring further imaging or biopsy in equivocal cases. In cirrhotic livers, careful application of CEUS LI-RADS criteria is essential.

When performed by experienced operators, CEUS provides a safe, radiation-free, and cost-effective first-line imaging modality for differentiating benign from malignant focal liver lesions.

9.4.1. Introduction

Focal liver lesions (FLL) are often discovered during abdominal US scans, with a reported incidence ranging from 2 to 19% (1) and CEUS is a fundamental tool in their differential diagnosis. CEUS examination should follow the same structured clinical approach as other imaging modalities, integrating patient history, symptoms, and risk factors before contrast administration. Characterization of FLL relies on real-time assessment of enhancement intensity (hypo-, iso-, or hyperenhancement), enhancement pattern (centrifugal, centripetal, or chaotic), and on dynamic vascular patterns across arterial, portal venous, and late phases. Differentiation between benign and malignant lesions is primarily based on portal and late-phase behavior: malignancies (with rare exceptions) show washout (being hypoenhancing), whereas benign solid lesions remain iso- or hyperenhancing, a principle validated in large multicenter studies demonstrating high diagnostic accuracy and performance comparable or superior to CT and MRI (2-4).

MPUS has emerged as a comprehensive, radiation-free diagnostic platform for liver imaging. Within this framework, CEUS plays a central role in the characterization of FLLs, particularly in differentiating benign from malignant entities. The liver's dual blood supply—approximately 70–75% portal venous and 25–30% arterial—forms the physiological basis for CEUS interpretation. Unlike CT and MRI contrast agents, microbubble ultrasound contrast agents (UCAs) remain strictly intravascular, allowing dynamic and continuous real-time evaluation of lesion vascularity. This fundamental property explains why CEUS provides highly specific vascular pattern recognition in benign lesions (5).

In daily practice, most incidentally detected FLLs are benign. A rapid, reliable, and safe characterization strategy is therefore essential to avoid unnecessary biopsies, cross-sectional imaging, patient anxiety, and healthcare costs. CEUS, integrated into MPUS, fulfils this requirement in the majority of cases.

9.4.2. CEUS Patterns of Common Benign Liver Lesions

a) Hemangiomas

Hemangioma is the most common benign liver tumor, with a prevalence ranging from 5 to 7% (1, 6) The typical aspect of hemangioma in B-mode US is of an hyperechoic, homogeneous, well delineated lesion, less than 3 cm in diameter. If this aspect is found in an asymptomatic patient (no history of malignancy or severe fibrosis/cirrhosis), no further imaging is needed (1). The problem is when the hemangioma is atypical (iso/hypoechoic, inhomogeneous, larger than 3 cm) and/or when the patient has a history of chronic liver disease with severe fibrosis/cirrhosis, or an oncologic history. This is when a contrast imaging method is needed and CEUS is really an useful tool with reported accuracy for diagnosing hemangioma ranging from 82.2% to 96.9% (4, 6, 7).

Typical CEUS features (Fig. 9.4.1) include (8):

- Peripheral, discontinuous, nodular enhancement in arterial phase
- Progressive centripetal fill-in ("iris diaphragm phenomenon")
- Sustained hyperenhancement in portal and late phases
- Absence of washout

Most hemangiomas present this typical enhancement pattern in CEUS, leading to its high specificity which can surpass 99% (6). However, large or giant hemangiomas may show heterogeneous B-mode appearance but maintain the characteristic dynamic enhancement pattern (6, 8). Atypical hemangiomas

(thrombosis, fibrosis) may lack typical nodular enhancement, presenting large unenhancing areas, however with sustained enhancing in the viable parts, and require MRI correlation (9). Another problem is continuous insonation, especially in superficial hemangiomas, which can lead to bubble destruction and a false wash-out, leading to a false diagnosis of malignancy (10) In a small percentage of cases, small hemangiomas (< 15 mm) present a rapid arterial enhancement due to having arterio-portal shunts ("high-flow hemangioma"), which can be a problem in the differential diagnosis with focal nodular hyperplasia (FNH) or hepatocellular carcinoma (HCC), the later especially in a cirrhotic liver (11).

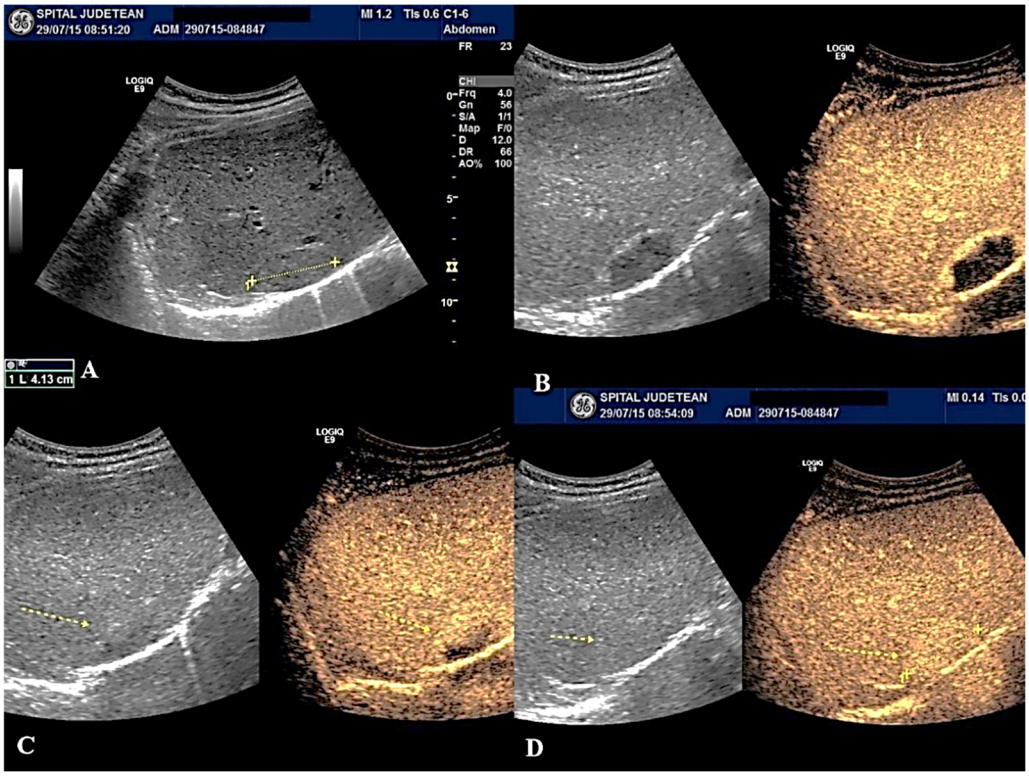


Fig. 9.4.1. On standard B-mode (A), a well-defined, homogeneous isoechoic lesion, with hyperechoic delineation, measuring approximately 4.1 cm is identified within the right hepatic lobe. On CEUS, the lesion demonstrates discontinuous peripheral, centripetal nodular hyperenhancement during the arterial phase (B). In the portal venous phase (C), progressive centripetal fill-in is observed, with increasing internal enhancement. In the late phase (D), the lesion shows persistent iso- to mild hyperenhancement relative to the surrounding liver parenchyma, without washout.

MPUS integration:

- Doppler: often minimal internal flow
- Elastography: typically soft
- CEUS: pathognomonic when classical

b) Focal Nodular Hyperplasia (FNH)

FNH is the second most frequent benign FLL, with an estimated prevalence of approximately 3% and is a hyperplastic response to localized vascular anomaly. In B-mode US it is usually isoechoic with a characteristic central scar. Doppler US typically shows a spoke-wheel pattern. CEUS is a very useful method for the diagnosis of FNH, with a specificity ranging from 94.3 to 100% (4, 8, 12).

CEUS features of FNH (8) (Fig. 9.4.2):

- Rapid centrifugal arterial filling from central artery
- "Wheel-spoke" vascular architecture
- Homogeneous hyperenhancement in arterial phase
- Iso- or hyperenhancement in portal venous phase and late phase
- No washout

The absence of wash-out is a decisive benign criterion (8, 12).

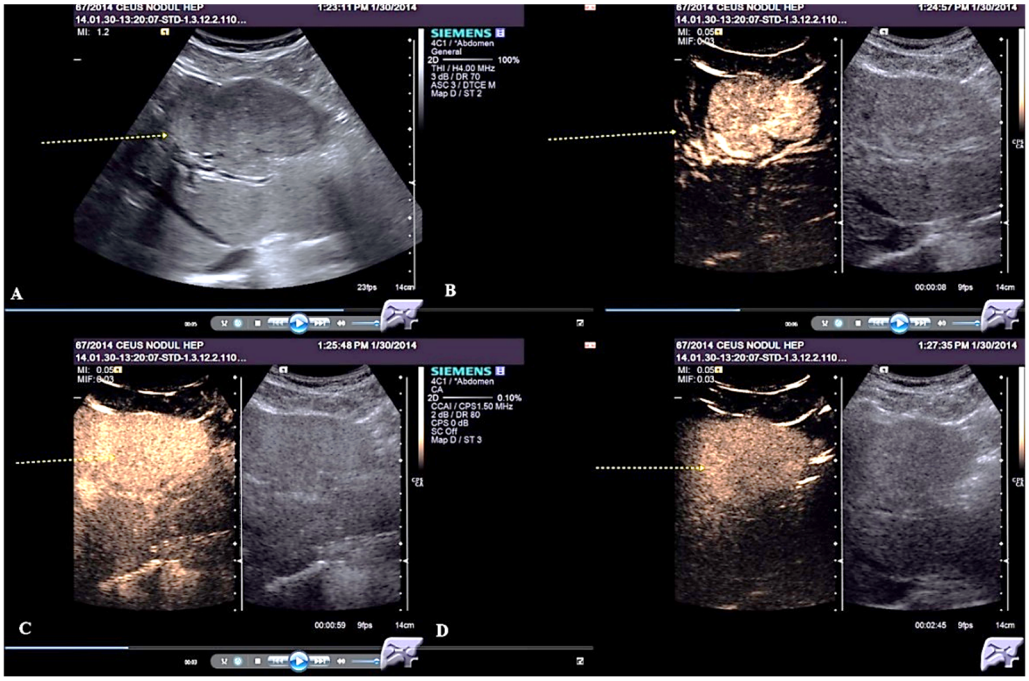


Fig. 9.4.2. On standard B-mode (A), a well-delineated, mildly hyperechoic lesion is identified within the hepatic parenchyma. (B–D) On CEUS examination, the lesion demonstrates intense, homogeneous hyperenhancement during the arterial phase, with a characteristic centrifugal filling pattern (B). In the portal venous (C) and late phases (D), the lesion remains hyperenhancing relative to the surrounding liver parenchyma, without washout. These enhancement characteristics are consistent with focal nodular hyperplasia.

MPUS integration:

- Doppler: central feeding artery, spoke wheel pattern
- Elastography: usually similar to surrounding liver
- CEUS: diagnostic in >90% of cases

The differentiation of FNH from hepatocellular adenoma (HCA) is crucial due to therapeutic implications (13). Both FNH and HCA show rapid arterial enhancement, but in FNH it is centrifugal, while in HCA it is centripetal (8). In HCA, due to the lack of portal vessels, a mild wash-out can occur in portal and late phases (1, 8).

Another differential diagnostic problem is with HCC, especially if the patient has an unrecognized chronic liver disease with severe fibrosis/cirrhosis. Both FNH and HCC have rapid arterial hyperenhancing, but in HCC it is a chaotic

one (8). Being malignant, HCCs usually present wash-out, but it is later and milder than in other malignant FLLs, usually after 60 seconds (8, 14) Especially well differentiated HCCs can present a very late wash-out, after 5-6 minutes, which can lead to a misdiagnosis of FNH. To diminish the risk of misdiagnosis in such cases, a thorough anamnesis as well as elastography are useful to demonstrate the presence of severe fibrosis/cirrhosis, to which HCCs are associated in more than 90% of the cases (1) Furthermore, the use of Li-RADS classification system has been proven to further enhance the ability of CEUS in the differential diagnosis of HCC (14, 15)

c) Hepatocellular Adenoma (HCA)

HCA is a rare benign tumor, in 90% of cases occurring in young women linked to birth control pills (16). There are three main subtypes according to phenotypic and genotypic traits (17) It must also be considered that in men there is a risk of malignant transformation, while in large adenomas there is a risk of hemorrhage and rupture. In B-mode US, HCA is difficult to diagnose since it is usually isoechoic (hypoechoic in patients with steatosis and thus easier to see).

CEUS characteristics of HCA (8) (Fig. 9.4 3):

- Homogeneous arterial hyperenhancement
- Mild portal venous hypoenhancement in many cases or isoenhancing
- Possible late phase washout (usually mild and late)
- Absence of central scar

If for hemangioma and FNH CEUS is a very accurate method, HCA it is not the same. In the DEGUM study, CEUS correctly diagnosed only 57.9% of liver adenomas (4). As shown before, the main problem for the differential diagnosis is FNH. From a clinical management standpoint, any doubt between FNH and HCA warrants further evaluation. Teleangiectatic (inflammatory) HCA may mimic FNH, being hyperenhancing in the late cases in up to 12% of cases (18). HCCs also have arterial hyperenhancement and may have very late and mild wash-out, thus making the differential diagnosis difficult (8), especially considering the risk of malignant transformation in HCA. In equivocal cases that could not be differentiated by hepato-specific contrast MRI, biopsy is recommended excepting large HCAs in men, where surgery is preferred (19, 20).

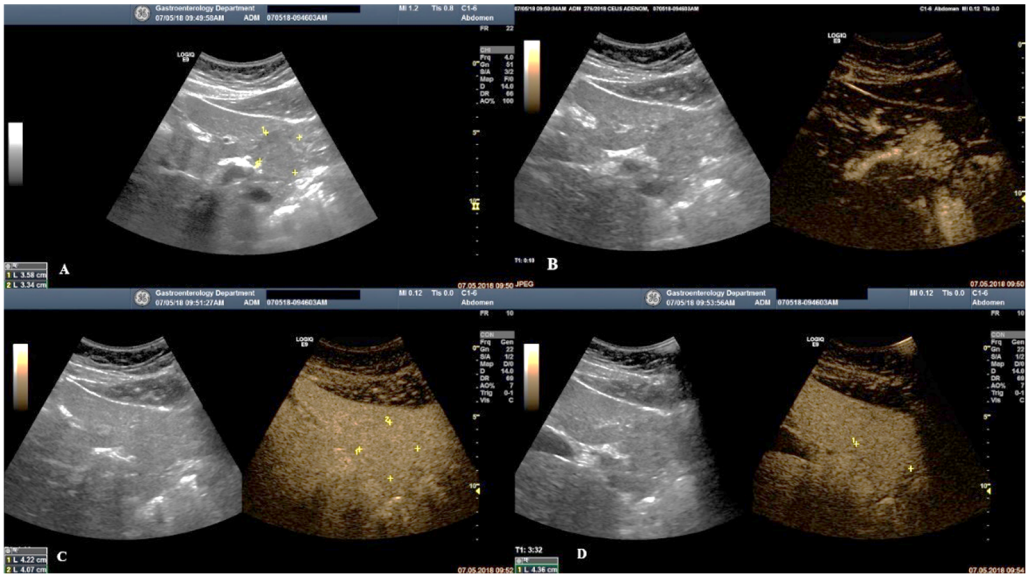


Fig. 9.4.3. On B-mode US (A), a well-defined, mildly heterogeneous lesion measuring approximately 4.2 × 4.1 cm is identified within the hepatic parenchyma. The lesion appears predominantly hypoechoic relative to the surrounding liver, with smooth margins and without evidence of capsular retraction or biliary dilatation. (B–D) On CEUS examination, the lesion demonstrates early arterial phase predominantly homogeneous hyperenhancement (B). In the portal venous (C) and late phases (D), mild washout is observed, with the lesion becoming slightly hypoenhancing as compared to the adjacent liver parenchyma. The presence of arterial phase hyperenhancement followed by late-phase washout, in the absence of a central scar, is compatible with hepatic adenoma.

MPUS considerations:

- Elastography may show relative softness as compared to the adjacent parenchyma
- If elastographic values of the adjacent parenchyma are high, above the cut-offs suggestive for severe fibrosis/cirrhosis, treat the lesion with extreme caution, as possibly malignant, until proven otherwise, including through liver biopsy.
- CEUS pattern is suggestive but not always definitive for HCA.

d) Focal fatty alterations: focal fatty infiltration and focal fatty sparing

Liver steatosis can be diffuse or can affect only parts of the liver. The mechanism of focal fatty alterations is presumed to be related to vascularity (21). In B-mode US, the aspect of focal fatty alterations is rather typical, they appear as

juxtaposition of well delineated areas with different echogenicity inside the liver, often with angular aspect and “geographical” delineation, never with mass effect on the adjacent structures, nor vessel invasion or alteration of the liver surface. They appear as hyperechoic areas in a normoechoic liver (focal fatty infiltration) or as hypoechoic areas on a steatotic, hyperechoic liver (focal fatty sparing). If they have this typical aspect, no further assessment is needed (1)When they have a more rounded shape, especially if hypoechoic, they may mimic neoplasia on B-mode US and further contrast enhanced imaging assessment is needed. Furthermore, focal fatty sparing can mask an underlying FLL in rare cases, especially small “shunt hemangiomas” that will only be visible by CEUS (22).

CEUS pattern of Focal Fatty Alterations (8) (Fig. 9.4.4):

- Isoenhancement in all phases
- No mass effect
- Preserved vascular architecture

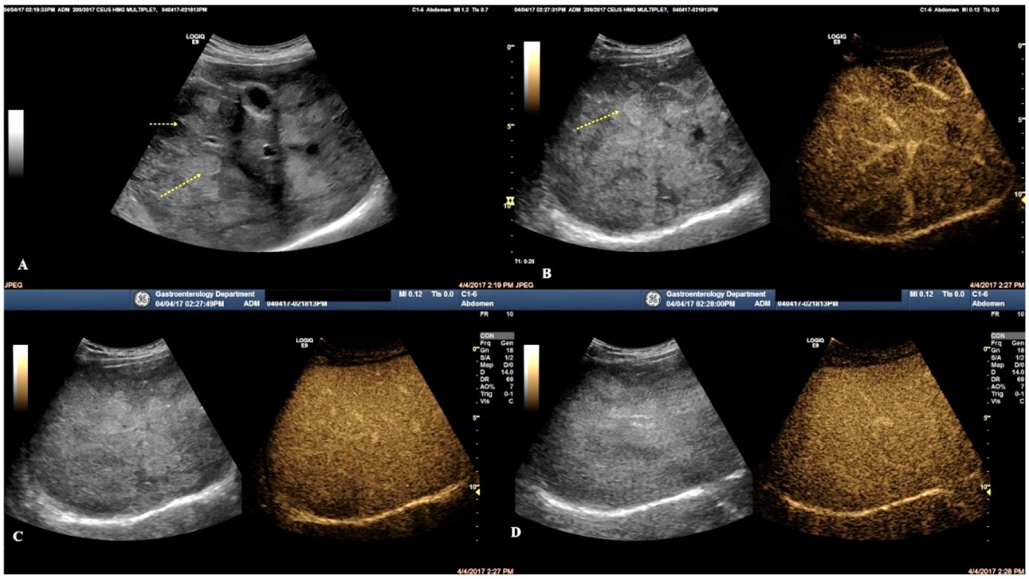


Fig. 9.4.4. On standard B-mode (A), a geographic, ill-defined hyperechoic area is observed within the hepatic parenchyma. The region does not exert mass effect, with preservation of normal vascular architecture and no displacement of intrahepatic vessels. (C–D) On CEUS examination, the area demonstrates isoenhancement relative to the surrounding liver parenchyma during the arterial phase. In the portal venous and late phases, persistent isoenhancement is noted, without washout or abnormal perfusion patterns. The absence of mass effect and the maintenance of vascular course, together with normal enhancement behavior on CEUS, are characteristic of focal fatty infiltration.

CEUS is particularly useful in oncology patients, preventing false diagnosis of metastases (3, 23). The performance of CEUS for diagnosing focal fatty alterations is similar to that of CE-CT, with Se exceeding 90% and Sp of 100% (24).

e) Liver Abscess

Liver abscess is a pus-containing lesion, usually caused by bacteria in the Western World (pyogenic abscess—the most frequent cause being E. Coli and Klebsiella) (25). The B-mode US aspect is of a hypoechoic, inhomogeneous, poorly delineated mass, with thick walls and sometimes with anechoic areas (necrotic liver tissue) and thick septa and/or with posterior amplification. Sometimes hyperechoic foci with posterior reverberation artifacts are observed within the lesion, consistent with intralesional gas formation. Very important is the clinical context: malaise, fever, and leucocytosis. The association of clinical features and B-mode US aspects that change over time are suggestive for the diagnosis; however, CEUS can be really helpful for a positive diagnosis and for the management of liver abscesses (8, 26).

CEUS features of liver abscess (8) (Fig. 9.4.5):

- Arterial rim hyperenhancement (consequence of perilesional hyperemia)
- Septal enhancement with a honeycomb appearance
- Non-enhancing central liquefaction
- Portal/late phase hypoenhancement

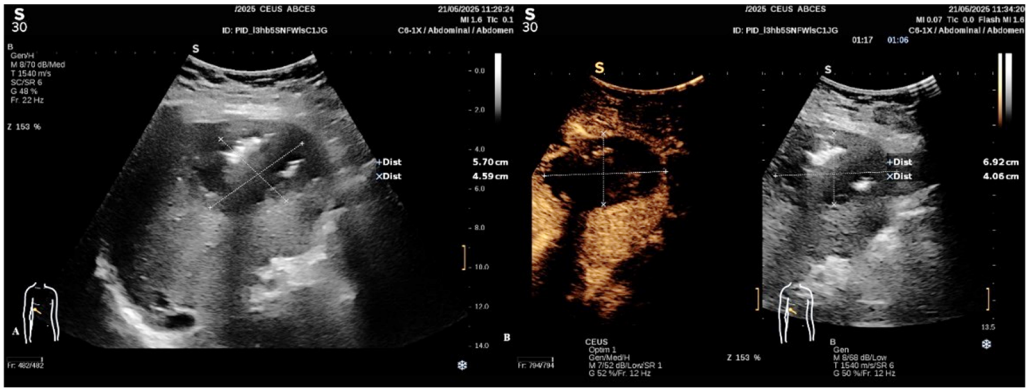


Fig. 9.4.5. On B-mode US (A), a large, heterogeneous lesion measuring approximately 5.7 × 4.6 cm is identified within the right hepatic lobe. The lesion demonstrates irregular margins and mixed echogenicity, with hypoechoic areas and internal echogenic debris suggestive of necrotic and purulent content. Additionally, hyperechoic foci with posterior reverberation artifacts are observed within the lesion, consistent with intralesional gas formation, a feature highly suggestive of a pyogenic abscess. (B) On CEUS during the arterial phase, the lesion exhibits peripheral rim-like hyperenhancement, while the central portion remains non-enhancing, consistent with avascular necrosis. The absence of central enhancement on CEUS, associated with peripheral inflammatory hyperenhancement, is highly suggestive of a pyogenic liver abscess.

CEUS is very useful for planning percutaneous drainage: it reveals the extent of necrotic areas and guides placement of the draining catheter. Furthermore, direct intracavitary injection of contrast shows possible communications among cavities in complex abscesses and the correct positioning of the needle, as well as presence of fistulas (27). Real-time imaging allows differentiation from necrotic tumors (3, 26).

f) Complex cystic lesions

In B-mode US, complex cystic lesions appear as anechoic/hypoechoic lesions with more or less well-defined margins, sometimes with inhomogeneous content or with echoic protrusions inside. They can be benign: hemorrhagic biliary cysts, “solid-like” hydatid cysts, cystadenomas; or malignant: cystadenocarcinomas, cystic metastases. B-mode US alone cannot differentiate them, and CEUS is a useful tool in the differential diagnosis.

CEUS features of complex cystic lesions (8) (Fig. 9.4.6):

- If the lesion and its walls are completely un-enhancing the possible diagnoses are hemorrhagic biliary cyst or "solid like" hydatic cyst
- If there is enhancing content and/or walls, that means there is neoformation tissue, so the possible diagnosis is cystadenoma, cystadenocarcinoma, or cystic metastases.
- If there is wash-out of the margins and content (in the absence of clinical symptoms of infection) that means that the lesion is malignant (cystadenocarcinoma, cystic metastases)

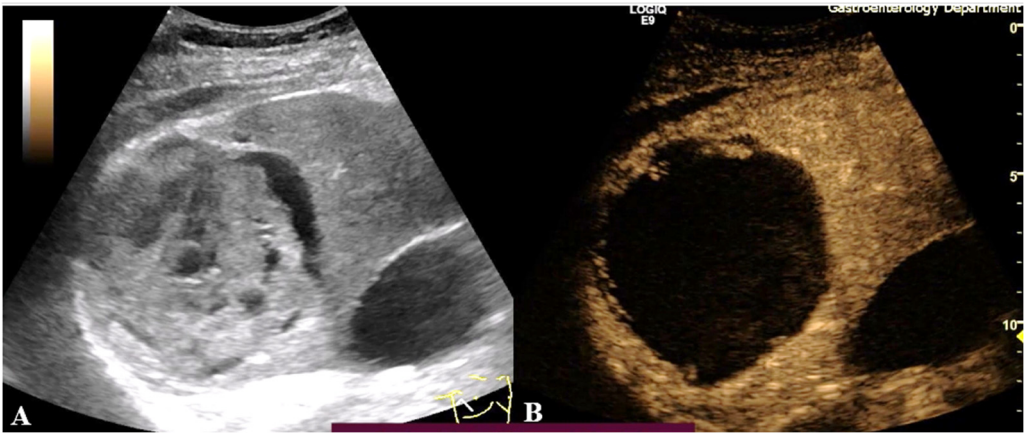


Fig. 9.4.6. On standard US (A), hemorrhagic biliary cysts are depicted like well-delineated cystic lesions containing echogenic material, without a definite solid mural component. At CEUS (B): The lesion demonstrates no internal contrast enhancement in any phase, confirming the avascular nature of the intracystic content.

g) Benign Lesions in Cirrhosis

Even if HCC is the most frequently new found lesion in a cirrhotic liver (78-86%) (28), benign lesions are also possible. Their interpretation is more challenging due to the heterogeneity of liver texture and to the modified vascular supply due to portal hypertension. Typical hemangiomas and cysts maintain classical patterns on B-mode US.

The regenerative nodules are usually hypoechoic, well delineated in B-mode US. In CEUS regenerative nodules are usually isoenhancing in all phases, with occasionally arterial hypoenhancement. In cirrhotic livers, CEUS LI-RADS criteria must be carefully applied for a correct differential diagnosis (8, 15).

9.4.3. Conclusion

When performed by experienced operators and integrated into a structured multiparametric approach, CEUS allows reliable differentiation between benign and malignant FLLs in the majority of patients, reduces healthcare costs, avoids radiation exposure, and accelerates patient management. From a modern hepatology perspective, CEUS is not an adjunct technique—it is an essential component of advanced liver imaging, a pivotal component of multiparametric ultrasound for the characterization of focal liver lesions.

The absence of washout in the portal venous and late phases is the most reliable indicator of benignity in solid liver lesions. Typical enhancement patterns—such as peripheral nodular fill-in in hemangioma and centrifugal arterial enhancement in FNH—allow confident, noninvasive differential diagnosis.

In non-cirrhotic patients with incidentally detected lesions, CEUS should be the first-line contrast imaging modality. When CEUS findings are inconclusive or suspicious, biopsy or complementary cross-sectional imaging remains mandatory. Integrated within MPUS, CEUS significantly reduces unnecessary investigations, radiation exposure, and patient anxiety.

References

1. Şirli R, Popescu A, Jenssen C, Möller K, Lim A, Dong Y, et al. WFUMB Review Paper. Incidental Findings in Otherwise Healthy Subjects, How to Manage: Liver. Cancers. 2024;16(16):2908.

2. Dietrich CF, Averkiou M, Nielsen MB, Barr RG, Burns PN, Calliada F, et al. How to perform Contrast-Enhanced Ultrasound (CEUS). Ultrasound Int Open. 2018;4(1):E2-e15.

3. Dietrich CF, Tana C, Caraiani C, Dong Y. Contrast enhanced ultrasound (CEUS) imaging of solid benign focal liver lesions. Expert Rev Gastroenterol Hepatol. 2018;12(5):479-89.

4. Strobel D, Seitz K, Blank W, Schuler A, Dietrich C, von Herbay A, et al. Contrast-enhanced ultrasound for the characterization of focal liver lesions--diagnostic accuracy in clinical practice (DEGUM multicenter trial). Ultraschall Med. 2008;29(5):499-505.

5. Moga TV, David C, Popescu A, Lupusoru R, Heredea D, Ghiuchici AM, et al. Multiparametric Ultrasound Approach Using a Tree-Based Decision Classifier for Inconclusive Focal Liver Lesions Evaluated by Contrast Enhanced Ultrasound. J Pers Med. 2021;11(12).

6. Sirli R, Sporea I, Săndulescu DL, Popescu A, Dănilă M, Săftoiu A, et al. Contrast enhanced ultrasound for the diagnosis of liver hemangiomas - results of a Romanian multicentre study. Med Ultrason. 2015;17(4):444-50.
7. Tranquart F, Le Gouge A, Correas JM, Ladam Marcus V, Manzoni P, Vilgrain V, et al. Role of contrast-enhanced ultrasound in the blinded assessment of focal liver lesions in comparison with MDCT and CEMRI: Results from a multicentre clinical trial. European Journal of Cancer Supplements. 2008;6(11):9-15.
8. Dietrich CF, Nolsøe CP, Barr RG, Berzigotti A, Burns PN, Cantisani V, et al. Guidelines and Good Clinical Practice Recommendations for Contrast-Enhanced Ultrasound (CEUS) in the Liver-Update 2020 WFUMB in Cooperation with EFSUMB, AFSUMB, AIUM, and FLAUS. Ultrasound Med Biol. 2020;46(10):2579-604.
9. Caserta MP, Fetzer DT, Swensson JK, Rodgers SK, Boyum JH. When Benign Behaves Badly: Atypical Hemangiomas on Contrast-Enhanced Ultrasonography. Ultrasound Q. 2022;38(2):133-41.
10. Giannetti A, Franci L, Grechi C, Giangregorio F. Contrast-enhanced sonography in the diagnosis of hepatic hemangiomas: atypical appearance due to the washout of microbubbles. J Clin Ultrasound. 2013;41(6):361-5.
11. Dietrich CF, Mertens JC, Braden B, Schuessler G, Ott M, Ignee A. Contrast-enhanced ultrasound of histologically proven liver hemangiomas. Hepatology. 2007;45(5):1139-45.
12. Şirli R, Sporea I, Popescu A, Dănilă M, Săndulescu DL, Săftoiu A, et al. Contrast-enhanced ultrasound for the assessment of focal nodular hyperplasia - results of a multicentre study. Med Ultrason. 2021;23(2):140-6.
13. Denis de Senneville B, Frulio N, Laumonier H, Salut C, Lafitte L, Trillaud H. Liver contrast-enhanced sonography: computer-assisted differentiation between focal nodular hyperplasia and inflammatory hepatocellular adenoma by reference to microbubble transport patterns. Eur Radiol. 2020;30(5):2995-3003.
14. Wilson SR, Lyshchik A, Piscaglia F, Cosgrove D, Jang HJ, Sirlin C, et al. CEUS LI-RADS: algorithm, implementation, and key differences from CT/MRI. Abdom Radiol (NY). 2018;43(1):127-42.
15. Ghiuchici AM, Dănilă M, Popescu A, Șirli R, Moga T, Topan M, et al. Contrast-enhanced ultrasound algorithm (ACR CEUS LI-RADSv 2017)- a valuable tool for the noninvasive diagnosis of hepatocellular carcinoma in patients with chronic liver disease. Med Ultrason. 2021;23(4):383-9.
16. González A, Canga F, Cárdenas F, Castellano G, García H, Cuenca B, et al. An unusual case of hepatic adenoma in a male. J Clin Gastroenterol. 1994;19(2):179-81.
17. Dietrich CF, Tannapfel A, Jang HJ, Kim TK, Burns PN, Dong Y. Ultrasound Imaging of Hepatocellular Adenoma Using the New Histology Classification. Ultrasound Med Biol. 2019;45(1):1-10.

18. Agarwal S, Fuentes-Orrego JM, Arnason T, Misdraji J, Jhaveri KS, Harisinghani M, et al. Inflammatory hepatocellular adenomas can mimic focal nodular hyperplasia on gadoxetic acid-enhanced MRI. AJR Am J Roentgenol. 2014;203(4):W408-14.
19. Garcovich M, Faccia M, Meloni F, Bertolini E, de Sio I, Calabria G, et al. Contrast-enhanced ultrasound patterns of hepatocellular adenoma: an Italian multicenter experience. J Ultrasound. 2019;22(2):157-65.
20. Dietrich CF, Schuessler G, Trojan J, Fellbaum C, Ignee A. Differentiation of focal nodular hyperplasia and hepatocellular adenoma by contrast-enhanced ultrasound. Br J Radiol. 2005;78(932):704-7.
21. Bhatnagar G, Sidhu HS, Vardhanabhuti V, Venkatanarasimha N, Cantin P, Dubbins P. The varied sonographic appearances of focal fatty liver disease: review and diagnostic algorithm. Clin Radiol. 2012;67(4):372-9.
22. Bartolotta TV, Taibbi A, Picone D, Anastasi A, Midiri M, Lagalla R. Detection of liver metastases in cancer patients with geographic fatty infiltration of the liver: the added value of contrast-enhanced sonography. Ultrasonography. 2017;36(2):160-9.
23. Dietrich CF, Sharma M, Gibson RN, Schreiber-Dietrich D, Jenssen C. Fortuitously discovered liver lesions. World J Gastroenterol. 2013;19(21):3173-88.
24. Janica J, Ustymowicz A, Lukasiewicz A, Panasiuk A, Niemcunowicz-Janica A, Turecka-Kulesza E, et al. Comparison of contrast-enhanced ultrasonography with grey-scale ultrasonography and contrast-enhanced computed tomography in diagnosing focal fatty liver infiltrations and focal fatty sparing. Adv Med Sci. 2013;58(2):408-18.
25. Sahu V, Pipal DK, Singh Y, Verma V, Singaria M, Pipal VR, et al. Epidemiology, Clinical Features, and Outcome of Liver Abscess: A Single-Center Experience. Cureus. 2022;14(10):e29812.
26. Popescu A, Sporea I, Şirli R, Dănilă M, Mare R, Grădinaru Taşcău O, et al. Does Contrast Enhanced Ultrasound improve the management of liver abscesses? A single centre experience. Med Ultrason. 2015;17(4):451-5.
27. Ignee A, Jenssen C, Cui XW, Schuessler G, Dietrich CF. Intracavitary contrast-enhanced ultrasound in abscess drainage--feasibility and clinical value. Scand J Gastroenterol. 2016;51(1):41-7.
28. Terzi E, Iavarone M, Pompili M, Veronese L, Cabibbo G, Fraquelli M, et al. Contrast ultrasound LI-RADS LR-5 identifies hepatocellular carcinoma in cirrhosis in a multicenter restropective study of 1,006 nodules. J Hepatol. 2018;68(3):485-92.

9.5. Contrast enhanced ultrasound (CEUS) for malignant lesions

Mirela Dănilă, Ana Maria Ghiuchici

Abstract

This chapter reviews the role of contrast-enhanced ultrasound (CEUS) in evaluating malignant focal liver lesions (FLLs), with particular emphasis on hepatocellular carcinoma (HCC), intrahepatic cholangiocarcinoma (iCCA), and liver metastases. CEUS provides real-time assessment of lesion vascularity, allowing differentiation between benign and malignant nodules based on vascular enhancement and washout patterns. Numerous studies and meta-analyses confirm the high diagnostic accuracy of CEUS for malignant liver lesions. Despite limitations, especially in small or deeply located lesions, CEUS remains a reliable, safe, and accessible first-line imaging modality in contemporary hepatology.

9.5.1. Introduction

CEUS can be used to characterize and classify liver lesions detected by standard ultrasound as benign or malignant (1).

The presence of washout in the portal or late phase of a CEUS examination typically indicates malignancy. Behavior in the arterial phase and the timing and degree of washout, compared with the surrounding liver, allow classification into specific malignant lesion types. Detection of hepatic lesions in patients with liver cirrhosis suggests HCC, whereas detection in patients with known malignancy indicates liver metastases.

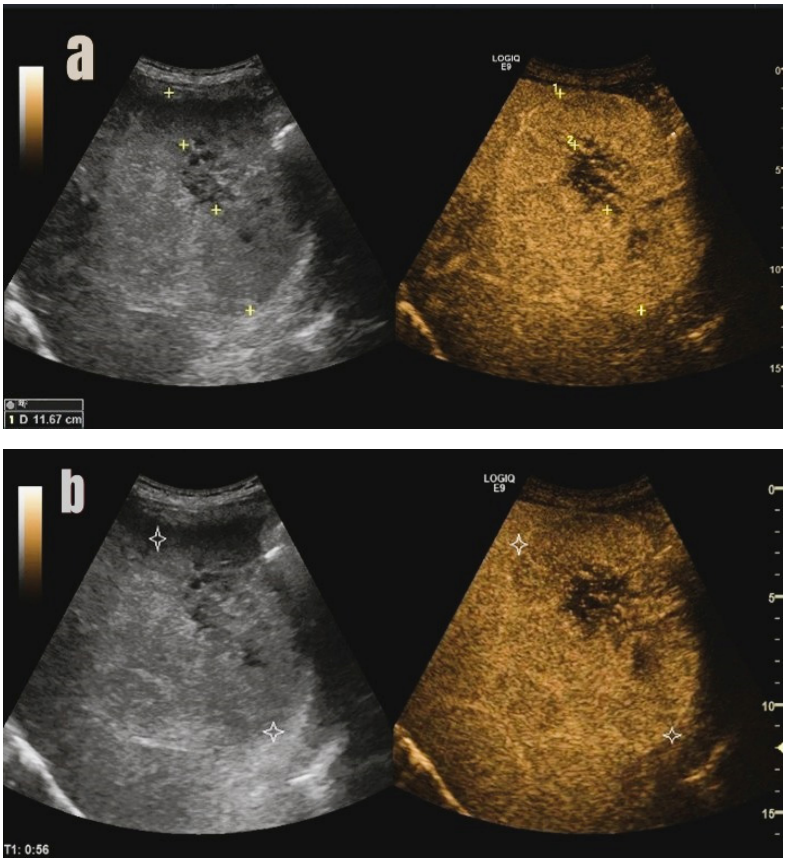
9.5.2. CEUS in hepatocellular carcinoma (HCC)

Liver cirrhosis represents the primary risk factor for HCC development. HCC develops through a multistep progression from regenerative nodules to low-grade dysplastic nodules, then to high-grade dysplastic nodules, culminating in overt carcinoma.

During this progression, significant alterations occur in the normal hepatic vascular architecture. Physiological portal venous vascularization progressively diminishes and is replaced by tumor neo-angiogenesis, characterized by the development of unpaired arteries and tumor-derived arterioles. This vascular remodeling results in malignant lesions predominantly supplied by arterial blood.

The imaging manifestation of this phenomenon is arterial phase hyperenhancement (APHE), a hallmark feature of HCC on contrast-enhanced imaging modalities, including CEUS (2). Since its introduction into clinical practice, CEUS has demonstrated substantial diagnostic value in HCC. Numerous studies and meta-analyses have highlighted its significant role in characterizing focal liver lesions in cirrhotic patients, supporting non-invasive diagnosis in typical cases.

The most common pattern of HCC on CEUS is arterial phase hyperenhancement, which may be homogeneous (Fig. 9.5.1). In larger HCCs, hyperenhancement often appears heterogeneous, with extensive non-enhancing areas due to tumor necrosis. Another enhancement pattern observed in HCC on CEUS is wheel-like enhancement. Several studies have reported increased sensitivity of CEUS in detecting arterial hyperenhancement, even in nodules as small as 2 cm (3).



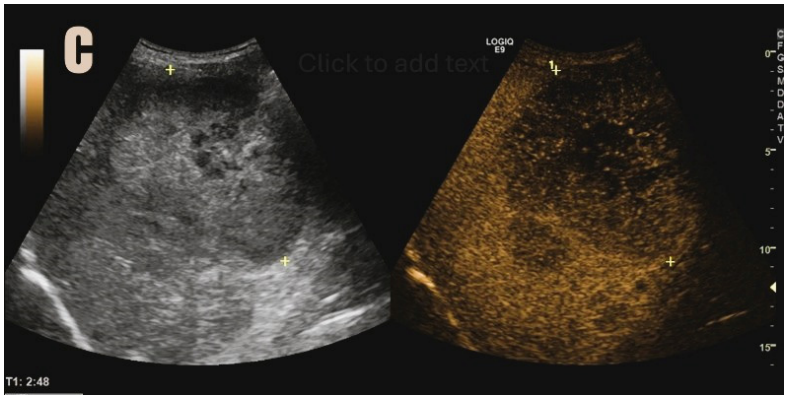


Fig. 9.5.1. Hepatocellular carcinoma. CEUS examination: the hyperechoic large HCC nodule (12 cm) in B-mode is showing homogeneous hyperenhancement and a central non-enhancing area in the arterial phase (a), isoenhancement in the portal venous phase (b) with mild and late washout in the late vascular phase (c). LR-5 lesion.

Arterial hyperenhancement is more commonly observed in moderately differentiated HCCs than in well- or poorly differentiated forms (4).

During the portal phase of a CEUS examination, HCC is typically isoenhancing. Washout is often not apparent until the last seconds of the portal phase, and mild washout occurs in the late phase. Washout occurs more rapidly during the portal and late phases in poorly differentiated HCC compared to well-differentiated lesions (4, 5).

The World Federation for Ultrasound in Medicine and Biology provides the following main recommendations for CEUS use in patients with cirrhosis (2):

- Characterization of focal liver lesions (FLLs) detected during surveillance and routine ultrasound in patients with liver cirrhosis to establish a diagnosis of malignancy.
- Evaluation of nodules unsuitable for biopsy when CT or MRI results are inconclusive.
- Assisting in the selection of nodules for biopsy when multiple lesions or varying contrast patterns are present.
- Monitoring changes in size and enhancement patterns over time for nodules under surveillance that are not diagnostic for HCC.
- Evaluation following inconclusive histological results.

Although numerous studies have demonstrated the strong performance of CEUS in diagnosing HCC (6, 7, 8), some have indicated that CEUS cannot reliably differentiate small (<3 cm) intrahepatic cholangiocarcinoma (ICC) in cirrhosis from HCC (9, 10). Consequently, CEUS was removed from earlier EASL guidelines as a diagnostic method for HCC.

In 2017, the American College of Radiology developed the CEUS LI-RADS algorithm to optimize the utility of CEUS for non-invasive diagnosis of hepatocellular carcinoma (HCC) and to align CEUS assessments with other liver imaging reporting systems, including CT/MRI LI-RADS (11).

The algorithm comprises eight distinct diagnostic categories:

- LR-1 (definitely benign): typical cystic lesions, hepatic fat deposition or sparing, and typical hemangiomas.
- LR-2 (probably benign) includes solid nodules under 10 mm exhibiting isoenhancement in all phases or non-mass-like isoenhancing observations of any size.
- LR-3: intermediate probability of malignancy.
- LR-4: probably HCC, but not definitive (Fig. 9.5.2).
- LR-5 (definitely HCC): liver nodules ≥1 cm with arterial phase hyperenhancement and mild late washout occurring after 120 seconds (Fig. 9.5.3 -9.5.5).
- LR-NC: lesions that cannot be categorized due to image degradation.
- LR-TIV (tumor in vein).
- LR-M (probably or definitely malignant, but not HCC specific). Liver nodules of varying sizes, with or without arterial hyperenhancement and lacking portal or late washout, correspond to LR-3 and LR-4 categories, indicating intermediate or increased probability of HCC.

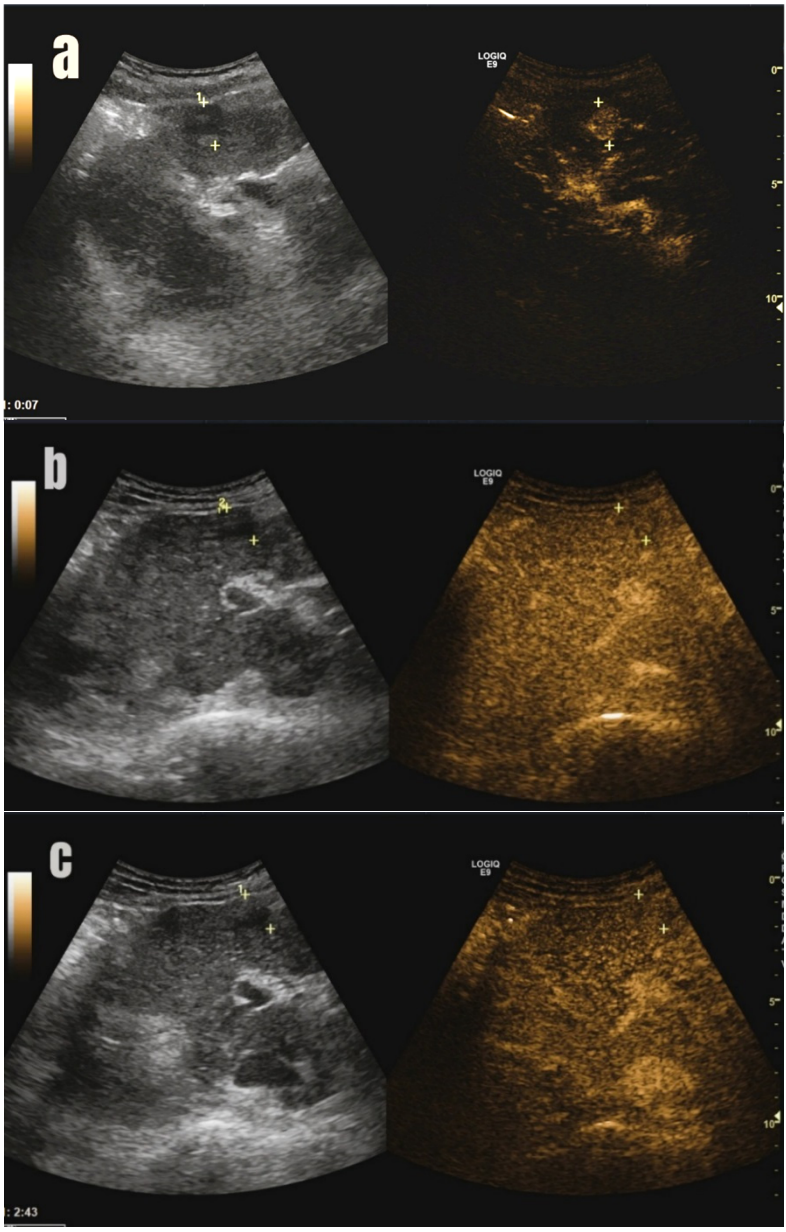


Fig. 9.5.2. Liver nodule in a cirrhotic patient corresponding to LR-4 category. CEUS examination: the hypoechoic small nodule measuring 1.7 cm in B-mode is showing homogeneous hyperenhancement in the arterial phase (a), isoenhancement in the portal venous (b), and late vascular phases (c). No washout is seen in the late vascular phase.

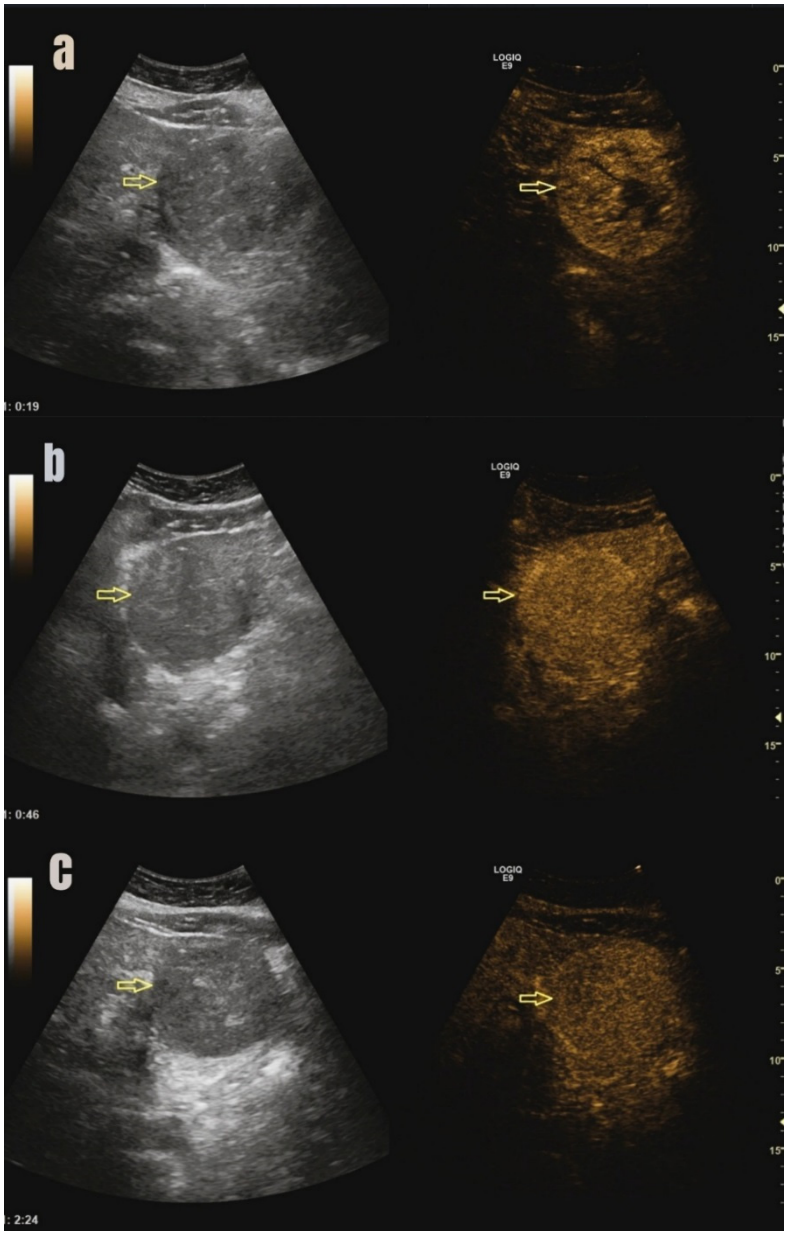


Fig. 9.5.3. Hepatocellular carcinoma. Liver nodule in a cirrhotic patient corresponding to LR-5 category. CEUS examination: the hypoechoic nodule measuring 6 cm in B-mode is showing homogeneous hyperenhancement in the arterial phase (a), isoenhancement in the portal venous phase (b), and mild and late washout in the late vascular phase (c).

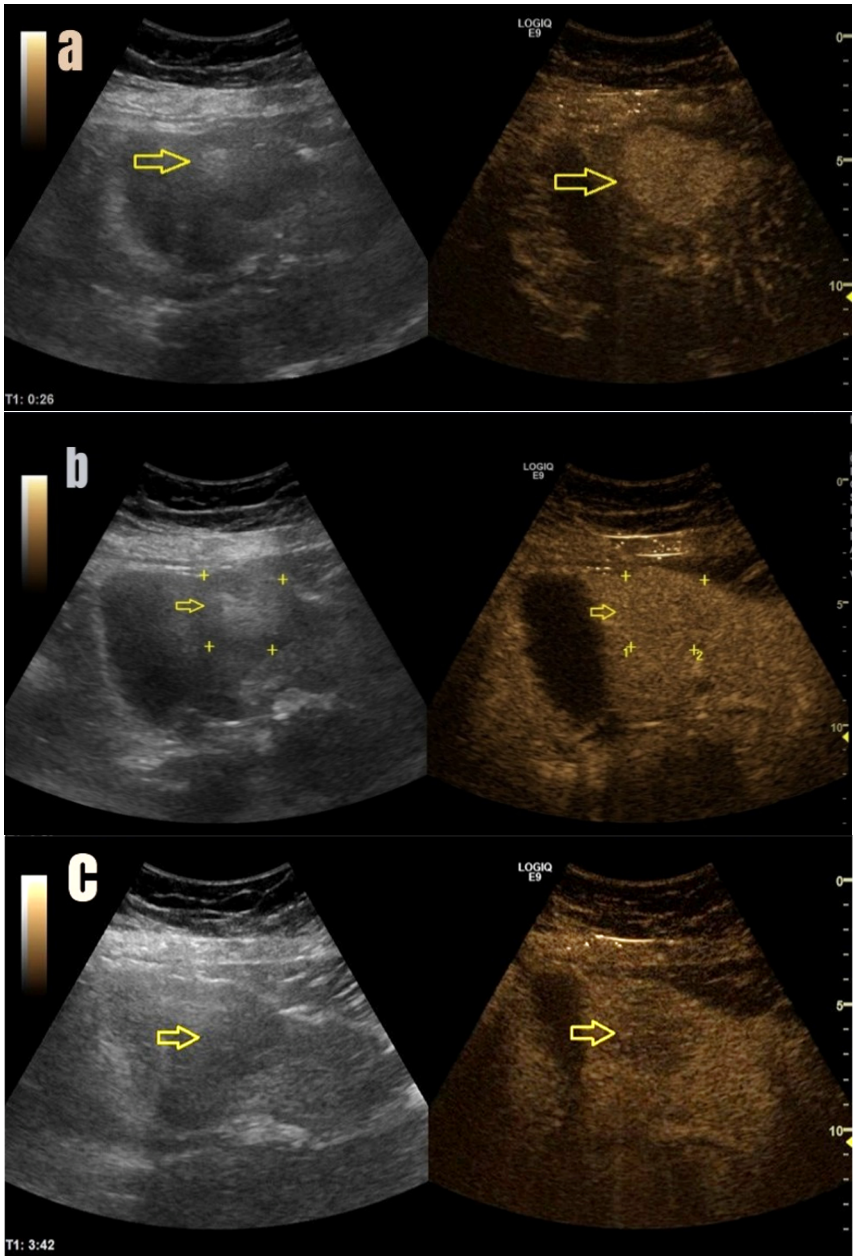


Fig. 9.5.4. Hepatocellular carcinoma. Liver nodule in a cirrhotic patient corresponding to LR-5 category. CEUS examination: the hypoechoic nodule measuring 4/4cm cm in B-mode is showing homogeneous hyperenhancement in the arterial phase (a), isoenhancement in the portal venous phase (b), and mild and late washout in the late vascular phase (c).

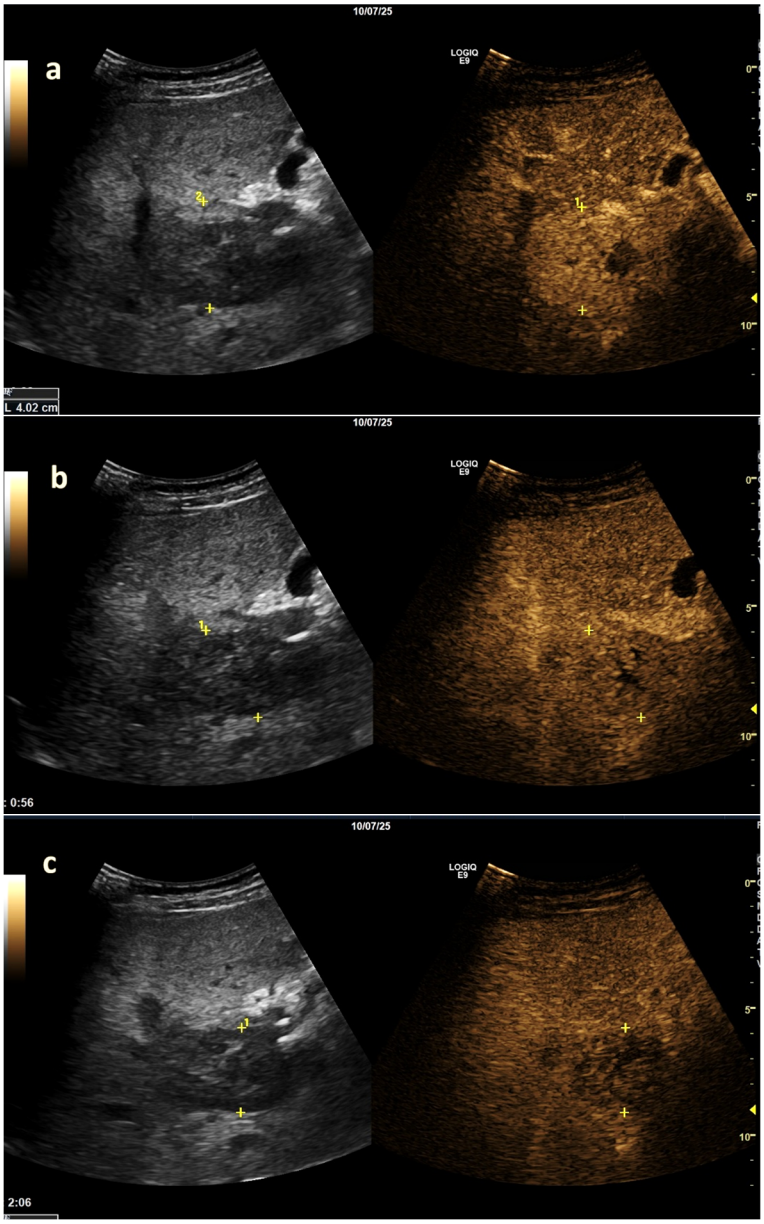


Fig. 9.5.5. Hepatocellular carcinoma. Liver nodule in a cirrhotic patient corresponding to LR-5 category. CEUS examination: the hypoechoic nodule measuring 4cm in B-mode is showing homogeneous hyperenhancement with a small central non-enhancing area in the arterial phase (a), isoenhancement in the portal venous phase (b), and mild and late washout in the late vascular phase (c).

The major features of CEUS LI-RADS for HCC include:

- ***Arterial phase hyperenhancement (APHE)*** occurring 10–20 or 30–45 seconds after contrast injection (Figs. 9.5.6–9.5.7). A liver mass visible on pre-contrast imaging that demonstrates a typical APHE pattern (excluding rim or peripheral discontinuous globular) should be characterized as hepatocellular in origin (CEUS LI-RADS LR-3, LR-4, or LR-5) (11).

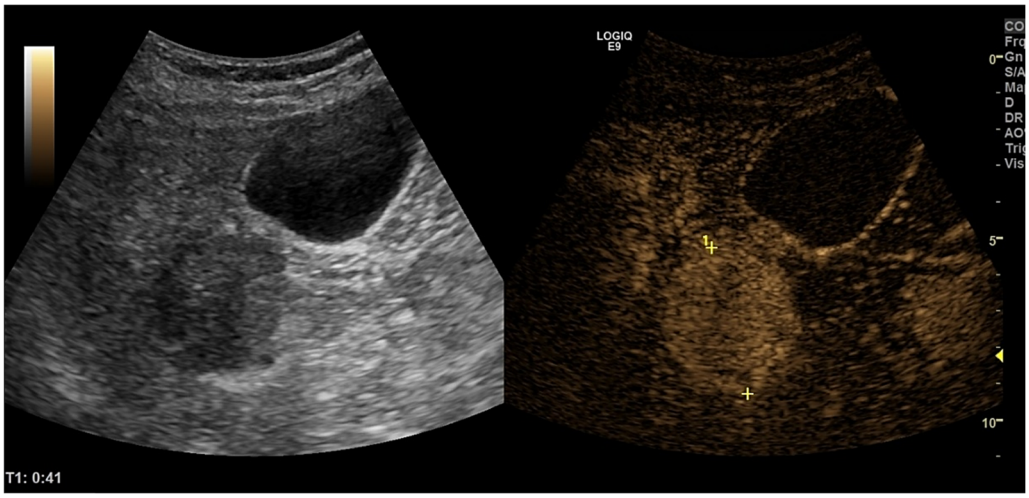


Fig. 9.5.6. Arterial phase hyperenhancement (APHE). CEUS examination: the hypoechoic liver nodule measuring 4 cm in B-mode is showing homogeneous hyperenhancement in the arterial phase.

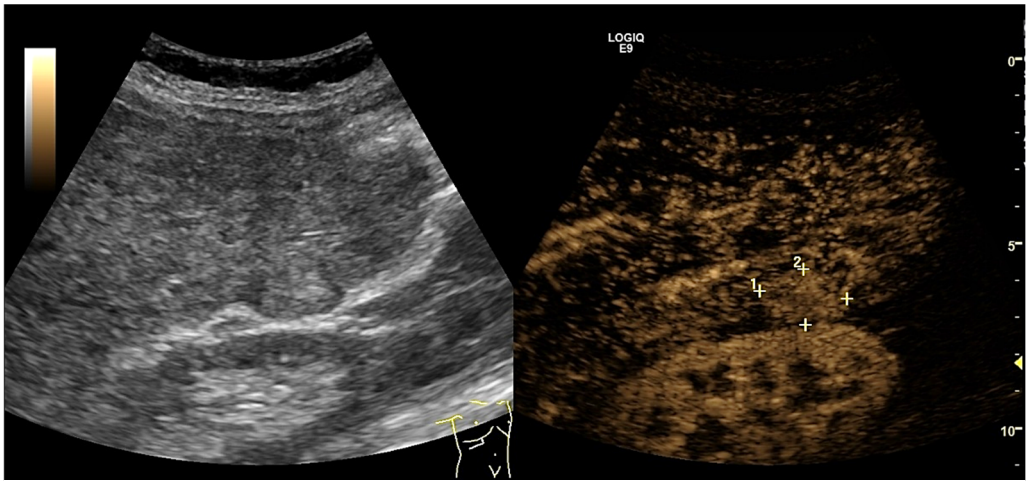


Fig. 9.5.7. Arterial phase hyperenhancement (APHE). CEUS examination: the slightly hyperechoic liver nodule measuring 1.3 cm in B-mode is showing homogeneous hyperenhancement in the arterial phase.

- ***Portal and late-phase washout onset:*** washout detected within 60 seconds of contrast injection is characterized as 'early onset', whereas washout occurring at or after 60 seconds is characterized as 'late onset' (Fig. 9.5.8).

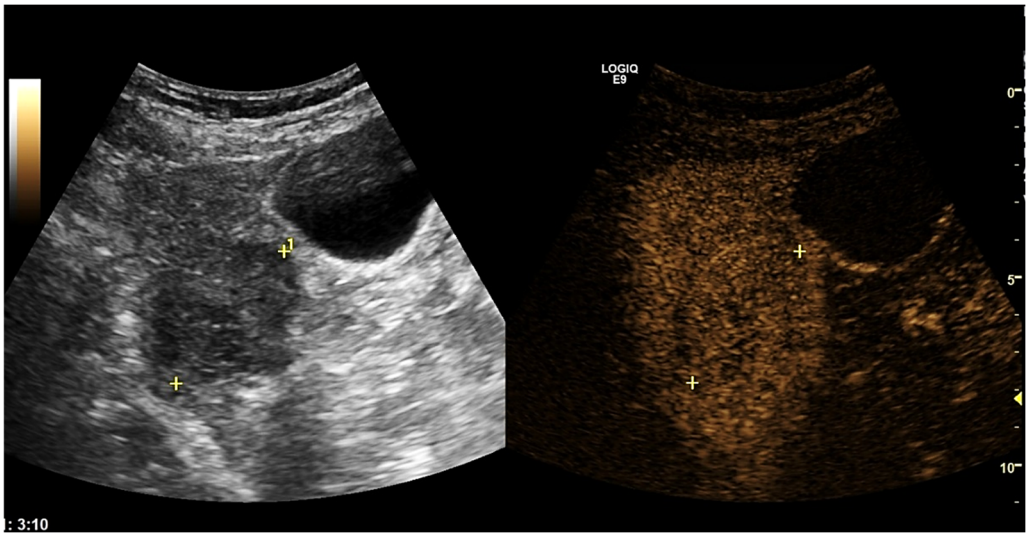


Fig. 9.5.8. Late onset and mild degree washout. CEUS examination: the hypoechoic liver nodule measuring 4 cm in B-mode shows mild and late washout in the late vascular phase.

Washout degree: marked washout suggests categorization as LR-M (Fig. 9.5.9).

HCC typically shows washout with late onset (60 s) and of mild degree, while nonhepatocellular lesions, including ICC, show early onset (<60 s) and/or marked washout.

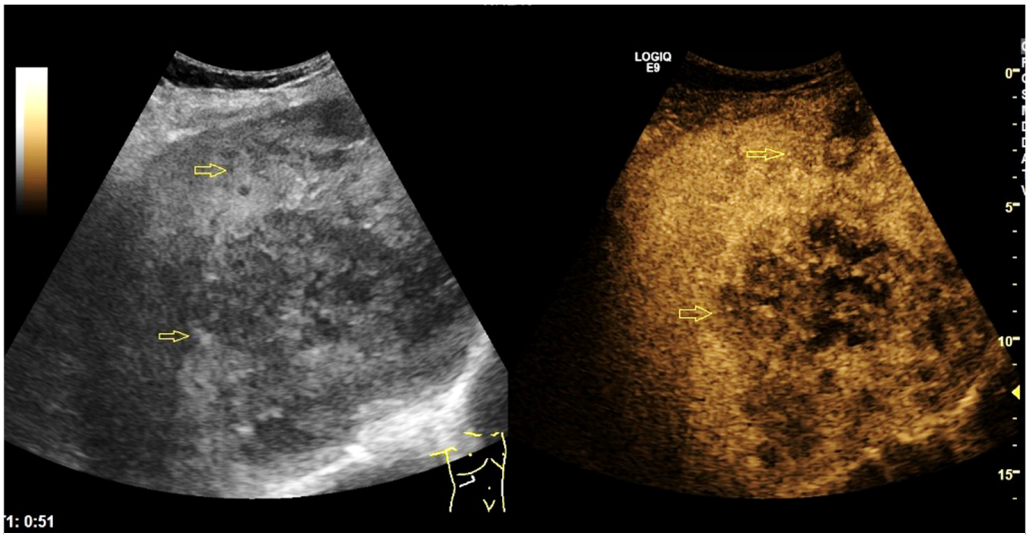


Fig. 9.5.9. Early onset and marked washout. CEUS examination: the heterogeneous hypoechoic liver tumor measuring 12 cm in B-mode shows early onset (<60 s) and marked washout, suggestive of an LR-M lesion.

Table 9.5.I presents the schematic CEUS LI-RADS diagnostic criteria for LR-3, LR-4, and LR-5 lesions, based on arterial phase hyperenhancement (APHE), nodule size, and washout characteristics.

Table 9.5.I. Schematic CEUS LI-RADS diagnostic criteria for LR-3, LR-4, and LR-5 lesions in high-risk patients.

Arterial phase hyperenhancement (APHE)	**No APHE Nodule < 20 mm**	**No APHE Nodule ≥ 20 mm**	**APHE present Nodule < 10 mm**	**APHE present Nodule ≥ 10 mm**
No washout of any type	CEUS LR-3	CEUS LR-3	CEUS LR-3	CEUS LR-4
Late and mild washout	CEUS LR-3	CEUS LR-4	CEUS LR-4	CEUS LR-5

Beyond these schematic criteria, it is important to note that CEUS LR-TIV (definite tumor in vein) is characterized by the presence of enhancing tissue within a vein, independent of liver tumor detection (Fig. 9.5.10). Differentiation between venous tumor invasion and bland thrombus can be achieved by evaluating the timing of microbubble contrast arrival in the vein.

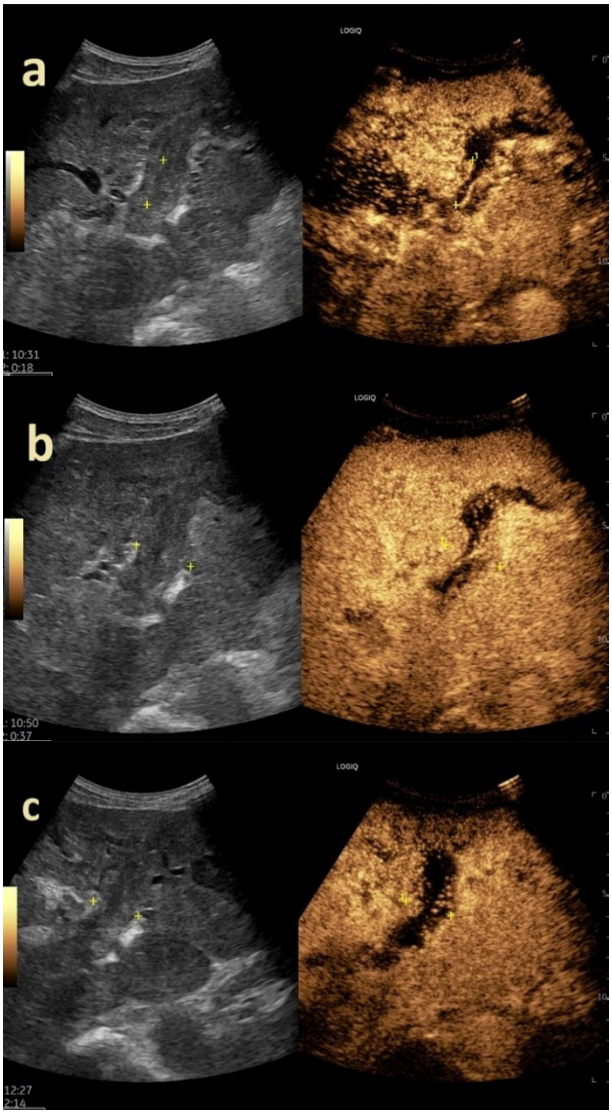


Fig. 9.5.10 CEUS LR-TIV (definite tumor in vein). CEUS examination of a complete portal vein thrombosis: the arterial phase (a, b) shows multilinear and multipunctate thrombus enhancement, followed by washout observed during the late phase (c).

CEUS has been incorporated into diagnostic algorithms for HCC by major international guidelines, including those of the European Association for the Study of the Liver (EASL) (12) and the World Federation for Ultrasound in Medicine and Biology (WFUMB) (2). In patients with cirrhosis and nodules ≥1 cm demonstrating CEUS hallmarks of arterial-phase hyperenhancement and non-rim APHE with late, mild washout, a non-invasive diagnosis of HCC can be established without biopsy.

The accuracy of the LI-RADS algorithm for diagnosing HCC has been assessed in multiple studies (13, 14). One study evaluated 1,000 liver nodules in high-risk patients using CEUS and classified them according to the CEUS LI-RADS algorithm. Using enhanced CT, contrast-enhanced MRI, or histopathology as reference standards, LR-5 was 98.5% predictive for HCC (13). The study also showed that the HCC rate increases progressively from LR-3 to LR-5. Furthermore, most intrahepatic cholangiocarcinomas (iCCAs) were classified as LR-M, along with mixed HCC-ICC tumors and metastases.

A study conducted in a tertiary gastroenterology and hepatology department evaluated 382 patients with 464 focal liver lesions and found that the LR-5 category had comparable accuracy for diagnosing HCC. The sensitivity, specificity, positive predictive value (PPV), and negative predictive value (NPV) were 71.9%, 94.3%, 97.7%, and 49.5%, respectively, resulting in an overall accuracy of 76.9% (14).

A comparative study found that the diagnostic performance of the CEUS LI-RADS algorithm is similar to that of the CT/MRI LI-RADS algorithm for HCC diagnosis (15).

CEUS has some limitations in the evaluation of liver nodules:

- Very small lesions may be missed due to the limited spatial resolution
- Deep located nodules can be difficult to detect, particularly in patients with hepatic steatosis, as this reduces acoustic penetration. Also, subdiaphragmatic lesions are often challenging to visualize due to their difficult anatomical location.
- Differentiating between HCC and other lesions with arterial hyperenhancement can sometimes be challenging (e.g., focal nodular hyperplasia).

Despite these limitations, CEUS plays an important role as a **first-line imaging modality** in the diagnosis of HCC. In clinical practice, when CEUS is performed by an experienced and properly trained physician, the likelihood of misdiagnosis is very low.

MPUS integration:

- *Doppler: HCC appears as a hypervascular tumor exhibiting a characteristic basket pattern on color Doppler imaging*
- *Elastography: usually softer than the surrounding liver parenchyma.*
- *CEUS pattern is suggestive but not always definitive for HCC. The most common features of HCC on CEUS are intense arterial hyper-enhancement and mild late washout.*

9.5.3. CEUS in the diagnosis of cholangiocarcinoma (CCA)

Several risk factors contribute to the development of cholangiocarcinoma, including chronic inflammation of the bile ducts caused by gallstones, sclerosing cholangitis, and environmental factors. Cirrhosis is a common risk factor for both intrahepatic cholangiocarcinoma (iCCA) and HCC, suggesting a shared pathogenesis for these primary liver cancers (16).

Imaging plays an important role in diagnosing cholangiocarcinoma. Despite its poor prognosis, this malignant tumor can be detected during routine imaging examinations. According to the CEUS Liver Imaging Reporting and Data System (LIRADS) algorithm, intrahepatic iCCA is classified as LR M due to rapid and intense washout, similar to liver metastases and poorly differentiated hepatocellular carcinomas. Metastases are diagnosed based on the patient's clinical context, whereas patients at risk of HCC require biopsy and histopathological examination to differentiate between cholangiocarcinoma and HCC.

Key predictive features on CEUS include peripheral-to-center progressive filling and rapid, intense washout (Fig. 9.5.11 -9.5.12).

In iCCA, various enhancement patterns are observed during the arterial phase of contrast-enhanced ultrasound examinations (17, 18, 19):

a) Peripheral, irregular, rim-like hyperenhancement
b) Heterogeneous hypoenhancement
c) Heterogeneous hyperenhancement
d) Homogeneous hyperenhancement

All iCCA shows washout during the portal and late phases.

A study involving 819 patients (HCC = 546; iCCA = 273) reported that the most common arterial phase pattern of iCCA was peripheral rim-like enhancement, observed in 68.5% of cases (17).

Chen et al. evaluated CEUS characteristics in 41 patients with histologically confirmed cholangiocarcinoma (18). The predominant arterial phase enhancement pattern was heterogeneous hyperenhancement, observed in 61.9% of lesions, followed by homogeneous hyperenhancement (19.0%), rim-like hyperenhancement (9.5%), isointense enhancement (4.8%), and hypointense enhancement (4.8%). Washout was present in 85.7% of lesions during the portal venous phase.

Xu et al. (19) found that most iCCAs smaller than 3 cm exhibit homogeneous enhancement, whereas larger tumors display heterogeneous enhancement or a peripheral enhancing rim, indicating that hyper-enhancement correlates with proliferation degree.

A meta-analysis by Chen et al. concluded that CEUS demonstrated excellent diagnostic capability in differentiating iCCA from HCC (21). The most important features of HCC include arterial hyperenhancement and mild, late washout (greater than 60 seconds), whereas rim-like enhancement and intense, early washout characterize iCCA.

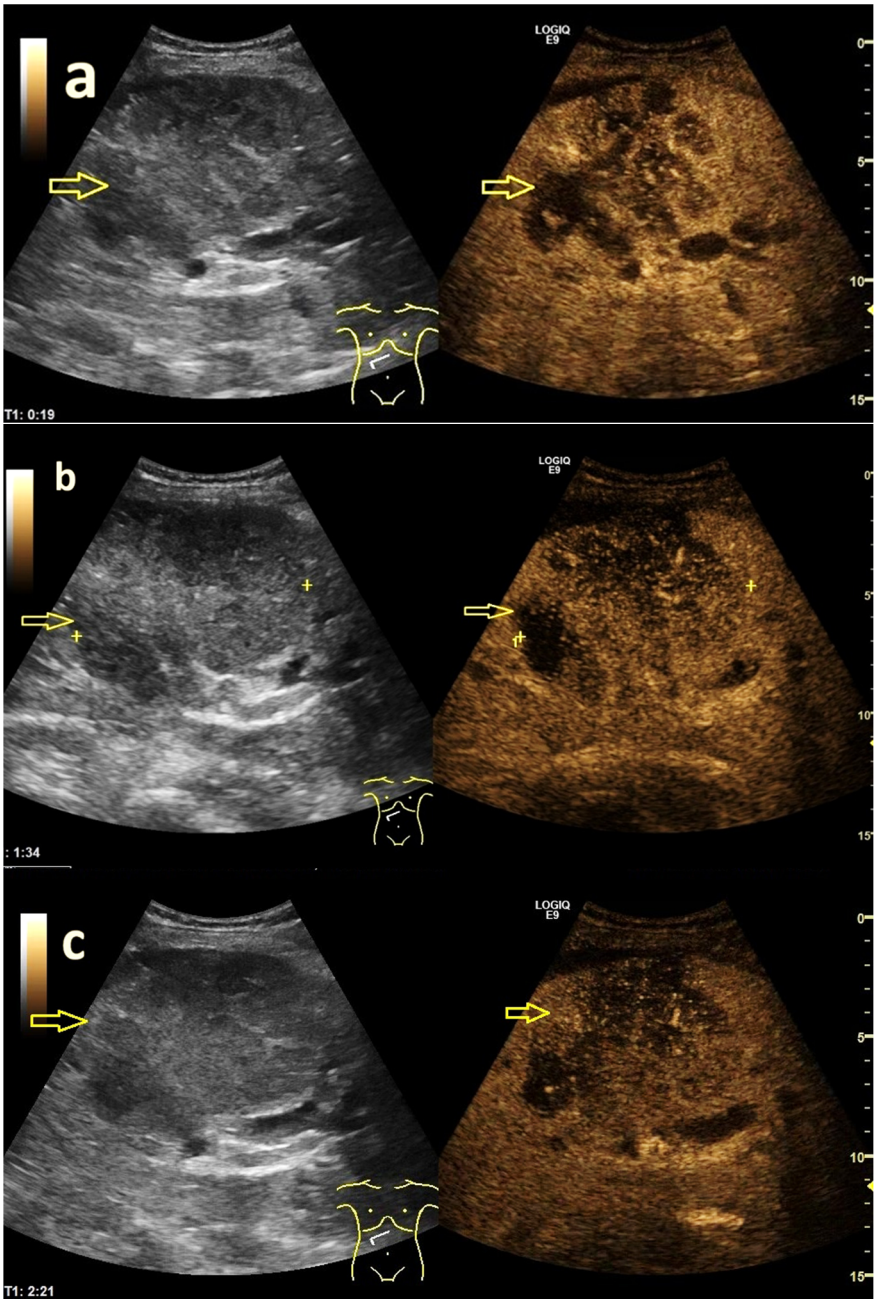


Fig. 9.5.11. Intrahepatic cholangiocarcinoma. CEUS examination: the large heterogeneous hypoechoic liver tumor in B-mode shows heterogeneous hyperenhancement in the arterial phase (a) and marked, rapid washout in the portal venous and late phases (b, c).

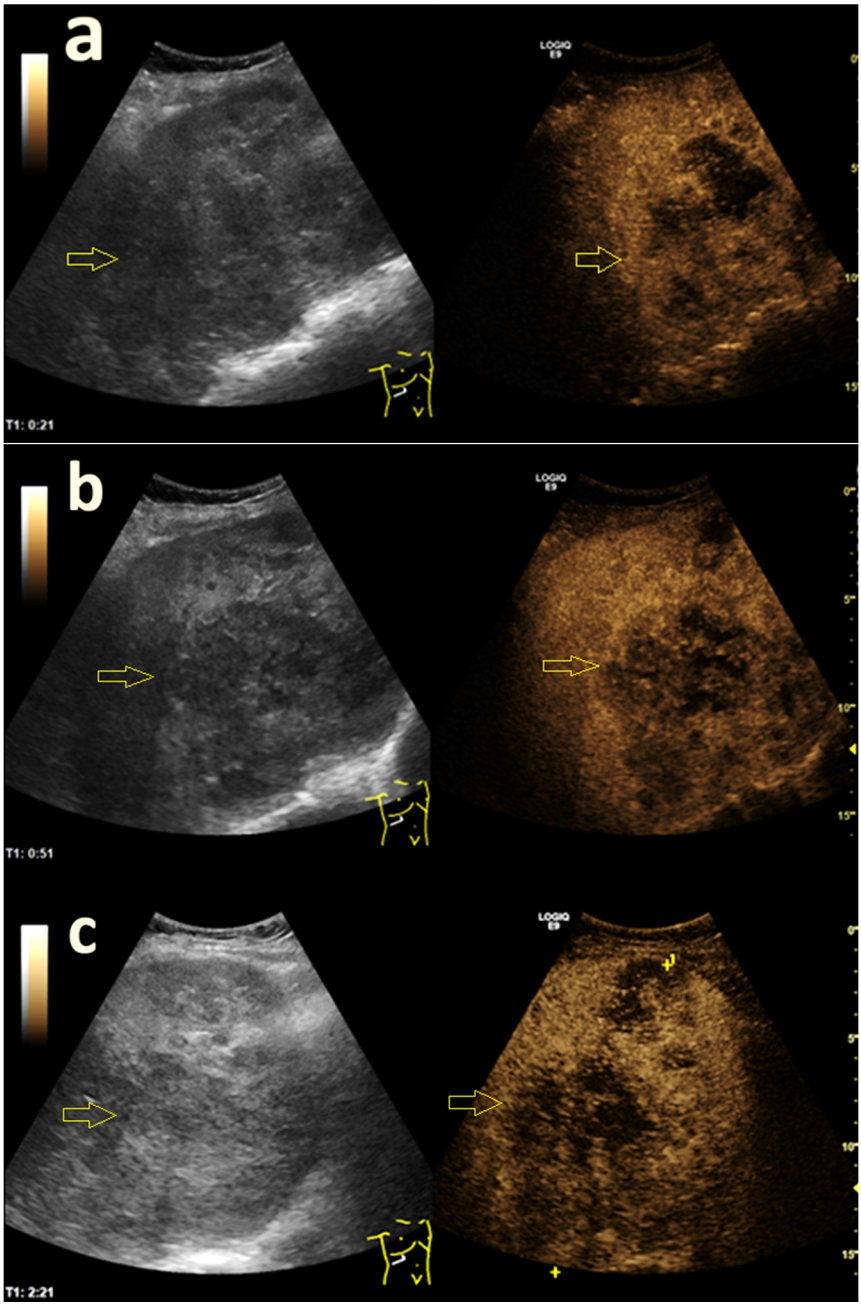
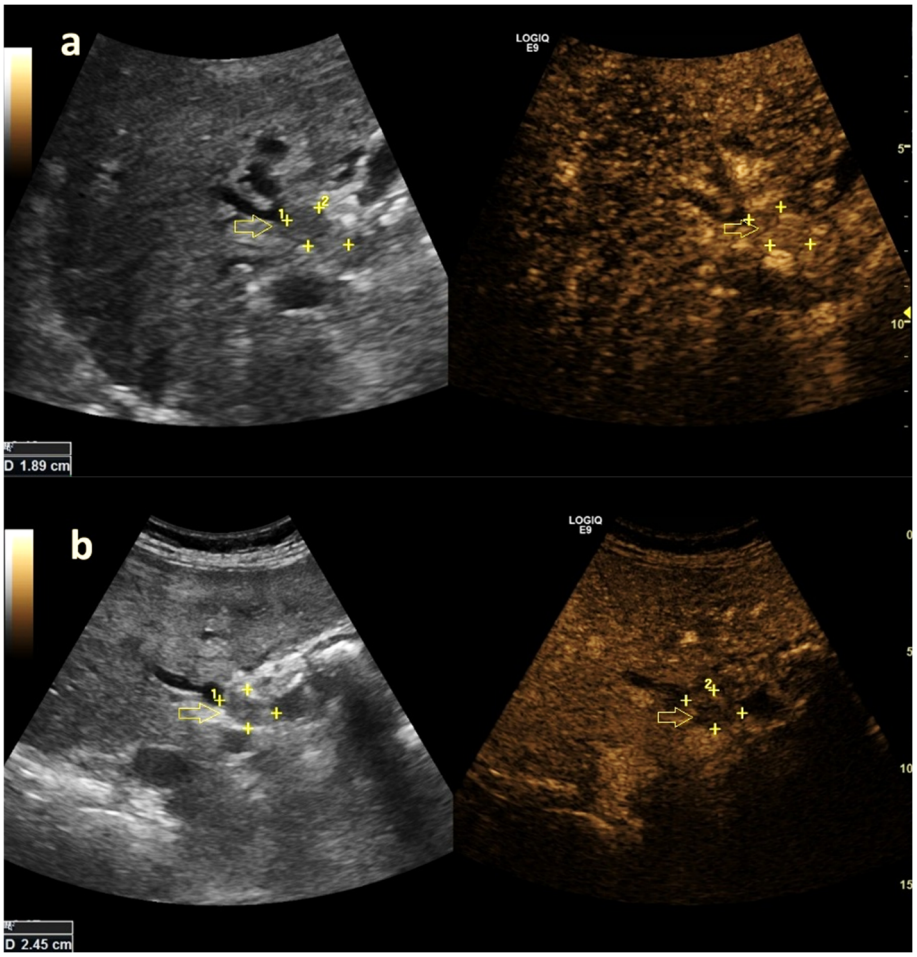


Fig. 9.5.12. Intrahepatic cholangiocarcinoma. CEUS examination: the large heterogeneous hypoechoic liver tumor in B-mode shows Peripheral, irregular, rim-like hyperenhancement in the arterial phase (a) and marked, rapid washout in the portal venous and late phases (b, c).

During CEUS examination, perihilar cholangiocarcinoma (pCCA) exhibits heterogeneous hyperenhancement in the arterial phase, while visible intraductal CCA shows homogeneous hyperenhancement (Fig. 9.5.13). Both lesion types demonstrate rapid and intense washout during the portal and late phases. The arterial enhancement of intraductal CCAs facilitates differentiation from avascular structures such as biliary sludge.



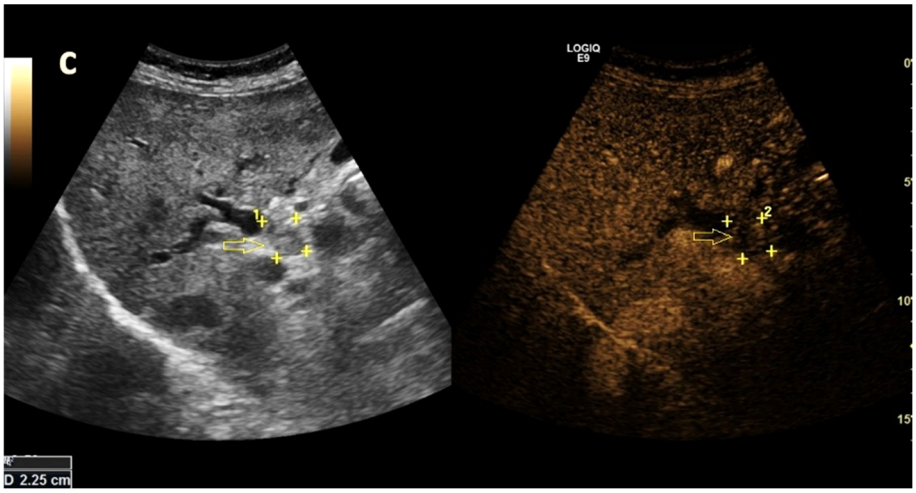


Fig. 9.5.13. Intraductal cholangiocarcinoma. CEUS examination: the hypoechoic area within the main biliary duct in B-mode shows homogeneous hyperenhancement in the arterial phase (a) and washout in the portal venous and late phases (b, c).

MPUS integration:

- *Doppler: iCCAs are solid tumors with low vascularity.*
- *Elastography: iCCA is stiffer on elastography due to its high fibrosis content.*
- *CEUS: The most characteristic pattern is rim enhancement in the arterial phase followed by a rapid and intense washout starting from the portal phase.*

9.5.4. CEUS in liver metastases

Ultrasound plays an important role in the surveillance of oncological patients. Liver metastases frequently complicate various cancers, particularly those originating from the gastrointestinal tract. The sensitivity of ultrasound for detecting metastases is reported in the literature as low and variable, ranging from 50% to 76% (21, 22).

Early detection of liver metastases is essential for optimizing treatment and improving prognosis in cancer patients.

Contrast-enhanced ultrasound (CEUS) is a valuable modality for detecting and characterizing liver metastases. Most studies report that CEUS is more sensitive and accurate than conventional grey-scale ultrasound for detecting metastases, particularly small nodules (23).

Numerous studies have demonstrated the high sensitivity of CEUS in diagnosing liver metastases. For instance, Friedrich-Rust's meta-analysis reported a CEUS sensitivity of 91%, while a Romanian multicenter study found sensitivity, specificity, and accuracy values of 87.1%, 82.9%, and 83.7%, respectively (24, 25).

A meta-analysis of 47 studies showed that CEUS has diagnostic capabilities comparable to those of diffusion-weighted imaging (DWI) and contrast-enhanced magnetic resonance imaging (CEMRI), particularly for lesions measuring 10 mm or larger (26).

A recent study compared the sensitivity of contrast-enhanced ultrasound (CEUS) for detecting liver metastases with that of multidetector computed tomography (MDCT), magnetic resonance imaging (MRI), and fluorodeoxyglucose (FDG) positron emission tomography (PET)/CT. MRI demonstrated higher sensitivity than CEUS, MDCT, and FDG PET/CT for lesions measuring 1 cm or less. The use of a hepatospecific contrast agent did not enhance diagnostic performance (27).

During CEUS, liver metastases display variable arterial-phase patterns, including peripheral rim-like enhancement, characteristic of hypovascular metastases (Fig. 9.5.14 – 9.5.16), and arterial hyperenhancement, typical of hypervascular metastases (Fig. 9.5.17 – 9.5.18) (28). Some metastases may present central non-enhancing areas in the arterial phase due to tumor necrosis. Washout typically begins early, often in the portal venous phase, and becomes evident in the portal and late phases, leading to metastases appearing as hypoechoic lesions within the liver. Consequently, CEUS can detect liver metastases that are not visible on standard ultrasound.

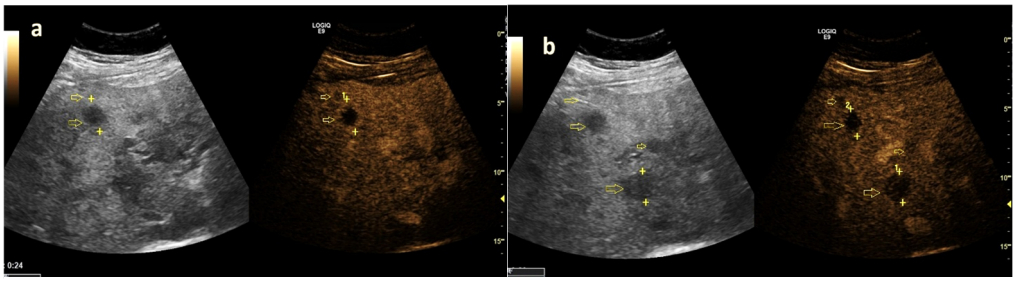


Fig. 9.5.14. Hypovascular metastases. CEUS: the hypoechoic lesions in B mode with peripheral rim-like enhancement in the arterial phase (a) and early washout in the portal venous phase (b).

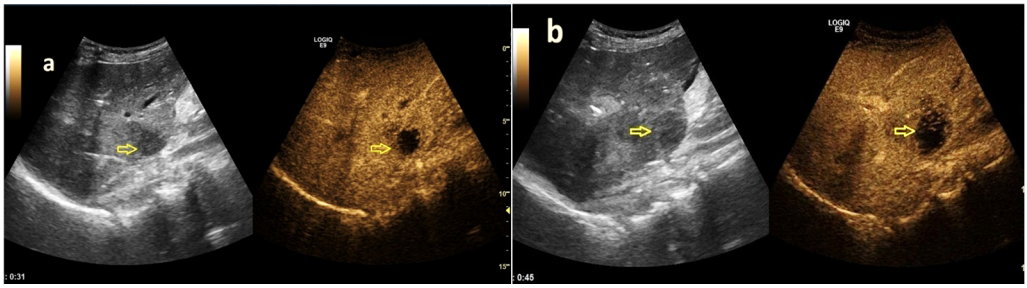


Fig. 9.5.15. Hypovascular metastasis. CEUS: the hypoechoic lesion in B mode with peripheral rim-like enhancement in the arterial phase (a) and early washout in the portal phase (b).

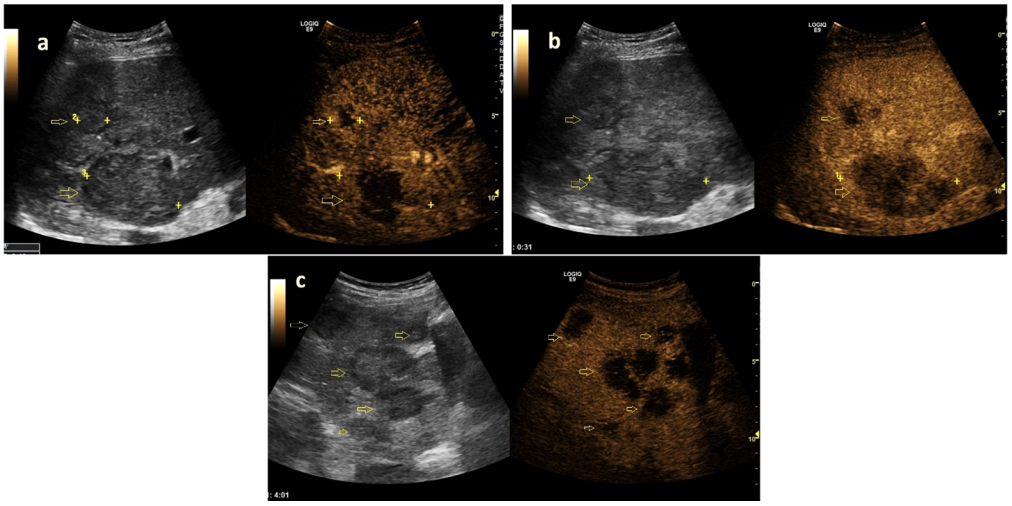


Fig. 9.5.16. Hypovascular metastases. CEUS: the hypoechoic lesions in B mode with peripheral rim-like enhancement (a) and early washout starting from the arterial phase (b); other multiple metastases with marked washout in the late phase (c).

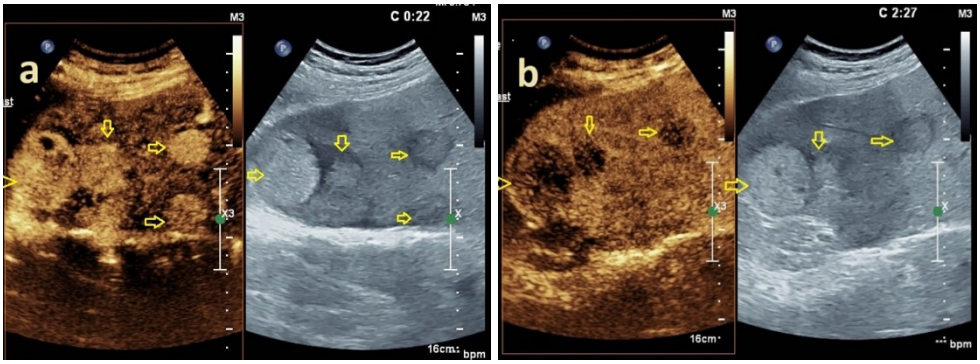


Fig. 9.5.17. Hypervascular metastases. CEUS: the hyperechoic lesions seen in B mode are hyperenhancing in the arterial phase (a) with marked washout in the late phase (b).

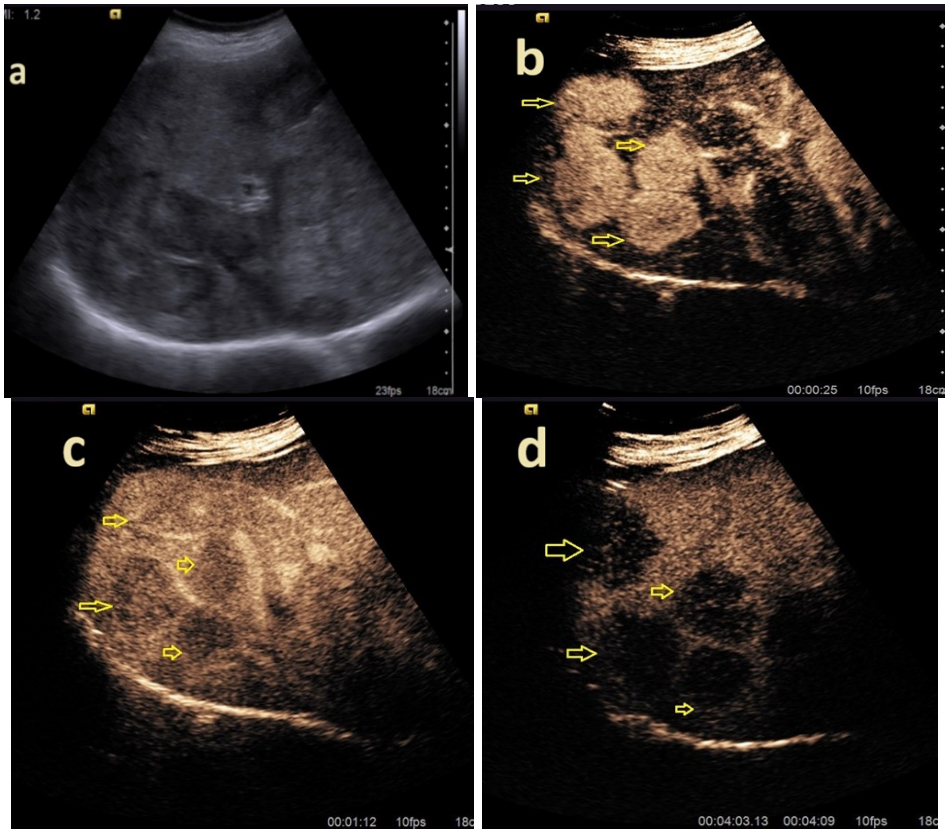


Fig. 9.5.18. Hypervascular metastases. Conventional US B-mode: multiple hyperechoic with hypoechoic halo FLLs suggestive for liver metastases (a). CEUS: the lesions are hyperenhancing in the arterial phase (b) with marked washout in the portal (c) and late phases (d).

The patterns of liver metastasis on CEUS can be influenced by factors such as primary malignant tumors with different biological behaviors and pathological changes associated with tumor growth (29) (Fig. 9.5.19).

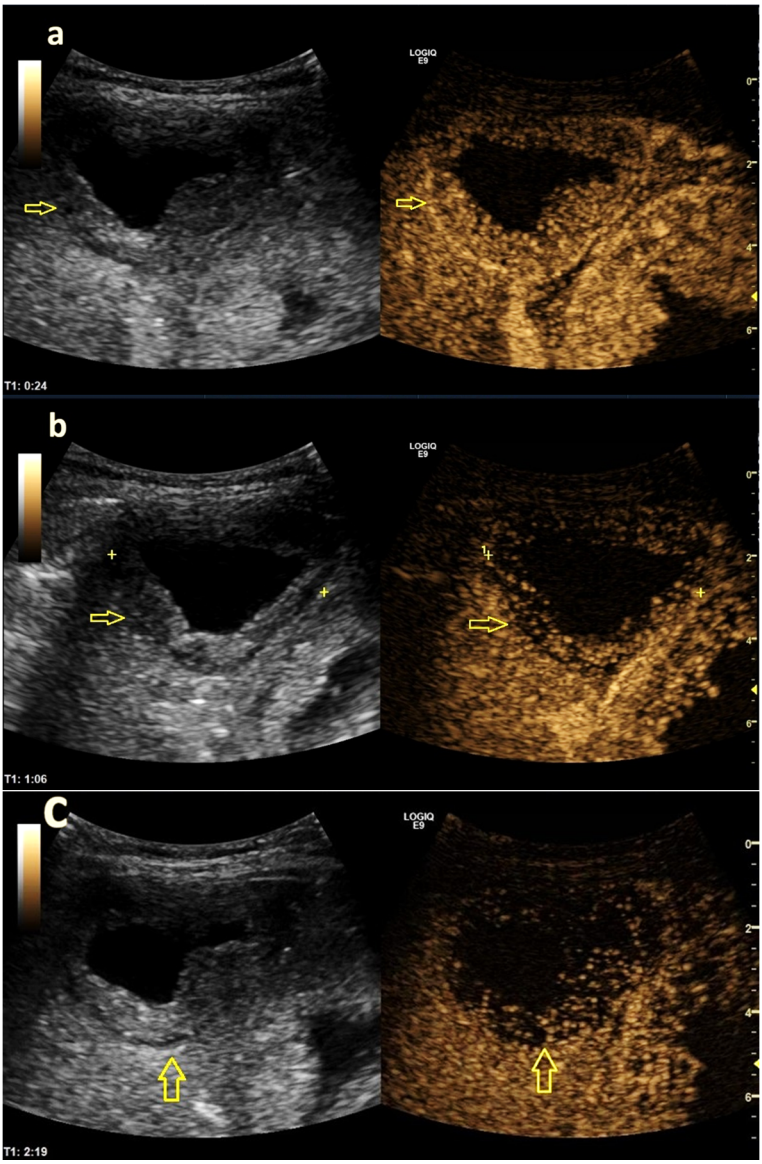


Fig. 9.5.19. Biopsy-confirmed liver metastasis in a patient with malignant GIST. CEUS shows that the lesion is hyperenhancing at the periphery, with a large central non-enhancing area in the arterial phase (a), and marked washout in the portal (b) and late phases (c).

Absence or delayed washout, commonly observed in hepatocellular carcinoma (HCC), may also occur in certain metastases, such as neuroendocrine metastases (30). This phenomenon results from the vascular and cellular characteristics of neuroendocrine tumor metastases, which are well vascularized primarily via the hepatic artery, leading to arterial phase hyperenhancement. The high cellular density of these tumors causes contrast retention during the portal and late phases, explaining the absence of washout (Fig. 9.5.20).

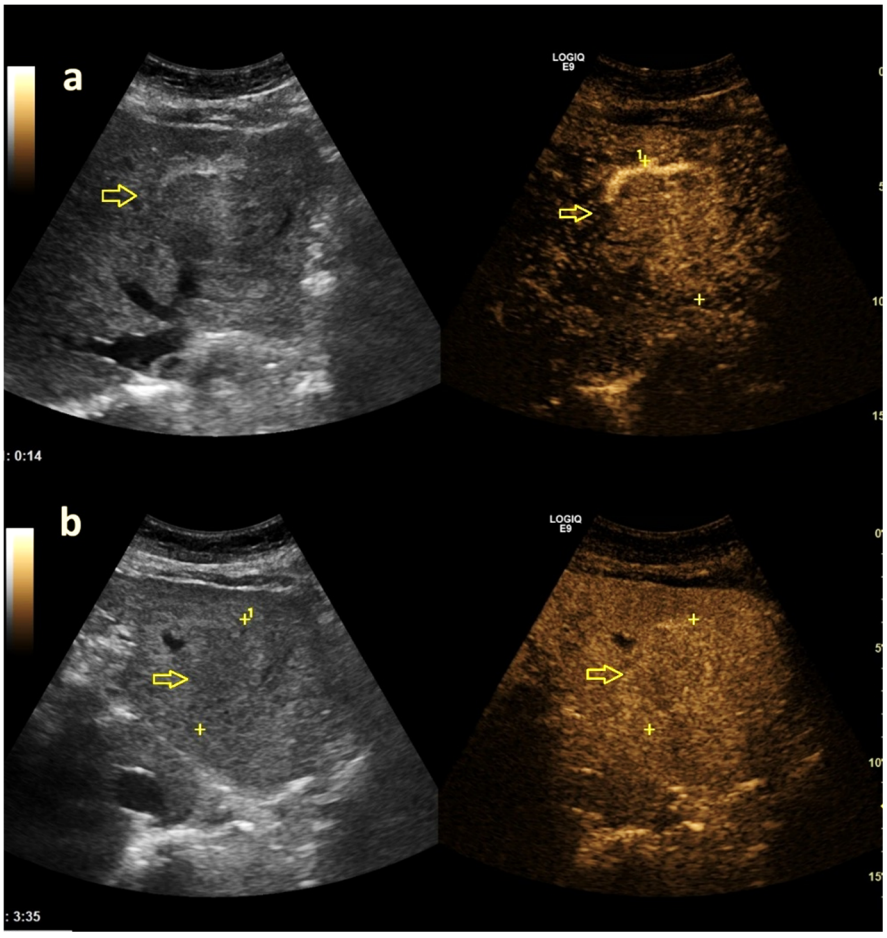


Fig. 9.5.20. Biopsy-confirmed liver metastasis in a patient with history of melanoma. CEUS shows that the lesion is hyperenhancing in the arterial phase (a) without washout in late phase (b).

MPUS integration:

- *Doppler: color Doppler can sometimes identify chaotic vascular architecture.*
- *Elastography: liver metastases appear as hard lesions.*
- *CEUS: the most characteristic feature is early washout.*

9.5.5. Take-home message

- The most common features of HCC on CEUS are intense arterial hyperenhancement and mild late washout.
- The use of the LI-RADS algorithm has allowed CEUS to be reintroduced as an alternative imaging method for diagnosing HCC in the EASL guidelines.
- The LR5 category demonstrates high predictive value for HCC.
- On CEUS examination, iCCA shows a distinct arterial phase enhancement pattern, most commonly characterized by peripheral rim-like enhancement. During the portal and late phases, iCCA presents intense washout.
- Liver metastases on CEUS can be classified as hypervascular (hyperenhancing in the arterial phase) or hypovascular (rim-like enhancement). The most common pattern of liver metastases is a rapid, intense washout that begins early in the portal phase.

References

1. Friedrich-Rust M, Klopffleisch T, Nierhoff J, Herrmann E, Vermehren J, Schneider MD, et al. Contrast-Enhanced Ultrasound for the differentiation of benign and malignant focal liver lesions: a meta-analysis. Liver Int. 2013 May;33(5):739-55.

2. Claudon M, Dietrich CF, Choi BI, Cosgrove DO, Kudo M, Nolsoe CP, et al. Guidelines and good clinical practice recommendations for Contrast Enhanced Ultrasound (CEUS) in the liver – update 2012: A WFUMB-EFSUMB initiative in cooperation with representatives of AFSUMB, AIUM, ASUM, FLAUS and ICUS. Ultrasound Med Biol 2013; 39: 187–210.

3. Giorgio A, Montesarchio L, Gatti P, Amendola F, Matteucci P, Santoro B, et al. Contrast-Enhanced Ultrasound: a simple and effective tool in defining a rapid diagnostic work-up for small nodules detected in cirrhotic patients during surveillance. J Gastrointestin Liver Dis, June 2016 Vol. 25 No 2: 205-211.

4. Jang HJ, Kim TK, Burns PN, Wilson SR. Enhancement patterns of hepatocellular carcinoma at contrast-enhanced US: comparison with histologic differentiation. Radiology. 2007 Sep;244(3):898-906.

5. Durot I, Wilson SR, Willmann JK. Contrast-enhanced ultrasound of malignant liver lesions. Abdom Radiol (NY). 2018;43: 819–847.
6. Sporea I, Sandulescu DL, Sirli R, Popescu A, Danilă M, Spârchez Z, et al. Contrast Enhanced Ultrasound for the characterization of malignant versus benign focal liver lesion in a prospective multicenter experience – The SRUMB Study. J Gastrointestin Liver Dis 2019;28: 191-196.
7. Strobel D, Seitz K, Blank W, Schuler A, Dietrich C, von Herbay A, et al. Contrast-enhanced ultrasound for the characterisation of focal liver lesions-diagnostic accuracy in clinical practice (DEGUM multicenter trial). Ultraschall Med 2008; 29:499-505.
8. Tranquart F, Le Gouge A, Correas JM, et al. Role of contrast-enhanced ultrasound in the blinded assessment of focal lesions in comparison with MDCT and CEMRI: Results from a multicentre clinical trial. EJC Supplements 2008; 6:9–15.
9. Vilana R, Forner A, Bianchi L, García-Criado A, Rimola J, de Lope CR, et al. Intrahepatic peripheral cholangiocarcinoma in cirrhosis patients may dysplasia vascular pattern similar to hepatocellular carcinoma on contrast-enhanced ultrasound. Hepatology 2010;51: 2020-2029.
10. Galassi M, Iavarone M, Rossi S, Bota S, Vavassori S, Rosa L, et al. Patterns of appearance and risk of misdiagnosis of intrahepatic cholangiocarcinoma in cirrhosis at contrast enhanced ultrasound. Liver Int 2013;33(5):771–779.
11. Wilson SR, Lyshchik A, Piscaglia F, Cosgrove D, Jang HJ, Sirlin C, et al. CEUS LI-RADS: Algorithm, implementation, and key differences from CT/MRI. Abdom Radiol (NY) 2018;43: 127-142.
12. EASL Clinical Practice Guidelines on the management of hepatocellular carcinoma European Association for the Study of the Liver et al. Journal of Hepatology, Volume 82, Issue 2, 315 – 374.
13. Terzi E, Iavarone M, Pompili M, Veronese L, Cabibbo G, Fraquelli M, et al. CEUS LI-RADS Italy study group collaborators: Contrast ultrasound LI-RADS LR-5 identifies hepatocellular carcinoma in cirrhosis in a multicenter restropective study of 1,006 nodules. J Hepatol. 2018 Mar;68(3):485-492.
14. Ghiuchici AM, Dănilă M, Popescu A, Șirli R, Moga T, Sporea I, et al. Contrast-enhanced ultrasound algorithm (ACR CEUS LI-RADSv 2017)- a valuable tool for the noninvasive diagnosis of hepatocellular carcinoma in patients with chronic liver disease. Med Ultrason. 2021 Nov 25;23(4):383-389.
15. Wang H, Cao J, Fan H, Huang J, Zhang H, Ling W. Compared with CT/MRI LI-RADS, whether CEUS LI-RADS is worth popularizing in diagnosis of hepatocellular carcinoma? -a direct head-to-head meta-analysis. Quant Imaging Med Surg. 2023 Aug 1;13(8):4919-4932.
16. Palmer WC, Patel T. Are common factors involved in the pathogenesis of primary liver cancers? A meta-analysis of risk factors for Intrahepatic cholangiocarcinoma. J Hepatol 2012;57: 69-76.

17. Liu GJ, Wang W, Lu MD, Xie XY, Xu HX, Xu Z F, et al. Contrast-Enhanced Ultrasound for the Characterization of Hepatocellular Carcinoma and Intrahepatic Cholangiocarcinoma. Liver Cancer. 2015 Dec;4(4):241-52.
18. Chen T, Chang X, Lv K, Wang Y, Fu X, Tan L, et al. Contrast-enhanced Ultrasound Features of Intrahepatic Cholangiocarcinoma: A New Perspective. Sci Rep. 2019 Dec 18;9(1):19363.
19. Xu HX, Chen LD, Liu LN, Zhang YF, Guo LH, Liu C. Contrast-enhanced ultrasound of intrahepatic cholangiocarcinoma: correlation with pathological examination. Br J Radiol 2012; 85: 1029-1037
20. Chen Y, Zhu Y, Chen K, Wang H, Zhang W, Bao J, et al. Differentiation between hepatocellular carcinoma and intrahepatic cholangiocarcinoma using contrast-enhanced ultrasound: A systematic review and meta-analysis. Clin Hemorheol Microcirc. 2021;79(2):293-309.
21. Albrecht T, Hohmann J, Oldenburg A, Skrok J, Wolf KJ. Detection and characterisation of liver metastases. Eur Radiol. 2004;14 Suppl 8: P25–P33.
22. Glover C, Douse P, Kane P, Karani J, Meire H, Mohammadtaghi S, et al. Accuracy of investigations for asymptomatic colorectal liver metastases. Dis Colon Rectum. 2002;45: 476–484.
23. Larsen LP, Rosenkilde M, Christensen H, Bang N, Bolvig L, Christiansen T, et al. The value of contrast enhanced ultrasonography in detection of liver metastases from colorectal cancer: a prospective double-blinded study. Eur J Radiol 2007; 62: 302– 307
24. Friedrich-Rust M, Klopffleisch T, Nierhoff J, Herrmann E, Vermehren J, Schneider MD, et al. Contrast-Enhanced Ultrasound for the differentiation of benign and malignant focal liver lesions: a meta-analysis. Liver Int 2013;33: 739-755.
25. Sporea I, Badea R, Popescu A, Spârchez Z, Sirli RL, Dănilă M, et al. Contrast-enhanced ultrasound (CEUS) for the evaluation of focal liver lesions – a prospective multicenter study of its usefulness in clinical practice. Ultraschall Med 2014;35: 259-266.
26. Zhang L, Zhang L, Wang H, Chen L, Sui G. Diagnostic performance of contrast-enhanced ultrasound and magnetic resonance imaging for detecting colorectal liver metastases: A systematic review and meta-analysis. Dig Liver Dis. 2019 Sep;51(9):1241-1248.
27. Tsili AC, Alexiou G, Naka C, Argyropoulou MI. Imaging of colorectal cancer liver metastases using contrast-enhanced US, multidetector CT, MRI, and FDG PET/CT: a meta-analysis. Acta Radiol. 2021 Mar;62(3):302-312.
28. Claudon M, Cosgrove D, Albrecht T, Bolondi L, Bosio M, Calliada F, et al. Guidelines and good clinical practice recommendations for contrast enhanced ultrasound (CEUS) - update 2008. Ultraschall Med. 2008 Feb;29(1):28-44.
29. Kong WT, Ji ZB, Wang WP, Cai H, Huang BJ, Ding H. Evaluation of Liver Metastases Using Contrast-Enhanced Ultrasound: Enhancement Patterns and Influencing Factors. Gut Liver. 2016 Mar;10(2):283-7.
30. Möller K, Sawatzki M, Jenssen C, Serra C, Bakken S, Görg C, et al. Pitfalls in contrast enhanced ultrasound: lack of washout in malignant liver lesions. A scoping review. Minerva Med. 2025 Oct;116(5):381-404.

9.6. Contrast-Enhanced Ultrasound (CEUS) for the Follow-Up of Percutaneous Treatment of Liver Tumors

Felix Bende, Tudor Moga

Abstract

Contrast-enhanced ultrasound (CEUS) has emerged as a valuable imaging modality for evaluating therapeutic response after percutaneous thermal ablation of liver tumors, particularly radiofrequency ablation (RFA) and microwave ablation (MWA). Owing to its real-time imaging capability and the purely intravascular nature of ultrasound contrast agents, CEUS enables accurate assessment of tissue perfusion and early detection of residual viable tumor. Following successful ablation, the treated area typically appears as a well-defined non-enhancing zone corresponding to coagulative necrosis, whereas nodular or irregular arterial phase enhancement indicates residual or recurrent tumor tissue. CEUS can be performed immediately after the procedure to assess treatment efficacy and guide additional ablation when necessary, and it can also be used during follow-up examinations to monitor local tumor control. Compared with contrast-enhanced CT and MRI, CEUS offers several advantages, including the absence of ionizing radiation, safety in patients with renal impairment, and the possibility of bedside real-time evaluation. Consequently, CEUS represents a reliable and increasingly integrated imaging tool in the post-treatment surveillance of patients undergoing percutaneous ablation of focal liver lesions.

9.6.1. Introduction

Percutaneous thermal ablation techniques, primarily radiofrequency ablation (RFA) and microwave ablation (MWA), have become established therapeutic options for hepatocellular carcinoma (HCC), liver metastases, and selected benign hepatic lesions in patients unsuitable for surgical resection or as bridging therapy to transplantation. The oncologic objective of local ablation is complete tumor necrosis with an adequate safety margin, generally considered to be at least 5–10 mm beyond the visible tumor boundary (1,2).

Accurate and early assessment of treatment response is critical to ensure complete tumor eradication and to identify residual viable tissue requiring retreatment. Traditionally, contrast-enhanced computed tomography (CE-CT) and contrast-enhanced magnetic resonance imaging (CE-MRI) have

been considered reference methods for post-ablation evaluation. However, CEUS has progressively gained a central role in this setting due to its real-time dynamic imaging capability, absence of ionizing radiation, and use of purely intravascular contrast agents.

Unlike iodinated or gadolinium-based contrast media, ultrasound contrast agents (UCAs) consist of microbubbles that remain confined to the vascular space. Therefore, CEUS provides a direct assessment of tissue perfusion and microvascularization, making it particularly suitable for distinguishing viable tumor tissue from post-ablative necrosis (3–5).

9.6.2. Principles of CEUS in the Post-Ablation Setting

1. Mechanism of Contrast Enhancement

Ultrasound contrast agents (e.g., sulfur hexafluoride microbubbles) enhance backscatter signals from blood flow, allowing visualization of microvascular perfusion in real time. In treated lesions, tissue viability directly correlates with perfusion. Necrotic tissue lacks microcirculation and appears non-enhancing across all vascular phases.

CEUS examination typically includes:

- Arterial phase (10–30 seconds after injection)
- Portal venous phase (30–120 seconds)
- Late phase (>120 seconds up to 4–6 minutes)

The interpretation of treatment response relies on dynamic enhancement behavior across these phases (5).

2. Expected Imaging Changes After Thermal Ablation

Thermal ablation induces coagulative necrosis within the target lesion and a surrounding safety margin. Immediately after treatment, the ablation zone appears as a sharply demarcated, avascular region on CEUS. The absence of intralesional enhancement is the fundamental imaging criterion of complete response.

However, perilesional reactive hyperemia frequently develops within the first 24–72 hours. This benign inflammatory response manifests as a thin, regular rim of arterial enhancement without washout in later phases and should not be misinterpreted as residual tumor (6, 7).

9.6.3. Timing of CEUS in the Follow-Up Protocol

1. Immediate Post-Procedural Assessment

CEUS can be performed immediately after ablation (Fig. 9.6.1) or within the first 24 hours. Early evaluation provides the opportunity to detect residual viable tumor tissue during the same treatment session.

Residual disease is suspected when:

- Nodular or irregular arterial phase enhancement is present within or at the periphery of the ablation zone
- Enhancement demonstrates washout in portal or late phases (particularly in HCC)

Immediate CEUS-guided retreatment significantly improves complete ablation rates and reduces the need for additional sessions (4,8).

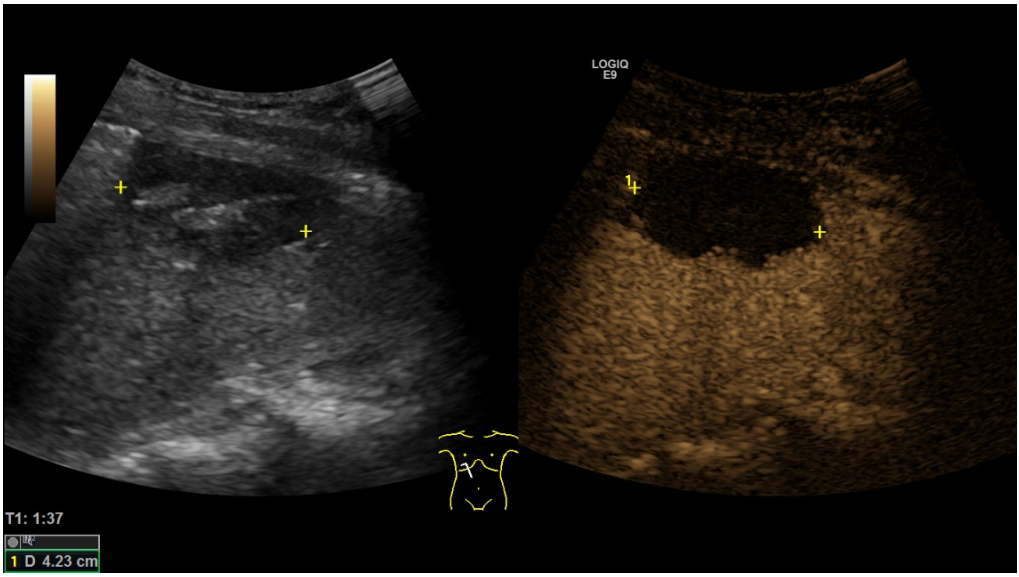


Fig. 9.6.1. Contrast-enhanced ultrasound (CEUS) performed within the first 24 hours after percutaneous microwave ablation (MWA) of a solitary liver metastasis. The grayscale B-mode image (left) demonstrates the post-ablation zone corresponding to the treated lesion. On contrast-specific imaging (right), the ablation area appears as a well-defined non-enhancing region, consistent with complete coagulative necrosis of the treated tumor.

2. Short-Term Follow-Up (4–6 Weeks)

Most international guidelines recommend contrast-enhanced cross-sectional imaging at 4–6 weeks after ablation to confirm treatment efficacy (1,5). CEUS may serve as:

- A primary follow-up tool in experienced centers
- A complementary modality when CT/MRI findings are equivocal
- An alternative imaging method in patients with renal insufficiency or contrast allergies

At this stage, inflammatory hyperemia has typically subsided, improving diagnostic specificity. If hypervascular enhancement adjacent to the necrotic area appears, it is highly suggestive of residual viable tumor (Fig. 9.6.2).

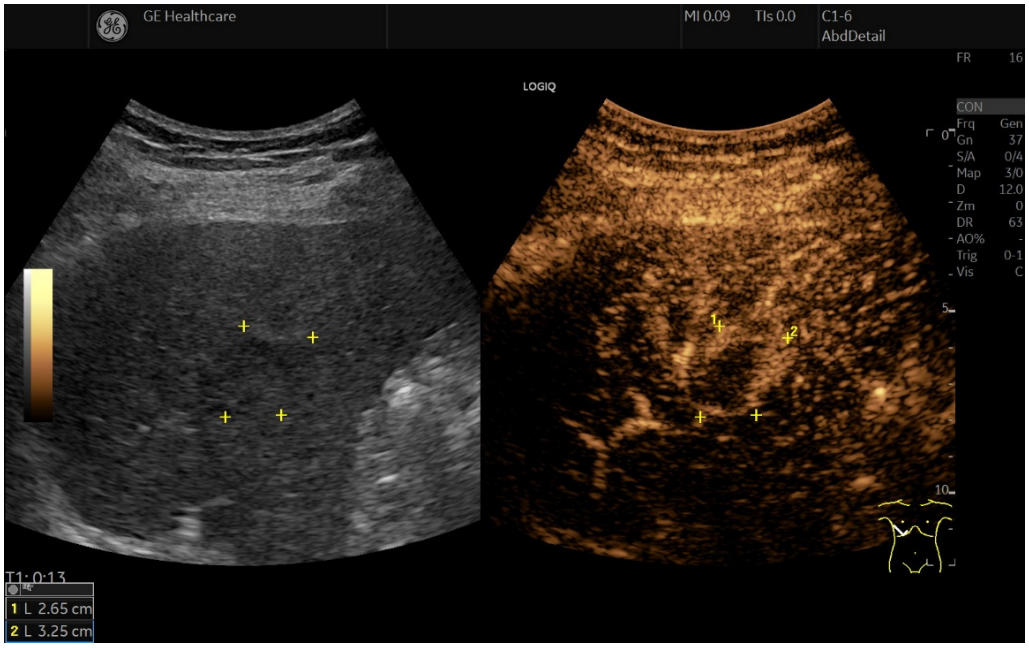


Fig. 9.6.2. Contrast-enhanced ultrasound (CEUS) evaluation performed 4 weeks after percutaneous microwave ablation (MWA) for hepatocellular carcinoma (HCC). The grayscale B-mode image (left) demonstrates the post-ablation zone within the liver parenchyma, corresponding to the treated lesion. On contrast-specific imaging (right), a focal area of arterial hyperenhancement is observed at the periphery of the ablation zone. This nodular hypervascular enhancement adjacent to the necrotic cavity is highly suggestive of residual viable tumor tissue rather than post-ablation reactive hyperemia.

3. Long-Term Surveillance

After confirmation of complete response, patients undergo periodic imaging every 3–6 months. CEUS is particularly advantageous in cirrhotic patients requiring repeated examinations, as it avoids cumulative radiation exposure and nephrotoxic contrast agents (9).

9.6.4. CEUS Criteria of Therapeutic Response

1. Complete Ablation

A complete therapeutic response is indicated when the treated area appears entirely avascular on CEUS. In these cases, the ablation zone demonstrates no arterial phase enhancement and remains non-enhancing throughout the portal and late phases. The treated area usually appears larger than the original lesion, reflecting the intended safety margin achieved during ablation (Fig 9.6.3).

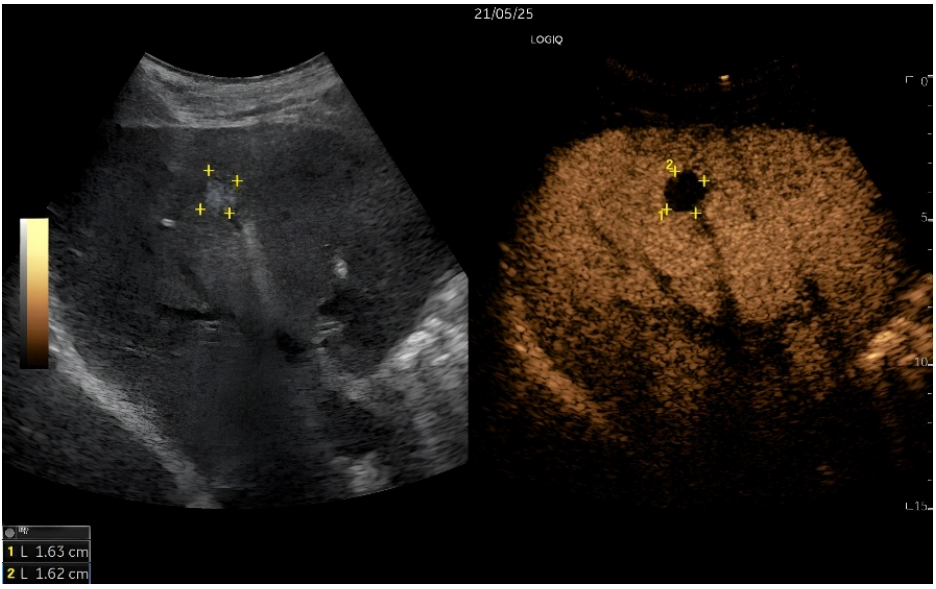


Fig. 9.6.3. CEUS performed 4 weeks after MWA of a liver metastasis. On B-mode ultrasound (left), the ablation zone appears as a well-defined heterogeneous hyperechoic area measuring approximately 1.6 cm, corresponding to the treated lesion. On CEUS (right), the ablation area shows complete absence of contrast enhancement throughout the vascular phases, indicating lack of tumoral vascularization. No nodular or irregular enhancing areas are identified within or at the margin of the ablation zone. These findings are consistent with complete ablation and absence of residual viable tumor.

2. Residual Tumor

Residual viable tumor tissue (Fig. 9.6.4) is typically characterized by the presence of focal enhancement within or adjacent to the ablation zone. This enhancement most often appears during the arterial phase and may demonstrate a nodular, eccentric, or irregular configuration. In hepatocellular carcinoma, this arterial enhancement is frequently followed by washout during the portal or late phase, a pattern that strongly suggests persistent tumor vascularization.

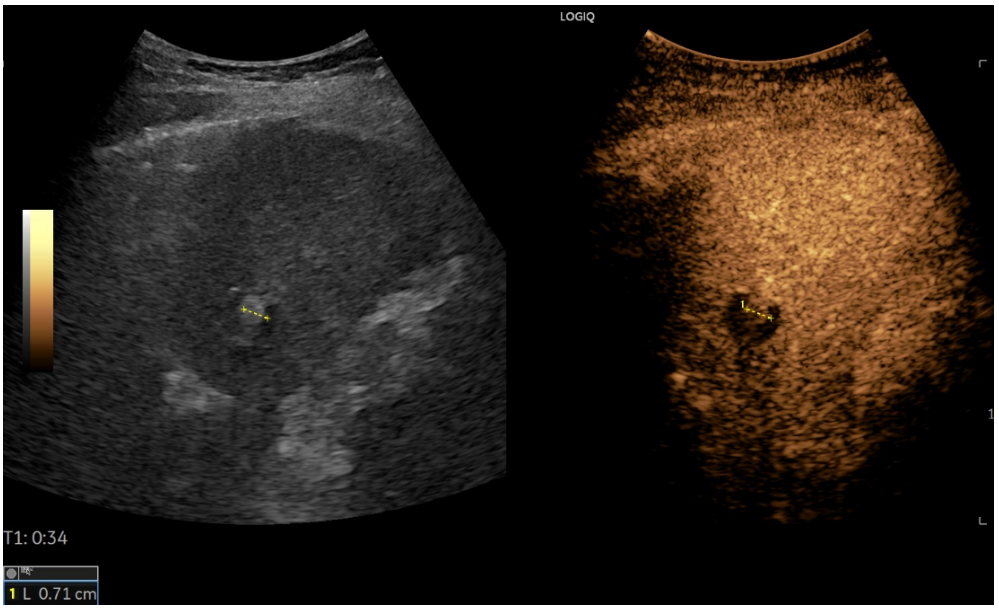


Fig. 9.6.4. CEUS performed 4 weeks after MWA for HCC. On B-mode ultrasound (left), a small nodular area measuring approximately 0.7 cm is identified within the ablation zone. On the arterial phase of CEUS (right), this area demonstrates nodular arterial enhancement, suggestive of persistent tumoral vascularization. These imaging findings are consistent with a residual viable tumor within the ablation zone.

3. Local Tumor Recurrence

Local tumor recurrence refers to the reappearance of viable tumor tissue at the margin of a previously treated lesion after an initial period during which complete necrosis was documented. On CEUS, recurrent tumor usually demonstrates enhancement characteristics similar to those observed in untreated lesions, including arterial phase hyperenhancement and, in the case of hepatocellular carcinoma, subsequent washout.

9.6.5. CEUS in Hepatocellular Carcinoma

In patients with hepatocellular carcinoma, CEUS evaluation is largely based on the well-established vascular profile of HCC, which typically consists of arterial phase hyperenhancement followed by washout in the portal or late phases. Because microbubble contrast agents remain confined to the vascular compartment, CEUS is particularly sensitive to the detection of arterial neovascularization associated with viable tumor tissue.

Several clinical studies have demonstrated that CEUS can achieve high diagnostic accuracy in detecting residual HCC after thermal ablation. Reported sensitivity ranges between approximately 80% and 95%, while specificity may reach 85% to 98% when compared with cross-sectional imaging techniques such as CT or MRI (8, 10). In cirrhotic patients who require repeated imaging evaluations, CEUS also offers the advantage of avoiding cumulative radiation exposure and the potential risks associated with repeated administration of nephrotoxic contrast agents.

9.6.6. CEUS in Liver Metastases

CEUS is also useful in evaluating the response of liver metastases treated with thermal ablation. The enhancement pattern of metastatic lesions varies depending on the type of primary tumor. For instance, colorectal liver metastases often demonstrate peripheral or rim-like arterial enhancement, whereas neuroendocrine metastases may exhibit intense and homogeneous arterial hyperenhancement. Hypovascular metastases may show more subtle perfusion patterns (11).

For this reason, knowledge of the baseline vascular characteristics of the lesion prior to treatment is essential when interpreting post-ablation CEUS findings. Residual tumor tissue usually preserves the same vascular behavior that was observed before treatment, which facilitates differentiation between viable tumor and benign post-procedural changes (5).

9.6.7. Comparison with CT and MRI

Advantages of CEUS

- Real-time dynamic evaluation
- High temporal resolution
- Bedside applicability
- Absence of ionizing radiation
- Safe in renal impairment
- Lower cost

Limitations

- Operator dependency
- Limited acoustic window in obese patients
- Difficulty assessing deeply located lesions
- Limited panoramic overview compared to CT/MRI

Comparative studies demonstrate similar diagnostic performance between CEUS and CE-CT/CE-MRI for early detection of residual tumor in selected patients (4, 8, 12).

9.6.8. Advanced Techniques: Fusion Imaging and Quantitative CEUS

Recent technological developments have further expanded the role of CEUS in the management of patients undergoing thermal ablation. Image fusion techniques allow real-time ultrasound images to be combined with previously acquired CT or MRI datasets, thereby improving lesion localization and facilitating accurate assessment of the ablation margins. This approach is particularly useful for lesions that are difficult to visualize with conventional ultrasound alone (10,13).

In addition, quantitative CEUS methods have been investigated as potential tools for assessing tissue perfusion more objectively. Although these techniques remain primarily within the research domain, they may in the future contribute to a more standardized evaluation of treatment response following liver tumor ablation (14). Quantitative CEUS techniques have been investigated as potential tools for assessing tissue perfusion more objectively. Dedicated perfusion-analysis software such as VueBox® (Bracco, Italy) enables the extraction of quantitative parameters from CEUS cine loops, including peak enhancement, time-to-peak, mean transit time, and wash-in area under the curve derived from time–intensity curves. These parameters provide an objective assessment of tumor microvascularization and may help reduce operator dependency associated with visual interpretation. Although quantitative CEUS remains primarily within the research domain, it may in the future contribute to a more standardized evaluation of treatment response following liver tumor ablation and other oncologic therapies (15).

9.6.9. Practical Recommendations

- CEUS should be performed by experienced operators.
- Baseline vascular pattern of the lesion should be documented before ablation.
- Immediate CEUS is recommended to detect residual disease.
- A 4–6 weeks follow-up examination is essential to confirm complete response.
- CEUS may be integrated into long-term surveillance protocols, particularly in cirrhotic patients.

References

1. European Association for the Study of the Liver. EASL Clinical Practice Guidelines on the management of hepatocellular carcinoma. J Hepatol. 2025 Feb;82(2):315-374.
2. Singal AG, Llovet JM, Yarchoan M, Mehta N, Heimbach JK, Dawson LA, et al. AASLD Practice Guidance on prevention, diagnosis, and treatment of hepatocellular carcinoma. Hepatology. 2023 Dec 1;78(6):1922-1965.
3. Piscaglia F, Bolondi L; Italian Society for Ultrasound in Medicine and Biology (SIUMB) Study Group on Ultrasound Contrast Agents. The safety of Sonovue in abdominal applications: retrospective analysis of 23188 investigations. Ultrasound Med Biol. 2006 Sep;32(9):1369-75.
4. Meloni MF, Andreano A, Zimbaro F, Lava M, Lazzaroni S, Sironi S. Contrast enhanced ultrasound: Roles in immediate post-procedural and 24-h evaluation of the effectiveness of thermal ablation of liver tumors. J Ultrasound. 2012 Sep 29;15(4):207-14.
5. Dietrich CF, Nolsøe CP, Barr RG, Berzigotti A, Burns PN, Cantisani V, et al. Guidelines and Good Clinical Practice Recommendations for Contrast-Enhanced Ultrasound (CEUS) in the Liver-Update 2020 WFUMB in Cooperation with EFSUMB, AFSUMB, AIUM, and FLAUS. Ultrasound Med Biol. 2020 Oct;46(10):2579-2604.
6. Solbiati L, Ahmed M, Cova L, Ierace T, Brioschi M, Goldberg SN. Small liver colorectal metastases treated with percutaneous radiofrequency ablation: local response rate and long-term survival with up to 10-year follow-up. Radiology. 2012 Dec;265(3):958-68.
7. Bartolotta TV, Taibbi A, Midiri M, Lagalla R. Contrast-enhanced ultrasound of hepatocellular carcinoma: where do we stand? Ultrasonography. 2019 Jul;38(3):200-214.
8. Wilson SR, Burns PN. Microbubble-enhanced US in body imaging: what role? Radiology. 2010 Oct;257(1):24-39.

9. Zheng SG, Xu HX, Lu MD, Xie XY, Xu ZF, Liu GJ ,et al. Role of contrast-enhanced ultrasound in follow-up assessment after ablation for hepatocellular carcinoma. World J Gastroenterol. 2013 Feb 14;19(6):855-65.
10. Minami Y, Kudo M. Imaging Modalities for Assessment of Treatment Response to Nonsurgical Hepatocellular Carcinoma Therapy: Contrast-Enhanced US, CT, and MRI. Liver Cancer. 2015 Mar;4(2):106-14.
11. Wu JY, Chen MH, Yang W, Lin SZ, Wu W, Yin SS, et al. Role of contrast enhanced ultrasound in radiofrequency ablation of metastatic liver carcinoma. Chin J Cancer Res. 2012 Mar;24(1):44-51. doi: 10.1007/s11670-012-0044-8. PMID: 23359761; PMCID: PMC3555259.
12. Mauri G, Cova L, De Beni S, Ierace T, Tondolo T, Cerri A, et al. Real-time US-CT/MRI image fusion for guidance of thermal ablation of liver tumors undetectable with US: results in 295 cases. Cardiovasc Intervent Radiol. 2015 Feb;38(1):143-51.
13. Xu E, Long Y, Li K, Zeng Q, Tan L, Luo L, et al. Comparison of CT/MRI-CEUS and US-CEUS fusion imaging techniques in the assessment of the thermal ablation of liver tumors. Int J Hyperthermia. 2019 Jan 1;35(1):159-167.
14. Gu DY, Zhang Y, Hu JX, Qin HY, Lu X, He GB, et al. The value of contrast-enhanced ultrasound quantitative parameters in the prognosis prediction of hepatocellular carcinoma after thermal ablation: a retrospective cohort study. J Gastrointest Oncol. 2022 Oct;13(5):2522-2531.
15. Dong Y, Koch JBH, Löwe AL, Christen M, Wang WP, Jung EM, et al. VueBox® for quantitative analysis of contrast-enhanced ultrasound in liver tumors1. Clin Hemorheol Microcirc. 2022;80(4):473-486.

9.7. Evidence-Based Proofs of the Value of Contrast-Enhanced Ultrasound (CEUS) for Focal Liver Lesions (FLL)

Ioan Sporea, Raluca Lupușoru

Abstract

Daily practice frequently detects focal liver lesions (FLL), which require rapid, accurate characterization to guide management. Computed tomography (CT) and magnetic resonance imaging (MRI) are established standards but have limitations related to radiation, nephrotoxicity, contrast allergy, availability, and cost. Contrast-enhanced ultrasound (CEUS) has emerged over the past 25 years as a robust, evidence-based tool for the characterization of FLL, supported by large multicenter cohorts, meta-analyses, and international guidelines.

CEUS allows real-time, high-temporal-resolution assessment of microvascularization with purely intravascular microbubble contrast agents, without nephrotoxicity and with an excellent safety profile.

Meta-analyses show pooled sensitivity around 90–92% and specificity around 85–88% for differentiating benign from malignant FLL, comparable to CT/MRI. CEUS reliably recognizes characteristic enhancement patterns of common benign lesions (hemangioma, focal nodular hyperplasia, liver abscesses) and malignant lesions (metastases, hepatocellular carcinoma, intrahepatic cholangiocarcinoma). Guidelines from EFSUMB and WFUMB now recommend CEUS as a first-line or problem-solving technique in many FLL scenarios, including incidentally detected lesions, nodules in cirrhosis, and indeterminate findings after CT/MRI. Recent developments such as dynamic or quantitative CEUS (D-CEUS), Sonazoid® with a post-vascular Kupffer phase, and integration into multiparametric ultrasound (MPUS) further strengthen its role.

9.7.1. Introduction

Focal liver lesions (FLL) are among the most common findings at abdominal imaging, discovered either incidentally or in the staging and follow-up of oncologic or cirrhotic patients. Conventional B-mode and Doppler ultrasound are usually the first-line modalities but often remain inconclusive, because many FLL share overlapping grayscale and Doppler features.

Since the early 2000s, second-generation ultrasound contrast agents (UCA) and contrast-specific imaging techniques have made CEUS a powerful tool for the real-time assessment of enhancement patterns of FLL (1). Early

guidelines from EFSUMB in 2004 and their subsequent updates in 2008 and 2012 established structured algorithms for CEUS in the liver, based on large clinical experience and prospective data (2). The latest WFUMB/EFSUMB joint update in 2020 (3) further consolidated CEUS as a key modality in the work-up of liver lesions worldwide.

Contrast-enhanced ultrasound (CEUS) provides unique diagnostic information due to the purely intravascular behavior of second-generation ultrasound contrast agents. Unlike iodinated or gadolinium-based contrast media used in CT and MRI, microbubble contrast agents remain strictly confined to the vascular space and do not diffuse into the interstitium. This characteristic allows real-time visualization of tumor microvascularization, with very high temporal resolution, enabling continuous assessment of arterial enhancement and later washout phenomena. Consequently, CEUS reflects true vascular perfusion dynamics and allows precise differentiation between benign and malignant focal liver lesions based on their hemodynamic behavior rather than delayed tissue enhancement patterns (4, 5).

9.7.2. Evidence for CEUS Diagnostic Performance in FLL

Overall benign vs. malignant differentiation

The strongest "proof" of CEUS value in FLL comes from meta-analyses and large multicenter series.

- In a meta-analysis published by Friedrich Rust (6) with a total of 45 studies with 8147 focal liver lesions, the overall sensitivity and specificity of CEUS for the diagnosis of *malignant liver lesions* was 93% (95% CI: 91–95%) and 90% (95% CI: 88–92%), respectively.
- In another large meta-analysis (7) with 25 studies, the pooled estimate sensitivity and specificity for liver CEUS studies were 87% and 89%, respectively. In this meta-analysis, CE-CT studies showed sensitivity and specificity of 86% and 82%, respectively, and CE-MRI studies showed sensitivity and specificity of 85% and 87%, respectively. And the conclusion of the study was: "The diagnostic performance of CEUS for FLLs is not significantly different than that of CE-CT and CE-MRI". CEUS is a highly specific and sensitive diagnostic modality in detecting FLLs and should be considered as the first evaluation of a new US lesion.
- In another meta-analysis (8) that compared liver CEUS with CE-CT and CE-MRI In 21 studies, it was shown that for SonoVue-enhanced ultrasound studies, sensitivity was 88% and specificity was 81%; for the

CE-CT studies, sensitivity was 90% and specificity was 77%; for the CE-MRI studies, sensitivity was 86% and specificity was 81%. In conclusion of this meta-analysis, in this comparison, SonoVue-enhanced ultrasound had high pooled sensitivity and pooled specificity and has no significant difference compared with CE-CT and CE-MRI.

- A comprehensive meta-analysis performed by Wu et al. (57 studies, >10,000 lesions) (9) reported pooled sensitivity of 0.92 and specificity of 0.87 for CEUS in differentiating malignant from benign FLL, with a diagnostic odds ratio >100, confirming high overall accuracy. The analysis also showed that second-generation UCAs significantly outperformed first-generation Levovist and that Sonazoid had particularly high diagnostic performance.
- A multicenter prospective Romanian study (14 Romanian centers, >2000 lesions) similarly demonstrated that CEUS can correctly classify >90% of FLL when typical enhancement criteria are applied, taking liver biopsy, CE-CT, or CE-MRI like standard (10). This study was preceded by others, some Romanian multicentric studies showing the same good results (11-14).
- A 2024 published meta-analysis of Sonazoid-enhanced CEUS (SZ-CEUS) reported high diagnostic accuracy for differentiating benign from malignant FLL, again with pooled sensitivity and specificity above 90% (15). This meta-analysis reported high pooled sensitivity (~94%) and specificity (~84%) for SZ-CEUS in differentiating benign and malignant lesions, demonstrating strong overall diagnostic performance.
- A 2025 published clinical study focused on lesions that remained indeterminate after CT/MRI/PET showed that CEUS could correctly reclassify most of these FLL as benign or malignant, with high positive and negative predictive values, underlining its role as a “problem-solving” modality (16).

Overall, the evidence consistently shows that CEUS is at least non-inferior to CT/MRI for characterizing FLL, and in some scenarios (e.g., “too small to characterize” nodules, patients with renal failure, or iodinated/gadolinium contrast allergy) it may be superior or uniquely feasible. National (17), European (3) or WFUMB (4) guidelines help people to use this method with success.

Cost-effectiveness studies in Europe have shown that CEUS as a second-line technique after inconclusive B-mode US reduces the need for CT/MRI and overall diagnostic costs while shortening time to diagnosis (18).

9.7.3. Clinical impact on patient management

Beyond diagnostic accuracy, the clinical value of CEUS is reflected in its direct impact on patient management. Because CEUS can be performed immediately following baseline ultrasound, diagnostic clarification is frequently achieved during the same examination session. This approach reduces diagnostic delays, minimizes patient anxiety, and allows rapid therapeutic decision-making. Moreover, accurate lesion characterization by CEUS may decrease the need for liver biopsy or additional imaging investigations, contributing to a more efficient diagnostic pathway. Several clinical experiences have demonstrated that integrating CEUS early in the diagnostic workflow shortens time to diagnosis while maintaining high diagnostic confidence (11).

Although numerous studies demonstrate the non-inferiority of CEUS compared with contrast-enhanced CT and MRI, certain clinical situations highlight potential advantages of CEUS. These include patients with renal insufficiency, allergy to iodinated or gadolinium-based contrast agents, and cases requiring repeated examinations without radiation exposure. Additionally, the real-time evaluation of enhancement allows improved assessment of small lesions and subtle vascular changes that may be missed with fixed-phase cross-sectional imaging. CEUS may also provide superior evaluation of treatment response following locoregional therapies, where early detection of residual vascularization is essential. In these specific contexts, CEUS represents not only an alternative but sometimes the preferred imaging modality (4).

Importantly, CEUS can be performed immediately, in the same room, without transferring the patient, avoiding delays and additional logistical burdens.

Limitations include operator performance and the need for specific training of the operator and reduced image quality in severely obese patients or in those with very poor acoustic windows. However, these limitations are shared with conventional ultrasound and can often be mitigated by high-end equipment and experienced operators.

9.7.4. CEUS as a problem-solving modality

Despite major advances in cross-sectional imaging, a proportion of focal liver lesions remains indeterminate after contrast-enhanced CT or MRI examinations. Published data suggest that approximately 5–15% of lesions cannot be confidently characterized using these modalities alone. In such scenarios, liver CEUS has demonstrated a significant added diagnostic value by enabling dynamic real-time evaluation of vascular patterns. Several recent

clinical studies have shown that liver CEUS can correctly reclassify most indeterminate lesions as benign or malignant, thereby reducing the need for additional imaging or invasive diagnostic procedures. This problem-solving role represents one of the strongest evidence-based arguments supporting the integration of CEUS into routine diagnostic algorithms (16).

9.7.5. Integration into multiparametric ultrasound (MPUS) and artificial intelligence (AI)

Recent WFUMB guidance on liver multiparametric ultrasound positions CEUS alongside B-mode, Doppler, elastography and attenuation imaging as part of a comprehensive, non-invasive assessment of liver parenchyma and focal lesions.

- Combining CEUS enhancement patterns with stiffness (shear wave elastography) and quantitative fat assessment may improve risk stratification in patients with chronic liver disease.
- Emerging artificial intelligence (AI) models are being trained on CEUS cine-loops to automatically classify FLL, potentially reducing inter-observer variability and supporting less experienced operators (19, 20). Early studies show promising results, but larger, multi-center validation is needed.
- Importantly, emerging artificial intelligence applications may also mitigate one of the traditionally cited limitations of CEUS—operator dependency. Machine learning models trained on CEUS cine-loops have demonstrated diagnostic performances comparable to experienced radiologists, suggesting that AI-assisted interpretation could standardize examinations and support less experienced operators. Such developments may facilitate wider adoption of CEUS, particularly in centers with limited expertise or restricted access to advanced cross-sectional imaging.

Despite the substantial body of evidence supporting CEUS, its adoption in daily clinical practice remains heterogeneous across different healthcare systems. Limited availability of ultrasound contrast agents, reimbursement restrictions, and unequal access to CEUS-capable equipment represent important barriers in some regions (21,22). In addition, operator dependency and variability in training opportunities may influence implementation rates. Addressing these challenges through education, guideline dissemination, and institutional support is essential to translate the strong evidence base of CEUS into broader clinical utilization.

Conclusions

From 2000 to 2025, a very large body of evidence - encompassing prospective cohorts, multicenter trials, meta-analyses, and multiple international guidelines - has firmly established CEUS as a core imaging modality for focal liver lesions.

.

References

1. Sirli R, Sporea I, Martie A, Popescu A, Dănilă M. Contrast enhanced ultrasound in focal liver lesions - a cost efficiency study. Med Ultrason. 2010 Dec;12(4):280-5.
2. Albrecht T, Blomley M, Bolondi L, Claudon M, Correas JM, Cosgrove D, et al. EFSUMB Study Group. Guidelines for the use of contrast agents in ultrasound. January 2004. Ultraschall Med. 2004 Aug;25(4):249-56.
3. Claudon M, Dietrich CF, Choi BI, Cosgrove DO, Kudo M, Nolsøe CP, et al. World Federation for Ultrasound in Medicine; European Federation of Societies for Ultrasound. Guidelines and good clinical practice recommendations for Contrast Enhanced Ultrasound (CEUS) in the liver - update 2012: A WFUMB-EFSUMB initiative in cooperation with representatives of AFSUMB, AIUM, ASUM, FLAUS and ICUS. Ultrasound Med Biol. 2013 Feb;39(2):187-210.
4. Dietrich CF, Nolsøe CP, Barr RG, Berzigotti A, Burns PN, Cantisani V, et al. Guidelines and Good Clinical Practice Recommendations for Contrast-Enhanced Ultrasound (CEUS) in the Liver-Update 2020 WFUMB in Cooperation with EFSUMB, AFSUMB, AIUM, and FLAUS. Ultrasound Med Biol. 2020 Oct;46(10):2579-2604.
5. Lee JY, Minami Y, Choi BI, Lee WJ, Chou YH, Jeong WK, et al. The AFSUMB Consensus Statements and Recommendations for the Clinical Practice of Contrast-Enhanced Ultrasound using Sonazoid. J Med Ultrasound. 2020 May 25;28(2):59-82.
6. Friedrich-Rust M, Klopffleisch T, Nierhoff J, Herrmann E, Vermehren J, Schneider MD, et al. Contrast-Enhanced Ultrasound for the differentiation of benign and malignant focal liver lesions: a meta-analysis. Liver Int. 2013 May;33(5):739-55.
7. Xie L, Guang Y, Ding H, Cai A, Huang Y. Diagnostic value of contrast-enhanced ultrasound, computed tomography and magnetic resonance imaging for focal liver lesions: a meta-analysis. Ultrasound Med Biol. 2011 Jun;37(6):854-61.
8. Guang Y, Xie L, Ding H, Cai A, Huang Y. Diagnosis value of focal liver lesions with SonoVue®-enhanced ultrasound compared with contrast-enhanced computed tomography and contrast-enhanced MRI: a meta-analysis. J Cancer Res Clin Oncol. 2011 Nov;137(11):1595-605.
9. Wu M, Li L, Wang J, Zhang Y, Guo Q, Li X, et al. Contrast-enhanced US for characterization of focal liver lesions: a comprehensive meta-analysis. Eur Radiol. 2018 May;28(5):2077-2088.

10. Sporea I, Săndulescu DL, Şirli R, Popescu A, Danilă M, Spârchez Z, et al. Contrast-Enhanced Ultrasound for the Characterization of Malignant versus Benign Focal Liver Lesions in a Prospective Multicenter Experience - The SRUMB Study. J Gastrointestin Liver Dis. 2019 Jun 1;28:191-196.
11. Sporea I, Badea R, Popescu A, Spârchez Z, Sirli RL, Dănilă M, et al. Contrast-enhanced ultrasound (CEUS) for the evaluation of focal liver lesions - a prospective multicenter study of its usefulness in clinical practice. Ultraschall Med. 2014 Jun;35(3):259-66.
12. Sporea I, Badea R, Popescu A, Spârchez Z, Sirli RL, Dănilă M, et al. Contrast-enhanced ultrasound (CEUS) for the evaluation of focal liver lesions - a prospective multicenter study of its usefulness in clinical practice. Ultraschall Med. 2014 Jun;35(3):259-66.
13. Sporea I, Badea R, Martie A, Dumitru E, Ioaniţescu S, Şirli R, et al. Contrast Enhanced Ultrasound for the evaluation of focal liver lesions in daily practice. A multicentre study. Med Ultrason. 2012 Jun;14(2):95-100.
14. Sporea I, Şirli R. Is Contrast Enhanced Ultrasound (CEUS) ready for use in daily practice for evaluation of focal liver lesions? Med Ultrason. 2014 Mar;16(1):37-40.
15. Tang Y, Sasaki SI, Hawley J, Peillon A, Sjöström A, Fuentes-Alburo A, et al. Diagnostic Test Accuracy of Contrast-Enhanced Ultrasound With Sonazoid for Assessment of Focal Liver Lesions: A Systematic Review and Meta-Analysis. J Clin Ultrasound. 2025 Mar-Apr;53(3):510-524.
16. Lyshchik A, Kuon Yeng Escalante C, Siu Xiao T, Piscaglia F, Kono Y, Medellin-Kowalewski A, et al. CEUS LI-RADS Trial Group; CEUS LI-RADS Trial Group Members. Contrast-enhanced US of High-Risk Indeterminate Focal Liver Observations Categorized as LR-4 or LR-M at CT/MRI. Radiology. 2025 Jan;314(1):e240916.
17. Sporea I, Badea R, Brisc C, Ioanițescu S, Moga T, Popescu A et, al. Romanian National Guidelines on Contrast Enhanced Ultrasound in clinical practice. Med Ultrason. 2017 Nov 29;19(4):401-415.
18. Sirli R, Sporea I, Martie A, Popescu A, Dănilă M. Contrast enhanced ultrasound in focal liver lesions--a cost efficiency study. Med Ultrason. 2010 Dec;12(4):280-5.
19. Hu HT, Wang W, Chen LD, Ruan SM, Chen SL, Li X, et al. Artificial intelligence assists identifying malignant versus benign liver lesions using contrast-enhanced ultrasound. J Gastroenterol Hepatol. 2021 Oct;36(10):2875-2883.
20. Ding W, Meng Y, Ma J, Pang C, Wu J, Tian J, et al. Contrast-enhanced ultrasound-based AI model for multi-classification of focal liver lesions. J Hepatol. 2025 Aug;83(2):426-439.
21. Sporea I. Why isn't Contrast Enhanced Ultrasound for Focal Liver Lesions used more in daily practice? Med Ultrason. 2016 Mar;18(1):5-6.
22. Yusuf GT, Sidhu PS. The benefits of CEUS and why we don't use more CEUS in clinical practice in the United Kingdom. Br J Radiol. 2026 Feb 3:tqag025.

9.8. Elastography for Focal Liver Lesions (FLL)

Ana-Maria Ghiuchici, Mirela Dănilă

Abstract

Ultrasound-based elastography represents a non-invasive imaging technique that complements conventional ultrasonography (US) in the evaluation of focal liver lesions (FLLs). By quantifying tissue stiffness, elastography provides additional data that can help differentiate benign from malignant liver tumors. Several elastographic methods are currently available, including strain elastography (SE) and Shear-Waves elastography (SWE), most of which are integrated into modern ultrasound systems. This chapter presents recent advances in US elastography for the assessment of FLLs.

9.8.1. Introduction

Conventional ultrasound (US) is the most commonly used imaging modality for liver evaluation, mainly because of its accessibility, safety, and cost-effectiveness. Focal liver lesions (FLLs) are often detected incidentally during routine US examinations. Accurate differentiation between benign and malignant lesions is essential for appropriate management (1–3).

However, additional diagnostic methods, including contrast-enhanced computed tomography (CT), magnetic resonance imaging (MRI), and liver biopsy, are often necessary to establish a definitive diagnosis (2, 4).

Technological advances in US have considerably improved its diagnostic performance for FLL. Techniques such as Doppler ultrasound, contrast-enhanced ultrasound (CEUS), and elastography now allow a more comprehensive assessment of focal and diffuse liver pathology (4, 5). Among these, US-based elastography has attracted increasing clinical interest due to its ability to non-invasively evaluate tissue stiffness (6).

The numerous advantages and well-validated performance of ultrasound elastography in assessing liver fibrosis have facilitated the expansion of its clinical applications (7–9). More recently, this technique has been investigated for characterizing focal liver lesions.

9.8.2. Ultrasound-based elastography for focal liver lesion evaluation

Elastography evaluates tissue mechanical properties by measuring the degree to which tissue deforms (changes shape) in response to applied stress

(external force). Soft tissues deform more easily than stiff ones. This makes elastography useful for detecting differences in elasticity (the ability to return to the original shape after deformation) between normal liver tissue and focal lesions (abnormal tissue areas) (10, 11).

Malignant transformation frequently induces structural alterations, including fibrosis, increased cellular density, and abnormal vascularization. These changes typically increase tissue stiffness, which can be detected using elastographic techniques (12).

Interpreting elastography results requires consideration of the clinical context, including chronic liver disease, cirrhosis, a history of malignancy, and other patient-specific factors. For example, hepatocellular carcinoma (HCC) develops in over 90% of cases within cirrhotic livers, where background liver tissue already shows increased stiffness (13).

The guidelines of the European Federation of Societies for Ultrasound in Medicine and Biology (EFSUMB) and the World Federation for Ultrasound in Medicine and Biology (WFUMB) classify ultrasound elastography techniques into two primary categories: strain elastography (SE) and Shear-Waves elastography (SWE) (6, 14-15). Both qualitative (SE) and quantitative (SWE) techniques assess tissue stiffness. These techniques fundamentally measure minimal tissue deformations induced by mechanical compression or acoustic radiation force impulses.

A. Strain Elastography

Strain elastography (SE) is a qualitative ultrasound technique that evaluates tissue displacement caused by mechanical compression or physiological motion. SE estimates tissue stiffness by comparing lesion deformation to that of the surrounding liver parenchyma (6, 10). Liver fibrosis may reduce the accuracy of focal liver lesion (FLL) assessment using SE.

Semi-quantitative parameters, including strain ratio and histogram analysis, provide estimates of tissue stiffness (16–18). Malignant lesions consistently demonstrate greater stiffness than benign lesions.

A prospective study assessing solid focal liver lesions reported significantly higher strain ratio values in malignant tumors compared to benign tumors (1.66 vs. 1.02) (16). Furthermore, another study demonstrated that strain index values were higher in malignant lesions than in benign lesions (2.82 ± 1.82 vs. 1.45 ± 1.28, $p < .0001$) (17).

Despite these findings, strain elastography has several limitations, including high interobserver variability, difficulties in patients with ascites or deeply located lesions, and significant overlap in stiffness values between benign and malignant lesions (6, 19). Consequently, current international guidelines do not recommend SE as a routine method for characterizing focal liver lesions (6, 15).

B. Shear-Waves Elastography

Shear-Waves elastography (SWE) provides a quantitative assessment of tissue stiffness by measuring the velocity of shear-waves induced by acoustic radiation force impulses. Since shear-waves propagate faster in stiffer tissues, shear-waves velocity serves as an indicator of tissue elasticity (20).

Measurements are reported as shear-waves velocity (m/s) or Young's modulus (kPa). SWE techniques comprise transient elastography (TE), point Shear-Waves elastography (pSWE), and two-dimensional Shear-Waves elastography (2D-SWE) (6, 15).

- **Point Shear-Waves Elastography (pSWE)**

Point shear-wave elastography enables targeted evaluation of stiffness within a selected region of interest under ultrasound guidance. This technique is among the most extensively studied for characterizing focal liver lesions (21–25).

Meta-analyses assessing SWE report sensitivities and specificities near 82% for distinguishing malignant from benign lesions (26, 27).

Reported typical stiffness values include:

1) Benign FLLs

- Focal nodular hyperplasia (FNH): approximately 2.0–2.7 m/s (21, 25).
- Hemangioma (HH): approximately 1.2–2.0 m/s, typically the softest lesions (Fig. 9.8.1) (28, 29).
- Hepatic adenoma (HA): intermediate stiffness values (24, 29).

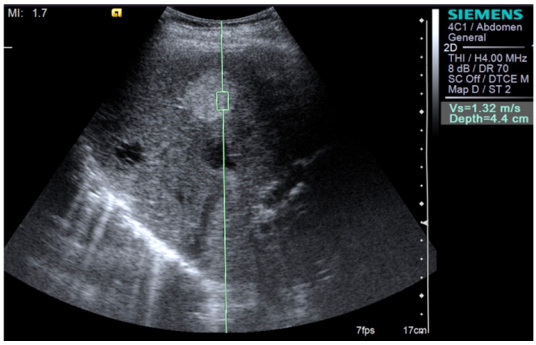


Fig. 9.8.1. pSWE measurement in a hepatic hemangioma using VTQ; Vs (velocity speed) = 1.32 m/s and ROI depth = 4.4 cm.

2) Malignant FLLs

- Liver metastases (LM): often 3.5–4.5 m/s or higher (Fig. 9.8.2) (21, 30)
- Intrahepatic cholangiocarcinoma (ICC): approximately 3.5–4.2 m/s (31–32)
- Hepatocellular carcinoma (HCC): approximately 2.1–3.1 m/s, varying with tumor differentiation and vascularization (Fig. 9.8.3) (33–34).

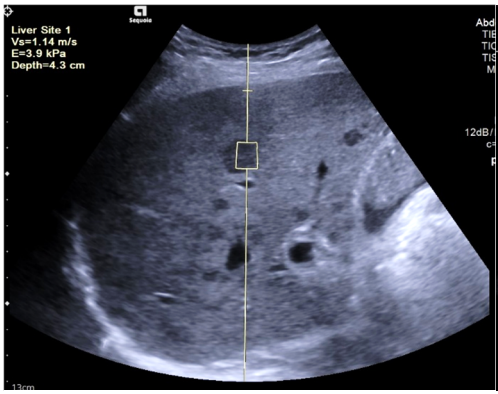


Fig. 9.8.2. pSWE measurement in a hepatic metastasis using VTQ; Vs (velocity speed) = 1.14 m/s and ROI depth = 4.3 cm.

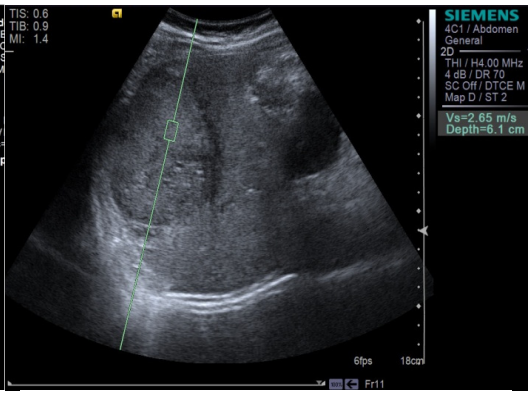


Fig. 9.8.3. pSWE measurement in a large hepatocellular carcinoma using VTQ; Vs (velocity speed) = 2.65 m/s and ROI depth = 6.1 cm.

The overall stiffness hierarchy observed in multiple studies is as follows: Metastases > ICC > HCC > FNH > Hemangioma (7).

Overlapping stiffness values between benign and malignant lesions are common, which limits the diagnostic accuracy of elastography (22–25).

- **Two-Dimensional Shear-Waves Elastography (2D-SWE)**

2D-SWE allows real-time visualization of tissue stiffness through color-coded elastographic maps superimposed on B-mode ultrasound images (35–37).

Reported stiffness values include:

- Benign lesions: median stiffness of 16.4 kPa (Fig. 9.8.4–9.8.5).
- Malignant lesions: median stiffness of 36 kPa (Fig. 9.8.6 – 9.8.7) (37).

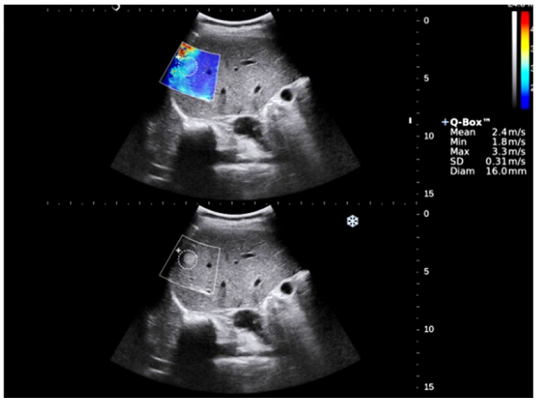


Fig. 9.8.4. 2D-SWE evaluation of a hepatic hemangioma using SSI–SuperSonic imagine; mean stiffness value = 2.4 m/s

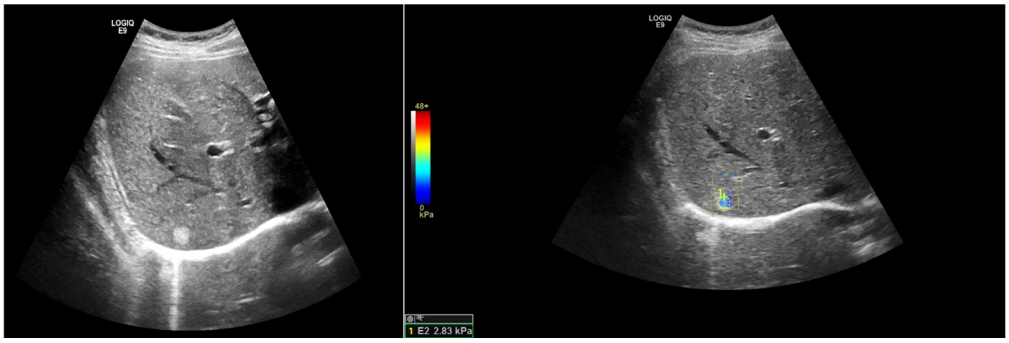


Fig. 9.8.5. 2D-SWE evaluation of a hepatic hemangioma using 2D-SWE.GE; mean stiffness value = 2.83 kPa

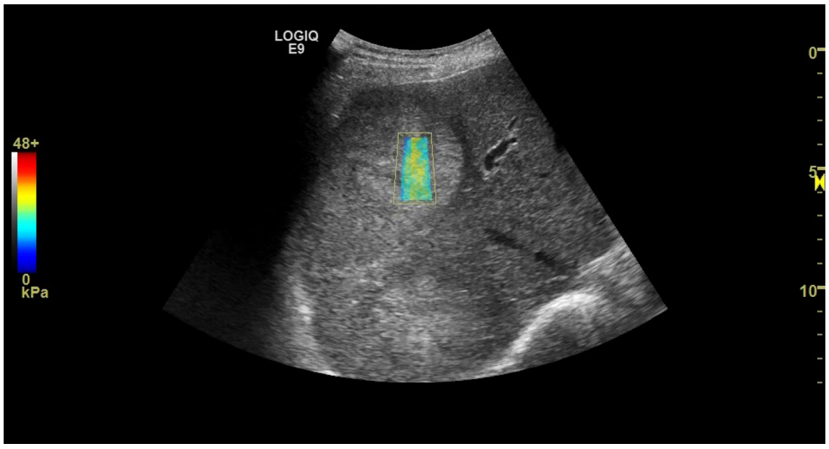


Fig. 9.8.6. 2D-SWE qualitative evaluation of a hepatocellular carcinoma using 2D-SWE.GE.

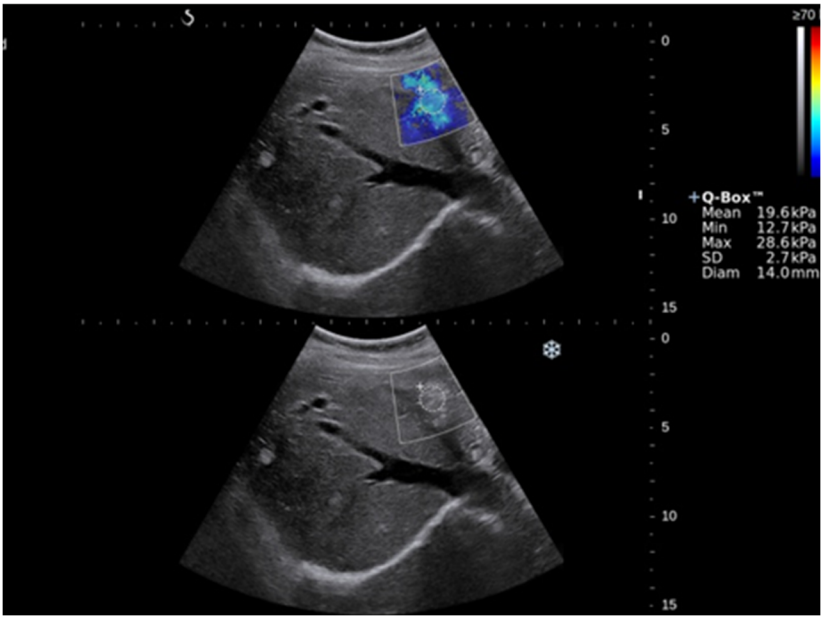


Fig. 9.8.7. 2D-SWE evaluation of a hepatic metastasis using SSI–SuperSonic imagine;
mean stiffness value = 19.6 m/s

The Liver Elastography Malignancy Prediction (LEMP) score demonstrated high diagnostic performance in differentiating benign from malignant lesions, using a cutoff value of 22.4 kPa (38).

Other studies have reported inconsistent results, underscoring the heterogeneity of elastographic measurements (35–37).

9.8.3. Limitations of US-based elastography in FLL evaluation

Although elastography is a promising imaging modality, several factors can influence measurement accuracy (6, 14, 39). Table 9.8.1 lists the most common factors that interfere with elastography assessment in FLLs.

Table 9.8.I Factors influencing elastographic measurements in focal liver lesions.

Category	**Factors influencing elastography**
Lesion-related factors	Tumor size and depth
	Heterogeneous tumor composition
	Presence of necrosis or cystic components
Patient-related factors	Obesity
	Narrow intercostal spaces
	Poor acoustic window
	Limited patient cooperation
Technical factors	Incorrect ROI placement
	Influence of large vessels or the liver capsule
	Lack of standardized measurement protocols
General limitation	Overlap between stiffness values of benign and malignant lesions

9.8.4. Take-home key messages

- US-based elastography provides additional information about tissue stiffness in FLLs.
- Malignant tumors have higher stiffness values than benign lesions.
- Variability in measurements and overlapping values between lesion types limits the use of elastography for FLL evaluation in every day practice.
- WFUMB and EFSUMB guidelines recommend to use elastography as an adjunct technique integrated with conventional US and contrast-enhanced imaging for improved characterization of FLLs.

References

1. Gore RM, Pickhardt PJ, Mortele KJ, Fishman EK, Horowitz JM, Fimmel CJ, et al. Management of incidental liver lesions on CT. J Am Coll Radiol. 2017;14:1429-1437.
2. Dietrich CF, Sharma M, Gibson RN, Schreiber-Dietrich D, Jenssen C. Fortuitously discovered liver lesions. World J Gastroenterol. 2013;19:3173-3188.
3. Kaltenbach TEM, Engler P, Kratzer W, Oeztuerk S, Seufferlein T, et al. Prevalence of benign focal liver lesions. Abdom Radiol. 2016;41:25-32.
4. Sporea I, Sandulescu DL, Sirli R, Popescu A, Danila M, Sparchez Z, et al. Contrast-enhanced ultrasound for focal liver lesions. J Gastrointestin Liver Dis. 2019;28:191-196.
5. Bartolotta TV, Taibbi A, Randazzo A, Gagliardo C. New frontiers in liver ultrasound. World J Gastrointest Oncol. 2021;13:1302-1316.
6. Dietrich CF, Bamber J, Berzigotti A, Bota S, Cantisani V, Castera L, et al. EFSUMB guidelines on liver ultrasound elastography. Ultraschall Med. 2017;38:e16-e47.
7. Lupsor-Platon M, Serban T, Silion AI, Tirpe A, Florea M. Hepatocellular carcinoma and NAFLD evaluation using elastography. Cancers. 2020;12:2778.
8. Grgurevic I, Tjesic Drinkovic I, Pinzani M. Multiparametric ultrasound in liver diseases. Postgrad Med J. 2019;95:425-432.
9. Fofiu R, Bende F, Popescu A, Şirli R, Lupușoru R, Ghiuchici AM, et al. Liver stiffness predicting varices in cirrhosis. Ultrasound Med Biol. 2021;47:76-83.
10. Shiina T, Nightingale KR, Palmeri ML, Hall TJ, Bamber JC, Barr RG, et al. WFUMB elastography guidelines: principles. Ultrasound Med Biol. 2015;41:1126-1147.
11. Yeh WC, Li PC, Jeng YM, Hsu HC, Kuo PL, Li ML, et al. Elastic modulus measurements of human liver. Ultrasound Med Biol. 2002;28:467-474.
12. Berzigotti A, Ferraioli G, Bota S, Gilja OH, Dietrich CF. Novel ultrasound methods for liver disease. Dig Liver Dis. 2018;50:107-112.
13. European Association for the Study of the Liver. EASL clinical practice guidelines: hepatocellular carcinoma. J Hepatol. 2018;69:182-236.
14. Ferraioli G, Filice C, Castera L, Choi BI, Sporea I, Wilson SR, et al. WFUMB guidelines for ultrasound elastography. Ultrasound Med Biol. 2015;41:1161-1179.
15. Ferraioli G, Wong VW, Castera L, Berzigotti A, Sporea I, Dietrich CF, et al. Liver ultrasound elastography update. Ultrasound Med Biol. 2018;44:2419-2440.
16. Cesario V, Accogli E, Domanico A, Di Lascio FM, Napoleone L, Gasbarrini A, et al. Sonoelastography for focal liver lesions. Dig Liver Dis. 2016;48:182-188.
17. Onur MR, Poyraz AK, Ucak EE, Bozgeyik Z, Özercan IH, Ogur E. Strain elastography of liver masses. J Ultrasound Med. 2012;31:1061-1067.
18. Emara DM, El Shafei MM, El-Gendi A, Yousif AA. Ultrasound elastography in focal hepatic lesions. Egypt J Radiol Nucl Med. 2019;50:103.
19. Rus G, Faris IH, Torres J, Callejas A, Melchor J. Clinical elastographic diagnosis. Sensors. 2020;20:2379.
20. Sigrist RMS, Liau J, Kaffas AE, Chammas MC, Willmann JK. Ultrasound elastography techniques. Theranostics. 2017;7:1303-1329.

21. Wu JP, Shu R, Zhao YZ, Ma GL, Xue W, He QJ, et al. ARFI evaluation of focal liver lesions. J Clin Ultrasound. 2016;44:347-353.
22. Dong Y, Wang WP, Xu Y, Cao J, Mao F, Dietrich CF. pSWE differentiation of liver lesions. Med Ultrason. 2017;19:259-264.
23. Zhang P, Zhou P, Tian SM, Qian Y, Li JL, Li RZ. CEUS and ARFI imaging of liver lesions. J Ultrasound Med. 2014;33:205-214.
24. Yu H, Wilson SR. ARFI differentiation of benign and malignant liver masses. Ultrasound Q. 2011;27:217-223.
25. Heide R, Strobel D, Bernatik T, Goertz RS. ARFI elastometry in focal liver lesions. Ultraschall Med. 2010;31:405-409.
26. Jiao Y, Dong F, Wang H, Zhang L, Xu J, Zheng J, et al. SWE meta-analysis for malignant liver lesions. Med Ultrason. 2017;19:16-22.
27. Hu X, Huang X, Chen H, Zhang T, Hou J, Song A, et al. SWE differentiation of malignant liver lesions. BMC Gastroenterol. 2019; 19:60.
28. Kim JE, Lee JY, Bae KS, Han JK, Choi BI. Acoustic radiation force impulse elastography for focal hepatic tumors: usefulness for differentiating hemangiomas from malignant tumors. Korean J Radiol. 2013;14(5):743-753.
29. Gallotti A, D'Onofrio M, Romanini L, Cantisani V, Pozzi Mucelli R. Acoustic Radiation Force Impulse (ARFI) ultrasound imaging of solid focal liver lesions. Eur J Radiol.2012;81(3):451-455.
30. Ying L, Lin X, Xie ZL, Tang FY, Hu YP, Shi KQ. Clinical utility of acoustic radiation force impulse imaging for identification of malignant liver lesions: a meta-analysis. Eur Radiol. 2012;22(12):2798-2805. doi:10.1007/s00330-012-2540-0.
31. Hasab Allah M, Salama RM, Marie MS, Mandur AA, Omar H. pSWE characterization of focal liver lesions. Expert Rev Gastroenterol Hepatol. 2018;1 2:201-207.
32. Akdoğan E, Yılmaz FG. ARFI elastography differentiation of liver masses. Turk J Gastroenterol. 2018;29: 456-463.
33. Ghiuchici AM, Sporea I, Dănilă M, Șirli R, Moga T, Bende F, et al. Is There a Place for Elastography in the Diagnosis of Hepatocellular Carcinoma?. J Clin Med. 2021;10(8):1710. Published 2021 Apr 15.
34. Guo LH, Wang SJ, Xu HX, Sun LP, Zhang YF, Xu JM, et al. Differentiation of benign and malignant focal liver lesions: value of virtual touch tissue quantification of acoustic radiation force impulse elastography. Med Oncol. 2015;32(3):68.
35. Ronot M, Di Renzo S, Gregoli B, Duran R, Castera L, Van Beers BE, et al. Characterization of fortuitously discovered focal liver lesions: additional information provided by shearwave elastography. Eur Radiol. 2015;25(2):346-358.
36. Guibal A, Boularan C, Bruce M, Vallin M, Pilleul F, Walter T, et al. Evaluation of shearwave elastography for the characterisation of focal liver lesions on ultrasound. Eur Radiol. 2013;23(4):1138-1149. doi:10.1007/s00330-012-2692-y

37. Gerber L, Fitting D, Srikantharajah K, Weiler N, Kyriakidou G, Bojunga J, et al. Evaluation of 2D-Shear-Waves elastography. J Gastrointestin Liver Dis. 2017;26:283-290.
38. Grgurevic I, Bokun T, Salkic NN, Brkljacic B, Vukelić-Markovic M, Stoos-Veic T, et al. Liver elastography malignancy prediction score for noninvasive characterization of focal liver lesions. Liver Int. 2018;38(6):1055-1063. doi:10.1111/liv.13611
39. Dong Y, Koch J, Alhyari A, Safai Zadeh E, Görg C, Wang WP, et al. Ultrasound Elastography for Characterization of Focal Liver Lesions. Z Gastroenterol. 2023 Apr;61(4):399-410.

10. Ultrasound for Hepatocellular Carcinoma (HCC) screening: when and how?

Mirela Dănilă, Ioan Sporea

Abstract

Hepatocellular carcinoma (HCC) is the most common primary liver malignancy and a major cause of cancer-related mortality worldwide, most frequently arising in the setting of liver cirrhosis and advanced chronic liver disease. Early detection through surveillance is essential because HCC is usually asymptomatic in its initial stages, and curative therapies are more effective when tumors are diagnosed early. Current guidelines recommend surveillance primarily in patients with cirrhosis (Child-Pugh A–B and selected C awaiting transplantation) and in selected high-risk non-cirrhotic populations, based on risk stratification models. Ultrasound every 6 months, together with alpha-fetoprotein (AFP), is the standard method for HCC screening. Despite the sensitivity of this screening not being high enough, it is still the method of choice. For selective cases, when ultrasound evaluation of the liver is not good enough, other imaging methods may be used (MRI and the more recent abbreviated MRI).

10.1. Introduction

Hepatocellular carcinoma (HCC) is by far the most common primary malignant liver tumor, accounting for 90% of all cases. It is one of the leading causes of cancer-related death worldwide, ranking third (1). It occurs in association with certain risk factors, the most important being liver cirrhosis. Therefore, monitoring these patients for the early detection of HCC is essential.

Chronic viral infections with hepatitis B virus (HBV) and hepatitis C virus (HCV) remain the leading cause of death from hepatocellular carcinoma (HCC) worldwide, with significant regional variations. In East Asia, endemic hepatitis B virus (HBV) infection is responsible for the majority of liver cancer–related deaths, while in North America, hepatitis C virus (HCV) infection and alcoholic liver disease (ALD) are the main causes. HCV is the main etiological factor in Western Europe, while ALD predominates in Central and Eastern Europe.

The recent increase in obesity and diabetes mellitus, particularly in developed countries, has led to a significant rise in the prevalence of MASLD

(metabolic dysfunction-associated steatotic liver disease), from 25.1% in Western Europe to 40% in the South America region, MASLD being associated with various complications, including HCC (2, 3).

The incidence of HCC in patients with liver cirrhosis varies slightly depending on the etiology but exceeds 1.5% per year; therefore, all current guidelines recommend screening in such patients.

The purpose of screening patients according to their risk of developing HCC is to enable early detection at stages when curative therapies are most effective, thereby improving prognosis and reducing mortality. In the early stages, HCC is typically asymptomatic, which makes active surveillance essential. A meta-analysis of 59 studies demonstrated that patients with hepatocellular carcinoma (HCC) who were detected through surveillance were more likely to undergo curative treatment than those diagnosed after the onset of symptoms (4).

When implementing a screening program, the potential benefits and negative effects of screening must be considered. Several cohort studies have evaluated the benefits of HCC surveillance, demonstrating an association between early detection and improved survival rates (5-7). However, two studies reported negative effects in around 20% of patients due to false-positive screening results that led to unnecessary invasive investigations (8, 9).

Parikh et al. evaluated the benefits and negative effects of screening for HCC (10). They concluded that surveillance increases the rate of early detection and that the cost-effectiveness of screening remains high, despite the potential harms.

10.2. Target populations for HCC surveillance

According to EASL (European Association for the Study of the Liver) guidelines, high-risk groups for which *HCC surveillance is recommended* are (11):

- *Patients with liver cirrhosis*, regardless of etiology, who are classified as Child-Pugh A or B, as well as patients with Child-Pugh C liver cirrhosis, who are awaiting liver transplantation. The new EASL guidelines on HCC management emphasize, “Patients with cirrhosis should be offered surveillance for HCC unless they have a relatively high risk of death from non-HCC causes, or they could not be offered a curative intent treatment for HCC" (11).

The risk of HCC in patients with cirrhosis varies according to the underlying etiology, being higher in viral-related cirrhosis than in cirrhosis associated with alcohol-induced liver disease. Variable incidences have been reported in MASLD (12-14). Given that the benefit of surveillance increases with higher baseline risk, a personalized surveillance based on risk assessment would be beneficial. Several risk models have been developed and are awaiting validation in clinical practice (15-18).

- *Patients with chronic liver disease and advanced fibrosis*
    - Patients with chronic hepatitis B virus infection are at risk of developing hepatocellular carcinoma (HCC), although this risk is lower than that associated with cirrhosis. To stratify the risk in these patients, both the EASL (11) and the American Association for the Study of Liver Diseases (AASLD) guidelines on HCC management (19) recommend using the Page B score. Patients with a Page B score (platelet count, age, gender) greater than 10 are at an increased risk of developing HCC within five years and should therefore be screened.
    - *Patients with chronic hepatitis C virus infection and advanced fibrosis* who are treated with direct-acting antivirals (DAAs) are at risk of developing hepatocellular carcinoma (HCC), but this risk depends on several factors, such as the patient's response to treatment and the presence of signs of liver cirrhosis before treatment begins. However, screening patients without cirrhosis for HCC is not considered cost-effective. Patients with cirrhosis who are treated successfully with DAAs continue to have an increased risk of developing HCC within 10 years of therapy. Beyond this period, the need for continued surveillance should be reassessed, based on individual risk factors.
    - *MASLD patients*. Patients with MASLD have a risk of developing HCC depending on the degree of fibrosis. The risk of hepatocellular carcinoma (HCC) in patients with MASLD without cirrhosis is0.03 per 100 person-years/ 0.03 cases per 100 person-years, compared with 3.48 cases per 100 person-years in those with MASLD-related cirrhosis (14).

As the number of patients with MASLD is very high, it is not considered cost-effective to screen all patients with MASLD without cirrhosis for HCC. With the increasing incidence of MASLD in developed countries, it is expected that

the incidence of HCC in the context of MASLD will also rise in the coming years. Therefore, risk stratification in this patient population is necessary.
The known risk factors for the progression of MASLD and HCC are type 2 diabetes, obesity and male sex (20).

In a review study, Mi K. and colleagues identified the following as independent risk factors for hepatocellular carcinoma (HCC) in the setting of MASLD: male sex; age over 65 years; body mass index (BMI) over 30 kg/m^2; waist circumference exceeding 110 cm; hypertension; type 2 diabetes mellitus (T2DM); alcohol intake; smoking; dyslipidemia; elevated alanine transaminase (ALT); and platelet counts of $150 \times 10^9/L$ or less (21). They also evaluated the role of risk scores in selecting MASLD patients for HCC screening. They found that the FIB-4 score had the highest sensitivity, at 95.20% (22), while the GALAD score [based on the patient's sex, age, and serum levels of AFP, AFP subtype L3 (AFP-L3), and des-gamma-carboxy prothrombin (DCP)] had the highest specificity, at 96.15% (23).

Many other risk scores have been created to select patients at high risk for HCC for surveillance: the Toronto HCC Risk Index, aMAP (age, male, albumin–bilirubin, platelets), HCC-RIFLE HCC, the NAFLD fibrosis score, with variable sensitivity.

A very recent study developed a novel risk prediction model for hepatocellular carcinoma in MASLD: the MASLD-HCC score. This score incorporates important cardiometabolic risk factors (such as overweight/obesity, central obesity, and prediabetes/diabetes) and fibrosis-related factors. It demonstrated superior predictive performance compared with existing models (24).

Using risk scores to stratify patient risk enables the identification of patients with MASLD without cirrhosis who nevertheless have a sufficiently high risk of developing HCC to justify surveillance (25).

The American Association of Gastroenterology (AGA) recommends monitoring patients with MASLD and severe fibrosis (F3). The assessment of liver fibrosis must be performed using at least two non-invasive tests, such as the FIB-4 index, the Enhanced Liver Fibrosis (ELF) Panel, Shear Wave Elastography (SWE), and MR elastography (MRE), among others (26).

10.3. Screening methods

Ultrasound at six-monthly intervals is the method recommended by all guidelines for monitoring patients at risk of hepatocellular carcinoma (HCC). The sensitivity of ultrasound as a screening method is influenced by several factors, including the expertise of the examiner, the acoustic window during examination, the proportion of the liver that can be evaluated, the presence of hepatic steatosis and extension of liver heterogeneity, and the size of HCC nodules. However, ultrasound has many advantages, such as being low-cost, non-invasive, readily available, and safe.

The role of ultrasound in hepatocellular carcinoma (HCC) screening has been evaluated in multiple studies. Singal et al. report that ultrasound is a very sensitive screening method (94%), but that sensitivity decreases to 63% for small lesions (27).

A 2018 meta-analysis indicates that ultrasound has 45% sensitivity in detecting small lesions when used as the sole surveillance method. Combining ultrasound with alpha-fetoprotein (AFP) testing increases sensitivity to 63% (28).

Regarding the role of ultrasound in patients with hepatic steatosis and cirrhosis, the American College of Radiology has introduced the LIRADS US score (ultrasound Liver Imaging Reporting and Data System) to standardize ultrasound reporting data. This algorithm includes three visualization scores (29, 30):

VIS-A: No or minimal limitations;

VIS-B: Moderate limitations due to heterogeneity of the liver parenchyma or moderate beam attenuation or difficulty in the visualization of some portion of the liver;

VIS-C: Severe limitations, with significantly impaired visualization due to marked parenchymal heterogeneity or severe beam attenuation, resulting in non-visualization of the majority of the liver.

After classification into one of the three visualization scores, patient follow-up is recommended as follows: patients with a good visualization score (VIS-A) are recommended to continue ultrasound surveillance at 6-month intervals; for patients with a VIS-B visualization score, a shortened surveillance interval of 3 months is recommended. If a lesion measuring <1 cm is suspected and remains stable or is no longer visualized on subsequent examinations, standard surveillance intervals may be resumed.

For the VIS-C visualization score, a repeat ultrasound examination within 3 months is recommended, along with consideration of alternative surveillance

modalities. This visualization score is frequently reported among patients with MASLD and cirrhosis (31).

The EASL guidelines recommend that US screening for HCC must be performed by an experienced examiner (Fig. 10.1).

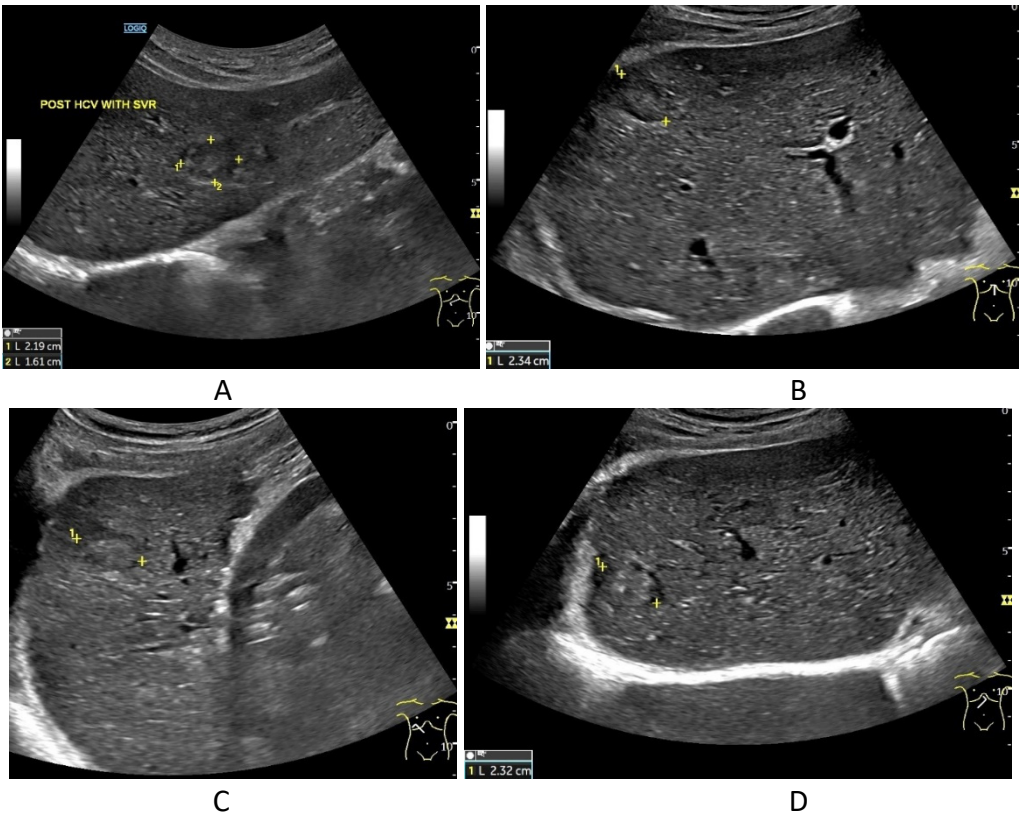


Fig. 10.1 A-D: Small HCCs found during the ultrasound screening in patients with liver cirrhosis.

Alpha-fetoprotein (AFP) is the most widely used biomarker for hepatocellular carcinoma (HCC) surveillance, but its sensitivity in detecting HCC is reduced by approximately 49.1% in early detection, with a specificity of 87.9% (32).

Combining AFP with ultrasound for HCC screening increases sensitivity from 51.6% for ultrasound alone to 74.1% for ultrasound plus AFP, with a specificity of 87.9% for ultrasound compared to 83.9% for ultrasound plus AFP (28).

Other biomarkers that were studied in relation to HCC are: AFP-L3, which measures a subfraction of AFP; and des-gamma-carboxy prothrombin (DCP), also known as vitamin K-dependent protein S (PIVKA-II), which is produced in excess by some types of HCC. AFP-L3% and DCP are not sensitive enough to detect early-stage HCC when used alone, but they are included in risk scores. The GALAD score, which includes patient sex, age, AFP-L3, AFP and DCP levels, has been found to have good sensitivity and specificity in the early detection of HCC (sensitivity of 65% and specificity of 82%, respectively) (33, 34, 35). A meta-analysis study found that the sensitivity and specificity of the GALAD score for diagnosing HCC (Barcelona stage 0/A) were 73% and 87%, respectively (35).

Contrast-enhanced MRI (CE-MRI). Studies have shown that CE-MRI is the most sensitive method for diagnosing small nodules, with the lowest false-negative rate (CE-MRI sensitivity: 84.8%; US sensitivity: 27.3%) (36). However, MRI remains costly, less widely accessible, and potentially uncomfortable for patients due to the prolonged examination time. In addition, the use of contrast agents carries a risk of adverse reactions. MRI-based surveillance may be recommended for certain HCC risk categories.

In their study, Nahon et al. suggest that surveillance using MRI at 6 months is cost effective for patients with an annual HCC risk >3%, as calculated using a scoring system that includes age, sex, platelet count, GGT >1.5 ULN, bilirubin >12 µmol/L and AFP >5 ng/ml (38).

Abbreviated MRI can be a solution for HCC screening. This protocol uses selected sequences from a full diagnostic protocol, reducing the examination time from ~45 minutes to ~15 minutes.

Studies evaluating the performance of abbreviated magnetic resonance imaging (aMRI) in hepatocellular carcinoma (HCC) screening have reported promising results (39, 40).

EASL supports risk-based surveillance. Accordingly, the choice of screening modality, the surveillance interval, and the decision to initiate surveillance should be guided by the individual patient's estimated risk of developing HCC. This strategy stratifies patients into three categories based on their risk level and the resulting need for monitoring. Patients classified as high risk are candidates for MRI-based surveillance, while those in the

medium-risk group are recommended to undergo standard monitoring (ultrasound and AFP at six months). Patients at low risk may not require monitoring.

We would like to emphasize that, when HCC screening is performed by ultrasound on patients at risk, the quality of the examination is essential. The quality of the ultrasound machine and the experience of the person performing this evaluation must be high enough (41). On the other hand, if the entire liver cannot be screened during a liver ultrasound examination, then another imaging technique must be recommended. Good cooperation from patients during the examination is important for improving visualization of the entire liver.

In conclusion, the aim of screening tests is to detect (HCCs) at an early stage, thereby enabling access to potentially curative treatment options.

The standard screening test involves an ultrasound examination of the liver performed alongside an AFP test at six-monthly intervals. However, ultrasound's sensitivity as a screening modality is influenced by multiple factors and remains suboptimal, particularly for detecting small or early-stage HCCs.

The most efficient approach to HCC monitoring is a risk-based surveillance strategy, as it allows for the individualized selection of surveillance modalities and intervals according to the patient’s estimated risk profile.

References

1. Ferlay J, Colombet M, Soerjomataram I, Parkin DM, Piñeros M, Znaor A, et al. Cancer statistics for the year 2020: An overview. Int J Cancer. 2021 Apr 5. doi: 10.1002/ijc.33588. Epub ahead of print. PMID: 33818764.

2. Younossi ZM, Golabi P, Paik JM, Henry A, Van Dongen C, Henry L. The global epidemiology of nonalcoholic fatty liver disease (NAFLD) and nonalcoholic steatohepatitis (NASH): a systematic review. Hepatology. 2023 Apr 1;77(4):1335-1347.

3. Mauro E, de Castro T, Zeitlhoefler M, Sung MW, Villanueva A, Mazzaferro V, et al. Hepatocellular carcinoma: Epidemiology, diagnosis and treatment. JHEP Rep. 2025 Sep 3;7(12):101571.

4. Singal AG, Zhang E, Narasimman M, Rich NE, Waljee AK, Hoshida Y, et al. HCC surveillance improves early detection, curative treatment receipt, and survival in patients with cirrhosis: A meta-analysis. J Hepatol. 2022 Jul;77(1):128-139.

5. van Meer S, de Man RA, Coenraad MJ, Sprengers D, van Nieuwkerk KM, Klümpen HJ, et al. Surveillance for hepatocellular carcinoma is associated with increased survival: Results from a large cohort in the Netherlands. J Hepatol. 2015 Nov;63(5):1156-63
6. Singal AG, Pillai A, Tiro J. Early detection, curative treatment, and survival rates for hepatocellular carcinoma surveillance in patients with cirrhosis: a meta-analysis. PLoS Med 2014;11:e1001624.
7. Choi DT, Kum HC, Park S, Ohsfeldt RL, Shen Y, Parikh ND, et al. Hepatocellular Carcinoma Screening Is Associated With Increased Survival of Patients With Cirrhosis. Clin Gastroenterol Hepatol. 2019 Apr;17(5):976-987.e4.
8. Konerman MA, Verma A, Zhao B, Singal AG, Lok AS, Parikh ND. Frequency and Outcomes of Abnormal Imaging in Patients With Cirrhosis Enrolled in a Hepatocellular Carcinoma Surveillance Program. Transpl 2019;25:369–379.
9. Atiq O, Tiro J, Yopp AC, Muffler A, Marrero JA, Parikh ND, et al. An assessment of benefits and harms of hepatocellular carcinoma surveillance in patients with cirrhosis. Hepatology. 2017 Apr;65(4):1196-1205.
10. Parikh ND, Singal AG, Hutton DW, Tapper EB. Cost-Effectiveness of Hepatocellular Carcinoma Surveillance: An Assessment of Benefits and Harms. Am J Gastroenterol. 2020 Oct;115(10):1642-1649.
11. European Association for the Study of the Liver. EASL Clinical Practice Guidelines on the management of hepatocellular carcinoma. J Hepatol. 2025 Feb;82(2):315-374.
12. West J, Card TR, Aithal GP, Fleming KM. Risk of hepatocellular carcinoma among individuals with different aetiologies of cirrhosis: a population-based cohort study. Aliment Pharmacol Ther. 2017 Apr;45(7):983-990.
13. Ioannou GN, Splan MF, Weiss NS, McDonald GB, Beretta L, Lee SP. Incidence and predictors of hepatocellular carcinoma in patients with cirrhosis. Clin Gastroenterol Hepatol. 2007 Aug;5(8):938-45, 945.e1-4.
14. Orci LA, Sanduzzi-Zamparelli M, Caballol B, Sapena V, Colucci N, Torres F, et al. Incidence of Hepatocellular Carcinoma in Patients With Nonalcoholic Fatty Liver Disease: A Systematic Review, Meta-analysis, and Meta-regression. Clin Gastroenterol Hepatol. 2022 Feb;20(2):283-292.e10.
15. Khan IM, Gjuka D, Jiao J, Song X, Wang Y, Wang J, et al. A Novel Biomarker Panel for the Early Detection and Risk Assessment of Hepatocellular Carcinoma in Patients with Cirrhosis. Cancer Prev Res (Phila). 2021 Jun;14(6):667-674.
16. Innes H, Jepsen P, McDonald S, Dillon J, Hamill V, Yeung A, et al. Performance of models to predict hepatocellular carcinoma risk among UK patients with cirrhosis and cured HCV infection. JHEP Rep. 2021 Oct 7;3(6):100384.
17. Ioannou GN, Green PK, Beste LA, Mun EJ, Kerr KF, Berry K. Development of models estimating the risk of hepatocellular carcinoma after antiviral treatment for hepatitis C. J Hepatol. 2018 Nov;69(5):1088-1098.

18. Sharma SA, Kowgier M, Hansen BE, Brouwer WP, Maan R, Wong D, et al. Toronto HCC risk index: A validated scoring system to predict 10-year risk of HCC in patients with cirrhosis. J Hepatol. 2017 Aug 24:S0168-8278(17)32248-1.
19. Singal AG, Llovet JM, Yarchoan M, Mehta N, Heimbach JK, Dawson LA, et al. AASLD Practice Guidance on prevention, diagnosis, and treatment of hepatocellular carcinoma. Hepatology. 2023 Dec 1;78(6):1922-1965.
20. Tovoli F, Ferri S, Piscaglia F. Hepatocellular carcinoma in nonalcoholic fatty liver disease. Curr Pharm Des 2020;26:3909–14
21. Mi K, Ye T, Zhu L, Pan CQ. Risk-stratified hepatocellular carcinoma surveillance in non-cirrhotic patients with MASLD. Gastroenterol Rep (Oxf). 2025 Feb 20;13:goaf018.
22. Imai K, Takai K, Unome S, Miwa T, Hanai T, Suetsugu A, et al. FIB-4 index and NAFLD fibrosis score are useful indicators for screening high-risk groups of non-viral hepatocellular carcinoma. Mol Clin Oncol. 2023 Aug 24;19(4):80.
23. Best J, Bechmann LP, Sowa JP, Sydor S, Dechêne A, Pflanz K, et al. GALAD Score Detects Early Hepatocellular Carcinoma in an International Cohort of Patients With Nonalcoholic Steatohepatitis. Clin Gastroenterol Hepatol. 2020 Mar;18(3):728-735.e4.
24. Chun HS, Lee M, Lee HA, Park ES, Choi JY, Baek HS, et al. A Novel Risk Prediction Model for Hepatocellular Carcinoma in MASLD: A Multinational, Multicenter Cohort Study. Clin Gastroenterol Hepatol. 2026 Mar;24(3):688-700.e17.
25. EASL Policy Statement Risk-based surveillance for hepatocellular carcinoma among patients with cirrhosis. Available at: https://easl.eu/wp-content/uploads/2023/04/ Policy-Statement-Liver-Cancer- Screening_VFF.pdf. Accessed July 15, 2024.
26. Loomba R, Lim JK, Patton H, El-Serag HB. AGA clinical practice update on screening and surveillance for hepatocellular carcinoma in patients with nonalcoholic fatty liver disease: expert review. Gastroenterology 2020;158:1822-30.
27. Singal A, Volk ML, Waljee A, Salgia R, Higgins P, Rogers MA, et al. Meta-analysis: surveillance with ultrasound for early-stage hepatocellular carcinoma in patients with cirrhosis. Aliment Pharmacol Ther. 2009 Jul;30(1):37-47.
28. Tzartzeva K, Obi J, Rich NE, Parikh ND, Marrero JA, Yopp A, et al. Surveillance Imaging and Alpha Fetoprotein for Early Detection of Hepatocellular Carcinoma in Patients With Cirrhosis: A Meta-analysis. Gastroenterology. 2018 May;154(6):1706-1718.e1.
29. American College of Radiology. ACR Ultrasound Liver Reporting and Data System. *J Am. Coll Radiol.* 2019;16(10):1421–1428.
30. Kamaya A, Fetzer DT, Seow JH, Burrowes DP, Choi HH, Dawkins AA, et al. LI-RADS US Surveillance Version 2024 for Surveillance of Hepatocellular Carcinoma: An Update to the American College of Radiology US LI-RADS. Radiology. 2024 Dec;313(3):e240169.
31. Kang JH, Kim NH, Kim DH, Choi Y, Choi JI. Ultrasound LI-RADS Visualization Scores on Surveillance Ultrasound for Hepatocellular Carcinoma: A Systematic Review With Meta-analysis. Ultrasound Med Biol. 2023 Oct;49(10):2205-2212.

32. Singal AG, Haaland B, Parikh ND, Ozbay AB, Kirshner C, Chakankar S, et al. Comparison of a multitarget blood test to ultrasound and alpha-fetoprotein for hepatocellular carcinoma surveillance: Results of a network meta-analysis. Hepatol Commun. 2022 Oct;6(10):2925-2936.
33. Berhane S, Toyoda H, Tada T, Kumada T, Kagebayashi C, Satomura S, et al. Role of the GALAD and BALAD-2 Serologic Models in Diagnosis of Hepatocellular Carcinoma and Prediction of Survival in Patients. Clin Gastroenterol Hepatol. 2016; 14:875–886 e876.
34. Mak LY, Yuen MF. Surveillance for Hepatocellular Carcinoma in Cirrhosis: End of Monopoly for Serum Alpha Fetoprotein. Gastroenterology. 2025 Feb;168(2):217-219.
35. Guan MC, Zhang SY, Ding Q, Li N, Fu TT, Zhang GX, et al. The Performance of GALAD Score for Diagnosing Hepatocellular Carcinoma in Patients with Chronic Liver Diseases: A Systematic Review and Meta-Analysis. J Clin Med. 2023 Jan 26;12(3):949.
36. Kim SY, An J, Lim YS, Han S, Lee JY, Byun JH, et al. MRI With Liver-Specific Contrast for Surveillance of Patients With Cirrhosis at High Risk of Hepatocellular Carcinoma. JAMA Oncol. 2017 Apr 1;3(4):456-463.
37. Rhee H, Kim MJ, Kim DY, An C, Kang W, Han K, et al. Noncontrast Magnetic Resonance Imaging vs Ultrasonography for Hepatocellular Carcinoma Surveillance: A Randomized, Single-Center Trial. Gastroenterology. 2025 Jun;168(6):1170-1177.e12.
38. Nahon P, Najean M, Layese R, Zarca K, Segar LB, Cagnot C, et al. Early hepatocellular carcinoma detection using magnetic resonance imaging is cost-effective in high-risk patients with cirrhosis. JHEP Rep. 2021 Nov 4;4(1):100390.
39. Gupta P, Soundararajan R, Patel A, Kumar MP, Sharma V, Kalra N. Abbreviated MRI for hepatocellular carcinoma screening: A systematic review and meta-analysis. J Hepatol. 2021; 75:108–19.
40. Park HJ, Kim SY, Singal AG, Lee SJ, Won HJ, Byun JH, et al. Abbreviated magnetic resonance imaging vs ultrasound for surveillance of hepatocellular carcinoma in high-risk patients. Liver Int. 2022;42:2080–92.
41. Dănilă M, Sporea I. Ultrasound screening for hepatocellular carcinoma in patients with advanced liver fibrosis. An overview. Med Ultrason. 2014 Jun;16(2):139-44.

11. Multiparametric Ultrasound for Portal Hypertension

11.1. Standard Ultrasound for Portal Hypertension

Ivica Grgurević

Abstract

Portal hypertension (PH) is defined by an increased portal venous pressure gradient, with clinically significant PH occurring at HVPG ≥10 mmHg. Although invasive measurement remains the gold standard, ultrasound is widely used for noninvasive evaluation.

Gray-scale ultrasound cannot measure portal pressure directly but detects morphological changes associated with PH, including portal and splenic vein dilatation, splenomegaly, portosystemic collaterals, and ascites. Additional findings such as umbilical vein recanalization or visceral congestion may also occur. These signs usually appear after the development of clinically significant PH and indicate increased risk of complications. However, while highly specific in cirrhosis, ultrasound findings have limited sensitivity, and their absence does not exclude portal hypertension.

11.1.1. Introduction

Portal hypertension (PH) is defined as an increase in pressure within the portal venous system, resulting in a rise of the pressure gradient between the portal vein and the inferior vena cava to more than 5 mmHg (1, 2). The current gold standard for quantifying the severity of PH is the invasive catheterization of the hepatic veins under fluoroscopic guidance, during which the hepatic venous pressure gradient (HVPG) is measured. HVPG represents the difference between the wedged hepatic vein pressure (WHVP) and the free hepatic vein pressure (FHVP). Portal hypertension is present when HVPG exceeds 5 mmHg; however, it is considered clinically significant (clinically significant portal hypertension, CSPH) only at values ≥10 mmHg, as complications related to portal hypertension—such as the development of esophageal and gastric varices, ascites, hepatic encephalopathy, and an increased risk of death—begin to occur above this threshold. HVPG is an indirect measure of portal pressure and correlates closely with it; however, it does not reliably reflect the true portal pressure in presinusoidal causes of PH, in which direct measurement of portal vein pressure would theoretically be more accurate.

Direct measurement can be performed via percutaneous transhepatic puncture of the portal vein using a Chiba needle connected to a manometer; however, due to its invasiveness and associated risks, this method is generally avoided (3). A potential alternative is the endoscopic ultrasound (EUS)-guided approach, in which a needle is used to puncture a branch of the hepatic vein and the portal vein, allowing pressure measurements whose difference represents the porto-caval pressure gradient (PCPG) (4). However, this technique remains under scientific evaluation and has inherent limitations.

11.1.2. Overview of the ultrasound modalities used for the portal hypertension assessment

Neither conventional ultrasonography nor Doppler ultrasound allows direct measurement of portal pressure (5). Nevertheless, ultrasonography enables morphological evaluation of the liver, spleen, associated vasculature, and other abdominal organs and structures that undergo changes in patients with PH. Gray-scale (B-mode) ultrasound can identify morphological signs characteristic of portal hypertension and its underlying causes.

The application of Doppler ultrasound, through analysis of blood flow features and hemodynamic changes in the hepatic and portal vasculature, may help determine certain etiologies of PH. In addition, the use of ultrasound contrast agents and analysis of perfusion dynamics—specifically dynamic contrast flow curves (time–intensity curves, TICs) in different hepatic vascular structures—may, according to some studies, establish the presence of PH and potentially stratify its severity into several categories (6,7).

Currently, however, the principal noninvasive modality used in the diagnostic work-up of PH is liver and spleen elastography. In combination with platelet count (e.g., according to the Baveno VII criteria, ANTICIPATE±NASH model, and NICER model), elastography enables accurate classification of CSPH in approximately 60-70% of patients with advanced chronic liver disease (ACLD) (8-11).

While elastography and Doppler techniques are discussed in separate chapters, the following section addresses the application of gray-scale ultrasonography in the diagnosis of PH. As these signs typically appear only after the development of CSPH, their detection by ultrasound also indicates the presence of CSPH and, consequently, a substantially increased prognostic risk in these patients.

11.1.3. Grey-scale (B-mode) ultrasound assessment of the portal hypertension

Morphological signs of CSPH include dilatation of the portal vein and its major tributaries (the splenic vein and the superior mesenteric vein), the presence of portosystemic venous collaterals, splenomegaly, edema of the wall of the gallbladder, stomach and intestines due to congestion, and ascites (5,12).

The portal vein is considered dilated when its diameter exceeds 12.5–13 mm at the hepatic hilum (Fig. 11.1.1). The splenic vein is dilated when its diameter exceeds 11 mm, typically accompanied by loss of respiratory variability in diameter (<40% collapse during expiration) due to high portal pressure (5).

Portosystemic venous collaterals represent pathways through which blood from the high-pressure portal system is diverted into the lower-pressure systemic (caval) circulation (13). Most commonly, serpiginous venous collaterals are observed at the splenic hilum or its cranial pole, communicating with the short gastric veins. A splenorenal shunt (between the splenic vein and the left renal vein) may also be present. In some cases, a dilated left gastric vein (LGV) can be visualized; this vessel drains blood along the lesser curvature of the stomach into the portal vein and communicates cranially with the submucosal esophageal veins. In PH, the LGV becomes dilated (>6 mm), and blood flow reverses to a hepatofugal direction, i.e., toward the esophagus, constituting the pathway for esophageal variceal filling (13).

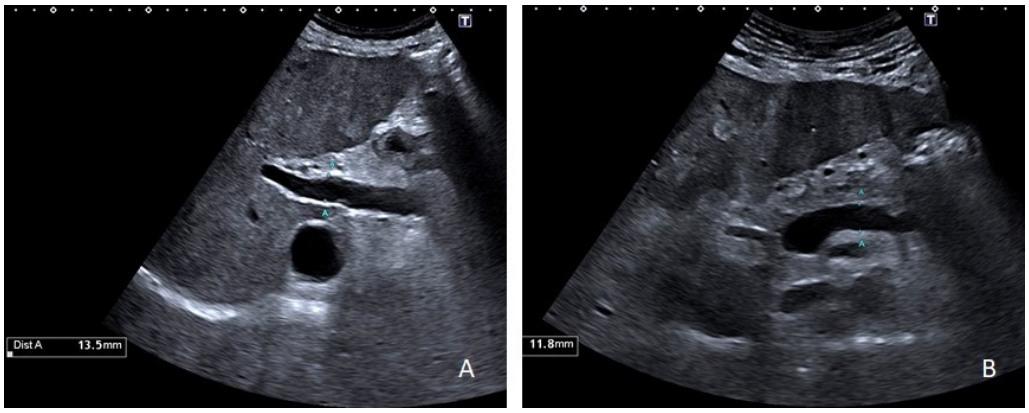


Fig. 11.1.1 Dilated (13.5 mm) portal vein (A), and splenic (11.8 mm) vein (B) in a patient with liver cirrhosis and portal hypertension.

In patients with liver cirrhosis, recanalization of the umbilical vein—normally obliterated after birth—may occur (Fig. 11.1.2). It originates from the left branch of the portal vein and courses along the falciform ligament, diverting blood from the liver toward the anterior abdominal wall, where it runs beneath the anterior abdominal wall toward the umbilical region. At the umbilicus, it communicates with the inferior epigastric veins and ultimately drains into the external iliac veins and subsequently the inferior vena cava, or alternatively with the superior epigastric vein, which drains via the thoracic veins into the superior vena cava. Dilated superficial branches of the superior and inferior epigastric veins in the umbilical region form the characteristic “caput medusae.”

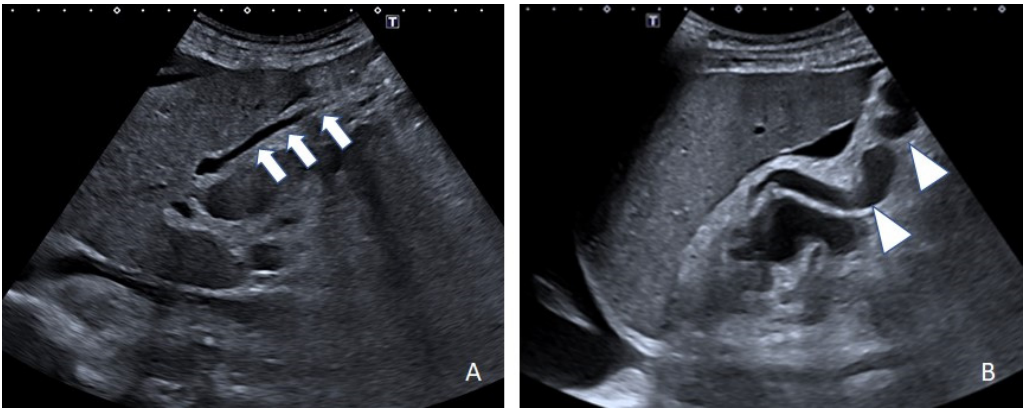


Fig. 11.1.2. Portosystemic collaterals in portal hypertension. A-Recanalized umbilical vein (longitudinal section through left liver lobe, sagittal plane, white arrows); B-collateral veins in the splenic hilum (white arrowheads).

Mesenteric collaterals connecting the superior mesenteric vein with retroperitoneal veins draining into the inferior vena cava may also be demonstrated; however, due to their deep location and the interposition of bowel gas and adipose tissue, they are more difficult to visualize by ultrasonography.

In PH the spleen becomes enlarged (>12–13 cm in longitudinal diameter, depending on body height) (Fig. 11.1.3). Splenomegaly is present in 50–80% of patients with cirrhosis, with higher prevalence among those with decompensated disease (14). A further increase in spleen size occurs in approximately 50% of patients and, in compensated individuals, is associated with a higher risk of decompensation. Due to hypersplenism and enhanced phagocytosis, hemosiderin accumulates within the splenic parenchyma, producing hyperechoic foci known as Gamna–Gandy bodies (15).

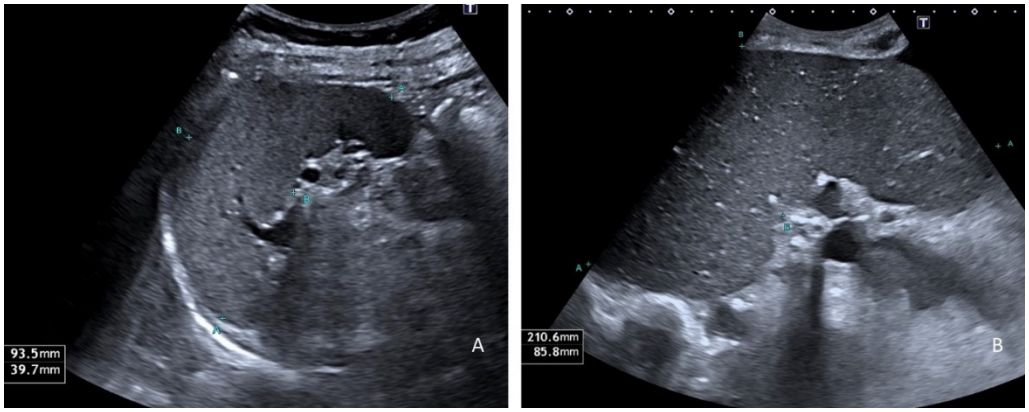


Fig. 11.1.3. Normal spleen and splenomegaly. A-normal spleen in a healthy person (cranio-caudal diameter<12 cm, homogeneous parenchyma); B-Splenomegaly (21 cm in cranio-caudal diameter) in a patient with liver cirrhosis and severe portal hypertension. Note Gamna-Gandy bodies in the splenic parenchyma (hyperechoic spots).

Ascites is a characteristic pathophysiological consequence of portal hypertension but occurs predominantly in patients with cirrhosis as the underlying cause of PH and only rarely in prehepatic etiologies (Fig. 11.1.4). Caution is warranted, as not all ascites are attributable to PH. In the absence of chronic liver disease, ascites may result from other etiologies, such as peritoneal carcinomatosis secondary to disseminated malignancies—most commonly originating from the gastrointestinal tract or gynecological organs. Ascites may also occur in systemic diseases, including polyserositis in systemic lupus erythematosus, protein-losing enteropathy, nephrotic syndrome, or heart failure. These conditions are typically accompanied by characteristic clinical features and lack ultrasonographic signs of PH or liver cirrhosis. In peritoneal carcinomatosis small nodules sticked to parietal peritoneum (which should otherwise be smooth) or mesentery may be observed by gray-scale ultrasound.

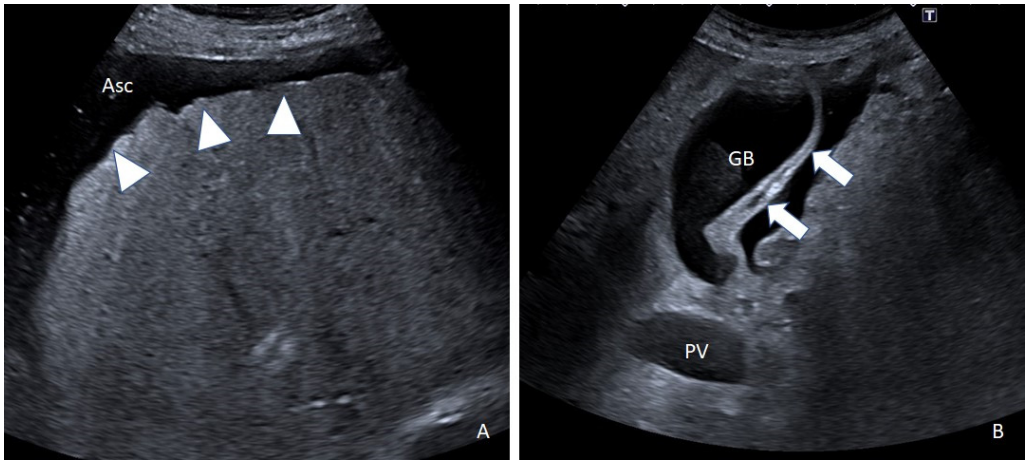


Fig. 11.1.4. Ascites and gallbladder edema. A-ascites in a patient with decompensated cirrhosis. Note the nodularity of the liver surface (arrowheads) and coarse parenchyma. The liver is surrounded by the anechoic ascitic fluid; B-Gallbladder wall edema (white arrows) in the same patient.

11.1.4. Limitations of grey-scale ultrasound in diagnosing portal hypertension

Highlighted morphological features as revealed by greyscale ultrasound are highly specific of PH when an underlying cause, such as cirrhosis, is present, but their sensitivity is limited; absence of these findings does not exclude PH (5). For instance, while splenomegaly is a recognized feature of PH, it is absent in approximately one-third of patients with cirrhosis and PH. Ascites is a specific indicator only in the context of chronic liver disease; otherwise, it may result from other causes such as peritoneal carcinomatosis. In the context of cirrhosis, the development of ascites indicates progression to the decompensated stage of the disease; however, the absence of ascites does not exclude the presence of CSPH. Similarly, a dilated PV is observed in PH secondary to cirrhosis, but it may also occur in non-cirrhotic conditions such as massive splenomegaly in some hematological conditions, where increased portal inflow coming from splenic vein leads to PV dilation and elevated flow velocity—contrasting with the reduced PV flow seen in cirrhosis

In conclusion, greyscale ultrasound can detect morphological signs of portal hypertension in chronic liver disease, including dilation of the portal and splenic veins, portosystemic collaterals, splenomegaly, ascites, and congestion-related edema of visceral organs. Although these ultrasound features are highly specific for PH when cirrhosis is present, their sensitivity is limited, and their absence does not exclude CSPH.

References

1. Abraldes JG, Sarlieve P, Tandon P. Measurement of portal pressure. Clin Liver Dis. 2014 Nov;18(4):779-92.
2. Boyer TD, Triger DR, Horisawa M, Redeker AG, Reynolds TB. Direct transhepatic measurement of portal vein pressure using a thin needle. Comparison with wedged hepatic vein pressure. Gastroenterology. 1977 Apr;72(4 Pt 1):584-9.
3. Hu Y, Duan S, Zhang Y, Hao L, Wang S, Xue F, et al. Feasibility and safety of ultrasound-guided percutaneous transhepatic measurement of portal venous pressure. PLoS One. 2024 Jul 19;19(7):e0305725.
4. Vanderschueren E, Laleman W, Bonne L, Maleux G, Wagner DR, Yeh C, et al. Endoscopic ultrasound-guided portosystemic pressure gradient measurement vs. transjugular balloon occlusion measurement in patients with cirrhosis (ENCOUNTER): A bicentric EU study. JHEP Rep. 2025 May 29;7(8):101466.
5. Berzigotti A, Piscaglia F. Ultrasound in portal hypertension--part 1. Ultraschall Med. 2011 Dec;32(6):548-68
6. Jeong WK, Kim TY, Sohn JH, Kim Y, Kim J. Severe portal hypertension in cirrhosis: evaluation of perfusion parameters with contrast-enhanced ultrasonography. PLoS One. 2015 Mar 23;10(3):e0121601.
7. Zocco MA, Cintoni M, Ainora ME, Garcovich M, Lupascu A, Iezzi R, et al. Noninvasive Evaluation of Clinically Significant Portal Hypertension in Patients with Liver Cirrhosis: The Role of Contrast-Enhanced Ultrasound Perfusion Imaging and Elastography. Ultraschall Med. 2023 Aug;44(4):428-435.
8. de Franchis R, Bosch J, Garcia-Tsao G, Reiberger T, Ripoll C; Baveno VII Faculty. Baveno VII - Renewing consensus in portal hypertension. J Hepatol. 2022 Apr;76(4):959-974.
9. Dajti E, Ravaioli F, Zykus R, Rautou PE, Elkrief L, Grgurevic I, et al; Spleen Stiffness—IPD-MA Study Group. Accuracy of spleen stiffness measurement for the diagnosis of clinically significant portal hypertension in patients with compensated advanced chronic liver disease: a systematic review and individual patient data meta-analysis. Lancet Gastroenterol Hepatol. 2023 Sep;8(9):816-828.
10. Jachs M, Odriozola A, Turon F, Moga L, Téllez L, Fischer P, et al; SSM-100Hz/ACLD Study Group; Baveno Cooperation. Spleen stiffness measurement by vibration-controlled transient elastography at 100 Hz for non-invasive predicted diagnosis of clinically significant portal hypertension in patients with compensated advanced chronic liver disease: a modelling study. Lancet Gastroenterol Hepatol. 2024 Dec;9(12):1111-1120.
11. Bañares J, Pons M, Reiberger T, Mandorfer M, Jachs M, Semmler G, et al; a study by the Baveno Cooperation: an EASL consortium. Refining the Baveno VII criteria for clinically significant portal hypertension: An individual patient data meta-analysis. J Hepatol. 2026 Mar;84(3):543-553.

12. Kennedy P, Bane O, Hectors SJ, Fischman A, Schiano T, Lewis S, et al. Noninvasive imaging assessment of portal hypertension. Abdom Radiol (NY). 2020 Nov;45(11):3473-3495.
13. Bandali MF, Mirakhur A, Lee EW, Ferris MC, Sadler DJ, Gray RR, et al. Portal hypertension: Imaging of portosystemic collateral pathways and associated image-guided therapy. World J Gastroenterol. 2017 Mar 14;23(10):1735-1746.
14. Berzigotti A, Zappoli P, Magalotti D, Tiani C, Rossi V, Zoli M. Spleen enlargement on follow-up evaluation: a noninvasive predictor of complications of portal hypertension in cirrhosis. Clin Gastroenterol Hepatol. 2008 Oct;6(10):1129-34.
15. Sagoh T, Itoh K, Togashi K, Shibata T, Nishimura K, Minami S, et al. Gamna-Gandy bodies of the spleen: evaluation with MR imaging. Radiology. 1989 Sep;172(3):685-7.

11.2. Value of Doppler ultrasound for the evaluation of Portal Hypertension

Ivica Grgurević

Abstract

Doppler ultrasonography is a key noninvasive tool for evaluating portal hypertension (PH), complementing grayscale ultrasound by providing information on hepatic and portal hemodynamics. It helps identify characteristic flow alterations in the portal, hepatic, and splenic vessels and supports the diagnosis of PH and its complications.

Doppler parameters such as portal vein velocity, congestion index, and arterial resistance indices reflect vascular remodeling associated with chronic liver disease. The technique is particularly useful for determining the etiology of PH, differentiating posthepatic, intrahepatic, and prehepatic causes, including congestive hepatopathy, Budd–Chiari syndrome, cirrhosis, and portal vein thrombosis. Doppler is also essential for monitoring the patency and function of transjugular intrahepatic portosystemic shunts (TIPS).

However, despite its high specificity, Doppler has limited sensitivity for detecting PH and cannot reliably grade its severity or assess response to beta-blocker therapy. Overall, Doppler ultrasound remains a valuable diagnostic and surveillance tool in the management of portal hypertension.

11.2.1. Introduction

In the evaluation of liver disease, grayscale ultrasound provides essential information on liver morphology, the vessels of the hepato-portal system, and other related organs. However, additional insights can be obtained through Doppler imaging, which allows assessment of hepatic and portal blood flow as well as the hemodynamic changes occurring within these structures. Accordingly, Doppler serves two primary purposes: 1- establishing a diagnosis by identifying the etiology of liver injury when vascular or circulatory causes are suspected, and 2- evaluating portal hypertension (PH), including its underlying causes and potential complications (1-5).

Guidelines from American societies focused on vascular ultrasound classify Doppler evaluation of visceral organs as Category A (Appropriate) for indications such as hepatomegaly or splenomegaly, ascites, assessment of patients with cirrhosis, evaluation of PH, and follow-up after transjugular

intrahepatic portosystemic shunt (TIPS) placement. Indications such as abnormal liver function tests, absence of an alternative liver disease diagnosis (e.g., drug-induced injury or viral hepatitis), unexplained jaundice (with biliary obstruction excluded), and abdominal pain are categorized as M (Maybe appropriate) (6). Similarly, the European Federation of Societies for Ultrasound in Medicine and Biology (EFSUMB) recommends Doppler for diagnosing PH, determination of its etiology, and monitoring patency of TIPS or surgical shunts (7,8). Current evidence does not support using Doppler to grade the severity of PH or to monitor hemodynamic response to nonselective beta-blockers (NSBB).

The role of Doppler in diagnosing vascular liver diseases will be discussed further in sections on the etiology of PH, including congestive liver disease and portal vein thrombosis or stenosis.

11.2.2. Doppler in the Evaluation of Portal Hypertension

Grayscale ultrasound often provides sufficient morphological information to establish the diagnosis of PH, or more specifically CSPH, and this was discussed in the previous chapter. On the other hand, grayscale ultrasound alone may be insufficiently sensitive to detect early cirrhosis, the most common cause of PH. In such cases, Doppler might reveal hemodynamic changes reflecting vascular remodeling within the cirrhotic liver. Typical Doppler parameters indicative of PH are summarized in Table 11.2.I.

Most analyses utilize simple parameters automatically calculated by ultrasound systems, including peak systolic velocity (PSV) and end-diastolic velocity (EDV) for arteries or over a defined interval in veins. These measurements yield flow velocities and indices such as the resistive index (RI) and pulsatility index (PI). More complex indices, including the congestion index of the portal vein (CI = PV cross-sectional area / time-averaged mean velocity, TAMV), may also be calculated, along with other indices outlined in Table 11.2.I (9-15).

Assessment of the splenic vessels is additionally valuable in PH evaluation. Portosystemic collaterals in the splenic hilum may form a splenorenal shunt. As the spleen hypertrophies morphologically and functionally, resistance to arterial flow increases, resulting in elevated RI (>0.63) and PI (>1) in intraparenchymal branches of the splenic artery (15-17).

However, as with morphological assessment, Doppler findings of PH are characterized by high specificity (80–100%) but limited sensitivity (50–80%); their absence does not exclude cirrhosis or PH (7,8,18). Moreover, many studies

evaluating Doppler for PH diagnosis have been criticized for using healthy controls rather than patients with chronic liver disease. For this reason, elastography is now preferred for reliably excluding cirrhosis, with a negative predictive value of approximately 95%, as discussed in the respective chapters on liver elastography.

Table 11.2.I. Hemodynamic Indicators of Portal Hypertension in Chronic Liver Disease.

Indicator	Abbreviation	Cut-off	Reference
Portal vein diameter		>12,5-13 mm	Haag K. 1999.
Time average maximum velocity (portal vein)	Tamax	<13-15 cm/s	Zironi G. 1992; Iwao T. 1997.
Congestion index (The cross-sectional area of the portal vein / Time-Averaged Mean Velocity (TAMV))	CI	>0,1 cm x s	Moriyasu F. 1986; Haag K. 1999.
Hepatic artery pulsatility index	HAPI	>1,1	Iwao T. 1997; Schneider AW. 1999.
Liver vascular index (TAMV/HARI)	LVI	<12 cm/s	Iwao T. 1997
Splenic artery resistive index (PSV-EDV)/PSV	SARI	>0,6	Bolognesi M. 1996.
Splenic artery pulsatility index (PSV-EDV)/TAMV	SAPI	>1	Bolognesi M. 1996.

Legend: TAMax – time-averaged maximal velocity; TAMV – time-averaged mean velocity; HAPI – hepatic artery pulsatility index; HARI – hepatic artery resistive index; CI – congestion index; SAPI – splenic artery pulsatility index; SARI – splenic artery resistive index; HCI – hepatic circulatory index; PSV – peak systolic velocity; EDV – end-diastolic velocity. According to references 9-15.

11.2.3. Determining the Etiology of Portal Hypertension Using Doppler Ultrasonography

Doppler ultrasonography plays a pivotal role in evaluating patients with suspected or established portal hypertension (PH). The etiology of PH can be categorized as posthepatic, intrahepatic, or prehepatic. Intrahepatic causes are further subdivided into postsinusoidal, sinusoidal, and presinusoidal by anatomical localization and underlying etiopathogenesis.

1. Posthepatic Causes of Portal Hypertension

The most common posthepatic etiologies include congestive heart failure and Budd-Chiari syndrome, both of which result in hepatic congestion and chronic ischemia, ultimately promoting fibrosis and the development of PH.

a) Congestive Heart Failure

Elevated right-heart filling pressures, the hallmark of congestive heart failure, lead to increased venous pressure in all upstream structures, including the hepatic veins (HV). This causes hepatic blood stasis, manifesting morphologically as hepatomegaly and HV dilation (>8 mm measured 2–3 cm from the junction with the inferior vena cava) (19). Characteristic Doppler findings include pronounced phasicity in hepatic veins, with the reversal of systolic "s" wave in case of tricuspidal regurgitation (Fig. 11.2.1). Increased phasicity of the portal vein (PV) flow due to retrograde transmission of pressure from HV via central veins and sinusoids may be observed as well (19, 20). Portal waveform may adopt an undulating pattern and, in severe cases, a biphasic morphology with one positive and one negative deflection, mirroring the HV spectrum (20).

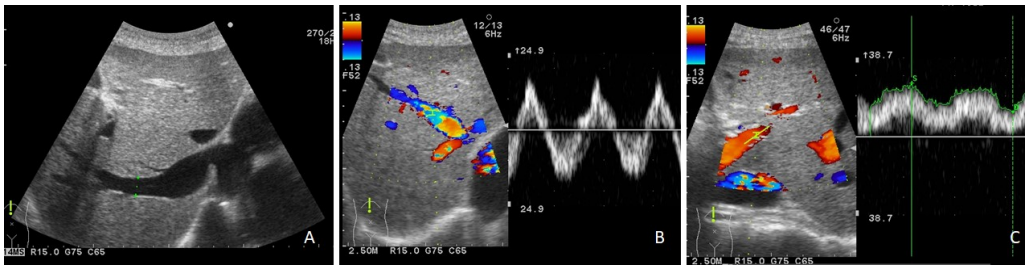


Figure 11.2.1. Ultrasound of a patient with tricuspidal regurgitation and liver congestion. A-dilated hepatic veins (>8 mm) on grey-scale imaging; B-increased phasicity of the waveform from hepatic vein-note the reversal of the systolic wave merging with the "a" wave of atrial contraction, making single deflection over the baseline ("a-s wave"), followed by "d" wave of ventricular diastole depicted as the deflection below the baseline; C-Increased phasicity of the waveform from the portal vein in the same patient.

In patients with elevated liver enzymes, typically displaying a cholestatic pattern, the triad of dilated HV with biphasic high-amplitude flow, and a highly phasic (often biphasic) PV Doppler waveform is pathognomonic for congestive hepatopathy. Even brief hypotensive episodes, such as a 15-minute arrhythmic event, may precipitate severe hepatic hypoperfusion, resulting in ischemic hepatitis with marked transaminase elevation and minimal bilirubin change, especially in patients with pre-existing liver congestion.

b) Budd-Chiari Syndrome

In Budd–Chiari syndrome (BCS), obstruction occurs in one or more hepatic veins, affecting either a short or a long segment (Fig. 11.2.2). The obstruction may also involve the inferior vena cava, most commonly in its retrohepatic segment. In the patent lumen of the hepatic veins proximal to the obstruction, blood flow loses its characteristic triphasic waveform and becomes monophasic, as pulsations from the right atrium are no longer transmitted (22). Additionally, a network of veno-venous collaterals develops, allowing blood from the obstructed vein to drain into a patent hepatic vein or, via short hepatic veins, directly into the inferior vena cava. Intrahepatic collaterals may assume a "hockey stick" configuration, characteristic of BCS. Short hepatic veins are also present under physiological conditions and normally drain the pericaval segments into the inferior vena cava, but their functional significance is minimal. However, when the main hepatic veins are obstructed, short hepatic veins become dilated and play a crucial role in maintaining hepatic circulation. One of the most commonly involved vessels is the vein draining the caudate lobe directly into the inferior vena cava. Complete retrohepatic IVC obstruction redirects flow caudally and then via retroperitoneal collaterals into the azygos system, contributing to esophageal varices formation. In some cases, macronodular regenerative changes may lead to stenosis of one or more hepatic veins, presenting on Doppler ultrasonography as focal increases in flow velocity.

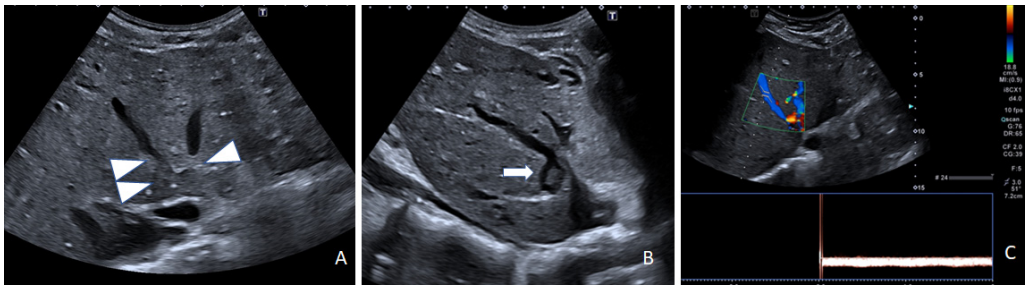


Figure 11.2.2. Doppler of the hepatic vein in a patient with Budd-Chiari syndrome. A-Note the lack of communication between the hepatic vein and inferior vena cava (arrowheads); B-Typical veno-venous collateral in the liver in the form of a hockey stick (white arrow); C-Monophasic waveform in the patent part of the hepatic vein, not transmitting the pulsatility from the right heart.

2. Intrahepatic Causes of Portal Hypertension

a) Postsinusoidal Causes – Sinusoidal Obstruction Syndrome

In Sinusoidal Obstruction Syndrome, thrombosis of the central veins occurs as a result of the toxic effects of chemotherapy on their endothelium. This leads to an increase in portal pressure and reversal of blood flow in the portal vein, which becomes hepatofugal, and may be accompanied by the development of gallbladder wall edema and ascites (23). The hepatic veins are usually not involved, and preserved blood flow can typically be demonstrated within them.

b) Sinusoidal Causes – Liver Cirrhosis

Liver cirrhosis can be diagnosed based on morphological features, including a nodular liver surface, coarse hyperechoic parenchyma, caudate lobe hypertrophy, irregular HV contours, and dilated PV and hepatic artery. Gallbladder wall edema due to congestion and hypoalbuminemia is often present. Development of PH with cirrhosis is associated with splenomegaly and portosystemic collateral formation, such as a recanalized umbilical vein or splenic hilum collaterals. Flow in a recanalized umbilical vein is hepatofugal and readily visualized on color Doppler (Fig. 11.2.3).

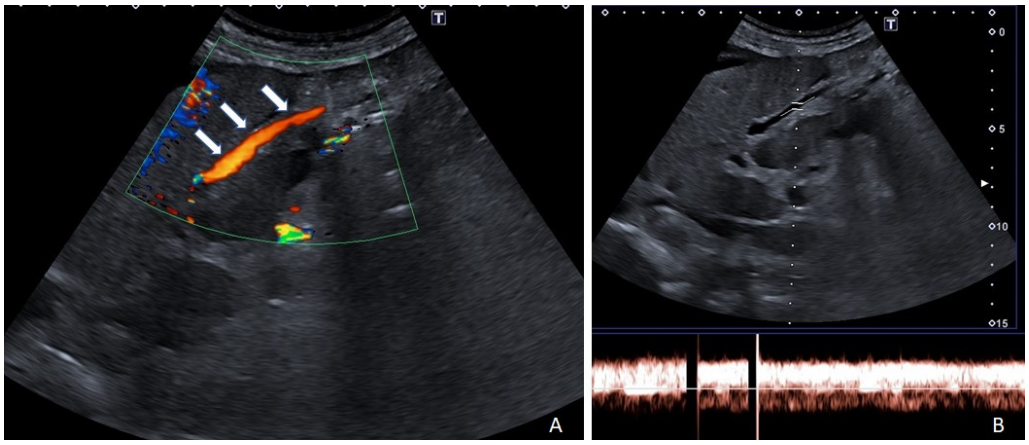


Figure 11.2.3. Recanalized umbilical vein in a patient with liver cirrhosis. A-On Color Doppler imaging, the umbilical vein is depicted in red color (white arrows) in keeping with the hepatofugal direction of blood flow (toward the ultrasound probe); B-Hepatofugal flow is also detected by pulsed (spectral) Doppler demonstrating a flat waveform over the baseline.

Hepatofugal flow may also be observed in the portal vein, but in the majority of patients it remains hepatopetal but with the reduced velocity (TAmax <15 cm/s) (Fig. 11.2.4).

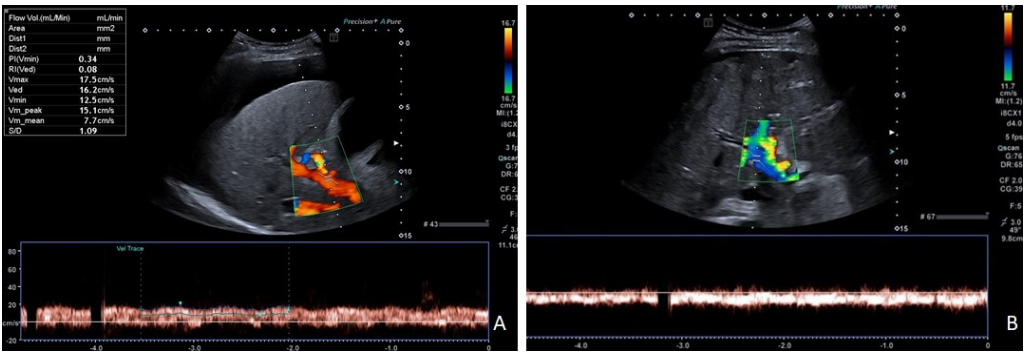


Figure 11.2.4. Spectral Doppler of the portal vein in patients with liver cirrhosis and portal hypertension. A-Decreased velocity in the portal vein, with normal hepatopetal direction (depicted in red color); B-hepatofugal direction of the flow in the portal vein (depicted in blue color).

Given that these, or very similar changes may also be observed in porto-sinusoidal vascular disease associated with nodular regenerative hyperplasia, in patients without a clear history of chronic liver disease, it is essential to perform liver stiffness measurements: in cirrhosis, values >15 kPa are typically recorded using transient elastography, whereas in PSVD they are usually below 10 kPa (24).

c) Presinusoidal Causes

Presinusoidal PH primarily involves portal tract structures, including terminal PV branches and bile ducts. Common examples include porto-sinusoidal vascular disease (PSVD, previously known as NRH/idiopathic non-cirrhotic portal hypertension (INCPH)), granulomatous liver diseases (e.g., sarcoidosis), and infections such as schistosomiasis. PSVD arises from terminal PV phlebitis, sometimes drug- or autoimmune-related, producing nodular regenerative lesions without fibrosis (24). Obstruction at terminal PV branches promotes prehepatic PH.

3. Prehepatic Causes of Portal Hypertension

Prehepatic causes encompass PV thrombosis, stenosis, and arteriovenous fistula. PV thrombosis is commonly multifactorial, related to local stasis, endothelial injury, and systemic thrombophilia. Thrombosis may be complete or partial, with variable extension along the portal vein trunk, branches and radicles (SMV or SV). Doppler detects absent flow in the thrombosed part of the PV in the acute phase, with progressive thrombus echogenicity aiding detection over time (25). In cases of chronic thrombosis, collateral venous circulation develops through the epi- and paracholedochal venous plexuses, allowing blood to bypass the obstructed segment of the portal vein. Epi-choledochal collaterals can lead to cavernous thickening of the choledochal wall, which may sometimes pose a differential diagnostic challenge compared to other causes of choledochal wall thickening (Fig. 11.2.5). However, in such thickened walls, color and pulsed Doppler ultrasonography typically reveal abundant venous-type flow, resolving these diagnostic dilemmas (26).

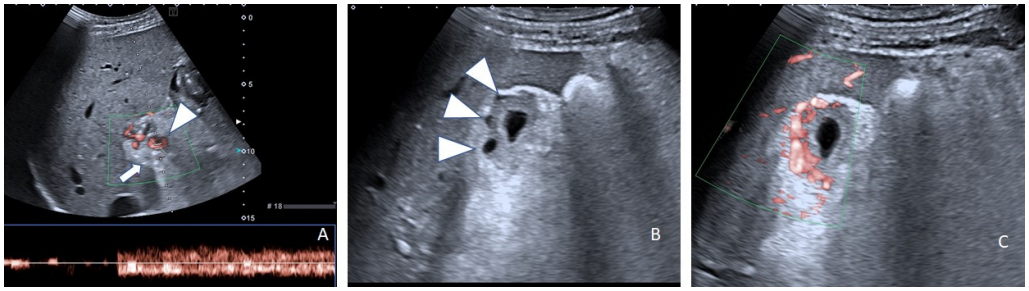


Figure 11.2.5. Chronic portal vein thrombosis with portal cavernoma. A - Thrombosed portal vein: note the lack of the lumen at the expected anatomical position of the portal vein, replaced with hyperechoic content and fibrous strands (white arrow), and tortuous veins around it (arrowhead); B - Edema of the gallbladder wall due to congestion, surrounded by anechoic structures representing collateral veins (arrowheads), confirmed by Color Doppler imaging as depicted at the C image.

Tumoral PV thrombosis, most often secondary to hepatocellular carcinoma (HCC), exhibits intrathrombus arterial flow on Doppler or contrast-enhanced ultrasonography (27). PV stenosis, usually iatrogenic following surgery, presents as focal acceleration at the site of stenosis and turbulent distal flow on Doppler, often with an “hourglass” appearance on B-mode imaging at the stenotic site (28).

11.2.4. Monitoring the patency of Transjugular Intrahepatic Portosystemic Shunt (TIPS)

Transjugular Intrahepatic Portosystemic Shunt (TIPS) creates a portosystemic connection between a HV branch and a PV branch to reduce portal pressures below 12 mmHg. Indications include variceal bleeding (when endoscopy fails, or varices with high-risk features for re-bleeding) and refractory ascites (Fig. 11.2.6). Absolute contraindications include right-sided heart failure, severe pulmonary hypertension, and polycystic liver disease. On ultrasound TIPS appears as a highly reflective, echogenic tubular structure, typically curved in the shape of an arch. Doppler evaluation of TIPS reveals uniform, typically monophasic flow, with peak systolic velocities of 90–190 cm/s and minimum velocities of 50–60 cm/s. Stenosis is suspected with focal velocity elevation or flow reduction below 50 cm/s (29,30). Complete occlusion is characterized by absent flow. Doppler surveillance is recommended at 7 and 14 days post-procedure, at 3 months, and biannually thereafter, ensuring timely intervention in cases developing complications such as TIPS stenosis or thrombosis (balloon angioplasty or thrombolysis).

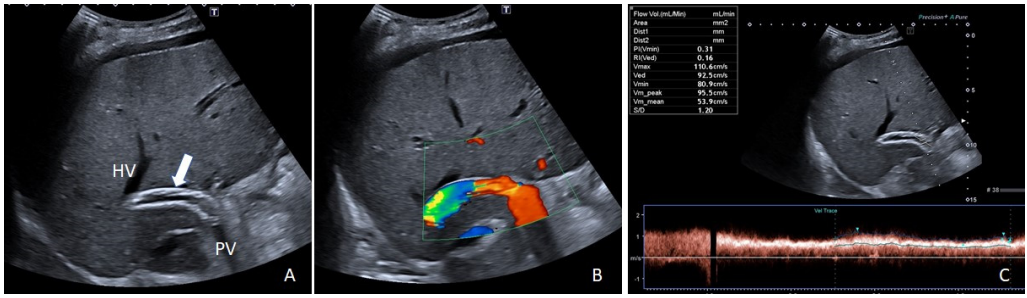


Figure 11.2.6. Doppler Ultrasound images of the transjugular intrahepatic portosystemic shunt (TIPS). A-Grey-scale image (longitudinal section, intercostal approach, right liver lobe) of TIPS (white arrow) traversing the portal vein (PV) and right hepatic vein (HV); B-On Color Doppler imaging note hepatopetal flow in the portal vein changing to hepatopetal in the portion of TIPS that enters right hepatic vein; C- Spectral Doppler analysis depicts normal velocity of the blood flow in the portal part of TIPS (mean peak velocity 95 cm/s), confirming normal patency and the function of the TIPS.

11.2.5. Assessing the Severity of Portal Hypertension Using Doppler

Although attempts have been made to correlate certain Doppler measurements with the severity of PH as defined by the hepatic venous pressure gradient (HVPG), this approach has not proven reliable and has not been adopted in clinical practice (7, 8, 18).

11.2.6. Monitoring Hemodynamic Response to Nonselective Beta-Blockers

This is an important clinical parameter in the management of patients with PH. Doppler was intuitively considered a logical method to evaluate hemodynamic parameters in the portal circulation and potentially correlate them with invasively measured portal pressure (HVPG). However, despite initial enthusiasm, Doppler has not proven reliable for this indication (7,8,18).

In conclusion, Doppler ultrasonography is essential for determining the etiology of portal hypertension, differentiating posthepatic, intrahepatic, and prehepatic causes based on characteristic flow patterns and vessel morphology. It enables noninvasive identification of conditions such as congestive hepatopathy, Budd-Chiari syndrome, cirrhosis, and portal vein thrombosis, guiding diagnosis, management, and surveillance, including TIPS follow-up. Accurate interpretation of Doppler findings allows early detection of complications and informs timely therapeutic interventions.

References

1. McNaughton DA, Abu-Yousef MM. Doppler US of the Liver Made Simple. RadioGraphics 2011; 31:161–188.
2. Grgurevic I, Boozari B, Kujundzic M, Brkljacic B. Color Doppler ultrasound of the liver circulation. Lijec Vjesn. 2009 Jul-Aug;131(7-8):211-7.
3. Grgurevic I, Tjesic Drinkovic I, Pinzani M. Multiparametric ultrasound in liver diseases: an overview for the practising clinician. Postgrad Med J. 2019;95(1126):425-432
4. Möller K., Hija RAE, Qi X, Jenssen C, Mutze S, Möller B, et al. Portal Hypertension—Noninvasive Multiparametric Ultrasound-Based Criteria and Measurements. Portal Hypertension & Cirrhosis 2025; 4: 44-65.
5. Allan R, Thoirs K, Phillips M. Accuracy of ultrasound to identify chronic liver disease. World J Gastroenterol. 2010 Jul 28;16(28):3510-20.
6. ACCF/ACR/AIUM/ASE/IAC/SCAI/SCVS/SIR/SVM/SVS/SVU 2013 Appropriate Use Criteria for Peripheral Vascular Ultrasound and Physiological Testing Part II: Testing for Venous Disease and Evaluation of Hemodialysis Access: A Report of the American College of Cardiology Foundation Appropriate Use Criteria Task Force. J Am Coll Cardiol. 2013;62(7):649-665.
7. Berzigotti A, Piscaglia F. Ultrasound in Portal Hypertension – Part 1. Ultraschall in Med 2011; 32: 548–571.

8. Berzigotti A, Piscaglia F. Ultrasound in Portal Hypertension – Part 2 – and EFSUMB Recommendations for the Performance and Reporting of Ultrasound Examinations in Portal Hypertension. Ultraschall in Med 2012; 33: 8–32
9. Haag K, Rossle M, Ochs A, Huber M, Siegestetter V, Oschewski M, et al. Correlation of Duplex sonography Findings and Portal Pressure in 375 Patients with Portal Hypertension. AJR 1999; 172: 631-5.
10. Zironi G, Gaiani S, Fenyves D, Rigamonti A, Bolondi L, Barbara L. Value of measurement of mean portal flow velocity by Doppler flowmetry in the diagnosis of portal hypertension. J Hepatol. 1992 Nov;16(3):298-303.
11. Iwao T, Toyonaga A, Oho K, Tayama C, Masumoto H, Sakai T, et al. Value of Doppler Ultrasound Parameters of Portal Vein and Hepatic Artery in the Diagnosis of Cirrhosis and portal Hypertension. Am J Gastroenterol 1997; 92(6): 1012-17.
12. Moriyasu F, Nishida O, Ban N, Nakamura T, Sakai M, Miyake T, et al. Congestion index" of the portal vein. AJR Am J Roentgenol. 1986 Apr;146(4):735-9.
13. Moriyasu F, Ban N, Nishida O, Nakamura T, Miyake T, Uchino H, et al. Clinical Application of an Ultrasonic Duplex System in the Quantitative Measurement of Portal Blood Flow. J Clin Ultrasound 1986; 14579-588.
14. Schneider AW, Kalk JF, Klein CP. Hepatic arterial pulsatility index in cirrhosis: correlation with portal pressure. J Hepatol 1999; 30(5): 876-81.
15. Bolognesi M, Sacerdoti D, Merkel C, Gerunda G, Maffei-Faccioli A, Angeli P, et al. Splenic Doppler impedance indices: influence of different portal hemodynamic conditions. Hepatology 1996; 23(5): 1035-40.
16. Piscaglia F, Donati G, Serra C, Muratori R, Solmi L, Gaiani S et al. Value of splanchnic Doppler ultrasound in the diagnosis of portal hypertension. Ultrasound Med Biol 2001; 27: 893–899
17. Bolognesi M, Sacerdoti D, Merkel C, Bombonato G, Gatta A. Noninvasive grading of the severity of portal hypertension in cirrhotic patients by echo-color-doppler. Ultrasound Med Biol 2001;27(7):901–7.
18. Kim G, Cho YZ, Baik SK, Kim MY, Hong WK, Kwon SO. The accuracy of ultrasonography for the evaluation of portal hypertension in patients with cirrhosis: a systematic review. Korean J Radiol. 2015 Mar-Apr;16(2):314-24.
19. Abu-Yousef MM. Duplex Doppler Sonography of the Hepatic Vein in Tricuspid regurgitation. AJR 1991; 156: 79-83.
20. Hosoki T, Arisawa J, Murukawa T, Tokunaga K, Kuroda C, Kozuka T, et al. Portal blood flow in congestive heart failure: pulsed doppler sonographic findings. Radiology 1990; 174: 733-6.
21. Duernickx AJ, Grant EG, Perrella RR, Szeto A, Tessler FN. The pulsatile portal vein in cases of congestive heart failure: correlation of duplex doppler findings with right atrial pressures. Radiology 1990; 176: 655-8.
22. Bargalló X, Gilabert R, Nicolau C, García-Pagán JC, Ayuso JR, Brú C. Sonography of Budd-Chiari Syndrome. American Journal of Roentgenology. 2006;187: W33-W41.

23. Herbetko J, Grigg AP, Buckley AR, Phillips GL. Venoocclusive liver disease after bone marrow transplantation: findings at duplex sonography. American Journal of Roentgenology. 1992;158:1001-1005.
24. Elkrief L, Lazareth M, Chevret S, Paradis V, Magaz M, Blaise L, et al; ANRS CO12 CirVir Group. Liver Stiffness by Transient Elastography to Detect Porto-Sinusoidal Vascular Liver Disease With Portal Hypertension. Hepatology. 2021 Jul;74(1):364-378.
25. Margini C, Berzigotti A. Portal vein thrombosis: The role of imaging in the clinical setting. Dig Liver Dis. 2017 Feb;49(2):113-120. doi: 10.1016/j.dld.2016.11.013.
26. Grgurevic I, Kujundzic M, Banic M, Kusec R, Bokun T, Vukelic-Markovic M, et al. Subtypes and clinical significance of common bile duct varices in portal vein thrombosis: diagnosis and follow-up by Doppler US and EUS. Abdom Radiol (NY). 2016 Mar;41(3):476-84.
27. Salman S. Portal vein thrombosis with contrast-enhanced ultrasound in a patient with hepatocellular carcinoma: a case study. Australasian Journal of Ultrasound in Medicine 2012; 15: 67-70.
28. Mullan CP, Siewert B, Kane RA, Sheiman RG. Can Doppler sonography discern between hemodynamically significant and insignificant portal vein stenosis after adult liver transplantation? AJR Am J Roentgenol. 2010 Dec;195(6):1438-43. doi: 10.2214/AJR.10.4636.
29. Bhogal KH, Sanyal JA. Transjugular intrahepatic portosystemic shunt: An overview. Clinical Liver Disease. 2012 Nov;1(5):173-6.
30. Perello PM, Mur PJ, Vives SM, Riutort MMJ, Artigues PA, Garcia NC, et al. Long-term follow-up of transjugular intrahepatic portosystemic shunt (TIPS) with stent-graft. Diagn Interv Radiol. 2019 Sep; 25(5):346-52.

11.3. Portal vein thrombosis: value of standard ultrasound and contrast enhanced ultrasound (CEUS)

Mirela Dănilă, Ana Maria Ghiuchici

Abstract

Portal vein thrombosis (PVT) refers to thrombotic material within the portal venous system and most commonly occurs in patients with liver cirrhosis. B-mode ultrasound (US) serves as the first-line imaging modality for detecting and evaluating thrombus extent. Doppler US and contrast-enhanced ultrasound (CEUS) improve diagnostic accuracy. Accurate characterization of PVT is essential for prognosis and therapeutic decision-making. Early imaging diagnosis facilitates timely anticoagulation in benign cases and appropriate oncologic management in malignant thrombosis.

11.3.1. Introduction and Clinical Background

Portal vein thrombosis (PVT) is defined as the presence of a thrombus within any segment of the portal venous system, including the main portal vein trunk, left and/or right intrahepatic portal vein branches, splenic vein, and superior and/or inferior mesenteric veins.

In clinical practice, PVT most frequently occurs in patients with liver cirrhosis, with or without hepatocellular carcinoma. The prevalence of PVT increases with the severity of liver disease, ranging from less than 1% in compensated cirrhosis to 8–25% among liver transplant candidates (1, 2). A meta-analysis by Stupia et al. reported a prevalence of 8.5% in patients with MASLD and advanced fibrosis, which is higher than in patients with non-MASLD etiologies (3).

The primary factors contributing to portal thrombosis in cirrhosis include portal hypertension, which reduces portal blood flow; endothelial vascular alterations; and a shift in coagulation balance favoring a procoagulant state.

A systematic review and meta-analysis identified several factors associated with increased risk of PVT, including Child-Pugh class B or C liver cirrhosis, elevated D-dimer levels, history of non-selective beta-blocker use, presence of moderate-to-severe esophageal varices, and ascites (4).

PVT in liver cirrhosis without hepatocellular carcinoma (HCC) is generally benign. In contrast, PVT associated with HCC in cirrhosis is often malignant and

indicates poor prognosis. Malignant PVT also occurs as a complication of other abdominal malignancies.

Benign PVT may complicate various pathological conditions, including acute pancreatitis, abdominal sepsis of diverse etiologies, and disorders affecting coagulation factors, such as thrombophilia and myeloproliferative neoplasms.

PVT classification includes acute or chronic, partial or complete, and benign or malignant categories. Additionally, classification considers the extent of involvement within the portal system: intrahepatic, extrahepatic, or both.

Abdominal pain is not present in all patients with acute PVT; however, early diagnosis during the acute phase (defined as thrombosis lasting less than six months) is essential to prevent complications such as variceal bleeding and intestinal ischemia. Patients with cirrhosis typically do not develop intestinal ischemia due to collateral vessel formation, but anticoagulation is required when this complication occurs (5). Early anticoagulant therapy in acute PVT has demonstrated recanalisation in 62% of patients after one week of treatment.

In patients presenting with thrombosis without known liver disease, hepatological evaluation is necessary to exclude cirrhosis. This assessment includes laboratory testing, liver elastography, and, when indicated, liver biopsy (6, 7).

For patients with or without cirrhosis, detailed characterization of PVT—including extent within the portal system, degree of occlusion, and thrombus morphology—is essential for guiding treatment and prognosis. Imaging modalities such as ultrasonography (US), contrast-enhanced computed tomography (CE-CT), and contrast-enhanced magnetic resonance imaging (CE-MRI) are employed for classification (6, 7).

11.3.2 Standard US and Doppler US in the detection of Portal Vein Thrombosis

US is often the first imaging examination used to detect PVT, particularly in patients with liver cirrhosis, but also in other pathological conditions associated with this complication. US generally performs well in detecting PVT, with reported sensitivities and specificities of 89–93% and 92–99%, respectively. However, ultrasound is operator-dependent, depending on the examiner's experience and the patient's characteristics (8-11).

In the standard US, a portal thrombus appears as echogenic material within the portal vein lumen and is frequently associated with dilatation of the

portal system. The thrombus echogenicity varies from hypo- to iso-echogenic, becoming increasingly hyperechoic as thrombosis progresses to a chronic stage. Portal vein thrombosis may be partial or complete. Ultrasound can assess the thrombus location and extent; however, color Doppler ultrasound more effectively differentiates complete from incomplete thrombosis by demonstrating the absence of blood flow in part or all of the lumen (Fig. 11.3.1- 11.3.6).

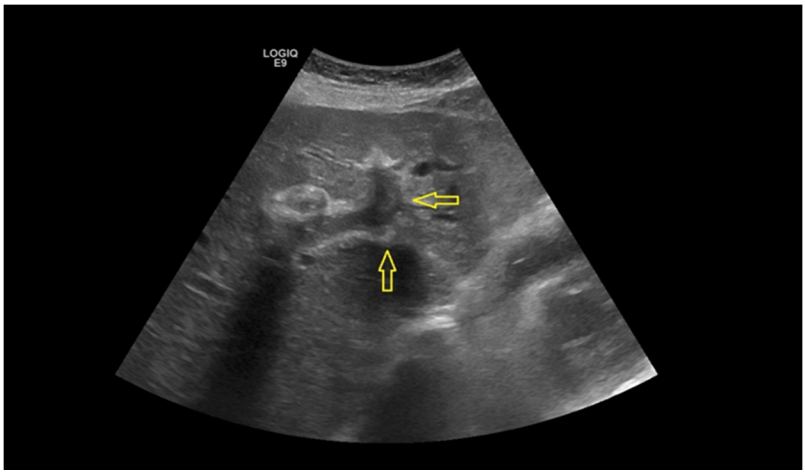


Fig. 11.3.1 B-mode US – Complete portal vein thrombosis; thrombus appears as hypoechoic material within the portal vein lumen

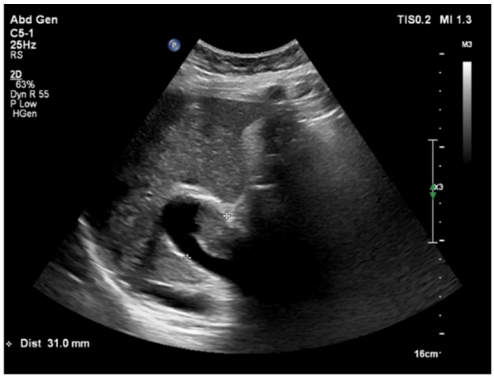


Fig. 11.3.2 B-mode US – Partial portal vein thrombosis; thrombus appears as slightly hyperechoic material within the portal vein lumen; portal hypertension with a large portal vein measuring 31 mm.

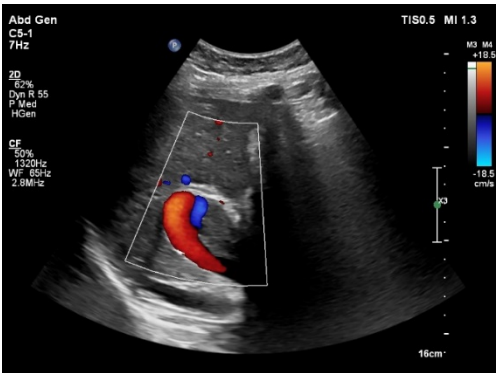


Fig. 11.3.3 Doppler color US – Partial portal vein thrombosis; absence of blood flow in part of the portal vein lumen; thrombus appears as hyperechoic material within the portal vein lumen.

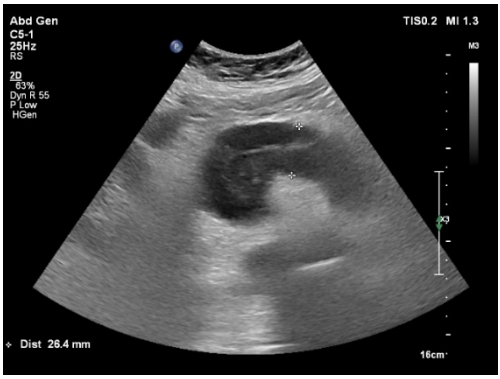


Fig. 11.3.4 B-mode US – Partial portal vein thrombosis; thrombus appears as hypoechoic material within the portal vein lumen; portal hypertension with a large portal vein measuring 26 mm.

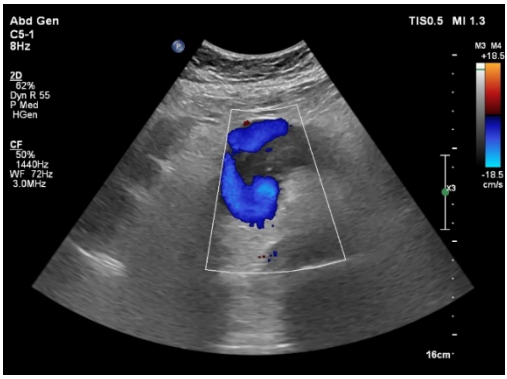


Fig. 11.3.5 Doppler color US – Partial portal vein thrombosis; absence of blood flow in part of the portal vein lumen; thrombus appears as hypoechoic material within the portal vein lumen.

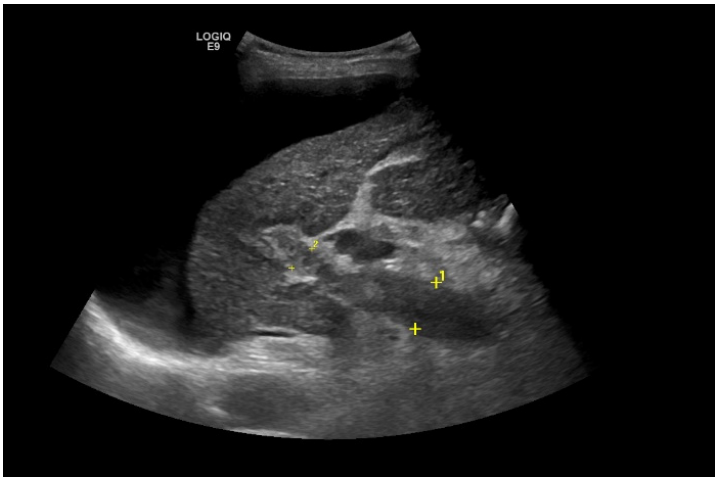


Fig. 11.3.6 B-mode US – Complete portal vein thrombosis; thrombus appears as hypoechoic material within the portal vein lumen

If PVT persists despite treatment or spontaneous resorption, collateral vessels develop around the obstruction. These vessels bypass the thrombosed portal vein segment, forming a portal cavernoma, which indicates chronic PVT (Fig. 11.3.7).

On US, cavernous transformation manifests as numerous tortuous vessels occupying the portal vein bed.

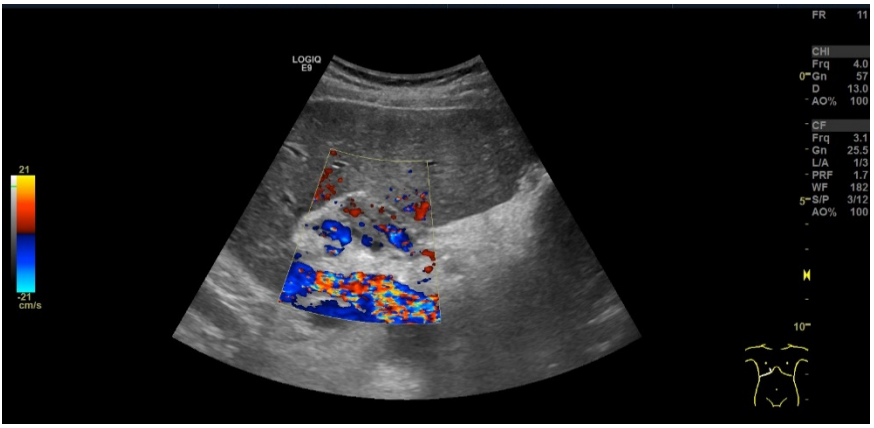


Fig. 11.3.7 Color Doppler US – Portal cavernoma; numerous tortuous vessels occupying the portal vein bed

Malignant portal vein thrombosis is commonly associated with hepatocellular carcinoma (HCC) or other malignancies. On standard ultrasound imaging, malignant thrombi typically appear heterogeneous and invade the portal vein wall (Fig. 11.3.8-11.3.9). HCC may be detected adjacent to the PVT; however, PVT can also be present without a circumscribed tumor, as observed in diffuse HCC. The presence of newly formed arterioles within the malignant thrombus allows detection of pulsatile flow using Doppler ultrasound, with reported sensitivities ranging from 66% to 100% (12-13).

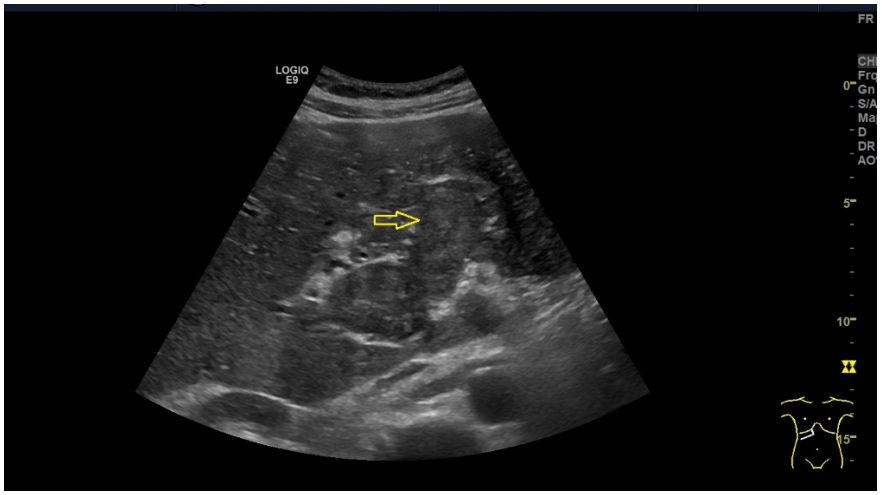


Fig. 11.3.8 B-mode US – Complete malignant portal vein thrombosis; thrombus appears as isoechoic heterogeneous material and invade the portal vein wall.

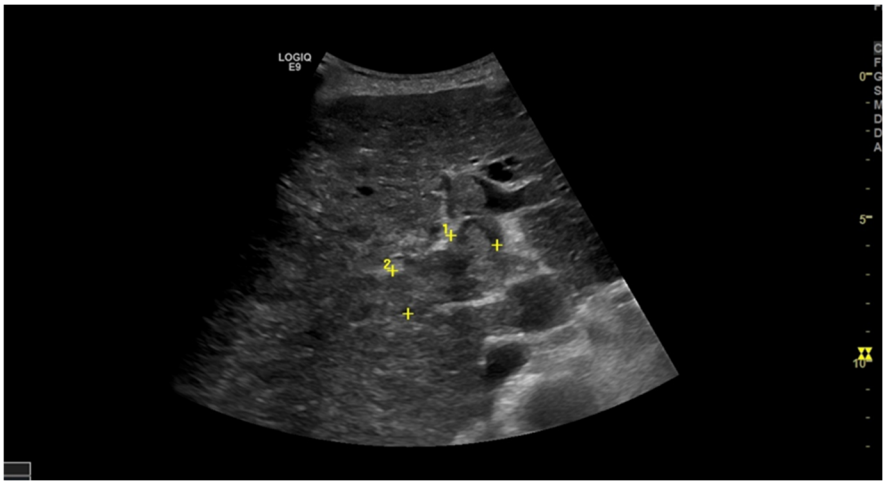


Fig. 11.3.9 B-mode US – Complete malignant portal vein thrombosis; thrombus appears as slightly hyperechoic heterogeneous material and invade the portal vein wall.

11.3.3. CEUS in the evaluation of Portal Vein Thrombosis

Contrast-enhanced ultrasound (CEUS) demonstrates superior diagnostic and characterization capabilities for portal vein thrombosis (PVT) compared to standard ultrasound and Doppler examinations. The EFSUMB guidelines recommend CEUS to differentiate benign from malignant thrombosis (tumor in vein). Numerous studies confirm CEUS's high effectiveness in characterizing PVT. Additionally, the CEUS-LI-RADS algorithm introduces the LI-RADS tumor-in-vein (LI-RADS TIV) category to assess malignant portal vein thrombosis in patients with liver cirrhosis (14, 15).

In benign PVT, CEUS reveals an absence of enhancement within the thrombosed segment of the portal vein (Fig. 11.3.10 - 11.3.12).

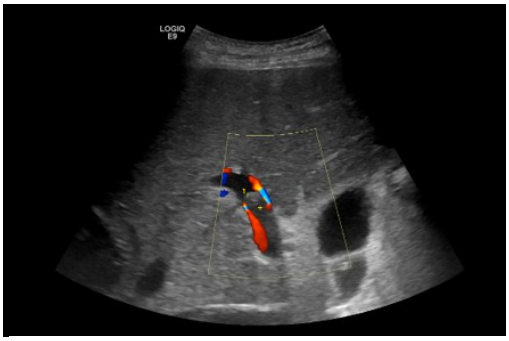


Fig. 11.3.10 Doppler color US – Partial acute portal vein thrombosis in a patient with liver abscess; absence of blood flow in part of the portal vein lumen; thrombus appears as hypoechoic material within the portal vein lumen.

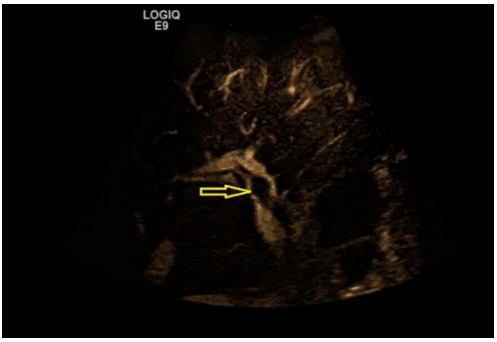


Fig. 11.3.11 CEUS arterial phase – Benign partial portal vein thrombosis; absence of enhancement within the thrombosed segment of the portal vein.

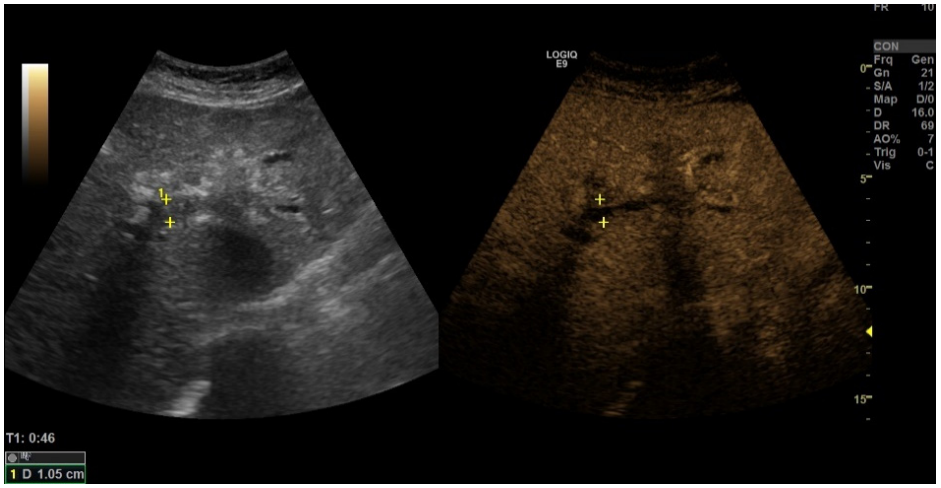


Fig. 11.3.12 CEUS arterial phase – Benign, acute complete portal vein thrombosis in a patient with acute cholangitis; absence of enhancement within the thrombosed segment of the portal vein.

Malignant PVT, or tumor in the vein, exhibits an enhancement pattern similar to that of the primary tumor. Malignant portal vein thrombosis demonstrates arterial-phase enhancement followed by washout in the late phase (Fig. 11.3.13 - 11.3.17) (14).

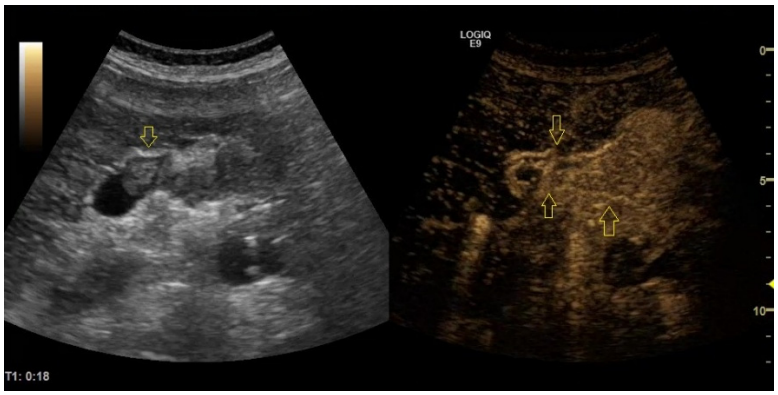


Fig. 11.3.13 CEUS arterial phase – Malignant portal vein thrombosis in a patient with liver cirrhosis and HCC; enhancement within the thrombosed segment of the portal vein.

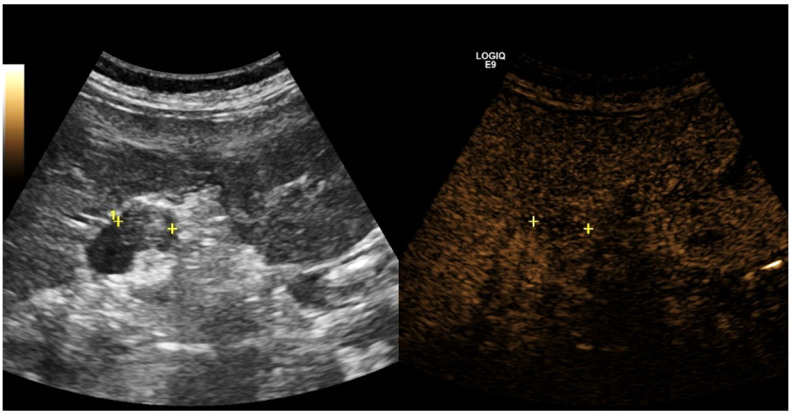


Fig. 11.3.14 CEUS late phase – Malignant portal vein thrombosis in a patient with liver cirrhosis and HCC; washout within the thrombosed segment of the portal vein.

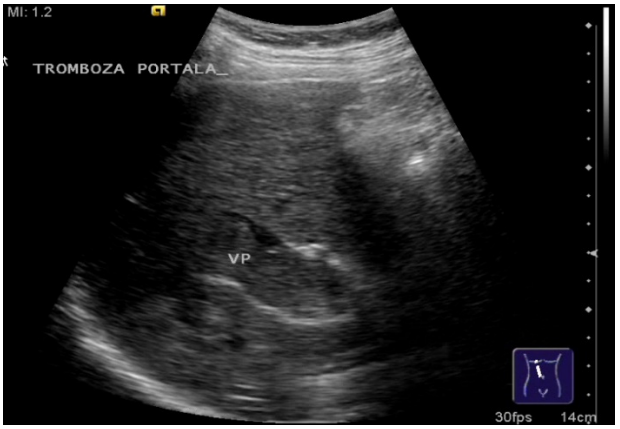


Fig. 11.3.15 B-mode US – Complete portal vein thrombosis; thrombus appears as heterogeneous hypoechoic material within the portal vein lumen.



Fig. 11.3.16 CEUS arterial phase – Malignant portal vein thrombosis in a patient; multilinear vascularized thrombus enhancement



Fig. 11.3.17 CEUS late phase – Malignant portal vein thrombosis; thrombus showing important washout.

Rossi et al. identified four arterial phase enhancement patterns in portal vein thrombosis (16):

- Pattern 1 corresponds to benign thrombus, characterized by the absence of enhancement in all phases.
- Pattern 2 involves thrombus enhancement similar to that of the originating tumour.
- Pattern 3: linear or dotted enhancement.
- Pattern 4: multilinear or multipunctate vascularized thrombus enhancement present during any CEUS phase.

Patterns 2, 3, and 4 correspond to malignant PVT.

Multiple studies have assessed CEUS performance in characterizing PVT and differentiating benign from tumor thrombosis, consistently demonstrating high sensitivity and specificity (9, 13, 16, 17).

A meta-analysis of 7 studies found that the sensitivity and specificity of CEUS for diagnosing TIV were 0.94 (95% CI, 0.89–0.97) and 0.99 (95% CI, 0.80–1.00), respectively. The study also concludes that CEUS is highly effective in differentiating TIV from benign PVT and represents a good alternative to CT and/or MRI (18). Cross-sectional imaging modalities such as CE-CT and CE-MRI are necessary to assess the extent of portal vein thrombosis and to stage the tumor.

Beyond characterizing portal vein thrombosis, CEUS is also utilized to guide percutaneous thrombus biopsy for anatomopathological confirmation (19).

Confirming whether a portal thrombus is benign or malignant is essential for predicting patient prognosis and guiding therapeutic decisions. Patients with liver cirrhosis who are candidates for liver transplantation require rigorous imaging surveillance to detect hepatocellular carcinoma (HCC) and portal thrombosis, benign or malignant, at an early stage.

Early therapeutic intervention is necessary for benign portal thrombosis to prevent thrombus extension and hepatic hemodynamic alterations, whereas malignant portal thrombosis may be a contraindication for liver transplantation.

In conclusion:

Ultrasound effectively detects portal vein thrombosis by identifying echogenic material within the portal vein lumen. When acoustic windows are adequate, the extent of thrombosis can be accurately assessed. Doppler ultrasound is useful for detecting flow in the portal vein lumen and, in the case of malignant thrombosis, it highlights pulsatile arterial flow within the PVT. CEUS is an excellent modality for characterizing portal vein thrombosis, with some studies indicating superior performance compared with CT.

References

1. Okuda K, Ohnishi K, Kimura K, Matsutani S, Sumida M, Goto N, et al. Incidence of portal vein thrombosis in liver cirrhosis. An angiographic study in 708 patients. Gastroenterology. 1985 Aug;89(2):279-86.
2. Francoz C, Belghiti J, Vilgrain V, Sommacale D, Paradis V, Condat B, et al. Splanchnic vein thrombosis in candidates for liver transplantation: usefulness of screening and anticoagulation. Gut. 2005 May;54(5):691-7.
3. Stupia R, Lombardi R, Cattazzo F, Zoncapè M, Mantovani A, De Marco L, et al. Prevalence of portal vein thrombosis in non-alcoholic fatty liver disease: a meta-analysis of observational studies. J Thromb Thrombolysis. 2024 Feb;57(2):330-336.
4. Pan J, Wang L, Gao F, An Y, Yin Y, Guo X, et al. Epidemiology of portal vein thrombosis in liver cirrhosis: A systematic review and meta-analysis. Eur J Intern Med. 2022 Oct;104:21-32.
5. Hernández-Gea V, De Gottardi A, Leebeek FWG, Rautou PE, Salem R, Garcia-Pagan JC. Current knowledge in pathophysiology and management of Budd-Chiari syndrome and non-cirrhotic non-tumoral splanchnic vein thrombosis. J Hepatol. 2019 Jul;71(1):175-199.
6. European Association for the Study of the Liver. EASL Clinical Practice Guidelines: Vascular diseases of the liver. J Hepatol. 2016 Jan;64(1):179-202.

7. Davis JPE, Lim JK, Francis FF, Ahn J. AGA Clinical Practice Update on Management of Portal Vein Thrombosis in Patients With Cirrhosis: Expert Review. Gastroenterology. 2025 Feb;168(2):396-404.e1.
8. Chawla Y, Duseja A, Dhiman RK. Review article: the modern management of portal vein thrombosis. Aliment Pharmacol Ther. 2009 Nov 1;30(9):881-94.
9. Danila M, Sporea I, Popescu A, Șirli R. Portal vein thrombosis in liver cirrhosis - the added value of contrast enhanced ultrasonography. Med Ultrason. 2016 Jun;18(2):218-33.
10. Tessler FN, Gehring BJ, Gomes AS, Perrella RR, Ragavendra N, Busuttil RW, et al. Diagnosis of portal vein thrombosis: value of color Doppler imaging. AJR Am J Roentgenol. 1991 Aug;157(2):293-6.
11. Bach AM, Hann LE, Brown KT, Getrajdman GI, Herman SK, Fong Y, et al. Portal vein evaluation with US: comparison to angiography combined with CT arterial portography. Radiology. 1996 Oct;201(1):149-54.
12. Chen H, Turon F, Hernández-Gea V, Fuster J, Garcia-Criado A, Barrufet M, et al. Nontumoral portal vein thrombosis in patients awaiting liver transplantation. Liver Transpl. 2016 Mar;22(3):352-65.
13. Tarantino L, Francica G, Sordelli I, Esposito F, Giorgio A, Sorrentino P, et al. Diagnosis of benign and malignant portal vein thrombosis in cirrhotic patients with hepatocellular carcinoma: color Doppler US, contrast-enhanced US, and fine needle biopsy. Abdom Imaging 2006 SepOct;31(5).
14. Claudon M, Dietrich CF, Choi BI, Cosgrove DO, Kudo M, Nolsoe CP, et al. Guidelines and good clinical practice recommendations for Contrast Enhanced Ultrasound (CEUS) in the liver – update 2012: A WFUMB-EFSUMB initiative in cooperation with representtatives of AFSUMB, AIUM, ASUM, FLAUS and ICUS. Ultrasound Med Biol 2013; 39: 187–210
15. Wilson SR, Lyshchik A, Piscaglia F, Cosgrove D, Jang HJ, Sirlin C, et al. CEUS LI-RADS: Algorithm, implementation, and key differences from CT/MRI. Abdom Radiol (NY) 2018;43:127-142.
16. Rossi S, Ghittoni G, Ravetta V, Torello Viera F, Rosa L, Serassi M, et al. Contrast-enhanced ultrasonography and spiral computed tomography in the detection and characterization of portal vein thrombosis complicating hepatocellular carcinoma. Eur Radiol 2008;18: 1749-1756.
17. Ueno N, Kawamura H, Takahashi H, Fujisawa N, Yoneda M, Kirikoshi H, et al. Characterization of portal vein thrombus with the use of contrast-enhanced sonography. J Ultrasound Med. 2006;25:1147–1152.
18. Chen J, Zhu J, Zhang C, Song Y, Huang P. Contrast-enhanced ultrasound for the characterization of portal vein thrombosis vs tumor-in-vein in HCC patients: a systematic review and meta-analysis. Eur Radiol. 2020 May;30(5):2871-2880.
19. Sparchez Z, Radu P, Zaharia T, Kacso G, Diaconu B, Grigorescu I, et al. B-mode and contrast enhanced ultrasound guided biopsy of portal vein thrombosis. Value in the diagnosis of occult hepatocellular carcinoma in liver cirrhosis. Med Ultrason. 2010 Dec;12(4):286-94.

11.4. Liver and Spleen elastography and combination for portal hypertension

Felix Bende, Renata Bende, Iulia Rațiu

Abstract

Portal hypertension (PH) is a major complication of advanced chronic liver disease and is associated with the development of esophageal varices, ascites, and clinical decompensation. Although hepatic venous pressure gradient (HVPG) measurement remains the gold standard for assessing PH severity, its invasive nature limits widespread use. In recent years, ultrasound-based elastography techniques—including transient elastography (TE), point shear-wave elastography (pSWE), and 2D/3D shear-wave elastography (SWE)—have shown good correlation with HVPG and promising performance in predicting clinically significant portal hypertension (CSPH) and high-risk varices.

Both liver stiffness and, particularly, spleen stiffness have emerged as valuable non-invasive markers and are incorporated into clinical algorithms such as the Baveno VI and VII criteria to reduce unnecessary endoscopic screening. Magnetic resonance elastography also demonstrates high diagnostic accuracy, although cost and availability remain limiting factors. Overall, elastography plays an essential role in the modern non-invasive assessment and risk stratification of portal hypertension in patients with compensated advanced chronic liver disease.

11.4.1. Introduction

Portal hypertension (PH) represents one of the most serious and clinically relevant complications of liver cirrhosis. It is defined by a hepatic venous pressure gradient (HVPG) exceeding 5 mmHg, while clinically significant portal hypertension (CSPH) is established when HVPG rises above 10 mmHg (1).

Regardless of the underlying etiology, cirrhosis remains the leading cause of portal hypertension. In patients with cirrhosis, the increase in portal pressure is primarily driven by structural alterations of the hepatic architecture, which disrupt the normal hepatic vascular structure. These structural abnormalities are responsible for nearly 70% of the increase in intrahepatic vascular resistance. The remaining proportion is attributed to a dynamic component involving the contraction of vascular smooth muscle cells and the

activation of hepatic stellate (Ito) cells, which together account for about 30% of the elevated portal resistance.

The combination of heightened intrahepatic resistance and compensatory mechanisms, including augmented splanchnic blood inflow and the development of a hyperdynamic circulatory state, perpetuates and further worsens portal hypertension (2,3).

The onset of CSPH marks a pivotal stage in the natural course of ***compensated advanced chronic liver disease (cACLD).*** At this point, patients become at risk for clinically relevant complications such as ascites and esophageal varices (EV). Variceal rupture typically occurs when wall tension surpasses the mechanical limits of the vessel, most often at HVPG values exceeding 12 mmHg (4).

In light of these considerations, evaluation of portal hypertension is recommended at the time of diagnosis in patients with advanced chronic liver disease, as it provides essential information for both treatment planning and prognostic assessment.

11.4.2. Invasive Approaches to Portal Hypertension Assessment

A) Hepatic Venous Pressure Gradient (HVPG) Measurement

Measurement of the hepatic venous pressure gradient (HVPG) remains the reference standard for the diagnosis of portal hypertension and for grading its severity. However, it is an invasive procedure that requires catheterization of a hepatic vein using a balloon-tipped catheter under imaging guidance. Vascular access is most commonly obtained through the right internal jugular vein, although femoral or antecubital approaches may also be used (5). HVPG is determined by calculating the difference between wedged hepatic venous pressure (WHVP) and free hepatic venous pressure (FHVP), according to the formula: **HVPG = WHVP – FHVP.** To improve accuracy and reproducibility, the final HVPG value is generally defined as the median of three consecutive measurements (6).

Based on robust clinical evidence, HVPG assessment is recommended at the time of diagnosis in patients with advanced chronic liver disease, as it provides valuable information for risk stratification and prognostic evaluation (7,8). Furthermore, HVPG is considered the most reliable tool for monitoring therapeutic response in patients with clinically significant portal hypertension (CSPH). Treatment goals include reducing HVPG to below 12 mmHg or achieving a decrease of at least 20% from baseline values (8,9). Failure to reach these

targets is recognized as the strongest independent predictor of first or recurrent variceal bleeding (10), with non-responders to non-selective beta-blockers exhibiting a two- to fourfold higher relative risk (11).

Although HVPG measurement has proven diagnostic and prognostic value, it also presents several limitations. The procedure is invasive, relatively expensive, and not universally available, and its complexity may reduce patient acceptance (12).

B) Upper Gastrointestinal Endoscopy

Upper gastrointestinal endoscopy is considered the reference method for the direct detection of esophageal and gastric varices, as well as portal hypertensive gastropathy. Although it is an invasive investigation, it offers essential diagnostic information by enabling detailed evaluation of variceal features such as size and the presence of red wale signs or other bleeding stigmata, which are strongly associated with the risk of variceal bleeding (13).

Nevertheless, in patients with advanced chronic liver disease, a substantial proportion of screening endoscopies do not reveal high-risk varices (HRV). As a result, the overall cost-effectiveness and practicality of universal endoscopic screening have been questioned.

In response to this concern, the Baveno VI consensus (12) recommended the use of non-invasive tools as an initial risk stratification strategy. These methods can reliably identify patients at very low risk of harboring esophageal or gastric varices requiring treatment, thereby safely reducing the need for unnecessary screening endoscopy. Moreover, the Baveno VII consensus (2022) firmly established non-invasive tests—particularly liver stiffness measurement combined with platelet count—as reliable tools to rule out (LSM ≤15 kPa and platelets ≥150 × 10^9/L) or rule in (LSM ≥25 kPa) clinically significant portal hypertension in patients with compensated advanced chronic liver disease, thereby reducing the need for invasive assessment (14).

11.4.3. Non-Invasive Diagnostic Approaches in Portal Hypertension

Over the past years, the diagnostic approach to portal hypertension (PH) has evolved substantially with the introduction of a variety of noninvasive markers that complement traditional invasive techniques. These advances have opened new opportunities for safer and more accessible evaluation strategies, particularly in patients with newly diagnosed compensated advanced chronic

liver disease (cACLD), where reliable and reproducible noninvasive methods are increasingly valuable.

In this clinical setting, an initial evaluation based on noninvasive markers is generally favored, as it helps determine the optimal timing for endoscopy or other invasive procedures.

The range of non-invasive methods used to predict portal hypertension includes biochemical markers, composite scoring systems, and various imaging techniques such as B-mode ultrasound, Doppler ultrasound, ultrasound-based elastography, computed tomography (CT), CT angiography, magnetic resonance imaging (MRI), MR angiography, and magnetic resonance elastography. In addition, emerging predictive models based on artificial intelligence are increasingly being explored (13).

Among these modalities, ultrasound-based elastography has been widely studied as a non-invasive method for evaluating the mechanical properties of tissues. These techniques provide both qualitative and quantitative information about tissue elasticity and stiffness. The increasing interest in ultrasound elastography is mainly driven by its practical benefits, including broad availability, good reproducibility, relatively low cost, and strong patient acceptance (15).

Although originally developed for the non-invasive staging of liver fibrosis in chronic liver diseases, numerous studies have subsequently evaluated their role in the assessment of portal hypertension by measuring liver and spleen stiffness, yielding encouraging results (16-24).

According to international guidelines (25, 26), elastography techniques are broadly classified into strain elastography—primarily used in breast, thyroid, and prostate applications—and shear-wave elastography (SWE). SWE relies on an externally generated impulse that induces shear waves within the examined organ, while ultrasound technology measures the propagation velocity of these waves, which correlates with tissue stiffness.

Depending on the type of external stimulus and the method used to measure shear-wave velocity, SWE techniques are further subdivided into:

- **Vibration Controlled Transient Elastography (VCTE)**, which uses a mechanical external impulse;
- **Point shear-wave elastography (pSWE)**, based on Acoustic Radiation Force Impulse (ARFI) technology, where shear-wave velocity is measured within a small, predefined region of interest;

- **Real-time shear-wave elastography**, including **2D-SWE and 3D-SWE**, which also use ARFI-generated impulses and allow stiffness quantification over a larger area while simultaneously displaying a color-coded elastogram (25,26).

It should be emphasized that stiffness cut-off values proposed for different fibrosis stages vary according to the specific ultrasound system used.

11.4.4. Ultrasound Elastography in Liver Evaluation

A) Vibration Controlled Transient Elastography (VCTE)

Vibration-Controlled Transient Elastography (VCTE) was the first elastographic method developed for the noninvasive evaluation of liver fibrosis and remains the most widely validated technique. Its underlying principle is based on the relationship between the velocity of a mechanical wave propagating through homogeneous tissue and tissue elasticity, which correlates with the degree of hepatic fibrosis (27).

The technique uses a dedicated transducer that produces low-frequency (approximately 50 Hz), low-amplitude mechanical vibrations, which generate shear waves that travel through the liver parenchyma. The propagation speed of these waves is measured by ultrasound and is directly related to the stiffness of the examined tissue, with higher velocities indicating increased tissue rigidity (28). Based on this principle, transient elastography provides quantitative measurements of liver stiffness, expressed in kilopascals (kPa). The measurable range typically extends from approximately 1.5 to 75 kPa, allowing the technique to capture a wide spectrum of liver stiffness values. In individuals with normal liver architecture, liver stiffness values are usually below 5 kPa (29–32).

Numerous studies have demonstrated a clear association between liver stiffness (LS) and the presence of esophageal varices (EV) (33–39), as well as a relationship between LS values and the size or severity of these varices (33, 36, 38, 40) These observations have stimulated further research exploring the potential of LS as a non-invasive surrogate marker for the assessment of portal hypertension (PH).

One of the early pivotal studies investigating liver stiffness as a predictor of portal hypertension demonstrated that a cut-off value of 13.6 kPa could accurately identify patients with HVPG ≥10 mmHg, showing excellent diagnostic performance (AUC 0.99, sensitivity 97%). For the prediction of HVPG ≥12 mmHg, a higher threshold of 17.6 kPa achieved an AUC of 0.92 with a

sensitivity of 94%. These findings suggest that LS shows a strong correlation with HVPG values up to around 10 mmHg; beyond this point, further increases in portal pressure appear to be more influenced by increased splanchnic blood flow rather than solely by intrahepatic vascular resistance (34). Similar results were subsequently reported in another study, where LS predicted HVPG ≥10 mmHg with an AUC of 0.945 using a cut-off value of 21 kPa (40). An important meta-analysis showed that liver stiffness (LS) measured by transient elastography (TE) has excellent diagnostic performance for detecting ***clinically significant portal hypertension (CSPH),*** with a pooled area under the curve (AUC) of 0.93. Another meta-analysis further confirmed a strong correlation between LS values and HVPG, highlighting the good diagnostic accuracy of LS for identifying CSPH (41).

Building on these observations, the Baveno VI consensus incorporated non-invasive parameters into clinical practice and suggested that patients with liver stiffness (LS) values below 20 kPa and a platelet count above 150 × 10^9/L could safely avoid screening upper gastrointestinal endoscopy. In this subgroup, the probability of harboring high-risk varices (HRV) is estimated to be below 5% when both criteria are met (12).

However, the number of endoscopies avoided using the original Baveno VI criteria was relatively limited. To address this issue, the criteria were later expanded and validated in additional cohorts in 2017 (42). In a study including 499 patients with compensated advanced chronic liver disease (cACLD) of different etiologies, alternative thresholds were evaluated to identify individuals with a very low risk (<5%) of HRV. The expanded criteria—platelet count >110 × 10^9/L and LS <25 kPa—were subsequently validated in two independent cohorts from London (309 patients) and Barcelona (117 patients). Using these modified thresholds, approximately 40% of screening endoscopies could be avoided, compared with 21% when applying the original Baveno VI criteria, while the risk of missing HRV remained very low (1.6%).

Despite these developments, the most recent EASL and AASLD guidelines have not yet reached a clear consensus regarding the optimal LS threshold (20 vs. 25 kPa) for predicting the risk of clinical decompensation. Addressing these uncertainties, a 2019 meta-analysis including 30 studies assessed the performance of both the original Baveno VI criteria (LS <20 kPa and platelets >150 × 10^9/L) and the expanded criteria (LS <25 kPa and platelets >110 × 10^9/L) for identifying HRV in patients with cACLD. The analysis concluded that both strategies demonstrate high sensitivity but limited specificity for detecting HRV (43).

More recently, the Baveno VII consensus reaffirmed that non-invasive tests are sufficiently accurate to identify CSPH (14). Specifically, LS ≤15 kPa combined with a platelet count ≥150 × 10^9/L can reliably exclude CSPH in patients with cACLD, with sensitivity and negative predictive value exceeding 90%.

Conversely, in patients with viral- or alcohol-related liver disease, as well as in non-obese individuals (BMI <30 kg/m²) with non-alcoholic steatohepatitis (NASH), an LS ≥25 kPa is considered adequate to rule in CSPH, with specificity and positive predictive value above 90%. In this population, the algorithm allows accurate risk stratification. Patients with intermediate values—LS between 20–25 kPa and platelets <150 × 10^9/L, or LS between 15–20 kPa and platelets <110 × 10^9/L—have an estimated 60% probability of harboring CSPH.

B) ARFI-Based Shear-Wave Elastography: Point Shear-Wave Elastography (pSWE)

Point shear-wave elastography (pSWE) is an ultrasound-based elastography technique that relies on Acoustic Radiation Force Impulse (ARFI) technology and is integrated into conventional ultrasound systems, allowing direct visualization of the examined liver parenchyma during the measurement. This method evaluates tissue stiffness within a predefined region of interest (ROI), whose dimensions depend on the specific ultrasound platform used.

Among pSWE techniques, the most extensively studied implementations include Virtual Touch Tissue Quantification (VTQ) available on Siemens systems and ElastPQ developed by Philips. In recent years, several other manufacturers have integrated ARFI-based point shear-wave elastography into their ultrasound platforms, including Samsung (S-Shearwave Point) (Fig. 11.4.1), Fujifilm-Hitachi (Shear Wave Measurement – SWM), Canon/Toshiba (SWE Point Measurement), and Esaote (ElaXtoQ) (44, 45).

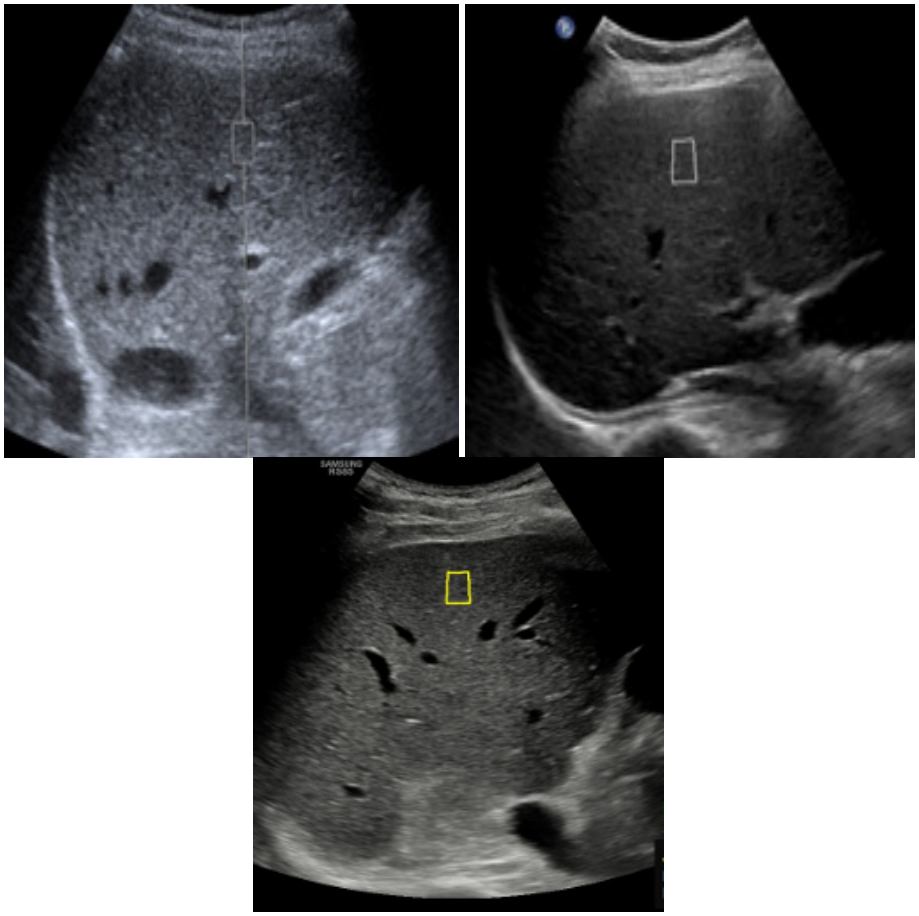


Fig. 11.4.1. Examples of liver stiffness measurements using point shear-wave elastography (pSWE) on different ultrasound platforms.

Representative ultrasound images illustrating liver stiffness assessment using ARFI-based pSWE techniques: **Left:** *Virtual Touch Tissue Quantification (VTQ) implemented on a Siemens system; Center***:** *ElastPQ implemented on a Philips ultrasound system;* **Right:** *S-Shearwave Point elastography implemented on a Samsung ultrasound platform. In all cases, liver stiffness is measured within a predefined region of interest (ROI) placed in the liver parenchyma.*

Clinical studies have shown that VTQ-based pSWE is a reliable method for diagnosing liver cirrhosis, even when liver biopsy is used as the reference standard. Reported cut-off values ranging from 1.55 to 2.0 m/s have demonstrated good diagnostic performance, with area under the curve (AUC) values between 0.89 and 0.93 (46–50). Furthermore, several meta-analyses

have confirmed the usefulness of pSWE for the diagnosis of cirrhosis, reporting pooled diagnostic accuracies above 0.91, which are comparable to those reported for transient elastography (TE) (51-53).

A study evaluating ElastPQ for the diagnosis of liver cirrhosis demonstrated a significant correlation between liver stiffness measurements and the stage of hepatic fibrosis ($r = 0.61$) (54). Likewise, pSWE implemented on the Samsung-Medison RS85 ultrasound system showed excellent diagnostic accuracy, with an AUC of 0.95 for detecting significant fibrosis and 0.98 for cirrhosis (55).

With regard to portal hypertension (PH), VTQ remains the most extensively investigated pSWE technique, although the reported results have been inconsistent across studies. In one of the earliest investigations, a cut-off value of 2.25 m/s was proposed for predicting large esophageal varices; however, the diagnostic performance was relatively modest, with an AUC of 0.596. Comparable findings were reported in another study evaluating the ability of VTQ to detect high-risk varices (HRV), where the AUC was 0.58 (56). These relatively low AUC values suggest that, although liver stiffness measured by VTQ may reflect portal hypertension to some extent, its ability to accurately discriminate patients with clinically relevant varices remains limited when used as a standalone parameter.

More encouraging findings were reported in another study that demonstrated a significant correlation between VTQ-derived liver stiffness values and HVPG measurements ($r = 0.646$; $p < 0.001$). In this study, the technique showed good diagnostic performance for identifying clinically significant portal hypertension (CSPH), with an AUC of 0.85 (57).

Similarly, in another study (58), liver stiffness assessed using VTQ showed moderate diagnostic performance for detecting esophageal varices. The reported AUC was 0.76 (cut-off 2.08 m/s) for identifying varices of any grade and 0.78 (cut-off 1.9 m/s) for predicting high-risk varices.

In contrast, evidence regarding the role of **ElastPQ** in the evaluation of portal hypertension remains relatively limited. However, a recent study reported a significant positive association between liver stiffness values obtained with ElastPQ and portal pressure measurements ($r = 0.482$; $p < 0.001$), suggesting a potential role for this technique in the non-invasive assessment of portal hypertension (59).

C) ARFI-Based Shear-Wave Elastography: Real-Time Shear-Wave Elastography (2D-SWE and 3D-SWE)

Real-time shear-wave elastography (2D-SWE) is an elastographic technique based on ARFI technology that has been incorporated into multiple ultrasound systems, enabling real-time assessment of shear-wave propagation within the examined tissue.

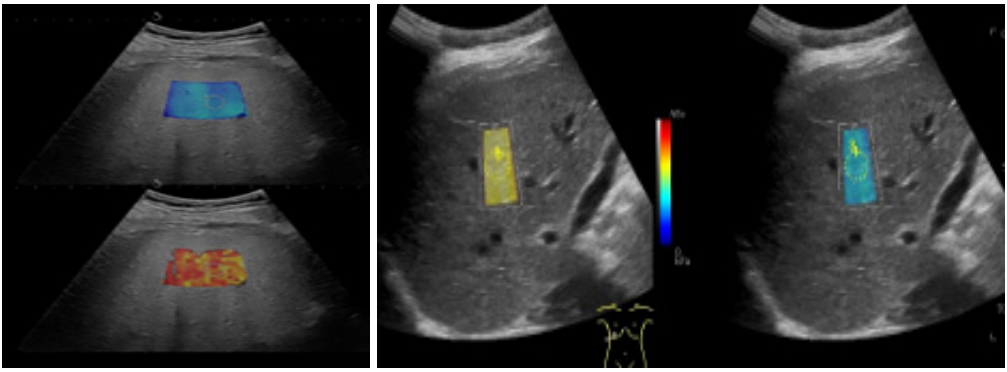


Fig. 11.4.2. Liver stiffness assessment using real-time shear-wave elastography (2D-SWE) on different ultrasound systems.

Representative images illustrating liver stiffness evaluation using **2D shear-wave elastography**. **Left:** *2D-SWE implemented on a* **Supersonic Imagine (Aixplorer) system***, showing a color-coded elastographic map superimposed on the B-mode image.* **Right:** *2D-SWE implemented on a* **GE Healthcare ultrasound system***, where liver stiffness is measured within a defined region of interest (ROI), with the stiffness scale displayed on the color bar.*

One of the main advantages of this method is the ability to display tissue stiffness as a color-coded elastogram superimposed on the conventional B-mode image, while simultaneously allowing quantitative measurement of liver stiffness (LS) within a defined region of interest. The results are typically expressed in kilopascals (kPa) or meters per second (m/s) (60). For optimal performance, good-quality B-mode imaging and sufficient operator expertise are required (61,62).

The 2D-SWE technique was initially developed by Supersonic Imagine (France) (2D-SWE.SSI) and incorporated into the Aixplorer® system. Subsequently, similar technologies were introduced by other manufacturers, including General Electric (2D-SWE.GE), Canon-Toshiba, Philips (ElastQ), and Samsung (Fig. 11.4.2) (60).

Multiple studies have demonstrated good diagnostic performance of 2D-SWE.SSI for identifying significant fibrosis and cirrhosis in patients with compensated advanced chronic liver disease (cACLD) of various etiologies (63–67). However, reported cut-off values vary considerably depending on the underlying liver disease.

A study including 331 subjects evaluated with 2D-SWE.GE (68) reported excellent diagnostic accuracy for significant fibrosis (AUC 0.95) and cirrhosis (AUC 0.96). Similar findings were observed in an Italian study that used liver biopsy as the reference standard (69).

More recently, a study investigating a **Samsung 2D-SWE** system reported a cut-off value of **7.6 kPa** for the diagnosis of cirrhosis, with excellent diagnostic performance (AUC 0.98) (55). Similarly, using the **ElastQ** technique, Villani et al. (70) identified a liver stiffness threshold of **12.65 kPa** for detecting cirrhosis, achieving a diagnostic accuracy reflected by an AUC of **0.89.**

Regarding the role of 2D-SWE in the assessment of portal hypertension (PH), most published studies have investigated the 2D-SWE.SSI platform. Kim et al. (22) demonstrated a significant correlation between LS values and HVPG in patients with clinically significant portal hypertension (CSPH) ($r = 0.574$; $p < 0.001$). A cut-off value of 15.2 kPa yielded an AUC of 0.819 (95% CI 0.725–0.892) for CSPH prediction. In another study (20), a similar threshold of 15.4 kPa achieved an AUC of 0.948 for detecting CSPH.

A multicenter meta-analysis including patients from seven different centers assessed the diagnostic performance of **2D-SWE.SSI** for detecting clinically significant portal hypertension (CSPH). In this analysis, **liver stiffness (LS) values below 14 kPa** were able to exclude CSPH with an overall accuracy of **85% (summary AUC 0.88),** whereas **LS values ≥32 kPa** were associated with a positive prediction of CSPH with an accuracy of **55% (summary AUC 0.83).** Based on these findings, the authors suggested that LS values below 14 kPa may be reliably used to rule out CSPH. However, liver stiffness alone did not demonstrate sufficient accuracy for predicting the presence of **high-risk varices (HRV)** (71).

Fewer studies have assessed the performance of 2D-SWE implemented on General Electric ultrasound system. A strong correlation between LS and HVPG was observed ($r = 0.704$; $p < 0.0001$) (72). Using a cut-off value of 11.3 kPa, the technique demonstrated very good performance for identifying CSPH (AUC 0.91).

Given the variability in reported cut-off values for both pSWE and 2D-SWE techniques, the Society of Radiologists in Ultrasound proposed a pragmatic and system-neutral approach known as the “rule of four” (5, 9, 13, and 17 kPa) (73). Developed primarily for viral etiologies and NAFLD, this framework can be interpreted as presented in Table 11.4.I.

Table 11.4.I. Interpretation of Liver Stiffness Values According to the “Rule of Four” for Ultrasound-Based Elastography

Liver Stiffness (kPa)	Approx. Velocity (m/s)	Clinical Interpretation
≤ 5 kPa	≈ 1.3 m/s	Highly suggestive of normal liver stiffness
≤ 9 kPa	≈ 1.7 m/s	In the absence of clinical signs, cACLD is unlikely
9–13 kPa	≈ 1.7–2.1 m/s	Possible cACLD – additional evaluation recommended
≥ 13 kPa	≈ 2.1 m/s	Strongly suggestive of cACLD
≥ 17 kPa	≈ 2.4 m/s	High probability of clinically significant portal hypertension (CSPH)

11.4.5. Ultrasound-Based Elastography in Spleen Evaluation

The spleen plays a crucial regulatory role in maintaining adequate portal venous inflow to the liver. In the setting of portal hypertension, splenomegaly arises from a complex interplay of mechanisms, including splenic congestion, as well as hyperplasia and increased activity of splenic lymphoid tissue. In parallel, enhanced processes of angiogenesis and fibrogenesis further contribute to structural remodeling of the spleen. This progressive fibrogenic transformation leads to increased splenic stiffness, which has attracted growing interest in the assessment of spleen stiffness (SS) as a non-invasive marker for the detection of portal hypertension and clinically significant portal hypertension (CSPH) (74).

Spleen stiffness has been evaluated using several ultrasound-based elastography techniques, including transient elastography and ARFI-based approaches such as point shear-wave elastography (pSWE) and two-dimensional shear-wave elastography (2D-SWE) (24, 25, 75, 76).

A) Vibration Controlled Transient Elastography (VCTE)

Over the past decade, growing scientific attention has been directed toward the spleen and its biomechanical properties, with numerous studies exploring the relationship between spleen stiffness and portal hypertension. Accumulating evidence has consistently demonstrated a strong and reproducible association between spleen stiffness (SS) measured by transient elastography and the presence of portal hypertension. These findings reflect the profound hemodynamic and structural changes occurring within the spleen in the setting of chronic liver disease. Early investigations in this field already reported significantly increased SS values in patients with liver cirrhosis, highlighting the spleen not merely as a passive bystander of portal hypertension, but as an active and informative marker of the underlying portal hemodynamic alterations (77).

Subsequent research further explored the clinical value of spleen stiffness in identifying complications of portal hypertension. In one study, an SS value exceeding **46.4 kPa** was shown to predict the presence of **esophageal varices in patients with liver cirrhosis**, with a diagnostic accuracy of **80.5% (AUC 0.78)** (78). These findings suggested that increased splenic stiffness reflects not only structural changes within the spleen but also the hemodynamic consequences of portal hypertension that contribute to variceal development.

To enhance diagnostic performance, investigators later proposed **multiparametric approaches** combining splenic and hepatic stiffness measurements. In this context, a predictive model incorporating **liver stiffness (LS ≥19 kPa)** together with **spleen stiffness (SS ≥55 kPa)** demonstrated improved accuracy for identifying patients with esophageal varices, reaching an overall diagnostic accuracy of **88.5%.** This combined approach highlights the complementary value of liver and spleen stiffness measurements in the non-invasive assessment of portal hypertension and its clinically relevant complications.

Another predictive model integrating spleen stiffness with the Baveno VI criteria proved useful in excluding high-risk varices (HRV). In a study involving 498 patients, an SS cut-off value ≤46 kPa was proposed to rule out HRV. Using either this threshold or the Baveno VI criteria alone, 35.8% and 21.7% of patients in the validation cohort, respectively, could have safely avoided upper gastrointestinal endoscopy, with a missed HRV rate below 2% in both scenarios. When both parameters were combined within the same predictive model, an

additional 22.5% of endoscopies could be avoided, increasing the overall proportion of avoided procedures to 43.8%, while maintaining excellent diagnostic performance and a missed HRV rate below 5% (79).

Another important study (23) evaluated the performance of SS measured by transient elastography in predicting portal hypertension. The authors concluded that SS represents a valuable noninvasive marker for identifying esophageal varices and CSPH. The reported AUC values were 0.94 for the prediction of esophageal varices and 0.95 for detecting HVPG ≥12 mmHg. More recently, Wang et al. (80) confirmed these findings, highlighting the high predictive accuracy of SS for esophageal varices. In a cohort of 102 cirrhotic patients evaluated using transient elastography, an SS cut-off value of 45.5 kPa yielded an AUC of 0.98 for predicting high-risk varices and an AUC of 0.92 for predicting variceal bleeding.

Most studies investigating spleen stiffness have been performed using **FibroScan®** equipped with the conventional spleen stiffness measurement mode (**SS@50 Hz**), which allows measurements up to a maximum value of **75 kPa**. While this system has demonstrated good feasibility and diagnostic performance in clinical studies, the upper measurement limit may restrict its ability to accurately capture very high stiffness values. As a result, in patients with advanced portal hypertension, spleen stiffness may reach values beyond this threshold, potentially leading to an underestimation of disease severity (81).

To overcome this limitation, **EchoSens** introduced a dedicated spleen stiffness measurement module (**SSM@100 Hz**), specifically designed to improve the evaluation of splenic stiffness in patients with portal hypertension. This updated technology enables a broader measurement range and enhances the technical feasibility of spleen stiffness assessment. In a comparative study evaluating the performance of the two approaches, the **SSM@100 Hz** module achieved a significantly higher rate of valid measurements compared with the conventional **SS@50 Hz** technique (**92.5% vs. 76.0%, $p < 0.001$**) (81). These findings suggest that the newer system may provide a more reliable assessment of spleen stiffness, particularly in patients with advanced disease, thereby improving the non-invasive evaluation of portal hypertension (81).

According to the **Baveno VII consensus**, spleen stiffness measured by transient elastography may be used in patients with **viral-related compensated advanced chronic liver disease (cACLD)** to non-invasively exclude or confirm the presence of **clinically significant portal hypertension (CSPH)**. Specifically,

spleen stiffness values **below 21 kPa** can be used to rule out CSPH, whereas values **above 50 kPa** are considered highly suggestive of its presence. However, these proposed thresholds still require additional validation in larger prospective studies (14). The Baveno VII recommendations also emphasize another important clinical implication of spleen stiffness assessment. In patients who are **not candidates for non-selective beta-blocker therapy** and who would otherwise be referred for **screening upper gastrointestinal endoscopy according to Baveno VI criteria**, endoscopic evaluation may potentially be avoided if **spleen stiffness is ≤40 kPa**, as the likelihood of **high-risk varices (HRV)** in this subgroup is considered low (14).

B) ARFI-Based Shear-Wave Elastography: Point Shear-Wave Elastography (pSWE)

Several studies have investigated the performance of spleen stiffness (SS) measured using pSWE techniques as a non-invasive predictor of portal hypertension (PH). Among the available pSWE methods (Fig. 11.4.3), the most extensively studied and validated technique for assessing SS is Virtual Touch Tissue Quantification (VTQ).

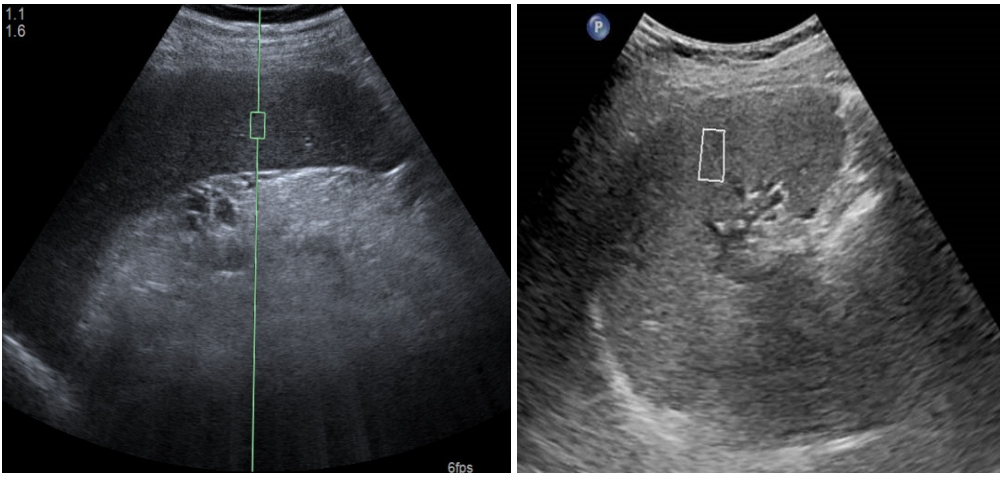


Fig. 11.4.3. Spleen stiffness assessment using point shear-wave elastography (pSWE).

Representative ultrasound images illustrating **spleen stiffness measurement using ARFI-based pSWE techniques***.* **Left:** *Virtual Touch Tissue Quantification (***VTQ***) implemented on a* **Siemens ultrasound system***.* **Right: ElastPQ** *implemented on a* **Philips ultrasound system***. In both techniques, stiffness is measured within a predefined* **region of interest (ROI)** *placed in the splenic parenchyma.*

In one study, spleen stiffness (SS) measured using **VTQ** showed lower diagnostic performance than liver stiffness (LS) for the detection of portal hypertension (PH), with an **AUC of 0.68 compared with 0.90** for LS (82). In contrast, another investigation reported that, in multivariate analysis, the relationship between SS assessed with VTQ and PH appeared to be stronger than that observed for LS, although the overall predictive accuracy of the two parameters remained similar (83).

One study demonstrated that **spleen stiffness (SS)** measured using **VTQ** showed good predictive performance for the diagnosis of liver cirrhosis; however, its ability to predict the presence or severity of **esophageal varices (EV)** was more limited (84). In the same analysis, a **multiparametric predictive model** was developed in which **liver stiffness (LS), spleen stiffness (SS)** measured by VTQ, and the **presence of ascites** were identified as independent predictors of **high-risk varices (HRV).** When these variables were combined into a predictive score, the model achieved a diagnostic accuracy of **69.6% for the detection of HRV (AUC 0.72)** (56).

Although the relative superiority of **spleen stiffness (SS)** compared with **liver stiffness (LS)** remains debated across individual studies, a meta-analysis including **16 studies** suggested that SS may offer **higher predictive accuracy for portal hypertension** (85). In another investigation, SS measured using **VTQ** demonstrated excellent diagnostic performance for predicting **high-risk varices (HRV),** with **AUC values ranging from 0.92 to 0.94**, depending on the underlying etiology of liver disease (86). Likewise, a separate study reported that VTQ-derived SS could predict HRV with an **AUC as high as 0.97**, further supporting the potential clinical utility of spleen stiffness assessment in patients with portal hypertension (87).

Evidence regarding the evaluation of **spleen stiffness (SS)** using other **pSWE techniques** remains relatively scarce. In a more recent study including **107 patients**, SS was assessed using another pSWE method (**ElastPQ**), with **HVPG** serving as the reference standard. The results demonstrated a **significant correlation between SS values and portal pressure** ($r = 0.489$, $p < 0.001$). Moreover, a **diagnostic algorithm combining SS values below 20 kPa with a platelet count ≥150 × 10^9/L** was able to **exclude clinically significant portal hypertension (CSPH)** with an accuracy of **92.9%** (59).

C) ARFI-Based Shear-Wave Elastography: Real-Time Shear-Wave Elastography (2D-SWE and 3D-SWE)

The available evidence regarding the use of **spleen stiffness (SS) measured by 2D shear-wave elastography (2D-SWE)** for the evaluation of portal hypertension remains relatively limited compared with liver stiffness measurements (Fig. 11.4.4). However, several studies have explored its potential role as a non-invasive marker of portal hypertension and its complications.

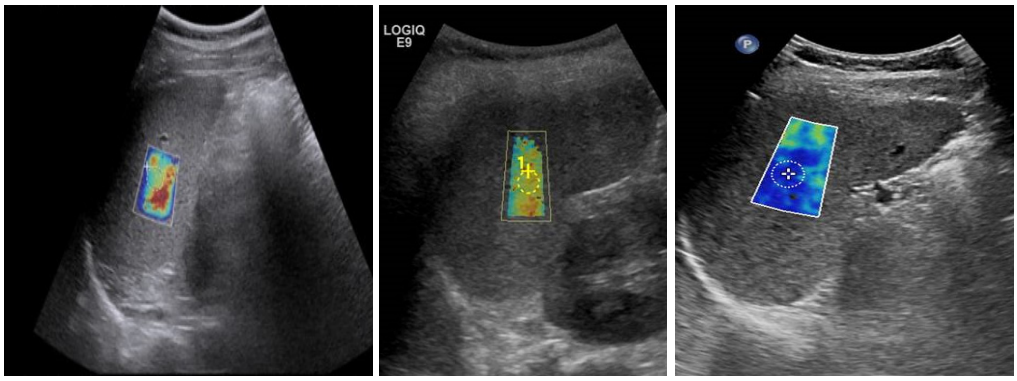


Fig. 11.4.4. Spleen stiffness assessment using real-time shear-wave elastography (2D-SWE) on different ultrasound platforms.

*Representative ultrasound images illustrating **spleen stiffness (SS) evaluation using 2D shear-wave elastography. Left:** 2D-SWE implemented on a **Supersonic Imagine (Aixplorer) system. Center: 2D-SWE.GE** performed on a **GE Healthcare LOGIQ system. Right: ElastQ 2D-SWE** implemented on a **Philips ultrasound system**. In all cases, stiffness measurements are obtained within a predefined region of interest placed in the splenic parenchyma.*

In one study including **77 patients**, SS assessed using **2D-SWE.SSI** demonstrated promising results for the identification of variceal risk. Specifically, **SS values below 35.8 kPa** were able to **exclude the presence of high-risk varices (HRV)** with good diagnostic performance, achieving an **AUC of 0.85** and a **negative predictive value of 91.3%** (88). These findings suggest that spleen stiffness measurements obtained with 2D-SWE may be useful for ruling out clinically relevant varices in selected patients. Similarly, another study conducted in a **larger patient population** reported that SS measurements showed **good predictive performance for the detection of esophageal varices**,

irrespective of their grade, with an **AUC of 0.80**. The same analysis demonstrated an **AUC of 0.78** for identifying **high-risk varices**, further supporting the potential role of spleen stiffness as a non-invasive tool for risk stratification in patients with portal hypertension (89). Together, these findings indicate that although the current evidence is still limited, **2D-SWE-based spleen stiffness assessment may represent a valuable adjunct in the non-invasive evaluation of portal hypertension and its complications**.

A noteworthy strategy for the non-invasive identification of **clinically significant portal hypertension (CSPH)** using **2D-SWE.SSI** was proposed through the development of a **sequential diagnostic algorithm combining liver stiffness (LS) and spleen stiffness (SS)** (90). This approach was evaluated in a cohort of **158 patients with liver cirrhosis**, all of whom also underwent **HVPG measurements**, which served as the reference standard for the diagnosis of portal hypertension.

In the first step of the algorithm, **liver stiffness** was assessed. When **LS exceeded 38 kPa, 36 out of 39 patients** were correctly classified as having CSPH, suggesting that very high LS values alone can reliably indicate clinically significant portal hypertension. For patients with **LS values below 38 kPa**, an additional evaluation of **spleen stiffness** was performed to improve diagnostic discrimination. When **LS <38 kPa and SS <27.9 kPa, 32 of 40 patients** were correctly identified as not having CSPH. In contrast, when **LS <38 kPa but SS exceeded 27.9 kPa, 35 of 37 patients** were accurately classified as having CSPH. Overall, this sequential algorithm achieved a **sensitivity of 89.2% and a specificity of 91.4%** for the detection of CSPH, highlighting the complementary diagnostic value of combining hepatic and splenic stiffness measurements.

Another investigation evaluated the performance of **2D-SWE implemented on a different ultrasound platform (General Electric)** for assessing **spleen stiffness as a predictor of high-risk varices (HRV)** and compared its performance with that of **pSWE (VTQ)** (91). In this study, the optimal **cut-off value for SS measured by 2D-SWE.GE was 13.2 kPa**, corresponding to an **AUC of 0.84**. By comparison, VTQ-derived measurements yielded a cut-off value of **2.91 m/s**, with an **AUC of 0.90**. Importantly, the difference in diagnostic performance between the two elastographic techniques was **not statistically significant (p = 0.1606),** suggesting that both methods may provide comparable diagnostic accuracy for identifying patients at risk of HRV.

The potential role of spleen stiffness as a marker of portal hypertension has also been supported by **several meta-analyses**. These analyses have demonstrated a **strong correlation between SS and HVPG values**, with a reported correlation coefficient of **r = 0.72**, indicating that splenic stiffness reflects the hemodynamic changes associated with increased portal pressure (92). In addition, pooled data have shown that **SS exhibits good diagnostic performance for the detection of high-risk varices**, further supporting its value as a non-invasive tool for risk stratification in patients with portal hypertension (93).

11.4.6. Magnetic Resonance Elastography (MRE)

Several meta-analyses have evaluated the diagnostic performance of magnetic resonance elastography (MRE) for assessing liver fibrosis, consistently demonstrating an accuracy exceeding 90% for the detection of advanced fibrosis and cirrhosis (94–96).

In addition to its excellent predictive value, MRE offers several important advantages. It allows evaluation of the entire hepatic parenchyma, enables quantification of hepatic steatosis, and facilitates the detection of focal liver lesions. Moreover, obesity does not significantly affect the feasibility or diagnostic accuracy of the technique (97). However, its main limitations remain the relatively high cost and limited availability.

A preliminary study involving 34 patients evaluated liver stiffness measured by MRE as a predictor of portal hypertension, using HVPG as the reference standard. Liver stiffness showed a weak but statistically significant correlation with HVPG values ($r = 0.478$, $p = 0.016$). Nevertheless, the predictive performance of liver stiffness for portal hypertension (AUC 0.809) and for clinically significant portal hypertension (CSPH) (AUC 0.742) was considered good (98).

Spleen stiffness measured by MRE has also been investigated together with liver stiffness for predicting the presence of esophageal varices (EV). Spleen stiffness values were significantly higher in patients with EV, and multivariate regression analysis identified spleen stiffness as an independent predictor of varices. In contrast, no significant association was found between liver stiffness and the presence of EV. Using a cut-off value of 9.53 for spleen stiffness, the diagnostic accuracy for detecting EV was high (AUC 0.853, sensitivity 84.4%, specificity 73.7%) (99).

These findings were further supported by two additional studies (100,101). More recently, a meta-analysis including 14 studies evaluated both spleen stiffness and liver stiffness as predictors of portal hypertension. The pooled and adjusted sensitivity, specificity, and AUC were 83%, 80%, and 0.88 for liver stiffness, respectively, compared with 79%, 90%, and 0.92 for spleen stiffness (102). Based on these results, the authors concluded that spleen stiffness may offer slightly higher specificity and overall diagnostic accuracy than liver stiffness for predicting portal hypertension.

References

1. Procopet B, Berzigotti A. Diagnosis of cirrhosis and portal hypertension: imaging, noninvasive markers of fibrosis and liver biopsy. Gastroenterol Rep (Oxf). 2017 May; 5(2): 79–89.
2. Iwakiri Y. Pathophysiology of Portal Hypertension. Clin Liver Dis. 2014 May; 18(2): 281–291.
3. García-Pagán J.C, Gracia-Sancho J, Bosch J. Functional aspects on the pathophysiology of portal hypertension in cirrhosis. J Hepatol 2012 Aug;57(2):458-61.
4. Dib N, Oberti F, Calès P. Current management of the complications of portal hypertension: variceal bleeding and ascites. CMAJ. 2006 May 9; 174(10): 1433–1443.
5. Perello A, Escorsell A, Bru C, Gilabert R, Moitinho E, Garcia-Pagan JC, et al. Wedged hepatic venous pressure adequately reflects portal pressure in hepatitis C virus-related cirrhosis. Hepatology. 1999;30(6):1393-1397
6. Bosch J, Abraldes JG, Berzigotti A, Garcia-Pagan JC. The clinical use of HVPG measurements in chronic liver disease. Nature Reviews. Gastroenterology & Hepatology. 2009;6(10):573-582
7. Groszmann RJ, Garcia-Tsao G, Bosch J, Grace ND, Burroughs AK, Planas R, et al. Beta-blockers to prevent gastroesophageal varices in patients with cirrhosis. N Engl J Med. 2005;353:2254– 2261.
8. Ripoll C, Groszmann R, Garcia-Tsao G, Grace N, Burroughs A, Planas R, et al. Hepatic venous pressure gradient predicts clinical decompensation in patients with compensated cirrhosis. Gastroenterology. 2007;133:481–488.
9. Garcia-Tsao G, Groszmann RJ, Fisher RL, Conn HO, Atterbury CE, Glickman M. Portal pressure, presence of gastroesophageal varices and variceal bleeding. Hepatology. 1985;5:419–424.
10. Boyer TD, Haskal JZ, American Association for the Study of Liver Diseases practice guidelines. The role of transjugular intrahepatic portosystemic shunt creation in the management of portal hypertension. Journal of Vascular and Interventional Radiology, 2005, vol. 16, no. 5, pp. 615–629.

11. Boyer TS, Haskal ZJ, and American Association for the Study of Liver Diseases. The role of transjugular intrahepatic portosystemic shunt (TIPS) in the management of portal hypertension: update. Hepatology,2010, vol. 51, no. 1, pp. 306–306.
12. De Franchis R, Baveno T. Faculty. Expanding consensus in portal hypertension: report of the Baveno VI consensus workshop: stratifying risk and individualizing care for portal hypertension. J Hepatol. 2015; 63(3): 743-752.
13. Ravaioli F, Montagnani M, Lisotti A, Festi D, Mazzella G, Azzaroli F. Noninvasive Assessment of Portal Hypertension in Advanced Chronic Liver Disease: An Update. Gastroenterol Res Pract 2018 Jun 7;2018:4202091
14. de Franchis R, Bosch J, Garcia-Tsao G, Reiberger T, Ripoll C; Baveno VII Faculty. Baveno VII - Renewing consensus in portal hypertension. J Hepatol. 2022 Apr;76(4):959-974
15. Sigrist R, Liau J, Ahmed El Kaffas, Chammas M.C., Willmann J.K. Ultrasound Elastography: Review of Techniques and Clinical Applications. Theranostics. 2017; 7(5): 1303–1329.
16. Carrión JA, Navasa M, Bosch J, Bruguera M, Gilabert R, Forns X. Transient elastography for diagnosis of advanced fbrosis and portal hypertension in patients with 99 hepatitis C recurrence after liver transplantation. Liver Transpl. 2006; 12(12): 1791-1798.
17. Karagiannakis DS, Voulgaris T, Siakavellas SI, Papatheodoridis GV, Vlachogiannakos J. Evaluation of portal hypertension in the cirrhotic patient: hepatic vein pressure and beyond. Scand J Gastroenterol. 2018; 53(10-11):1153-1164.
18. Castera L, Pinzani M, Bosch J. Non invasive evaluation of portal hypertension using transient elastography. J Hepatol. 2012; 56(3): 696-703.
19. Lemoine M, Katsahian S, Ziol M, Nahon P, Ganne-Carrie N, Kazemi F, et al. Liver stifness measurement as a predictive tool of clinically signifcant portal hypertension in patients with compensated hepatitis C virus or alcoholrelated cirrhosis. Aliment Pharmacol Ther. 2008; 28(9): 1102-1110.
20. Yu JB, Xiong H, Yuan XC, Zhou AY. Liver Stiffness Detected by Shear Wave Elastography Predicts Esophageal Varices in Cirrhotic Patients. Ultrasound Q. 2019.
21. Procopet B, Berzigotti A, Abraldes JG, Turon F, Hernandez-Gea V, García-Pagán JC, et al. Real-time shear-wave elastography: applicability, reliability and accuracy for clinically significant portal hypertension. J Hepatol. 2015; 62(5): 1068-1075.
22. Elkrief L, Rautou PE, Ronot M, Lambert S, Dioguardi Burgio M, Francoz C, et al. Prospective comparison of spleen and liver stiffness by using shear-wave and transient elastography for detection of portal hypertension in cirrhosis. Radiology 2015; 275(2): 589-598.
23. Kim TY, Jeong WK, Sohn JH, Kim J, Kim MY, Kim Y. Evaluation of portal hypertension by real-time shear wave elastography in cirrhotic patients. Liver Int. 2015; 35(11): 2416-2424.

24. Colecchia A, Montrone L, Scaioli E, Bacchi-Reggiani ML, Colli A, Casazza G, et al. Measurement of spleen stiffness to evaluate portal hypertension and the presence of esophageal varices in patients with HCV-related cirrhosis. Gastroenterology 2012; 143(3): 646-654.
25. Bamber J, Cosgrove D, Dietrich CF, Fromageau J, Bojunga J, Calliada F, et al. EFSUMB guidelines and recommendations on the clinical use of ultrasound elastography. Part 1: Basic principles and technology. Ultraschall in der Medizin—European Journal of Ultrasound. 2013;34(2):169-184
26. Shiina T, Nightingale KR, Palmeri ML, Hall TJ, Bamber JC, Barr RG, et al.WFUMB guidelines and recommendations for clinical use of ultrasound elastography: Part 1: Basic principles and terminology. Ultrasound in Medicine & Biology. 2015;41(5):1126-1147
27. Yeh WC, Li PC, Jeng YM, Hsu HC, Kuo PL, Li ML, et al. Elastic modulus measurements of human liver and correlation with pathology. Ultrasound Med Biol. 2002;28:467–474.
28. Castera L, Forns X, Alberti A. Non-invasive evaluation of liver fibrosis using transient elastography. J Hepatol 2008;48:835–847.
29. Roulot D, Czernichow S, Le Clesiau H, Costes JL, Vergnaud AC, Beaugrand M. Liver stiffness values in apparently healthy subjects: influence of gender and metabolic syndrome. J Hepatol 2008;48:606–613.
30. Kim SU, Choi GH, Han WK, Kim BK, Park JY, Kim DY, et al. What are true normal‘ liver stiffness values using FibroScan?: a prospective study inhealthy living liver and kidney donors in South Korea. Liver Int 2010;30:268–274.
31. Colombo S, Belloli L, Zaccanelli M, Badia E, Jamoletti C, Buonocore M, et al. Normal liver stiffness and its determinants in healthy blood donors. Dig Liver Dis 2011;43:231–236.
32. Das K, Sarkar R, Ahmed SM, Mridha AR, Mukherjee PS, Das K, et al. Normal‘‘ liver stiffness measure (LSM) values are higher in both lean and obese individuals: a population-based study from a developing country. Hepatology 2012;55:584–593.
33. Castera L, Bail B.L, Roudot-Thoraval F, Bernard PH, Foucher J, Merrouche W, et al. Early detection in routine clinical practice of cirrhosis and oesophageal varices in chronic hepatitis C: comparison of transient elastography (FibroScan) with standard laboratory tests and non-invasive scores. Journal of Hepatology, 2009,vol. 50, no. 1, pp. 59–68.
34. Vizzutti F, Arena U, Romanelli RG, Rega L, Foschi M, Colagrande S, et al. Liver stiffness measurement predicts severe portal hypertension in patients with HCV-related cirrhosis. Hepatology. 2007;45:1290–1297.
35. Reiberger T, Ferlitsch A, Payer BA, Pinter M, Homoncik M, Peck-Radosavljevic M. Non-selective β-blockers improve the correlation of liver stiffness and portal pressure in advanced cirrhosis. J Gastroenterol. 2012;47:561–568

36. Kazemi F, Kettaneh A, N'kontchou G, Pinto E, Ganne-Carrie N, Trinchet JC, et al. Liver stiffness measurement selects patients with cirrhosis at risk of bearing large oesophageal varices. J Hepatol, 45 (2006), pp. 230-23
37. Pineda JA, Recio E, Camacho A, Macías J, Almodóvar C, González-Serrano M, et al; Grupo Andaluz de Hepatitis Vírica (HEPAVIR) de la Sociedad Andaluza de Enfermedades Infecciosas (SAEI). Liver stiffness as a predictor of esophageal varices requiring therapy in HIV/hepatitis C virus-coinfected patients with cirrhosis.J Acquir Immune Defic Syndr, 51 (2009), pp. 445-449
38. Pritchett S., Cardenas A., Manning D., Curry M., Afdhal N.H. The optimal cut-off for predicting large oesophageal varices using transient elastography is disease specific. J Viral Hepat, 18 (2011), pp. e75-e80
39. Malik R, Lai M, Sadiq A, Farnan R, Mehta S, Nasser I, et al. Comparison of transient elastography, serum markers and clinical signs for the diagnosis of compensated cirrhosis. J Gastroenterol Hepatol, 25 (2010), pp. 1562-1568
40. Bureau C, Metivier S, Peron JM, Selves J, Robic MA, Gourraud PA, et al. Transient elastography accurately predicts presence of significant portal hypertension in patients with chronic liver disease. Aliment Pharmacol Ther 2008;27:1261–1268.
41. Shi KQ, Fan YC, Pan ZZ, Lin XF, Liu WY, Chen YP, et al. Transient elastography: a meta-analysis of diagnostic accuracy in evaluation of portal hypertension in chronic liver disease. Liver Int. 2013 Jan;33(1):62-71.
42. Augustin S, Pons M, Maurice JB, Bureau C, Stefanescu H, Ney M, et al. Expanding the Baveno VI criteria for the screening of varices in patients with compensated advanced chronic liver disease. Hepatology. 2017 Dec;66(6):1980-1988.
43. Stafylidou M, Paschos P, Katsoula A, Malandris K, Ioakim K, Bekiari E, et al. Performance of Baveno VI and Expanded Baveno VI Criteria for Excluding High-Risk Varices in Patients With Chronic Liver Diseases: A Systematic Review and Meta-analysis. Clin Gastroenterol Hepatol. 2019 Aug;17(9):1744-1755.e11.
44. Şirli R, Sporea I, Popescu A, Dănilă M. Ultrasound-based elastography for the diagnosis of portal hypertension in cirrhotics. World J Gastroenterol. 2015 Nov 7; 21(41): 11542–11551.
45. Dietrich CF, Bamber J, Berzigotti A, Bota S, Cantisani V, Castera L, et al. EFSUMB Guidelines and Recommendations on the Clinical Use of Liver Ultrasound Elastography, Update 2017 (Long Version). Ultraschall Med. 2017; 38(4): e48.
46. Lupsor M, Badea R, Stefanescu H, Sparchez Z, Branda H, Serban A, et al. Performance of a new elastographic method (ARFI technology) compared to unidimensional transient elastography in the noninvasive assessment of chronic 106 hepatitis C. preliminary results. Journal of Gastrointestinal and Liver Diseases. 2009;18(3):303-310
47. Friedrich-Rust M, Wunder K, Kriener S, Sotoudeh F, Richter S, Bojunga J, et al. Liver fibrosis in viral hepatitis: noninvasive assessment with acoustic radiation force impulse imaging versus transient elastography. Radiology 2009; 252: 595-604.

48. Sporea I, Sirli R, Bota S, Fierbinţeanu-Braticevici C, Petrişor A, Badea R, et al. Is ARFI elastography reliable for predicting fibrosis severity in chronic HCV hepatitis? World J Radiol. 2011;3:188–193 168.
49. Sporea I, Badea R, Sirli R, Lupsor M, Popescu A, Danila M, et al. How efficient is acoustic radiation force impulse elastography for the evaluation of liver stiffness? Hepat Mon. 2011;11:532–538
50. Rizzo L, Calvaruso V, Cacopardo B, Alessi N, Attanasio M, Petta S, et al. Comparison of transient elastography and acoustic radiation force impulse for noninvasive staging of liver fibrosis in patients with chronic hepatitis C. Am J Gastroenterol. 2011;106:2112–2120.
51. Friedrich-Rust M, Nierhoff J, Lupsor M, Sporea I, Fierbinteanu-Braticevici C, Strobel D, et al. Performance of Acoustic Radiation Force Impulse imaging for the staging of liver fibrosis: a pooled meta-analysis. J Viral Hepat. 2012;19:e212–e219
52. Nierhoff J, Chávez Ortiz AA, Herrmann E, Zeuzem S, Friedrich-Rust M. The efficiency of acoustic radiation force impulse imaging for the staging of liver fibrosis: a metaanalysis. Eur Radiol. 2013;23:3040–3053 108
53. Bota S, Herkner H, Sporea I, Salzl P, Sirli R, Neghina AM, et al. Meta-analysis: ARFI elastography versus transient elastography for the evaluation of liver fibrosis. Liver Int. 2013;33:1138–1147
54. Ferraioli G, Tinelli C, Lissandrin R, Zicchetti M, Dal Bello B, Filice G, et al. Point shear wave elastography method for assessing liver stiffness. World Journal of Gastroenterology. 2014;20(16):4787-4796
55. Foncea C.G., Popescu A., Lupusoru R., Fofiu R., Sirli R., Danila M, et al. Comparative study between pSWE and 2D-SWE techniques integrated in the same ultrasound machine, with Transient Elastography as the reference method. Med Ultrason 2020 Mar 1;22(1):13-19.
56. Bota S, Sporea I, Sirli R, Focsa M, Popescu A, Danila M, et al. Can ARFI elastography predict the presence of significant esophageal varices in newly diagnosed cirrhotic patients? Annals of Hepatology. 2012;11(4):519-525
57. Salzl P, Reiberger T, Ferlitsch M, Payer BA, Schwengerer B, Trauner M, et al. Evaluation of portal hypertension and varices by acoustic radiation force impulse imaging of the liver compared to transient elastography and AST to platelet ratio index. Ultraschall Med 2014;35:528-533.
58. Park Y, Kim SU, Park SY, Kim BK, Park JY, Kim DY, et al. A novel model to predictesophageal varices in patients with compensated cirrhosis using acoustic radiation force impulse elastography. PLoS One 2015;10:e0121009.
59. Bucsics T., Grasl B., Schwabl P., Mandorfer M, Dmitrieva J., Peck-Radosavljevic M., et al. The novel point shear-wave elastography method ElastPQ® is accurate for non-invasive evaluation of liver fibrosis and portal hypertension. May 2017 Zeitschrift für Gastroenterologie 55(05):e28-e56

60. Popescu A, Şirli R, Sporea I. Ultrasound elastography.2D Shear Wave Elastography for Liver Fibrosis Evaluation Chapter, March 2020, ISBN: 978-1-78985-710-8, Print ISBN: 978-1-78985-709-2, eBook (PDF) ISBN: 978-1-83880-015-4
61. Grădinaru-Taşcău O, Sporea I, Bota S, Jurchiş A, Popescu A, Popescu M, et al. Does experience play a role in the ability to perform liver stiffness measurements by means of supersonic shear imaging (SSI)? Medical Ultrasonography. 2013;15:180-183 185.
62. Ferraioli G, Tinelli C, Dal Bello B, Zicchetti M, Filice G, Filice C; Liver Fibrosis Study Group. Accuracy of real-time shear wave elastography for assessing liver fibrosis in chronic hepatitis C: A pilot study. Hepatology. 2012;56:2125-2133
63. Lupșor-Platon M, Badea R, Gersak M, Maniu A, Rusu I, Suciu A, et al. Noninvasive assessment of liver diseases using 2D shear wave Elastography. Journal of Gastrointestinal and Liver Diseases. 2016;25(4):525-532
64. Sporea I, Bota S, Gradinaru-Taşcău O, Sirli R, Popescu A, Jurchiş A. Which are the cut-off values of 2D-shear wave Elastography (2D-SWE) liver stiffness measurements predicting different stages of liver fibrosis, considering transient Elastography (TE) as the reference method? European Journal of Radiology. 2014;83:e118-e122
65. Jeong JY, Kim TY, Sohn JH, Kim Y, Jeong WK, Oh YH, et al. Real time shear wave elastography in chronic liver diseases: Accuracy for predicting liver fibrosis, in comparison with serum markers. World Journal of Gastroenterology. 2014;20:13920-13929
66. Deffieux T, Gennisson JL, Bousquet L, Corouge M, Cosconea S, Amroun D, et al. Investigating liver stiffness and viscosity for fibrosis, steatosis and activity staging using shear wave elastography. Journal of Hepatology. 2015;62:317-324
67. Cassinotto C, Boursier J, de Lédinghen V, Lebigot J, Lapuyade B, Cales P, et al. Liver stiffness in nonalcoholic fatty liver disease: A comparison of supersonic shear imaging, FibroScan, and ARFI with liver biopsy. Hepatology. 2016;63:1817-1827
68. Bende F, Sporea I, Sirli R, Popescu A, Mare R, Miutescu B, et al. Performance of 2D-SWE.GE for predicting different stages of liver fibrosis, using Transient Elastography as the reference method. Med Ultrason. 2017 Apr 22;19(2):143-149.
69. Serra C, Grasso V, Conti F, Felicani C, Mazzotta E, Lenzi M, et al. A new two-dimensional shear wave Elastography for noninvasive assessment of liver fibrosis in healthy subjects and in patients with chronic liver disease. Ultraschall in der Medizin. 2018;39:432-439
70. Villani R.,Cavallone F., Davide Romano A., Bellanti F., Serviddio G. Two-Dimensional Shear Wave Elastography versus Transient Elastography: A Non-Invasive Comparison for the Assessment of Liver Fibrosis in Patients with Chronic Hepatitis C. Diagnostics (Basel). 2020 May; 10(5): 313.
71. Thiele M, Hugger MB, Kim Y, Rautou PE, Elkrief L, Jansen C, et al. 2D shear wave liver elastography by Aixplorer to detect portal hypertension in cirrhosis: An individual patient data meta-analysis. Liver International. 2020;40(6):1435-1446

72. Stefanescu H., Rusu C., Lupsor-Platon M., Nicoara Farcau O., Fischer P, Grigoras C, et al. Liver Stiffness Assessed by Ultrasound Shear Wave Elastography from General Electric Accurately Predicts Clinically Significant Portal Hypertension in Patients with Advanced Chronic Liver Disease. Ultraschall Med. 2020 Oct;41(5):526-533.
73. Barr RG, Wilson SR, Rubens D, Garcia-Tsao G, Ferraioli G. Update to the society of radiologists in ultrasound liver Elastography consensus statement. Radiology. 2020;296(2):263-274
74. Bolognesi M, Merkel C, Sacerdoti D, Nava V, Gatta A. Role of spleen enlargement in cirrhosis with portal hypertension. Dig Liver Dis. 2002 Feb;34(2):144-50.
75. Ferraioli G, Wong VW, Castera L, Berzigotti A, Sporea I, Dietrich CF, et al. Liver ultrasound elastography: An update to the world federation for ultrasound in medicine and biology guidelines and recommendations. Ultrasound in Medicine & Biology. 2018;44(12):2419-2440
76. Saftoiu A, Gilja OH, Sidhu PS, Dietrich CF, Cantisani V, Amy D, et al. The EFSUMB guidelines and recommendations for the clinical practice of elastography in non-hepatic applications: Update 2018. Ultraschall in der Medizin—European Journal of Ultrasound. 2019;40(4):425-453
77. Stefanescu H, Lupsor M, Grigorescu M, Procopet B, Maniu A, Badea R. Transient elastography of the spleen as non-invasive assessment of portal hypertension in liver cirrhosis patients. Poster abstract nr 63, Proceedings of EASL Monothematic Conference Portal Hypertension: Advances in Knowledge, Evaluation and Management, Budapest, 2009, p. 130
78. Stefanescu H , Grigorescu M, Lupsor M, Procopet B, Maniu A, Badea R. Spleen stiffness measurement using Fibroscan for the noninvasive assessment of esophageal varices in liver cirrhosis patients. J Gastroenterol Hepatol. 2011; 26(1):164-170.
79. Colecchia A, Ravaioli F, Marasco G, Colli A, Dajti E, Di Biase AR, et al. A combined model based on spleen stiffness measurement and Baveno VI criteria to rule out high-risk varices in advanced chronic liver disease. J Hepatol. 2018 Aug;69(2):308-317.
80. Wang X.K., Wang P., Zhang Y., Sheng-Lin Q., Chi K.; Wang G.C. A study on spleen transient elastography in predicting the degree of esophageal varices and bleeding. Medicine (Baltimore). 2019 Mar;98(9):e14615.
81. Stefanescu H, Marasco G, Calès P, Fraquelli M, Rosselli M, Ganne-Carriè N, et al. A novel spleen-dedicated stiffness measurement by FibroScan® improves the screening of high-risk oesophageal varices. Liver Int. 2020 Jan;40(1):175-185.
82. Rifai K, Cornberg J, Bahr M, Mederacke I, Potthoff A, Wedemeyer H, et al. ARFI elastography of the spleen is inferior to liver elastography for the detection of portal hypertension. Ultraschall in der Medizin. 2011;32(Suppl 2):E24-E30
83. Vermehren J, Polta A, Zimmermann O, Herrmann E, Poynard T, Hofmann WP, et al. Comparison of acoustic radiation force impulse imaging with transient elastography for the detection of complications in patients with cirrhosis. Liver Int. 2012;32:852–858.

84. Bota S, Sporea I , Şirli R , Popescu A , Dănilă M , Şendroiu M, et al. Spleen assessment by Acoustic Radiation Force Impulse Elastography (ARFI) for prediction of liver cirrhosis and portal hypertension. Med Ultrason.2010;12(3):213-7
85. Ma X, Wang L, Wu H, Feng Y, Han X, Bu H, et al. Spleen Stiffness Is Superior to Liver Stiffness for Predicting Esophageal Varices in Chronic Liver Disease: A MetaAnalysis. PLoS One. 2016;11(11):e0165786.
86. Takuma Y, Nouso K, Morimoto Y, Tomokuni J, Sahara A, Toshikuni N, et al. Measurement of spleen stiffness by acoustic radiation force impulse imaging identifies cirrhotic patients with esophageal varices. Gastroenterology. 2013 ;144(1):92-101.e2
87. Fierbinteanu-Braticevici C, Tribus L, Peagu R, Petrisor A, Baicus C, Cretoiu D, et al. Spleen Stiffness as Predictor of Esophageal Varices in Cirrhosis of Different Etiologies. Sci Rep. 2019;9(1):16190.
88. Karagiannakis DS, Voulgaris T, Koureta E, Chloupi E, Papatheodoridis GV, Vlachogiannakos J. Role of Spleen Stiffness Measurement by 2D-Shear Wave Elastography in Ruling Out the Presence of High-Risk Varices in Cirrhotic Patients. Dig Dis Sci. 2019 Sep;64(9):2653-2660.
89. Cassinotto C, Charrie A, Mouries A, Lapuyade B, Hiriart JB, Vergniol J, et al. Liver and spleen elastography using supersonic shear imaging for the non-invasive diagnosis of cirrhosis severity and oesophageal varices. Digestive and Liver Disease. 2015;47(8):695-701
90. Jansen C, Bogs C, Verlinden W, Thiele M, Möller P, Görtzen J, et al. Shear-wave elastography of the liver and spleen identifies clinically significant portal hypertension: A prospective multicentre study. Liver Int 2016;37:396- 405.
91. Fofiu R, Bende F, Popescu A, Şirli R, Lupușoru R, Ghiuchici AM, et al. Spleen and Liver Stiffness for Predicting High-Risk Varices in Patients with Compensated Liver Cirrhosis. Ultrasound Med Biol. 2021 Jan;47(1):76-83.
92. Song J, Huang J, Huang H, Liu S, Luo Y. Performance of spleen stiffness measurement in prediction of clinical significant portal hypertension: A meta-analysis. Clin Res Hepatol Gastroenterol. 2018 Jun;42(3):216-226.
93. Singh S, Eaton JE, Murad MH, Tanaka H, Iijima H, Talwalkar JA. Accuracy of spleen stiffness measurement in detection of esophageal varices in patients with chronic liver disease: Systematic review and meta-analysis. Clinical Gastroenterology and Hepatology. 2014;12(6):935-45e4
94. Wang QB, Zhu H, Liu HL, Zhang B. Performance of magnetic resonance elastography and diffusion-weighted imaging for the staging of hepatic fibrosis: A meta-analysis. Hepatology. 2012;56(1):239-247
95. Singh S, Venkatesh SK, Wang Z, Miller FH, Motosugi U, Low RN, et al. Diagnostic performance of magnetic resonance elastography in staging liver fibrosis: a systematic review and meta-analysis of individual participant data. Clin Gastroenterol Hepatol. 2015 Mar;13(3):440-451.e6.

96. Friedrich-Rust M, Poynard T, Castera L. Critical comparison of elastography methods to assess chronic liver disease. Nature Reviews Gastroenterology & Hepatology. 2016;13(7):402-411
97. European Association for the Study of the Liver. EASL clinical practice guidelines on non-invasive tests for evaluation of liver disease severity and prognosis. Journal of Hepatology. 2021;75(3):659-689
98. Wagner M, Hectors S, Bane O, Gordic S, Kennedy P, Besa C, et al. Noninvasive prediction of portal pressure with MR elastography and DCE-MRI of the liver and spleen: Preliminary results. J Magn Reson Imaging. 2018 Oct;48(4):1091-1103.
99. Jhang ZE, Wu KL, Chen CB, Chen YL, Lin PY, Chou CT. Diagnostic value of spleen stiffness by magnetic resonance elastography for prediction of esophageal varices in cirrhotic patients. Abdominal Radiology (NY). 2021;46(2):526-533
100. Abe H, Midorikawa Y, Matsumoto N, Moriyama M, Shibutani K, Okada M, et al. Prediction of esophageal varices by liver and spleen MR elastography. Eur Radiol. 2019 Dec;29(12):6611-6619.
101. Hoffman DH, Ayoola A, Nickel D, Han F, Chandarana H, Babb J, et al. MR elastography, T1 and T2 relaxometry of liver: role in noninvasive assessment of liver function and portal hypertension. Abdom Radiol (NY). 2020 Sep;45(9):2680-2687.
102. Singh R, Wilson MP, Katlariwala P, Murad MH, McInnes MDF, Low G. Accuracy of liver and spleen stiffness on magnetic resonance elastography for detecting portal hypertension: A systematic review and meta-analysis. European Journal of Gastroenterology & Hepatology. 2021;32(2):237-245

12. Point of Care Ultrasound (PoCUS) in Hepatology: when to use it and how to use it?

Ioan Sporea, Roxana Șirli

Abstract

Point-of-care ultrasound (PoCUS) has become a cornerstone diagnostic modality in modern hepatology. It allows rapid, bedside evaluation of liver morphology, steatosis, fibrosis, inflammation, portal hypertension, and focal liver lesions. The integration of B-mode ultrasound, Doppler techniques, Fatty Quantification, Shear-Wave Elastography (SWE), Contrast-Enhanced Ultrasound (CEUS) into Multiparametric Ultrasound (MPUS), transformed ultrasound into a comprehensive non-invasive imaging platform.

12.1. Introduction

Ultrasound has evolved from a simple anatomical imaging tool into an advanced, multiparametric diagnostic method. In hepatology, PoCUS offers unique advantages, because liver diseases often requires dynamic bedside assessment. PoCUS allows hepatologists to immediately evaluate the liver morphology in case of abnormal liver tests, to screen for cirrhosis complications, to find liver focal lesions and to characterize them (1). Its safety, portability, repeatability, and low cost make it superior to CT or MRI for routine longitudinal evaluation. The introduction of ultrasound based elastography and CEUS (Contrast Enhanced Ultrasound) further broadened its capabilities.

12.2. Evolution of PoCUS in Hepatology

The acceptance of ultrasound performed by clinicians, rather than radiologists, in several countries (such as Germany, Italy, Japan or Romania) accelerated the evolution of PoCUS. Modern ultrasound systems now incorporate Doppler, fatty quantification, real-time shear-wave elastography, microvascular flow imaging, CEUS into a single platform. Multiparametric ultrasound (MPUS) parallels multiparametric MRI by combining morphological, vascular, and tissue property evaluation. AI-driven analysis enhances lesions detection and fibrosis and steatosis quantification.

12.3. Technique of Liver Ultrasound

High-quality PoCUS requires standardized methodology. The operator must assess liver size, contour, parenchymal texture, echogenicity, vascular structures, spleen size and structure, and presence of ascites. Multiple sections in transverse, longitudinal, oblique subcostal or intercostal sections are needed. The substantial advantage of ultrasound examination is that it is a real time technique and every section is possible. The entire liver must be screened to be sure that no mass is missed during examination. A good ultrasound window is necessary and, of course, a good personal experience of the examiner (but this can be obtained through daily use of ultrasound for clinical practice).

Key B-Mode Assessment Components

B-mode ultrasound provides fundamental morphological information. Critical components include: parenchymal homogeneity, surface smoothness or nodularity, echogenicity relative to the kidney (for fatty quantification), caudate and quadrate lobe sizes, portal vein diameter and flow (with Doppler), spleen size and echotexture, the presence of ascites and its volume, the presence of focal liver lesions (FLL).

12.4. Diffuse Liver Diseases

Diffuse liver diseases encompass steatosis, fibrosis, and cirrhosis. PoCUS is the first-line imaging modality for each of these conditions. Its ability to non-invasively quantify steatosis and fibrosis by using new techniques such as quantitative ultrasound for steatosis (QUS) and ultrasound based elastography for fibrosis, has reduced the need for biopsy for staging MASLD and viral hepatitis (2).

12.4.1. Steatosis Assessment

Standard ultrasound is highly accurate for detecting moderate-to-severe steatosis, reaching 84.8% sensitivity and 93.6% specificity as compared to liver biopsy (3). Increased echogenicity, posterior attenuation, and vessel blurring are hallmark signs. Quantitative ultrasound methods (QUS), allow reliable grading of steatosis. More details in the dedicated chapter.

12.4.2. Fibrosis Assessment

Elastography has transformed the staging of fibrosis. Shear Wave Elastography (SWE) including VCTE (Vibration Controlled Transient Elastography), pSWE (uni-dimensional), and 2D-SWE (bi-dimensional) (ARFI-

based methods for last two) correlate strongly with histologic fibrosis. Meta-analyses calculated AUROCs above 0.85 for detecting significant fibrosis (F2) (4) and more for liver cirrhosis. The “Rule of 5” (VCTE) and “Rule of 4” (ARFI-based methods) guide interpretation (5-7). Liver stiffness values higher than 12–15 kPa suggest advanced fibrosis, while values higher than 20–25 kPa suggest portal hypertension ((in VCTE). Elastography reduces the need for liver biopsy in MASLD, HBV, HCV, and alcohol-associated liver disease.

12.4.3. Multiparametric Ultrasound (MPUS)

MPUS in chronic liver diseases refers to combining Attenuation coefficient or quantitative ultrasound (QUS) for steatosis evaluation, Shear-wave elastography for fibrosis assessment and Shear-wave dispersion to assess the viscoelastic properties of liver tissue as markers of inflammation. This results in a comprehensive noninvasive tissue characterization, improving detection of MASH (Metabolic Associated Steato-hepatitis) and clinically significant fibrosis.

Important steps have been made in the last few years for the evaluation by ultrasound of the viscoelastic properties of the liver as markers of inflammation, and it was demonstrated that Dispersion slope correlates with hepatic inflammation in MASLD (8). Semiquantitative steatosis quantification is possible with standard ultrasound liver examination, while QUS (quantitative ultrasound) allows a more precise assessment of liver fat content (9, 10). Liver stiffness assessment by SWE as a marker of fibrosis is a “normality” in every hepatology department, while spleen stiffness assessment is useful when portal hypertension is suspected (or combination of liver and spleen elastography).

12.5. Portal Hypertension

B-mode ultrasound identifies key features of portal hypertension, including splenomegaly (>12-13 cm), portal vein dilation (>13–14 mm), recanalized umbilical vein, ascites and hepato-fugal flow by Doppler. Elastography also contributes significantly for predicting portal hypertension: in VCTE, liver stiffness >25 kPa and spleen stiffness >40 kPa strongly predict clinically significant portal hypertension (CSPH) (6), allowing safe avoidance of screening endoscopy in many patients.

12.6. Focal Liver Lesions

PoCUS is valuable for identifying Focal Liver Lesions (FLL). B-mode is a good method to detect most lesions (especially hyperechoic or hypoechoic ones, more difficult for isoechoic lesions), but may not always allow their characterization. Doppler ultrasound assessment helps to distinguish hypervascular lesions, especially focal nodular hyperplasia (FNH). Elastography can measure FLL's stiffness, to calculate a ratio between the lesion and the rest of the liver. However, CEUS provides the highest accuracy for FLL's characterization, with sensitivity and specificity often exceeding 90% (9,10).

CEUS Enhancement Patterns

CEUS provides real-time perfusion imaging which allows an accurate diagnosis for several types of FLL:

- Hemangioma: peripheral nodular centripetal slow arterial enhancement without washout in the portal and late phases.
- Focal Nodular Hyperplasia (FNH): very rapid arterial centrifugal enhancement, with a spoke-wheel pattern and no washout in the portal and late phases.
- Hepatocellular carcinoma (HCC): arterial hyperenhancement with late or very late washout.
- Metastases: rim or diffuse arterial enhancement, with early washout.

CEUS is comparable to CT/MRI for many indications and is especially valuable in cirrhotic livers when CT/MRI may be equivocal (10) and in patients with incidentally found FLL (11).

12.7. One-Stop-Shop Hepatology

Modern ultrasound systems allow clinicians to completely evaluate the liver in a single session: morphology, Doppler, microflow, fat quantification (QUS), elastography, CEUS, and interventional guidance (1, 4, 12-14). This reduces radiation exposure (like in CT), costs, and diagnostic delays. It is ideal too for biannual screening for HCC in patients with advanced chronic liver disease (15, 16).

12.8. When to Use PoCUS

Indications include patients with abnormal liver enzymes, with suspected MASLD/MASH (patients with overweight or obesity, metabolic syndrome, type 2 diabetes or dyslipidemia), patients with chronic viral hepatitis

or alcohol-associated liver disease (ALD), for portal hypertension assessment, in patients with ascites, for HCC screening and surveillance, as well as in emergency settings: acute abdominal pain, suspected portal thrombosis.

Very recently (17), in a paper published in Clinical Gastroenterology and Hepatology in 2025, American authors underline the role of PoCUS in Hepatology and Gastroenterology. For Hepatology, ultrasound was recommended for ascites and hepatic hydrothorax assessment, for steatosis and fibrosis quantification and for HCC screening programs. This is a new concept in American Hepatology, stating that PoCUS should be a method used by clinicians.

12.9. Practical Recommendations for Liver PoCUS

Practical recommendations:

- Convex multifrequency probes (1–6 MHz) should be generally used, but linear high frequency probes should be used when necessary (superficial structures, liver surface assessment, others).
- Optimize depth, gain, and harmonics for an optimal US image.
- For accurate elastographic measurements, the patient should be fasting for at least 3 hours; vessels, FLLs should be avoided during acquisition; 5-10 LSMs should be obtained with an IQR/Median less than 30%.
- For CEUS: evaluate arterial, portal, late phases; avoid deep lesions >12 cm depth.
- Document all measurements and save cine loops.

12.10. Conclusion

PoCUS is now a core competency in Hepatology (18,19). It enables real-time, non-invasive evaluation of diffuse liver disease, of portal hypertension, and of FLL. With CEUS, and MPUS, PoCUS rivals with more expensive imaging modalities for many indications.

References

1. Sporea I. Ultrasound: “one stop shop” in hepatology. Med Ultrason 2016;18:143-144.
2. Peltec A, Sporea I. Multiparametric ultrasound as a new concept of assessment of liver tissue damage. World J Gastroenterol. 2024 Mar 28;30(12):1663-1669.

3. Hernaez R, Lazo M, Bonekamp S, Kamel I, Brancati FL, Guallar E, et al. Diagnostic accuracy and reliability of ultrasonography for the detection of fatty liver: a meta-analysis. Hepatology. 2011 Sep 2;54(3):1082-1090.
4. Dietrich CF, Bamber J, Berzigotti A, Bota S, Cantisani V, Castera L, et al. EFSUMB Guidelines and Recommendations on the Clinical Use of Liver Ultrasound Elastography, Update 2017 (Short Version). Ultraschall Med. 2017 Aug;38(4):377-394.
5. de Franchis R; Baveno VI Faculty. Expanding consensus in portal hypertension: Report of the Baveno VI Consensus Workshop: Stratifying risk and individualizing care for portal hypertension. J Hepatol. 2015 Sep;63(3):743-52.
6. de Franchis R, Bosch J, Garcia-Tsao G, Reiberger T, Ripoll C; Baveno VII Faculty. Baveno VII - Renewing consensus in portal hypertension. J Hepatol. 2022 Apr;76(4):959-974. Erratum in: J Hepatol. 2022 Jul;77(1):271.
7. Barr RG, Wilson SR, Rubens D, Garcia-Tsao G, Ferraioli G. Update to the Society of Radiologists in Ultrasound Liver Elastography Consensus Statement. Radiology. 2020 Aug;296(2):263-274.
8. Sugimoto K, Moriyasu F, Oshiro H, Takeuchi H, Abe M, Yoshimasu Y, et al. The Role of Multiparametric US of the Liver for the Evaluation of Nonalcoholic Steatohepatitis. Radiology. 2020 Sep;296(3):532-540.
9. Friedrich-Rust M, Klopffleisch T, Nierhoff J, Herrmann E, Vermehren J, Schneider MD, et al. Contrast-Enhanced Ultrasound for the differentiation of benign and malignant focal liver lesions: a meta-analysis. Liver Int. 2013 May;33(5):739-55.
10. Xie L, Guang Y, Ding H, Cai A, Huang Y. Diagnostic value of contrast-enhanced ultrasound, computed tomography and magnetic resonance imaging for focal liver lesions: a meta-analysis. Ultrasound Med Biol. 2011 Jun;37(6):854-61.
11. Şirli R, Popescu A, Jenssen C, Möller K, Lim A, Dong Y, et al. WFUMB Review Paper. Incidental Findings in Otherwise Healthy Subjects, How to Manage: Liver. Cancers (Basel). 2024 Aug 21;16(16):2908.
12. European Association for Study of Liver; Asociacion Latinoamericana para el Estudio del Higado. EASL-ALEH Clinical Practice Guidelines: Non-invasive tests for evaluation of liver disease severity and prognosis. J Hepatol. 2015 Jul;63(1):237-64.
13. Eddowes PJ, Sasso M, Allison M, Tsochatzis E, Anstee QM, Sheridan D, et al. Accuracy of FibroScan Controlled Attenuation Parameter and Liver Stiffness Measurement in Assessing Steatosis and Fibrosis in Patients With Nonalcoholic Fatty Liver Disease. Gastroenterology. 2019 May;156(6):1717-1730.
14. Fujiwara Y, Kuroda H, Abe T, Ishida K, Oguri T, Noguchi S, et al. The B-Mode Image-Guided Ultrasound Attenuation Parameter Accurately Detects Hepatic Steatosis in Chronic Liver Disease. Ultrasound Med Biol. 2018 Nov;44(11):2223-2232.
15. Gu W, de Lédinghen V, Aubé C, Krag A, Strassburg C, Castéra L, et al. Hepatocellular Cancer Surveillance in Patients with Advanced Chronic Liver Disease. NEJM Evid. 2024 Nov;3(11):EVIDoa2400062.

16. Dănilă M, Sporea I. Ultrasound screening for hepatocellular carcinoma in patients with advanced liver fibrosis. An overview. Med Ultrason. 2014 Jun;16(2):139-44.
17. Shankar N, Kuo L, Krugliak Cleveland N, Galen B, Samel NS, et al. Point-of-Care Ultrasound in Gastroenterology and Hepatology. Clin Gastroenterol Hepatol. 2025 Jul;23(8):1277-1290.
18. Sporea I. Point of care or clinical ultrasound? Med Ultrason. 2012 Mar;14(1):3-4.
19. Popescu A, Bende F, Sirli R, Sporea I. Redefining Diagnosis and Management in Hepatology with Multiparametric Ultrasound. EMJ Hepatol. 2025;13(1):66-75.

13. Handheld ultrasound devices: How to Use Them?

Alina Popescu, Tudor Moga

Abstract

Handheld ultrasound devices (HHUSDs) have accelerated the clinical adoption of point-of-care ultrasound (POCUS), enabling ultrasound to be performed at the bedside and interpreted immediately by the treating clinician. HHUSDs are excellent for *binary or rule-in/rule-out bedside questions*, but they should trigger timely referral to comprehensive ultrasound when a finding needs full characterization. They are best viewed as ***extensions of bedside examination*** that answer focused, time-sensitive clinical questions. When used within clearly defined indications, with appropriate training and hygiene measures, they can improve workflow and access.

13.1. Introduction

Handheld ultrasound devices (HHUSDs) have accelerated the clinical adoption of point-of-care ultrasound (POCUS), enabling ultrasound to be performed at the bedside and interpreted immediately by the treating clinician (1). This paradigm improves speed of decision-making and may broaden access to imaging, but HHUSDs must be used with a clear understanding of their purpose: focused clinical questions, not comprehensive imaging.

International statements consistently emphasize that POCUS/handheld ultrasound does not replace a full diagnostic ultrasound examination performed on high-end systems when the clinical scenario requires detailed characterrization or when findings may change management substantially (2-4).

Currently, ultrasound represents a widely available, cost-effective, versatile, and non-invasive imaging modality that can enhance bedside patient evaluation when applied within the POCUS framework. Clinicians may perform focused examinations guided by clinical findings; although these do not replace comprehensive imaging studies, they support timely and cost-effective clinical decision-making.

Advances in digitization and device miniaturization over the past decade have led to the development of pocket-sized HHUSDs suitable for routine bedside use. This technological progress has prompted suggestions that HHUSDs could complement or potentially replace the traditional stethoscope.

In recent years, HHUSDs have further evolved through the integration of wireless transducers and Doppler capabilities (3, 5).

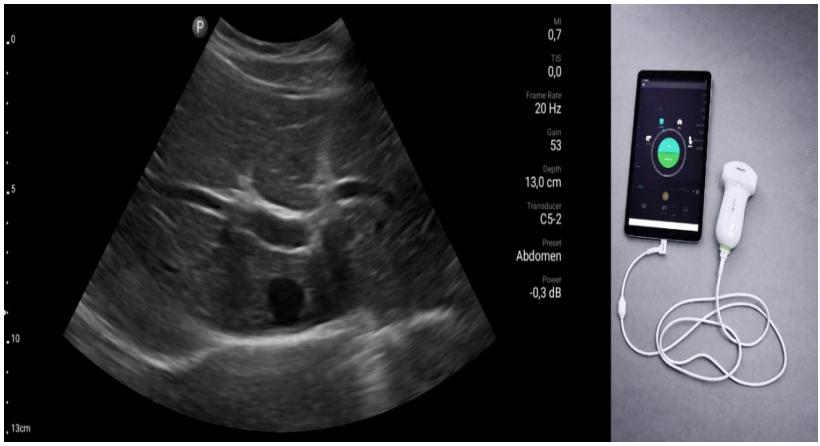


Fig. 13.1. Handheld ultrasound examination using the Philips Lumify system. Left: Right subcostal abdominal ultrasound image obtained with the Philips Lumify handheld ultrasound device, demonstrating liver parenchyma and vascular structures. Right: The Philips Lumify handheld ultrasound system, consisting of a portable probe connected to a tablet interface used for point-of-care imaging.

13.2. What handheld ultrasound devices can (and cannot) do (2, 6)

13.2.1 Typical capabilities

Most HHUSDs provide:

- B-mode imaging (Fig. 13.1, 13.2)
- Basic Doppler (color/power, sometimes PW Doppler depending on model)
- Simple measurements and image archiving/export (device- and platform-dependent)

13.2.2 Typical limitations

Compared with cart-based/high-end systems, HHUSDs often have:

- Lower overall imaging performance (especially in demanding patients and deep targets)
- Less sensitive Doppler for low-flow states
- Limited advanced applications (commonly no CEUS, no shear-wave elastography)

These limitations are repeatedly highlighted in society statements and performance evaluations, which show measurable reductions in imaging performance for abdominal and cardiac applications versus cart-based units (6).

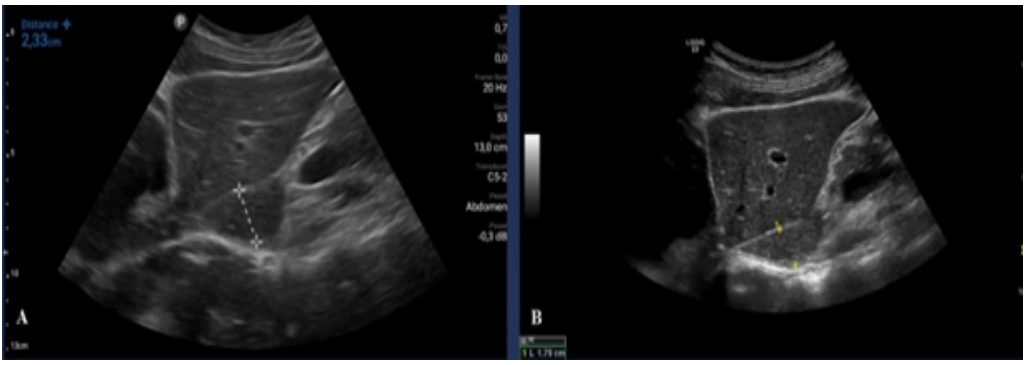


Fig. 13.2. Longitudinal section obtained in the epigastric region, demonstrating the caudate lobe of the liver. Comparison between handheld ultrasound device (HHUD) and high-end ultrasound system. Representative abdominal ultrasound images obtained with a handheld ultrasound device (A) and a high-end ultrasound system (B). The HHUD provides adequate visualization for rapid point-of-care assessment, while the high-end system offers higher resolution and improved image detail, supporting more precise diagnostic evaluation.

The immediate practical implication is that HHUSDs are excellent for *binary or rule-in/rule-out bedside questions*, but they should trigger timely referral to comprehensive ultrasound when a finding needs full characterization.

A useful way to define appropriate HHUSD use is: *"Will a focused answer change immediate bedside decisions?"* This aligns with WFUMB/EFSUMB positioning (2, 4).

13.3. Appropriate clinical indications (focus on GI/hepatology)

13.3.1. High-yield indications in gastroenterology/hepatology

Ascites

- Detection and semi-quantitative assessment
- Procedural support (e.g., paracentesis planning)

Biliary tract screening

- Gallbladder: stones/sludge (with caution in difficult habitus)
- Screening for biliary dilatation in jaundice

Gross liver and spleen assessment

- Hepatomegaly/splenomegaly
- Screening for obvious focal lesions (not characterization)

Aorta screening (where appropriate training exists)

- Rapid exclusion of major aneurysm patterns in symptomatic patients (system-dependent scope)

These are consistent with EFSUMB's abdominal HHUSD positioning and ESR's discussion of safe deployment and patient-safety boundaries (6).

13.3.2. Indications that require escalation to high-end ultrasound (7, 8)

Handheld findings should prompt comprehensive imaging when:

- A focal liver lesion is detected or suspected (need characterization pathways; often CEUS/MRI/CT depending)
- Vascular questions are critical (portal vein thrombosis, subtle flow changes)
- The patient is technically difficult (obesity, bowel gas, limited windows)
- Management depends on detailed staging/quantification

13.4. How to use handheld devices correctly: a practical workflow (1, 9)

13.4.1. Step 1 — Define a focused clinical question

Examples:

- "Is there free fluid (ascites)?"
- "Is the common bile duct clearly dilated?"
- "Is there a gross mass explaining palpable hepatomegaly?"

This approach is consistent with POCUS principles described by WFUMB (2).

13.4.2. Step 2 — Optimize the environment and patient position

- Light control (reduce glare on phone/tablet)
- Patient position changes (supine, left lateral, semi-erect) to improve acoustic windows
- Adequate gel and stable hand positioning (small devices magnify motion artifacts)

13.4.3. Step 3 — Choose probe/preset and actively optimize the image

Even with "auto" settings, actively adjust:

- Depth (do not scan "too deep" by default)
- Gain and time-gain compensation (if available)
- Focus position
- Doppler scale and wall filter when Doppler is used (avoid false negatives in low-flow states)

13.4.4. Step 4 — Scan systematically (avoid "one-window ultrasound")

Use a simple protocol:

- RUQ: liver surface, gallbladder, portal hilum, bile ducts (where visible)
- Perihepatic and pelvic windows for ascites
- Epigastric window for aorta (if within scope)
- Documentation: store representative stills/clips and key measurements

13.4.5. Step 5 — Interpret conservatively and integrate clinically

A central message from society documents: patient safety must not be compromised, and the user should recognize HHUSD boundaries (10).

The most common error is not a missed lesion—it is overconfidence after a technically limited scan. A "negative" HHUSD exam in a difficult patient should be documented as *limited* and escalated when clinical suspicion persists.

13.5. Evidence on performance vs. cart-based devices

Recent comparative work suggests handheld devices can achieve clinically meaningful accuracy in selected applications and contexts, but performance may vary by target organ, operator experience, and device generation (11).

- A randomized prospective comparison found **similar overall diagnostic accuracy** between handheld and cart-based POCUS across several exam types in a clinical setting, though exact sensitivity/specificity varied (10).
- Technical and imaging-performance assessments report **notable reductions** in imaging performance of HHUSDs versus cart-based systems, including abdominal imaging contexts—supporting the recommendation that HHUSDs be used for focused questions and appropriate triage rather than comprehensive diagnostics (12).
- More recent abdominal-focused research continues to examine diagnostic accuracy vs high-end scanners and emphasizes the ongoing need for conventional ultrasound training alongside HHUSD expansion (13).

13.6. Infection prevention and device hygiene (often underestimated)

Portable and handheld systems introduce additional surfaces (smartphones/tablets) into the patient-care environment. ESR emphasizes that portable devices must undergo **appropriate decontamination protocols** analogous to standard equipment to maintain patient safety (10).

13.7. Training, competency, and governance

Handheld ultrasound is highly operator-dependent, thus governance should include:

- Structured training and supervision
- Defined scopes of practice (what the operator is credentialed to answer)
- Documentation standards (images, interpretation, limitations)
- Quality assurance (peer review, correlation with definitive imaging)

The WFUMB position paper underscores variability in training and implementation and the need for structured teaching frameworks; WFUMB also addresses broader ultrasound education principles relevant to HHUSD adoption (2, 13).

13.8. Future directions

HHUSD development is moving toward AI-supported acquisition and interpretation, tele-ultrasound supervision, and improved portability-performance trade-offs. These trends may reduce barriers but will not remove the need for clinical reasoning, competency frameworks, and escalation pathways.

13.9. Conclusion

Handheld ultrasound devices are best viewed *as* ***extensions of bedside examination*** that answer focused, time-sensitive clinical questions. When used within clearly defined indications, with appropriate training and hygiene measures, they can improve workflow and access. Their limitations—particularly in image quality, Doppler sensitivity, and advanced characterization tools—justify a low threshold for referral to comprehensive ultrasound when findings are uncertain or clinically significant.

References

1. Moore CL, Copel JA. Point-of-care ultrasonography. N Engl J Med. 2011;364(8):749-57.
2. Dietrich CF, Goudie A, Chiorean L, Cui XW, Gilja OH, Dong Y, et al. Point of Care Ultrasound: A WFUMB Position Paper. Ultrasound Med Biol. 2017;43(1):49-58.
3. Herzog M, Arsova M, Matthes K, Husman J, Toppe D, Kober J, et al. Technical assessment of resolution of handheld ultrasound devices and clinical implications. Ultraschall Med. 2024;45(4):405-11.
4. Nürnberg D, Jenssen C, Lucius C, Klingenberg-Noftz R, Wüstner M, Worlicek H, et al. [Clinical Ultrasound (ClinUS) - Concepts and Controversies]. Z Gastroenterol. 2025;63(3):279-92.
5. Piscaglia F, Dietrich CF, Nolsoe C, Gilja OH, Gaitini D. Birth of „Echoscopy"– The EFSUMB Point of View. Ultraschall. 2013;34:92.
6. Nielsen MB, Cantisani V, Sidhu PS, Badea R, Batko T, Carlsen J, et al. The Use of Handheld Ultrasound Devices - An EFSUMB Position Paper. Ultraschall Med. 2019;40(1):30-9.
7. Merkel D, Züllich TF, Schneider C, Yousefzada M, Beer D, Ludwig M, et al. Prospective Comparison of Handheld Ultrasound Devices from Different Manufacturers with Respect to B-Scan Quality and Clinical Significance for Various Abdominal Sonography Questions. Diagnostics (Basel). 2023;13(24).
8. Blaivas M, Brannam L, Theodoro D. Ultrasound image quality comparison between an inexpensive handheld emergency department (ED) ultrasound machine and a large mobile ED ultrasound system. Acad Emerg Med. 2004;11(7):778-81.
9. Díaz-Gómez JL, Mayo PH, Koenig SJ. Point-of-Care Ultrasonography. N Engl J Med. 2021;385(17):1593-602.
10. ESR statement on portable ultrasound devices. Insights Imaging. 2019;10(1):89.
11. Rykkje A, Carlsen JF, Nielsen MB. Hand-Held Ultrasound Devices Compared with High-End Ultrasound Systems: A Systematic Review. Diagnostics (Basel). 2019;9(2).
12. Moran CM, McLeod C, Inglis S, Pye SD. An Assessment of the Imaging Performance of Hand-Held Ultrasound Scanners Using the Edinburgh Pipe Phantom. Ultrasound Med Biol. 2024;50(8):1178-82.
13. Segura-Grau A, Salcedo-Joven I, Montes-Belloso E, Cinza-Sanjurjo S, Segura-Fragoso A, Segura-Grau E. Usefulness of handheld ultrasound devices in the assessment of abdominal pathology and comparison with high-end ultrasound devices. Ultrasound J. 2025;17(1):38.

14. Comparison between Imaging Methods for Liver Evaluation

Durim Cela, Blerina Saraci, Denis Qirinxhi

Abstract

Imaging plays a fundamental role in the evaluation of liver diseases, providing non-invasive assessment of hepatic morphology, vascularization, and functional changes. Ultrasonography is the primary diagnostic method due to its accessibility, safety, and real-time capability, while Doppler and elastography enhance evaluation of hepatic hemodynamics and fibrosis.

Computed tomography offers high spatial resolution and multiphasic contrast imaging, making it valuable for trauma assessment, vascular pathology, and oncologic staging.

Magnetic resonance imaging provides superior soft-tissue contrast and multiparametric analysis, enabling accurate characterization of focal liver lesions and quantification of fat or iron deposition.

Nuclear medicine techniques add functional and metabolic information, particularly in oncologic evaluation.

Because each modality has specific strengths and limitations, optimal liver imaging requires a multimodal approach tailored to the clinical context.

14.1. Introduction

Imaging examinations play a central role in hepatology, as they provide a non-invasive, repeatable, and comprehensive evaluation of the hepatic parenchyma, biliary tract, and portal–systemic vasculature. In modern clinical practice, imaging is often the “first gateway” to diagnosis: it identifies steatosis, focal lesions, biliary dilatation, signs of portal hypertension, and complications of cirrhosis (ascites, splenomegaly, portosystemic collaterals), often before significant laboratory or clinical changes appear. Furthermore, imaging allows risk stratification and guides therapeutic decision-making, helping determine the need for biopsy, endoscopy, endoscopic intervention, or surgery.

Ultrasonography remains the basic method due to its accessibility and safety, but the integration of advanced techniques such as Doppler for hepatic hemodynamics, elastography for non-invasive fibrosis assessment, contrast-enhanced CT, and multiparametric MRI for lesion characterization and disease staging has significantly increased diagnostic accuracy. In biliary and pancreatic

pathology, MRCP provides detailed anatomical mapping without radiation, while procedures such as ERCP retain a specific role when diagnosis is combined with treatment.

In the context of cirrhosis, imaging is essential for screening and early detection of hepatocellular carcinoma and for monitoring treatment response. Thus, imaging examinations are not only diagnostic tools but also strategic instruments for monitoring, prognosis, and personalized management of the hepatology patient.

14.2. Liver Ultrasonography

14.2.1. Principles and Techniques

Ultrasound is a coherent mechanical vibration with high frequency (2–20 MHz in diagnostic applications) that propagates in tissues as longitudinal waves with sequences of compression and rarefaction. It is generated by piezoelectric crystals, mainly lead zirconate titanate (PZT), which deform under electrical voltage and, reciprocally, produce electrical signals when struck by the reflected wave. The crystal, polarized above the Curie point and equipped with electrodes, matching layers, and focusing elements, constitutes the transducer. Resonance frequency is determined by crystal thickness; thinner crystals produce higher frequencies and better resolution but with more limited penetration. Propagation in tissues at an average speed of 1540 m/s allows depth calculation according to the formula $f = c/\lambda$, while attenuation increases with frequency (approximately 1 dB/cm/MHz in soft tissues). Reflection occurs at any interface with a change in acoustic impedance; in soft tissues it is partial, while at tissue–gas or tissue–bone interfaces it is almost total, creating acoustic shadowing. Echoes may be specular (from smooth surfaces) or scattered (from parenchyma). Under nonlinear conditions, harmonics are generated and exploited in harmonic imaging to increase contrast and reduce noise.

14.2.2. Ultrasound Methods

Imaging is based on the pulse–echo principle, where depth is determined by the time between pulse emission and echo return. A-scan displays echo amplitude in one dimension; M-mode shows depth as a function of time and is particularly used for evaluating rapid cardiac motion; B-mode (grayscale) forms a two-dimensional tomographic image by displaying echo intensity as shades of gray and represents the basic clinical modality. Beam

steering is achieved mechanically (single rotating element transducer, mainly in intracavitary applications) or electronically with phased arrays, where very small-time delays between elements create interference patterns that steer and focus the beam. Linear arrays produce a rectangular image suitable for superficial structures, while sector arrays provide a triangular field of view with minimal skin contact. Pulse repetition frequency is limited by the need to avoid range ambiguity; typically, around 1000 pulses/s, with a compromise between depth, line density, and frame rate.

Resolution. Axial resolution depends on pulse length and improves with shorter pulses and higher frequencies. Lateral resolution is determined by beam width and controlled by larger aperture and mechanical or electronic focusing. Near and far fields define the optimal focal zone; dynamic focusing during reception allows continuous optimization of resolution at different depths. However, the real beam is not ideal: its bell-shaped profile, side lobes, and far-field divergence limit spatial and contrast resolution, especially outside the imaging plane (azimuthal direction), where control is more limited in one-dimensional probes.

Artifacts. Artifacts arise when assumptions of linear propagation and constant speed are violated. Speed differences in fat (lower than in soft tissues) or silicone cause depth overestimation and distortion of deep structures. Refraction at tissue–fat interfaces may create duplicate images. Beam scattering and defocusing in heterogeneous tissues reduce contrast, partially mitigated by harmonic imaging. Multiple reflections produce false parallel images; gas collections, calcifications, or foreign bodies generate the “comet-tail” artifact. Mirror-image artifact occurs when the wave is deflected by an oblique reflector and returns along an alternative path, displaying structures deeper than their real position. These limitations represent significant challenges in clinical interpretation and modern transducer design.

Advantages of Ultrasonography. Ultrasonography represents the basic method in liver imaging evaluation due to its safety, accessibility, and ability to provide real-time information. The absence of ionizing radiation makes it suitable for repeated examinations, screening, and long-term follow-up, including sensitive populations such as pregnant women and pediatric patients. It enables assessment of liver size, contours, and parenchymal echotexture,

effectively identifying diffuse pathologies such as steatosis and cirrhosis, as well as indirect signs of portal hypertension.

Integration of Doppler significantly expands diagnostic value by enabling hemodynamic analysis of the portal vein, hepatic veins, and hepatic artery, important in portal vein thrombosis, Budd–Chiari syndrome, and portosystemic shunts. Elastography has added a quantitative dimension, providing non-invasive fibrosis assessment. In focal lesions, ultrasonography is the first detection method, while contrast-enhanced ultrasound (CEUS) allows dynamic perfusion analysis and aids benign–malignant differentiation. For these reasons, it remains a central tool in modern hepatology practice.

Clinical Applications. Abdominal ultrasonography is widely used to examine the liver and surrounding structures, offering comprehensive morphological and vascular evaluation. It enables identification of normal anatomy, including portal vein branching, hepatic veins, and their relationship with the inferior vena cava. Recognition of anatomical variants is essential to avoid diagnostic errors, especially in the context of living donor liver transplantation.

Normally, the hepatic parenchyma is homogeneous and slightly more hyperechoic than the renal cortex. Portal flow is continuous and antegrade, while hepatic vein flow reflects cardiac cycle variations.

Hepatic steatosis, the most common diffuse pathology, manifests with increased echogenicity and reduced deep vascular visualization. However, these findings require clinical correlation due to overlap with fibrosis. In cirrhosis, ultrasonography shows nodular contour, heterogeneous texture, and signs of portal hypertension, while Doppler demonstrates reduced portal flow velocity and, in advanced stages, hepatofugal flow.

Portal hypertension is assessed by analyzing flow direction and velocity and identifying portosystemic collaterals. Portal vein thrombosis is primarily diagnosed by absence of Doppler signal within the lumen, distinguishing acute from chronic phases. In Budd–Chiari syndrome, ultrasound may reveal thrombosis or indirect signs of hepatic venous obstruction.

The method is also useful in identifying portal gas or pneumobilia and differentiating them, as well as in evaluating benign cystic lesions. Simple cysts appear as typical anechoic structures with posterior enhancement, whereas abscesses show dynamic evolution and may be treated under ultrasound guidance.

Limitations of Ultrasonography. Although it is a first-line method, ultrasonography has significant limitations. It is highly operator-dependent and influenced by technical quality. Limited acoustic penetration, particularly in obese patients or those with intestinal gas, may reduce sensitivity for small lesions or deep structures.

In diffuse diseases, it is more sensitive for advanced stages than early ones; mild steatosis and early fibrosis may be indistinguishable. In focal lesions, specificity is limited, as many benign and malignant entities have overlapping B-mode appearances, requiring confirmation with CT or MRI. Although CEUS improves characterization, its availability is not universal.

14.2.3. Doppler Ultrasound

Doppler is an essential component of liver examination, providing information on direction, velocity, and character of blood flow. Spectral Doppler graphically displays velocity changes over time, while color Doppler visualizes flow distribution and direction within the 2D image. Both modalities are used complementarily.

Under physiological conditions, portal flow is continuous and low resistance, whereas arterial flow reflects distal vascular bed resistance. Doppler is crucial in diagnosing stenosis, thrombosis, and hemodynamic disorders of portal hypertension. Accurate interpretation requires attention to insonation angle, sample volume placement, and technical parameters, as errors may lead to over- or underestimation of velocities.

Artifacts such as aliasing, inappropriate filtering of low-frequency signals, and inclusion of more than one vessel in the sample volume may create false hemodynamic patterns. In color Doppler, color reversal often represents a technical limitation rather than true reversed flow. Awareness of these pitfalls is essential for correct clinical interpretation.

14.2.4. Elastography

Elastography has transformed the assessment of hepatic fibrosis by providing a non-invasive method to measure parenchymal stiffness. It complements conventional ultrasonography, which focuses on morphology, by adding functional information directly related to fibrosis severity.

The method is widely used in chronic viral hepatitis, non-alcoholic fatty liver disease, and monitoring of cirrhotic patients. It enables staging, therapeutic follow-up, and prognostic evaluation, reducing the need for

repeated biopsies. In cirrhosis, high stiffness values correlate with the risk of portal hypertension and complications, making elastography an essential component of the modern hepatologic diagnostic algorithm.

14.3. Computed Tomography (CT)

14.3.1. Principles and Techniques

CT is an X-ray–based imaging modality that creates axial slices and volumetric 3D datasets of the body. Tissue density is expressed in Hounsfield units (HU), with water = 0, air ≈ −1000, and bone having high positive values. Modern systems are helical and multidetector (MDCT), allowing rapid acquisition and multiplanar reconstructions (MPR, MIP, VR). Image reconstruction is performed using filtered back projection (FBP) or iterative algorithms, the latter reducing noise and radiation dose.

Image quality depends on resolution, noise, and artifacts; noise is inversely related to dose and slice thickness. The use of iodinated contrast significantly increases diagnostic value but requires evaluation of renal function, allergy history, and thyroid status; complications range from mild reactions to rare serious emergencies.

Protocol optimization is guided by the clinical indication and the ALARA principle, limiting unnecessary phases to reduce radiation exposure. Interpretation is based on density analysis (HU), partial volume effect, and relationships with surrounding structures. CT is also widely used for image-guided interventions (biopsy, drainage, ablation).

Advanced techniques include cardiac CT with ECG synchronization, dual-energy CT for material characterization and iodine mapping, and CT perfusion for hemodynamic assessment, particularly in stroke and oncology.

Intravenous Contrast Administration

Iodinated contrast media are essential for multiphasic CT examinations, including:

- Arterial phase
- Portal venous phase
- Delayed phase

These phases allow optimal evaluation of vascular structures, parenchymal enhancement patterns, and lesion characterization.

Pre-Contrast Evaluation

Prior to contrast administration, the following factors must be assessed:

- History of allergic reactions
- Renal function (serum creatinine, eGFR)
- Presence of thyroid disease
- Use of metformin

Contrast-Related Complications

Extravasation requires immediate cessation of contrast injection, elevation of the affected limb, and clinical monitoring.

Systemic reactions may range from mild manifestations, such as urticaria, to severe and potentially life-threatening reactions, including laryngeal edema and hypotension.

14.3.2. Advantages of Computed Tomography (CT)

CT is a central modality in hepatic diagnostics due to its high anatomical resolution, rapid acquisition, and the possibility of multiphasic contrast studies. It accurately depicts hepatic morphology (segmental atrophy/hypertrophy, capsular deformities, signs of cirrhosis) and is well suited for longitudinal follow-up due to high reproducibility.

Dynamic arterial–portal–delayed imaging enables non-invasive characterization of focal lesions according to enhancement pattern (e.g., hepatocellular carcinoma with arterial enhancement and delayed washout; metastases typically hypovascular in the portal phase). CT evaluates pre-contrast density (fat, blood, calcifications), aiding benign/malignant differentiation.

In hepatic trauma, CT is the method of choice for identifying lacerations, hematomas, and active hemorrhage, guiding management. CT angiography clearly demonstrates hepatic arteries and the portal system, diagnosing thrombosis, stenosis, and portal hypertension collaterals.

It plays a key role in tumor staging, assessment of vascular involvement, and therapeutic planning (surgery, ablation, systemic therapy, transplantation), as well as in monitoring treatment response. Wide availability, protocol standardization, and modern dose reduction make CT a practical and reliable modality in daily clinical practice.

14.3.3. Clinical Applications of Computed Tomography (CT)

CT is widely used in hepatic pathology due to high anatomical resolution, multiphasic contrast evaluation, and global abdominal assessment. It is particularly indicated when ultrasound is limited, when precise lesion characterization or vascular assessment is required, for oncologic staging, or in emergency situations.

In diffuse steatosis, CT evaluates reduced parenchymal density on non-contrast studies (loss of liver–spleen attenuation difference), but quantification is limited by factors such as fibrosis or metal deposition. In cirrhosis, CT documents nodular contour, segmental volume changes, and signs of portal hypertension (ascites, collaterals), although it is insensitive to early fibrosis. In viral hepatitis, its role is mainly for complication assessment and exclusion of obstructive pathology.

In iron overload (e.g., hemochromatosis), CT may show increased hepatic attenuation, but this finding is not specific. In Wilson's disease, CT mainly demonstrates structural consequences (cirrhosis), without direct characteristic signs.

In non-neoplastic focal lesions, CT is highly sensitive for calcifications and gas (pneumobilia, portal gas, abscess). Simple cysts appear hypodense without enhancement; in hydatid disease, calcifications and daughter cysts are assessed. Abscess typically shows rim enhancement but requires clinical correlation to differentiate from necrotic metastases.

In oncology, CT is essential for detection, characterization, and staging. Metastases are usually hypodense in the portal phase; some hypervascular metastases are better seen in the arterial phase. Hepatocellular carcinoma presents arterial enhancement with delayed washout; CT also evaluates vascular invasion (e.g., portal tumor thrombus).

In vascular pathology, CT diagnoses portal vein thrombosis, arterioportal shunts, and Budd–Chiari syndrome, demonstrating parenchymal congestion and volumetric changes. In hepatic trauma, CT is the method of choice for identifying lacerations, hematomas, and active bleeding, as well as for follow-up of complications.

Finally, CT is used in interventional procedures (biopsy, drainage) when precise anatomical guidance is required. Overall, CT remains a key modality in the diagnosis and management of liver diseases, particularly in emergency and oncologic contexts.

14.3.4. Limitations of Computed Tomography (CT)

Although CT is fundamental in hepatic imaging, it has important diagnostic and practical limitations. The main limitation is low sensitivity to early microscopic changes (early fibrosis, chronic hepatitis without cirrhosis), where examination may appear normal despite clinically relevant disease.

In steatosis, non-contrast densitometric evaluation is indicative but not precise, as it is influenced by fibrosis, iron deposition, medications, and perfusion changes. Coexistence of steatosis and fibrosis further limits reliable quantification.

CT has limited sensitivity for very small lesions (<3–5 mm) and often cannot reliably differentiate regenerative nodules, biliary hamartomas, or microscopic metastases. Enhancement patterns may overlap between benign and malignant pathologies (e.g., abscess vs necrotic metastasis), requiring clinical correlation or additional imaging. In cirrhotic liver, early detection of hepatocellular carcinoma remains challenging due to parenchymal heterogeneity and atypical vascularization.

CT is primarily an anatomical modality and provides limited functional information (it does not directly assess hepatocellular function or biliary flow), restricting differentiation of some pathologies with similar architecture.

A significant practical limitation is exposure to ionizing radiation, especially in frequent follow-up (cirrhosis, oncology, pediatrics), particularly with multiphasic protocols. Additionally, iodinated contrast may be contraindicated in renal insufficiency or allergy, reducing diagnostic value.

In interventional procedures, CT is less flexible than ultrasound due to lack of continuous real-time imaging and dependence on breath-holding; CT fluoroscopy improves guidance but increases radiation dose.

In summary, CT remains a powerful modality, but with limitations in early diagnosis, characterization of very small lesions, functional assessment, and radiation exposure considerations.

14.4. Magnetic Resonance Imaging (MRI)

14.4.1. Principles and Techniques of MRI

MRI is based on the resonance of nuclei with “spin” (primarily the hydrogen proton) within a static magnetic field (B0). Protons behave as magnetic dipoles; within B0 they become polarized and process at the Larmor frequency ($\omega 0 = \gamma B0$). Application of a radiofrequency (RF) pulse at this frequency excites them (flip angle), creating detectable transverse

magnetization. The return to equilibrium generates signal through T1 relaxation (spin–lattice, longitudinal recovery) and T2 relaxation (spin–spin, transverse dephasing); T2* additionally incorporates magnetic field inhomogeneities.

Image formation requires spatial encoding using gradients (slice selection, frequency encoding, and phase encoding) and reconstruction via Fourier transformation from k-space. The parameters TR (repetition time) and TE (echo time) determine image weighting:

- T1-weighted (short TR/TE)
- T2-weighted (long TR/TE)
- PD-weighted (long TR, short TE)

Main sequences include:

- Spin-echo (SE) and Fast/Turbo SE (FSE/TSE) for stable T2 contrast
- Gradient-echo (GRE) for rapid acquisition and T2* weighting
- Inversion recovery (IR) for selective signal suppression (e.g., fat/fluid)
- 2D and 3D acquisitions (isotropic voxels, multiplanar reconstructions)
- Rapid techniques such as echo planar imaging for high temporal resolution and diffusion imaging

MRI contrast depends on proton density, T1, T2/T2*, magnetic susceptibility, and the chemical shift phenomenon (water/fat separation, in-phase/out-of-phase imaging). Gadolinium-based agents primarily shorten T1 relaxation and enable dynamic perfusion studies and MR angiography.

The MRI system consists of a superconducting magnet (typically 1.5–3T), gradient coils for spatial encoding, and transmitting/receiving RF coils. Increasing B0 improves the signal-to-noise ratio but also increases susceptibility artifacts and homogeneity challenges.

Advanced techniques include MR angiography (time-of-flight, phase-contrast, contrast-enhanced), perfusion imaging (dynamic T1/T2*), and diffusion-weighted imaging (DWI) with ADC maps, which assess microscopic water motion and assist in identifying diffusion restriction.

In essence, MRI provides superior soft-tissue contrast and extensive technical flexibility through manipulation of physical parameters and pulse sequences.

14.4.2. Advantages of Using MRI in Liver Examination

MRI plays a central role in liver evaluation because it provides high soft-tissue contrast without ionizing radiation and enables multiple contrast mechanisms (T1, T2, T2*, proton density, diffusion, perfusion). This makes it

particularly valuable for detection, characterization, and staging of liver diseases, with superior capability to identify subtle parenchymal changes and differentiate lesions according to composition (water, fat, blood, fibrosis, paramagnetic deposits), often without the need for invasive procedures.

Contrast Flexibility

By modifying sequence parameters:

- ***T2-weighted imaging*** increases sensitivity to processes with high water content (inflammation, edema, necrosis, cystic components).
- ***T1-weighted imaging*** assists in anatomical evaluation, identification of subacute hemorrhage, and dynamic post-contrast analysis.
- ***T2**** is useful for magnetic susceptibility phenomena (blood products, metal deposits), providing diagnostic information often not obtainable from radiation-based modalities.

Assessment of Fat and Intracellular Deposits

MRI exploits the chemical shift phenomenon and water/fat techniques (in-phase/out-of-phase, Dixon), making it the most reliable method for:

- Non-invasive confirmation and quantification of steatosis
- Monitoring NAFLD/NASH
- Differentiating focal fat from solid lesions

Similarly, through T2/T2* analysis, MRI provides information on metallic deposits and their effects on the parenchyma (relevant in certain metabolic diseases or after multiple transfusions).

Functional Information – Diffusion

Diffusion-weighted imaging (DWI) and ADC maps provide information on cellularity and microarchitecture:

- Increase sensitivity for detecting small lesions
- Assist in differentiating lesion nature (diffusion restriction in highly cellular tissues)
- Serve as a guiding sequence for localization and further characterization

Dynamic Perfusion Assessment

Multiphase studies following gadolinium administration (arterial, portal, delayed phases) allow analysis of enhancement patterns and washout, key elements in liver lesion characterization. Dynamic contrast-enhanced (DCE)

techniques correlate imaging with hemodynamic parameters and vascular permeability, particularly useful in oncology and treatment response evaluation.

Non-Invasive Vascular Assessment

MR angiography (with or without contrast) enables analysis of hepatic and portal vessels:

- Vessel patency and flow direction
- Flow parameters (in dedicated protocols)
- Evaluation of hemodynamic changes in chronic liver disease and portal hypertension

Safety and Long-Term Monitoring

The absence of ionizing radiation makes MRI suitable for:

- Repeated follow-up examinations
- Young patients
- Long-term surveillance of chronic liver disease and focal lesions

Value in Clinical Planning

Good spatial resolution (especially with 3D acquisitions), superior tissue contrast, and multiplanar reconstructions allow integration of anatomical, biological, and hemodynamic information within a single examination, improving diagnostic accuracy and reducing clinical uncertainty.

In summary: MRI combines superior contrast, functional information, and high safety, making it the most comprehensive modality for modern evaluation of liver pathology.

14.4.3. Clinical Applications

Based on its physical principles, advanced sequence techniques, and contrast mechanisms described in contemporary radiological literature, MRI represents the most informative imaging modality for selected liver diseases, particularly where detailed characterization of parenchyma, focal lesions, fat or metal content, and vascular and biliary architecture is required.

A primary indication is evaluation of hepatic steatosis and fat-related liver disease. MRI is widely used due to its high sensitivity and specificity, especially with chemical shift and Dixon techniques. The typical imaging finding is signal drop on out-of-phase sequences compared to in-phase imaging,

reflecting intracellular triglycerides. Modern Dixon and IDEAL techniques allow not only diagnosis but also quantification of hepatic fat content, essential in non-alcoholic steatosis and treatment monitoring.

MRI also plays a central role in evaluating fibrosis and cirrhosis. Although early fibrosis may be subtle on conventional T1- and T2-weighted sequences, advanced stages demonstrate parenchymal heterogeneity, lobar morphological changes (posterior right lobe atrophy and caudate lobe hypertrophy), and indirect signs of portal hypertension. Magnetic resonance elastography, based on mechanical wave propagation and tissue stiffness measurement, is increasingly used for non-invasive fibrosis assessment, providing quantitative parameters comparable to liver biopsy.

MRI is widely used for characterization of benign and malignant focal liver lesions. Hepatic hemangiomas represent a classic indication, showing very high T2 signal intensity and characteristic progressive centripetal enhancement after contrast administration. This combination often allows near-definitive diagnosis without invasive procedures.

Focal nodular hyperplasia (FNH) is another condition where MRI is the modality of choice. The lesion is typically iso- or mildly hyperintense on T2, isointense on T1, and shows strong homogeneous arterial enhancement, with a central scar demonstrating high T2 signal and delayed enhancement. Hepatocyte-specific contrast agents are particularly valuable, as FNH shows uptake and retention during the hepatobiliary phase, differentiating it from hepatic adenoma.

Hepatic adenomas are also important indications due to the risk of hemorrhage and malignant transformation. On MRI, they demonstrate marked arterial enhancement and typically become isointense during the portal phase, remaining hypointense during the hepatobiliary phase due to absence of functional biliary ducts. Intralesional fat, hemorrhage, or necrosis contribute to signal heterogeneity on T1 and T2 sequences.

MRI is extensively used in diagnosis and staging of hepatocellular carcinoma (HCC). The principal imaging feature is early arterial enhancement followed by washout in the portal or delayed phase, often associated with a peripheral enhancing capsule. Diffusion-weighted imaging shows diffusion restriction due to high cellular density, increasing sensitivity for small lesions. Hepatocyte-specific contrast agents assist in identifying premalignant lesions and differentiating regenerative from dysplastic nodules.

Another important indication is evaluation of iron overload disorders, particularly hemochromatosis. Iron deposition causes marked signal reduction on T2 and especially T2* sequences due to susceptibility effects. MRI allows both diagnosis and quantification of hepatic iron content, playing a key role in monitoring treatment with phlebotomy or chelation therapy.

MRI also has a specific role in biliary diseases such as primary sclerosing cholangitis through MRCP. This heavily T2-weighted technique demonstrates segmental strictures and alternating dilatations of the bile ducts, providing a non-invasive overview of the entire biliary system without intravenous contrast.

14.4.4. Disadvantages of MRI

Although MRI is one of the most advanced modalities for liver examination, its use is associated with several disadvantages and limitations.

A major limitation is the relatively long examination time compared with CT and ultrasound. Hepatic protocols include multiple sequences and dynamic phases, requiring good patient cooperation, particularly breath-holding. Patients with dyspnea, severe ascites, pain, poor general condition, or inability to cooperate often produce motion-degraded images that significantly reduce diagnostic quality.

Motion artifacts represent a significant challenge in hepatic MRI. Respiratory motion, cardiac pulsation, and bowel peristalsis particularly affect T2-weighted, diffusion-weighted, and dynamic post-contrast sequences. Despite modern techniques such as breath-hold imaging and respiratory triggering, artifacts remain a limiting factor, especially in advanced liver disease.

MRI is also sensitive to magnetic field inhomogeneities and susceptibility effects, particularly problematic in the abdomen. Air–tissue interfaces in the gastrointestinal tract cause signal distortion, local signal loss, and geometric artifacts, especially in gradient-echo and diffusion-weighted sequences. These effects are more pronounced at higher field strengths (e.g., 3T).

Use of gadolinium-based contrast agents constitutes an additional limitation. In patients with severe renal insufficiency, gadolinium is restricted due to the risk of nephrogenic systemic fibrosis, significantly reducing diagnostic potential. Concerns about gadolinium deposition have also increased caution regarding repeated contrast use.

MRI has limitations in availability and cost. Equipment is less widespread than CT, particularly in peripheral centers, and examinations are more

expensive. This influences accessibility and limits MRI as a first-line modality in hepatic emergencies, where CT is often preferred for speed and availability.

Absolute and relative contraindications represent another important limitation. Patients with non-compatible ferromagnetic devices, older pacemakers, certain cochlear implants, or intraocular metallic fragments cannot undergo MRI. Even with MRI-compatible implants, special protocols and monitoring may be required.

From a diagnostic standpoint, MRI is not always superior in every aspect. Very early fibrosis may not be detectable on conventional sequences, and although MR elastography is promising, it is not yet widely available. Some findings remain non-specific and require clinical, laboratory, or histologic correlation.

Finally, the technical complexity and sequence variability make interpretation highly dependent on radiologist experience. Variations in protocols, technical parameters, and magnetic field strength may significantly affect image appearance, creating potential inter-center variability and standardization challenges.

14.5. Nuclear Medicine

Nuclear medicine represents a distinct branch of diagnostic imaging based on the use of radionuclides to evaluate functional, metabolic, and hemodynamic processes of tissues and organs, rather than their anatomical structure. In hepatology, this characteristic makes nuclear medicine an important complementary method to morphological techniques such as ultrasonography, computed tomography (CT), and magnetic resonance imaging (MRI), particularly in situations where functional alterations precede structural changes.

The fundamental principle of nuclear medicine consists of the administration of a radiopharmaceutical, which is composed of a radionuclide bound to a biologically active molecule. After administration, usually intravenously, the radiopharmaceutical distributes throughout the body according to its physicochemical and biological properties, accumulating in specific organs or tissues. The radionuclide emits gamma radiation, which is detected by imaging equipment and processed to create a functional map of radioactivity distribution. In the case of the liver, this distribution reflects hepatocellular function, reticuloendothelial system activity, and the integrity of portal and hepatic circulation.

The principal device used in nuclear medicine is the gamma camera, which consists of a collimator, a scintillation crystal (usually sodium iodide activated with thallium), photomultiplier tubes, and computer systems for signal processing. The collimator allows only photons traveling in a specific direction to reach the crystal, thereby improving spatial localization. When gamma photons strike the crystal, they produce light impulses that are converted into electrical signals and subsequently into images. The development of tomographic techniques such as Single Photon Emission Computed Tomography (SPECT) has significantly improved spatial resolution and the ability to evaluate the three-dimensional distribution of radiopharmaceuticals in the liver.

In liver imaging, the most commonly used radiopharmaceuticals are technetium-99m–labeled colloids, which are taken up by Kupffer cells of the reticuloendothelial system. This allows assessment of global hepatic function and its distribution. Under normal conditions, homogeneous accumulation of the radiopharmaceutical is observed in the hepatic parenchyma, while the spleen and bone marrow demonstrate lower uptake. Any deviation from this pattern suggests diffuse or focal pathology.

In diffuse hepatic diseases, such as cirrhosis, nuclear medicine demonstrates reduced and heterogeneous hepatic uptake of the radiopharmaceutical, often accompanied by increased accumulation in the spleen and bone marrow as a consequence of portal hypertension and redistribution of reticuloendothelial function. In advanced stages, morphological changes such as reduced hepatic volume and redistribution of radioactive activity may also be observed.

In focal hepatic lesions, nuclear medicine has a more limited role compared to CT and MRI, but it remains useful in specific contexts. Lesions that do not contain Kupffer cells, such as metastases and most primary malignant tumors, appear as photopenic areas on hepatic scintigraphy. Conversely, certain benign lesions containing reticuloendothelial components may demonstrate relative radiopharmaceutical uptake, assisting in their differentiation.

A particular application of nuclear medicine in hepatology is the evaluation of hepatic function prior to surgical interventions, including hepatic resections and liver transplantation. Scintigraphic techniques can provide quantitative information regarding residual hepatic function, which cannot be directly assessed with morphological imaging methods.

The main advantages of nuclear medicine include the ability to directly evaluate hepatic function, high sensitivity to early functional changes, and the possibility of global organ assessment. The method is relatively non-invasive and uses low radiation doses, particularly with modern radionuclides such as technetium-99m.

However, nuclear medicine also has important disadvantages. Spatial resolution is limited compared to CT and MRI, making it less suitable for detailed anatomical characterization of small lesions. Findings are often non-specific and must always be interpreted in clinical context and in combination with other imaging modalities. Furthermore, availability of equipment and radiopharmaceuticals may be limited in certain centers.

14.6. Innovations in Imaging

14.6.1. Artificial Intelligence

Artificial Intelligence (AI) is becoming a fundamental component of modern hepatic imaging, significantly influencing the way liver diseases are diagnosed, classified, and monitored. The global rise in the prevalence of chronic liver diseases—particularly metabolic dysfunction–associated steatotic liver disease (MASLD/NAFLD), chronic viral hepatitis, and hepatocellular carcinoma—has created the need for more accurate, standardized, and non-invasive diagnostic methods. In this context, AI, especially through machine learning and deep learning techniques, offers promising solutions by analyzing large volumes of imaging data beyond the capacity of human visual interpretation.

One of the fields in which AI has demonstrated direct clinical impact is the diagnosis of hepatic steatosis. A meta-analysis published in *Scientific Reports* (2025) showed that AI models applied to ultrasonography, CT, and MRI achieve high sensitivity and specificity in detecting steatosis, often comparable or superior to experienced radiologists. Deep learning models are capable of identifying subtle parenchymal texture changes that are not easily perceived by the human eye, enabling not only binary detection of steatosis but also grading of its severity. This development has significant clinical relevance, as it reduces dependence on liver biopsy and increases the use of non-invasive methods in the management of NAFLD.

The development of AI in NAFLD has been comprehensively analyzed in a bibliometric study published in *Frontiers in Radiology* (2025), which demonstrates an exponential increase in research activity in this field over the

past decade. The study highlights that AI is not only used for detecting steatosis but is increasingly applied to assess fibrosis and predict progression to steatohepatitis and cirrhosis. The integration of radiomics with advanced algorithms enables extraction of quantitative imaging parameters that correlate with histopathological changes. This positions AI as an important tool for risk stratification and longitudinal follow-up of patients with chronic liver disease.

Another area in which AI is transforming clinical practice is the characterization of focal liver lesions, particularly in contrast-enhanced ultrasound (CEUS). An article published in the World Journal of Gastroenterology (2025) describes the use of AI algorithms for automated analysis of vascular phases in CEUS, improving differentiation between benign and malignant lesions. AI can analyze contrast enhancement dynamics in real time, identifying perfusion patterns characteristic of hepatocellular carcinoma, metastases, or hemangioma. This enhances diagnostic reproducibility and reduces inter-operator variability, a traditional limitation of ultrasonography.

In the field of magnetic resonance imaging, AI has shown particular potential in the diagnosis of hepatocellular carcinoma. A 2025 study reported by *AuntMinnie* demonstrated that explainable deep learning models applied to hepatocyte-specific contrast-enhanced MRI achieve high accuracy in identifying HCC, including small lesions that are often difficult to characterize using conventional criteria. The advantage of “explainable” models lies in their ability to highlight the imaging regions contributing to the diagnostic decision, thereby increasing clinician and radiologist confidence in AI as an assistive tool rather than a replacement.

Beyond focal lesion diagnosis, AI is playing an increasingly important role in the management of chronic liver diseases. Recently there are many published articles describing the use of AI-based systems for integrating imaging data with clinical, laboratory, and genetic parameters. These systems are capable of predicting fibrosis progression, risk of decompensation, and the development of complications such as hepatocellular carcinoma. This multidimensional approach makes AI a key component of personalized medicine in hepatology.

An important aspect emerging from these studies is the role of AI in standardizing imaging interpretation. Inter-radiologist variability and dependence on individual experience have always been challenges in hepatic imaging. AI algorithms, trained on large and heterogeneous databases, provide consistent and reproducible interpretation, reducing subjective errors.

Nevertheless, authors emphasize that AI should be considered an assistive tool rather than a substitute for clinical judgment, as clinical context and pathophysiological understanding remain essential.

In *conclusion*, recent literature clearly demonstrates that artificial intelligence is transforming the paradigm of hepatic imaging. From detection of steatosis and assessment of fibrosis to characterization of focal lesions and early diagnosis of hepatocellular carcinoma, AI significantly enhances diagnostic accuracy and clinical efficiency. Its further integration into daily practice is expected to improve the management of patients with liver diseases, making diagnosis earlier, more precise, and more personalized.

14.6.2. Radiomics

Radiomics represents a paradigm shift in contemporary medical imaging, transforming radiological images from primarily descriptive tools into rich sources of quantitative data. In the context of liver diseases, radiomics has gained particular importance due to the biological heterogeneity of hepatic tissues and the limitations of traditional non-invasive methods for their assessment. By systematically analyzing numerical features extracted from CT, MRI, and ultrasound images, radiomics enables the identification of imaging biomarkers that reflect the liver's microarchitecture, vascularization, and molecular alterations.

In diffuse liver diseases such as fibrosis, steatosis, and cirrhosis, radiomics has demonstrated a high capacity to capture subtle changes that are often not visually distinguishable by the radiologist. Radiomic models based on MRI and multimodal ultrasound have shown strong correlation with histopathological grades of fibrosis and inflammation. This is particularly important in patients with chronic viral hepatitis, where radiomics offers potential for non-invasive assessment of disease progression and prediction of hepatic clinical events such as decompensation or the development of portal hypertension. In several recent studies, MRI-based radiomic models have achieved superior prognostic performance compared to traditional clinical parameters and standalone elastography.

Another field where radiomics has significant impact is the characterization of focal liver lesions. Differentiation between dysplastic nodules, early hepatocellular carcinoma (HCC), and benign lesions remains a persistent diagnostic challenge, especially in cirrhotic livers. By analyzing intratumoral and peritumoral features from dynamic contrast-enhanced MRI

sequences, radiomics has demonstrated the ability to distinguish early HCC from premalignant lesions with higher sensitivity and specificity than conventional visual criteria. This capability is related to the fact that radiomics captures structural and perfusion heterogeneity of the tumor, reflecting early biological changes in angiogenesis and cellular density.

In the context of hepatocellular carcinoma, radiomics also plays an important prognostic role. MRI-based radiomic models have been successfully used to predict early recurrence of HCC after surgical resection or ablation. By integrating features derived from both the tumor tissue and the surrounding liver parenchyma, these models reflect not only the intrinsic aggressiveness of the tumor but also the hepatic microenvironment, which plays a key role in disease recurrence. Such predictive capacity has direct clinical relevance, as it may influence post-therapeutic follow-up strategies and decisions regarding adjuvant therapy.

Radiomics has also demonstrated considerable potential when integrated with artificial intelligence and machine learning models. Advanced algorithms are capable of processing hundreds to thousands of radiomic features and combining them with clinical, laboratory, and demographic data to generate personalized predictive models. In chronic liver diseases, these models have shown the ability to predict severe hepatic events, surpassing traditional approaches based solely on biochemical markers or clinical scoring systems. This approach supports the concept of precision medicine, in which diagnostic and therapeutic decision-making is tailored to the individual characteristics of each patient.

An important aspect of radiomics is its expansion beyond MRI and CT into ultrasonography. Ultrasound-based radiomics, particularly when combined with contrast enhancement or elastography, offers an affordable and accessible alternative for evaluating diffuse liver diseases. Ultrasound texture analysis has demonstrated potential in grading hepatic steatosis and fibrosis, reducing the need for invasive biopsy in selected patient groups. This is particularly relevant in resource-limited settings, where MRI may not always be available.

However, despite its great potential, radiomics still faces methodological challenges. Standardization of imaging protocols, lesion segmentation, and reproducibility of radiomic features remain critical issues for broad clinical implementation. Inter-scanner and inter-center variability can significantly affect the performance of radiomic models. For this reason, recent studies

emphasize the need for multicenter validation and integration of radiomics into the routine radiological workflow.

In conclusion, radiomics represents a powerful and promising tool in hepatic imaging, providing in-depth information about the structure, function, and biology of liver diseases. It expands the role of imaging from visual diagnosis toward prediction, risk stratification, and treatment personalization. With further development of artificial intelligence and methodological standardization, radiomics is expected to become an integral component of clinical practice in hepatology and diagnostic radiology.

1*4.6.3. Hybrid Imaging*

Hybrid imaging represents one of the most significant developments in contemporary radiology, combining anatomical information with functional and metabolic data within a single examination. In the evaluation of hepatic diseases, this approach has transformed the way liver pathologies are diagnosed, staged, and monitored, particularly in the context of malignant and chronic diffuse diseases. Hybrid imaging is not merely a technical combination of modalities, but rather a conceptual integration that substantially enhances the diagnostic value of modern imaging.

Fundamentally, hybrid imaging includes modalities such as PET/CT, SPECT/CT, and more recently PET/MRI, which enable the fusion of morphological imaging with functional and metabolic tissue assessment. In hepatology, this is particularly important due to the biological heterogeneity of the liver and the complexity of its vascular and biliary circulation. Metabolic alterations often precede structural changes visible on conventional CT or MRI, making hybrid imaging a powerful tool for early disease detection.

In malignant hepatic diseases, especially hepatocellular carcinoma and liver metastases, PET/CT with 18F-FDG has found widespread application for assessing tumor metabolic activity. Although primary hepatocellular carcinoma may show variability in FDG uptake due to cellular differentiation, hybrid imaging provides valuable prognostic information. Tumors with high metabolic activity are frequently associated with greater biological aggressiveness, a higher risk of vascular invasion, and poorer prognosis. Integrating these metabolic data with anatomical information from CT allows for more accurate evaluation of disease spread and assists in selecting patients for curative or palliative treatment strategies.

Another important advantage of hybrid imaging in liver evaluation is its role in staging and restaging oncologic disease. Liver metastases originating from colorectal, neuroendocrine, or pancreatic tumors may be small or isodense on conventional CT, making detection challenging. Hybrid imaging, by combining the high metabolic sensitivity of PET with the anatomical resolution of CT or MRI, increases diagnostic sensitivity for detecting secondary hepatic lesions and assessing response to systemic or local therapies.

PET/MRI represents a further evolutionary step in hybrid imaging, particularly in liver assessment. The combination of the superior soft-tissue contrast provided by MRI with the metabolic information from PET makes this modality especially valuable in the cirrhotic liver, where differentiation of focal lesions is challenging. Recent studies indicate that PET/MRI offers high performance in characterizing hepatic lesions while reducing exposure to ionizing radiation compared with PET/CT—an aspect of particular importance in patients requiring long-term follow-up.

In diffuse liver diseases, hybrid imaging is gaining increasing importance. Although its use is not yet routine in the evaluation of fibrosis or steatosis, research studies have demonstrated that metabolic changes detected by PET may correlate with inflammatory activity and fibrotic progression. This opens new perspectives for monitoring chronic liver diseases and evaluating the effectiveness of antifibrotic therapies in the future.

A fundamental aspect of hybrid imaging is its ability to improve therapeutic planning. In hepatocellular carcinoma, hybrid imaging assists in selecting patients for surgical resection, liver transplantation, or locoregional therapies such as ablation or chemoembolization. Assessment of tumor metabolic activity and extrahepatic spread is essential to avoid unnecessary invasive interventions and to optimize clinical outcomes.

Beyond oncology, hybrid imaging also has applications in the evaluation of hepatic infections and inflammatory processes. PET/CT may help identify liver abscesses or active inflammatory foci, particularly in immunocompromised patients, in whom anatomical findings may be nonspecific. This approach increases diagnostic sensitivity and contributes to rapid and accurate patient management.

However, despite its numerous advantages, hybrid imaging has limitations. High cost, limited availability, and the need for multidisciplinary expertise are factors that currently restrict its widespread use. Furthermore, interpretation of hybrid data requires in-depth knowledge of both radiology and

nuclear medicine, emphasizing the importance of interdisciplinary collaboration.

In conclusion, hybrid imaging represents an essential tool in the modern evaluation of hepatic diseases, providing an integrated anatomical and functional perspective that surpasses the limitations of individual modalities. It plays a particularly important role in hepatic oncology, disease staging, therapeutic planning, and treatment response monitoring. With further technological development and integration of artificial intelligence, hybrid imaging is expected to assume an increasingly central role in precision-based hepatology.

14.7. Comparative Analysis of Imaging Modalities

14.7.1. Sensitivity and Specificity

Ultrasonography is the first-line and most widely used method in the initial evaluation of the liver, owing to its broad availability, absence of ionizing radiation, and low cost. It demonstrates high sensitivity for the detection of moderate to severe hepatic steatosis, with reported values exceeding 85%. However, its specificity decreases in the presence of fibrosis or chronic inflammation, where echotextural changes are nonspecific. For focal liver lesions, ultrasonography has limited sensitivity, particularly for lesions smaller than 1 cm, and its specificity is insufficient for definitive characterization without the use of additional modalities or contrast-enhanced ultrasound.

Computed tomography represents a key modality in the morphological evaluation of the liver, especially in focal and vascular pathologies. Multiphase contrast-enhanced CT demonstrates high sensitivity for detecting hepatocellular carcinoma in intermediate and advanced stages, often exceeding 80–90% for lesions larger than 2 cm, with good specificity based on characteristic patterns of arterial enhancement and portal venous washout. However, CT sensitivity decreases significantly for small lesions and early-stage hepatocellular carcinoma, as well as in differentiating regenerative from dysplastic nodules in cirrhosis. For diffuse liver diseases, CT is relatively insensitive in the early stages of fibrosis but is valuable in assessing complications of cirrhosis and portal hypertension.

Magnetic resonance imaging is considered the modality with the highest sensitivity and specificity in liver examination, particularly when multiparametric protocols and hepatocyte-specific contrast agents are used. MRI demonstrates superior sensitivity for detecting hepatic steatosis, even at

minimal levels, and for quantifying fat and iron content. In the diagnosis of hepatocellular carcinoma, MRI surpasses CT, especially for lesions smaller than 2 cm, with sensitivity and specificity often exceeding 90% when dynamic criteria and the hepatobiliary phase are applied. Moreover, MRI is the most specific modality for characterizing benign lesions such as hemangioma, focal nodular hyperplasia, and hepatic adenoma, significantly reducing the need for biopsy. Techniques such as diffusion-weighted imaging and magnetic resonance elastography further enhance its diagnostic value in the assessment of fibrosis and inflammation.

Nuclear medicine, including hepatic scintigraphy and hybrid imaging modalities such as PET/CT and PET/MRI, has limited sensitivity for primary hepatic lesions but plays an important role in detecting metastases, assessing tumor metabolic activity, and evaluating response to therapy. PET/CT with 18F-FDG demonstrates high specificity for liver metastases originating from extrahepatic tumors but lower sensitivity for well-differentiated hepatocellular carcinoma. The combination of PET with MRI significantly improves both sensitivity and specificity, providing functional and morphological information within a single examination.

As summarized below, the comparative diagnostic performance of the principal liver imaging modalities reflects their complementary roles in clinical practice.

Table 14.I. Comparative Sensitivity and Specificity of Liver Imaging Modalities

Imaging Modality	**Diffuse Liver Disease (Steatosis / Fibrosis)**	**Focal Liver Lesions**	**Hepato-cellular Carcinoma (HCC)**	**Benign Lesion Characteri-zation**	**Meta-stases Detection**	**Principal Limitation s**
Ultra-sonography (US)	High sensitivity (>85%) for moderate–severe steatosis; reduced specificity in fibrosis and chronic inflammation	Limited sensitivity, especially for lesions <1 cm	Limited sensitivity for early HCC; improves with contrast-enhanced US	Insufficient specificity without contrast enhancement	Moderate sensitivity	Operator-depen-dent; reduced accuracy in obesity and fibrosis; limited small-lesion detection

Computed Tomography (CT)	Low sensitivity in early fibrosis; valuable for cirrhosis complications and portal hypertension	High sensitivity for lesions >2 cm	Sensitivity 80–90% for lesions >2 cm with good specificity based on arterial hyperenhancement and washout	Moderate specificity; limited differentiation in cirrhosis	High sensitivity	Reduced sensitivity for lesions <2 cm and early HCC; radiation exposure
Magnetic Resonance Imaging (MRI)	Very high sensitivity and specificity for steatosis; accurate fat and iron quantification; high performance in fibrosis (MRE)	Superior sensitivity for lesions <2 cm	Sensitivity and specificity often >90% with multi-parametric and hepato-biliary phase imaging	Highest specificity for hemangioma, focal nodular hyperplasia, and adenoma; reduces biopsy need	Very high sensitivity	Higher cost; longer acquisition time; limited availability
Nuclear Medicine (Scintigraphy, PET/CT, PET/MRI)	Limited role	Limited sensitivity for primary lesions	Lower sensitivity for well-differentiated HCC; high specificity in metabolically active tumors	Limited role	High specificity for metastases (especially FDG-avid tumors); PET/MRI improves sensitivity	Limited sensitivity for primary tumors; radiation exposure (PET/CT); high cost

4.7.2. Safety

Safety represents a fundamental criterion in selecting the appropriate imaging modality for liver examination, particularly in patients with chronic liver disease, renal insufficiency, the need for repeated examinations, and in vulnerable populations such as children and pregnant women. The main imaging modalities differ significantly with respect to exposure to ionizing radiation, use of contrast agents, and short- and long-term risk profiles.

Ultrasonography is considered the safest modality for liver evaluation. It does not use ionizing radiation, does not require contrast agents in its standard

form, and is not associated with known harmful biological effects. For this reason, ultrasound is the preferred method for screening, long-term follow-up, and examination of vulnerable patients, including pregnant women and pediatric patients. Even the use of contrast-enhanced ultrasound (microbubble-based contrast agents) has a very favorable safety profile, with an extremely low incidence of anaphylactic reactions and no nephrotoxicity, making it suitable for patients with renal insufficiency.

Computed tomography presents important safety limitations due to its use of ionizing radiation. Exposure to cumulative radiation doses is particularly concerning in patients with chronic liver disease, who often require repeated examinations for surveillance of hepatocellular carcinoma or complications of cirrhosis. Furthermore, the use of intravenous iodinated contrast agents is associated with a risk of contrast-induced nephropathy, especially in patients with impaired renal function, diabetes mellitus, or dehydration. Allergic reactions to iodinated contrast agents, although relatively rare, remain a clinical concern and require specific safety protocols.

Magnetic resonance imaging has a considerably more favorable safety profile compared with CT, as it does not use ionizing radiation. This makes MRI particularly suitable for repeated examinations and long-term follow-up of patients with chronic liver disease. However, MRI safety is influenced by the use of gadolinium-based contrast agents. Although gadolinium is generally safe, an association has been reported between some older agents and the development of nephrogenic systemic fibrosis in patients with advanced renal insufficiency. Currently, the use of macrocyclic and hepatocyte-specific contrast agents has significantly reduced this risk, but assessment of renal function remains an essential step prior to contrast administration. MRI also has safety limitations in patients with non-compatible metallic implants, older cardiac devices, or severe claustrophobia.

Nuclear medicine, including hepatic scintigraphy and hybrid techniques such as PET/CT and PET/MRI, involves exposure to ionizing radiation through radiopharmaceuticals. Radiation doses are generally moderate but become relevant in the context of repeated examinations and in younger patients. PET/CT, in particular, combines radiation from CT and the radioisotope, resulting in a higher effective dose compared with PET/MRI. On the other hand, PET/MRI significantly reduces total radiation exposure and represents a safer alternative, although it has limited availability and higher cost.

Table 14.II. Safety Profile of Liver Imaging Modalities

Imaging Modality	Ionizing Radiation	Contrast Agent Use	Contrast-Related Risks	Suitability for Repeated Examinations	Use in Renal Insufficiency	Use in Pregnancy & Pediatrics	Principal Safety Limitations
Ultrasonography (US)	None	Not required (standard US); microbubble contrast in CEUS	Extremely low risk of anaphylaxis; no nephrotoxicity	Excellent	Safe; preferred modality	Preferred modality	Operator dependency; limited by body habitus
Computed Tomography (CT)	Yes (moderate to high cumulative dose)	Iodinated intravenous contrast	Risk of contrast-induced nephropathy; allergic reactions possible	Limited due to cumulative radiation	Caution required; risk increased in renal impairment, diabetes, dehydration	Not preferred due to radiation	Ionizing radiation exposure; contrast nephrotoxicity; allergic reactions
Magnetic Resonance Imaging (MRI)	None	Gadolinium-based contrast agents (optional but often used)	Very low risk; rare nephrogenic systemic fibrosis (mainly with older linear agents in severe renal failure)	Very good; suitable for long-term follow-up	Caution in advanced renal failure; renal function assessment required	Generally safe; caution in first trimester	Contraindicated in non-compatible implants; claustrophobia; longer examination time
Nuclear Medicine (Scintigraphy, PET/CT, PET/MRI)	Yes (radiopharmaceuticals; PET/CT higher dose than PET/MRI)	Radiotracers (e.g., FDG)	Minimal allergic risk; radiation-related stochastic risk	Limited in repeated exams, especially in younger patients	Generally safe; no nephrotoxicity but radiation considered	Not preferred due to radiation	Radiation exposure; higher dose with PET/CT; limited availability (PET/MRI)

Ultrasonography represents the safest modality and is the preferred method for screening, follow-up, and vulnerable populations.

CT carries significant safety concerns related to ionizing radiation and iodinated contrast nephrotoxicity.

MRI offers an excellent safety profile without radiation exposure, though gadolinium administration requires renal function assessment.

Nuclear medicine techniques involve radiation exposure, with PET/MRI offering a lower-dose alternative compared with PET/CT.

14.7.3. According to Diagnostic Indications

In diffuse liver diseases (metabolic steatosis/steatohepatitis, fibrosis/cirrhosis, iron deposition), ultrasonography (US) is often used as the initial examination because it identifies general signs of steatosis (increased echogenicity, reduced acoustic penetration, blurring of vascular contours), but it has limitations in precise quantification and in differentiating steatosis from advanced fibrosis. For fibrosis and non-invasive staging, elastography (TE/2D-SWE) is preferred, as it measures hepatic stiffness as a biomarker of fibrosis and has been widely integrated into chronic liver disease assessment algorithms. Magnetic resonance imaging, particularly with quantitative techniques such as proton density fat fraction (PDFF) and T2*/R2* sequences, has an advantage in quantifying steatosis and iron overload. Computed tomography may suggest steatosis through reduced hepatic density, but it is less reliable when fibrosis or deposits coexist and, due to radiation exposure, is generally not selected as a first-line method solely for assessing fat percentage.

In cholestasis and biliary pathology, the practical algorithm begins with US to confirm bile duct dilation and suggest the level of obstruction. When detailed evaluation of the biliary tree is required (e.g., strictures, anatomical anomalies, unclear choledocholithiasis), magnetic resonance cholangio-pancreatography (MRCP), as part of MRI, is considered a key choice because it provides non-invasive mapping of the biliary ducts without radiation or iodinated contrast. CT is used when a tumoral etiology or extrahepatic complications are suspected, or when rapid abdomen–pelvis assessment is needed; however, for intraductal morphology, MRCP is often more informative.

For focal liver lesions, the indication depends on the clinical scenario (incidental finding, patient with cirrhosis, oncologic patient). US often detects the lesion, but characterization requires a contrast-based modality. Multiphase CT (arterial, portal-venous, delayed phases) is widely used due to accessibility

and speed, especially for staging and surgical planning. However, MRI with contrast—particularly with hepatocyte-specific agents such as gadoxetic acid—has an important advantage in differentiating focal nodular hyperplasia (FNH) from adenoma, in characterizing hemangioma, and in detecting very small lesions or subcentimeter metastases. Radiological guidelines emphasize the role of contrast-enhanced CT/MRI for characterization, while the choice between them depends on availability, contraindications, and the clinical question.

In patients with cirrhosis or high risk for hepatocellular carcinoma (HCC), standard screening is performed with US every 6 months (with or without AFP depending on local practice) due to its simplicity and cost-effectiveness. When a suspicious nodule is detected, multiphase CT or dynamic MRI are used for non-invasive diagnosis based on the typical vascular pattern (arterial hyperenhancement and delayed washout). The LI-RADS system standardizes CT/MRI interpretation in the cirrhotic liver. MRI often provides higher sensitivity for small lesions and additional information (diffusion-weighted imaging, hepatobiliary phase), whereas CT is strong for rapid vascular and extrahepatic assessment.

In oncology (e.g., staging of liver metastases), contrast-enhanced portal-venous CT is a basic method for whole-body staging in many tumors. However, liver MRI with diffusion-weighted imaging (DWI) and hepatobiliary contrast is preferred when higher sensitivity for small lesions is required or when surgical decision-making depends on the number and size of metastases. Expert documents on the use of gadoxetic acid emphasize its value for detecting subcentimeter lesions and for therapeutic planning.

In infections (pyogenic abscess, complex collections), CT is widely used because it rapidly identifies collections, intraparenchymal gas, and extrahepatic spread, and guides percutaneous drainage. US is often the first step, but CT becomes the decisive modality when precise anatomical mapping is required. MRI is reserved for selected cases; in emergencies, CT predominates.

In hepatic vascular pathologies (portal vein thrombosis, Budd–Chiari syndrome, arterioportal shunts), Doppler US is the first examination because it provides real-time hemodynamic information (flow direction and velocity). When complete anatomical assessment is required, CT angiography/venography or MRI/MRA are used to confirm thrombus, assess extent, and evaluate collaterals. The choice depends on the need for hemodynamic analysis (Doppler) versus anatomical mapping (CT/MR).

In hepatic trauma, contrast-enhanced CT is the practical standard for rapid evaluation of injury grade, active hemorrhage, and associated abdominal injuries due to its availability and emergency standardization. US (FAST) is used for screening free fluid but does not replace CT for full staging; MRI is generally not used in the acute phase.

For specific benign lesions, modality selection is linked to their imaging characteristics. Hemangioma is often suggested on US, but MRI (with prolonged T2 signal and dynamic post-contrast behavior) is highly reliable for confirmation; dynamic CT may demonstrate the typical centripetal fill-in pattern. FNH and adenoma often require MRI with hepatobiliary contrast for differentiation, as behavior in the hepatobiliary phase allows safer distinction and guides clinical management.

In nuclear medicine and hybrid imaging, modalities such as PET/CT and PET/MRI have a selective role, mainly in oncology for systemic evaluation, detection of extrahepatic disease, and monitoring treatment response. However, for detailed characterization of hepatic lesions, liver-protocol CT/MRI remain the primary modalities, while functional hepatobiliary scans (e.g., HIDA) have a more limited role in strictly parenchymal pathologies.

Table 14.III. ***Decision Algorithm for Imaging Selection in Liver Disease***

Clinical Scenario	**Step 1 (Initial Test)**	**If Positive / Suspicious**	**If Inconclusive**	**Preferred Definitive Modality**	**Special Considerations**
Diffuse liver disease (steatosis, fibrosis, iron overload)	US	If steatosis suspected → Quantification needed	Unclear differentiation steatosis vs fibrosis	MRI (PDFF, T2*/R2*); Elastography (TE / 2D-SWE)	Avoid CT for fat quantification due to radiation
Cholestasis / Biliary dilation	US	Duct dilation present	Level/cause unclear	MRCP (MRI-based)	CT if tumor or urgent abdomen–pelvis evaluation suspected
Incidental focal liver lesion (non-cirrhotic)	US detection	Lesion >1 cm or indeterminate	Characterization required	Contrast-enhanced MRI (preferred) or multiphase CT	MRI superior for small or indeterminate lesions

Cirrhosis – HCC surveillance	US every 6 months	Nodule ≥1 cm detected	Indeterminate US finding	Dynamic MRI (preferred) or multiphase CT	Apply LI-RADS criteria for CT/MRI interpretation
Oncologic patient – staging for metastases	Portal-venous CT	Suspicious hepatic lesions	Need higher sensitivity for small lesions	MRI with DWI + hepatobiliary contrast	PET/CT or PET/MRI for systemic disease evaluation
Suspected hepatic abscess / infection	US	Collection suspected	Mapping required or emergency setting	Contrast-enhanced CT	CT guides drainage planning
Portal vein thrombosis / vascular disorder	Doppler US	Flow abnormality detected	Extent unclear	CT angiography or MRI/MRA	Doppler = functional; CT/MR = anatomical mapping
Acute hepatic trauma	FAST US	Free fluid present	Injury grading required	Contrast-enhanced CT	MRI not used in acute trauma setting
Benign lesion differentiation (FNH vs adenoma)	US	Lesion indeterminate	Characterization required	MRI with hepatocyte-specific contrast	Hepatobiliary phase critical for differentiation
Renal insufficiency / need for repeated imaging	US	Further evaluation required	Avoid nephrotoxic agents	MRI without contrast or CEUS	Avoid iodinated contrast CT when possible

Simplified Flow Concept for liver evaluation

1. **Start with Ultrasound** in most liver indications (screening, detection, biliary dilation, trauma screening).
2. **Escalate to MRI** when:
    - Lesion characterization is required
    - Small HCC suspected
    - Quantification of fat/iron is necessary
    - Radiation avoidance is important
3. **Use CT** when:
    - Rapid emergency assessment is needed
    - Whole-body staging required
    - Trauma or abscess suspected

4. **Use Doppler US first for vascular questions**, confirm with CT/MR angiography if anatomical detail required.
5. **Use PET-based imaging selectively in oncology** for systemic evaluation and therapy response.

14.8. Conclusions

There is no universal imaging modality for all hepatic diseases; the choice must be tailored to the clinical question, the patient's context, and the diagnostic objective (screening, characterization, staging, or follow-up).

Ultrasonography (US) remains the first-line method for initial evaluation and screening (especially for hepatocellular carcinoma), owing to its safety, accessibility, and low cost. However, it has limitations in obese patients and in the characterization of focal lesions. Elastography has significantly improved the non-invasive assessment of hepatic fibrosis and the monitoring of chronic liver diseases.

Computed tomography is particularly valuable in emergency settings, trauma, complex pathologies, and oncologic staging, but it is limited by exposure to ionizing radiation and the use of iodinated contrast agents.

Magnetic resonance imaging provides the most advanced characterization of liver parenchyma and focal lesions, with high sensitivity for small lesions and a key role in therapeutic decision-making. Magnetic resonance cholangiopancreatography (MRCP) represents the non-invasive standard for evaluation of the biliary tree. MRI limitations are related to cost, examination time, and specific contraindications.

PET/CT and PET/MRI have a selective role, mainly in oncology for systemic staging and treatment monitoring.

In ***clinical practice***, the optimal approach is multimodal and multidisciplinary, combining imaging methods according to clinical needs and integrating imaging data with clinical, laboratory, and histopathological information. Advances in artificial intelligence and radiomics are expected to further strengthen the role of hepatic imaging toward quantitative and predictive analysis.

References

1. Adam A, Dixon AK, Gillard JH, Schaefer-Prokop C. Grainger & Allison's Diagnostic Radiology: A Textbook of Medical Imaging. 7th ed. Elsevier; 2021.
2. European Association for the Study of the Liver. EASL Clinical Practice Guidelines: Management of hepatocellular carcinoma. J Hepatol. 2018;69(1):182-236.
3. American College of Radiology. ACR Manual on Contrast Media. 2023 ed. Reston, VA: American College of Radiology; 2023.
4. Boellaard R, Delgado-Bolton R, Oyen WJ, Walrand S, Knešaurek K, Campesato R, et al. FDG PET/CT: EANM procedure guidelines for tumour imaging: version 2.0. Eur J Nucl Med Mol Imaging. 2015;42(2):328-354.
5. Mitchell DG, Bruix J, Sherman M, Sirlin CB, Abbattista T, Brancatelli G, et al. LI-RADS (Liver Imaging Reporting and Data System): Summary, Updates, and Future Directions. Radiology. 2018;289(3):638-650.
6. Barr RG, Wilson SR, Lyshchik A, Dietrich CF, Cosgrove D, Piscaglia F, et al. Contrast-enhanced ultrasound of the liver: clinical applications. Abdom Radiol (NY). 2018;43(5):1061-1082.
7. Singh S, Venkatesh SK, Wang Z, Miller FH, Motosugi U, Low RN, et al. Diagnostic performance of magnetic resonance elastography in staging liver fibrosis: a systematic review and meta-analysis of individual participant data. Clin Gastroenterol Hepatol. 2015;13(3):440-451.
8. Vilgrain V, Ronot M, Abdel-Rehim M, Zappa M, d'Assignies G, Bruno O, et al. MRI of focal liver lesions: current concepts and future directions. Radiology. 2012;264(3):641-659.
9. Barr RG, Cosgrove D, Dietrich CF, Jenssen C, Kolokythas O, Cantisani V, et al. WFUMB-EFSUMB guidelines and recommendations on the clinical use of liver ultrasound elastography: Part 1: Basic principles and terminology. Ultrasound Med Biol. 2015;41(5):1126-1147.
10. Wang J, Zhou J, Dong Y, Fan M, Wang W. Artificial intelligence in contrast-enhanced ultrasound: a new era for liver lesion assessment. World J Gastroenterol. 2025;31(42):112196.
11. Singh Y, Hathaway Q, Salehi S, Alkhouri N, Sanyal AJ. Artificial intelligence–based agents in chronic liver disease. Nat Rev Gastroenterol Hepatol. 2025;22:1-15.
12. Dietrich CF, Bamber J, Berzigotti A, Bota S, Church V, Castera L, et al. EFSUMB guidelines and recommendations on the clinical use of liver ultrasound elastography, update 2017 (Long Version). Ultraschall Med. 2017;38(4):e16-e47.
13. Hertzberg BS, Middleton WD. Ultrasound: The Requisites. 4th ed. St. Louis, MO: Elsevier; 2015.

15. Recent development of ultrasound for liver (PAT, Micro-flow, Image fusion ultrasongraphy, Drug delivery)

Felix Bende, Tudor Moga, Raluca Lupuşoru

Abstract

Recent technological advances have significantly expanded the diagnostic and therapeutic capabilities of ultrasound in liver diseases. Emerging techniques such as parametric arrival time imaging (PAT), microflow imaging, image fusion ultrasonography, and ultrasound-mediated drug delivery are improving the evaluation of hepatic perfusion, microvascular architecture, and image-guided interventions.

Contrast-enhanced ultrasound (CEUS) with parametric arrival time analysis allows assessment of hepatic microcirculatory changes associated with liver fibrosis by mapping contrast arrival dynamics, providing functional information that complements stiffness-based techniques such as elastography.

Microflow imaging enables visualization of slow blood flow within small vessels without the need for contrast agents, improving the characterization of tumor vascularity and potentially aiding in treatment monitoring.

Image fusion ultrasonography integrates real-time ultrasound with previously acquired CT or MRI datasets, enhancing lesion localization and procedural guidance, particularly during liver tumor ablation or biopsy.

In addition, ultrasound-mediated drug delivery represents a rapidly developing therapeutic approach in which acoustic energy and microbubbles facilitate targeted drug release and improved tissue penetration.

Together, these innovations highlight the evolving role of multiparametric ultrasound as a comprehensive platform for liver imaging, interventional guidance, and emerging therapeutic applications.

15.1. Parametric Arrival Time (PAT) / Arrival-Time Parametric Imaging (At-PI) in CEUS for Liver Fibrosis

Rationale for Perfusion-Based Assessment of Liver Fibrosis. Liver fibrosis is not only a structural remodeling process but also a hemodynamic disorder characterized by sinusoidal capillarization, increased intrahepatic resistance, and portal–systemic shunting (1, 2). These vascular alterations modify hepatic perfusion dynamics and can be evaluated using contrast-

enhanced ultrasound (CEUS), which provides real-time visualization of microbubble transit within the hepatic microcirculation (3).

Technical Principles of CEUS-PAT. Parametric Arrival Time (PAT), also referred to as Arrival-Time Parametric Imaging (At-PI), converts temporal contrast enhancement data into spatially coded perfusion maps (4). After intravenous administration of sulfur hexafluoride microbubbles (SonoVue®), low mechanical index imaging is performed. The arrival time of contrast in the liver is normalized using a systemic reference organ (e.g., the right kidney), reducing interindividual hemodynamic variability. Breath-holding during the early arterial phase improves reproducibility.

Evolution of CEUS in Fibrosis Assessment. Early CEUS applications relied on the "red color ratio" obtained using external image-processing software (4). Later, structured analysis using time–intensity curves (TIC) and arrival times in the hepatic vein, hepatic artery, portal vein, and parenchyma became a standard investigative approach (5, 6).

Shortened hepatic vein arrival time has consistently been associated with increasing fibrosis severity (5). Ridolfi et al. demonstrated that hepatic vein arrival time decreases progressively with fibrosis stage in chronic hepatitis C (6). Similar inter-organ comparisons between liver and kidney perfusion were described by Fujita et al. in alcoholic liver disease (7).

Ying et al. evaluated early cirrhosis using SonoVue and showed shorter hepatic vein arrival times and prolonged peak times in cirrhotic patients compared with controls (8). A systematic review and meta-analysis by Kim et al. concluded that CEUS demonstrates promising diagnostic potential but requires further validation (5).

Cocciolillo et al. reported that perfusion alterations detected by CEUS may precede measurable fibrosis in MASLD (9), while additional biopsy-correlated studies confirmed that CEUS may help exclude severe fibrosis (10). CEUS has also been used to predict esophageal varices through TIC-derived parameters (11).

Yoshimine et al. applied At-PI in primary biliary cholangitis and reported AUROC values of 0.77 and 0.92 for F2 and F3 fibrosis, respectively (12).

Diagnostic Performance of CEUS-PAT. High diagnostic performance has been reported in individual studies, with AUROC values approaching 0.98 in

selected cohorts, with a strong correlation observed between CEUS-PAT and VCTE (r = 0.81) (13).

Newer elastographic techniques have shown similar or slightly lower diagnostic performance compared with CEUS-PAT in cirrhosis detection (14, 15). Although elastography remains well validated for fibrosis staging (16, 17), perfusion-based imaging provides complementary functional information.

Pathophysiological Interpretation. Advanced fibrosis shortens microvascular transit time due to increased intrahepatic resistance and arterialization of hepatic blood supply (1). Additionally, sinusoidal remodeling may alter microbubble retention dynamics. PAT imaging captures these functional perfusion changes rather than purely mechanical stiffness alterations.

Conclusion on this topic. Parametric Arrival Time (PAT) / Arrival-Time Parametric Imaging (At-PI) is a promising CEUS-based technique for assessing hepatic microcirculatory changes associated with liver fibrosis. By converting contrast arrival times into perfusion maps, this method provides functional information on intrahepatic hemodynamics that complements stiffness-based techniques such as elastography.

Several studies have shown that shortened contrast arrival times correlate with increasing fibrosis severity and cirrhosis, reflecting progressive vascular remodeling and intrahepatic shunting in chronic liver disease. Although elastography remains the standard noninvasive method for fibrosis staging, CEUS-PAT may provide additional diagnostic value within a multiparametric ultrasound approach.

15.2. Microflow Imaging

Microflow imaging represents a recent advancement in Doppler ultrasound technology that enables visualization of slow blood flow within small vessels that are often undetectable using conventional colour Doppler or power Doppler techniques. Traditional Doppler imaging uses wall filters to suppress motion artifacts caused by tissue movement; however, these filters may also eliminate signals originating from low-velocity blood flow in microvessels. Microflow imaging technologies use advanced clutter suppression algorithms that can differentiate true blood-flow signals from tissue motion artifacts, thereby allowing improved visualization of microvascular circulation (18).

Technical Principles. Modern microvascular Doppler techniques rely on adaptive filtering methods that preserve slow flow signals while removing background tissue motion. Several ultrasound manufacturers have developed proprietary microvascular imaging technologies, including Superb Microvascular Imaging (SMI), Microvascular Flow Imaging (MV-Flow), and Microvascular Imaging (MVI). These techniques allow detailed visualization of small vessels without the need for contrast agents and with improved spatial resolution compared with conventional Doppler techniques (18, 19).

Because tumor angiogenesis often involves the development of abnormal microvascular networks, visualization of microvascular flow may provide valuable diagnostic information. Microflow imaging can therefore reveal vascular patterns that may not be detectable with standard Doppler imaging (20).

Clinical Applications. Microflow imaging has been increasingly applied in the evaluation of focal lesions in various organs. In hepatology, it may improve visualization of intratumoral vascularity in hepatocellular carcinoma and metastatic liver lesions. Malignant tumours typically demonstrate irregular, tortuous microvascular patterns reflecting tumour angiogenesis, whereas benign lesions may exhibit more organized vascular structures (20, 21).

In addition to liver imaging, microflow techniques have been studied in several other clinical fields, including breast and thyroid. Improved visualization of microvascular architecture may assist in differentiating benign from malignant lesions and may enhance diagnostic confidence during ultrasound examinations (19-22).

Microflow imaging may also contribute to treatment monitoring following locoregional therapies such as radiofrequency or microwave ablation of hepatocellular carcinoma. The detection of residual intratumoral vascular signals may indicate the presence of viable tumor tissue after treatment (22).

Limitations. Despite its advantages, microflow imaging has certain limitations. Visualization of microvascular flow may be affected by patient motion, respiratory movement, lesion depth, and acoustic window. In addition, the technique remains operator dependent and may require optimized ultrasound settings to achieve optimal image quality (18, 19).

Conclusion on this topic. Microflow imaging represents a valuable advancement in Doppler ultrasound technology, allowing improved visualization of microvascular circulation without the need for contrast agents. When combined with other advanced ultrasound techniques such as contrast-enhanced ultrasound and elastography, it may contribute to a more comprehensive assessment of tissue perfusion and tumour vascularity in clinical practice.

15.3. Image Fusion Ultrasonography

Image fusion ultrasonography combines real-time ultrasound with previously acquired computed tomography (CT) or magnetic resonance imaging (MRI), allowing simultaneous visualization of live sonographic images and cross-sectional datasets. This approach improves lesion localization, diagnostic confidence, and procedural guidance, especially in hepatology, oncology, and interventional radiology (23).

Ultrasound offers several advantages, including real-time imaging, wide availability, and the absence of ionizing radiation. However, conventional ultrasound may have limited sensitivity for detecting small or deeply located lesions. In contrast, CT and MRI provide superior anatomical detail and higher sensitivity for lesion detection but cannot offer real-time procedural guidance. Image fusion ultrasonography overcomes these limitations by synchronizing ultrasound with CT or MRI datasets, enabling accurate targeting of lesions detected on cross-sectional imaging during ultrasound-guided interventions (23, 24).

Principles of Fusion Imaging. The basic principle of fusion imaging is spatial co-registration between real-time ultrasound and previously acquired CT or MRI images. This process allows the ultrasound probe position to correspond precisely to the correct anatomical location within the cross-sectional dataset. Registration is typically achieved by identifying anatomical landmarks such as vascular structures or organ contours and by using electromagnetic tracking systems that monitor the position and orientation of the ultrasound probe (23, 25).

Once the datasets are aligned, the ultrasound system continuously updates the corresponding CT or MRI plane as the probe moves, allowing simultaneous visualization of both imaging modalities. This real-time

correlation facilitates accurate lesion localization and improves procedural guidance during interventional procedures (25).

Fusion imaging can be further enhanced by contrast-enhanced ultrasound (CEUS). The administration of microbubble contrast agents allows dynamic evaluation of lesion vascularization and perfusion patterns, thereby improving lesion conspicuity and characterization. CEUS is particularly useful in the evaluation of focal liver lesions and in the detection of residual viable tumour tissue following ablation therapies (26).

Clinical Applications. One of the most important clinical applications of fusion imaging is in liver oncology, particularly in patients with hepatocellular carcinoma (HCC). Fusion imaging improves the targeting of lesions that are difficult to visualize on conventional ultrasound and increases confidence during percutaneous ablation procedures (24, 27).

Several studies have demonstrated that fusion imaging allows accurate localization and treatment of hepatic tumours that are visible on CT or MRI but poorly visible on ultrasound alone. This approach has been shown to improve the feasibility and technical success of radiofrequency ablation and other percutaneous therapies (25, 28).

Fusion imaging is also useful for image-guided biopsies and other interventional procedures because it allows correlation between the needle trajectory and lesions previously characterized on CT or MRI. As a result, fusion imaging may improve diagnostic yield and reduce the need for CT-guided procedures, thereby lowering radiation exposure (25).

Limitations. Despite its advantages, fusion imaging presents certain technical challenges. Registration errors may occur due to differences in patient positioning, respiratory motion, or organ deformation between the time of CT or MRI acquisition and the ultrasound examination. These factors may affect spatial alignment and require manual adjustment during the procedure (23, 25).

In addition, successful use of fusion imaging requires operator experience and familiarity with both ultrasound and cross-sectional imaging interpretation. The availability of dedicated hardware and software may also limit the widespread implementation of this technique in some institutions (23).

Future Perspectives. Recent technological developments aim to improve the accuracy and usability of fusion imaging systems. Advances in

navigation systems, artificial intelligence, and automated image-registration algorithms may further enhance multimodal image alignment and reduce operator dependency (29, 30).

These innovations may expand the role of fusion imaging in interventional radiology and precision medicine, particularly in the management of focal liver lesions and minimally invasive oncologic therapies.

Conclusion on this topic. Image fusion ultrasonography represents an important advancement in diagnostic and interventional imaging. By integrating real-time ultrasound with high-resolution cross-sectional imaging modalities such as CT and MRI, fusion imaging improves lesion detection, procedural accuracy, and treatment guidance. Continued technological developments are expected to further expand its clinical applications in the future.

15.4. Ultrasound-Mediated Drug Delivery

Ultrasound-mediated drug delivery has emerged as a promising strategy for targeted therapy by combining imaging guidance with localized drug release. This technique uses acoustic energy to enhance the penetration and accumulation of therapeutic agents in specific tissues, thereby increasing treatment efficacy while reducing systemic toxicity (31). Ultrasound-assisted drug delivery has attracted considerable interest in oncology, neurology, and hepatology, where conventional systemic therapies often suffer from limited drug penetration and significant side effects.

Mechanisms of Ultrasound-Enhanced Drug Delivery. The most important mechanism involved in ultrasound-mediated drug delivery is sonoporation, a process in which ultrasound waves temporarily increase cell membrane permeability. This effect allows drugs, nucleic acids, or nanoparticles to enter cells more efficiently. Sonoporation is often facilitated by the presence of microbubbles, which oscillate under ultrasound exposure and generate mechanical forces that enhance vascular permeability and drug extravasation (32).

Two main cavitation phenomena are involved in this process: stable cavitation, characterized by oscillation of microbubbles, and inertial cavitation, which involves bubble collapse and the generation of strong mechanical forces. These acoustic effects can transiently disrupt endothelial barriers and facilitate the penetration of therapeutic molecules into the surrounding tissue (32, 33).

Microbubbles and Nanocarriers. Recent advances in nanotechnology have led to the development of ultrasound-responsive carriers, including drug-loaded microbubbles and nanodroplets. These carriers can transport chemotherapeutic agents, genes, or proteins through the circulation and release them locally when exposed to ultrasound. This targeted release allows spatial and temporal control of drug delivery and may significantly improve therapeutic specificity (34).

New strategies also include theragnostic microbubbles, which combine imaging and therapeutic functions. These agents can be visualized using ultrasound imaging while simultaneously acting as drug carriers, enabling real-time monitoring of drug delivery and treatment response (35).

Emerging Clinical Applications. Recent research has explored ultrasound-mediated drug delivery in several clinical fields. In oncology, this technique has been investigated for improving the delivery of chemotherapeutic agents into solid tumours, where abnormal tumour vasculature often limits drug penetration. Ultrasound-activated microbubbles can increase intratumoral drug uptake and improve local therapeutic effects (34, 36).

Another promising application involves the temporary opening of biological barriers, such as the blood–brain barrier (BBB). Focused ultrasound combined with microbubbles has been shown to safely and reversibly increase BBB permeability, allowing therapeutic agents to reach brain tissue that is normally inaccessible to many drugs (37).

Future Perspectives. Recent studies highlight the rapid development of ultrasound-responsive nanocarriers and targeted microbubble systems. These technologies may enable more precise drug delivery and support personalized treatment strategies. Advances in ultrasound physics and microbubble engineering are also improving control over drug release kinetics and tissue targeting (35, 38).

With continued technological progress and improved understanding of acoustic bioeffects, ultrasound-mediated drug delivery is expected to become an important component of image-guided therapies in oncology and other fields.

Conclusion on the topic. Ultrasound-mediated drug delivery represents a rapidly evolving therapeutic strategy that combines imaging guidance with targeted drug release. Through mechanisms such as sonoporation and microbubble-mediated cavitation, ultrasound can enhance drug penetration and improve therapeutic efficacy. Ongoing developments in nanotechnology and ultrasound physics are likely to expand the clinical applications of this approach in the coming years.

References

1. Mueller S. Does pressure cause liver cirrhosis? World J Gastroenterol. 2016;22:10482–10501.
2. Friedman SL. Evolving challenges in hepatic fibrosis. Nat Rev Gastroenterol Hepatol. 2010;7:425–436.
3. Claudon M, Dietrich CF, Choi BI, Cosgrove DO, Kudo M, Nolsøe CP, et al. Guidelines and good clinical practice recommendations for contrast enhanced ultrasound (CEUS) in the liver--update 2012: a WFUMB-EFSUMB initiative in cooperation with representatives of AFSUMB, AIUM, ASUM, FLAUS and ICUS. Ultraschall Med. 2013;34(1):11-29.
4. Wakui N, Takayama R, Kanekawa T, Ichimori M, Otsuka T, Shinohara M, et al. Usefulness of arrival time parametric imaging in chronic hepatitis C. J Ultrasound Med. 2012;31:373–382.
5. Kim G, Shim KY, Baik SK. Diagnostic accuracy of hepatic vein arrival time for cirrhosis: systematic review and meta-analysis. Gut Liver. 2017;11:93–101.
6. Ridolfi F, Abbattista T, Marini F, Vedovelli A, Quagliarini P, Busilacchi P, et al. CEUS to evaluate severity of chronic hepatitis C. Dig Liver Dis. 2007;39:929–935.
7. Fujita Y, Watanabe M, Sasao K, Wakui N, Shinohara M, Ishii K, et al. Investigation of liver parenchymal flow using CEUS in alcoholic liver disease. Alcohol Clin Exp Res. 2004;28:169S–173S.
8. Ying M, Leung G, Lau TY, Tipoe GL, Lee ES, Yuen QW, et al. Evaluation of liver fibrosis using CEUS: an animal study. J Clin Ultrasound. 2012;40:462–470.
9. Cocciolillo S, Parruti G, Marzio L. CEUS and Fibroscan in NAFLD/NASH. World J Hepatol. 2014;6:496–503.
10. Nasr P, Hilliges A, Thorelius L, Kechagias S, Ekstedt M. CEUS differentiation of fibrosis stages in NAFLD. Scand J Gastroenterol. 2016;51:1126–1132.
11. Li J, Feng JC, Peng XY, Wu XW, Du TT, Wang JJ, et al. CEUS for predicting esophageal varices in HBV cirrhosis. Med Sci Monit. 2017;23:2241–2249.
12. Yoshimine N, Wakui N, Nagai H, Igarashi Y. Arrival-Time Parametric Imaging in Contrast-Enhanced Ultrasound for Diagnosing Fibrosis in Primary Biliary Cholangitis. Ultrasound Q. 2022 Jun 1;38(2):191-199.

13. Lupușoru R, Sporea I, Rațiu I, Lungeanu D, Popescu A, Dănilă M**, et al.** Contrast-enhanced ultrasonography with arrival time parametric imaging as a non-invasive diagnostic tool for liver cirrhosis. **Diagnostics (Basel).** 2022;12(12):3013.
14. Sporea I, Sirli R, Deleanu A, Tudora A, Curescu M, Cornianu M, et al. Comparison of liver stiffness measurement by transient elastography with biopsy. World J Gastroenterol. 2008;14:6513–6517.
15. Friedrich-Rust M, Ong MF, Martens S, Sarrazin C, Bojunga J, Zeuzem S, et al. Performance of transient elastography: meta-analysis. Gastroenterology. 2008;134:960–974.
16. Ferraioli G, Filice C, Castera L, Choi BI, Sporea I, Wilson SR, et al. WFUMB guidelines for liver elastography. Ultrasound Med Biol. 2015;41:1161–1179.
17. Ferraioli G, Wong VW, Castera L, Berzigotti A, Sporea I, Dietrich CF, et al. Liver ultrasound elastography update. Ultrasound Med Biol. 2018;44:2419–2440.
18. Aziz MU, Eisenbrey JR, Deganello A, Zahid M, Sharbidre K, Sidhu P, et al. Microvascular Flow Imaging: A State-of-the-Art Review of Clinical Use and Promise. Radiology. 2022 Nov;305(2):250-264.
19. Zhan J, Diao XH, Jin JM, Chen L, Chen Y. Superb Microvascular Imaging-A new vascular detecting ultrasonographic technique for avascular breast masses: A preliminary study. Eur J Radiol. 2016 May;85(5):915-21.
20. Machado P, Segal S, Lyshchik A, Forsberg F. A Novel Microvascular Flow Technique: Initial Results in Thyroids. Ultrasound Q. 2016 Mar;32(1):67-74.
21. Wilson A, Lim AKP. Microvascular imaging: new Doppler technology for assessing focal liver lesions. Is it useful? Clin Radiol. 2022 Dec;77(12):e807-e820.
22. Ota Y, Aso K, Yokoo H, Fujiya M. Noninvasive Visualization of Tumor Blood Vessels within Hepatocellular Carcinoma by Application of Superb Microvascular Imaging to Contrast-Enhanced Ultrasonography. Diagnostics (Basel). 2024 Mar 23;14(7):678.
23. Ewertsen C, Săftoiu A, Gruionu LG, Karstrup S, Nielsen MB. Real-time image fusion involving diagnostic ultrasound. AJR Am J Roentgenol. 2013 Mar;200(3):W249-55.
24. Minami Y, Kudo M. Ultrasound fusion imaging of hepatocellular carcinoma: a review of current evidence. Dig Dis. 2014;32(6):690-5.
25. Mauri G, Cova L, De Beni S, Ierace T, Tondolo T, Cerri A, et al. Real-time US-CT/MRI image fusion for guidance of thermal ablation of liver tumors undetectable with US: results in 295 cases. Cardiovasc Intervent Radiol. 2015 Feb;38(1):143-51.
26. Dietrich CF, Nolsøe CP, Barr RG, Berzigotti A, Burns PN, Cantisani V, et. Guidelines and Good Clinical Practice Recommendations for Contrast Enhanced Ultrasound (CEUS) in the Liver - Update 2020 - WFUMB in Cooperation with EFSUMB, AFSUMB, AIUM, and FLAUS. Ultraschall Med. 2020 Oct;41(5):562-585.
27. Makino Y, Imai Y, Igura T, Ohama H, Kogita S, Sawai Y, et al. Usefulness of the multimodality fusion imaging for the diagnosis and treatment of hepatocellular carcinoma. Dig Dis. 2012;30(6):580-7.

28. Song KD, Lee MW, Rhim H, Cha DI, Chong Y, Lim HK. Fusion imaging-guided radiofrequency ablation for hepatocellular carcinomas not visible on conventional ultrasound. AJR Am J Roentgenol. 2013 Nov;201(5):1141-7.
29. European Society of Radiology (ESR). Abdominal applications of ultrasound fusion imaging technique: liver, kidney, and pancreas. Insights Imaging. 2019 Jan 28;10(1):6.
30. York B, Beutler BD, Lewis LM, Chang EY, Shah I, Ballard A, et al. Ultrasound Fusion in Interventional Radiology: A Practical Guide to Procedural Applications. J Vasc Interv Radiol. 2026 Jan;37(1):107799.
31. Bouakaz A, Michel Escoffre J. From concept to early clinical trials: 30 years of microbubble-based ultrasound-mediated drug delivery research. Adv Drug Deliv Rev. 2024 Mar;206:115199.
32. Tu J, Yu ACH. Ultrasound-Mediated Drug Delivery: Sonoporation Mechanisms, Biophysics, and Critical Factors. BME Front. 2022 Jan 29;2022:9807347.
33. Li X, Liu Y. Focused ultrasound in modern medicine: bioengineering interfaces, molecular effects, and clinical breakthroughs. Front Bioeng Biotechnol. 2025 Aug 29;13:1610846.
34. Shakya G, Cattaneo M, Guerriero G, Prasanna A, Fiorini S, Supponen O. Ultrasound-responsive microbubbles and nanodroplets: A pathway to targeted drug delivery. Adv Drug Deliv Rev. 2024 Mar;206:115178.
35. Zhang C, Zhang Q, Xu Q, Jiang X, Ma Y, Liu C, et al. Ultrasound targeted microbubbles for theranostic applications in liver diseases: from molecular imaging to targeted therapy. Drug Deliv. 2025 Dec;32(1):2541656.
36. Ibsen S, Schutt CE, Esener S. Microbubble-mediated ultrasound therapy: a review of its potential in cancer treatment. Drug Des Devel Ther. 2013 May 3;7:375-88.
37. Wei HJ, Upadhyayula PS, Pouliopoulos AN, Englander ZK, Zhang X, Jan CI, et al. Focused Ultrasound-Mediated Blood-Brain Barrier Opening Increases Delivery and Efficacy of Etoposide for Glioblastoma Treatment. Int J Radiat Oncol Biol Phys. 2021 Jun 1;110(2):539-550..
38. Patel PB, Latt S, Ravi K, Razavi M. Clinical Applications of Micro/Nanobubble Technology in Neurological Diseases. Biomimetics (Basel). 2024 Oct 20;9(10):645.

16. Artificial Intelligence in Liver Ultrasound

Ioan Sporea, Alexandru Popa

Abstract

Ultrasonography has undergone rapid modernization driven by artificial intelligence (AI), transitioning from an operator-dependent, predominantly qualitative modality to a more quantitative, automated, and increasingly standardized diagnostic tool. These advances have been particularly impactful for liver ultrasound, which is widely used for screening, diagnosis, and longitudinal monitoring of chronic liver diseases. Modern AI applications encompass (i) ultrasomics (radiomics applied to ultrasound), (ii) automated identification of standard scan planes and anatomical structures, (iii) AI-assisted detection and characterization of focal liver lesions (FLLs), (iv) interpretation of contrast-enhanced ultrasound (CEUS), (v) optimization and quality control of shear-wave elastography (SWE), and (vi) multiparametric ultrasound (MPUS) models that integrate B-mode, Doppler, CEUS kinetics, attenuation and backscatter parameters, and elastography into clinically actionable outputs.

Additional emerging areas include robotic/telerobotic ultrasound, simulation and virtual reality (VR)-enhanced teaching, and new ethical challenges related to AI-generated images and algorithmic bias. Overall, the literature suggests that AI can improve workflow efficiency, repeatability, and diagnostic accuracy across a range of liver applications, while supporting—rather than replacing—clinical expertise. As the field moves from proof-of-concept to broader clinical integration, robust prospective validation, transparent reporting, and responsible governance remain essential.

16.1. Introduction

Artificial intelligence (AI) has become a major driver of innovation in medical imaging, including ultrasound. In this context, AI broadly refers to computational methods that enable machines to perform tasks typically requiring human intelligence, while machine learning (ML) and deep learning (DL) represent subsets that learn patterns from data. Deep learning architectures—particularly convolutional neural networks (CNNs)—have been instrumental for image classification, segmentation, and detection, while newer attention-based models can capture complex spatial relationships in imaging data.

Ultrasound has historically been considered subjective and operator-dependent, with variability introduced by acquisition technique, equipment settings, patient habitus, and interpretation. AI is reshaping this landscape by enabling automated image enhancement, standardized acquisition guidance, quantitative feature extraction, and decision support. Liver ultrasound is a prominent beneficiary because it is commonly used worldwide for chronic liver disease screening and follow-up, including steatotic liver disease and fibrosis assessment, evaluation of portal hypertension surrogates, and characterization of focal lesions. AI now supports multiple steps of the ultrasound pathway: (i) acquisition (scan-plane recognition and guidance), (ii) image optimization (noise/speckle reduction and parameter standardization), (iii) analysis (segmentation, quantification, and lesion detection), and (iv) reporting (structured outputs and risk stratification).

16.2. Evolution of AI in ultrasonography

The evolution of AI in ultrasound in our local experience, can be summarized in pragmatic stages, reflecting both computational progress and clinical translation:

2013–2017: ***Early computer-assisted diagnosis (CAD) with handcrafted features*****.**

During this period, CAD systems primarily relied on predefined texture descriptors and classical ML classifiers (e.g., random forests, support vector machines). In liver ultrasound, early approaches addressed tasks such as steatosis grading using B-mode texture and echogenicity-related features (1). These systems were limited by variability in image quality, vendor-specific post-processing, and relatively modest dataset sizes.

2017–2021: ***Deep learning enables robust classification, segmentation, and detection.***

The expansion of DL—particularly CNNs—enabled more powerful feature learning directly from ultrasound images. This period saw growth in automatic organ identification, scan-plane recognition, and lesion localization. In parallel, AI support for CEUS interpretation and lesion characterization began to mature, including prototypes aiming to aid less-experienced operators in FLL assessment (2). Multiparametric strategies integrating several ultrasound dimensions were also explored (3).

2021–present: ***Real-time AI embedded in ultrasound platforms and workflow.***

Modern ultrasound systems increasingly include AI modules that operate in real time, such as:

- automatic enhancement of B-mode images,
- recognition of standard abdominal cross-sections and anatomy (4),
- lesion detection/measurement with automated contouring and quantification,
- quality-guided SWE acquisition with automated ROI selection and artifact avoidance,
- CEUS curve extraction and perfusion-kinetic analysis.

These developments aim to reduce interobserver variability and improve reproducibility, but they also introduce new requirements for validation across devices, centers, and patient subgroups, as well as transparency regarding training data, failure modes, and human–AI interaction.

16.3. Ultrasomics: a modern paradigm for quantification

Ultrasomics refers to the extraction of high-dimensional quantitative features from ultrasound data - analogous to radiomics in CT/MRI - but adapted to ultrasound's unique properties (speckle, operator dependence, and vendor variability). Ultrasomics can leverage B-mode, Doppler, elastography, and CEUS cine loops to generate feature signatures reflecting texture, shape, stiffness distribution, and temporal enhancement patterns.

16.3.1 Ultrasomics Workflow

A typical ultrasomics pipeline includes:

1. ***Standardized data acquisition*** (B-mode, Doppler, elastography, CEUS), ideally with harmonized presets and consistent probe/frequency settings.
2. Segmentation of the organ region or the focal lesion—manual, semi-automatic, or automated using DL segmentation networks. Scan-plane recognition and anatomy labeling can further support standardization (4).
3. **Feature extraction**, including:
    - first-order intensity statistics,

- textural features (e.g., gray-level co-occurrence/run-length matrices),
- shape/morphology descriptors,
- elastography-derived stiffness distributions and heterogeneity metrics,
- CEUS temporal features (wash-in, peak, wash-out, time-to-peak).

4. ***Model building and integration*** using ML/DL, optionally combining imaging signatures with clinical variables, laboratory data, and biomarkers to produce interpretable outputs (risk estimates, probability scores, or ordinal staging).

16.3.2 Clinical Applications

Ultrasomics has been explored for:

- FLL characterization (benign vs malignant; subtype discrimination), including performance comparable to expert radiologists in selected tasks and incremental gains when combined with radiologist assessment (5).
- Steatosis quantification, leveraging pixel-level patterns and attenuation-related signatures; systematic reviews report promising performance, but emphasize heterogeneity and limited external validation (6).
- Fibrosis staging and portal hypertension prediction, using B-mode features, surface nodularity surrogates, and elastography maps to improve staging and reduce measurement variability (7-9).
- **Therapy response assessment**, particularly in oncology, where CEUS kinetics and textural changes may serve as early biomarkers.
- ***Personalized models*** combining imaging features with biomarkers, to support individualized risk stratification.

16.4. AI for chronic liver disease (fatty liver and fibrosis assessment)

Steatotic liver disease, now framed within the MASLD/MASH nomenclature, represents a major global health burden. Contemporary guidelines emphasize structured case-finding strategies, use of non-invasive tests, and risk stratification for advanced fibrosis (10). Epidemiologic data suggest a high and increasing global prevalence of fatty liver disease, reinforcing the need for scalable, reproducible imaging tools (11).

16.4.1. AI in Fatty Liver Detection

Traditional B-mode ultrasound detects steatosis based on qualitative surrogates (increased echogenicity, attenuation, vessel blurring), but performance depends on operator skill and steatosis severity. AI approaches attempt to:

- standardize B-mode interpretation,
- quantify echogenicity/attenuation patterns,
- reduce dependence on subjective grading.

Systematic reviews indicate that AI can achieve high diagnostic performance for fatty liver detection and quantification, but underline challenges such as dataset heterogeneity, lack of consistent reference standards, and limited multicenter validation (6). In parallel, MPUS approaches that incorporate attenuation and backscatter-based quantitative ultrasound (QUS) parameters are increasingly aligned with international guidance on liver fat quantification (12).

16.4.2. AI for Fibrosis Assessment

Fibrosis staging is central for prognosis and management decisions. SWE provides quantitative stiffness but remains susceptible to technical variability (respiration, obesity, inflammation, congestion) and operator dependence. AI can enhance fibrosis assessment by:

- analyzing B-mode features (surface nodularity, texture heterogeneity),
- using elastography maps (stiffness distribution, quality indices),
- integrating multi-source features into robust staging models.

Recent automated ultrasound image-based frameworks have reported reliable fibrosis stage classification (7). In SWE specifically, DL-radiomics approaches have shown improved diagnostic performance in multicenter prospective settings (8). International guidance also supports structured acquisition and quality control principles that AI modules can help implement in routine practice (13, 14).

16.5. AI for focal liver lesions (FLL) detection and characterization

FLLs remain a frequent indication for ultrasound examinations, spanning incidental findings to surveillance-detected nodules in at-risk patients. AI contributes at two clinical levels: improving ***detection*** and assisting ***characterization***, particularly when multimodal ultrasound data are available.

16.5.1. Automated Lesion Detection

Real-time detection models can highlight suspected lesions, delineate boundaries, and automate measurement (size, shape, growth). This may be valuable for surveillance workflows and follow-up comparisons, especially when combined with scan-plane standardization and structured reporting. However, detection performance can be influenced by background parenchymal heterogeneity (e.g., cirrhosis), lesion conspicuity, and operator scanning coverage—factors that require careful evaluation in prospective settings.

16.5.2. CEUS Interpretation

CEUS provides real-time assessment of enhancement patterns and lesion vascular kinetics. AI tools can analyze:

- enhancement pattern classes,
- wash-in/wash-out behavior,
- quantitative time – intensity curves,
- microbubble distribution dynamics.

Systematic reviews support a growing evidence base for AI-assisted FLL classification using ultrasound/CEUS data, while highlighting variability across study design and reference standards (15). Clinical perspective papers also emphasize that AI may reshape future ultrasound-based HCC detection and characterization, but must be integrated responsibly with existing diagnostic pathways (16). Recently, CEUS-based AI models have been reported for multi-class FLL classification, approaching high diagnostic performance in specialized cohorts (17). These developments align conceptually with international recommendations for CEUS use in the liver, which stress standardized acquisition and interpretation - an area where AI may provide consistency and decision support (18).

16.6. AI in liver elastography

SWE and related elastography techniques have transformed fibrosis assessment, but remain affected by operator dependency and technical artifacts. AI offers important improvements by supporting acquisition quality, ROI placement, and automated interpretation.

16.6.1. AI-Based Frame Selection

Real-time algorithms can evaluate cine loops and exclude frames affected by motion, poor coupling, breathing artifacts, or propagation failure. Such approaches mirror consensus recommendations emphasizing quality control, reliable acquisition conditions, and standardized reporting for liver elastography (14).

16.6.2. Automatic ROI Placement

AI can position ROIs in homogeneous parenchyma while avoiding vessels, biliary structures, and artifact-prone areas. Automated guidance can reduce variability between operators and potentially improve feasibility in difficult examinations. These functions are consistent with WFUMB guidance emphasizing standardized elastography methodology and reliability (13).

16.6.3. Evidence

DL-radiomics applied to SWE has demonstrated improved diagnostic performance for liver fibrosis assessment in prospective multicenter cohorts, particularly in chronic hepatitis B (8). Beyond accuracy, a key clinical gain is improved repeatability and robustness—attributes crucial for longitudinal monitoring and population-level screening.

16.7. Multiparametric ultrasound (MPUS) of the liver and AI

MPUS integrates multiple ultrasound modalities into unified diagnostic models, aiming to approximate the "granularity" of histologic phenotyping using non-invasive data. A typical MPUS framework may combine:

- B-mode morphologic features,
- Liver (and increasingly spleen) Shear Wave Elastography,
- QUS fat metrics (attenuation/backscatter-related parameters),
- Doppler-derived hemodynamic surrogates,
- CEUS kinetics and pattern-based interpretation (17, 19).

Recent WFUMB guidance explicitly addresses liver multiparametric ultrasound (MPUS), emphasizing standardized methodology and interpretation for elastography and for liver fat quantification, thereby creating a foundation for clinically reliable MPUS-AI models (13, 12).

Destrempes et al. demonstrated that combining quantitative ultrasound parameters with elastography and ML can support simultaneous assessment of steatosis, inflammation, and fibrosis, approaching biopsy-like

stratification in selected cohorts (19). Importantly, future MPUS translation will depend not only on performance metrics, but also on interpretability, calibration, and clinically meaningful outputs (e.g., probability of clinically significant fibrosis, risk categories, and monitoring thresholds).

16.8. AI in ultrasound education and training

AI is increasingly used to support ultrasound education through simulation, structured feedback, and individualized learning pathways.

Virtual Reality (VR).

VR can recreate scanning scenarios for repeated practice without patient risk. Randomized studies suggest that immersive VR training can be non-inferior to traditional instruction, for certain ultrasound skills acquisition (20). In CEUS education, VR simulation has been used to develop competency-based assessments and validity evidence for core skill testing (21).

Intelligent Tutor Systems

AI-enabled tutor systems can provide real-time feedback, identify scanning errors, and guide learners toward standard views. WFUMB state-of-the-art work highlights the role of simulators in improving learning outcomes and reducing pressure on clinical lists, providing a framework for broader adoption of AI-enhanced simulation (22).

16.9. Radiomics and machine learning in chronic liver disease

Radiomics - high-dimensional feature extraction coupled with ML - can generate signatures associated with disease stage and prognosis. In liver disease, ultrasound radiomics has been explored for:

- early fibrosis detection (9),
- prediction of clinically significant fibrosis and portal hypertension surrogates,
- risk of decompensation,
- prediction of hepatocellular carcinoma development in high-risk populations.

A critical challenge is reproducibility: radiomics features can be sensitive to acquisition parameters, vendor differences, and preprocessing. Therefore, robust external validation, harmonization strategies, and transparent reporting are necessary to avoid overfitting and ensure clinical utility.

16.10. AI-generated ultrasound images and ethics

Generative AI can synthesize ultrasound-like images, potentially aiding education, data augmentation, and method development. However, it raises concerns about:

- ***data provenance and authenticity,***
- ***misuse in research*** (fabrication or undisclosed synthetic data),
- ***bias amplification,***
- ***blurred boundaries between educational and diagnostic content.***

Research integrity and publication ethics discussions increasingly address AI-related risks, emphasizing transparency, disclosure, and rigorous review mechanisms (23,24). To support trustworthy translation, AI ultrasound research should align with established reporting and evaluation frameworks. Widely cited guidance includes the CLAIM 2024 update for medical imaging AI (25), TRIPOD+AI for prediction models (26), STARD-AI for AI-centered diagnostic accuracy studies (27), CONSORT-AI for AI clinical trials (28), SPIRIT-AI for trial protocols (29), and DECIDE-AI for early-stage clinical evaluation of decision support systems (30).

16.11. Robotic and autonomous ultrasound

Robotic ultrasound combines AI-driven optimization with probe navigation and force control, with applications in:

- ***telemedicine/telerobotic scanning,***
- ***standardized acquisition*** in screening programs,
- ***reduction of operator physical strain,***
- ***autonomous scanning research*** (semi-autonomous and fully autonomous systems).

Recent surveys describe teleoperated and autonomous robotic ultrasound systems and highlight key technical barriers (path planning, force control, safety, and real-time image quality assessment) as well as promising clinical directions (31). Early studies of autonomous robotic scanning pipelines suggest potential improvements in reproducibility and observer consistency, though liver-specific autonomous workflows still require careful validation across anatomy, body habitus, and breathing variability (32).

16.12. Conclusion

AI is reshaping hepatic ultrasonography by improving standardization, diagnostic performance, and reproducibility across steatosis assessment, fibrosis staging and elastography quality control, lesion detection/characterization, CEUS interpretation, and multiparametric modeling. The clinical trajectory points toward “precision hepatology” supported by quantitative ultrasound and integrated decision support - expanding access to consistent, high-quality imaging without replacing clinician expertise. The next stage of progress requires rigorous prospective validation, careful assessment of generalizability, and adherence to transparent reporting and ethical governance frameworks to ensure safe and responsible clinical integration.

References

1. Mihăilescu DM, Gui V, Toma CI, Popescu A, Sporea I. Computer aided diagnosis method for steatosis rating in ultrasound images using random forests. Med Ultrason. 2013;15(3):184-90.
2. Moga TV, Popescu A, Sporea I, Danila M, David C, Gui V, et al. Is Contrast Enhanced Ultrasonography a useful tool in a beginner’s hand? How much can a Computer Assisted Diagnosis prototype help in characterizing the malignancy of focal liver lesions? Med Ultrason. 2017;19(3):252-258.
3. Moga TV, David C, Popescu A, Lupusoru R, Heredea D, Ghiuchici AM, et al. Multiparametric Ultrasound Approach Using a Tree-Based Decision Classifier for Inconclusive Focal Liver Lesions Evaluated by Contrast Enhanced Ultrasound. J Pers Med. 2021;11(9):1388.
4. Lawley A, Hampson R, Worrall K, Dobie G. Analysis of neural networks for routine classification of sixteen ultrasound upper abdominal cross sections. Abdom Radiol (NY). 2024;49:651-661.
5. Li W, Lv X, Zheng X, Ruan S, Hu H, Chen J, et al. Machine learning-based ultrasomics improves the diagnostic performance in differentiating focal nodular hyperplasia and atypical hepatocellular carcinoma. Front Oncol. 2021;11:544979.
6. Alshagathrh FM, Househ MS. Artificial Intelligence for Detecting and Quantifying Fatty Liver in Ultrasound Images: A Systematic Review. Bioengineering (Basel). 2022;9(12):748.

7. Park HC, Joo Y, Lee OJ, Lee K, Song TK, Choi C, et al. Automated classification of liver fibrosis stages using ultrasound imaging. BMC Med Imaging. 2024;24(1):36.
8. Wang K, Lu X, Zhou H, Gao Y, Zheng J, Tong M, et al. Deep learning Radiomics of shear wave elastography significantly improved diagnostic performance for assessing liver fibrosis in chronic hepatitis B: a prospective multicentre study. Gut. 2019;68(4):729-741.
9. Al-Hasani M, Sultan LR, Sagreiya H, Cary TW, Karmacharya MB, Sehgal CM. Ultrasound Radiomics for the Detection of Early-Stage Liver Fibrosis. Diagnostics (Basel). 2022;12(11):2737.
10. European Association for the Study of the Liver (EASL); European Association for the Study of Diabetes (EASD); European Association for the Study of Obesity (EASO). EASL-EASD-EASO Clinical Practice Guidelines on the management of metabolic dysfunction-associated steatotic liver disease (MASLD). J Hepatol. 2024 Sep;81(3):492-542.
11. Younossi ZM, Golabi P, Paik JM, Henry A, Van Dongen C, Henry L. The global epidemiology of nonalcoholic fatty liver disease (NAFLD) and nonalcoholic steatohepatitis (NASH): a systematic review. Hepatology. 2023 Apr 1;77(4):1335-1347.
12. Ferraioli G, Barr RG, Berzigotti A, Sporea I, Wong VWS, Reiberger T, et al. WFUMB Guidelines/Guidance on Liver Multiparametric Ultrasound. Part 2: Guidance on Liver Fat Quantification. Ultrasound Med Biol. 2024;50(8):1088-1098.
13. Ferraioli G, Barr RG, Berzigotti A, Sporea I, Wong VWS, Reiberger T, et al. WFUMB Guideline/Guidance on Liver Multiparametric Ultrasound: Part 1. Update to 2018 Guidelines on Liver Ultrasound Elastography. Ultrasound Med Biol. 2024;50(8):1071-1087.
14. Barr RG, Wilson SR, Rubens D, Garcia-Tsao G, Ferraioli G. Update to the Society of Radiologists in Ultrasound Liver Elastography Consensus Statement. Radiology. 2020 Aug;296(2):263-274.
15. Vetter M, Waldner MJ, Zundler S, Klett D, Bocklitz T, Neurath MF, et al. Artificial intelligence for the classification of focal liver lesions in ultrasound - a systematic review. Ultraschall Med. 2023;44(4):395-407.
16. Waldner MJ, Strobel D. Ultrasound Diagnosis of Hepatocellular Carcinoma: Is the Future Defined by Artificial Intelligence? Ultraschall Med. 2024;45(1):8-12.

17. Ding W, Meng Y, Ma J, Pang C, Wu J, Tian J, et al. Contrast-enhanced ultrasound-based AI model for multi-classification of focal liver lesions. J Hepatol. 2025;83(2):426-439.
18. Dietrich CF, Nolsøe CP, Barr RG, Berzigotti A, Burns PN, Cantisani V, et al. Guidelines and Good Clinical Practice Recommendations for Contrast-Enhanced Ultrasound (CEUS) in the Liver-Update 2020 WFUMB in Cooperation with EFSUMB, AFSUMB, AIUM, and FLAUS. Ultrasound Med Biol. 2020 Oct;46(10):2579-2604.
19. Destrempes F, Gesnik M, Chayer B, Roy-Cardinal MH, Olivié D, Giard JM, et al. Quantitative ultrasound, elastography, and machine learning for assessment of steatosis, inflammation, and fibrosis in chronic liver disease. PLoS One. 2022;17(1):e0262291.
20. Andersen NL, Jensen RO, Konge L, Laursen CB, Falster C, Jacobsen N, et al. Immersive Virtual Reality in Basic Point-of-Care Ultrasound Training: A Randomized Controlled Trial. Ultrasound Med Biol. 2023 Jan;49(1):178-185.
21. Jacobsen N, Larsen JD, Falster C, Nolsøe CP, Konge L, Graumann O, et al. Using Immersive Virtual Reality Simulation to Ensure Competence in Contrast-Enhanced Ultrasound. Ultrasound Med Biol. 2022 May;48(6):912-923.
22. Dietrich CF, Lucius C, Nielsen MB, Burmester E, Westerway SC, Chu CY, et al. The ultrasound use of simulators, current view, and perspectives: Requirements and technical aspects (WFUMB state of the art paper). Endosc Ultrasound. 2023 Jan-Feb;12(1):38-49.
23. Chen Z, Chen C, Yang G, He X, Chi X, Zeng Z, et al. Research integrity in the era of artificial intelligence: Challenges and responses. Medicine (Baltimore). 2024 Jul 5;103(27):e38811.
24. Kocak Z. Publication Ethics in the Era of Artificial Intelligence. J Korean Med Sci. 2024 Aug 26;39(33):e249.
25. Tejani AS, Klontzas ME, Gatti AA, Mongan JT, Moy L, Park SH, et al. Checklist for Artificial Intelligence in Medical Imaging (CLAIM): 2024 Update. Radiol Artif Intell. 2024;6(4):e240300.
26. Collins GS, Moons KGM, Dhiman P, Riley RD, Beam AL, Van Calster B, et al. TRIPOD+AI statement: updated guidance for reporting clinical prediction models that use regression or machine learning methods. BMJ. 2024;385:e078378.

27. Sounderajah V, Guni A, Liu X, Collins GS, Karthikesalingam A, Markar SR, et al; STARD-AI Steering Committee. The STARD-AI reporting guideline for diagnostic accuracy studies using artificial intelligence. Nat Med. 2025 Oct;31(10):3283-3289.
28. Liu X, Rivera SC, Moher D, Calvert MJ, Denniston AK. Reporting guidelines for clinical trial reports for interventions involving artificial intelligence: the CONSORT-AI extension. BMJ. 2020;370:m3164.
29. Rivera SC, Liu X, Chan AW, Denniston AK, Calvert MJ, et al. Guidelines for clinical trial protocols for interventions involving artificial intelligence: the SPIRIT-AI Extension. BMJ. 2020;370:m3210.
30. Vasey B, Nagendran M, Campbell B, Clifton DA, Collins GS, Denaxas S, et al; DECIDE-AI expert group. Reporting guideline for the early stage clinical evaluation of decision support systems driven by artificial intelligence: DECIDE-AI. BMJ. 2022 May 18;377:e070904.
31. Jiang Z, Salcudean SE, Navab N. Robotic ultrasound imaging: State-of-the-art and future perspectives. Med Image Anal. 2023;89:102878.
32. Lin XX, Li MD, Ruan SM, Ke WP, Zhang HR, Huang H, et al. Autonomous robotic ultrasound scanning system: a key to enhancing image analysis reproducibility and observer consistency in ultrasound imaging. Front Robot AI. 2025 Feb 5; 12:1527686.

„MPUS for the assessment of the liver" provides a relatively comprehensive introduction into the available tools and applications for the ultrasonic evaluation of the liver.
The authors and editors are to be congratulated on putting together an up-to-date text on this topical subject, stimulating further exploration through extensive references.
The text is supplemented with useful figures, illustrations and key take-home messages at the end of each chapter.
Overall, this textbook represents a valuable compendium for both trainees and experienced clinicians performing liver ultrasound in routine practice.

Adrian Lim
March 2026, London, UK

Professor Adrian Lim MD FRCP FRCR
Imperial College London and NHS Trust
President-Elect, EFSUMB

ISBN 978-606-786-556-1